Design and Synthesis of Novel CYP51 Inhibitors as Therapeutics for *Candida Albicans* Infections.

A thesis submitted to Cardiff University for the Degree of Doctor of Philosophy

PhD Thesis (2022)

By

Marwa Naser Alsulaimany

School of Pharmacy and Pharmaceutical Sciences, Cardiff University

Supervisor: Dr. Claire Simons

Table of Contents

List of Figures:

List of Tables:

viii

List of Abbreviations:

CaCYP51: *candida albicans* cytochrome P51

CDI: 1,1′-carbonyldiimidazole

DMF: dimethylformamide

EtOAc: ethyl acetate

HPLC: high performance liquid chromatography

HTIB: hydroxy(tosyloxy)iodobenzene

IC$_{50}$: half maximum inhibitory concentration

MIC: minimum inhibitory concentration

MD: molecular dynamic simulation

NADPH: nicotinamide adenine dinucleotide phosphate

Pd/C: palladium in carbon

Pd(PPh$_3$)$_4$: tetrakis(triphenylphosphine)-palladium(0)

R*f*: retention factor

RMSD: root mean square deviation

THF: tetrahydrofuran

TLC: thin layer chromatography

TMSOI: trimethylsulfoxonium iodide

TPP: triphenylphosphine

Twenty Amino Acids:

Name (Amino acid)	3 Letter Code	1 Letter Code
Cystine	Cys	C
Glycine	Gly	G
Glutamic acid	Glu	E
Leucine	Leu	L
Lysine	Lys	K
Methionine	Met	M
Phenylalanine	Phe	F
Serine	Ser	S
Tyrosine	Tyr	Y
Aspartic acid	Asp	D
Arginine	Arg	R
Histidine	His	H
Threonine	Thr	T
Asparagine	Asn	N
Glutamine	Gln	Q
Proline	Pro	P
Alanine	Ala	A
Valine	Val	V
Isoleucine	Ile	I
Tryptophan	Trp	W

Acknowledgments

Abstract

Lanosterol 14α-demethylase, CYP51, is an important target enzyme in fungal diseases. *Candida albicans* (*C. albicans*) is one of the fungal pathogens prevalent in human infections, which causes infections that range from superficial to life-threatening systemic infections, a particular challenge in immunocompromised patients. Although azoles (especially Fluconazole) have been used as a first choice for the treatment in many fungal infections and as a prophylactic, issues of drug resistance to this class of antifungals are increasing. The aim of this study was to design and synthesise novel CYP51 inhibitors that can counteract the azole resistance mechanism in *C. albicans*.

Drug design employed computational methods: Molecular Operating Environment (MOE) for docking and binding studies and Desmond Maestro for Molecular Dynamic (MD) simulations to determine optimal fit in the CaCYP51 active site and binding interactions. From the computational docking study, thiazole, hydroxy-propyl benzamide and non-hydroxy-propanamide novel compounds were selected for synthesis; a short series (fluconazole type), a mid-sized and an extended series (posaconazole type), which showed promising docking results. The extended series was observed to have optimal filling of the active site and additional binding interactions (H-bonding and π-π/hydrophobic) at the access channel that were anticipated to counteract the loss of one key H-bonding interaction with Tyr132, a common mutation in *C. albicans* azole resistant strains (Y132H, Y132F). Using 4-8 step synthetic schemes, all series were obtained and compounds subject to structure (^{1}H and ^{13}C NMR, mass spectroscopy) and purity (HPLC) analysis.

All final compounds for the thiazole (Chapter 2 and 3), chloro and dichloro of the hydroxy-propyl benzamide (Chapter 4) were evaluated against *C. albicans* strains (MIC) and promising compounds evaluated further for CaCYP51 binding affinity (K_d) and inhibitory activity (IC$_{50}$) in comparison with the standards fluconazole. Owing to the COVID-19 situation, the fluoro and difluoro compounds of the hydroxy-propyl benzamide series (Chapter 4) were screened first against the model organism *Saccharomyces cerevisiae* wildtype and single mutant strains using disk diffusion assay, and the most promising compounds were progressed for evaluation against C. *albicans* strains using disk diffusion assay and MIC in comparison with posaconazole. The hydroxy-propyl benzamide extended compounds (Chapter 4) (**57**, **59**, **69** and **70**) were found to be active against *C. albicans* strains. The biological assessment of the non-hydroxy-propanamide compounds (Chapter 5) is still in progress. Those compounds with optimal activity will be further evaluated against CaCYP51 mutant strains as

well for selectivity against human CYP51. Further testing against a wide range of fungal strain will be done for future work.

Chapter I

(Introduction)

Introduction:

The kingdom of fungi includes yeasts, mushrooms, molds and rusts, which are characterised as eukaryotic organisms.[1] Some of these organisms are harmful while others are beneficial.[1] For instance, the beneficial fungi play a major role in the production of certain drugs as well as cheese, beer and other food.[1] Also, fungi are considered an important source of nutrients for humans because they can initiate the production of many vitamins and proteins.[1] On the other hand, some of these fungi can cause a wide range of infections if they enter the human body by inhalation or through wounds.[1] In 2017, a study found that nearly a billion people were estimated to have mild (skin, nail, and hair) fungal infections while 150 millions had serious fungal diseases globally; moreover, the mortality from fungal infections are now recognised to be over 1.6 million people annually which is 3-fold more than malaria and similar to tuberculosis.[2] Unfortunately, fungal diseases are still a neglected area of public health even though 80 % of patients' lives could be saved from dying by early detection.[2] The most common fungal pathogens that cause the majority of serious fungal disease are *Candida*, *Aspergillus*, *Pneumocysti* and *Cryptococcus* species.[2,3] The annual incidence of fungal infections from the Leading International Fungal Education (LIFE) portal, reported 50% of invasive candidiasis (candidemia, 78,778 cases) in Asia, followed by Central and South America (40,613 and 33,962 cases, respectively), Europe (29,130 cases; the United Kingdom had the highest number of cases ≅ 5142, 8.1 cases per 100,000 population) and Africa (19,602 cases).[2] Additionally, Asian countries had 50% of the cases of invasive aspergillosis (81,927 cases) with Vietnam reporting the highest number of cases (14,523 cases), followed by Europe (24,201 cases) with Germany reporting the highest number of cases (4280 cases).[2] *Cryptococcus* infections are most common in the Africa continent.[2]

According to Centers for Disease Control and prevention (CDC) in 2020, patients with severe COVID-19 symptoms have developed aspergillosis or invasive candidemia regardless if the patient was an immunocompromised or normal patient.[4,5,6] Different studies reported invasive aspergillosis in patients with severe COVID-19 occurred in 43 cases from several countries, but mostly from Europe and 4 cases from South America, specifically Argentina.[6–8] Moreover, 39% of invasive candidemia has been reported in COVUD-19 patients in China (38 cases of 96) followed by Brazil which reported 36% (9 cases of 25), Italy 2.1% (21 cases of 989) and 0.4% in Spain (4 cases of 989).[5,9] Importantly, COVID-19 fungal coinfection can increase the incidence of the mortality worldwide.[4,5]

Candida species ranked fourth in infections after the common bacterial pathogens.[2,3] There are more than 20 Candida species involved in human fungal infections. These species vary in the site of infection and the geography.[10] Globally, the number of cases of invasive candidiasis is about 700,000 cases annually.[2] Some of the prevalent Candida species are Candida albicans (C. albicans), Candida glabrata (C. glabrata), Candida parapsilosis (C. parapsilosis), Candida tropicalis (C. tropicalis), Candida krusei (C. krusei) and Candida auris (C. auris). These species are opportunistic pathogens that cause superficial and systemic infections.[11] The pathogenicity of Candida species results from the production of hydrolytic enzymes, formation of biofilms by adhering to medical devices or host mucosal epithelum.[11] Biofilms can contain one or more types of microorganisms, which are organised and are embedded in an extracellular matrix.[11] The difference between all Candida species depends mainly on the structure of the biofilms and the extracellular matrix compositions.[11]

Candidiasis is the terminology used generally to describe the fungal diseases that occur from Candida species, all of which are yeasts.[1,12] Of all these species, C. albicans is the most frequent cause of fungal infections.[3,13,14] Moreover, C. albicans is one of the fungi that can exist normally in the human flora, which mostly resides as a lifelong/harmless commensal.[15,16] One of the essential sterols that plays a major role in fungal cell life is ergosterol, which means that fungi cannot survive without ergosterol, for this reason ergosterol biosynthesis is an important target of antifungal drugs.[17]

Ergosterol Biosynthesis:

Sterols are essential lipids of most eukaryotic cells, and they play a major role in cell structure and signaling.[18] In fungi, ergosterol is the main sterol component of the cell membrane that protects the permeability and the fluidity of the membrane.[19,20] The biosynthetic pathway of ergosterol synthesis in C. albicans is a long multistep synthesis that starts from squalene, which is a precursor of sterol biosynthesis in fungi as well as in human, and gives the sterol end product (ergosterol).[18] One of the most important cytochrome P450 (CYP) enzymes involved in the synthesis of ergosterol is lanosterol 14α-demethylase (CYP51), which is also known as Erg11.[21,22] The demethylated intermediates resulting from the catalytic reaction of this enzyme are essential in the ergosterol biosynthesis pathway (Figure 1).

However, there is another pathway that supports the viability of C. albicans when CYP51 is mutated. This pathway involves the conversion of lanosterol into the 14α-methyl

fecosterol intermediate, which protects the stability of the cell membrane in the absence of Erg3 (Figure 1). [10,6,21] Erg3 , a desaturase enzyme, cannot initiate the desaturation step when Erg11 is mutated, thus Erg3 will convert 14α-methyl fecosterol into a toxic sterol 14α-methylergosta-8,24(28)-dien-3β,6α-diol (Figure 1).[4,23] This is one of the pathways that controls the survival of *C. albicans* in humans and as a result, overgrowth of *C. albicans* will lead to different types of fungal infections called candidiasis.
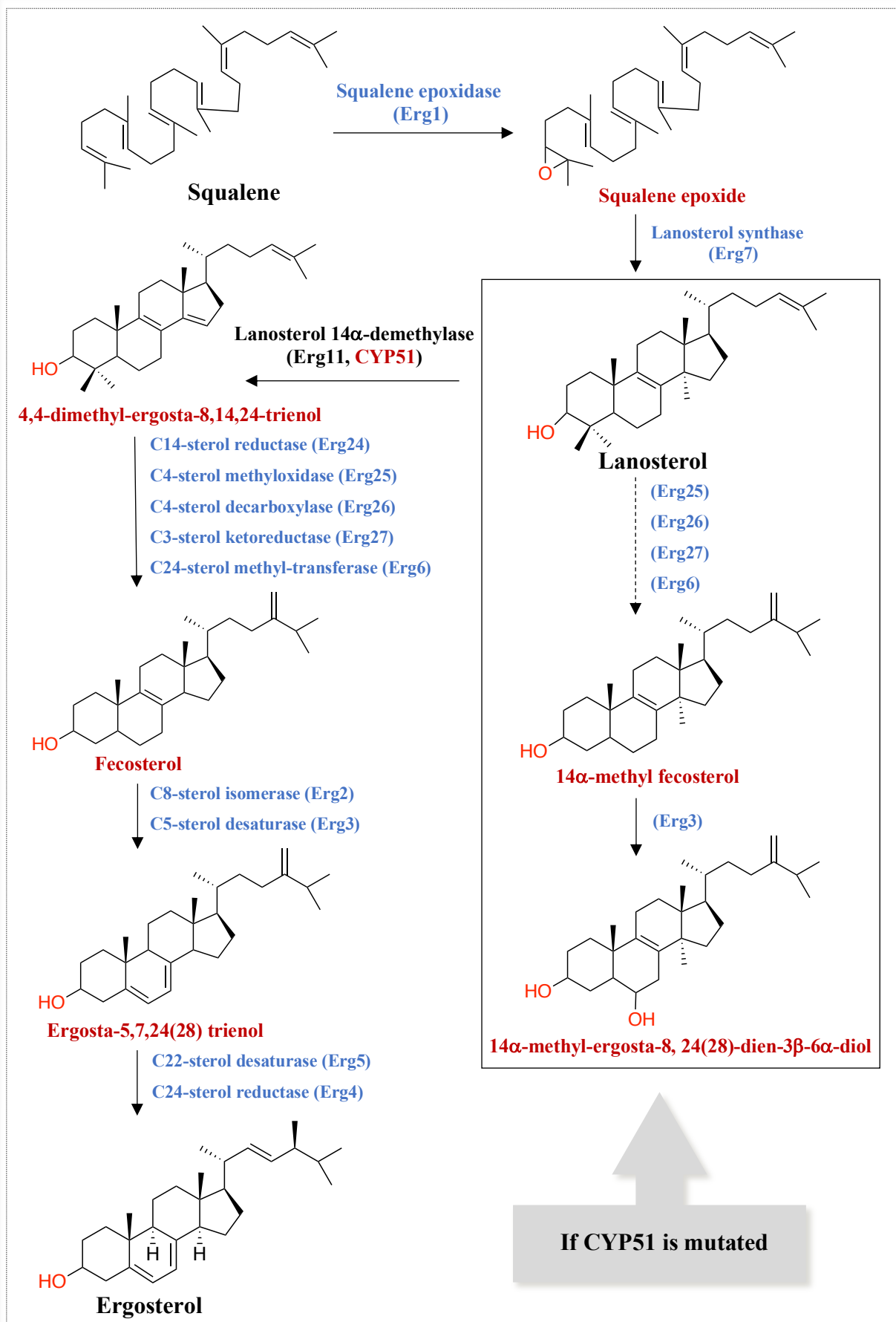
Figure 1: Ergosterol biosynthesis in *C. albicans.*

Candidiasis:

Candidiasis is a yeast infection caused predominantly by *C. albicans*, which resides in different parts of the human body such as the gastrointestinal tract, genitourinary tract, oropharynx, and surrounding the skin.[8,15] Under certain conditions, *C. albicans* can cause infections that range from superficial to life-threatening infections such as candidemia.[15,24] There are several factors that increase yeast growth and lead to candidiasis, one of the factors is overuse of antibiotics, which can kill the beneficial bacteria that control the growth of these yeasts.[6,7,25] Another factor is an impaired immune system, which can occur due to treatment with cancer chemotherapy, organ transplantation, and using different types of implantable medical devices.[6,7,25] In addition, there are different types of candidiasis, which include candida of the mouth/throat, and this is known as thrush or oropharyngeal candidiasis, respectively.[26,27] Vaginal candidiasis is another type referred to as vaginal yeast infection or vulvovaginal candidiasis.[26,27] The most dangerous type is known as invasive candidiasis, which is life-threatening because it can affect the heart, brain, bone, blood and other organs.[26,27] Furthermore, immunocompromised patients are very susceptible to invasive fungal infection, and the treatment is preventive.[28,29] Worldwide, one of the most common healthcare associated bloodstream infections in intensive care units (ICU) with a mortality of 30-50% is candidemia.[25,30] As a result, it is important to increase research in this area of candidiasis in order to discover a promising antifungal treatment as the current number of effective antifungal agents is limited with drug resistance associated with current antifungals.[3,13]

Classification of antifungal treatments:

Sterol is a major structural component of fungal and human cell membranes, however cholesterol is the essential sterol in human cell membranes while the predominant sterol in fungal cell membranes is ergosterol.[24] Another significant difference is that fungi have a cell wall while the human cell does not.[31] These biochemical differences can be exploited for drug design. There are five major classes of antifungal agents: polyenes, echinocandins, allylamines, antimetabolite (flucytosine) and azoles (Figure 2). Novel classes of antifungals with novel targets are also being actively developed and some are in clinical trials.[32,33]
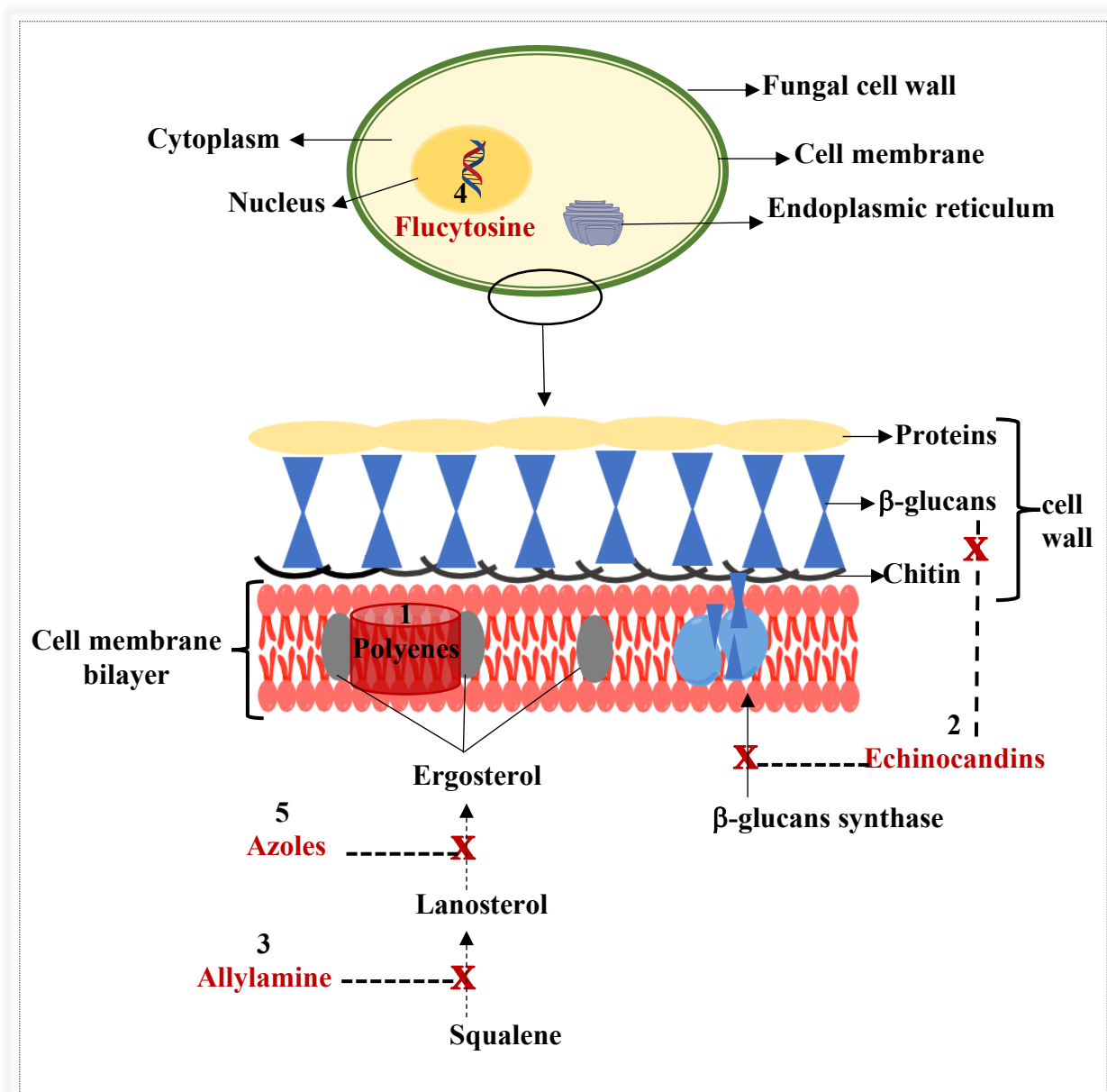
Figure 2: Targets for antifungal treatments in *C. albicans*.

1) Polyenes:

The polyenes are macromolecules that contain hydrophilic and hydrophobic regions. The mechanism of action of this class first involves the lipophilic region that crosses the cell lipid bilayer and binds to ergosterol to form a pore. Through this pore, potassium and other cellular ions are lost leading to cellular death.[24,31] In addition, polyene antifungals have a higher affinity to ergosterol containing cell membranes than cholesterol membranes, resulting in selective toxicity to fungal cells.[24,31] The antifungal drugs in this class include Amphotericin B (AmpB) and Nystatin, which differ from each other according to the route of administration, and

whether used for local or systemic treatment (Figure 3).[24,31] AmpB is taken intravenously and can maintain a broad spectrum of fungicidal activity. However, although these drugs could be the first choice in many serious fungal infections, especially life-threatening infections, they have limited use because of the severe renal and host toxicity.[34,35] Moreover, AmpB rarely develops resistance with only two Candida species (*C. lusitaniea* and *C. auris*) with resistance to AmpB as observed by increase in MIC value.[32,36] The resistance developed from the two species resulted from the low membrane ergosterol content which leads to reduced susceptibility and low reactive oxygen species (ROS) level, as AmpB usually produces high levels of ROS in fungal cells in normal condition, in addition to production of different sterols.[32,36] AmpB cochleate, a new orally available formulation is currently under investigation for the treatment of vulvovaginal candidiasis.[37] AmpB cochleate is a lipid bilayer based drug delivery system, which consist of phosphatidylserine and calcium precipitate, that form a spiral without internal aqueous space to improve drug absorption across the GIT.[37] Once the cochleate reaches the circulation, the calcium concentration is decreased and the drug releases from the opened spiral.[37]
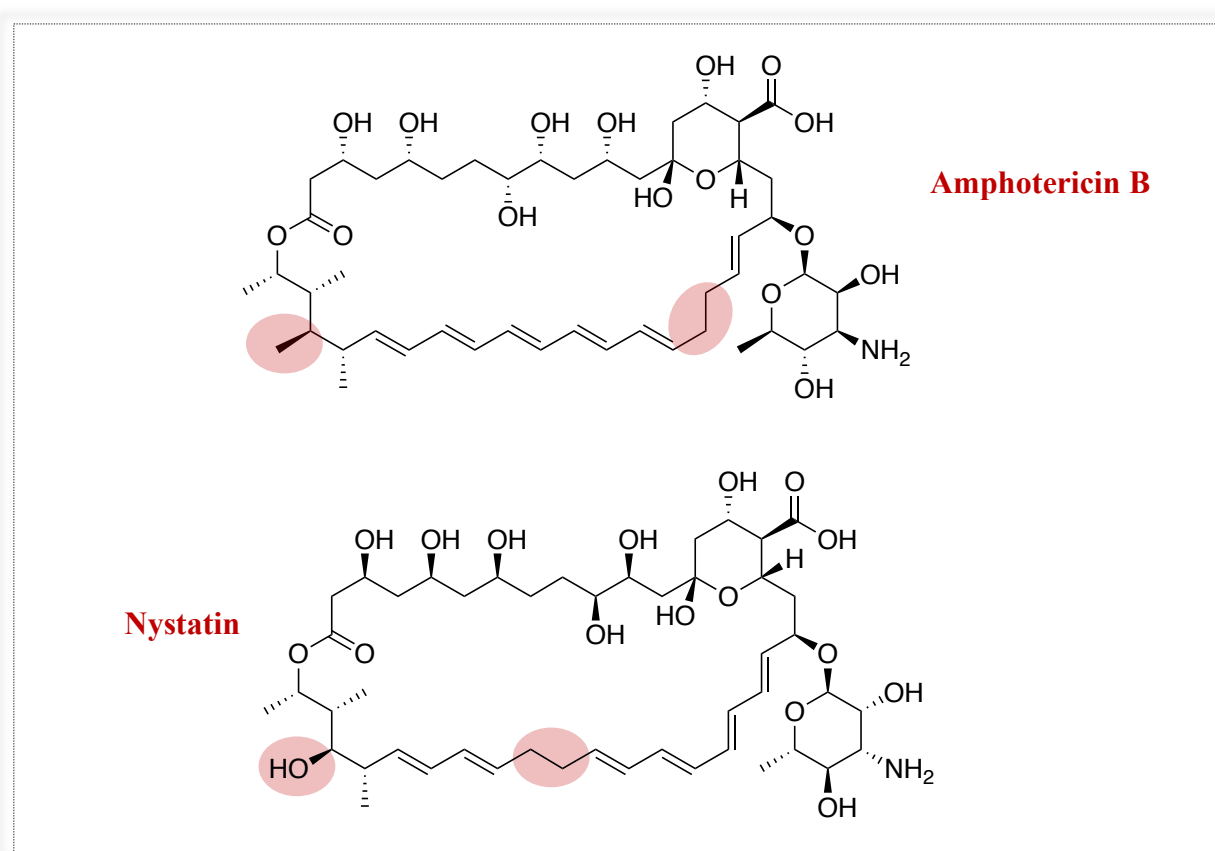
Figure 3: Examples of polyene compounds.

2) Echinocandins:

Echinocandins are group of cyclic peptides with side chains of lipophilic molecules.[24] Echinocandins were the first novel selective antifungal agents that inhibit fungal cell wall biosynthesis, through inhibiting the enzyme β-1,3-glucan synthase (Fks1), which is encoded by the *FKS1* gene.[24,38,39] Furthermore, the main function of this enzyme is catalysing the formation of β-glucan, which is a natural component of the fungal cell wall. Thus, reduction in the level of β-glucan will lead to cell wall stress and the integrity of the cell will be lost.[24,40] The antifungal drugs in this class include Caspofungin, Anidulafungin and Micafungin, which have been used to treat life-threatening/systemic fungal infections (Figure 4).[24,31] Due to the serious side effects of this class, specifically hepatotoxicity, as well as the absence of oral activity, they have limited use in the clinic.[24,41] In addition, the resistance of Candida species to echinocandins is due to a single mutation in the Fks1 protein, which leads to reduced enzyme activity.[32,36,38] For *C. albicans*, the resistance occurred less than 3% compared to other Candida species and the common amino acid mutation in *C. albicans's* Fks1 hot spot Phe641-Pro649 is Phe641Ser.[38,42] *C. glabrata* resistance to echinocandins is the most significant compared to other Candida species with 8% occur and the single mutation in Fks1 is Ser629Pro.[38,42] Owing to the low bioavailability and the high frequency of IV dosing of this class, a second generation of inhibitors (Rezafungin/CD101) with improvements in the molecule stability, solubility, frequency of use and toxicity is in phase II clinical trial.[37,38] Structurally, rezafungin is similar to anidulfungin in chemical structure but with modification to improve the pharmacological properties.[37] Another inhibitor of β-1,3-glucan synthase is Ibrexafungerp (SCY-078), which has a unique structure.[37] This inhibitor shows high bioavailability as well as broad spectrum activity against different fungal pathogens, including azole resistance strains, and it can be administered either orally or intravenously.[37,38] Ibrexafungerp was approved by FDA in June 2021 for treating vulvovaginal candidiasis.[43,44]
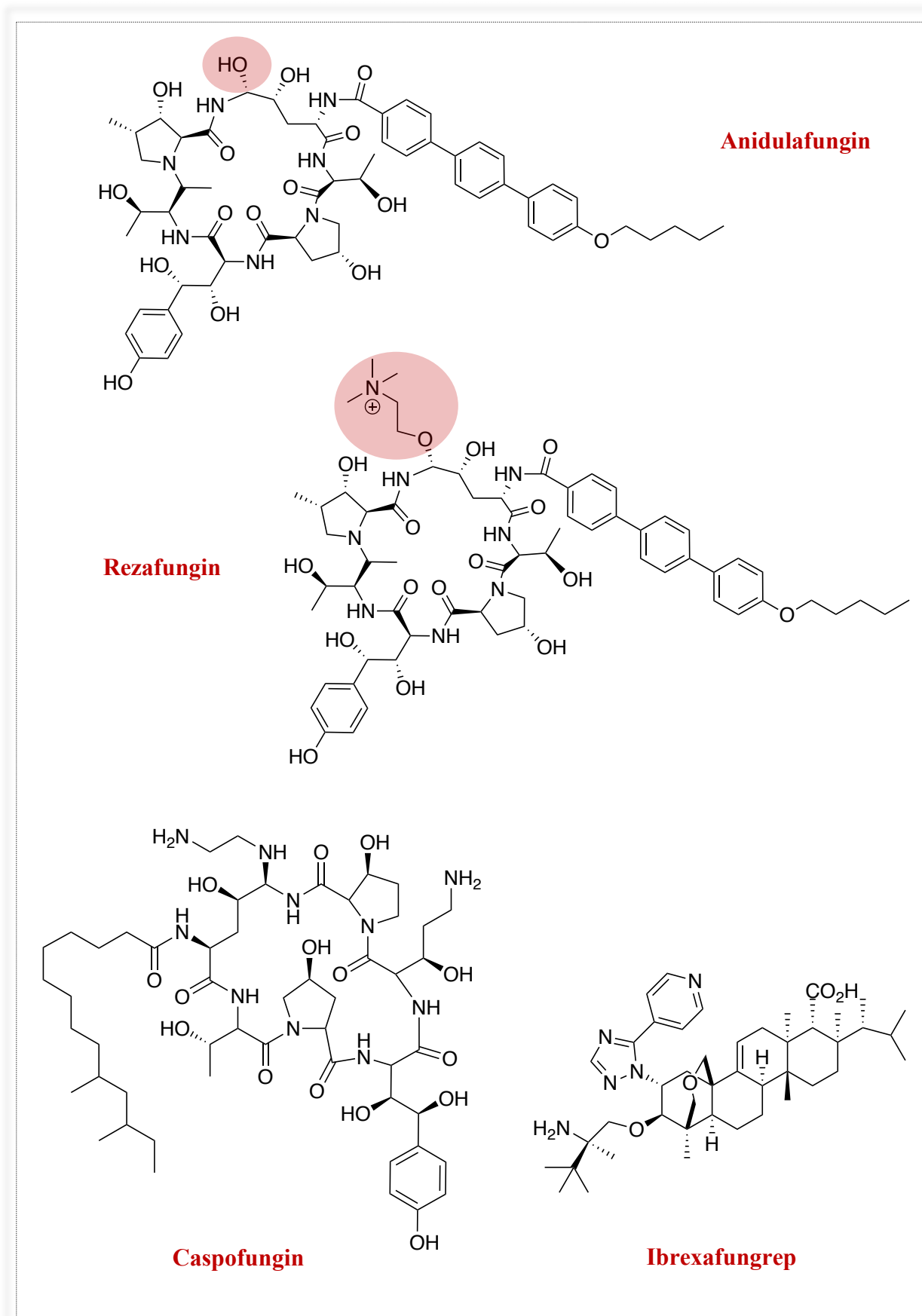
Figure 4: Examples of echinocandins compounds.

3) Allylamines:

Allylamines are mostly used for dermal infections, and usually prescribed in the treatment of fungal infections of the nail and skin.[35] Therefore, they have a limited spectrum of activity compared with the other antifungal classes. All of the drugs in this group act by inhibiting the biosynthesis of ergosterol through the inhibition of squalene epoxidase.[25,45] The first allylamine discovered was Naftifine, which is only available in topical dosage form, while terbinafine is available in oral and topical dosage forms (Figure 5).[46] The limitation in this class varies with the drug itself. In the case of Naftifine, it is not available orally because it goes through extensive first pass metabolism.[45] The most implicated enzymes in first-pass metabolism are CYP enzymes, which includes CYP2D6, CYP3A4, CYP1A2, and CYP2C19, and this class of antifungal treatments can be metabolised by the microsomal CYPs through several pathways such as aromatic hydroxylation, aliphatic hydroxylation and N-dealkylation.[45,47,48] Terbinafine, is involved in drug-drug interactions with other CYP enzymes such as CYP2D6, which is an important enzyme for metabolising many drugs.[24] No resistance has been reported for allylamines used in the clinic.[37]

Figure 5: Examples of allylamines compounds.

4) Antimetabolite:

Any drug, similar to the structure of a natural chemical metabolite or enzymatic substrate, which can interfere with the reactions/functions of an enzyme necessary for DNA synthesis is known as an antimetabolite. Flucytosine (FC) is a fluorinated analogue of cytosine used in the treatment of serious systemic fungal infections, such as Cryptococcus and Candida species.[24,39] FC a prodrug that is metabolised by fungal cytidine deaminase to the active form, 5-flurouracil (5-FU). 5-FU is metabolised to 5-fluorodeoxyuridine (5-FdU) and then to 5-fluorodeoxyuridine monophosphate (5-FdUMP) by thymidine kinase. 5-FdUMP is a competitive inhibitor of thymidylate synthase, which is important for protein and RNA biosynthesis.[24,39] Inhibition of thymidylate synthase blocks the formation of thymidine monophosphate from deoxyuridine monophosphate leading to inhibition of DNA synthesis (Figure 6).[24,39] However, the cytidine deaminase enzyme only exists in fungi and selective

fungal suppression is achieved.[24,39] Resistance to FC rapidly develops when used alone, therefore, FC is normally used in conjunction with AmpB, which results in an increase fungal uptake of FC owing to a synergistic effect.[24,39] Human toxicity from FC arises from intestinal flora that convert FC to 5-FU, but the major toxicity is depression of the bone marrow which leads to anaemia, leukopenia, and thrombocytopenia.[24,39] Moreover, hepatotoxicity is another side effect of FC and its incidence is not clear. Some studies reported that hepatotoxcicity from FC is concentration-dependent, therefore dosage needs to be maintained and managed for each patient. [24,39] Owing to the toxicity of FC, azoles antifungals are the preferred therapeutics for systemic infections.[24,39]
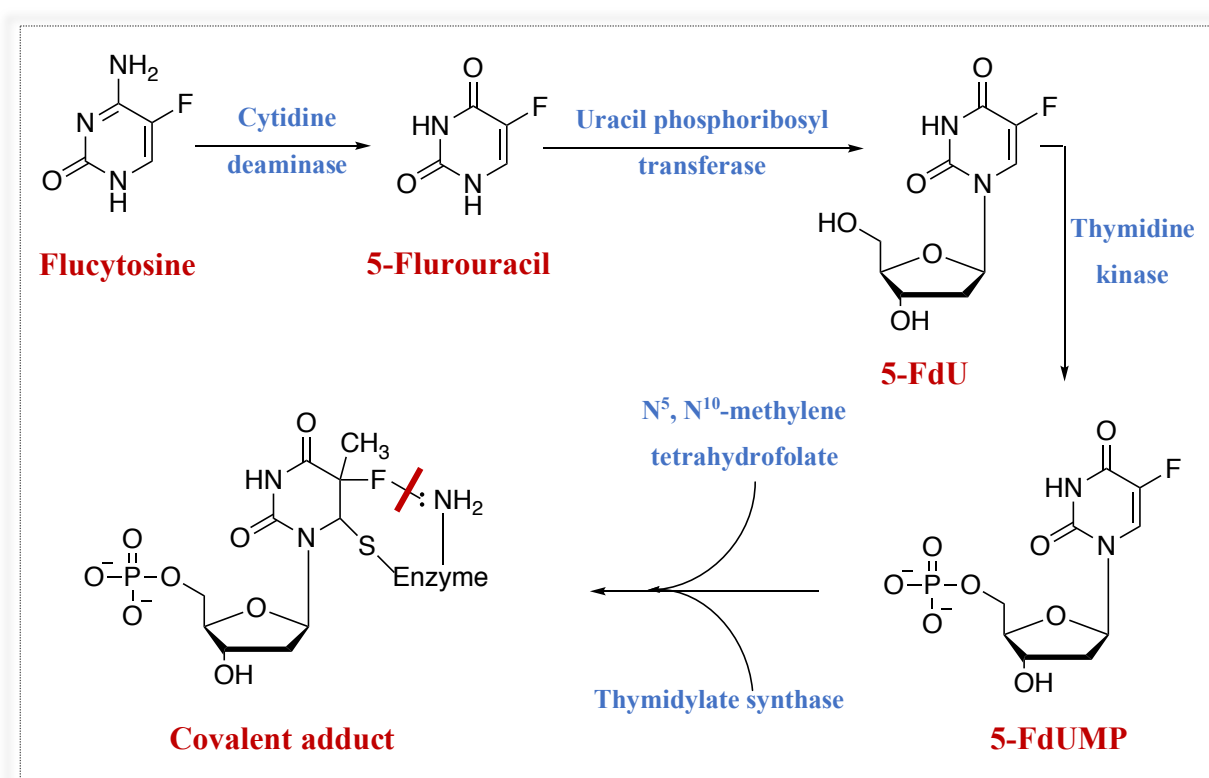
Figure 6: Flucytosine reaction mechanism in fungi.

5) Azoles:

The largest class of antifungals is the azole antifungal drugs, which contain either an imidazole or triazole ring. The basic nitrogen of the azole ring forms a bond with the haemactive site (haem iron) of the 14α-demethylase (CYP51) enzyme.[25] The mechanism of action of all azoles is inhibition of the biosynthesis of ergosterol through inhibition of CYP51, leading to fungal cell death.[4,9] In order to enhance the selectivity of azoles to the fungal CYP51

enzyme, the triazole nucleus has replaced the imidazole in the active pharmacophore.[46] The antifungal agents in this class includes (Figure 7):[38]

    1. First generation azoles ketoconazole, clotrimazole, and chlormidazole, which have an imidazole ring,

    2. Second and third generation azoles fluconazole, itraconazole, voriconazole and posaconazole, which have a triazole ring,

Some of these medications are used systemically and/or topically and for superficial and life threatening fungal infections.[33] Comparing with the other mentioned classes, the high oral bioavailability, low toxicity, selectivity, tolerability by patient and the broad spectrum of activity of this class allows the widespread use in treating serious fungal infections.[24,31] However, there are some limitations for the use of these azoles. For example, *C. krusei* is naturally resistant to fluconazole and must be treated with other azoles.[32] Voriconazole has a broad spectrum of activity against most Candida species and fungal pathogens over fluconazole, but voriconazole has more adverse effects and drug-drug interactions than fluconazole.[32] The low bioavailability of itraconazole and posaconazole, which have broad spectrum activities against candidiasis, has limited clinical use.[37] As the traditional oral itraconazole has poor bioavailability, this led to the development of an oral capsule with a pH dependent polymer matrix to enhance dissolution and absorption.[36] SUBA-itraconazole has been approved by the FDA for specific cases, especially in fungal strains that develop resistance to AmpB therapy.[36]

Based on the inhibitory effect of the available azoles on human CYPs (CYP3A4 and CYP2C9) and fluconazole resistance, new compounds with a tetrazole ring have been developed in order to increase specificity to fungal CYP51.[37,49] Quilseconazole (VT-1129), is a new azole compound showing activity against Cryptococcus infections by inhibiting CYP51 and is in the preclinical stage,[37,49] while oteseconazole (VT-1161) showed high potency against two Candida species that are extremely resistant to fluconazole (*C. glabrata* and *C. krusei)*.[25,32,50] In addition, oteseconazole has specific affinity for fungal CYP51 versus human, fewer off-target effects and fewer drug-drug interactions compared with other azoles.[32] Currently, oteseconazole is in phase 3 clinical trials for the treatment of recurrent vulvovaginal candidiasis.[32,51] Although azoles (especially fluconazole) have been used as the first choice of treatment in many fungal infections and as a prophylactic, issues of drug resistance to this class of antifungals, especially in *C. albicans*, are increasing.[3,19]
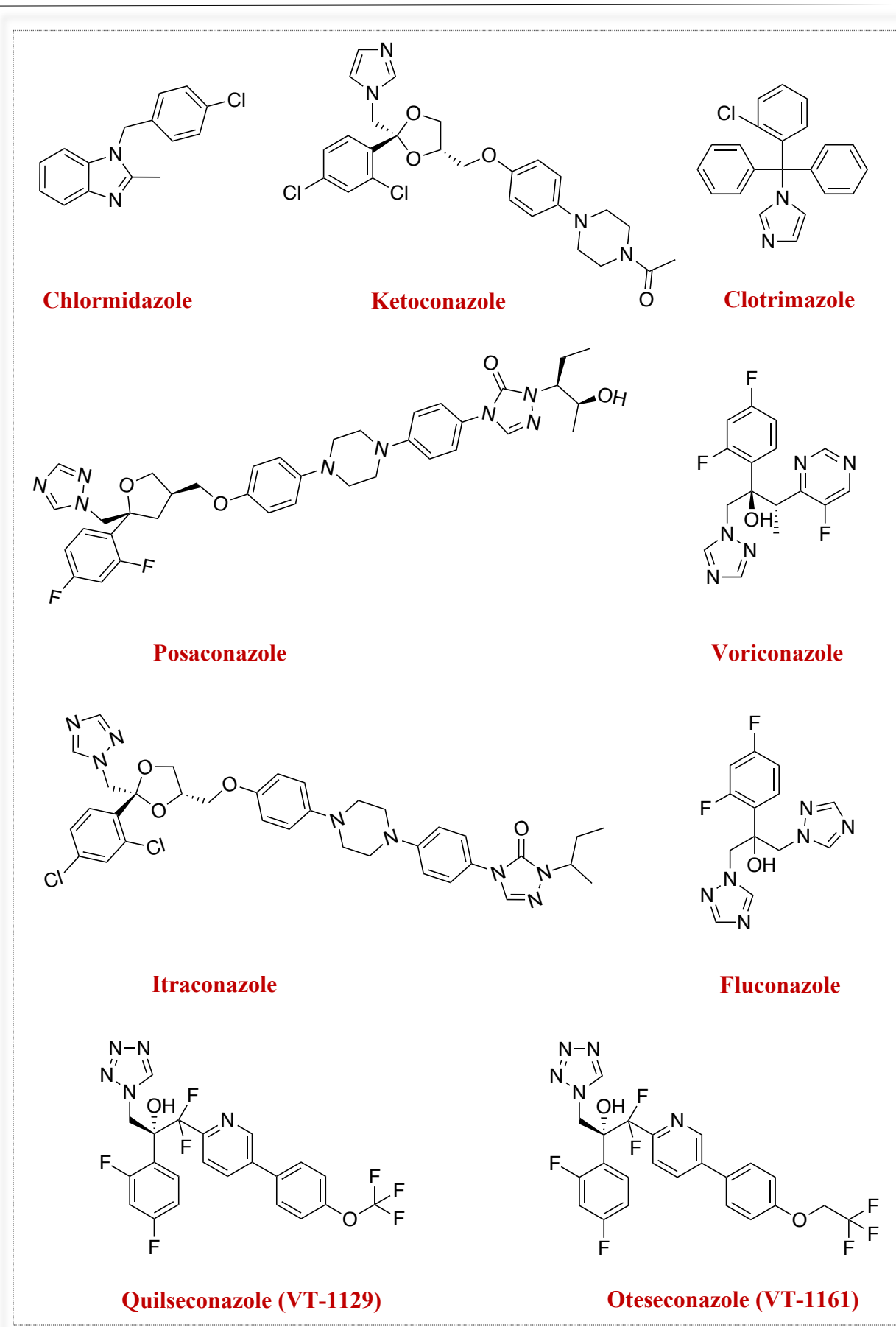
Figure 7: Examples of azole compounds.

Azole resistance:

The development of drug resistance to the available medications, especially to azole antifungals in yeast and other fungi is increasing.[52] This is attributed to the long treatment administration of azole antifungals in the clinic, the prophylactic use, and the widespread use of agricultural azole fungicides to protect crops.[13] In addition, azole drugs are fungistatic rather than fungicidal, and that could be another factor in developing drug resistance.[22]

Susceptible dose dependent (SDD indicates the maximum drug dose required for optimal treatment, which has been identified by measuring the minimum inhibitory concentration of fluconazole (MIC, μg/mL).[13,14,32] The SDD for fluconazole in Candida species such as *C. albicans*, *C. tropicalis*, and *C. parapsilosis* is in the range of 0.125-4 μg/mL while for *C. glabrata* it is ≤ 32 μg/mL.[32,53–55] The breakpoint of fluconazole resistance in Candida species occurs when the MIC value for *C. albicans*, *C. tropicalis*, and *C. parapsilosis* is ≥ 4 μg/mL while an MIC greater than 32 μg/mL in *C. glabrata* is considered resistant.[32]

One of the most common yeast that causes a wide range of human infections in the clinic from mucosal to life-threatening infections is *C. albicans*.[13,14] According to the Centre of Disease Control and Prevention, there are 46,000 hospitalised patients yearly worldwide owing to *C. albicans* fluconazole resistance.[19] However, there are four major mechanisms of azole resistance in *C. albicans* (see Figure 8):[13,19,46-28]

1. Overexpression CaCYP51:

Overexpression of the enzyme is due to upregulation of the *ERG11* gene. This requires more drug to inhibit the enzyme and contributes directly to reduced susceptibility to *C. albicans*. [33,36,38] The transcription factor UPC2 is responsible for the regulation of most ergosterol biosynthesis genes, thus activating mutations in the *UPC2* gene contributes to azole resistance, whereas disruption of *C. albicans UPC2* increases azole susceptibility.[33,36,38]

2. Overexpression of efflux pump proteins (transporters):

Overexpression of the membrane efflux pumps play a major role in reducing the intracellular concentration of azoles leading to azole resistance. There are two main efflux pump classes responsible for the development of antifungal/azole resistance with different mechanistic strategies to efflux drugs: the ATP-binding cassette (ABC) proteins and major facilitator superfamily (MFS) efflux pumps.[56]

a. ATP-binding cassette (ABC) proteins:

ABC proteins, which have five known subfamilies, are primary active transporters, and the driving force to efflux the drugs is the energy produced from the hydrolysis of ATP.[56] The subfamily associated with *C. albicans* resistance is the pleiotropic drug resistance (PDR) family, which include seven proteins Cdr1, Cdr2, Cdr3, Cdr4, Cdr11, Snq2p, and Ca4531.[56] Upregulation of ABC efflux pumps Cdr1 and Cdr2, specifically Cdr1, which represents a major drug transporter of *C. albicans*, leads to azole resistance by overexpression of the encoding gene (*CDR1/CDR2*).[32,56]

b. Major facilitator superfamily (MFS):

The secondary active transporter MFS, which has 17 families of proteins, act by utilising the electrochemical gradient.[56] The electrochemical gradient is a difference in hydrogen ion concentration across a membrane which will produce a concentration gradient and an electrical potential gradient.[56,57] These gradients together store potential energy in the cell to be used for drug efflux.[56,57] However, of all 17 MFS proteins, Mdr1 is known to efflux azole drugs in *C. albicans*, and the overexpression of its gene (*MDR1*) can be enhanced by other drugs leading to azole resistant clinical isolates.[56]

One of the major mechanisms that contribute to azole resistance in *C. albicans* is the ABC drug-efflux system, leading to a new approach, which is the development of chemosensitisers to the cell by inhibiting Cdr1 and Cdr2 to restore the activity of fluconazole resistant strains of *C. albicans*.[33]

3. Secondary mutation:

Secondary mutations in the ergosterol biosynthetic pathway, especially mutations in the *ERG3* gene, occurs commonly.[13,39] The Erg3 enzyme has two important roles in the ergosterol biosynthesis pathway:

1. Catalysing one of the final steps of the pathway to form ergosterol.

2. Converting non-toxic sterol (14α-methyl-fecosterol), which accumulates during Erg11 mutation, to a toxic sterol (14α-methylergosta-8,24(28)-dien-3β,6α-diol) that eliminated rapidly by the cell.[10]

Thus the lack or deactivation of Erg3 allows the accumulation of 14α-methyl-fecosterol which is capable of protecting the fungal cell membrane functions.[10,58,59]

4. CaCYP51 mutations:

Mutations in the amino acid sequence of the enzyme Erg11 (CYP51), which is the main target of azole drugs, results in reduced affinity of the drugs to the mutated CYP51 protein. This is the most common mechanism for azole resistance in *C. albicans* determined from the clinical isolates.[13,14,32] Different studies have found that the isolates could have at least one mutation or more.[14,60] Several studies reported that *C. albicans* fluconazole resistance is related to single and double mutations within CYP51.[13,14] The most serious single amino acid mutations include Y132F, K143R, and S279F, which are located within the haem active site, and also the G450E single mutation located within the electron transfer area of NADPH-P450 reductase.[13,14,52] The greatest increase in the IC_{50} compared with the wild-type CaCYP51enzyme was observed with the double mutations Y132H/K143R (22.1-fold), Y132F/K143R (15.3-fold), and G307S/G450E (13-fold),).[13,14,52] The single mutations Y132F, K143R, D278N, S279F, S405F, G448E, and G450E showed at least 2-fold increases in the fluconazole IC_{50} and MIC. The double mutation Y132F/K143R showed the strongest increase in MIC (32-fold), owing to high resistance to fluconazole.[14]

Another resistance mechanism related to biofilm formation has been reported.[38,39] The last step in biofilm formation is maturation, which is controlled by the gene *FKS1* in the presence of glucose, followed by the production of extracellular matrix that plays a major role in protecting the cells from phagocytic cells and acting as a barrier to drugs.[38] The high levels of β-1,3-glucan synthase (Fks1) in the matrix has been observed and found to contribute to fluconazole resistance in *C. albicans*.[38] Finally, most drug resistance problems depend on fungal species and the type of antifungal agent.[15,20,23] According to CDC, patients with severe COVID-19 fungal-coinfection have developed resistance against current antifungal treatment owing to immunity suppression by the virus.[4,9] As a result, the need for novel antifungal drugs to be identified is high as well as alternative therapeutic approaches.
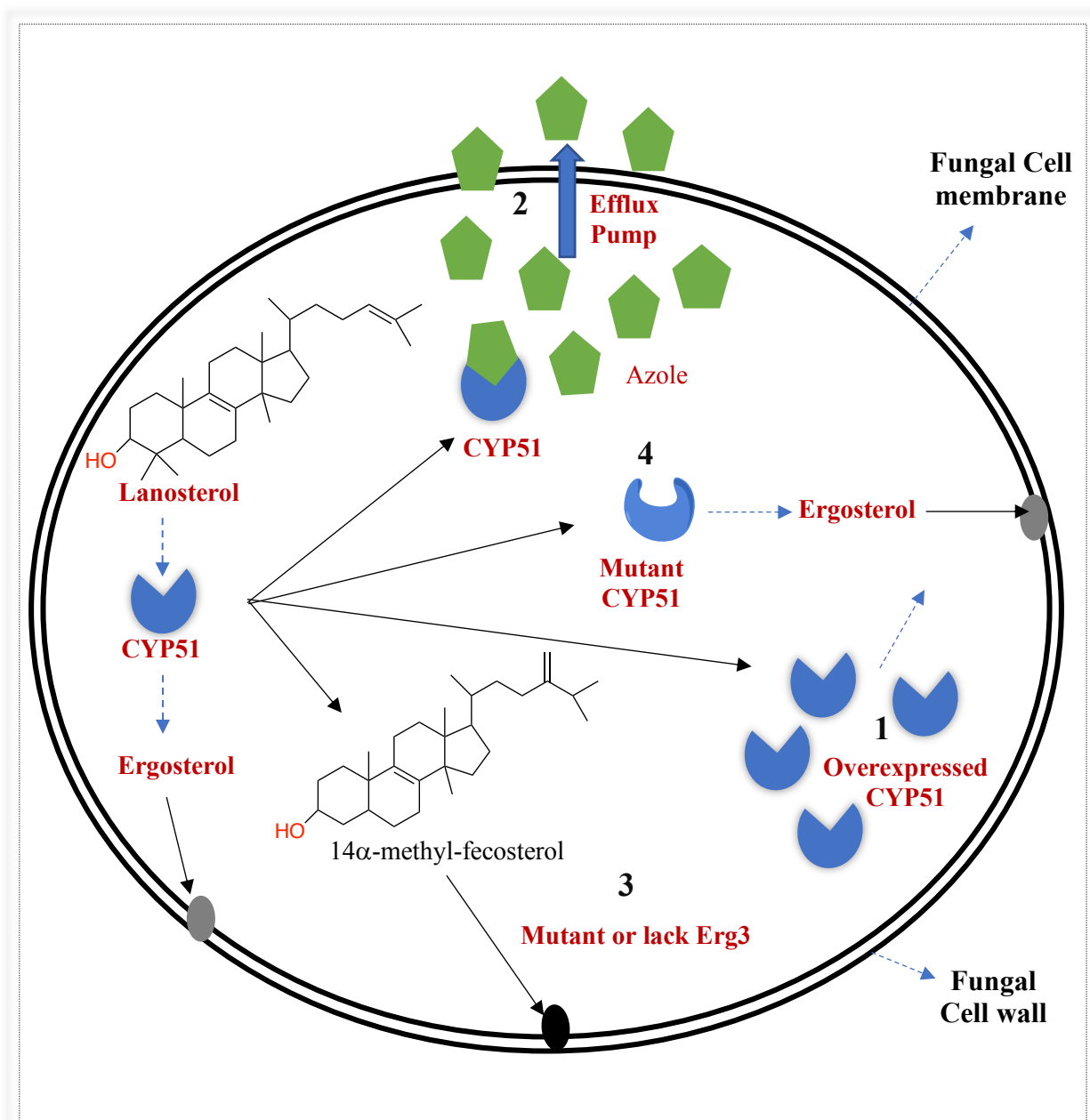
Figure 8: The different mechanisms of azole resistance in *C. albicans*. 1- Overexpression of CaCYP51. 2- Overexpression of efflux pump proteins. 3- Secondary mutation. 4- CaCYP51 mutations.[13] The black and gray dots on the cell membrane represent the protective role of ergosterol and 14α-methyl fecosterol, respectively. Modified from (Parker et al., 2014)[13]

Cytochrome P450 (CYP):

CYP is an iron carrying enzyme discovered in the 1960s.[61,62] The meaning of cytochrome includes two parts: cyto-, which comes from cell, and chrome from colour, while P means pigment.[63] This enzyme when reduced and bound to carbon monoxide absorbs light at a wavelength of 450nm, and from that the name of cytochrome P450 (CYP) was derived.[63,64] In addition, CYP enzymes exist everywhere in human tissue except red blood cells and skeletal muscle but the greater proportion is found in the hepatocytes.[64,65]

In human, there are 57 CYP genes divided into 18 subfamilies, with different isozymes/forms depending on the substrate oxidised.[1,64] The nomenclature of CYP enzymes follows a systematic method. First, the symbol of "CYP" is given an Arabic number, which indicates the family and is based on $\geq 40\%$ amino acid similarity. Second, a letter is given for the subfamily, that has 55% similarity in the amino acid sequence, followed by an Arabic number, which represents the individual gene.[63,64,66] However, when describing the gene, all letters and numbers must be italicised i.e. *CYP3A4*, while the non-italic CYP3A4 represents the enzyme itself.[63,65,66]

CYP enzymes play numerous roles in the biosynthesis and metabolism of lipids as well as metabolism of foreign compounds such as natural products, therapeutic drugs and carcinogens.[63–65] Approximately 75% of enzymatic reactions that occur in drug metabolism are performed by CYP enzymes.[67] These enzymes are known as monooxygenase because they convert an oxygen molecule into a very reactive oxygen species and then insert the oxygen into the substrate in order to make it polar and facilitate its elimination.[65] In addition, CYP catalytic reactions play a major role in converting prodrugs into the active form, which means CYP enzymes can produce both active and inactive metabolites and even toxic reactive metabolites.[63,64,68] A very small number of CYP families such as 1, 2, 3 and 4 were found to be involved in the metabolism of most drugs, and the main enzymes are CYP1A2, CYP2D6 and CYP3A4.[63,69] These enzymes have several ways to metabolise drugs:[63]

- A single CYP enzyme can metabolise a wide range of drugs with different structures.
- A drug could be metabolised by multiple CYP enzymes at different sites resulting in several metabolites.
- A single drug could be metabolised only at one site by multiple CYP enzymes, but it differs depending on the catalytic rates.

1. Structure and Catalytic Cycle of CYP:

Based on genetic analysis, these enzymes are classified as cytochrome P450s because of the signature (motif) sequence of 10 amino acids Phe-XX-Gly-X_bXX-Cys-X-Gly, which includes the invariant cysteine residue while X_b is usually a basic amino acid that plays a key role with the reductase partner.[62,70] The most important structural feature of the CYP active site is the iron-porphyrin complex, which is known as the fourth ligand, that controls the spin state equilibrium during the catalytic cycle.[61,65,71,72] Another unique feature is that the cysteine residue forms the fifth ligand with the haem iron while the water molecule represents the sixth ligand during the enzyme rest state (Figure 9).[65,71,72]
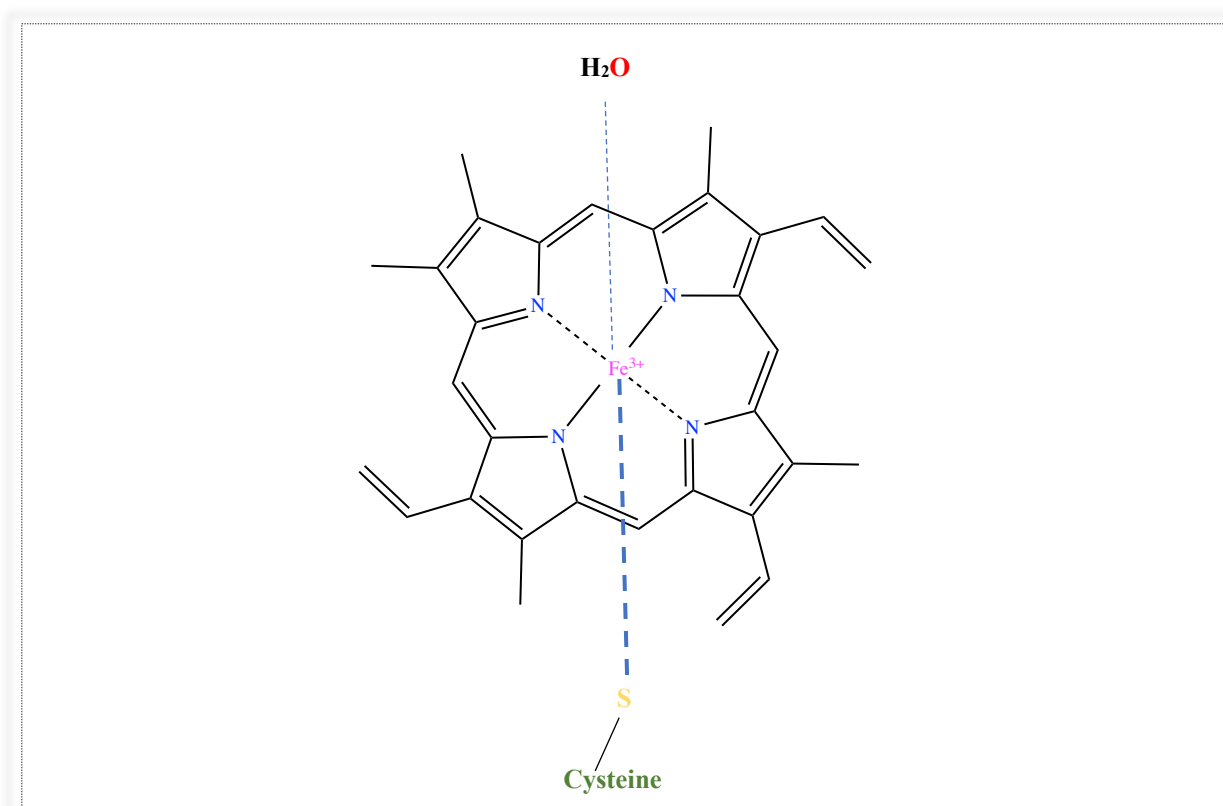
Figure 9: Structure of cytochrome P450 haem moiety.

Iron is very reactive chemically in any form, and is able to produce reactive oxygen species (ROS), which are harmful for human health.[65,66] However, CYP enzymes can regulate reactivity by binding the substrate to the haem that stabilises the ROS, which is produced when the oxygen (O_2) binds, with subsequent oxygenation of the substrate.[65,66,73] Moreover, the monooxygenase reactions performed by CYP enzymes require a combination of oxygen and the substrate (RH) to form the hydroxylated metabolite (ROH) and a water molecule.[65,73] The reaction requires two reducing equivalents (two electrons and two protons), which are supplied

by nicotinamide adenine dinucleotide (NADH) or nicotinamide adenine dinucleotide phosphate (NADPH) depending on the redox system.[65,71,74] The general reaction catalysed by CYP enzymes can be represented as follows:

$$RH + O_2 + 2e^- + 2H^+ \longrightarrow ROH + H_2O$$
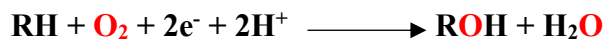
The CYP catalytic cycle begins with a water molecule bound to the ferric ion (Fe^{3+}), and this is the resting state (Figure 10). When the substrate enters the active site of the enzyme, it displaces the water molecule and forms a complex with ferric ion (Fe^{3+}), which leads to a change in the coordination number of Fe^{3+} from six to five. The ferric complex slightly increases the redox reaction potential, and that allows the acceptance of electrons from NADPH P450 reductase. The first addition of electrons results in reducing the ferric ion (Fe^{3+}) to the ferrous state (Fe^{2+}) then, binding of molecular oxygen gives the ferric peroxide complex (Fe^{3+}-O_2^-). This activates a second reduction of the previous complex to generate the ferric-peroxo anion (Fe^{3+}-O_2^{2-}). The ferric-peroxo anion complex is rapidly protonated to form the hydrogen peroxide intermediate (Fe^{3+}-H_2O_2), and this intermediate initiates the formation of a water molecule and the hydroxylated substrate (Fe^{3+}-ROH) by a free radical reaction. In Figure 10, the free radical reaction mechanism (**A**) is explained while the proposed mechanism in the presence of CYP enzyme, and the initiator factor in the case of the enzyme, which is the ferric complex with H_2O_2 is illustrated in (**B**). Finally, when the last reaction is complete, the hydroxylated substrate will leave the enzyme reactive centre and a water molecule will enter to restore the enzyme resting state.[64,65,75]

Consequently, the mechanism by which the complex is protonated is not clear, but it is suggested that a water molecule could play a role in the protonation of the complex as the water available within the active site of the enzyme.[65] Moreover, some studies suggested that the protonation could occur through a catalytic triad.[70,75] A catalytic triad is a group of three amino acids, with a specific feature, that exist in the active site of some CYP enzymes.[38] The three amino acids must be in a specific sequence which is acid-base-nucleophile in order to catalyse the reaction. The most common sequence found in CYP enzymes is Asp251-Lys178/Arg186-Thr252, which plays a role during the protonation step in the CYP cycle.[70] Nonetheless, there are different mechanisms of how the substrate is oxygenated depending on the differences between CYP enzymes and its ability to form various products with the same substrate.[64,65,75] Also, the molecular size of the substrate, its orientation and the conformational changes of the enzymes play a key role in having different mechanisms.[65,73]
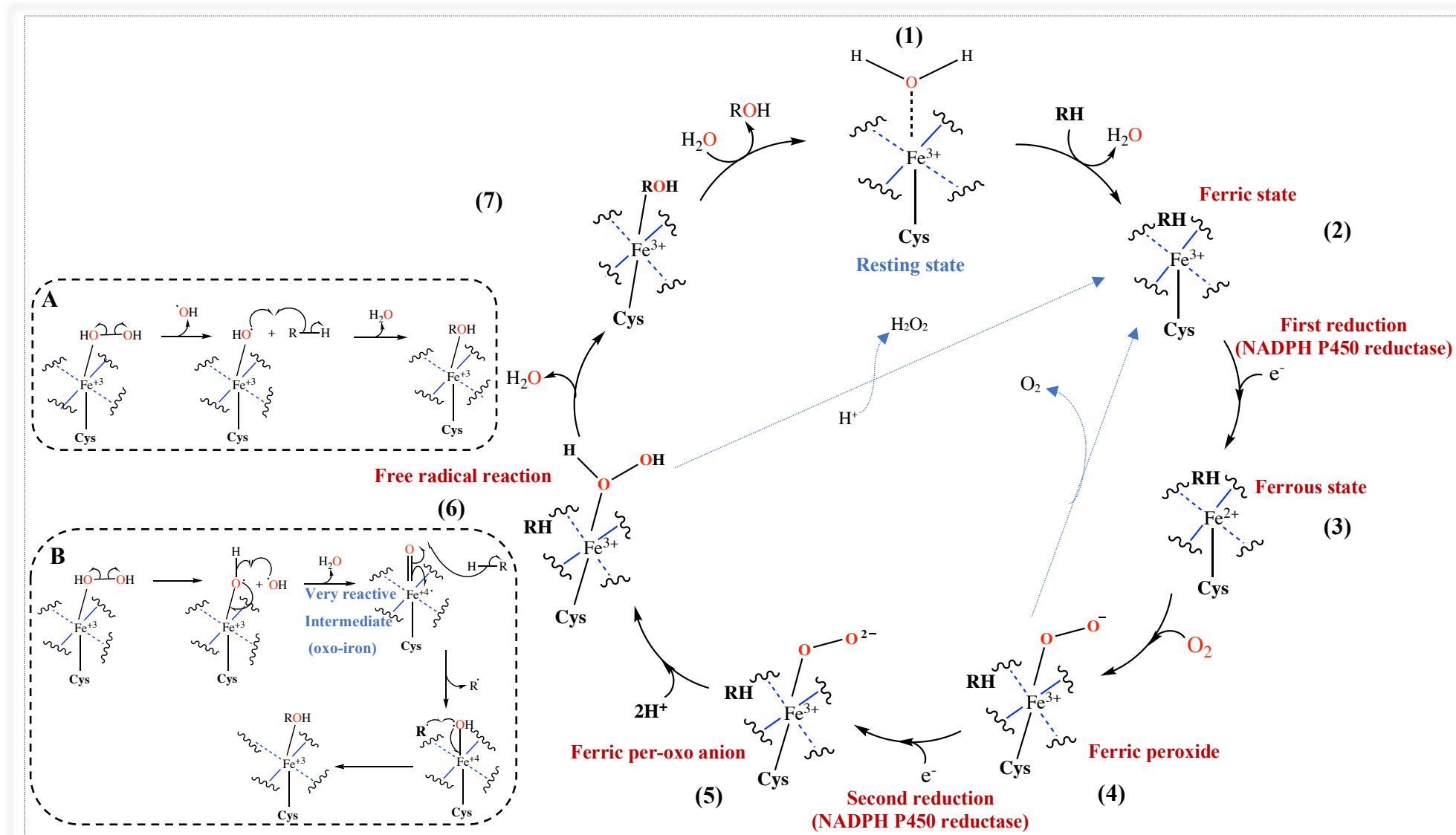
Figure 10: Cytochrome P450 catalytic cycle. (**A**) The general free radical reaction mechanism. (**B**) Proposed mechanism in the presence of CYP enzymes

2. Catalysis by CYP:

Most CYP reactions are oxidations, which generally include insertion of oxygen into the substrate.[65,74,76] There are several types of CYP reactions that are involved in the metabolism of many drugs and biosynthesis of macromolecules. The most common reactions include:

a. Aromatic/Aliphatic hydroxylation:

Aromatic hydroxylation means converting a benzene ring into a phenolic ring while aliphatic hydroxylation means converting a saturated hydrocarbon into an alcohol. In both cases, the reaction is still an oxidation because an oxygen atom is inserted into a C-H bond.
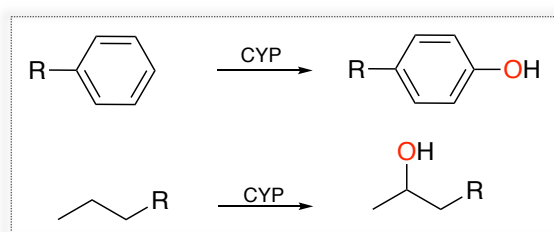
b. Oxidative dealkylation:

Oxidative dealkylation results in the removal of an alkyl group from a molecule. Also, it includes heteroatom dealkylation, which means removing an alkyl group from heteroatoms such as O, N and S. In some cases, removal of the alkyl group leads to inactivation of the compound such as caffeine.[62,4]

caffeine
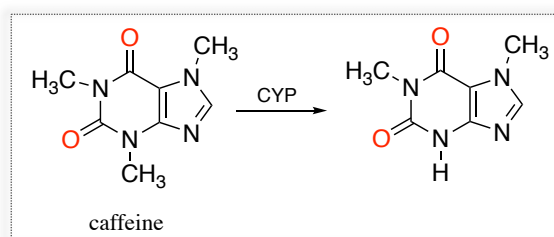
c. Oxidative deamination:

Oxidative deamination is the removal of a nitrogen atom in order to deactivate the molecule, however sometimes it can generate very toxic molecules.[64]
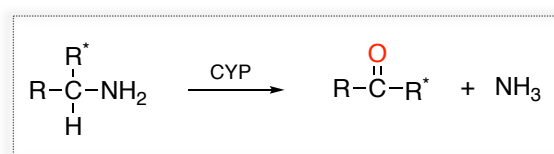
3. Sterol 14α- demethylase (CYP51):

CYP51, also known as lanosterol 14α-demethylase, is one of the ancient CYP enzyme families.[25,77,20] CYP51 is possibly the only enzyme that is found in all biological kingdoms. CYP51 is essential for the sterol biosynthesis pathway, which produces the most important sterol necessary for cell membrane function in human and fungi as previously described.[25] However, both human and fungi share the same CYP51 catalytic reaction, which involves a three sequential CYP catalytic cycle.[20,78] This occurs by removal of the 14α-methyl group from lanosterol, which is the precursor for the final sterol product.[25] As mentioned previously, each cycle requires two electrons provided by NADPH and two protons (Figure 11).
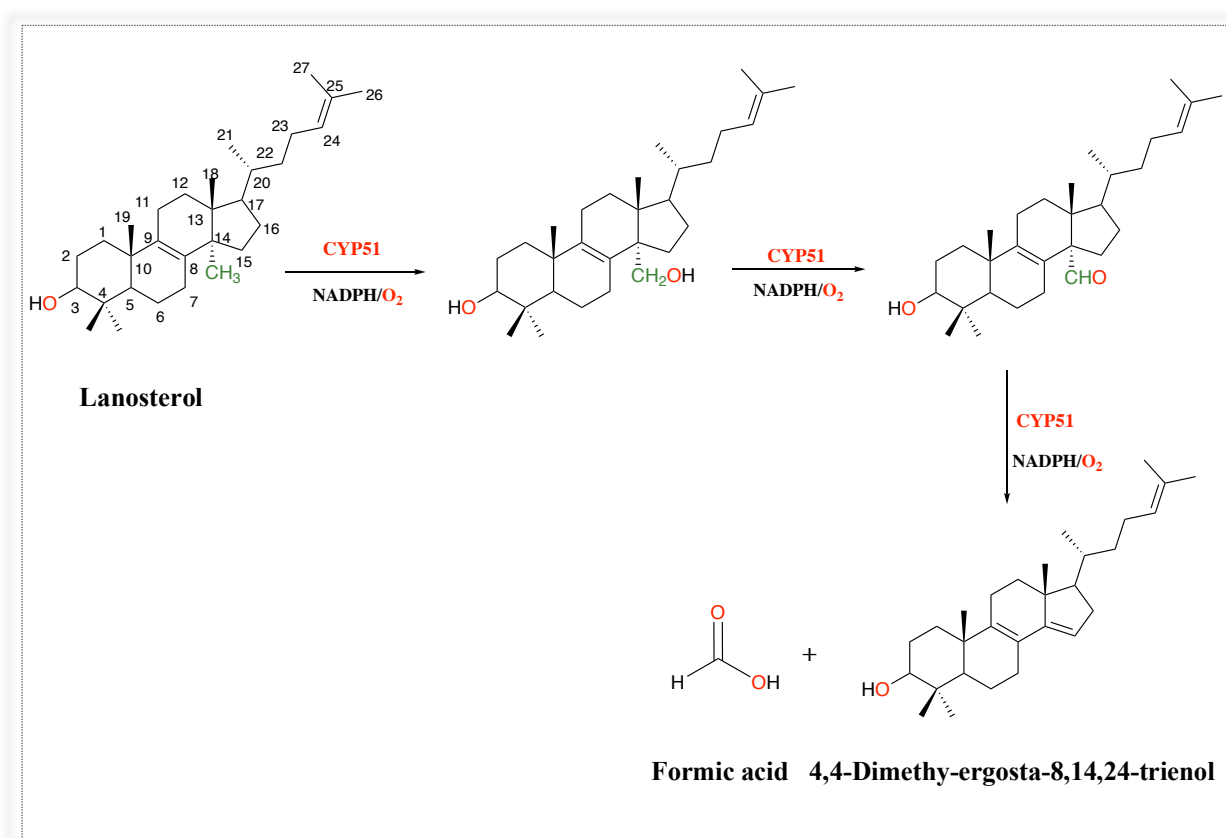
Figure 11: 14α-demethylation reaction by CYP51.

CYP51 in *C. albicans* (CaCYP51) contains 528 amino acids while in human (hCYP51) 503 amino acids (Figure 12), and the amino acid sequence identity is less than 35%,[25,78] therefore there is sufficient difference in the enzyme active site structure to allow development of selective CaCYP51 inhibitors with respect to hCYP51.
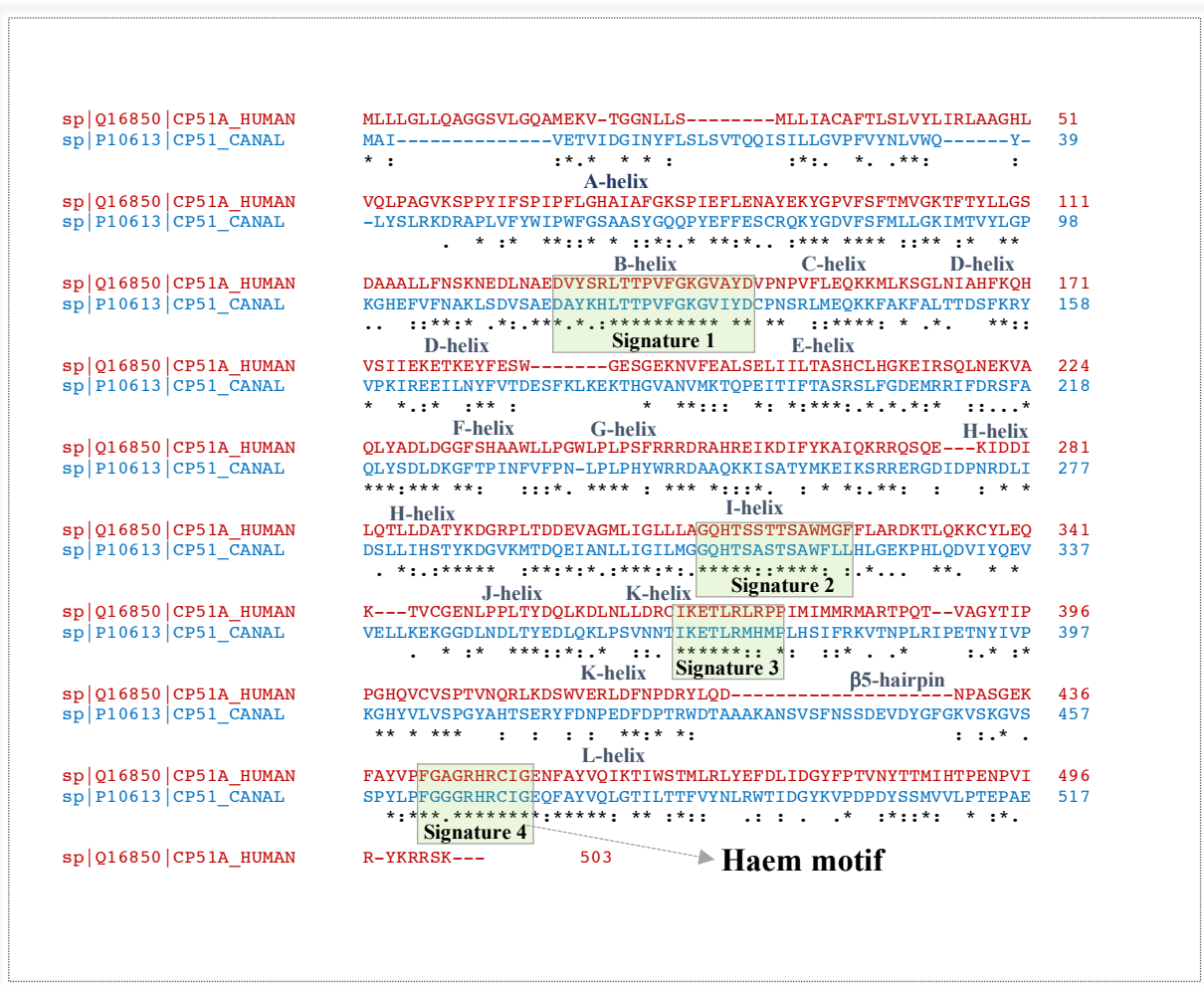
Figure 12: Amino acid sequence alignment of CYP51 in human and *C. albicans*, using Clustal Omega in which "*" means that the residues are identical, ":" means that conserved substitutions have been observed, "." means that semi-conserved substitutions are observed.

4. Structural features of CaCYP51:

The core of the protein is the most important structural conservation in CYP enzymes, which exists around the haem.[71] Also, the core has the essential mechanisms of electron/proton transfer and oxygen activation.[71] CaCYP51 has four similar signature motifs to hCYP51 (Figure 12), which are a common feature in CYP enzymes. The first signature is located in the B-helix, which has two important amino acids (Tyr118 and Tyr132) that form H-bonds with the haem propionates.[14,25] The second signature is the I-helix, which is located just above the right site of the distal surface of the haem and parallel to the haem plane. The I-helix has the two proton delivery residues (His310 and Thr311), and forms a wall in the substrate-binding cavity.[25,71] The third signature, which is important for supporting the core structure of the protein (Glu-XX-Arg), is located in the K-helix.[71] The last motif is the prosthetic haem, which is located between the L-helix (proximal surface) and the I helix (distal surface), and binds to Cys470 as the fifth ligand with the haem iron (Figures 13A and 13B).

The β5-hairpin, a feature that exists only in *C. albicans,* is located above the haem motif moiety within the proximal surface of the enzyme and is expected to play a role in the interaction of CaCYP51 with NADPH-cytochrome P450 reductase.[25] The A/F-helices are located at the channel entrance, and the common residues in A-helix and F-helix are shown in Table 1. The F-helix, which is positively charge, forms a salt bridge with aspartic acid (Asp294) and glutamic acid (Glu296) in the I-helix.[25] The role of the salt bridge in CaCYP51 is still not clear and the effect of amino acids mutations in F/I- helices have not been determined.[25] Finally, the FG loop plays an important role in stabilising the inhibitors within the channel, and the two residues that support this stabilisation are Tyr118 and Ser378.[79]

A

Distal Surface
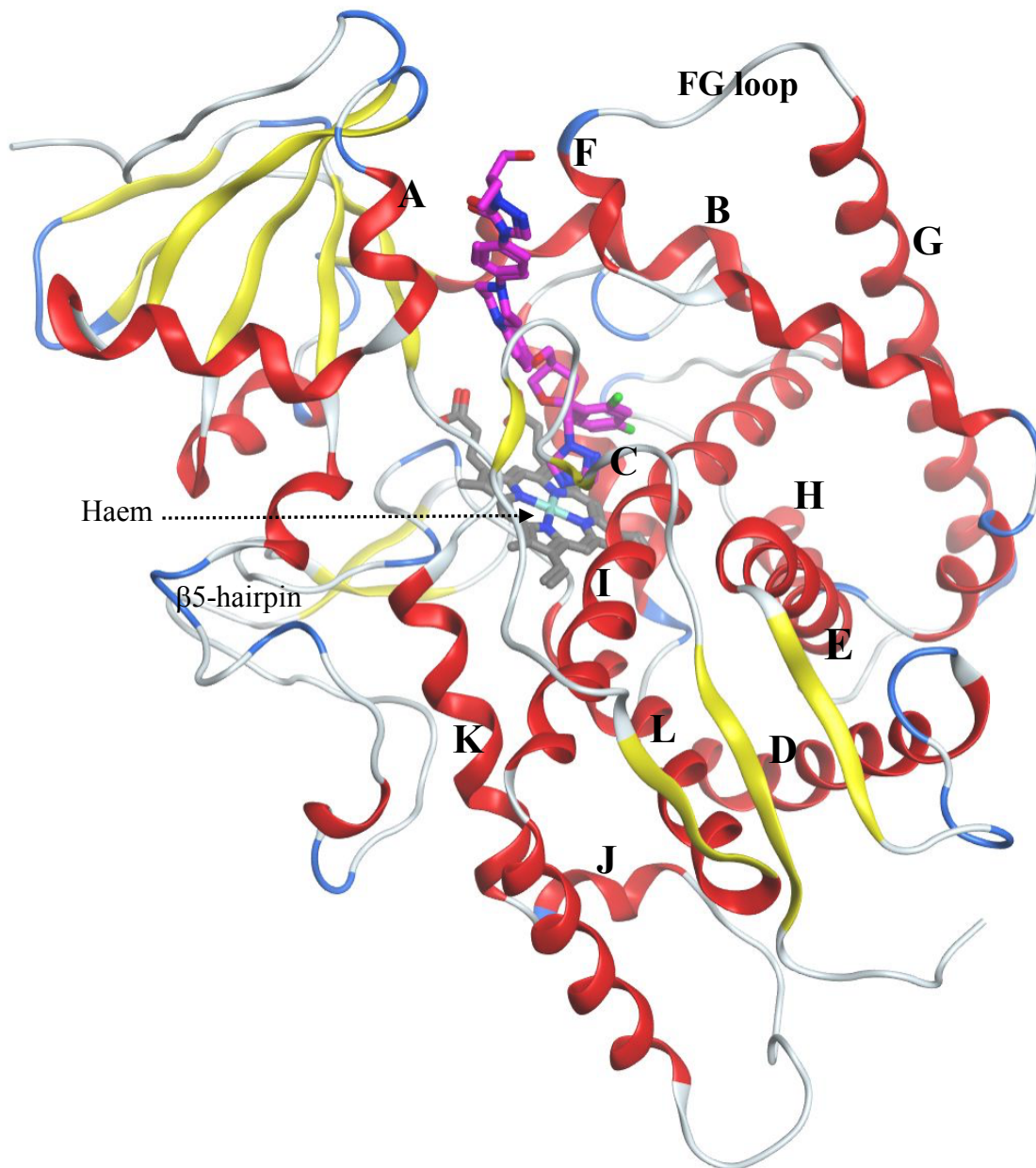
Proximal Surface
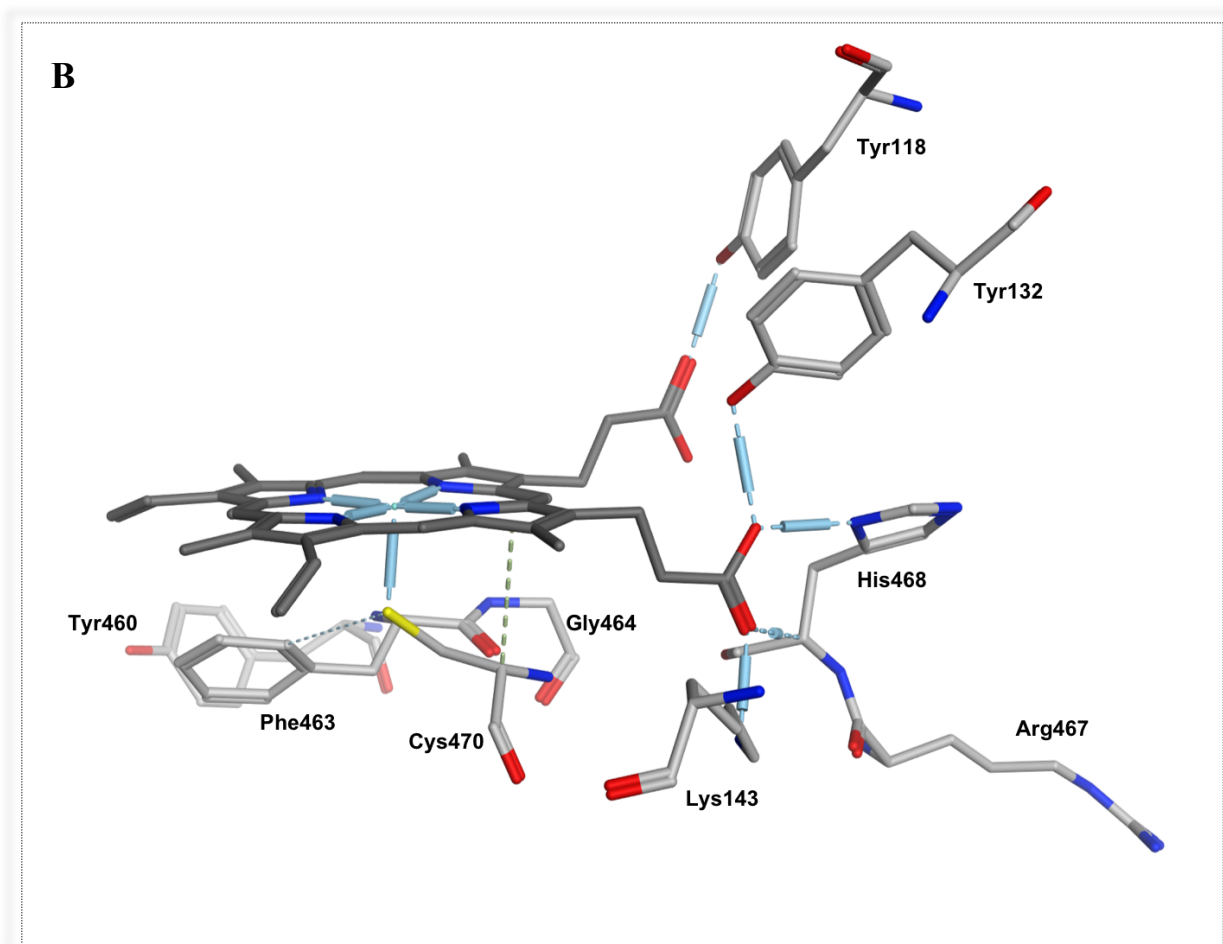
Figure 13: Crystal structure of *C. albicans* CYP51 with posoconazole (magenta) (pdb 5FSA). (**A**) Helices of the protein and the haem are shown: haem (dark gray), helices (red) and β5-hairpin (light gray and blue). (**B**) Residues that form H-bonds with the haem propionates and examples of some amino acid residues binding with the haem moiety.

Table 1: Most common residues in CaCY51 secondary structure.

CaCYP51 Secondary Structure	Residues
A-helix	Phe58/ Ala61/ Ala62/ Tyr64/ Gly65/ Leu88
B-helix	Tyr118/ Leu121/ Thr122/ Phe126/Tyr132
C-helix	Lys143/ Phe145
F-helix	Asp226/ Phe-228/ Pro230/ Phe233
I-helix	Asp294/ Glu296/Gly303/ Ile304/ Gly307/Gly308/ Thr311
β5-hairpin	Tyr447/ Gly448/ Gly450

According to the data provided by the Centre for Cytochrome P450 Biodiversity, Swansea University Medical School, the majority of the mutations in CaCYP51 cluster in three hot spots located within residues 105 to 165, 266 to 287, and 405 to 488.[80,81] The most important residues located in the enzyme active site cavity showing significant mutations are Tyr132, Lys143, Gly307, and Ser405. As mentioned previously, the most significant mutations that showed resistance to fluconazole are the double mutants Y132H/K143R, Y132F/K143R, G307S/G450E, Y132F/F145L and D278N/G464S.[80,81]

Mutation of Tyr132 (Y132), which is most common in the double mutants, resulted in lowering the strength or eliminating the H-bond between Tyr132 and the OH group of fluconazole. The iron-porphyrin complex forms H-bond with Tyr118, Tyr132 and Lys143, thus mutation to these amino acids could results in loss of the H-bond.[82] Moreover, the double mutations Y132H/K143R, Y132F/K143R and Y132F/F145L, located within the enzyme active site at the B and C-helices, as mentioned previously, could eliminate the binding interaction between the azole nitrogen and the haem iron as well as change the conformation of the active site cavity, which in addition to loss of the Tyr132 bond with the OH of fluconazole, results in fluconazole resistance.

On the other hand, the G307S/G450E mutation, located in the proximal site of the enzyme specifically at the I-helix and β5-hairpin, with high molecular weight amino acids (Ser and Glu) could influence the active site volume leading to a change in the position of the haem or fluconazole, and disturb the binding between them.[82,83] In addition, a study has reported that mutation to G450E could contribute to fluconazole resistance by influencing the CYP51 catalytic cycle as the monooxygenase reaction still persists.[84] As a result, the double mutation G307S/G450E plays a role in the CaCYP51 tridimensional conformation without affecting the catalytic cycle, but might affect the entrance of fluconazole to the enzyme active site.[83,84,85]

However, the new azole drug oteseconazole is active against different Candida species by forming H-bond with His-377 of CaCYP51(Figure 14). All Candida species CYP51 have a conserved His-377 residue in the K-helix.[32] Thus, the X-ray structure of CaCYP51 will help with a more efficient structure based design of novel and potent azole inhibitors to overcome the resistance resulting from amino acid mutations.
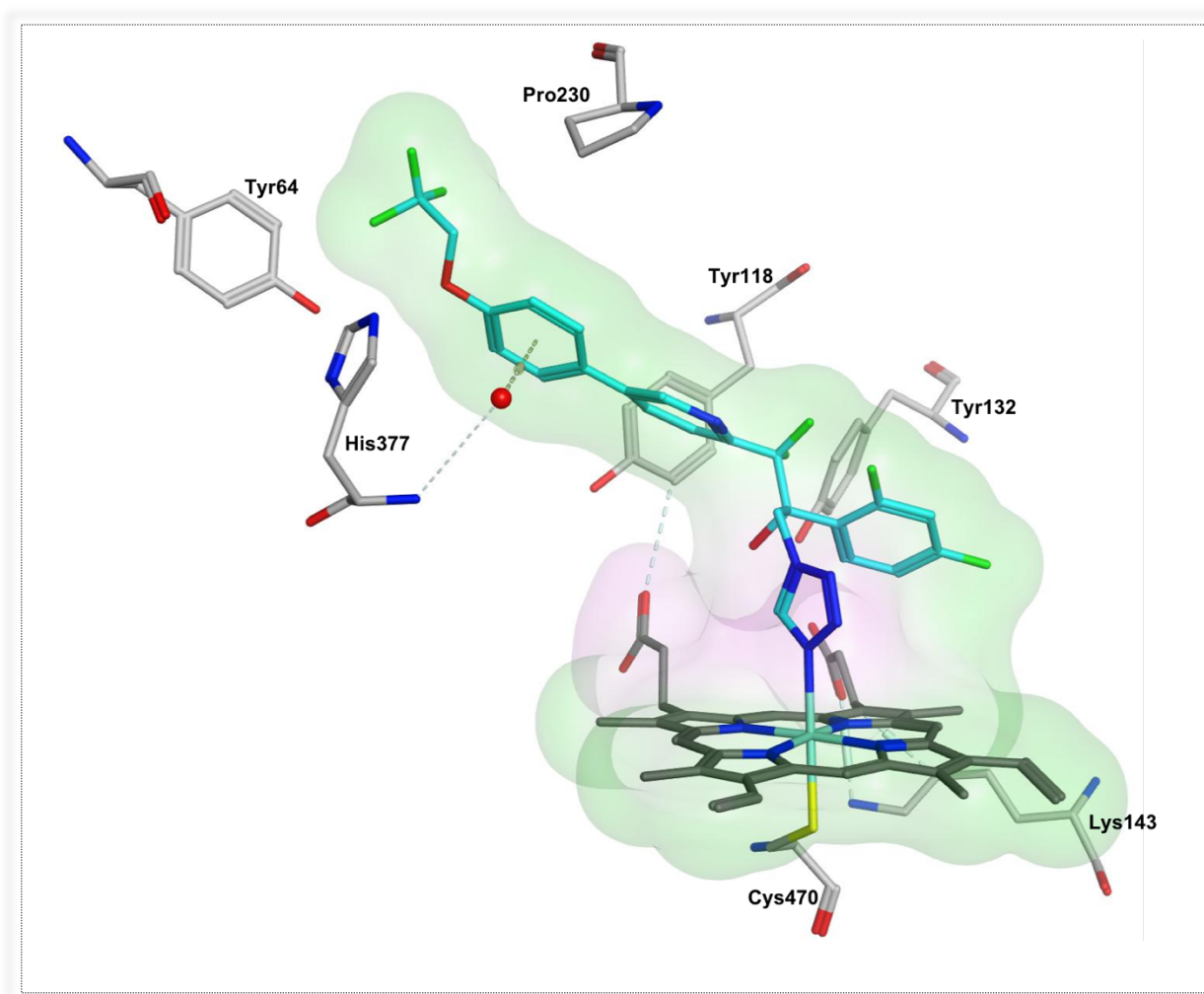
Figure 14: 3D visualisation of oteseconazole within CaCYP51 active site showing key H-bonding with His377.

Hypothesis:

Fungal infections are an emerging medical issue especially for immunocompromised patients, for example cancer or organ transplan patients, as these infections are potentially life threatening. Developing new antifungal agenst is difficult compared with antibacterial agents owing to the nature of the fungal cells.[33,36] The discovery of new CYP51 inhibitors as potent antifungal agents remains an active research area owing to the severe resistance to the azole drugs in different fungal species, especially candida. However, some of the clinically available azole drugs have several major drawbacks, such as limited potency, toxicity and non-optimal pharmacokinetics. As a result, our focus was to develop a drug targeting CaCYP51with selectivity and reduced side effects, the ability to overcome the resistance resulting from amino acid mutations, and also administered orally as well as intravenously. The big question is:

Can we design novel compounds to optimise occupancy and binding interactions in the CaCYP51 active site with both efficacy and activity in resistant *C. albicans* strains?

Aims and Objectives:

Aims:

To design and synthesise novel CYP51 inhibitors as therapeutics for *C. albicans* infections.

Objectives:

1. To understand the binding requirements determined from the X-ray structure of CaCYP51, at the active binding sites and use the knowledge gained to design inhibitors selective for CaCYP51 by performing a detailed docking analysis of the novel azole inhibitors with CaCYP51, which will provide useful information for rational drug design.

2. To study the predicted physicochemical properties of the designed inhibitors such as solubility and LogP characteristics as well as the ADME properties of the proposed inhibitors.

3. To develop synthetic routes to synthesise novel inhibitors with not more than 8 reaction steps and perform analysis, e.g. NMR, HPLC-MS, elemental analysis, to confirm structure and purity.

4. To perform biological assays including susceptibility, IC_{50} and binding affinity to assess the efficacy of the novel inhibitors as well as selectivity against hCYP51.

The rationale of the project:

The CaCYP51 active site has a structure of two short arms, which include the haem iron binding site for the substrate, and a long hydrophobic tunnel, which allows the entrance of the substrate.[77] Three types of novel compounds were explored, a short series' of compounds which are similar to fluconazole in length (as well as design), mid-sized and an extended series', which includes modifications on the short series compounds. Thus, the main aim was to design inhibitors with a "Y-shape" that might allow the occupancy of both short arms at the haem active site as well as the long access channel and increase the binding interactions with key amino acids at the access channel (Figure 15).
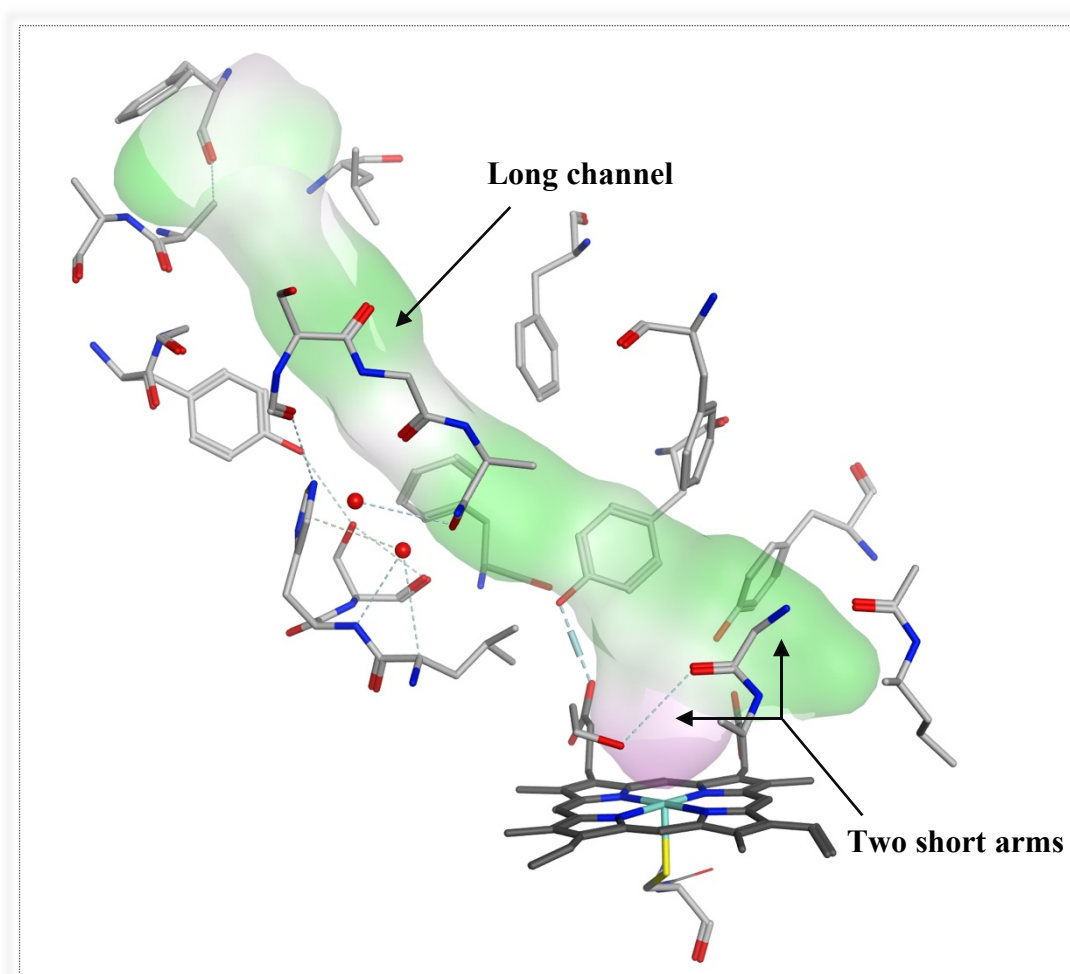
Figure 15: CaCYP51 active site image.

In this project, in order to improve the efficiency and to overcome the resistance associated with the azole drugs, our strategy was to design inhibitors by using fluconazole (Figure 7) as a pharmacophore (such as, the azole ring with the CH_2 was kept because of the

coordination with haem iron binding and the aryl ring are important for the hydrophobic binding at the active site)[86].

New modifications in the pharmacophore include:

1. In chapter II and chapter III, replacement of one of the triazoles and the OH groups of the fluconazole with a thiazole nucleus to explore the antifungal activity.
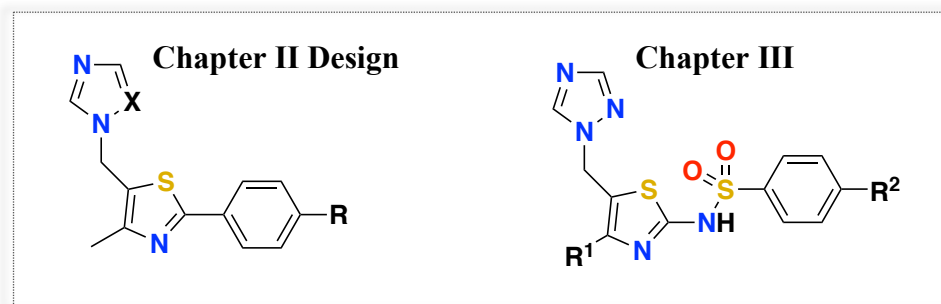
2. In chapter IV, the OH group is kept, and one azole of fluconazole replaced with an amide functional group attached to a ring system (five, six, fused and bi-phenyl) at R^3 to explore binding interaction with different residues in the CaCYP51 active site as well as improve inhibitory activity.
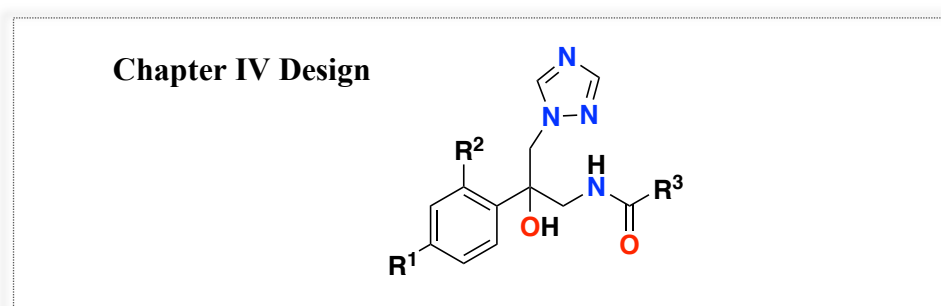
3. In chapter V, the design is similar to chapter IV however the amide group with the CH_2 was reversed, and the OH group replaced with a hydrogen. In addition, the amide linker is connected with a substituted phenyl benzamide moiety to explore binding interaction with different amino acid in the access channel, specifically with His377.
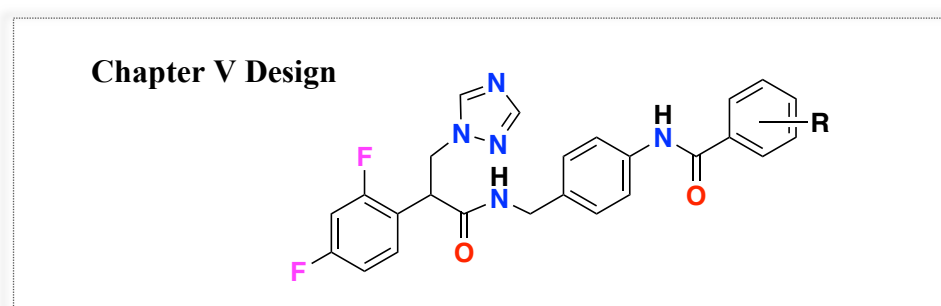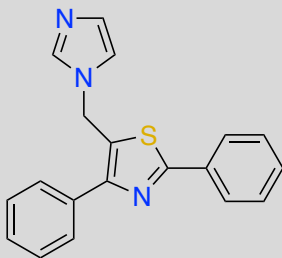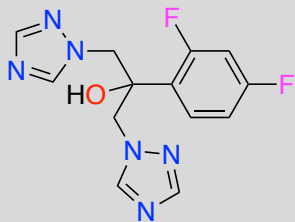
Chapter II

(Phenyl thiazole derivatives)

1. Introduction:

Based on previous work done in our lab by Safaa Kishk,[87] a lead compound with a thiazole core as a possible lead compound was identified. As shown in Table 2, the lead compound showed IC$_{50}$ against CaCYP51 of 10.06 μM, however did not show antifungal activity below 16 μg/mL.

Table 2: The lead compound with CAI4 susceptibility and CaCYP51 inhibitory data.

	SK-oxa23	Fluconazole
MIC (μg/mL)	>16	0.125
IC$_{50}$ (μM)	10.06	0.6

Modifications to the lead compound was needed in order to optimise the activity and selectivity profiles of the new prepared compounds. Two series of phenyl thiazole inhibitors were synthesized, a short series and an extended series.

For the short series, three common modifications on SK-oxa23 were applied (Figure 16):

1. Replacing the phenyl ring at position 4 in the thiazole ring by an alkyl group to explore effects on binding affinity and activity against fungal strains.

2. *Para*-substitutions on the phenyl ring at position 2 of the thiazole ring to explore structure-activity relationships (SAR). The R-group could be an electron donating or electron withdrawing group.

3. Triazole was introduced in position 5 of the thiazole ring to obtain selectivity for CaCYP51.
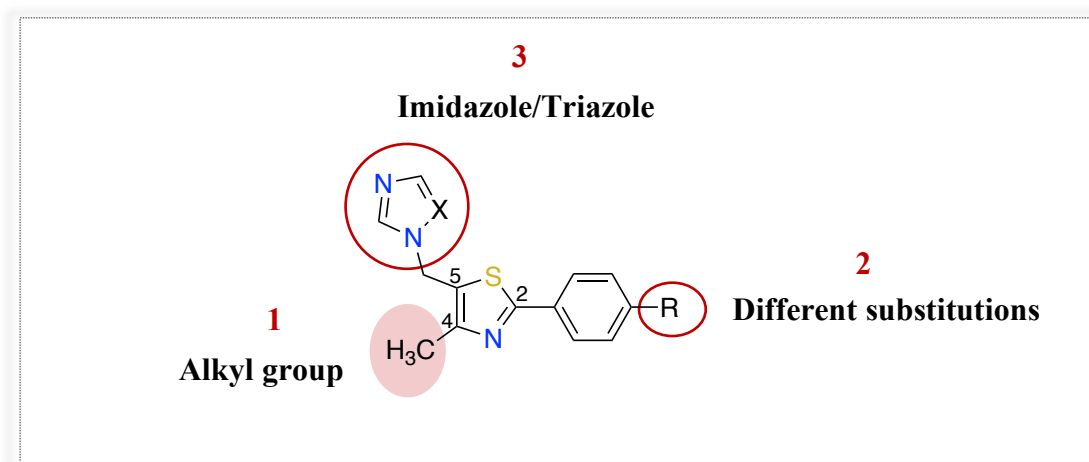
Figure 16: General structure of phenyl thiazole short inhibitors.

The extended series was designed based on only one modification of the short series, through elongating the structure by adding a sulfonamide linker to allow the occupancy of the access channel (Figure 17).
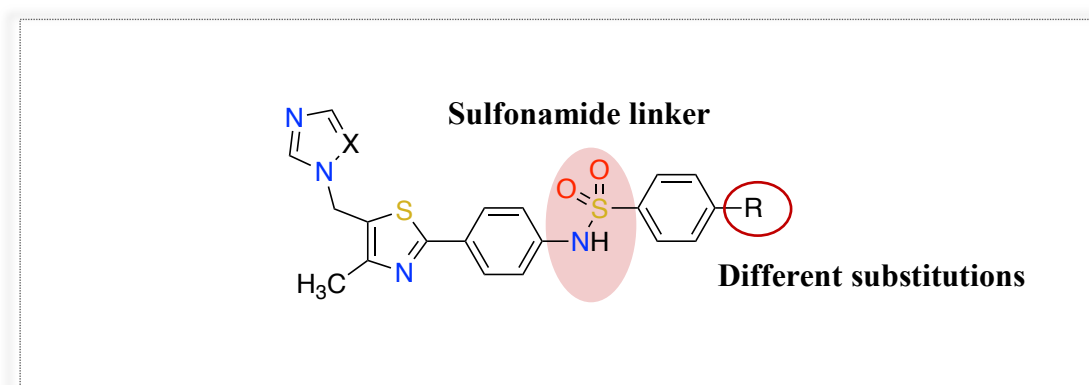
Figure 17: General structure of phenyl thiazole extended inhibitors.

2. Results and discussion

a. Molecular modelling:

To perform the docking studies, posaconazole, one of the known inhibitors of CaCYP51, which was co-crystallised with CaCYP51 in the crystal structure 5FSA,[88] was used with the designed inhibitors to compare the positions and the binding interactions within the enzyme active site. As shown in Figure 18A, posaconazole has binding interactions with 29 amino acids in the active site, predominantly hydrophobic interactions and one H-bond between the carbonyl oxygen of the triazolone ring and Ala61, and a direct binding with the haem iron with a distance of 2.08 Å (Figure 18B).
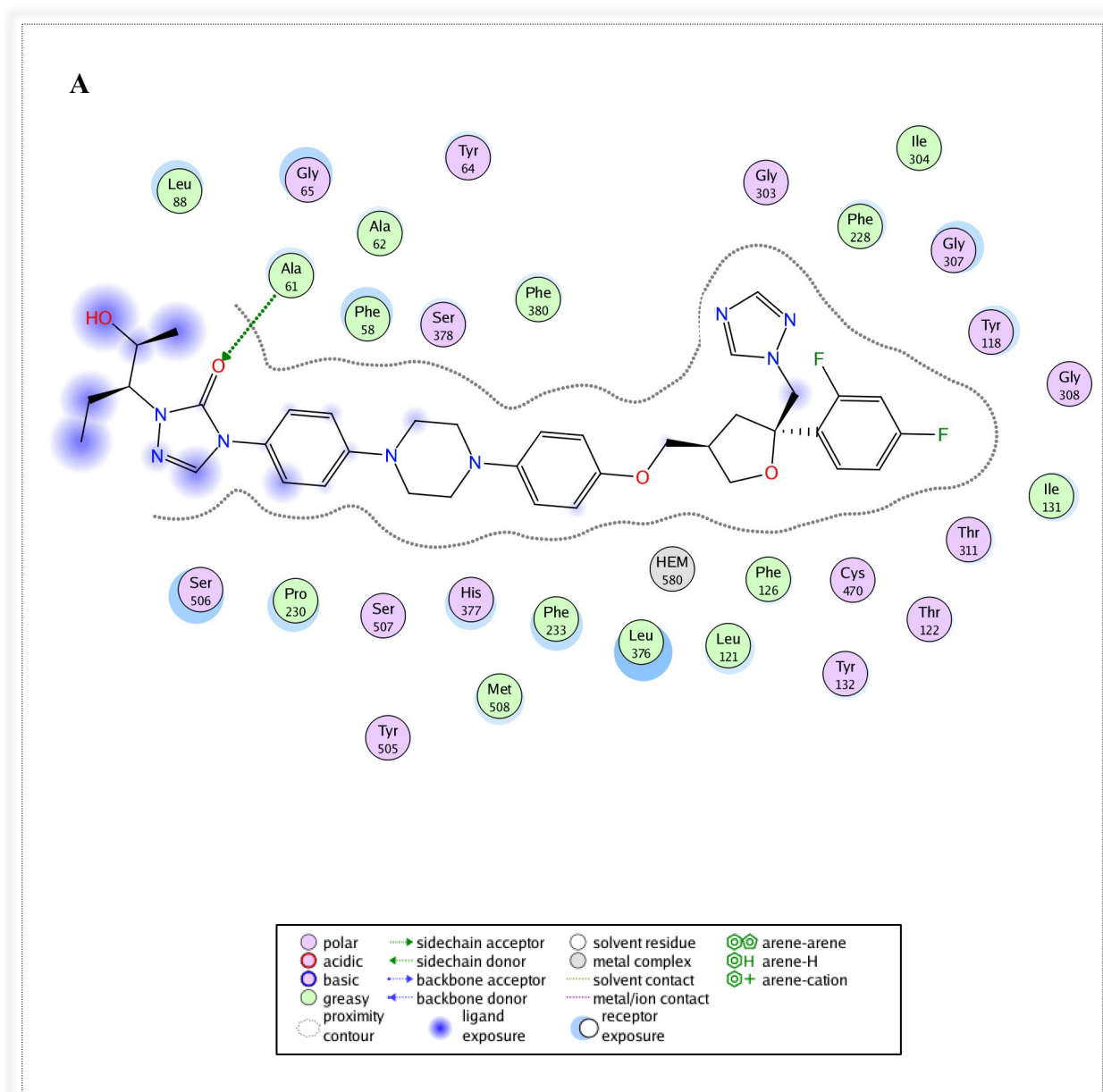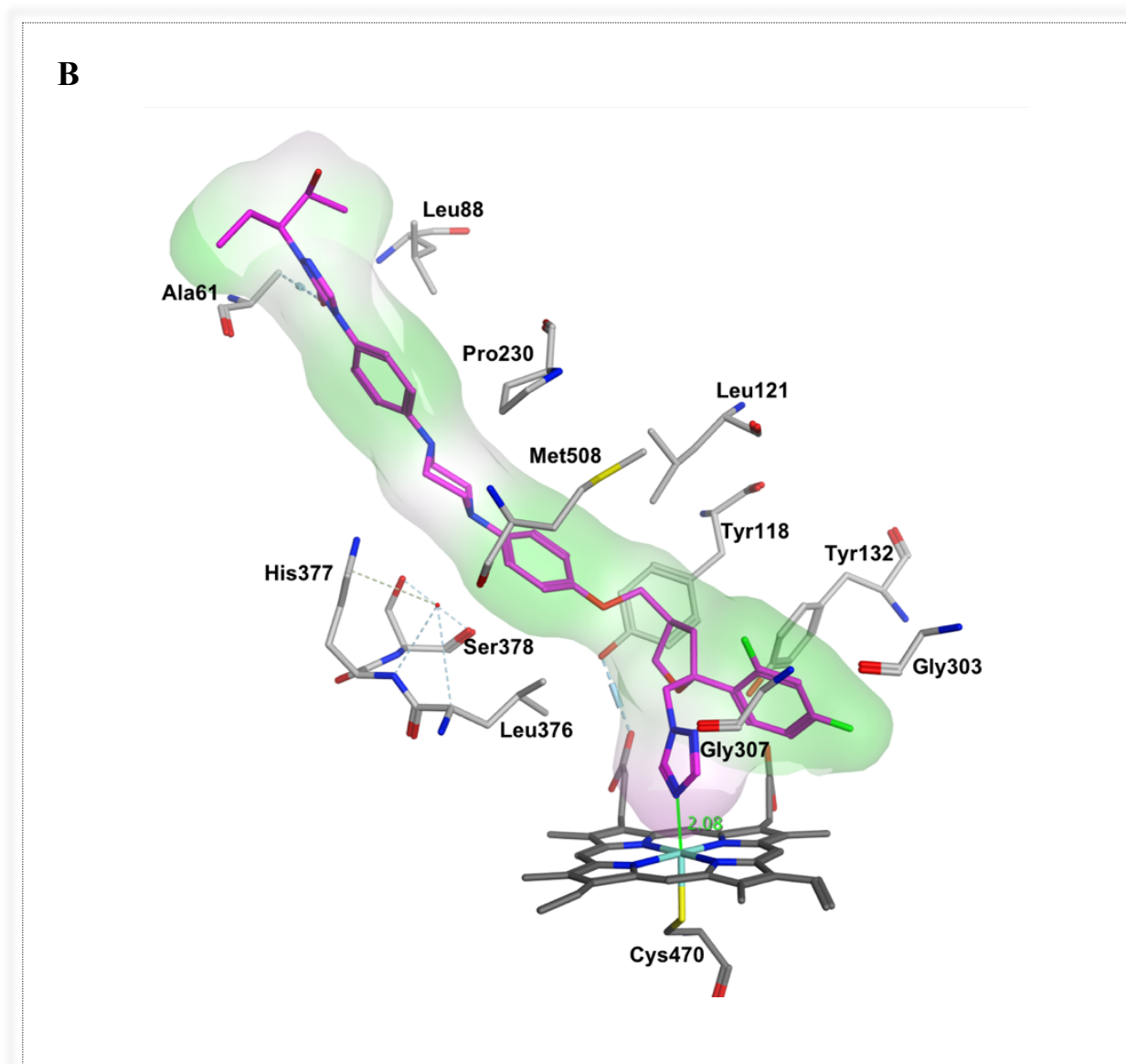
Figure 18: (**A**) 2D and (**B**) 3D representative images of posaconazole (magenta) binding interactions with CaCYP51 protein. In the 3D image the lipophilic regions are green while the hydrophilic regions are pink.

Moreover, the crystal structure for fluconazole with CaCYP51 in the protein data bank (PDB) was not available, therefore fluconazole was docked in the CaCYP51 crystal structure. The docking result showed hydrophobic binding interactions with 12 amino acid residues (Figure 19A) and fluconazole occupies the haem area as well as interacts perpendicularly with the haem iron with a distance of 2.74 Å (Figure 19B).
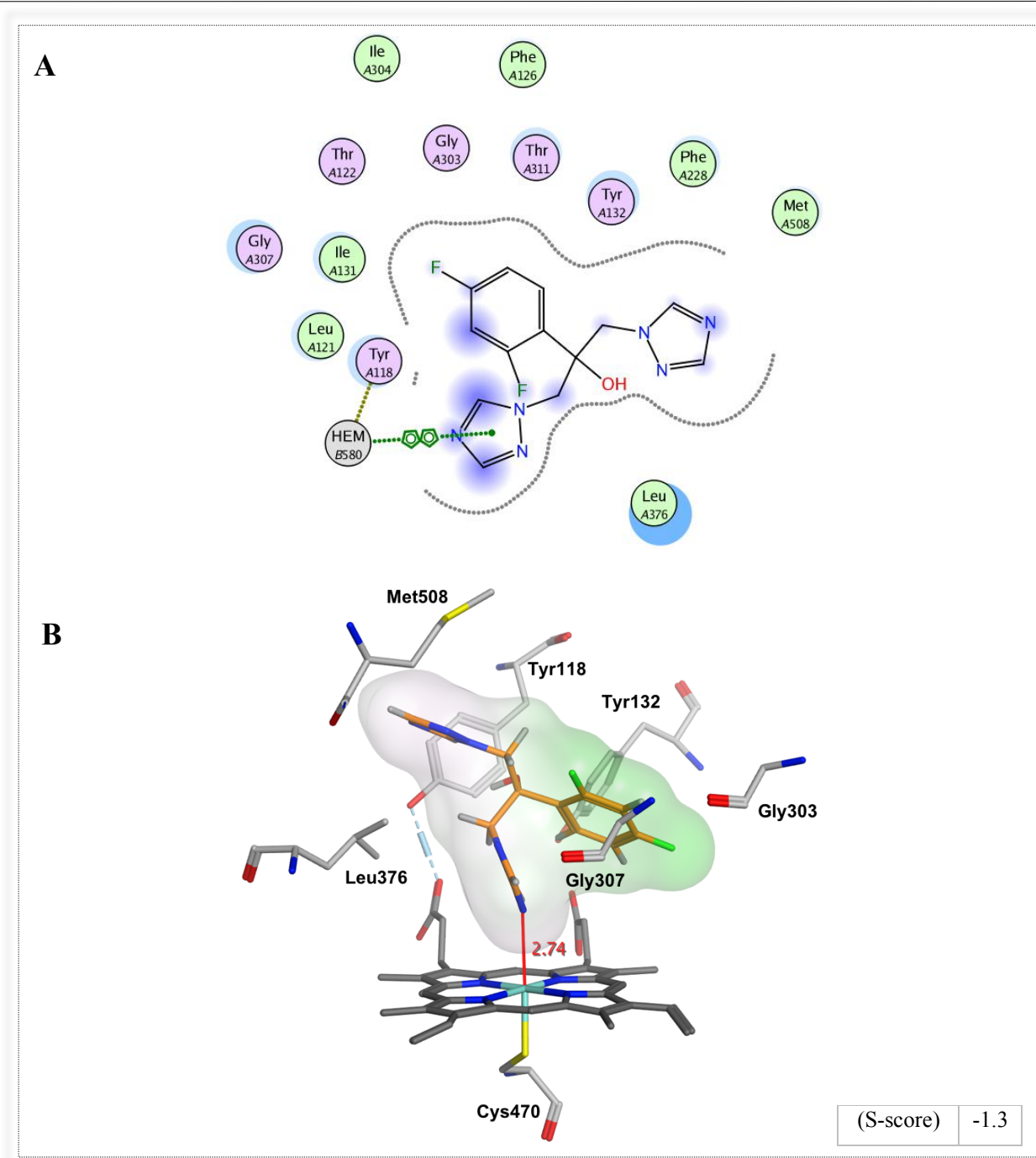
Figure 19: (**A**) 2D and (**B**) 3D representative images of fluconazole (orange) binding interactions with CaCYP51 protein.

From the docking study of the short series, which is similar in length to fluconazole, the compounds showed a good fit in the active site pocket, and the distance between the azole nitrogen and the haem iron is approximately 2.6 Å. Binding is through multiple hydrophobic interactions with Gly307, Tyr132, Leu376, His377, Ser378, Phe380, Phe233, Met508, Phe228, Leu121 and Thr311 (Figure 20).

| (S-score) | -1 |
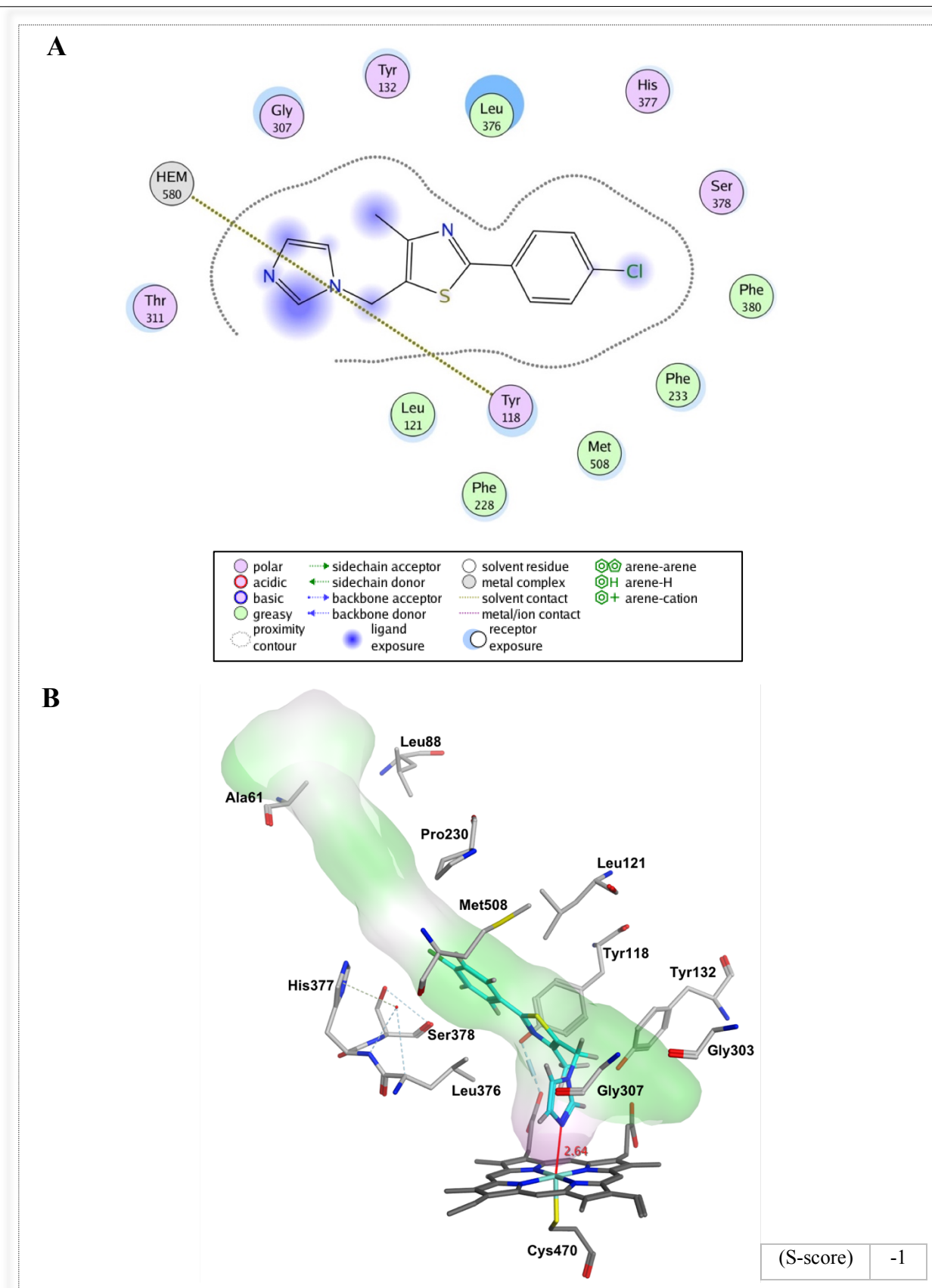
Figure 20: Example of phenyl thiazole short compound **6b** 2D and 3D visualisation. Binding interactions in (**A**) 2D ligplot and (**B**) 3D image illustrating fit within the enzyme active site.

On the other hand, the docking study of the extended series, which is similar in length to posaconazole, showed good position and fit in the active site pocket, and the distance between the azole nitrogen and the haem iron is approximately 2.70 Å. In addition, the inhibitor (compound **10c**) formed hydrogen bonding with Leu376, Met508, Pro375, His377, Pro230, and Ser507 through water molecule as well as multiple hydrophobic interactions with 14 amino acid residues (Figure 21).
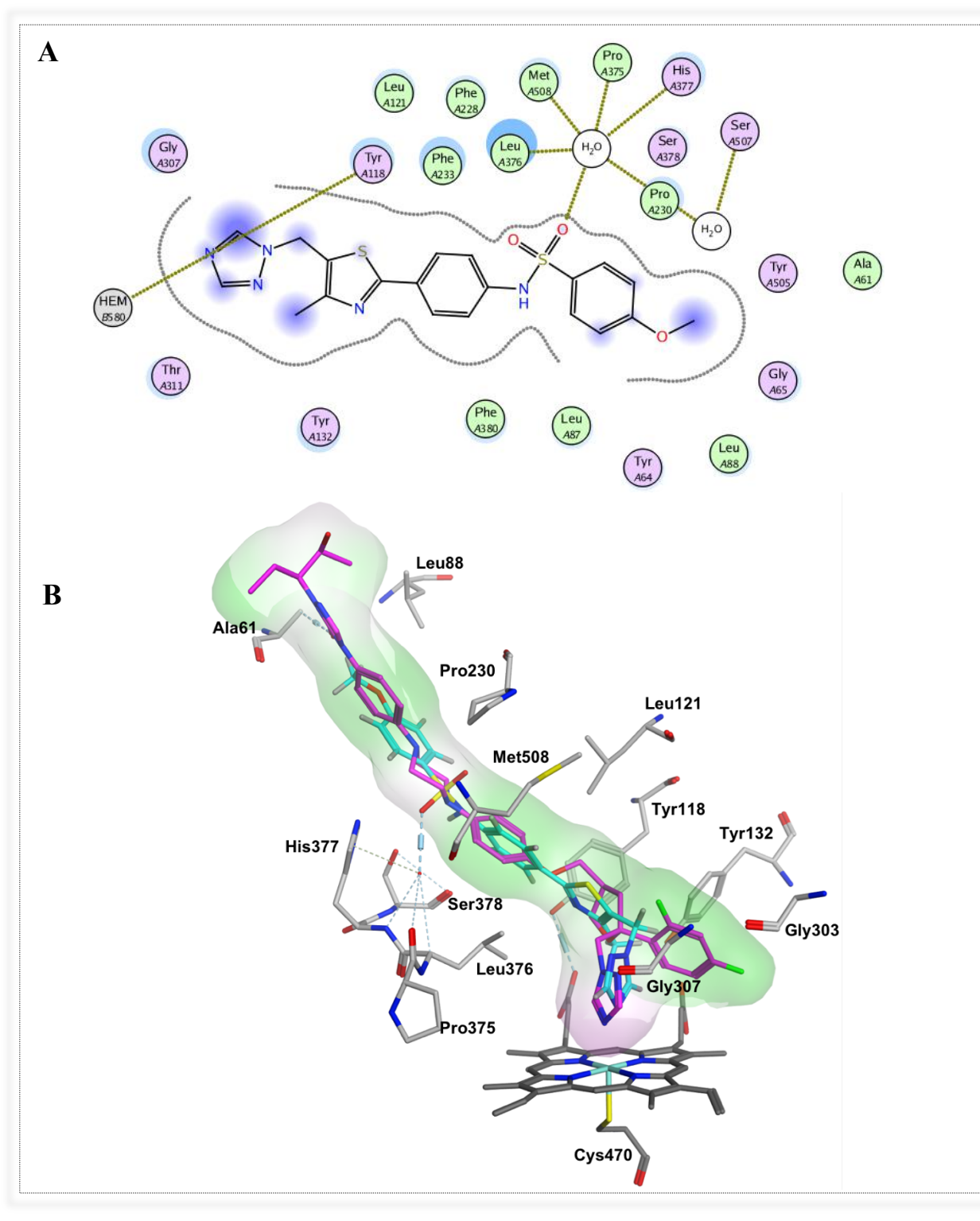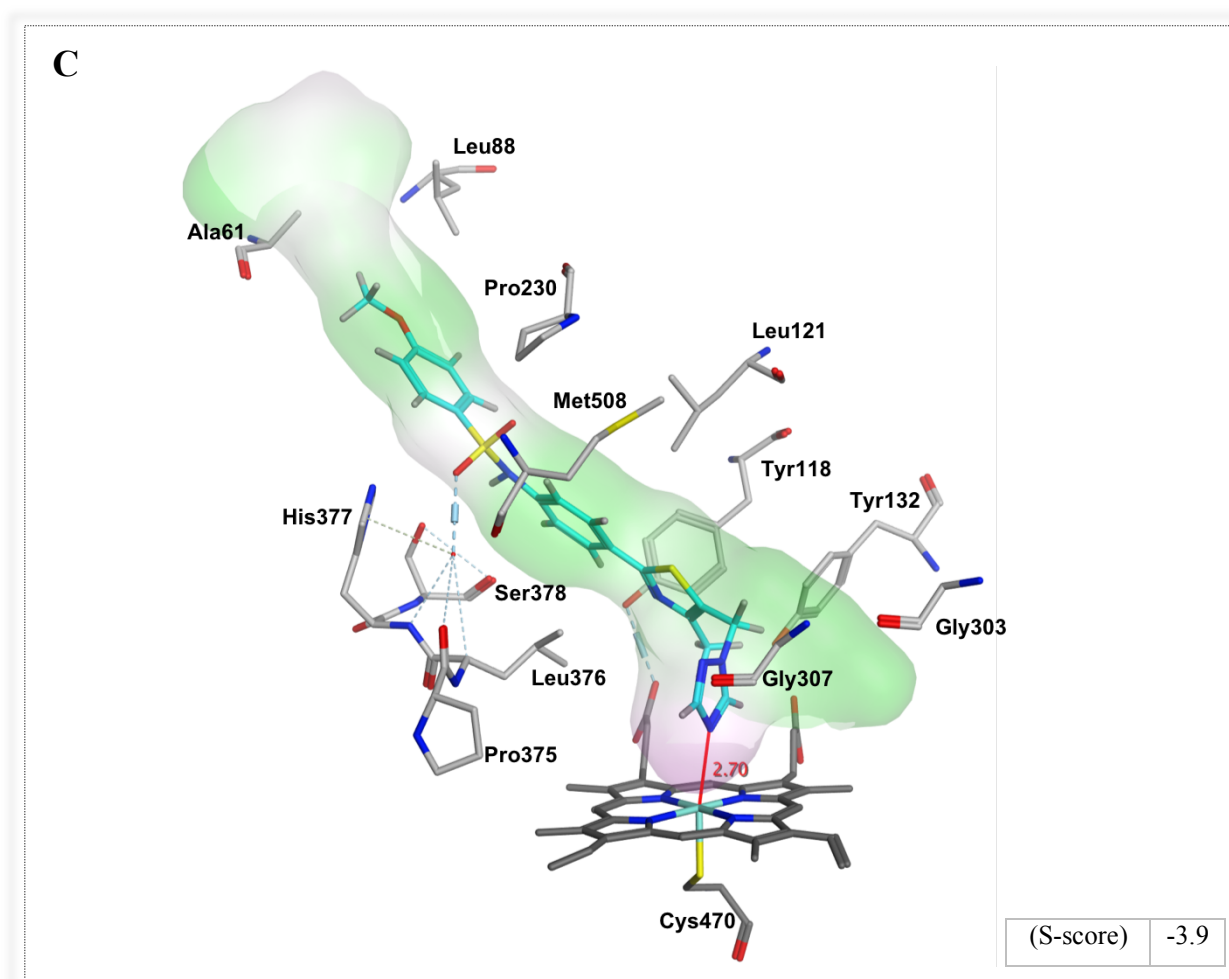
Figure 21: Example of phenyl thiazole extended compound **10c** binding interactions with CaCYP51: (**A**) 2D ligplot illustrating binding interactions with amino acids in the protein. (**B**) Overlap of compound **10c** and posaconazole to view filling of binding cavities. (**C**) 3D image illustrating key H-bonding interactions with Leu376, Met508, Pro375, His377, and Pro230 as well as the distance between the N atom of the triazole ring and the haem iron was approximately 2.70 A°.

b. Chemistry:

1. Phenyl thiazole short compounds:

From the results of the docking studies, different novel inhibitors were chosen for synthesis. After optimisation of the reaction conditions, which included temperature, time, and the reagent equivalents, the short compounds with different substitutions were synthesised. These compounds are 5-((1H-imidazol-1-yl)methyl)-4-methyl-2-phenyl/(4-substituted-phenyl)thiazoles (**6**) and 5-((1H-1,2,4-triazol-1-yl)methyl)-4-methyl-2-phenyl/(4-substituted-phenyl)thiazoles (**7**) (Scheme 1).To synthesise the novel compounds (**6**, **7**), four reaction steps were used (Scheme 1)[87]:

1. Hantzsch thiazole synthesis with thiobenzamide.
2. Reduction reaction by NaBH$_4$.
3. Chlorination reaction using thionyl chloride.
4. Nucleophilic substitution of imidazole/triazole.
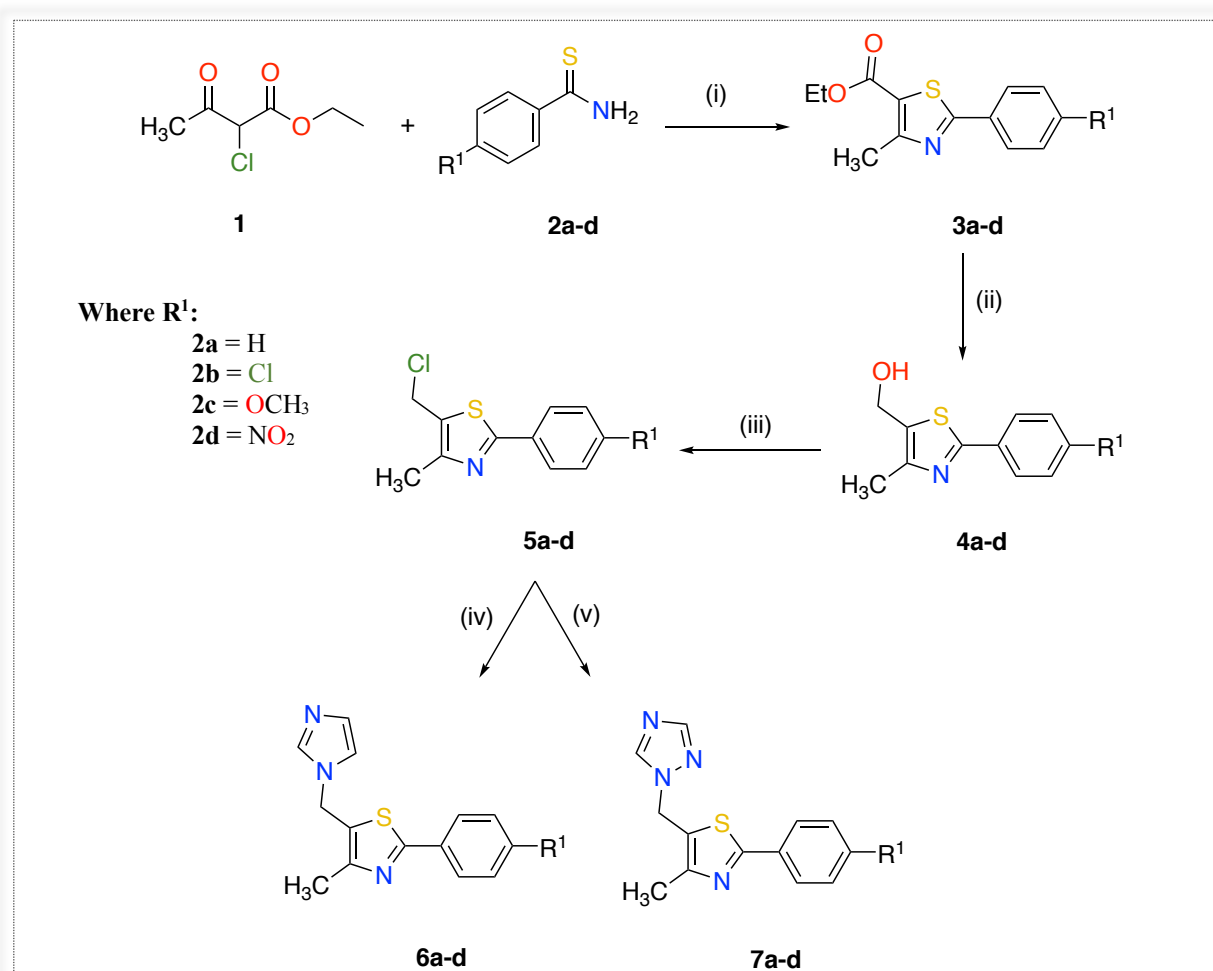
Scheme 1: *Reagents and conditions*: (i) EtOH, 80 °C, o/n (ii) THF, NaBH$_4$, 69 °C, 7 h, r.t., o/n (iii) CH$_2$Cl$_2$, SOCl$_2$, 40 °C, 4 h (iv) (a) CH$_3$CN, K$_2$CO$_3$, imidazole, 45 °C, 1 h (b) 70 °C, o/n (v) (a) CH$_3$CN, K$_2$CO$_3$, triazole, 45 °C, 1 h (b) 70 °C, o/n.

Synthesis of ethyl-4-methyl-2-phenyl/(4-substituted-phenyl) thiazole-5-carboxylate (3):
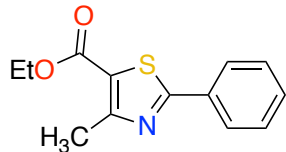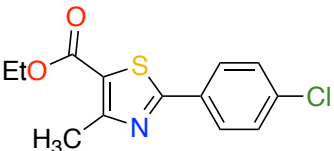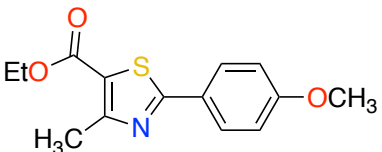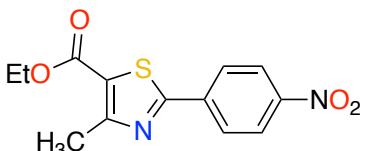
The synthesis of ethyl-4-methyl-2-phenyl/(4-substituted-phenyl)thiazole-5-carboxylate (**3**) involved a cyclisation reaction known as the Hantzsch thiazole synthesis, which includes a condensation of an α-haloketone and thioamide derivative.[89] This compound was prepared by adding thiobenzamide to ethyl 2-chloroacetoacetate (**1**), in dry EtOH and heating at 80 °C overnight.[90] The reaction mechanism involves two steps, the first is a nucleophilic attack of the sulfur atom at the α-chloroketone to form a C-S bond, with elimination of Cl⁻. Second is the five membered ring formation, which is achieved by the removal of a water molecule (Figure 22).
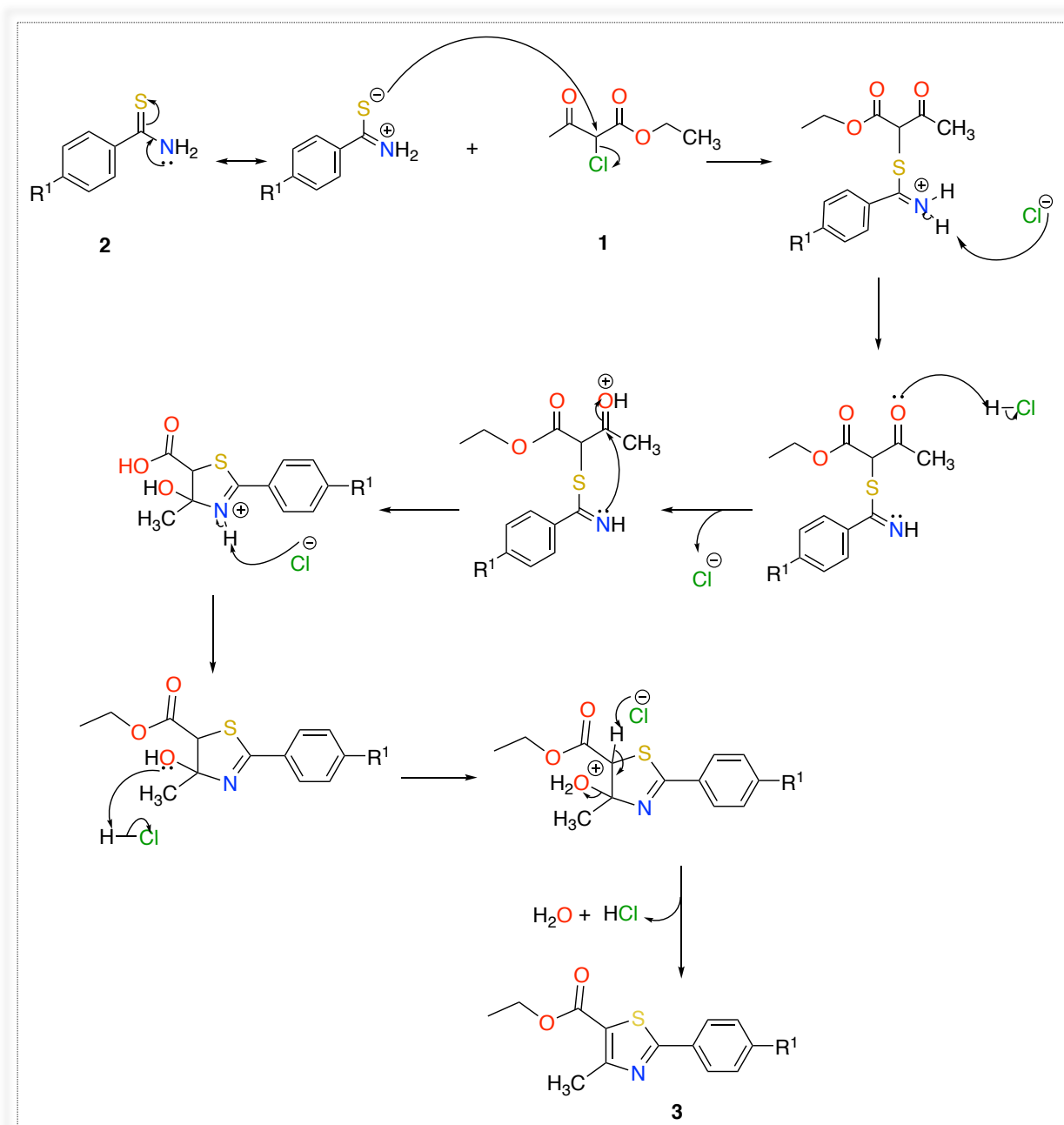
Figure 22: Reaction mechanism of thiazole ring formation.

Both the chloro (**1**) and tosyl (**13a**) reagents (see Table 11 in chapter III) were investigated for this reaction with product (**3a**) obtained with both reagents, however the yield was much better when the ethyl 2-chloroacetoacetate (**1**) was used as starting reagent (yield $\cong$ 63%) rather than ethyl-3-oxo-2(tosyloxy)butanoate (**13a**) (yield $\cong$ 51%). For this reason, the chloro (**1**) was used for the synthesis of the thiazole, which were all obtained in good yields (Table 3).

Table 3: Chemistry of the prepared thiazole compounds (**3**).

Compound	Structure	Yield (%)	M.P. (°C)
3a		63	Oil
3b		61	84 – 86 (Lit. m.p. not found)
3c		86	78 -80 (Lit. m.p. not found)
3d		78	147 – 149 (Lit. m.p. not found)
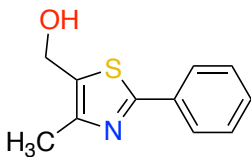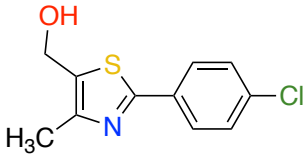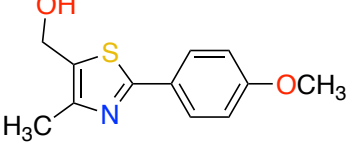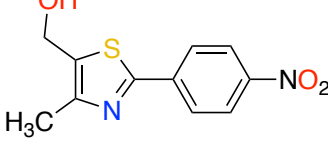
Synthesis of (4-methyl-2-phenylthiazole-5-yl)methanol (4):

NaBH$_4$ is a reducing agent that is used mainly in the reduction of aldehyde and ketone.[91,92] In addition, NaBH$_4$ is a weak reducing agent compared with LiAlH$_4$ owing to the strong electronegativity of boron, which withdraws more electrons toward itself, resulting in the low availability of the hydride ion compared with Al. Carboxylic acids, esters and amides are less reactive because of the resonance and the high electronegativity of the O and N, thus the reduction needs a strong reducing agent such as LiAlH$_4$. In our case, the reduction of ethyl-4-methyl-2-phenyl/(4-substituted-phenyl)thiazole-5-carboxylate (**3**), which has an ester functional group was reduced to (4-methyl-2-phenylthiazole-5-yl)methanol (**4**) with NaBH$_4$ in THF with a few drops of MeOH under 7 h of reflux.[90]

The esters (**3**) were all successfully reduced to the alcohols (**4**), however compounds **4a-4c** were found to be unstable (decomposition occurred when left at room temperature

overnight) so were used immediately in the next reaction. The nitro derivative (**4d**) was stable and therefore subject to further purification by column chromatography. The yields of **4a-4c** are high as they are crude yields (Table 4).

Table 4: Yields of the prepared alcohol compounds (**4**).

Compound	Structure	Yield (%)	Comment
4a		88	Decomposed on standing therefore used in the next step without further purification.
4b		96	Decomposed on standing therefore used in the next step without further purification.
4c		92	Decomposed on standing therefore used in the next step without further purification.
4d		60	Purified by gradient column chromatography.
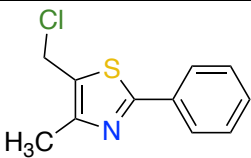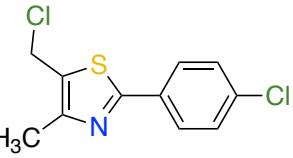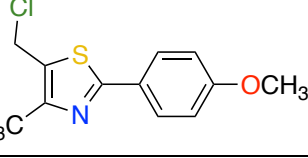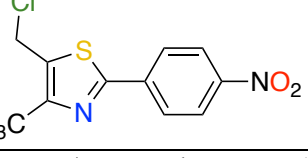
Synthesis of 5-(chloromethyl)-4-methyl-2-phenylthiazole (5):

To obtain the final desired compounds, the OH group must be converted into a good leaving group to synthesise the imidazole/triazole novel compounds. This synthesis was accomplished by a chlorination reaction involving the addition of thionyl chloride to the alcoholic compounds (**4**) in CH_2Cl_2 under heat for 4 h.[93]

To confirm synthesis of the chlorinated compounds (**5**), ^{1}H NMR was applied and a singlet peak for R-C$\underline{H_2}$Cl appeared at δ 5.11 while the R- CH$_2$O$\underline{H}$ triplet peak of the starting alcohols (**4**) at δ 5.54 had disappeared.

The chlorinated intermediates (**5**) were pure enough to be used immediately in the next reaction, and the retention factor for the intermediates range from 0.42-0.55 (Table 5).

Table 5: Chemistry of the prepared chlorinated compounds (**5**).

Compound	Structure	M.P. (°C)	TLC R$_f$*
5a		82-85 (Li. m.p.: 68-69)[94]	0.55
5b		116-118 (Lit. m.p. not found)	0.52
5c		86-90 (Lit. m.p. not found)	0.55
5d		122-124 (Lit. m.p. not found)	0.42

*TLC eluent (9.5:0.5 v/v CH$_2$Cl$_2$- MeOH).

Synthesis of 5-((1*H*-imidazol/1,2,4-triazol)-1-yl)methyl)-4-methyl-2-phenyl/(4-substituted-phenyl)thiazole (6 and 7):

The final compounds were obtained by reacting the imidazole/triazole anion with the previous chlorinated compound (**5**). To prepare the imidazolate/triazolate anions, a solution of imidazole/triazole in dry acetonitrile and potassium carbonate was heated for 1 h at 45 °C to deprotonate the imidazole/triazole. The resulting anion was added to the chlorinated compounds and heated at 70 °C overnight resulting in the displacement of Cl.[95]

After the work up, the crude products were purified by gradient flash column chromatography and structures confirmed by ^{1}H NMR. Three broad singlet peaks were observed for the imidazole ring to confirm the imidazole products (**6**) while two singlet peaks were observed for the triazole ring to confirm the triazole products (**7**) (e.g. compounds **6b** and **7b**, Figure 23). The pure compounds showed good yields and purity percent except the methoxy derivatives (Table 6). The difficulty in purifying compound **6c** and **7c** resulted in the low yields.
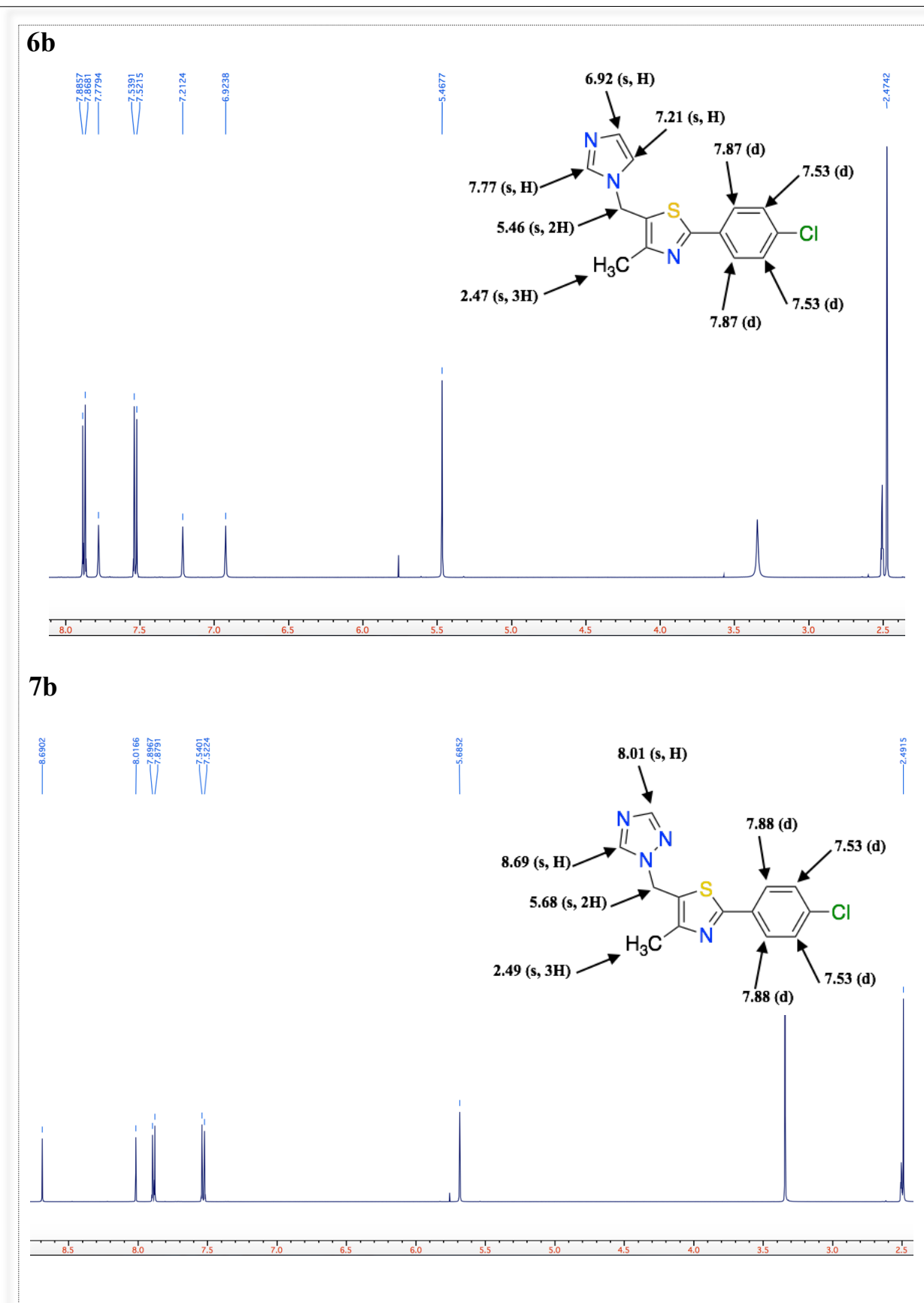
Figure 23: ^{1}H NMR (DMSO-d$_6$/ 500 MHz) for imidazole and triazole final compounds (**6b** and **7b**) that illustrating the three singlet peaks of imidazole vs the two singlet peaks of triazole.

Table 6: List of the final phenyl thiazole short compounds.

Code	Structure	Yield (%)	Melting point (°C)	HPLC purity (%)
6a		50	90-93	98
6b		52	139-142	98
6c		28	106-108	97
7a		45	116-118	98
7b		59	162-165	100
7c		26	113-115	98
7d		53	198-200	99

2. Phenyl thiazole extended compounds:

The nitro derivative in the phenyl thiazole short series, (5-((1*H*-1,2,4-triazol-1-yl)methyl)-4-methyl-2-(4-nitrophenyl) thiazole) (**7d**), provided a route to synthesise a new linker to allow extension of the short derivatives (Scheme 2). The reactions involved were:

1. Hydrogenation reaction using Pd/C catalyst.
2. Formation of sulfonamide linker.
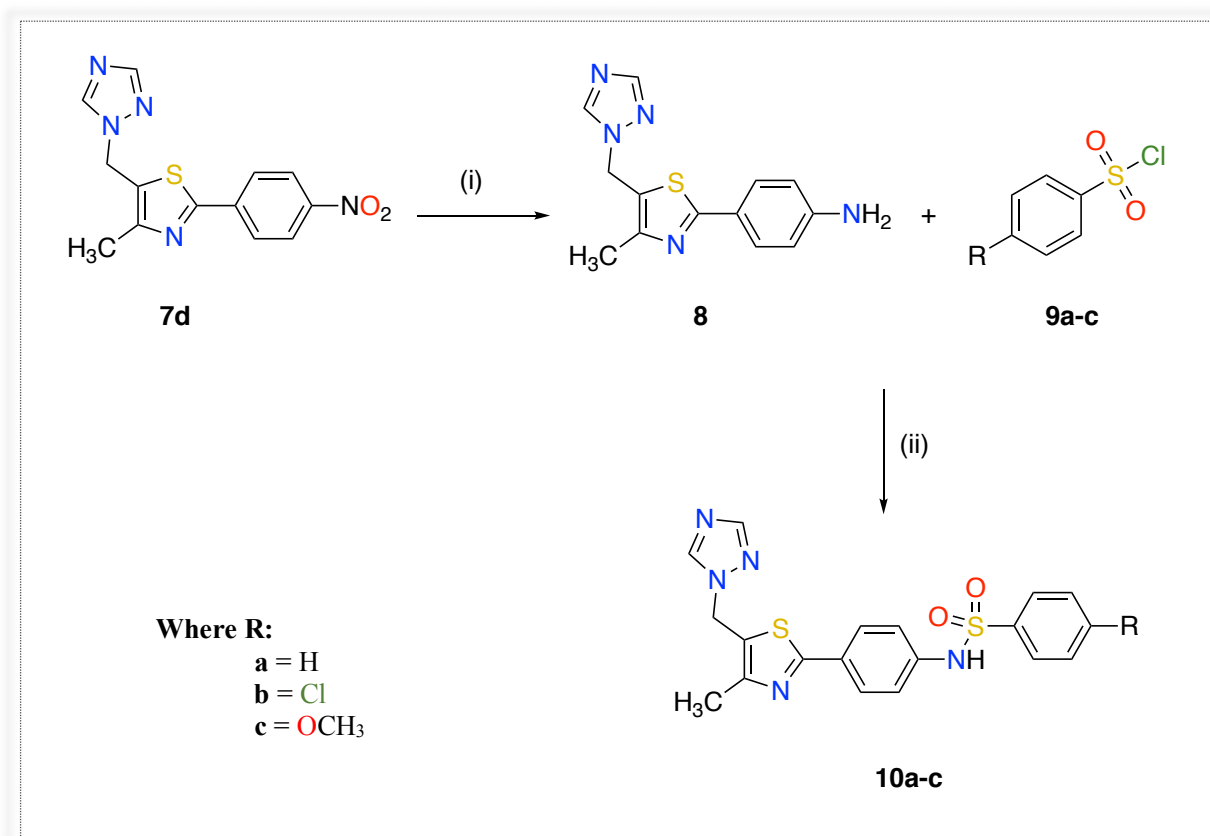
Scheme 2: *Reagents and conditions:* (i) H$_2$, Pd/C, EtOH, r.t., 3 h (ii) Pyridine, r.t., o/n.
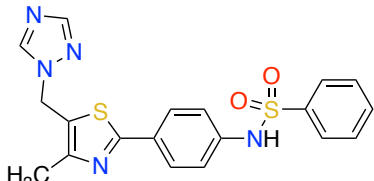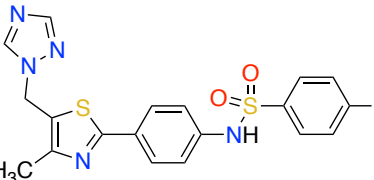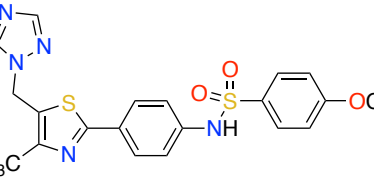
Synthesis of 4-(5-((1*H*-1,2,4-triazol-1-yl)methyl)-4-methylthiazol-2-yl) aniline (8):

The synthesis of 4-(5-((1*H*-1,2,4-triazol-1-yl)methyl)-4-methylthiazol-2-yl)aniline (**8**) was obtained by a reduction reaction using 10% palladium on carbon (Pd/C) in dry MeOH, and the reaction atmosphere filled with H$_2$ using H$_2$ balloons. The mixture was stirred at room temperature for 3 h.[96] The product was confirmed by ^{1}H NMR with the primary amine proton observed as a broad singlet at δ 5.66 ppm. The crude product (**8**) was obtained in 100 % yield and used in the next step without any further purification.

Synthesis of *N*-(4-(5-((1*H*-1,2,4-triazol-1-yl)methyl)-4-methylthiazol-2-yl)phenyl) benzenesulfonamide derivatives (10):

Sulfonyl chloride derivatives are very reactive functional groups especially with amines leading to formation of a sulfonamide bond. The synthesis of *N*-(4-(5-((1*H*-1,2,4-triazol-1-yl) methyl)-4-methylthiazol-2-yl)phenyl)benzenesulfonamide derivatives (**10**) was achieved by using benzene sulfonyl chloride derivatives (**9**) in dry pyridine, and the mixture was left at room temperature overnight.[97] The desired products were purified by column chromatography to give a pale-yellow solid with good yields (Table 7), and the products were confirmed by ^{1}H NMR with the amide proton observed at δ 10.46 ppm.
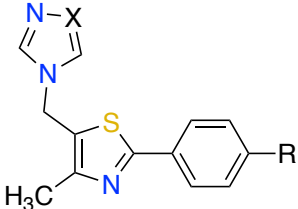
Table 7: List of the novel phenyl thiazole extended compounds.
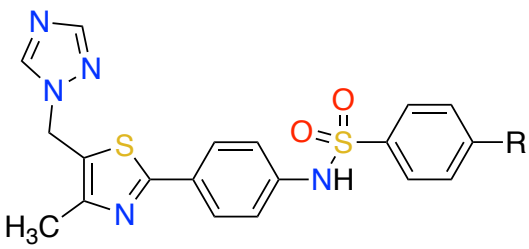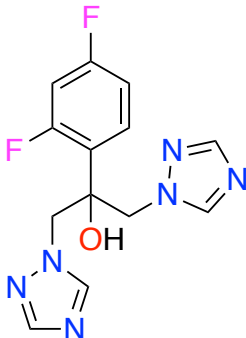
Compound	Structure	Yield (%)	M.P. (°C)	HPLC purity (%)
10a		41	175 - 178 °C	97
10b		58	172 – 174 °C	99
10c		59	86 – 88 °C	99

c. Biological evaluation:

1. *C. albicans* susceptibility testing:

The final phenyl thiazole short and extended derivatives were screened against *C. albicans* wild-type clinical isolate CAI4 and *C. albicans* laboratory strain SC5314. As reported in Table 8, the MIC for all synthesised compounds were very high (>16 µg/mL) compared with fluconazole (0.125 µg/mL). This might be due to the failure of the compounds to penetrate *C. albicans* biofilm, which could be related to the presence of the bacterial matrix material in the extracellular medium that makes a barrier for the diffusion of the novel inhibitors.[98] Moreover, the failure of the compounds to be taken up into the microorganism may be a result of enzymatic degradation of the compounds or a transporters issue.[98]

Table 8: MIC values for compounds **6**, **7** and **10**.

Phenyl thiazole short derivatives

Compounds	X	R	MIC (µg/mL)
6a	C	H	>16
6b	C	Cl	>16
6c	C	OCH_3	>16
7a	N	H	>16
7b	N	Cl	>16
7c	N	OCH_3	>16

7d	N	NO$_2$	>16

Phenyl thiazole extended derivatives	

Compounds	R	MIC (µg/mL)
10a	H	>16
10b	Cl	>16
10c	OCH$_3$	>16
Fluconazole		0.125

2. Binding affinity:

In CaCYP51, protein binding affinity is a type of analytical test used to measure the interaction between the novel azole molecule and the haem iron. Moreover, figure 24A showed the absolute spectra of CaCYP51 at the enzyme resting state when the water molecule binds to Fe^{3+} as the sixth ligand. However, there are two modes of binding, Type I and Type II, which have been studied using UV spectroscopy.[99] Type I binding suggests that the potential substrate (sterol) binds at the hydrophobic channel of the CaCYP51 active site without direct coordination to the haem iron, which results in small shift in the water molecule rather than displacement.[100] While type II binding suggest that the potential inhibitor binds directly to the Fe^{3+} and expelled the water molecule.[100] In addition, the difference between Type I and Type

II ligand binding is in the change of the haem-soret absorption band. The binding of the natural substrate (sterol) to CaCYP51 hydrophobic pocket resulted in the blue shift of the soret peak from 419 to 385 nm indicative of Type I binding (Figure 24B). In contrast, the binding coordination of the antifungal fluconazole (sixth ligand) to CaCYP51 haem iron is Type II binding mode, which results in a red shift of the soret peak from 413 to 429 nm (Figure 24C).[99,100]
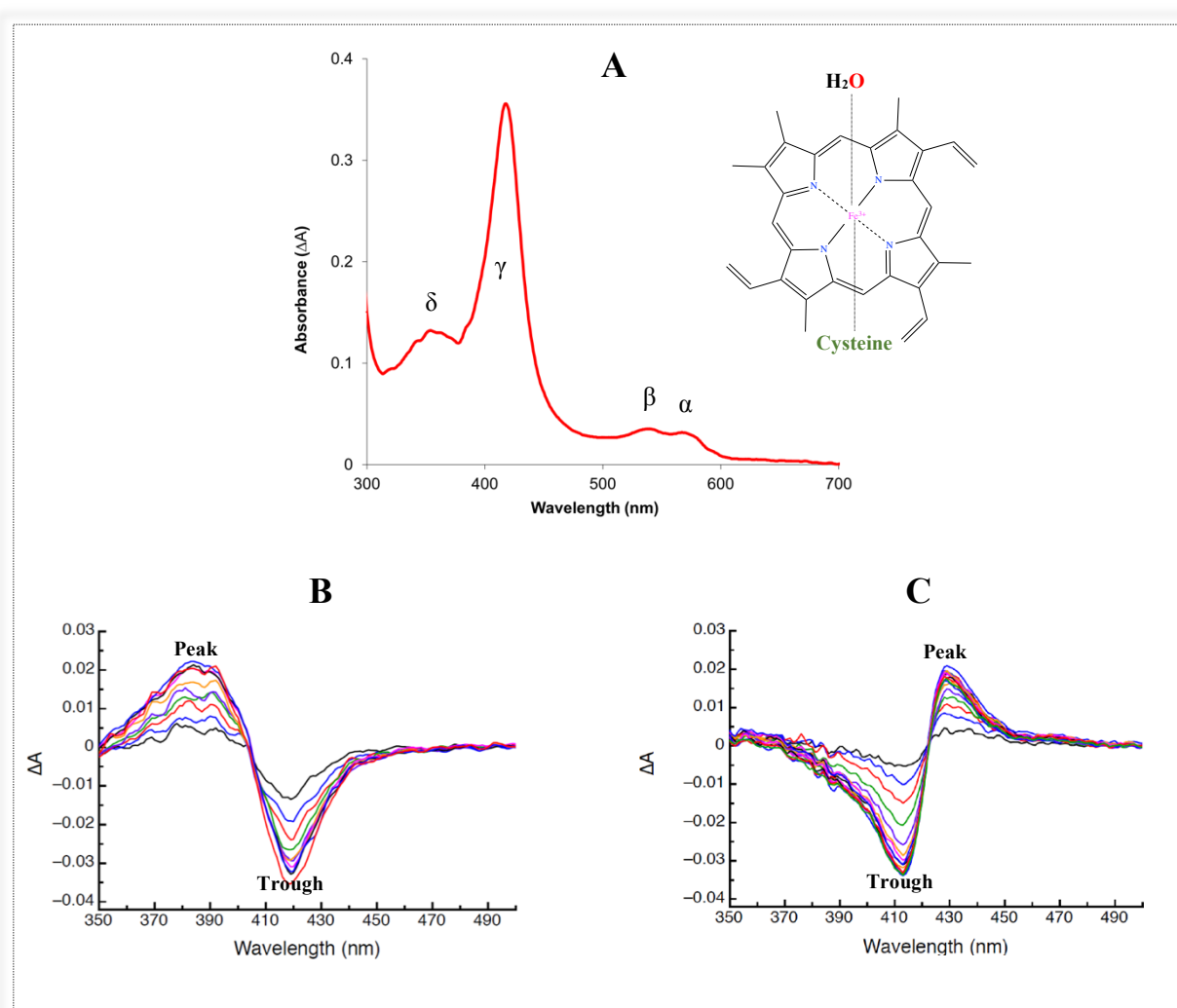
Figure 24: **A**) Absolute spectra of CaCYP51 at resting state and the absorbance peaks: α-band: ~570 nm, β-band: ~540 nm, γ-band: ~418 nm and δ-band: ~350 nm (soret). **B**) Absorbance difference spectra were measured during the titration of 5 μM CaCYP51 with sterol (Type I binding). **C**) Absorbance difference spectra were measured during the titration of 5 μM CaCYP51 with Fluconazole (Type II binding).

The novel azole compounds were designed to cause Type II binding in CaCYP51. To determine binding affinity (K_d) value for fluconazole as well as the novel inhibitors, a binding saturation curve was created from the change in the absorbance (ΔA peak-trough) which was

plotted against the antifungal concentration for CaCYP51. Moreover, the K_d value for Type II binding of the azole was determined by a rearrangement of the Morrison equation ($\Delta A = \Delta A_{max}$ x ([E$_t$] + [azole] + K_d) − {([E$_t$] + [azole] + K_d)^2 − 4[E$_t$][L]}$^{0.5}$ /2[E$_t$] where E$_t$ means total enzyme) while the Michaelis-Menten equation ($\Delta A = (\Delta A_{max}$ x[azole]) / (K_d + [azole])) was used to determine Type I binding. However, fluconazole has excellent MIC and IC$_{50}$ values against CaCYP51 (0.125 µg/mL and 0.35µM, respectively), additionally the binding affinity showed tight binding or Type II binding to CaCYP51 (K_d = 60 ± 40 nM) as shown in Figure 25.
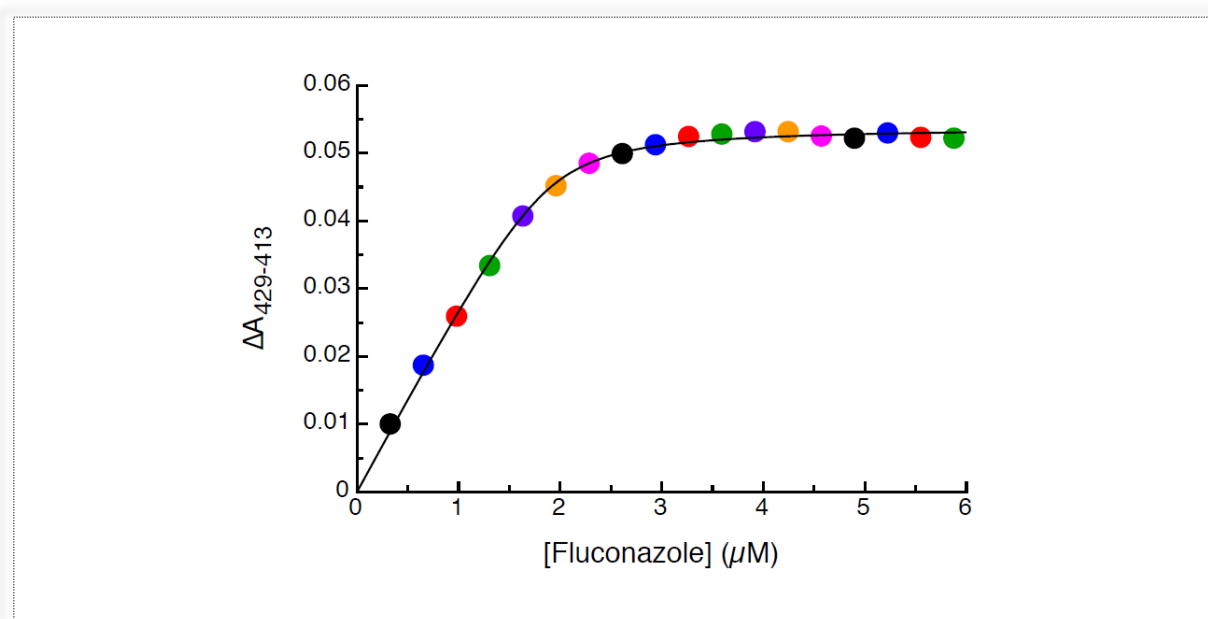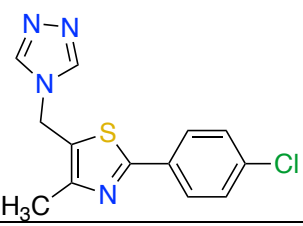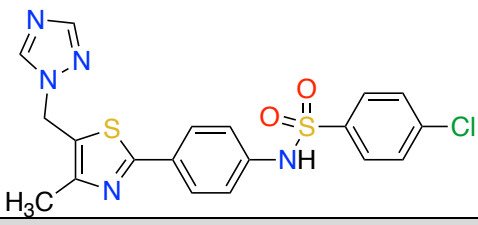
Figure 25: CaCYP51 fluconazole saturation curve derived from type II difference spectra in previous figure 23C with 5 µM CaCYP51. Fluconazole titration was performed in triplicate although only one replicate is shown.

Although the MIC of phenyl thiazole compounds did not show any inhibitory activity, studying the binding affinity of the synthesised compounds will provide answers as to whether:

1. There is a direct binding between the azole nitrogen of the novel compounds and the haem iron of CaCYP51, and
2. How the designed compounds fit in the enzyme active site.

Two compounds (**7b** and **10b**) of the novel phenyl thiazole short and extended derivatives, respectively, were evaluated for binding type and binding affinity by titrating against CaCYP51. As a result, the binding spectra and the binding saturation curve for compound **7b** showed Type II binding and weak binding (less tight) affinity compared to fluconazole (Table 9 and Figure 26A). While compound **10b** showed non-standard binding with trough and no peak as well as very weak binding affinity, compared to fluconazole (Table 9 and Figure 26B).

Table 9: K_d value for compounds **7b** and **10b**.

Compounds	Structure	K_d (nM)
7b		684
10b		4717
Fluconazole		60 ± 40
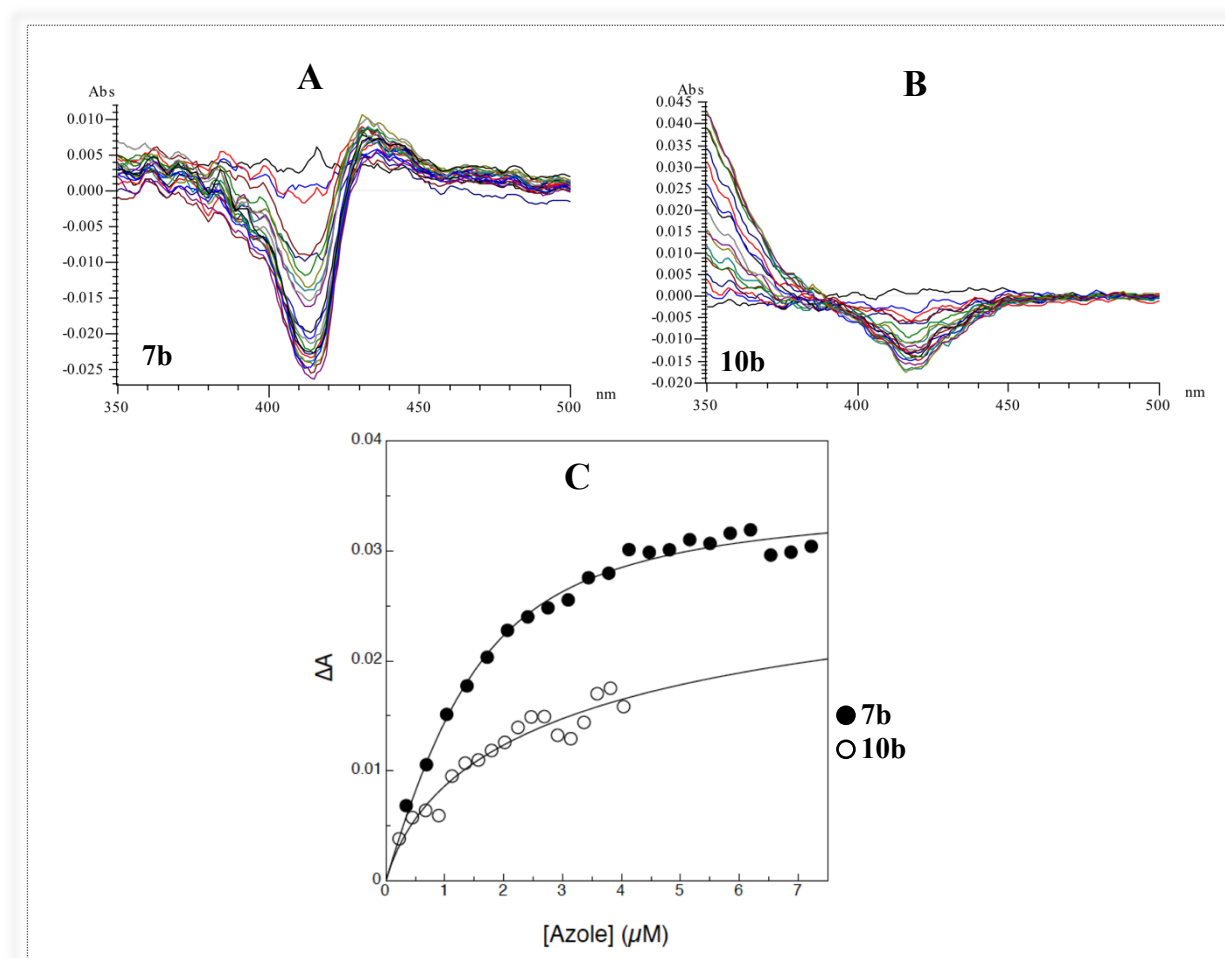
Figure 26: **A**) Compound **7b** Type II binding spectra. **B**) Compound **10b** non-standard binding spectra. **C**) CaCYP51 azole saturation curve. Compound **7b** and **10b** binding saturation curve derived from type II difference spectra with 5 μM CaCYP51. Azole titration was performed in triplicate although only one replicate is shown.

As a result, compound **7b** showed Type II binding but the binding affinity (K_d = 684 nM) was less tight to CaCYP51. Also, compound **10b** showed unknown binding spectra with decreased affinity. This could be related to the rigidity of the designed compounds, which would decrease the chance of direct binding with the haem iron especially for the extended compound **10b**.

3. Molecular Dynamic (MD) simulation:

Further investigations on compound **7b** and **10b** were done using computational studies to correlate the biological results. Molecular dynamic (MD) is a computer simulation tool used in this project for studying the stability of protein-ligand complex as well as analysing the physical movements of both CaCYP51 and the novel inhibitor atoms. The dynamic system will allow the atoms and CaCYP51 molecule to interact for a specific period of time in nanoseconds (ns).[101] The favorable pose of the inhibitor with CaCYP51 crystal structure (PDB 5FSA)[88], obtained from MOE, was subjected to a 200 ns molecular dynamic simulations using the Desmond programme of Maestro.

Both compounds (**7b** and **10b**) formed a coordination interaction between the triazole N and the haem Fe^{3+}. However, the binding profile of compound **7b** showed 64 % binding interaction between the triazole N and the haem Fe^{3+} during the 200 ns simulation while compound **10b** showed only 35 % binding interaction (Figure 27A and 27B). In addition, both compounds formed π-π stacking with Phe380 but compound **10b** had an advantage of forming H-bonding interaction with Ser378 and Met508 through water molecules. Moreover, the 3D visualisation of both compounds after the MD simulation illustrated how far the inhibitors have moved from the haem active site, which may explain the weak binding interaction percentage with the haem iron (Figure 26D). In addition, the distance between the triazole N and the haem Fe^{3+} of both compounds (**7b** and **10b**) at 0 ns was 2.72 and 2.56 Å, respectively (Figure 26C). After MD simulation, a large shift between the triazole N and the iron was observed for both compounds (Table 10). Subsequently, the molecular dynamic results of compound **7b** and **10b** provided evidence to support that both compounds had very weak binding affinity compared to fluconazole (Table 9). Thus, the rigidity of the structure might play a major role in lowering the binding interaction with haem iron as well as with the amino acid residues.

Table 10: The distance between the N-azole ring and the haem iron in the wild type of CaCYP51 active site at 0 ns and 100 ns MD stimulation for compound **7b** and **10b**.

Compounds	N-Fe^{3+} (Å) 0 ns	N-Fe^{3+} (Å) 200 ns
7b	2.72	5.15
10b	2.56	5.00
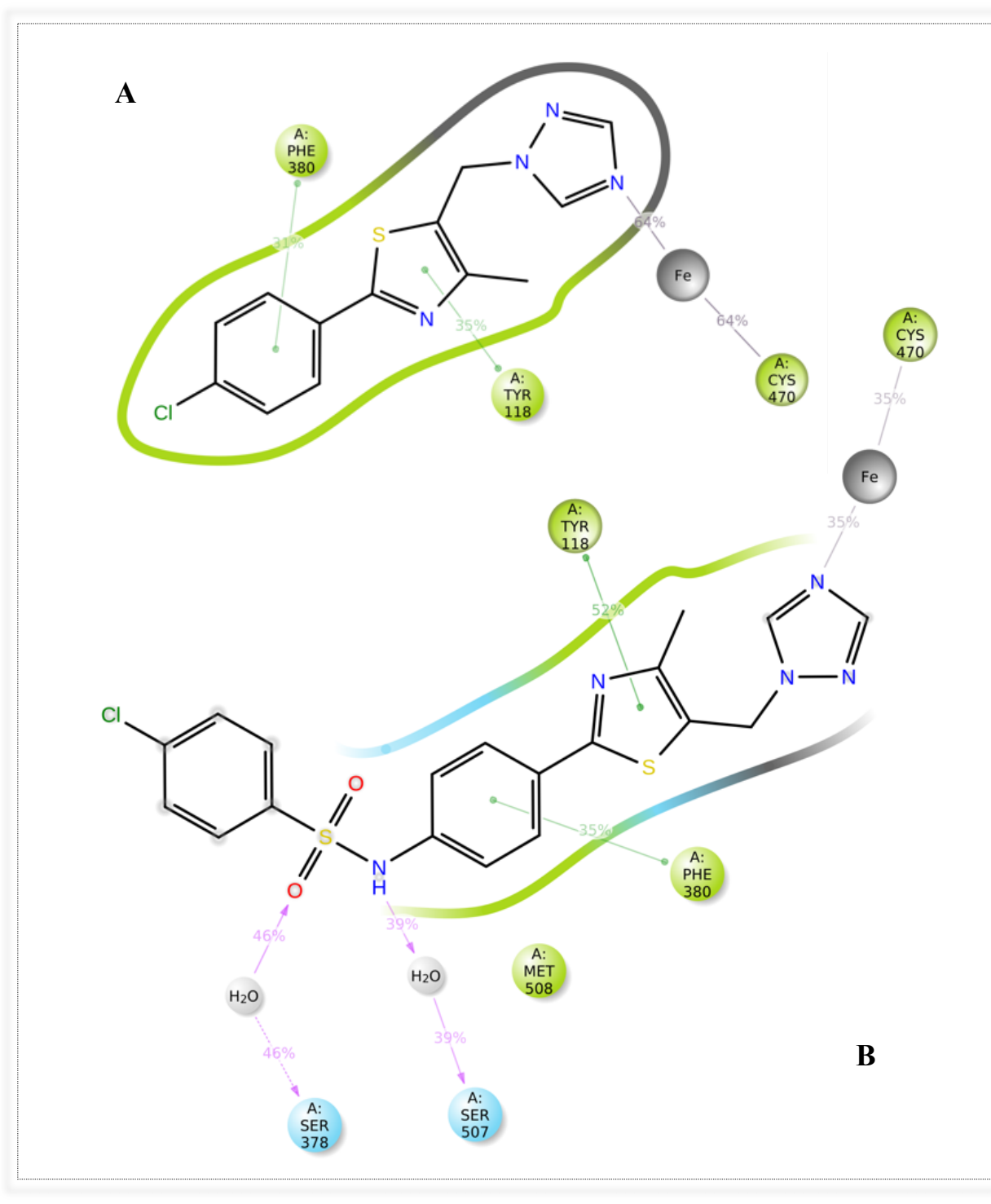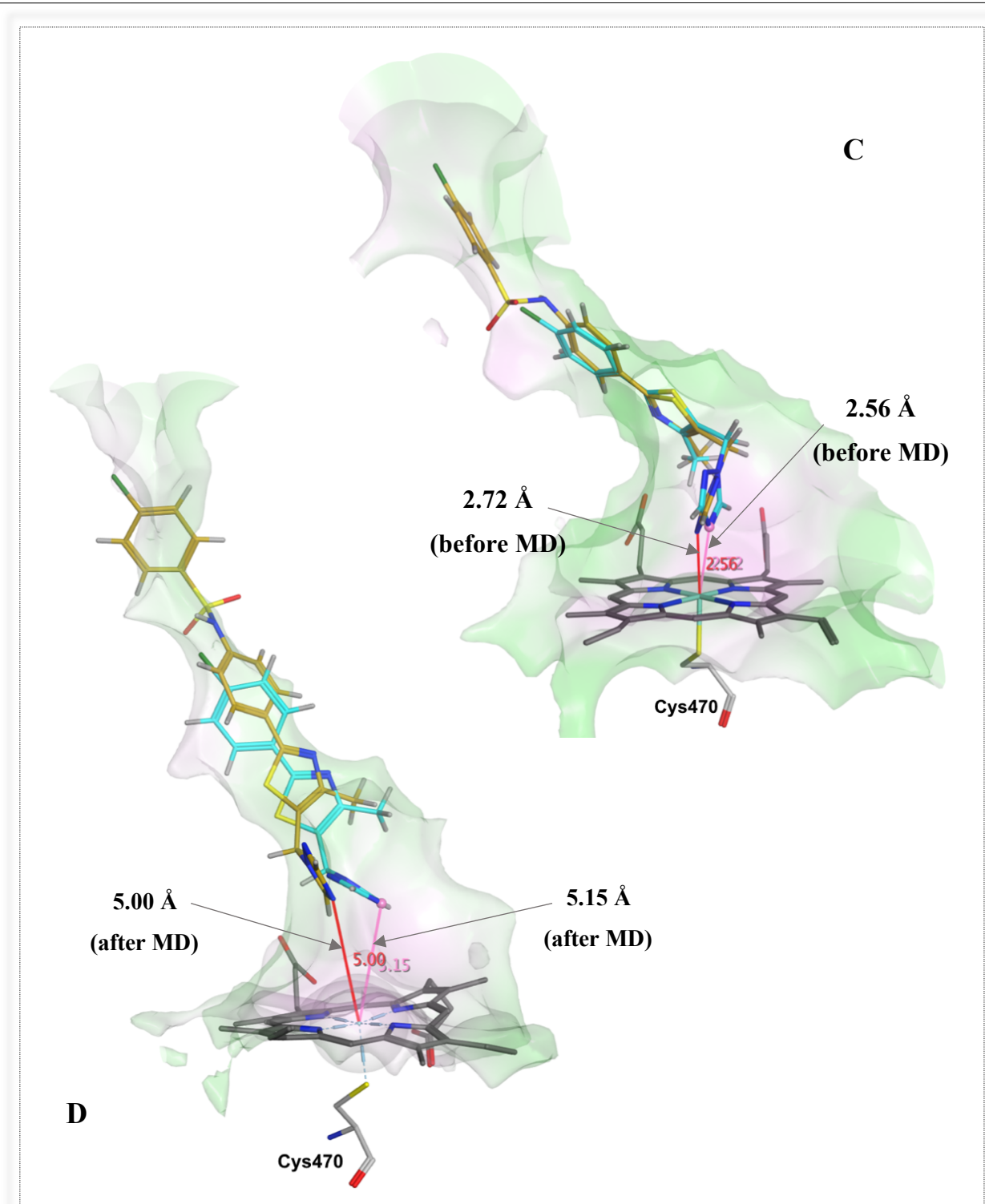
Figure 27: A) 2D detailed ligand interaction between the triazole N of compounds **7b** and **10b** and the haem Fe^{3+} as well as interaction with amino acids of CaCYP51 active site that occur more than 30% of the simulation time in the selected trajectory (0 through 200 ns). **C)** 3D visualisation of both compounds **7b** (cyan) and **10b** (yellow) showing the occupancy and the distance between the N-azole ring and the haem iron before MD simulation and **D)** after MD simulation.

3. Conclusion:

In this chapter, the docking results for the phenyl thiazole short derivatives, which include the thiazole backbone, showed a good fit in the enzyme active site. In addition, extension to phenyl thiazole short series with a sulfonamide linker was performed to fill the long access channel, and it showed water-mediated binding interactions between the sulfonamide and a few amino acids. The synthetic scheme of phenyl thiazole derivatives was designed and optimised with four to six reaction steps as well as with a few changes depending on each derivative. However, the biological results for both short and extended phenyl thiazole derivatives did not show any activity against wild-type *C. albicans* at the MIC level. Moreover, the binding affinity testing for both derivatives showed very weak binding to CaCYP51. The lack of biological activity could be owing to the lack of the flexibility in the phenyl thiazole short and extended series, which might be explained from the MD simulation studies, that showed that the inhibitors moved far away from the haem active site. In the next chapter, a modified thiazole backbone series with a more flexible linker between the thiazole and aryl ring were synthesised to improve the antifungal activity.

4. Experimental

a. Molecular Modelling:

The crystal structure of the wild-type CaCYP51 (PDB 5FSA) was downloaded from the protein data bank.[88] The process of creating the ligands was done by using ChemDraw professional (16.0) and introduced into the Molecular Operating Environment (MOE) programme. All compounds were protonated at physiological pH ($\approx$7.4), to mimic the physiological condition in *C. albicans* endoplasmic reticulum and used in the docking studies. The MOE program was used to perform molecular docking and was found to closely replicate the position and binding interactions of posaconazole, as observed in the crystal structure.

All minimisations were performed with MOE with MMFF94 forcefield and partial charges were automatically calculated. The charge of the haem iron at physiological pH was set to 3^+ (geometry d2sp3) through the atom manager in MOE. The London ΔG scoring function estimates the free energy of binding of the ligand from a given pose. The binding score (S-score) of all used poses was between (-1 to -5). Refinement of the results using MMFF94 forcefield and scoring of the refined results using the London ΔG scoring function was applied. The output database dock file was created with different poses for each ligand and arranged according to the final S-score function, which is the score of the last stage that was not set to zero.

The CaCYP51 double mutants models were built by Dr. Claire and Dr. Esraa Tatar using SWISS-MODEL software. The mutated CYP51 models, which were created and saved for docking studies, included Y132H/K143R and Y132F/F145L.

b. Molecular Dynamics (MD)Simulatin:

Molecular dynamics simulations were performed on CaCYP51-ligand complexes, which were optimised with protein preparation wizard in Maestro (Schrödinger release 2020-1)[102], by assigning bond orders, adding hydrogen, and correcting incorrect bond types. A default quick relaxation protocol was used to minimise the MD systems with the Desmond programme.[102] In Desmond, the volume of space in which the simulation takes place, the global cell, is built up by regular 3D simulation boxes, which was utilised as part of this system for protein interactions. The orthorhombic water box allowed for a 10 Å buffer region between protein atoms and box sides. Overlapping water molecules were deleted, and the systems were neutralised with Na^+ ions and salt concentration 0.15 M.

Force-field parameters for the complexes were assigned using the OPLS_ 2005 forcefield, that is a 200 ns molecular dynamic run in the NPT ensemble (T = 300 K) at a constant pressure of 1 bar. Energy and trajectory atomic coordinate data were recorded at each 1.2 ns.

c. Chemistry General information:

All chemicals, reagents and solvents were purchased from Sigma-Aldrich, Alfa Aesar, VWR, Acros and Fluka. Solvents were dried prior to use over molecular sieves (4 Å). For column chromatography, a glass column was slurry packed in the appropriate eluent with silica gel (Fluka Kieselgel 60), column chromatography was performed with the aid of a bellow. Analytical thin layer chromatography (TLC) was carried out on pre-coated silica plates (ALUGRAM® SIL G/UV254) with visualisation via UV light (254 nm). Melting points were determined on an electrothermal instrument (Gallenkamp melting point apparatus) and were uncorrected. cLogP obtained from Chem Draw (Professional 16.0) using Crippen's fragmentation.[103]

^{1}H and ^{13}C-NMR spectra were recorded on a Bruker Advance DP500 spectrometer operating at 500 MHz and 125 MHz, respectively and auto calibrated to the deuterated solvent reference peak. NMR solvents were chloroform-d ($CDCl_3$), methanol-d4 (CD_3OD), DMSO-d$_6$ (($CD_3)_2SO$). Chemical shifts are given in parts per million (ppm) relative to the internal standard tetramethylsilane (Me_4Si); coupling constants (J) were given in Hertz (Hz). Splitting of the peaks in the ^{1}H NMR spectra are denoted as s (singlet), d (doublet), dd (doublet of doublet), t (triplet), q (quartet), and m (multiplet). All NMR characterisations were made by comparison with previous NMR spectra of the appropriate structure class and/or predictions from ChemDraw.

High performance liquid chromatography (HPLC)/ high resolution mass spectra (HRMS) were performed by Shaun Reeksting, Department of Pharmacy & Pharmacology, University of Bath, Bath, UK or Cardiff University. HPLC (Method A) was performed on a Zorbax Eclipse Plus C18 Rapid Resolution 2.1 x 50 mm, 1.8 μm particle size using a 7.5-minute gradient method 5:95 v/v water: methanol with 0.1% formic acid as additive; (Method B, Cardiff University) was performed on a Shimadzu LC-2030C Plus C18 Rapid Resolution 250 x 4.6 mm, 5 μm particle size using a 7-10 minute gradient method 5:95 v/v water: methanol.

General method:

Ethyl-4-methyl-2-phenylthiazole-5-carboxylate (3a)[93]

(C$_{13}$H$_{13}$NO$_2$S, M.W. 247.31)

(1)	**(2a)**	**(3a)**
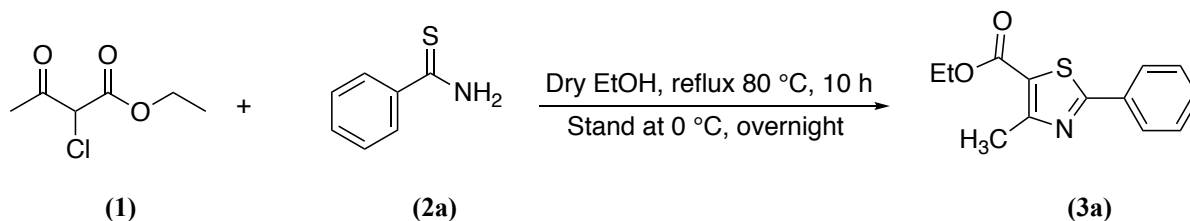
Method: A solution of thiobenzamide (**2a**) (0.5 g, 3.64 mmol) and ethyl 2-chloroacetoacetate (**1**) (1.01 g, 6.18 mmol) in dry EtOH (15 mL) was refluxed at 80 °C for 10 h. Then, the mixture was allowed to stand at 0 °C for another night. The solvent was evaporated under vacuum then saturated aqueous NaHCO$_3$ (50 mL) was added, and the mixture was extracted with EtOAc (2 x 50 mL). The organic layer was washed with H$_2$O (2 x 50 mL), dried (MgSO$_4$), and concentrated under reduced pressure. The residue was purified by using gradient column chromatography and the pure compound was eluted with 10 % EtOAc in petroleum ether.

Yield: 0.57 g (63 %) as a colourless oil.

R$_f$: 0.62 (4:1 v/v petroleum ether-EtOAc).

^{1}H NMR (DMSO-d$_6$): δ 8.01 (dd, J = 1.4, 9.7 Hz, 2H, Ar), 7.56-7.50 (m, 3H, Ar), 4.29 (q, J = 7.1Hz, 2H, C$\underline{H_2}$CH$_3$), 2.70 (s, 3H, CH$_3$), 1.30 (t, J = 7.1 Hz, 3H, CH$_2$C$\underline{H_3}$).

Using this procedure, the following compounds were prepared:

Ethyl-4-methyl-2-phenylthiazole-5-carboxylate (3a)[87]

(C$_{13}$H$_{13}$NO$_2$S, M.W. 247.31)

(13a)	**(2a)**	**(3a)**
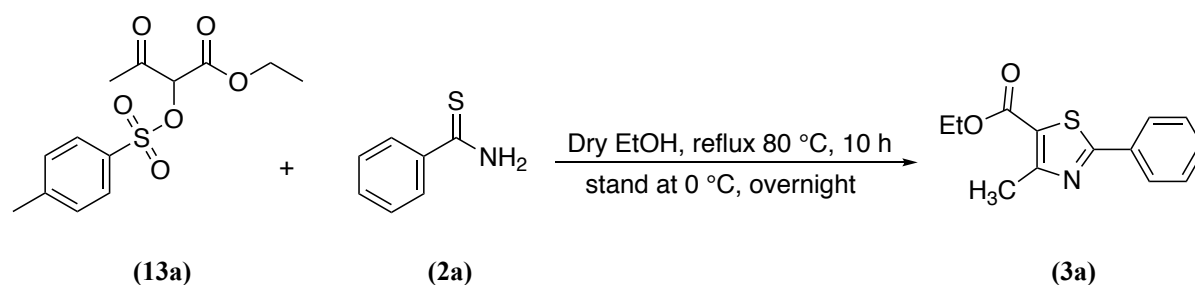
Reagents: thiobenzamide (**2a**) (0.45 g, 3.27 mmol) and ethyl-3-oxo-2-(tosyloxy)butanoate (**13a**) (1.5 g, 4.9 mmol).

Yield: 0.41 g (51 %) as colorless oil.

R$_f$: 0.53 (5:1 v/v petroleum ether-EtOAc).

¹H NMR (DMSO-d₆): δ 7.99 (dd, J = 1.4, 8.1 Hz, 2H, Ar), 7.56-7.50 (m, 3H, Ar), 4.31 (q, J = 7.1 Hz, 2H, C$\underline{H_2}$CH₃), 2.68 (s, 3H, CH₃), 1.31 (t, J = 7.1 Hz, 3H, CH₂C$\underline{H_3}$).

Ethyl 2-(4-chlorophenyl)-4-methylthiazole-5-carboxylate (3b)[93]
(C₁₃H₁₂ClNO₂S, M.W. 281.75)

| (1) | (2b) | (3b) |
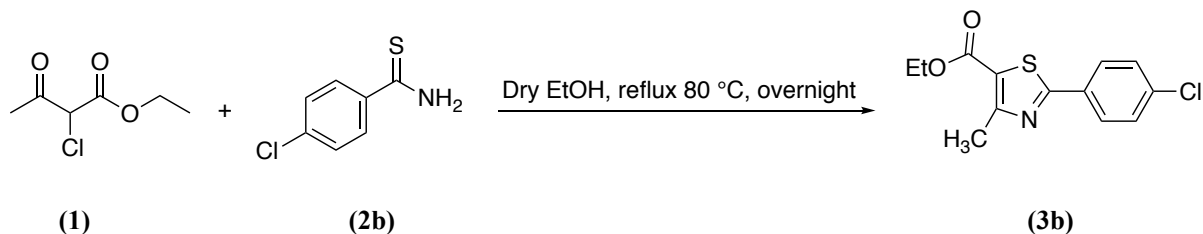
Reagents: 4-chlorothiobenzamide (**2b**) (1 g, 5.82 mmol) and ethyl 2-chloroacetoacetate (**1**) (1.36 mL, 9.89 mmol). The residue was purified by gradient column chromatography and the pure compound was eluted with 5% EtOAc in petroleum ether. (A fraction with impurities was recrystallised with EtOH to recover the compound and to improve the yield).

Yield: 0. 98 g (61%) as a white solid.

m.p.: 84-86 °C.

R$_f$: 0.72 (4:1v/v petroleum ether-EtOAc).

¹H NMR (DMSO-d₆): δ 8.01 (d, J = 8.8 Hz, 2H, Ar), 7.58 (d, J = 8.8 Hz, 2H, Ar), 4.30 (q, J = 7.1Hz, 2H, C$\underline{H_2}$CH₃), 2.69 (s, 3H, CH₃), 1.31 (t, J = 7.1 Hz, 3H, CH₂C$\underline{H_3}$).

Ethyl 2-(4-methoxyphenyl)-4-methylthiazole-5-carboxylate (3c)[93]
(C₁₄H₁₅NO₃S, M.W. 277.34)

| (1) | (2c) | (3c) |
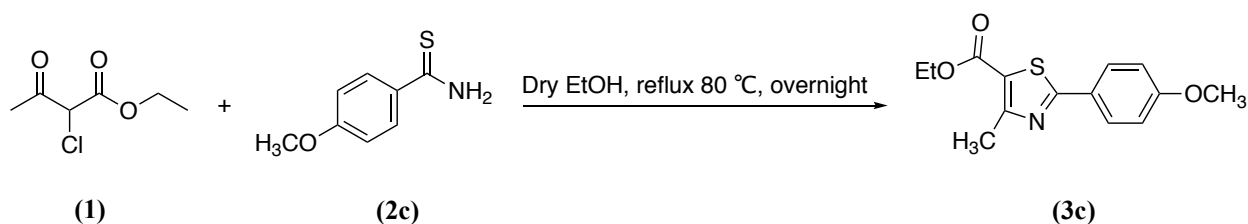
Reagents: 4-methoxybenzothioamide (**2c**) (1 g, 5.97 mmol) and ethyl 2-chloroacetoacetate (**1**) (1.39 mL, 10.14 mmol).

Yield: 0.1.42 g (86 %) as a white solid.

m.p.: 78-80 °C.

R$_f$: 0.52 (4:1 v/v petroleum ether-EtOAc).

¹H NMR (DMSO-d₆): δ 7.93 (d, J = 9.0 Hz, 2H, Ar), 7.06 (d, J = 9.0 Hz, 2H, Ar), 4.28 (q, J = 7.1Hz, 2H, C$\underline{H_2}$CH₃), 3.83 (s, 3H, O-CH₃), 2.66 (s, 3H, CH₃), 1.31 (t, J = 7.1 Hz, 3H, CH₂C$\underline{H_3}$).

Ethyl 4-methyl-2-(4-nitrophenyl) thiazole-5-carboxylate (3d)[93]
(C₁₃H₁₂N₂O₄S, M.W. 292.31)
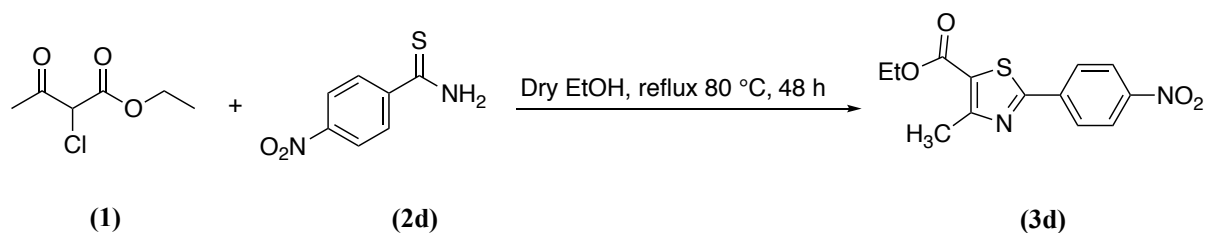
Prepared as described for 3a with some modifications:

A solution of 4-nitrobenzothioamide (**2d**) (0.5 g, 2.74 mmol) and ethyl 2-chloroacetoacetate (**1**) (0.63 mL, 4.65 mmol) in dry EtOH (15 mL) was heated at 80 °C for 48 h.[93] Then, a pale yellow solid was formed when the mixture reached room temperature. The mixture was filtered, and the solid was washed several times with EtOH, then dried in the oven (40 °C) to obtain the desired product.

Yield: 0.63 g (78 %) as a pale yellow solid.

m.p.: 147-149 °C.

R$_f$: 0.5 (4:1 v/v petroleum ether-EtOAc).

¹H NMR (DMSO-d₆): δ 8.32 (d, J = 9.1 Hz, 2H, Ar), 8.24 (d, J = 9.0 Hz, 2H, Ar), 4.32 (q, J = 7.1 Hz, 2H, C$\underline{H_2}$CH₃), 2.71 (s, 3H, CH₃), 1.32 (t, J = 7.1 Hz, 3H, CH₂C$\underline{H_3}$).

(4-Methyl-2-phenylthiazole-5-yl) methanol (4a)[93]
(C₁₁H₁₁NOS, M.W. 205.28)
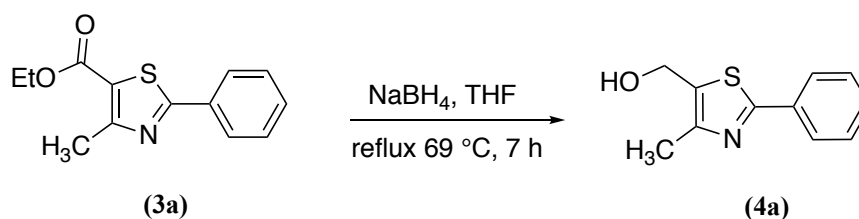
Method: To a stirred mixture of ethyl-4-methyl-2-phenylthiazole-5-carboxylate (**3a**) (0.41 g, 1.7 mmol) in a dry THF (10 mL), NaBH₄ (0.19 g, 5.1 mmol) was added. During the reflux, MeOH (0.5 mL) was added and the mixture was refluxed for 7 h at 69 °C. The solution was left at room temperature overnight, then the reaction mixture was poured into ice/cold H₂O (10

mL) and extracted with EtOAc (3 x 15 mL). The organic layer was collected and washed with saturated brine (2 x 15 mL), dried (MgSO₄) and concentration under reduced pressure to give a white solid, which was used in the next step without any further purification.

Yield: 0.3 g (88 %) as a white solid.

m.p.: 108-111°C (94-95 °C)[104].

R$_f$: 0.1 (5:1 v/v petroleum ether-EtOAc).

¹H NMR (DMSO-d₆): δ 7.88 (dd, J = 1.7, 8.2 Hz, 2H, Ar), 7.49-7.43 (m, 2H, Ar), 5.54 (t, J = 5.6 Hz, 1H, OH, ex), 4.64 (d, J = 5.5 Hz, 2H, CH₂), 2.35 (s, 3H, CH₃).

Using this procedure, the following compounds were prepared:

(2-(4-Chlorophenyl)-4-methylthiazol-5-yl)methanol (4b)[93]
(C₁₁H₁₀ClNOS, M.W. 239.72)

(3b)   NaBH₄, THF / reflux 69 °C, 7 h   **(4b)**
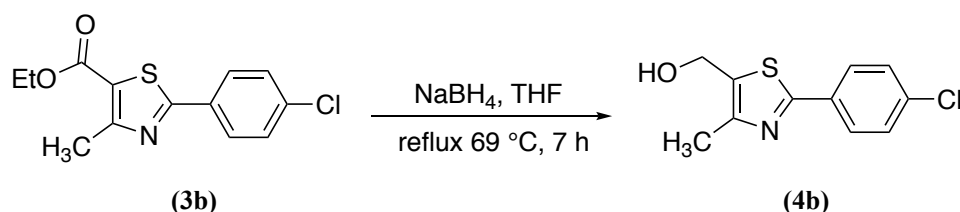
Reagents: ethyl 2-(4-chlorophenyl)-4-methylthiazole-5-carboxylate (**3b**) (0.98 g, 3.47 mmol).

Yield: 0.8 g (96 %) as a white solid.

m.p.: 148-150 °C (134-136 °C)[104].

R$_f$: 0.17 (4:1 v/v petroleum ether-EtOAc)

¹H NMR (DMSO-d₆): δ 7.89 (d, J = 8.8 Hz, 2H, Ar), 7.53 (d, J = 8.8 Hz, 2H, Ar), 5.57 (t, J = 5.6 Hz, 1H, OH, ex), 4.64 (d, J = 5.5 Hz, 2H, CH₂), 2.34 (s, 3H, CH₃).

(2-(4-Methoxyphenyl)-4-methylthiazol-5-yl)methanol (4c)[93]
(C₁₂H₁₃NO₂S, M.W. 235.30)

(3c)   NaBH₄, THF / reflux 69 °C, 7 h / room temp. overnight   **(4c)**
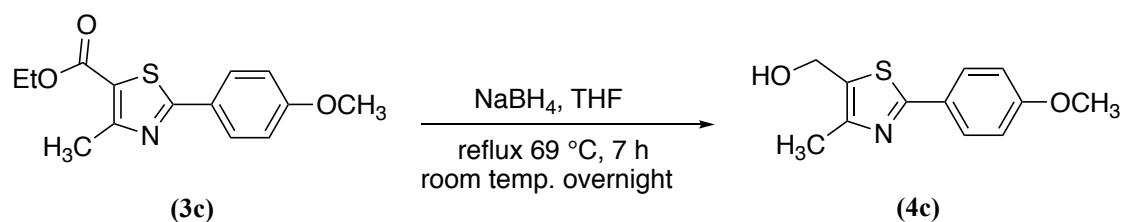
Reagents: ethyl 2-(4-methoxyphenyl)-4-methylthiazole-5-carboxylate (**3c**) (1.42 g, 5.12 mmol).

Yield: 1.10 g (92 %) as a white solid.

m.p.: 116-119 °C.

R$_f$: 0.15 (4:1 v/v petroleum ether-EtOAc)

¹H NMR (DMSO-d$_6$): δ 7.81 (d, J = 8.9 Hz, 2H, Ar), 7.02 (d, J = 9.0 Hz, 2H, Ar), 5.48 (t, J = 5.6 Hz, 1H, OH, ex), 4.61 (d, J = 5.1 Hz, 2H, CH$_2$), 3.81 (s, 3H, O-CH$_3$), 2.32 (s, 3H, CH$_3$).

(4-Methyl-2-(4-nitrophenyl) thiazol-5-yl)methanol (4d)[93]
(C$_{11}$H$_{10}$N$_2$O$_3$S, M.W. 250.27)

(3d)   **(4d)**
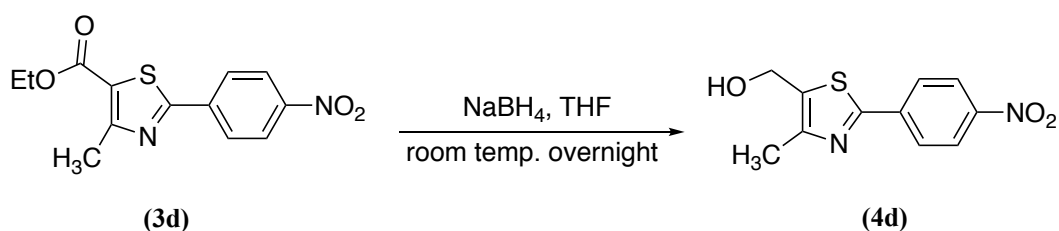
Variation: The reaction was stirred at room temperature overnight and the crude product purified by gradient column chromatography eluting with 1.5 % MeOH in CH$_2$Cl$_2$.

Reagents: ethyl 4-methyl-2-(4-nitrophenyl)thiazole-5-carboxylate **(3d)** (1.13 g, 3.86 mmol).

Yield: 0.71g (60%) as a yellow crystalline solid.

m.p.: 184-187 °C.

R$_f$: 0.37 (9.5: 0.5 v/v CH$_2$Cl$_2$-MeOH).

¹H NMR (DMSO-d$_6$): δ 8.31 (d, J = 9.1 Hz, 2H, Ar), 8.14 (d, J = 9.0 Hz, 2H, Ar), 5.69 (t, J = 5.6 Hz, 1H, OH, ex), 4.68 (d, J = 5.1 Hz, 2H, CH$_2$), 2.38 (s, 3H, CH$_3$).

5- (Chloromethyl)-4-methyl-2-phenylthiazole (5a)
(C$_{11}$H$_{10}$ClNS, M.W. 223.72)

(4a)   **(5a)**
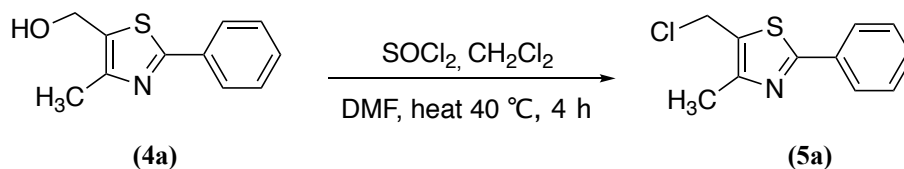
Method: To a solution of (4-methyl-2-phenylthiazole-5-yl)methanol **(4a)** (0.3 g, 1.5 mmol) in dry CH$_2$Cl$_2$ (10 mL), thionyl chloride (0.65 mL, 9 mmol) was added slowly, and a catalytic amount of DMF (2 drops) were added at room temperature. The mixture was heated at 40 °C for 4 h.[93] The reaction was concentrated under reduced pressure and the residue extracted with CH$_2$Cl$_2$ (50 mL), and saturated NaHCO$_3$ (50 mL) was added with caution. The organic layer

was washed with H_2O (2 x 50 mL), dried ($MgSO_4$) and concentrated under reduced pressure to give a pale yellow solid, which was used in the next step without any further purification.

Yield: 0.3 g (90 %) as a pale yellow solid.

m.p.: 82-85 °C (68-69 °C)[94].

R$_f$: 0.55 (5:1 v/v petroleum ether-EtOAc).

^{1}H NMR (DMSO-d$_6$): δ 7.91-7.89 (m, 2H, Ar), 7.52-7.48 (m, 3H, Ar), 5.11 (s, 2H, CH$_2$), 2.43 (s, 3H, CH$_3$).

Using this procedure, the following compounds were prepared:

5-(Chloromethyl)-2-(4-chlorophenyl)-4-methylthiazole (5b)[93]
(C$_{11}$H$_9$Cl$_2$NS, M.W. 258.16)

(4b)　　　　　　　　　　　　　　　　　　　(5b)
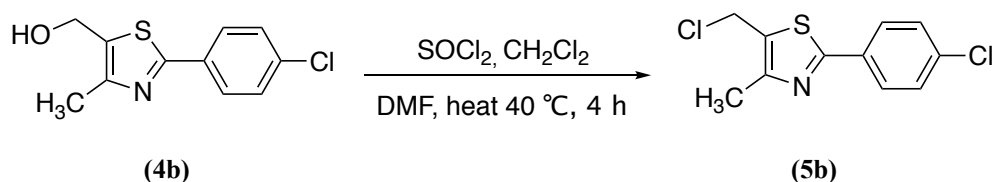
Reagents: (2-(4-chlorophenyl)-4-methylthiazol-5-yl)methanol (**4b**) (0.8 g, 3.33 mmol).

Yield: 0.75 g (87 %) as a pale-yellow solid.

m.p.: 116-118 °C.

R$_f$: 0.52 (4:1 v/v petroleum ether-EtOAc).

^{1}H NMR (DMSO-d$_6$): δ 7.92 (d, $J = 8.8$ Hz, 2H, Ar), 7.55 (d, $J = 8.8$ Hz, 2H, Ar), 5.11 (s, 2H, CH$_2$), 2.43 (s, 3H, CH$_3$).

5-(Chloromethyl)-2-(4-methoxyphenyl)-4-methylthiazole (5c)[93]
(C$_{12}$H$_{12}$ClNOS, M.W. 253.74)

(4c)　　　　　　　　　　　　　　　　　　　(5c)
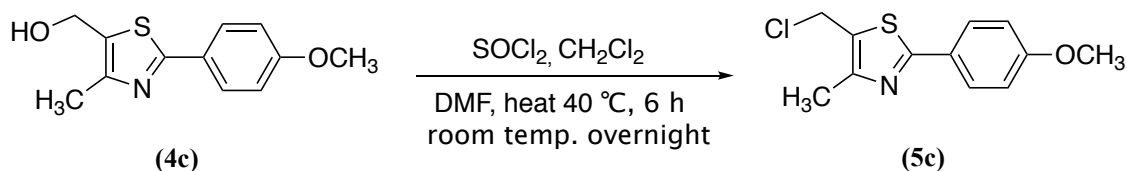
Reagents: (1.10 g, 4.67 mmol) 2-(4-methoxyphenyl)-4-methylthiazol-5-yl)methanol (**4c**).

Yield: 1g (84 %) as a pale yellow solid.

m.p.: 86-90 °C.

R$_f$: 0.55 (4:1 v/v petroleum ether-EtOAc).

^{1}H NMR (DMSO-d$_6$): δ 7.84 (d, J = 8.9 Hz, 2H, Ar), 7.04 (d, J = 9.0 Hz, 2H, Ar), 5.09 (s, 2H, CH$_2$), 3.82 (s, 3H, O-CH$_3$), 2.40 (s, 3H, CH$_3$).

5-(Chloromethyl)-4-methyl-2-(4-nitrophenyl)thiazole (5d)[93]
(C$_{11}$H$_9$ClN$_2$O$_2$S, M.W. 268.72)

(4d)   SOCl$_2$, CH$_2$Cl$_2$ / DMF, heat 40 ℃, 4 h   **(5d)**
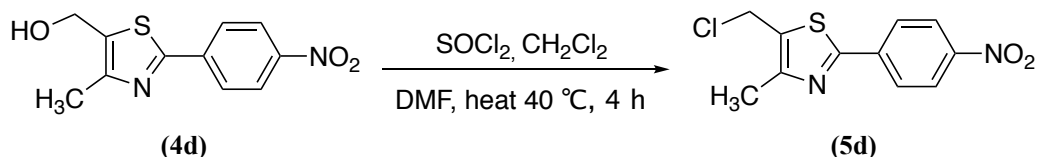
Reagents: (4-methyl-2-(4-nitrophenyl)thiazol-5-yl)methanol (0.71 g, 2.83 mmol) (**4d**).

Yield: 0.71 g (100 %) as a pale yellow solid.

m.p.: 122-124 °C.

R$_f$: 0.42 (4:1 v/v petroleum ether-EtOAc).

^{1}H NMR (DMSO-d$_6$): δ 8.33 (d, J = 9.1 Hz, 2H, Ar), 8.17 (d, J = 9.0 Hz, 2H, Ar), 5.17 (s, 2H, CH$_2$), 2.47 (s, 3H, C$\underline{H}_3$).

5-((1H-Imidazol-1-yl) methyl)-4-methyl-2-phenylthiazole (6a)
(C$_{14}$H$_{13}$N$_3$S, M.W.255.34)

(5a)   I. K$_2$CO$_3$, imidazole, CH$_3$CN heat 45 °C, 1 h / II. Heat 70 °C, overnight   **(6a)**
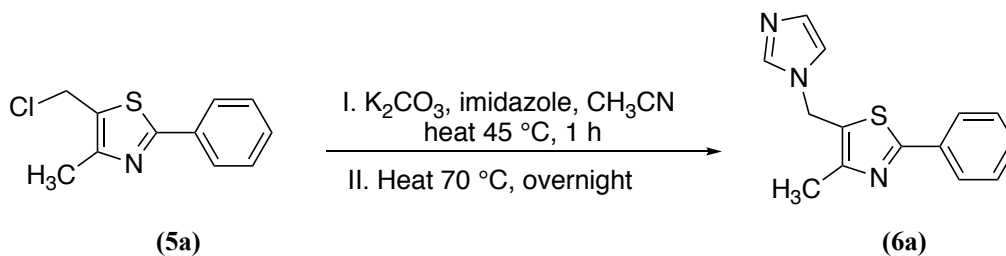
Method: A suspension of K$_2$CO$_3$ (0.62 g, 4.48 mmol) and imidazole (0.30 g, 4.48 mmol) in dry CH$_3$CN (10 mL) was heated at 45 °C for 1 h. After cooling to room temperature, 5-(chloromethyl)-4-methyl-2-phenylthiazole (**5a**) (0.25 g, 1.12 mmol) was added and the mixture was heated at 70 °C overnight.[87] The solvent was evaporated under vacuum and the residue was extracted with EtOAc (50 mL), and washed with brine (3 x 50 mL) and H$_2$O (2 x 50 mL). The organic layer was dried (MgSO$_4$) and evaporated under vacuum. The crude product was purified by gradient column chromatography and the pure compound was eluted with 3 % MeOH in CH$_2$Cl$_2$.

Yield: 0.14 g (50 %) as a yellow solid.

m.p.: 90-93 °C.

R$_f$: 0.27 (9.5: 0.5 v/v CH$_2$Cl$_2$-MeOH).

^{1}H NMR (DMSO-d$_6$): δ 8.52 (s, 1H, imidazole), 7.90-7.88 (m, 2H, Ar), 7.46-7.43 (m, 3H, Ar), 7.22 (s, 1H, imidazole), 7.03 (s, 1H, imidazole), 5.49 (s, 2H, C$\underline{H}_2$), 2.55 (s, 3H, CH$_3$).

^{13}C NMR (DMSO-d$_6$): δ 176.6 (CH, imidazole), 167.7 (C, thiazole), 153.0 (C, thiazole), 132.9 (C, thiazole), 130.5 (2 x CH, Ar), 129.0 (2 x CH, Ar), 126.48 (CH, para-Ar), 126.43 (CH, imidazole), 123.6 (C, Ar), 119.2 (CH, imidazole), 43.5 (CH$_2$), 15.3 (CH$_3$).

HPLC (Method A): 98 %, RT = 3.51 min.

HRMS (ESI, m/z): theoretical mass: 278.0727 [M+Na]$^+$, observed mass: 278.0722 [M+Na]$^+$.

Using this procedure, the following compounds were prepared:

5-((1H-Imidazol-1-yl) methyl)-2-(4-chlorophenyl)-4-methylthiazole (6b)
(C$_{14}$H$_{12}$ClN$_3$S, M.W. 289.78)

(5b)   **(6b)**
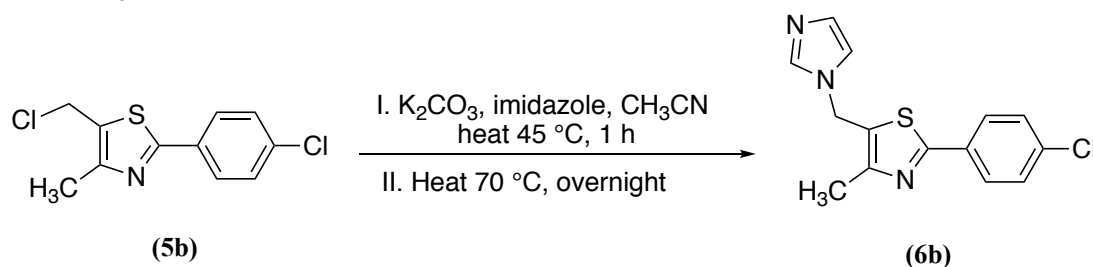
Reagents: 5-(chloromethyl)-2-(4-chlorophenyl)-4-methylthiazole (**5b**) (0.4 g, 1.54 mmol).

Yield: 0.23 g (52 %) as a white solid.

m.p.: 139-142 °C.

R$_f$: 0.47 (9.5: 0.5 v/v CH$_2$Cl$_2$-MeOH).

^{1}H NMR (DMSO-d$_6$): δ 7.87 (d, J = 8.8 Hz, 2H, Ar), 7.77 (s, 1H, imidazole), 7.53 (d, J = 8.8 Hz, 2H, Ar), 7.21 (s, 1H, imidazole), 6.92 (s, 1H, imidazole), 5.46 (s, 2H, C$\underline{H}_2$), 2.47 (s, 3H, CH$_3$).

^{13}C NMR (DMSO-d$_6$): δ 164.0 (C, thiazole), 151.7 (C, thiazole), 137.5 (CH, imidazole), 135.2 (C, Ar), 132.1 (C, Ar para-Cl), 129.7 (2 x CH, Ar), 129.3 (CH, imidazole), 129.0 (C, thiaazole), 128.0 (2 x CH, Ar), 119.6 (CH, imidazole), 41.4 (CH$_2$), 15.3 (CH$_3$).

HPLC (Method A): 99 %, RT = 3.75 min.

HRMS (ESI, m/z): theoretical mass: $^{35/37}$Cl 290.0518/292.0518 [M+H]$^+$, observed mass: $^{35/37}$Cl 290.0518/292.0487 [M+H]$^+$.

5-((1*H*-Imidazol-1-yl)methyl)-2-(4-methoxyphenyl)-4-methylthiazole (6c)

(C$_{15}$H$_{15}$N$_3$OS, M.W. 285.37)
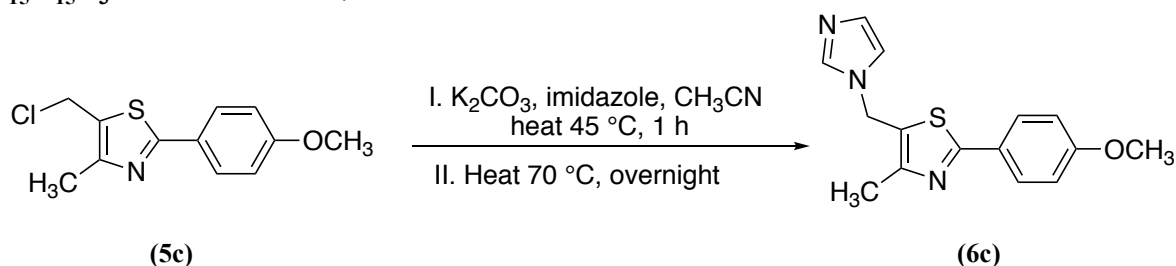
(5c)   I. K$_2$CO$_3$, imidazole, CH$_3$CN heat 45 °C, 1 h   II. Heat 70 °C, overnight   **(6c)**

Reagents: 5-(chloromethyl)-2-(4-methoxyphenyl)-4-methylthiazole (**5c**) (0.5 g, 1.97 mmol). The pure compound was eluted with 2.5 % MeOH in CH$_2$Cl$_2$.

Yield: 0.16 g (28 %) as a pale yellow solid.

m.p.: 106-108 °C.

R$_f$: 0.3 (9.5: 0.5 v/v CH$_2$Cl$_2$-MeOH).

^{1}H NMR (DMSO-d$_6$): δ 7.79 (d, J = 9.0 Hz, 2H, Ar), 7.78 (s, 1H, imidazole), 7.19 (s,1H, imidazole), 7.01 (d, J = 9.0 Hz, 2H, Ar), 6.91 (s, 1H, imidazole), 5.42 (s, 2H, C*H$_2$*), 3.80 (s, 3H, O-CH$_3$), 2.44 (s, 3H, CH$_3$).

^{13}C NMR (DMSO-d$_6$): δ 165.3 (C, thiazole), 161.3 (C, Ar), 151.2 (C, thiazole), 137.5 (CH, imidazole), 129.3 (CH, imidazole), 127.9 (2 x CH, Ar), 127.1 (C, Ar),126.1 (C, thiazole), 119.6 (CH, imidazole), 115.0 (2 x CH, Ar), 55.8 (CH$_3$, Ar para O-CH$_3$), 41.5 (CH$_2$), 15.3 (CH$_3$).

HPLC (Method A): 97 %, RT = 3.55 min.

HRMS (ESI, m/z): theoretical mass: 308.0833 [M+Na]$^+$, observed mass: 308.0825 [M+Na]$^+$.

Triazole derivatives prepared as described for 6 replacing imidazole with triazole:

5-((1*H*-1,2,4-Triazol-1-yl) methyl)-4-methyl-2-phenylthiazole (7a)

(C$_{13}$H$_{12}$N$_4$S, M.W.256.33)

(5a)   I. K$_2$CO$_3$, triazole, CH$_3$CN heat 45 °C, 1 h   II. Heat 70 °C, overnight   **(7a)**
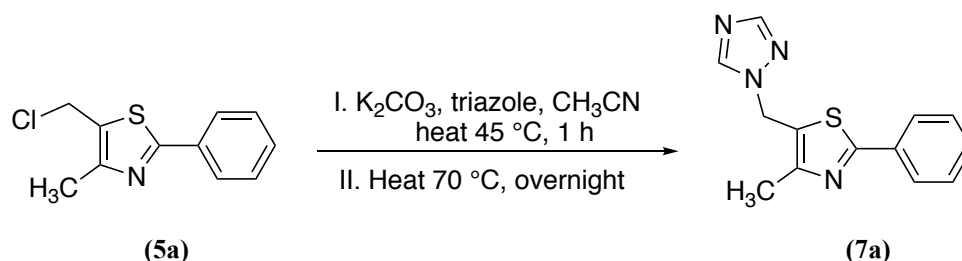
Reagents: 5-(chloromethyl)-4-methyl-2-phenylthiazole (0.29 g, 1.29 mmol) (**5a**).

Yield: 0.15 g (45 %) as a white solid.

m.p.: 116-118 °C

R*f*: 0.20 (9.5:0.5 v/v CH$_2$Cl$_2$-MeOH).

^{1}H NMR (DMSO-d$_6$): δ 8.69 (s, 1H, triazole), 8.01 (s, 1H, triazole), 7.88-7.86 (m, 2H, Ar), 7.48-7.46 (m, 3H, Ar), 5.68 (s, 2H, C*H$_2$*), 2.49 (s, 3H, CH$_3$).

^{13}C NMR (DMSO-d$_6$): δ 165.8 (C, thiazole), 152.34 (CH, triazole), 152.31 (C, thiazole), 144.3 (CH, triazole), 133.2 (C, thiazole), 130.7 (CH, para-Ar), 129.6 (2 x CH, Ar), 126.3 (C, Ar), 126.1 (2 x CH, Ar), 44.1 (CH$_2$), 15.4 (CH$_3$).

HPLC (Method A): 98 %, RT = 4.11 min.

HRMS (ESI, m/z): theoretical mass: 257.0860 [M+H]$^+$, observed mass: 257.0857 [M+H]$^+$.

5-((1*H*-1,2,4-Triazol-1-yl)methyl)-2-(4-chlorophenyl)-4-methylthiazole (7b) (C$_{13}$H$_{11}$ClN$_4$S, M.W. 290.77)
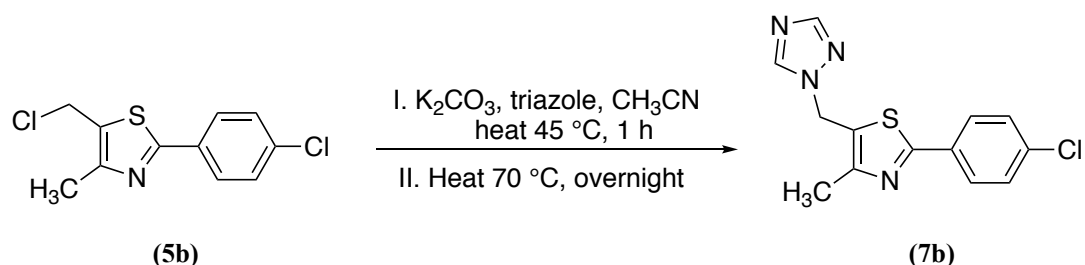
Reagents: 5-(chloromethyl)-2-(4-chlorophenyl)-4-methylthiazole (**5b**) (0.29 g, 1.29 mmol).

Yield: 0.26 g, (59 %) as a white solid.

m.p.: 162-165 °C.

R*f*: 0.52 (9.5: 0.5 v/v CH$_2$Cl$_2$-MeOH).

^{1}H NMR (DMSO-d$_6$): δ 8.69 (s, 1H, triazole), 8.01 (s, 1H, triazole), 7.88 (d, *J* = 8.8 Hz, 2H, Ar), 7.53 (d, *J* = 8.8 Hz, 2H, Ar), 5.68 (s, 2H, C*H$_2$*), 2.49 (s, 3H, CH$_3$).

^{13}C NMR (DMSO-d$_6$): δ 164.4 (C, thiazole), 152.3 (CH, triazole), 152.3 (C, thiazole), 144.4 (CH, triazole), 135.2 (C, Ar), 132.0 (CH, para-Ar), 129.7 (2 x CH, Ar), 128.2 (2 x CH, Ar), 126.9 (C, thiazole), 44.1 (CH$_2$), 15.4 (CH$_3$).

HPLC (Method A): 100 %, RT = 4.36 min.

HRMS (ESI, m/z): theoretical mass: $^{35/37}$Cl 291.0471/ 293.0471 [M+H]$^+$, observed mass: $^{35/37}$Cl 291.0468/ 293.0438 [M+H]$^+$.

5-((1*H*-1,2,4-Triazol-1-yl)methyl)-2-(4-methoxyphenyl)-4-methylthiazole (7c)

(C$_{14}$H$_{14}$N$_4$OS, M.W. 286.35)
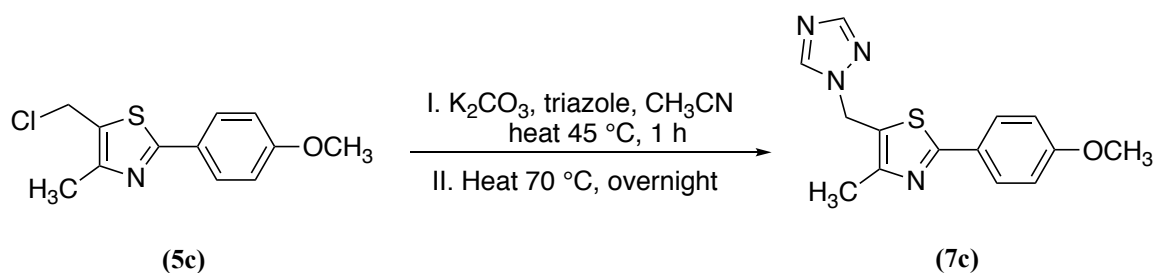
(5c)   **(7c)**

Reagents: 5-(chloromethyl)-2-(4-methoxyphenyl)-4-methylthiazole (**5c**) (0.5 g, 1.97 mmol). The pure compound was eluted with 2 % MeOH in CH$_2$Cl$_2$.

Yield: 0.15 g (26 %) as a pale yellow solid.

m.p.: 113-115 °C.

R$_f$: 0.27 (9.5: 0.5 v/v CH$_2$Cl$_2$-MeOH).

^{1}H NMR (DMSO-d$_6$): δ 8.67 (s, 1H, triazole), 8.00 (s,1H, triazole), 7.81 (d, J = 9.0 Hz, 2H, Ar), 7.02 (d, J = 8.9 Hz, 2H, Ar), 5.64 (s, 2H, C*H*$_2$), 3.81 (s, 3H, O-CH$_3$), 2.46 (s, 3H, CH$_3$).

^{13}C NMR (DMSO-d$_6$): δ 165.8 (C, thiazole), 161.3 (C, Ar), 152.3 (CH, triazole), 151.9 (C, thiazole), 144.3 (CH, triazole), 127.9 (2 x CH, Ar), 126.0 (C, Ar),125.2 (C, thiazole), 115.0 (2 x CH, Ar), 55.8 (CH$_3$, Ar para O-CH$_3$), 41.5 (CH$_2$), 15.4 (CH$_3$).

HPLC (Method A): 98 %, RT = 4.13 min.

HRMS (ESI, m/z): theoretical mass: 287.0966 [M+H]$^+$, observed mass: 287.0960 [M+H]$^+$.

5-((1*H*-1,2,4-Triazol-1-yl)methyl)-4-methyl-2-(4-nitrophenyl)thiazole (7d)

(C$_{13}$H$_{11}$N$_5$O$_2$S, M.W. 301.32)

(5d)   **(7d)**
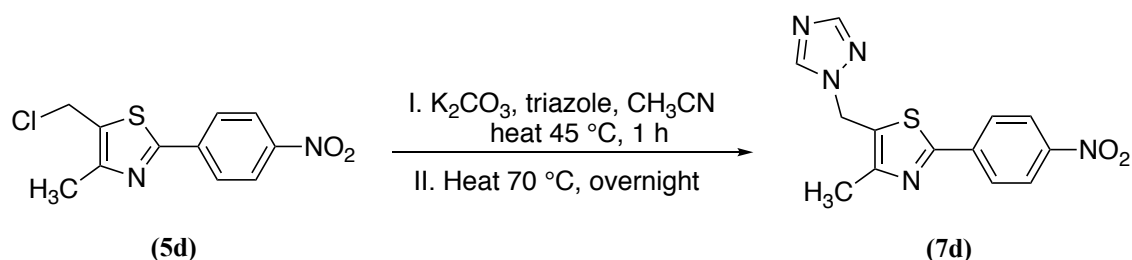
Reagents: 5-(chloromethyl)-4-methyl-2-(4-nitrophenyl) thiazole (**5d**) (0.71 g, 2.64 mmol). The pure compound was eluted with 2 % MeOH in CH$_2$Cl$_2$.

Yield: 0.3 g (37 %) as a pale yellow solid.

m.p.: 198-200 °C.

R$_f$: 0.37 (9.5: 0.5 v/v CH$_2$Cl$_2$-MeOH).

¹H NMR (DMSO-d₆): δ 8.71 (s, 1H, triazole), 8.30 (d, J = 9.1 Hz, 2H, Ar)*,* 8.14 (d, J = 9.0 Hz, 2H, Ar), 8.03 (s,1H, triazole), 5.73 (s, 2H, C*H*₂), 2.53 (s, 3H, CH₃).

¹³C NMR (DMSO-d₆): δ 163.1 (C, thiazole), 153.2 (C, thiazole),152.4 (CH, triazole), 148,4 (C, Ar), 144.5 (CH, triazole), 138.6 (C, Ar), 129.1 (C, thiazole), 127.4 (2 x CH, Ar), 124.9 (2 x CH, Ar), 44.1 (CH₂), 15.4 (CH₃).

HPLC (Method A): 99 %, RT = 4.37 min.

HRMS (ESI, m/z): theoretical mass: 302.0711 [M+H]⁺, observed mass: 302.0714 [M+H]⁺.

4-(5-((1*H*-1,2,4-Triazol-1-yl)methyl)-4-methylthiazol-2-yl)aniline (8)

(C₁₃H₁₃N₅S, M.W. 271.34)

(7d)   **(8)**
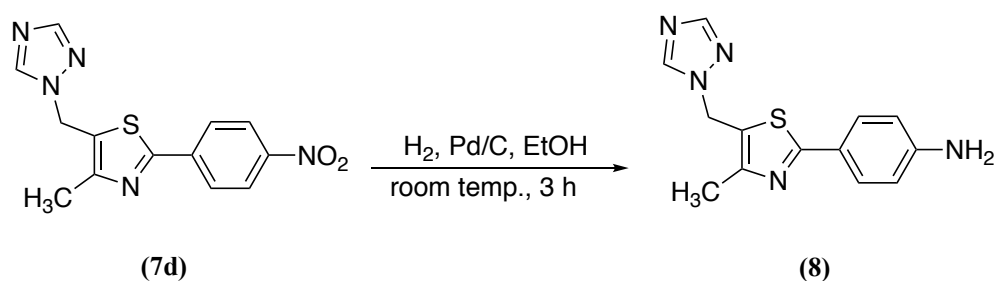
Method: To a solution of 5-((1*H*-1,2,4-triazol-1-yl)methyl)-4-methyl-2-(4-nitrophenyl) thiazole (**7d**) (0.3 g, 0.99 mmol) in dry MeOH (15 mL) was added 10 % Pd/C (30 mg). Then, the reaction was degassed and the atmosphere filled with H₂ using H₂ balloons, and the mixture was stirred at room temperature for 3 h.[96] The suspension was filtered through a pad of celite and the filtrate was evaporated under reduced pressure to give the desired product, which was used in the next step without any further purification.

Yield: 0.26 g (100 %) as a yellow solid.

m.p.: 175-178 °C.

R*f*: 0.37 (9.5: 0.5 v/v CH₂Cl₂-MeOH).

¹H NMR (DMSO-d₆): δ 8.64 (s, 1H, triazole), 7.99 (s, 1H, triazole), 7.53 (d, J = 8.7 Hz, 2H, Ar)*,* 6.57 (d, J = 8.7Hz, 2H, Ar), 5.66 (s, 2H, NH₂), 5.59 (s, 2H, C*H*₂), 2.41 (s, 3H, CH₃).

¹³C NMR (DMSO-d₆): δ 166.62 (C, thiazole), 152.20 (CH, triazole), 151.56 (C, thiazole), 144.22 (CH, triazole), 127.74 (2 x CH, Ar), 123.10 (C, Ar), 120.97 (C, Ar), 114.01 (2 x CH, Ar), 44.30 (CH₂), 15.41 (CH₃).

N-(4-(5-((1H-1,2,4-Triazol-1-yl)methyl)-4-methylthiazol-2yl)phenyl)benzenesulfonamide (10a)

(C₁₉H₁₇N₅O₂S₂, M.W. 411.50)
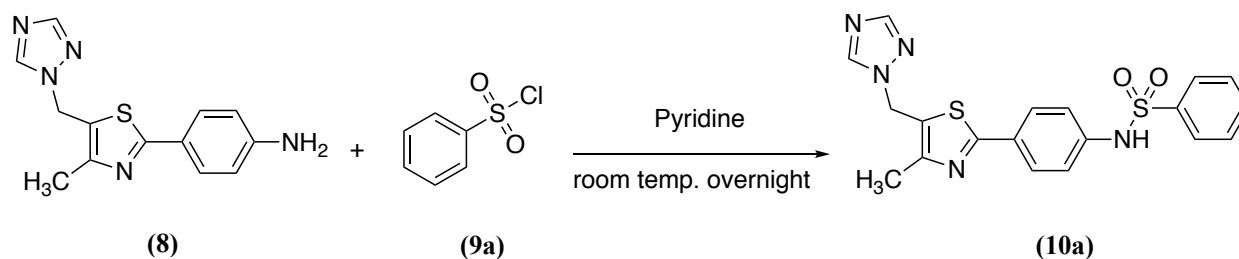
Method: To a cooled (ice bath) solution of 4-(5-((1H-1,2,4-triazol-1-yl)methyl)-4-methylthiazol-2-yl) aniline (**8**) (0.26 g, 0.95 mmol) in dry pyridine (5 mL) was added benzene sulfonyl chloride (**9a**) (0.14 mL, 1.14 mmol) in portions.[59, 97] Then, the mixture was left at room temperature overnight. The solvent was evaporated, and the resulting oil was extracted with CH_2Cl_2 (50 mL), washed with 1M aq. HCl (25 mL), H_2O (2 x 25 mL), and dried ($MgSO_4$). The organic layer was evaporated under reduced pressure to give a crude yellow-orange oil. The desired product was purified by gradient column chromatography to give a pale yellow solid which eluted at 3 % MeOH in CH_2Cl_2.

Yield: 0.23 g (58 %) as a pale yellow solid.

m.p.: 175-178 °C.

R$_f$: 0.32 (9.5: 0.5 v/v CH_2Cl_2-MeOH).

¹H NMR (DMSO-d₆): δ 10.46 (s, 1H, NH), 8.65 (s, 1H, triazole), 7.99 (s, 1H, triazole), 7.80 (d, J = 7.1 Hz, 2H, Ar), 7.73 (d, J = 8.9 Hz, 2H, Ar), 7.63-7.60 (m, 1H, Ar), 7.57-7.54 (m, 2H, Ar), 7.18 (d, J = 8.9 Hz, 2H, Ar), 5.63 (s, C$\underline{H}_2$), 2.44 (s, C$\underline{H}_3$).

¹³C NMR (DMSO-d₆): δ 165.2 (C, thiazole), 152.1 (C, thiazole), 152.1 (CH, triazole), 144.3 (CH, triazole), 140.0 (C, Ar), 139.7 (C, Ar), 133.5 (CH, Ar), 129.8 (2 x CH, Ar), 128 (C, Ar), 127.4 (2 x CH, Ar), 127.0 (2 x CH, Ar), 125.9 (C, thiazole), 120.0 (2 x CH, Ar), 44.1 (CH₂), 15.4 (CH₃).

HPLC (Method A): 97 %, RT = 3.73 min.

HRMS (ESI, m/z): theoretical mass: 412.0902 [M+H]⁺, observed mass: 412.0902 [M+H]⁺.

Using this procedure, the following compounds were prepared:

N-(4-(5-((1H-1,2,4-Triazol-1-yl)methyl)-4-methylthiazol-2-yl)phenyl)-4-chlorobenzenesulfonamide (10b)

(C$_{19}$H$_{16}$ClN$_5$O$_2$S$_2$, M. W. 445.94)

(8)   **(9b)**   **(10b)**
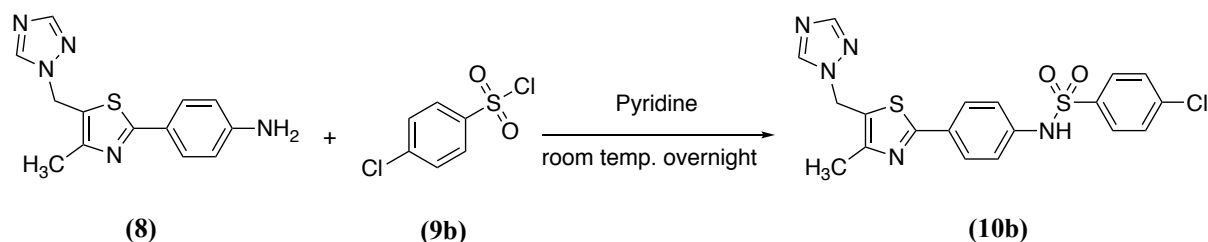
Reagents: 4-chlorobenzene sulfonyl chloride (**9b**) (0.14 g, 0.66 mmol). The pure compound was eluted with 2.5 % MeOH in CH$_2$Cl$_2$.

Yield: 0.14 g (58 %) as a white solid.

m.p.: 172-174 °C.

R$_f$: 0.3 (9.5: 0.5 v/v CH$_2$Cl$_2$-MeOH).

^{1}H NMR (DMSO-d$_6$): δ 10.70 (s, 1H, NH), 8.65 (s, 1H, triazole), 7.99 (s, 1H, triazole), 7.79-7.74 (m, 4H, Ar), 7.64 (d, J = 8.9 Hz, 2H, Ar), 7.18 (d, J = 8.9 Hz, 2H, Ar), 5.64 (s, C$\underline{H}_2$), 2.44 (s, C$\underline{H}_3$).

^{13}C NMR (DMSO-d$_6$): δ 165.1 (C, thiazole), 152.1 (C, thiazole), 152.1 (CH, triazole), 144.3 (CH, triazole), 139.6 (C, Ar), 138.5 (C, Ar), 138.4 (C, Ar), 130.0 (2 x CH, Ar), 129.1 (C, Ar), 129.0 (2 x CH, Ar), 127.5 (2 x CH, Ar), 126.0 (C, thiazole), 120.4 (2 x CH, Ar), 44.1 (CH$_2$), 15.4 (CH$_3$).

HPLC (Method A): 99 %, RT = 4.20 min.

HRMS (ESI, m/z): theoretical mass: $^{35/37}$Cl 446.0512/448.0512 [M+H]$^+$, observed mass: $^{35/37}$Cl 446.0510/448.0486 [M+H]$^+$.

N-(4-(5-((1H-1,2,4-triazol-1-yl)methyl)-4-methylthiazol-2-yl)phenyl)-4-methoxybenzenesulfonamide (10c)

(C$_{20}$H$_{19}$N$_5$O$_3$S$_2$, M.W. 441.52)

(8)   **(9c)**   **(10c)**
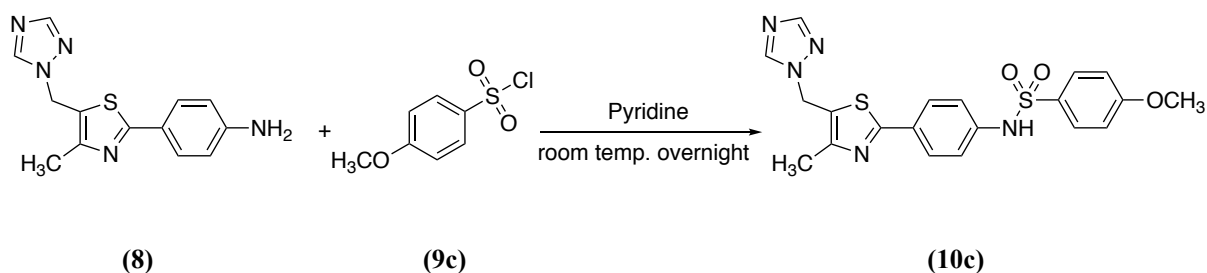
Reagents: 4-methoxybenzene sulfonyl chloride (**9c**) (0.20 g, 1.00 mmol). The pure compound was eluted with 3.5 % MeOH in CH_2Cl_2.

Yield: 0.22 g (59 %) as a white solid.

m.p.: 86-88°C.

R$_f$: 0.27 (9.5: 0.5 v/v CH_2Cl_2-MeOH).

^{1}H NMR (DMSO-d$_6$): δ 10.49 (s, 1H, NH), 8.65 (s, 1H, triazole), 7.99 (s, 1H, triazole), 7.72 (d, J = 9 Hz, 4H, Ar), 7.17 (d, J = 8.9 Hz, 2H, Ar), 7.06 (d, J = 9 Hz, 2H, Ar), 5.63 (s, C$\underline{H}_2$), 3.78 (s, O-C$\underline{H}_3$), 2.44 (s, C$\underline{H}_3$).

^{13}C NMR (DMSO-d$_6$): δ 165.3 (C, thiazole), 163.0 (C, Ar), 152.1 (C, thiazole), 152.1 (CH, triazole), 140.3 (C, Ar), 134.2 (CH, triazole), 131.3 (C, Ar), 129.3 (2 x CH, Ar), 128.5 (C, Ar), 127.4 (2 x CH, Ar), 125.8 (C, thiazole), 119.8 (2 x CH, Ar), 114.9 (2 x CH, Ar), 56.0 (CH$_3$, O-CH$_3$), 44.1 (CH$_2$), 15.4 (CH$_3$).

HPLC (Method A): 99 %, RT = 3.78 min.

HRMS (ESI, m/z): theoretical mass: 442.1007 [M+H]$^+$, observed mass: 442.1009 [M+H]$^+$

c. Biological evaluation:

All methods were performed at the Center for Cytochrome P450 Biodiversity, Swansea University Medical School by Dr. Josie Parker and Dr. Andrew Warrilow.

1. CaCYP51 susceptibility testing:

Antifungal MIC testing was performed according to the CLSI microdilution method for yeasts.[105] *C. albicans* strains CAI4 and SC5314 were tested in triplicate. Cultures were diluted to 2.5 x 10^3 cells/mL in RPMI 1640 (Sigma), buffered with 0.165 M MOPS, pH 7.0. Antifungal compounds were dissolved in DMSO and added at a final concentration of 1% v/v DMSO. Plates were incubated at 37 °C and read at 48 h.

2. Binding affinity (K_d):

The ligand-CaCYP51 complex was determined by non-linear regression (Levenberg-Marquardt algorithm) using a rearrangement of the Morrison equation for tight ligand binding.[52,106] While weak ligand binding was calculated by the Michaelis-Menten equation. Curve fitting for novel azole saturation curves was performed using the computer program ProFit 6.1.12 (QuantumSoft, Zurich, Switzerland) for Mac OSX. K_d values were determined for each of the three replicate titrations per azole compound and then mean K_d values and standard deviations calculated.[52,106]

Chapter III

(Thiazole sulfonamide derivatives)

1. Introduction:

The CaCYP51 active site has a "Y-shape" structure, which includes the haem iron binding site for the substrate, and a long hydrophobic channel that allows the entrance of the substrate.[77] Modifications of phenyl thiazole series were needed in order to optimise the activity, flexibility, selectivity profiles of the new prepared compounds and improve the occupancy of both short arms at the haem active site as well as the long access channel. Thus, Table 11 showed four derivatives (A-D) of modified phenyl thiazole series, which were designed and investigated using computational programs Molecular Operating Environment (MOE) and Molecular Dynamic (MD) simulation to determine and explore binding interactions within the CaCYP51 active as well as direct binding with the haem Fe^{3+}.

Table 11: The four proposed derivatives (A-D).
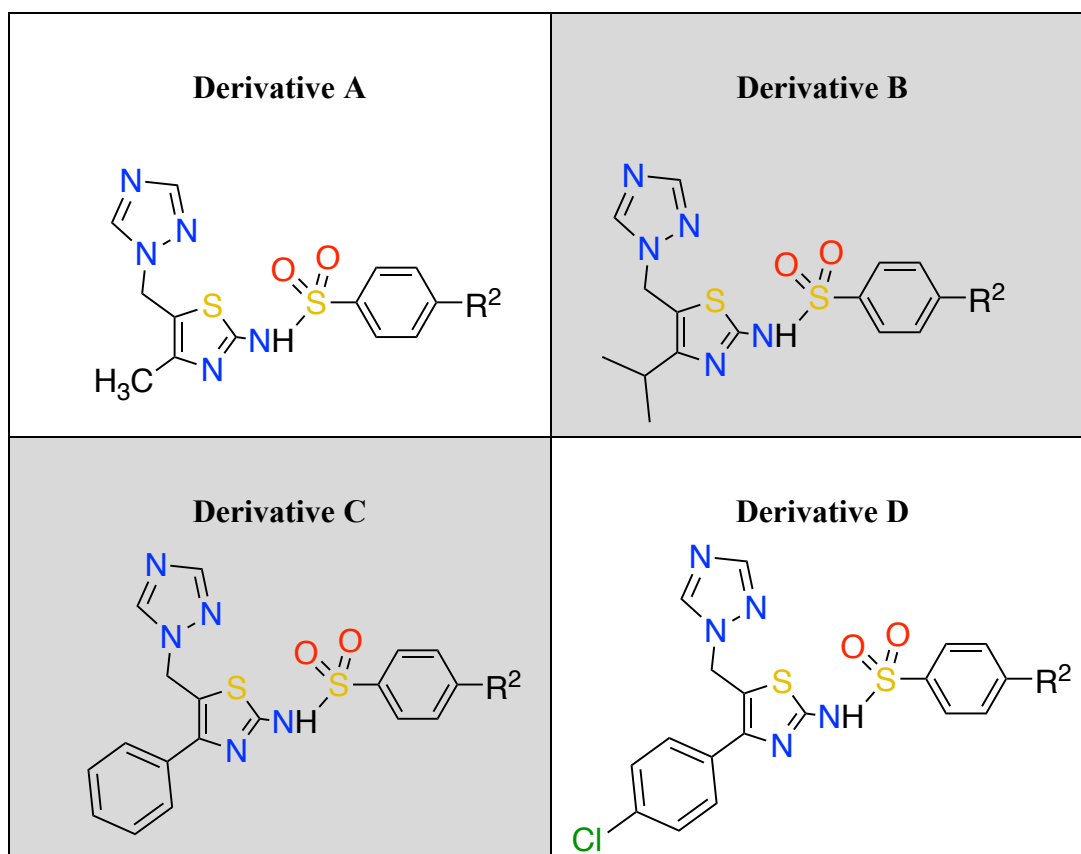
The modifications on phenyl thiazole series included (Figure 28):

1. R^1 will be alkyl/phenyl substitution at position 4 in the thiazole ring to explore effects on binding affinity and activity against fungal strains.
2. Sulfonamide linker at position 2 in the thiazole ring to provide more flexibility.

3. Different *para*-substitutions on the phenyl ring to explore the structure-activity relationships (SAR). The R^2 group could be an electron donating or electron withdrawing group.

4. Triazole was kept in position 5 of the thiazole ring to obtain selectivity for CaCYP51.
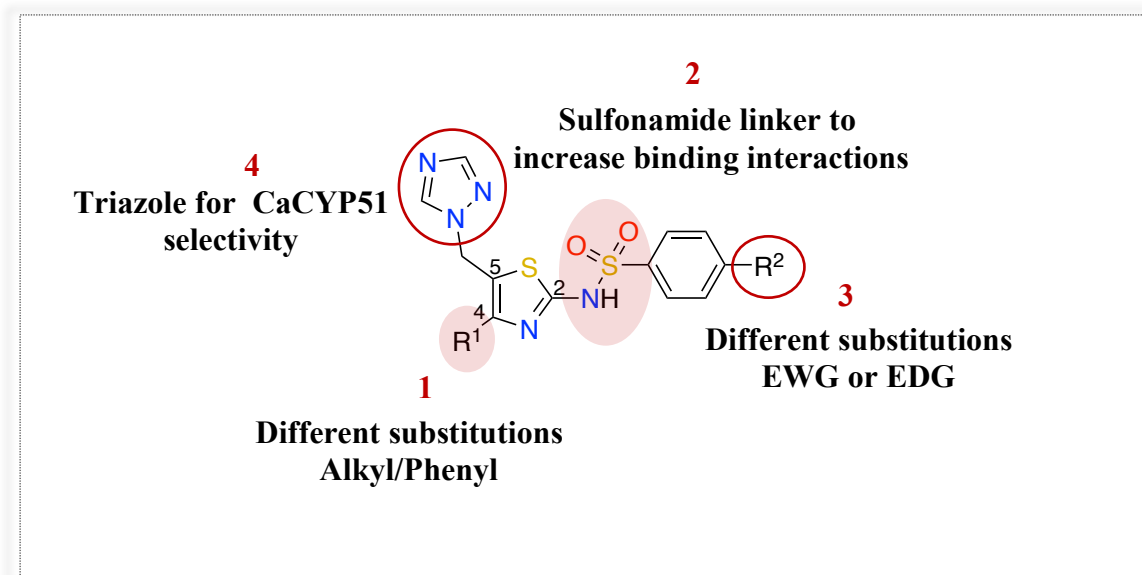
Figure 28: General structure of thiazole sulfonamide series.

2. Results and discussion

a. Computational studies:

1. Molecular modelling:

1.1 Wild type docking:

The molecular docking result for all derivatives (A-D) in wild-type CaCYP51 showed high similarity with posaconazole with respect to the position, and the most common amino acid residues involved in the binding interactions with the new inhibitors were Met508, Pro375, Leu376, His377, Ser507 and Ser378. The H-bonding interactions occur either through water molecules and/or directly between the novel inhibitors and the amino acids.

Derivative B (Figure 29A) is used as an exemplar to illustrate water mediated interactions between the sulfonyl oxygen and Met508, Pro375, Leu376, His377 and Ser507 as well as Met508 formed direct H-bonding with the substituted phenyl ring and the sulfonamide N. Moreover, the distance between the N atom of the triazole ring and the haem iron was approximately 2.74 Å as shown in the 3D visualisation (Figure 29B).
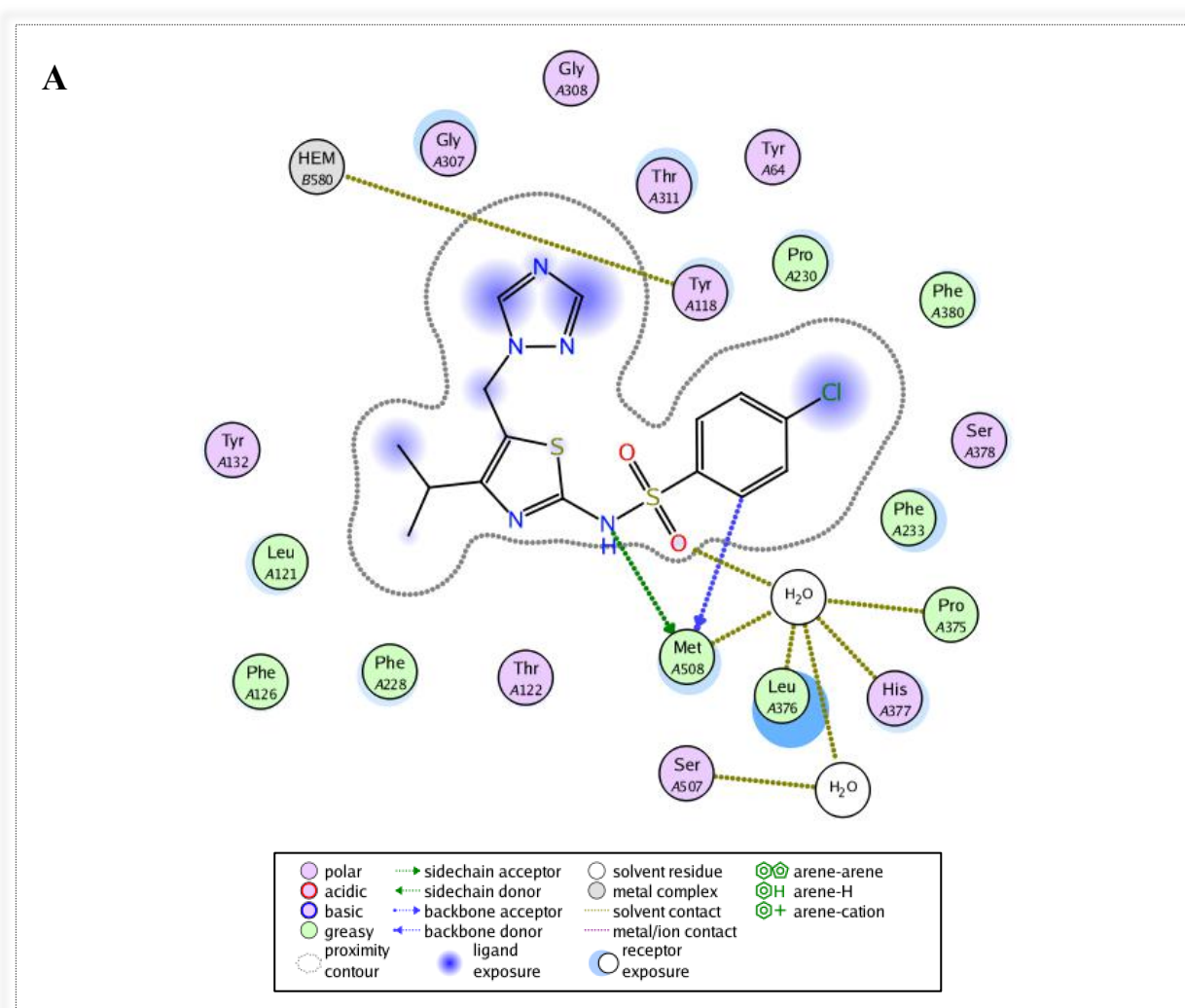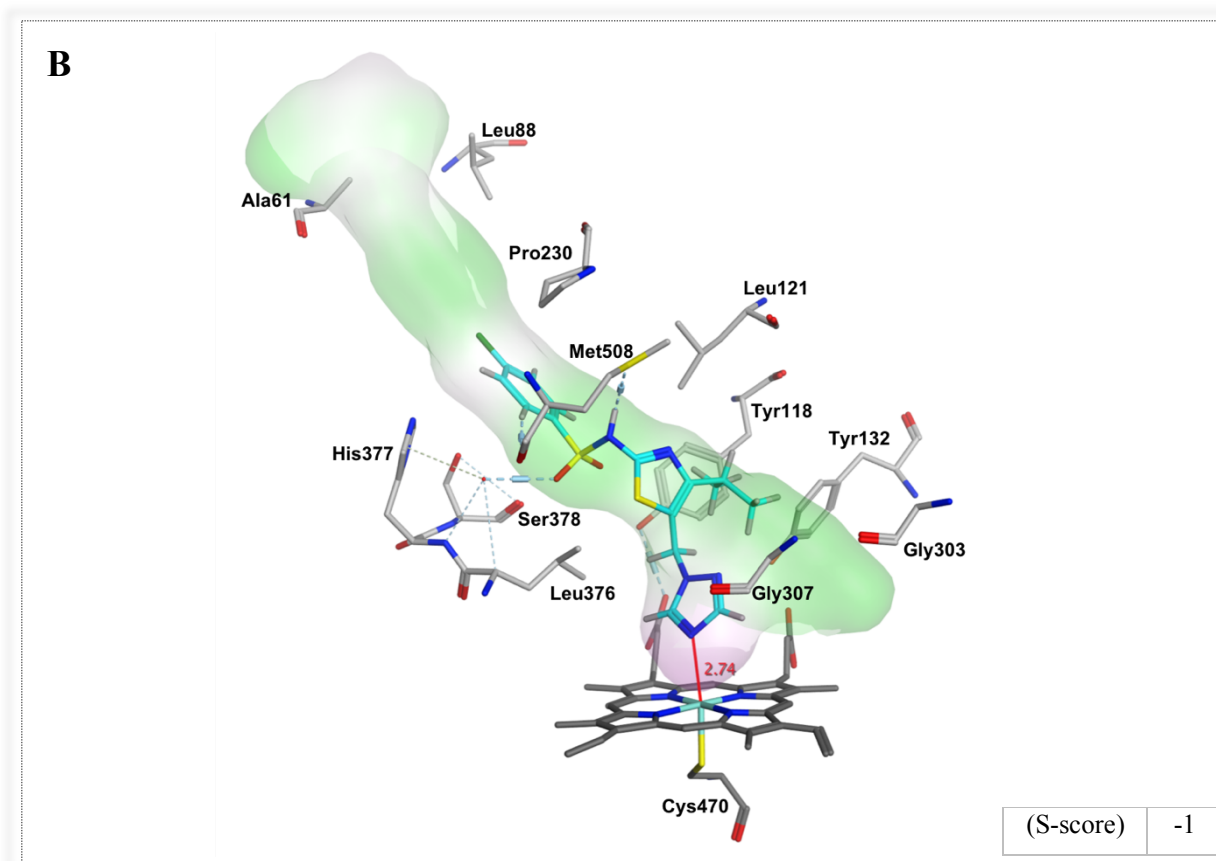
Figure 29: Example of derivative B binding interactions with CaCYP51: (**A**) 2D ligplot illustrating binding interactions with amino acids in the protein. (**B**) 3D image illustrating key H-bonding interactions with Met508, Leu376, and His377 as well as the distance between the N atom of the triazole ring and the haem iron, which was approximately 2.74 Å.

1.2 Mutated CaCYP51 docking:

In this chapter, the molecular docking studies of derivative C and D with phenyl/Cl-phenyl substitution in the fourth position on the thiazole ring appeared to be more promising for optimal fill of the binding cavity in the double mutant CaCYP51(Y132H/K143R). Both derivatives showed high similarity with fluconazole with respect to the position in the enzyme active site. In addition, the most common amino acid residues involved in the binding interactions with the inhibitors were Met508, Leu376 and His377. The H-bonding interactions with Met508, Pro375, Leu376 and His377 occur through water molecules while the direct H-bond interaction occurs between the phenyl ring and the NH of the sulfonamide with Met 508 as shown in the 2D and 3D visualisations of derivative D (Figure 30).
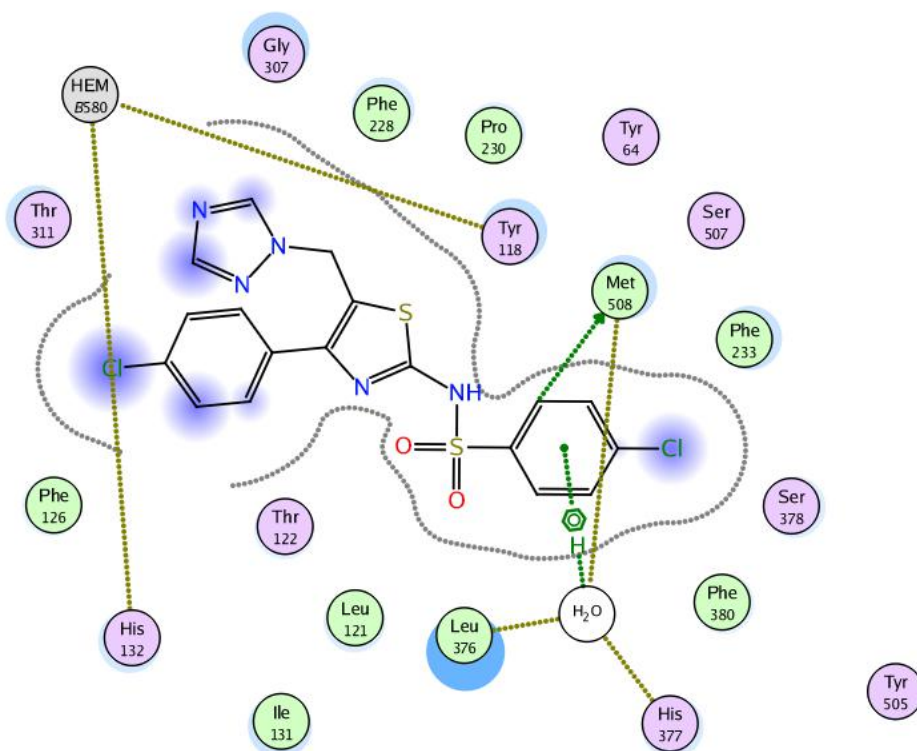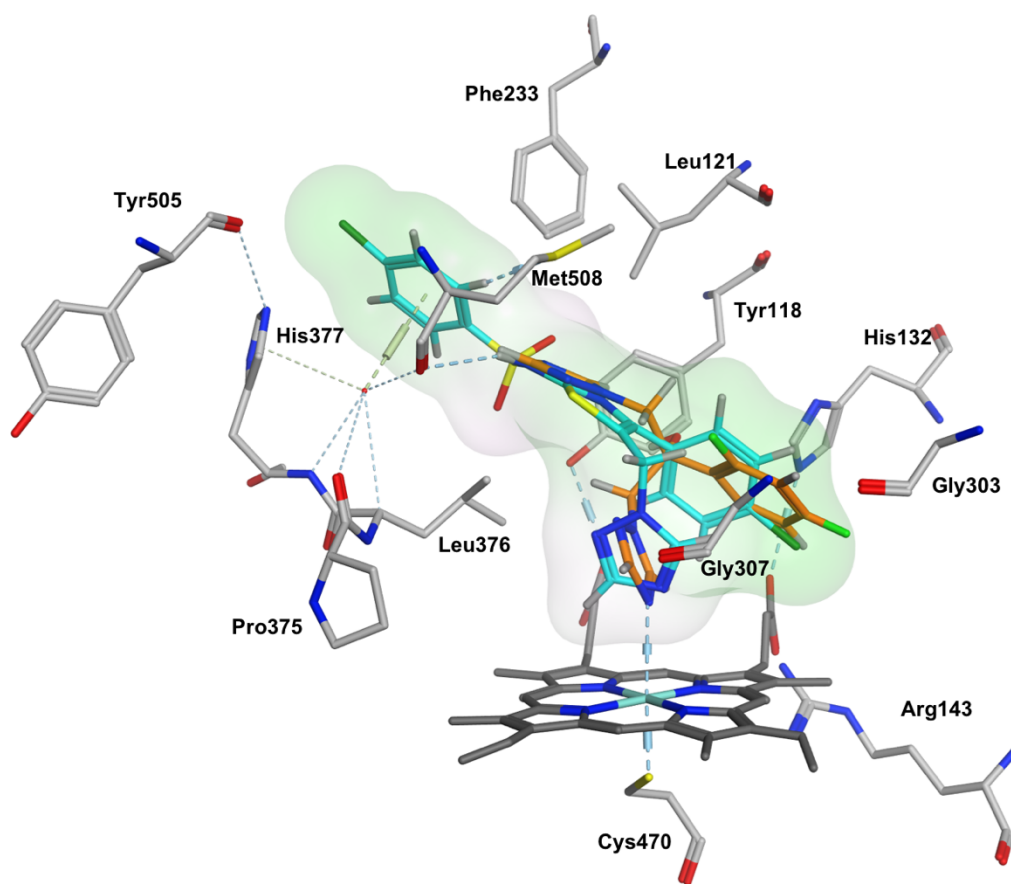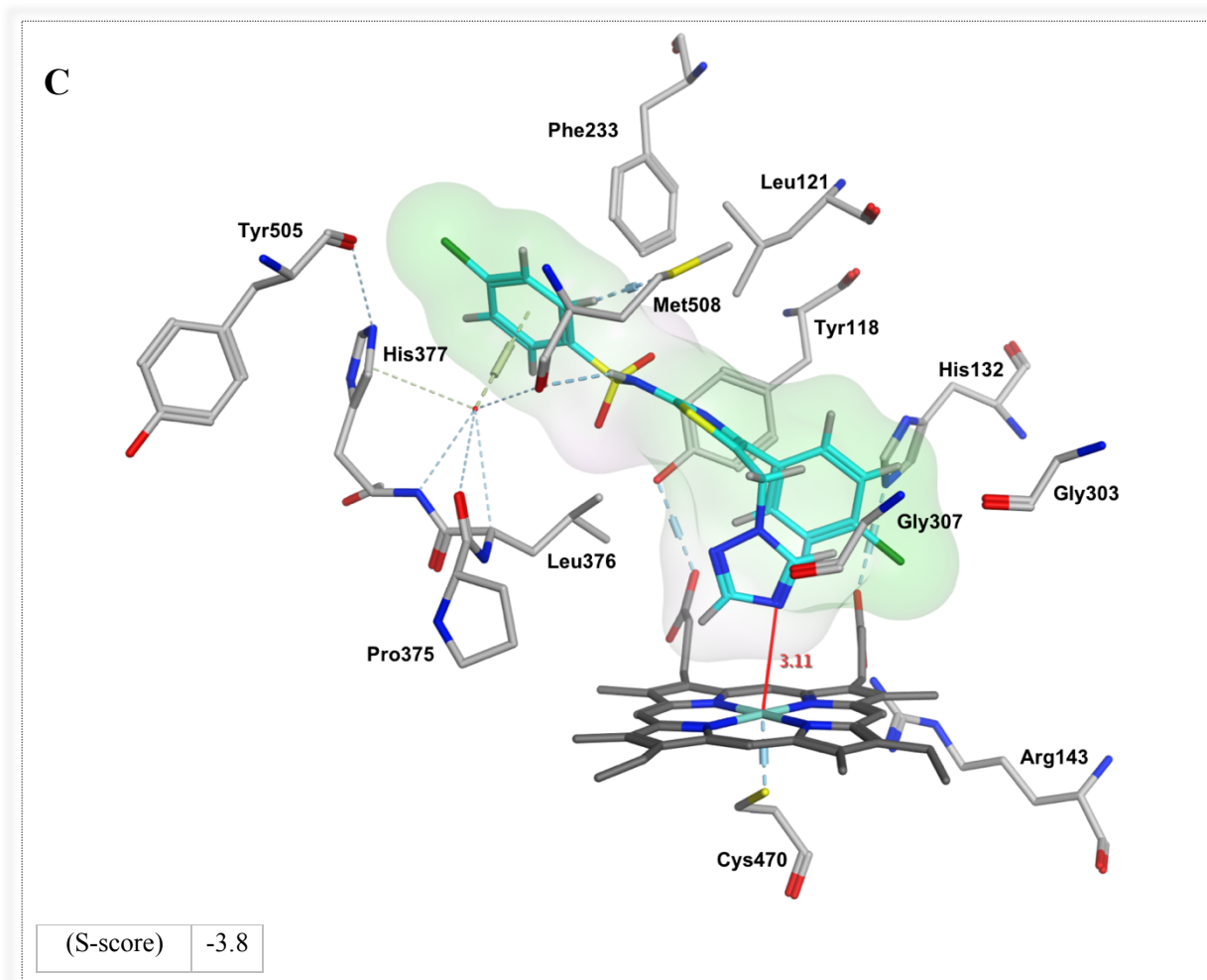
Figure 30: Example of derivative D binding interactions with CaCYP51 double mutant (Y132H/K143R): (**A**) 2D ligplot illustrating of derivative D binding interactions with amino acids in the CaCYP51 protein. (**B**) Overlap of derivative D (cyan) and fluconazole (orange) to view filling of binding cavities as well as fitting. (**C**) 3D image illustrating key H-bonding interactions with Met508, Pro375, Leu376 and His377 and the distance between the N of the triazole and the haem iron approximately 3.11 Å.

2. Molecular dynamic (MD) simulations:

Molecular dynamics (MD) is a computer simulation tool used in this project for studying the stability of protein-ligand complexes as well as analysing the physical movements of both CaCYP51 and the novel inhibitor atoms through computational method. The dynamic system will allow the inhibitor and CaCYP51 to interact for a specific period of time in nanoseconds (ns).[101] For all derivatives (A-D), the favourable pose of the inhibitor with the CaCYP51 crystal structure obtained from MOE, was subjected to a 200 ns molecular dynamic simulation using the Desmond programme of Maestro.[102,106]

The binding profile of all derivatives (A-D) in the wild-type were similar in forming a coordination interaction between the haem Fe^{3+} and the triazole N. Moreover, all derivatives showed direct or water mediated binding interactions with Met508, His 377, Ser 378 and Leu376 as well as hydrophobic interactions with different residue as shown in the 2D ligand interaction of derivative D is shown as an exemplar. However, derivative B molecular dynamic simulations also formed a direct H-bonding with His377 and Ser378 through the sulfonyl oxygen and H-bonding between NH of the sulfonamide and Met508 as shown in the 2D ligand interaction (Figure 31).
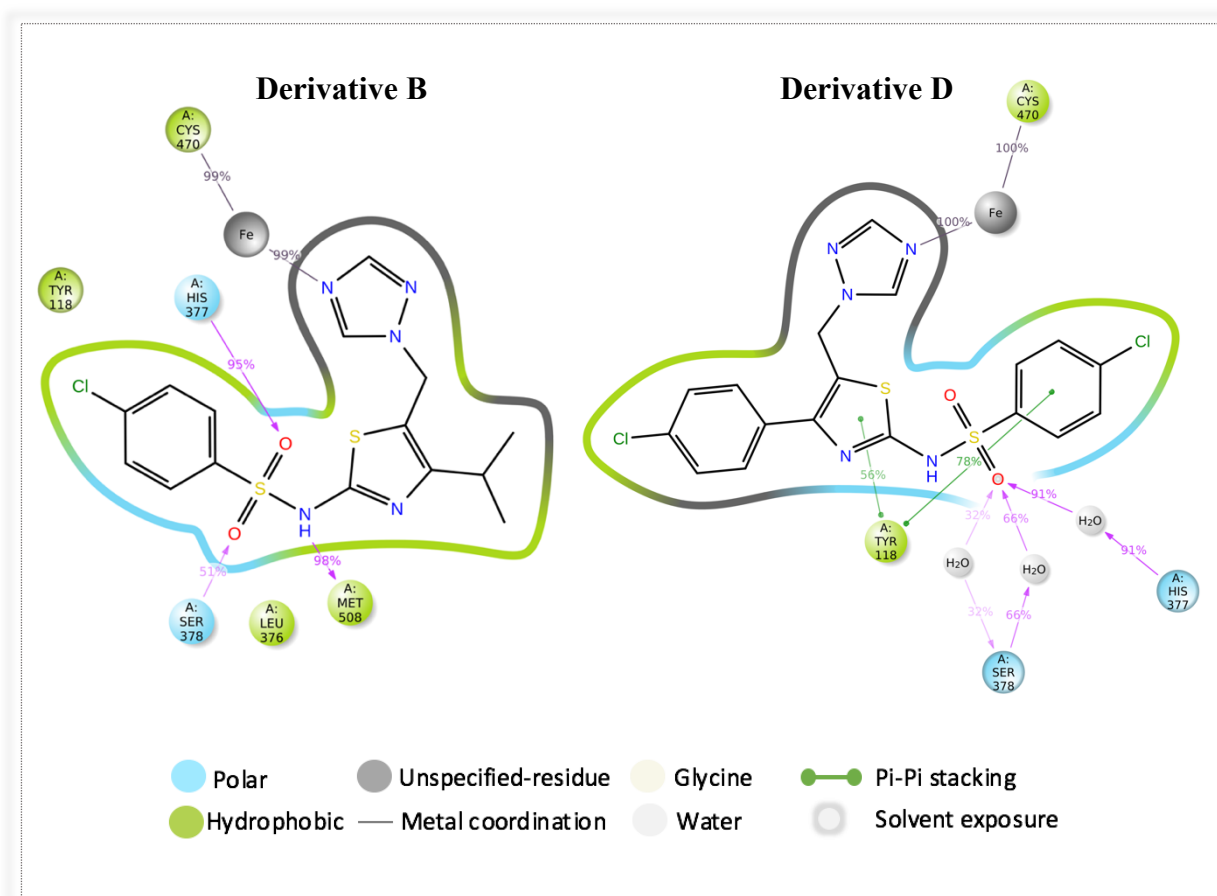
Figure 31: 2D detailed ligand interaction of derivative B and D with amino acids of CaCYP51 active site that occur more than 30% of the simulation time in the selected trajectory (0 through 200 ns).

The root mean square deviation (RMSD) is a quantitative measurement (in angstrom) used to address protein-ligand complex stability over a fixed time.[107] There are two main concept of the RMSD:

1. The change in the RMSD of the protein between the starting time and the final time must be within the acceptable range (1-3 Å).

2. If the ligand RMSD value observed is significantly larger than the RMSD of the protein that means the ligand has diffused away from its initial binding site or protein pocket.

As shown in Table 12, derivative B RMSD started at 0.9 Å at 0 ns and rapidly equilibrated with CaCYP51 with a final RMSD of 1.39 Å at 200 ns. Similarly, derivative D-complex showed rapid equilibration of CaCYP51 with the ligand and a RMSD for CaCYP51-derivative D complex at 200 ns of 2.75 and 2.49 Å, respectively (Figure 32).
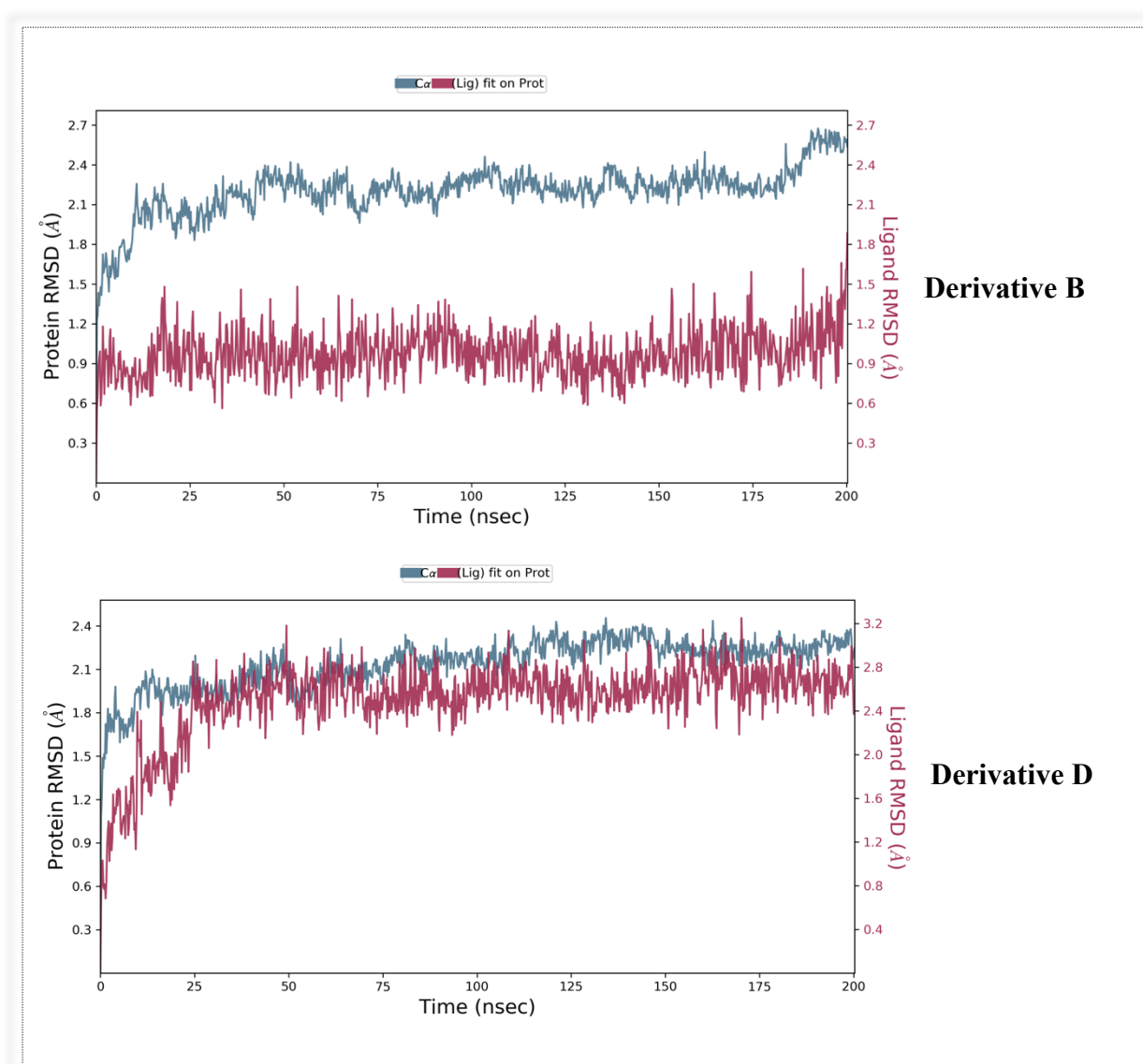
Figure 32: RMSD plot with respect to time over the 200 ns simulation of CaCYP51-derivative B/D complex.

Table 12: Protein-ligand complex RMSD (Å) at 0 and 200 ns for derivative B and D.

Ligand -complex	RMSD (Å) at 0 ns		RMSD (Å) at 200 ns	
	CaCYP51	Ligand	CaCYP51	Ligand
Derivative B	1.32	0.9	2.61	1.39
Derivative D	1.57	0.88	2.75	2.49

While in the CaCYP51 double mutants (Y132H/K143L), the binding profiles for all derivatives (A-D) formed a coordination interaction between the haem Fe^{3+} and the triazole N. Moreover, derivative D, used as an exemplar for the molecular dynamic (MD) simulation showed only direct H-bonding with Met508, His377 and Ser378 in high percentage (>85%) during the 200 ns simulation. The RMSD for the ligand-protein complex showed high stability between CaCYP51 and derivative D during the 200 ns MD simulation. The ligand RMSD started from 2.68 Å at 0 ns and rapidly reached the equilibrium plateau with a final RMSD of 2.49 Å at 200 ns. The protein (CaCYP51)-ligand (derivative D) plot illustrated the high stability of the complex (Figure 33)
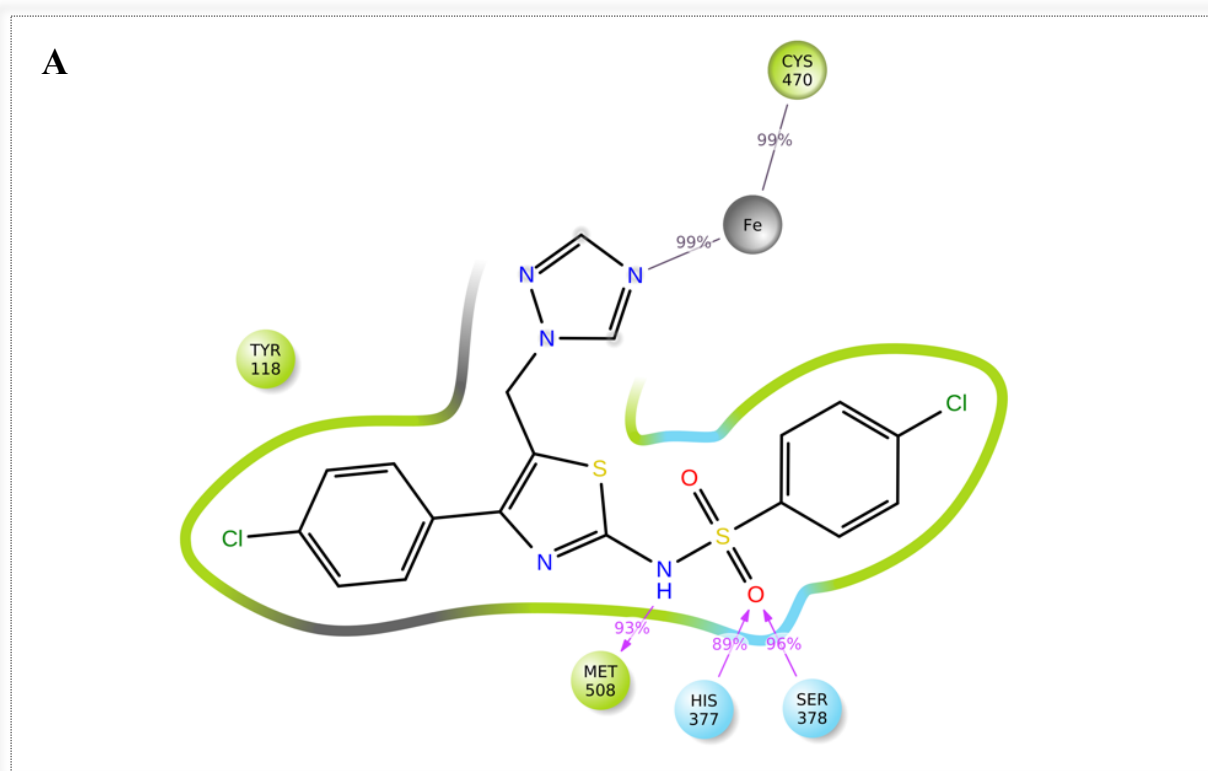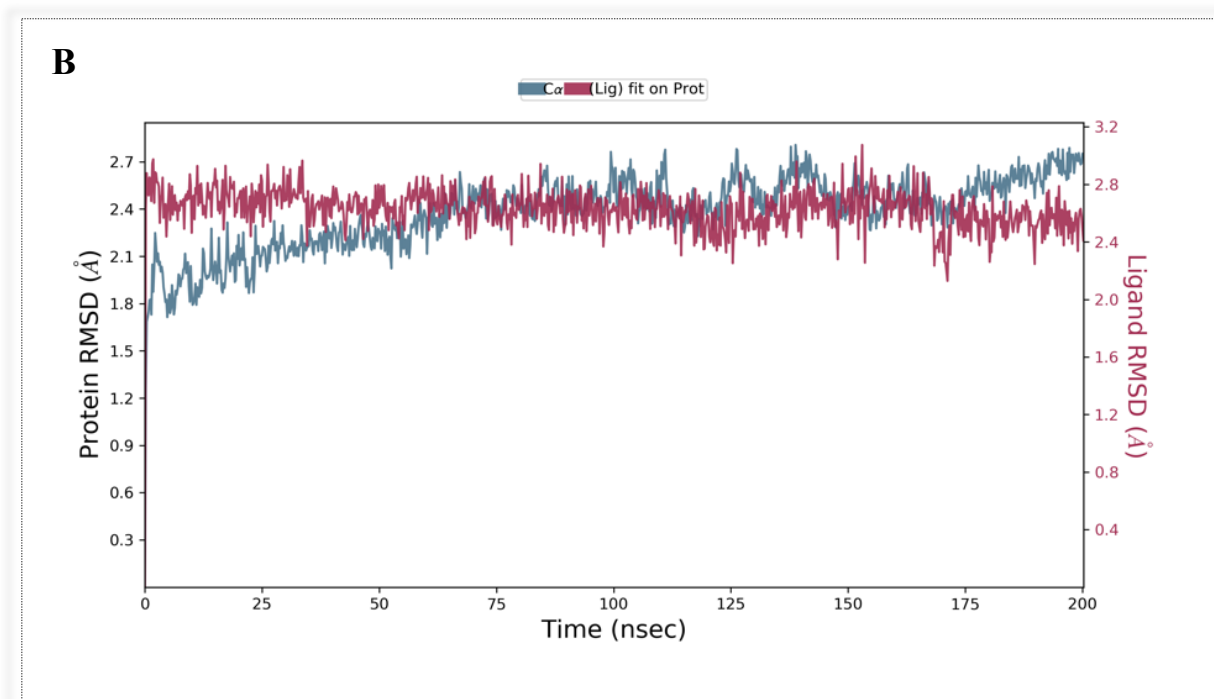
Figure 33: A) 2D ligand interactions of molecular dynamic (MD) simulation of CaCYP51(Y132H/K143L)-derivative D complex illustrating the binding interactions that occur more than 30% of the simulation time in the selected trajectory (0 through 200 ns). **B)** Protein-ligand RMSD of CaCYP51(Y132H/K143L)-derivative D complex over 200 ns MD simulation.

b. Chemistry:

To synthesise the novel thiazole sulfonamide compounds (derivative A-D), six reaction steps were used (Scheme 3):

1. Koser's reaction with different ethyl acetoacetate derivatives.

2. Hantzsch thiazole synthesis with thiourea.

3. Sulfonamide linker formation.

4. Reduction reaction with LiAlH$_4$.

5. Chlorination reaction using thionyl chloride or Appel (iodination) reaction using triphenylphosphine (TPP) and imidazole.

6. Nucleophilic substitution of triazole.

Scheme (3): *Reagents and conditions:*
(i) HTIB, CH₃CN 75 °C, o/n
(ii) EtOH, reflux at 80 °C, 4 h
(iii) Pyridine, 80 °C, aryl sulfonyl chloride 3-48 h, r.t., o/n
(iv) THF, LiAlH₄, r.t., o/n
(v) CH₂Cl₂, TPP, imidazole, iodine 0 °C, r.t., o/n
(vi) (a) CH₃CN, K₂CO₃, triazole, 45 °C, 1 h, b. 70 °C, overnight.
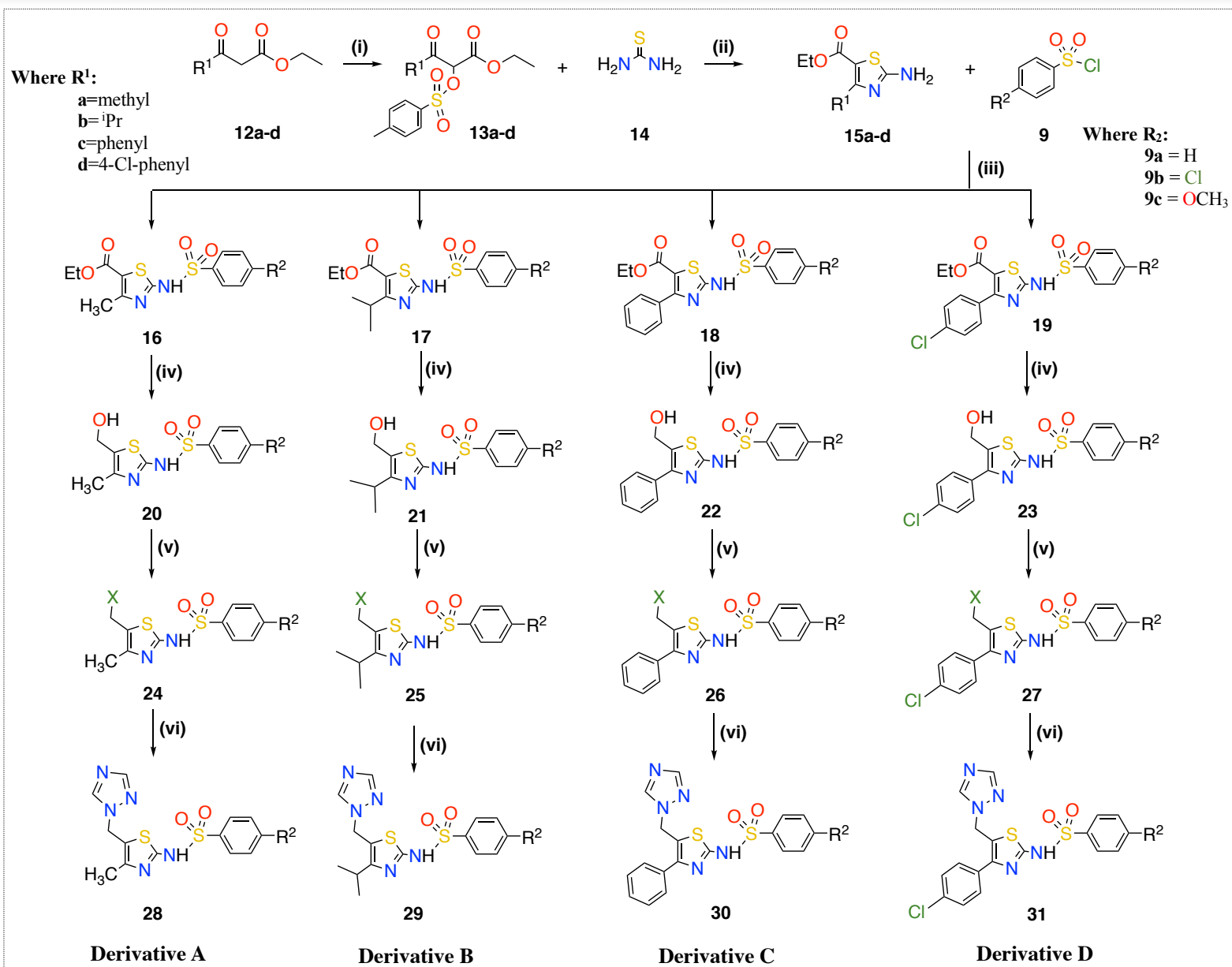
1. First Method:

Synthesis of ethyl 3-oxo-2 (tosyloxy)butanoate (13a):
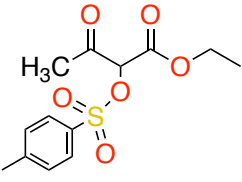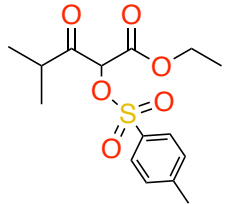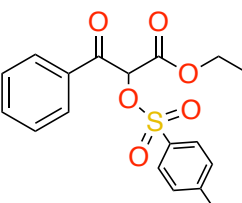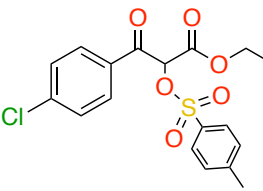
Hydroxy(tosyloxy)iodobenzene (HTIB, Koser's reagent) is a widely used reagent to generate a good leaving group, commonly HTIB is used for the α-tosylation of ketones.[90] The synthesis of ethyl 3-oxo-2-(tosyloxy)butanoate (**13**) was obtained by adding HTIB (**11**) to ethyl acetoacetate (**12**) in portions in dry CH_3CN, and the colourless solution was heated overnight at 75 °C.[87]

The reaction mechanism involves electrophilic addition of HTIB, which has an electrophilic iodine, to the enol tautomer of ethyl acetoacetate. Then, the intermediate α-phenyliodide ketone is attacked by the tosylate via S_N2 mechanism to give the desired product as shown in Figure 34. Purification by column chromatography afforded the desired product. This method was also applied to the synthesis of ethyl 4-methyl-3-oxo-2-(tosyloxy) pentanoate (**13b**), ethyl 3-oxo-3-phenyl-2-(tosyloxy) propanoate (**13c**) and ethyl 3-oxo-3-(4-chlorophenyl)-2-(tosyloxy) propanoate (**13d**) (Table 13).
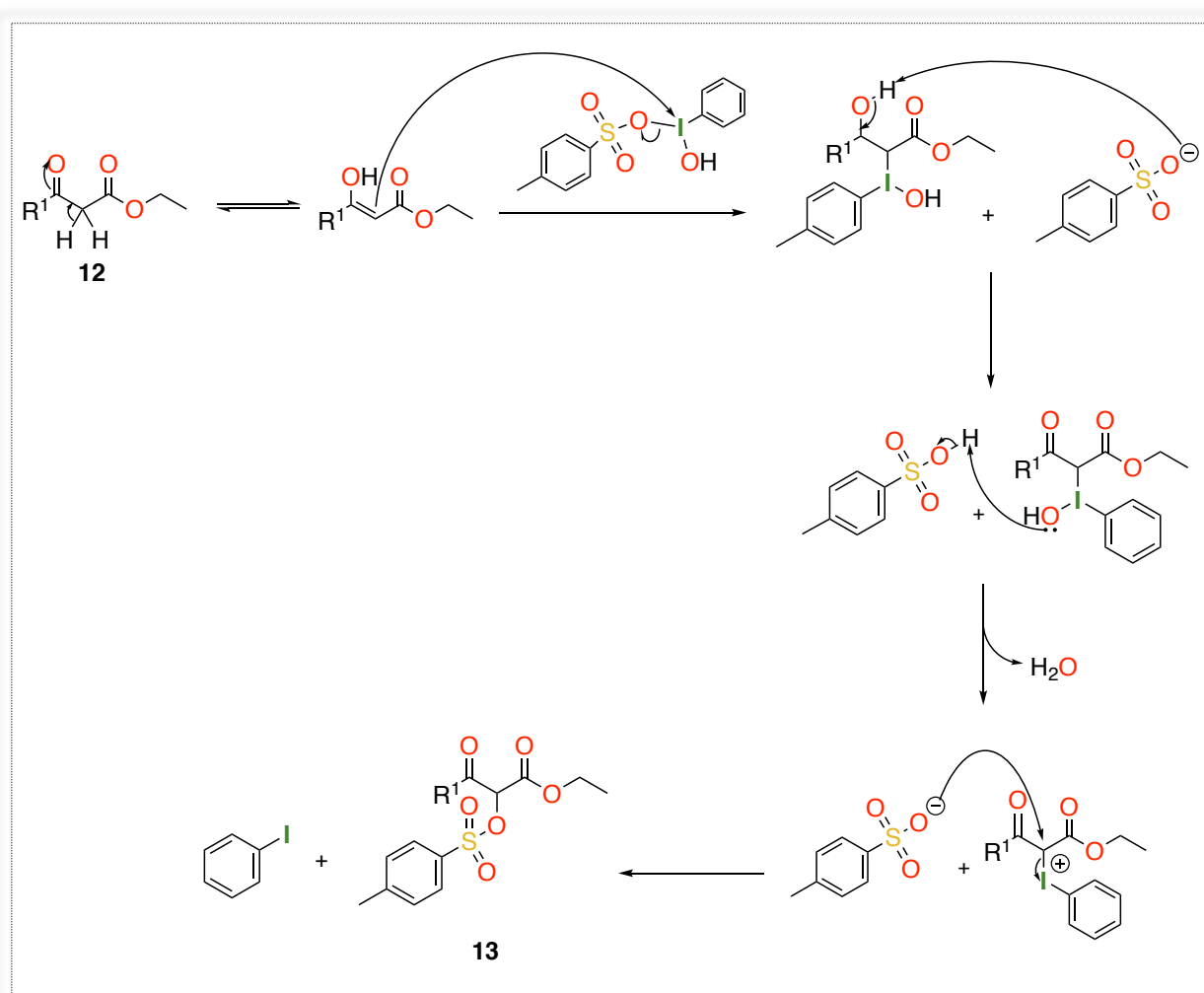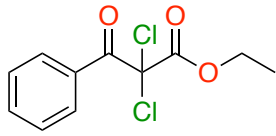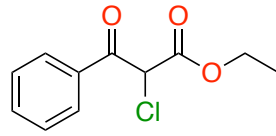
Figure 34: Reaction mechanism of tosylation using HTIB.

Table 13: Yields of the prepared tosyloxy compounds (**13**).

Compound	Structure	Yield (%)
13a		52
13b		83
13c		88
13d		34

Another method was used to convert compound **12** into a chloro derivative, providing a good leaving group in order to form the thiazole ring. As described in the literature for the synthesis of ethyl 2-chloro-3-oxo-3-phenylpropanoate (**13c**, R^1 = phenyl), a chlorination reaction was performed using sulfuryl chloride, which was added dropwise at 0°C to ethyl benzoyl acetate (**12d**) in dry CHCl₃ solution. The resulting mixture was allowed to reach room temperature and stirred for 30 min.[108] After that, the mixture was refluxed at 63 °C and monitored for 48 h, however the reaction did not go to completion. The work up was done after 48 h and column chromatography was applied to purify the desired compound. The ¹H NMR data showed that the dichlorinated product (Yield = 67%) was obtained as well as the required mono-chlorinated product (Yield = 19%). The dichlorinated product can be distinguished from the mono-chlorinated product, which has a singlet peak at δ 5.75 ppm for CHCl (Table 14). Unfortunately, ¹³C NMR was not applied for both derivatives.

Table 14: The major and minor product of the reaction.

Product	Structure	Yield (%)	^{1}H NMR Data
Di-chlorinated Major		67	**^{1}H NMR (DMSO-d$_6$):** δ 7.93 (d, J = 7.3 Hz, 2H, Ar), 7.78-7.76 (m, 1H, Ar), 7.63-7.61 (m, 2H, Ar), 4.33 (q, J = 7.1 Hz, C$\underline{H_2}$CH$_3$), 1.09 (t, J = 7.0 Hz, 3H, CH$_2$C$\underline{H_3}$).
Mono-chlorinated Minor		19	**^{1}H NMR (DMSO-d$_6$):** δ 7.93 (d, J = 7.3 Hz, 2H, Ar), 7.78-7.76 (m, 1H, Ar), 7.63-7.61 (m, 2H, Ar), 5.75 (s, C$\underline{H}$), 4.33 (q, J = 7.1 Hz, C$\underline{H_2}$CH$_3$), 1.09 (t, J = 7.0 Hz, 3H, CH$_2$C$\underline{H_3}$).
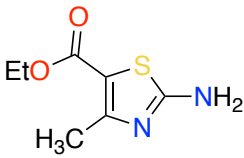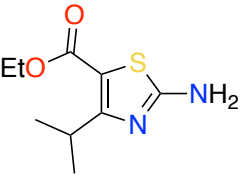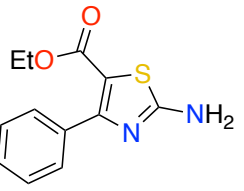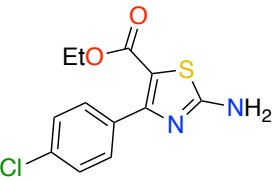
Synthesis of ethyl 2-amino-4-(alkyl/aryl)thiazole-5-carboxylate (15):

Ethyl 2-amino-4-(alkyl/aryl)thiazole-5-carboxylate (**15**) was obtained by Hantzsch thiazole synthesis with thiourea, where thiourea was added into the solution of ethyl 2-(chloro/tosylate)acetoacetate in dry EtOH and refluxed at 80°C for 4 h.[95]

The reaction mechanism of the thiazole formation involves two major steps as previously described (Figure 22). First, the nucleophilic attack of sulfur atom at the α-tosyloxyketone to form the C-S bond. Then, formation of a five membered ring, which is achieved by the removal of a water molecule. In this reaction tosylate takes the same role as Cl (ethyl 2-chloroacetoacetate (**1**)).

The reaction was worked up by quenching with water, then the resulting mixture was neutralised with NH$_4$OH (28 %) to pH 9 to provide a white precipitate. The free amine compounds were obtained in very good yields and used in the next step without further purification (Table 15).
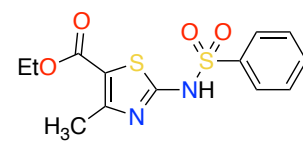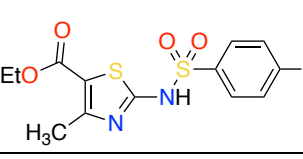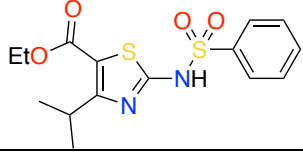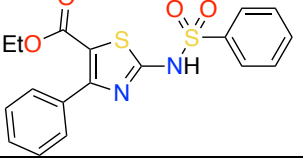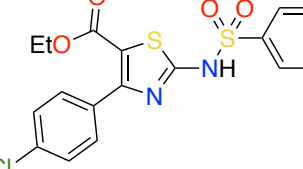
Table 15: Yields and melting points of the prepared thiazole amines (**15**).

Compound	Structure	Yield (%)	M.P. (°C) (Lit. m.p.)
15a		87	180- 182 (174-176)[67]
15b		94	180- 182 (179- 181)[109]
15c		74	168- 171 (170- 172)[109]
15d		60	194- 196 (198- 200)[110]

Synthesis of ethyl 4-(alkyl/aryl)-2-(phenylsulfonamido)thiazole-5-carboxylate (16-19):

The sulfonamide linker was obtained by adding ethyl 2-amino-4-(alkyl/aryl)thiazole-5-carboxylate (**15**) and benzensulfonyl chloride derivatives (**9**) in dry pyridine with heating at 80 °C for 3 h for alkyl derivatives, then the mixture was left at room temperature overnight,[111] and for the aryl derivatives after 48 h at room temperature. All derivatives except compound **19a** were achieved in good yields (Table 16).

Table 16: Yields and melting points of the prepared sulfonamide and amide linkers.

Compound	Structure	Yield (%)	M.P. (°C) (Lit. M.P.)
16a		86	190 -192 (157-158°C)[68]
16b		96	185-187 (Li. m.p. not found)
17a		92	Oil
18a		61	Semisolid
19a		8	226-229 (Li. m.p. not found)

The reaction of compound **19a**, which is part of derivative D synthesis, did not reach completion even after several optimisations with the equivalents of reagents used, time and heat. This could be owing to the electron withdrawing effect (Cl) on the phenyl ring at position 4 of thiazole which played a role in lowering the availability of the lone pair of electrons on the amino N of compound **15d**, resulted in reducing the nucleophilicity of the NH_2. Moreover, Compound **19a** was achieved in a very low yield (8%) because of the difficulty in the purification as well as incomplete reaction. Unfortunately, the synthesis of derivative D not continued after this stage (Figure 35).
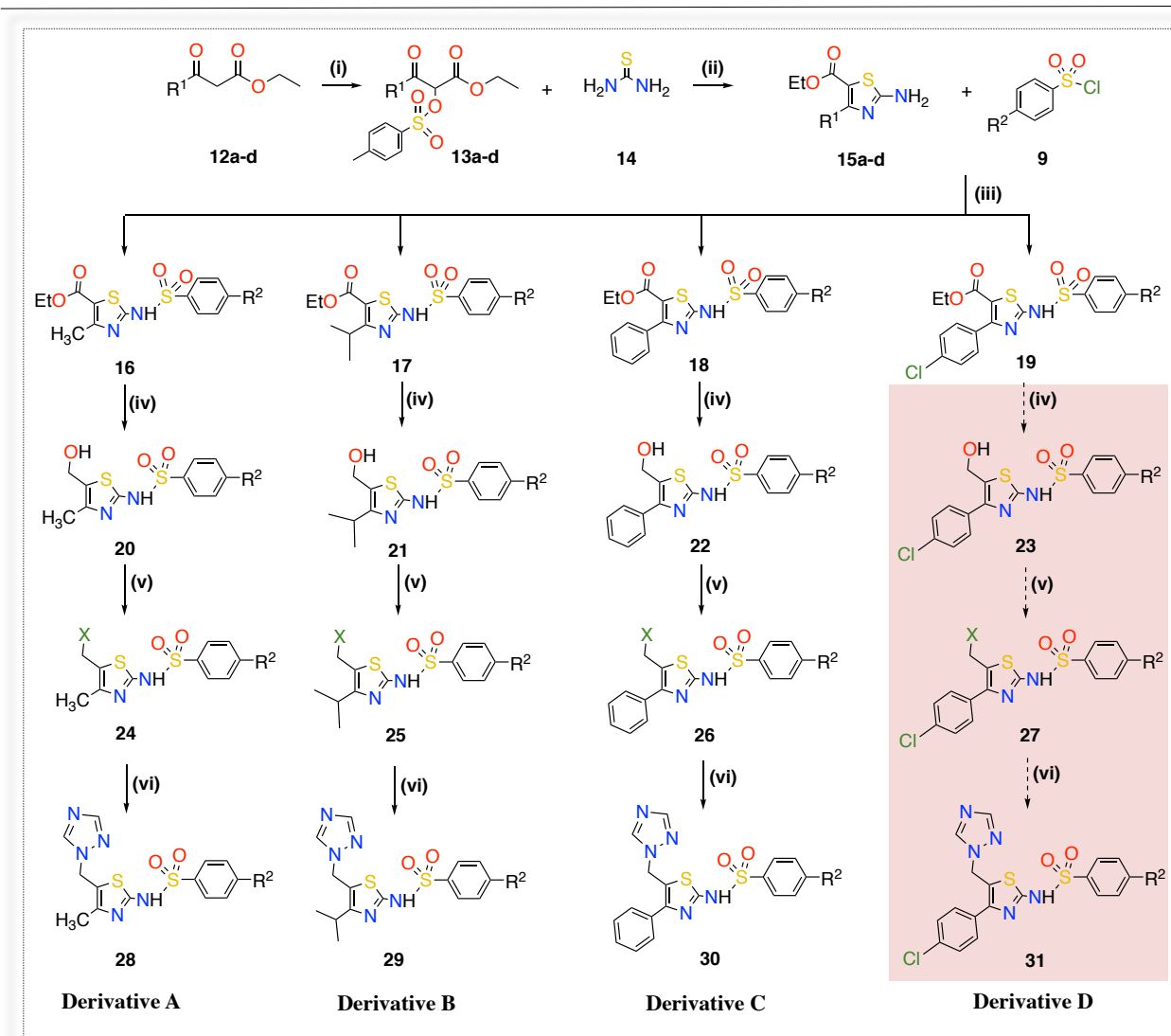
Figure 35: The cut off for derivative D synthesis.
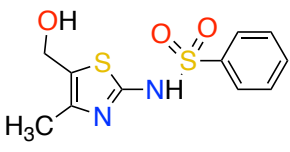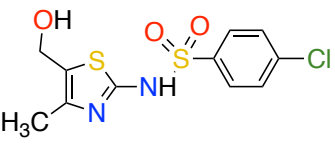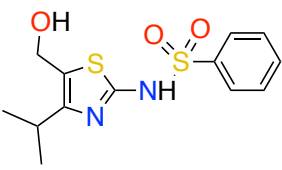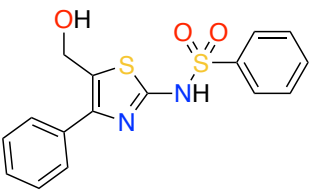
Synthesis of *N*-(5-(hydroxymethyl)-4-(alkyl/aryl) thiazol-2-yl)benzenesulfonamide (20-22):

To synthesise *N*-(5-(hydroxymethyl)-4-(alkyl/aryl)thiazol-2-yl)benzenesulfonamides (**20-22**) several optimisation methods of the reduction reaction were done. First, NaBH$_4$ (3 and 6 equivalents) was used in THF with reflux at 69 °C for 7 h as usual and left overnight, but the reaction did not reach completion. Second, LiAlH$_4$ (1.5 equivalent) was used with caution in THF and the reaction was left at room temperature overnight.[87] The resulting mixture was quenched carefully with H$_2$O in an ice-bath until cession of effervescence, the solid residue was filtered, and the desired product was extracted with ethyl acetate from the filtrate solution several times. Unfortunately, the crude yield for derivative A and B was very low ranging from 23-27%, as the desired product extracted into both the water and organic layer after work up. In contrast, derivative C was only found in the organic layer owing to having a higher cLogP

than derivative A and B, additionally the yield after purification with column chromatography was acceptable (54%) (Table 17).

Table 17: Yields and cLogP of the reduction reaction.

Compound	Structure	Yield (%)	Comment	cLog P[*]
20a		27	Due to the low lipophilicity of the compound, the product remained in the aqueous layer	0.79
20b		37	This compound was extracted about 10 times from the aqueous layer, but the yield was low and contained impurities.	1.35
21a		23	Due to the low lipophilicity of the compound, recovery from the aqueous layer was difficult resulting in a poor recovery.	1.67
22a		54	The compound was only found in the organic layer.	2.86

[*]cLogP done by Crippen's fragmentation.[103]

Synthesis of *N*-(5-(chloro/iodomethyl)-4-alkyl/arylthiazol-2-yl) benzenesulfonamide (24-26):

For the final step of the reactions scheme, the OH group must be converted into a good leaving group that can be displaced with triazole. Several methods were applied: first, a chlorination reaction using either thionyl chloride or oxalyl chloride, which involved the addition of thionyl chloride or oxalyl chloride to the alcoholic derivatives (A-C) in CH₂Cl₂ under heat for 4 h and then at room temprature overnight.[93] However, there was no reaction and when DMF was added a complex mixture was obtained. After isolation of the crude products, it was found that the amide linker in all derivative (A-C) had broken to give the free amine and an aldehyde byproduct.

A suggested reaction mechanism involves a nucleophilic attack of (O⁻) of the DMF on the carbonyl carbon of the oxalyl chloride which resulted in formation of the Vilsmeier-Haack reagent. Then, a nucleophilic attack by the alcoholic O at the alkyl halide bond resulted in displacement of the chloride ion. The chloride ion may then attack the C-O carbon resulting in formation of intermediate I and the chlorinated product with the free amine. Ultimately, another nucleophilic attack by the lone pair of the free amine on the methylidene will give the formamide byproduct and dimethylamine (Figure 36).
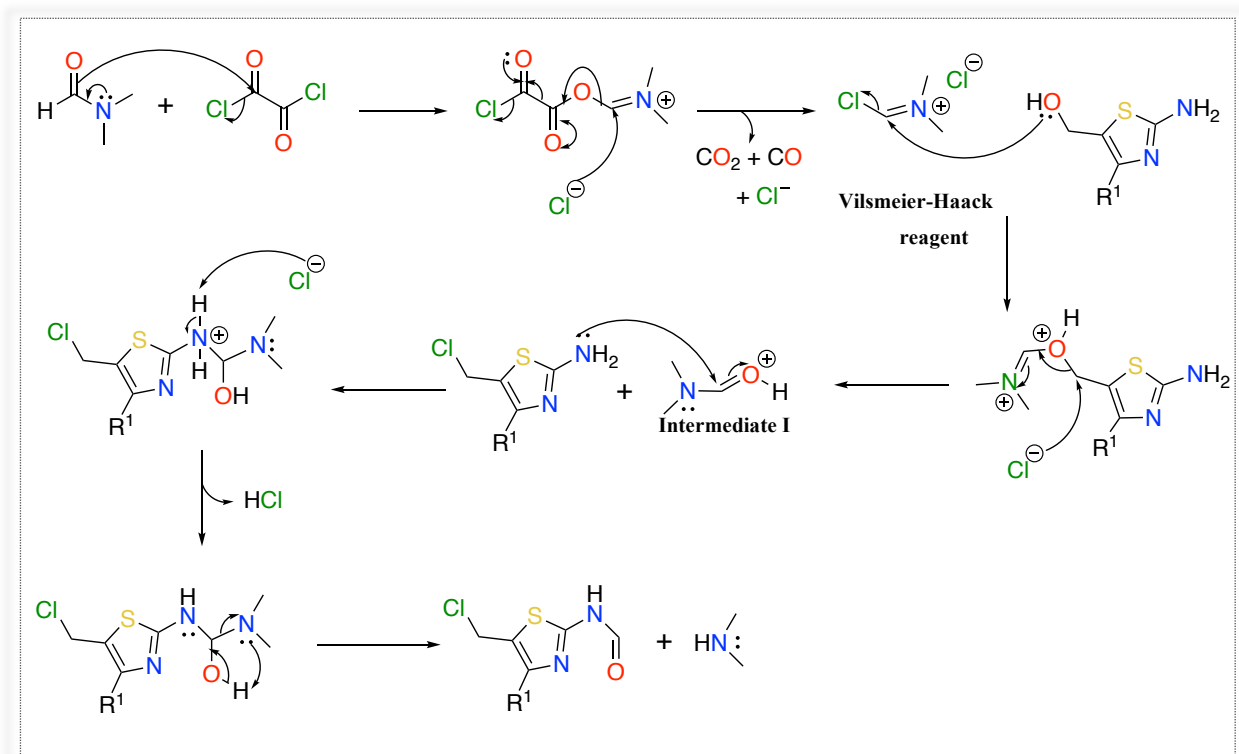
Figure 36: Proposed mechanism for chlorination reaction byproduct.

The next method applied was to convert the alcohol into either a mesylate or tosylate leaving group. The mesylation or tosylation reaction was performed by adding either mesyl or tosyl chloride reagent to the alcoholic compound in dry CH_2Cl_2, which was stirred at room temperature overnight. Unfortunately, a complex mixture was obtained, and the desired product could not be identified.

The last trial was an iodination reaction, which was applied by adding iodine to a solution of TPP and imidazole in dry CH_2Cl_2 at 0°C. Then, the reaction was warmed to room temperature for 10 min, after that the solution was cooled to 0°C and the alcohol derivative added.[112,113] The reaction was stirred at room temperature overnight, however the reaction did not obtain completion even after the addition of 1 more equivalent of iodine. The crude iodine intermediate was used in the next step without further purification.

This reaction of converting an alcohol into an alkyl halide is known as the Appel reaction.[114] The reaction mechanism involves a nucleophilic attack of the lone pair of the oxygen of a hydroxy group on the iodotriphenylphosphonium iodide to displace the iodide. Then, another nucleophilic attack by the iodide on the C-O bond to give the iodination product and triphenylphosphine oxide byproduct. The imidazole played a role as a scavenger for the iodide (Figure 37).
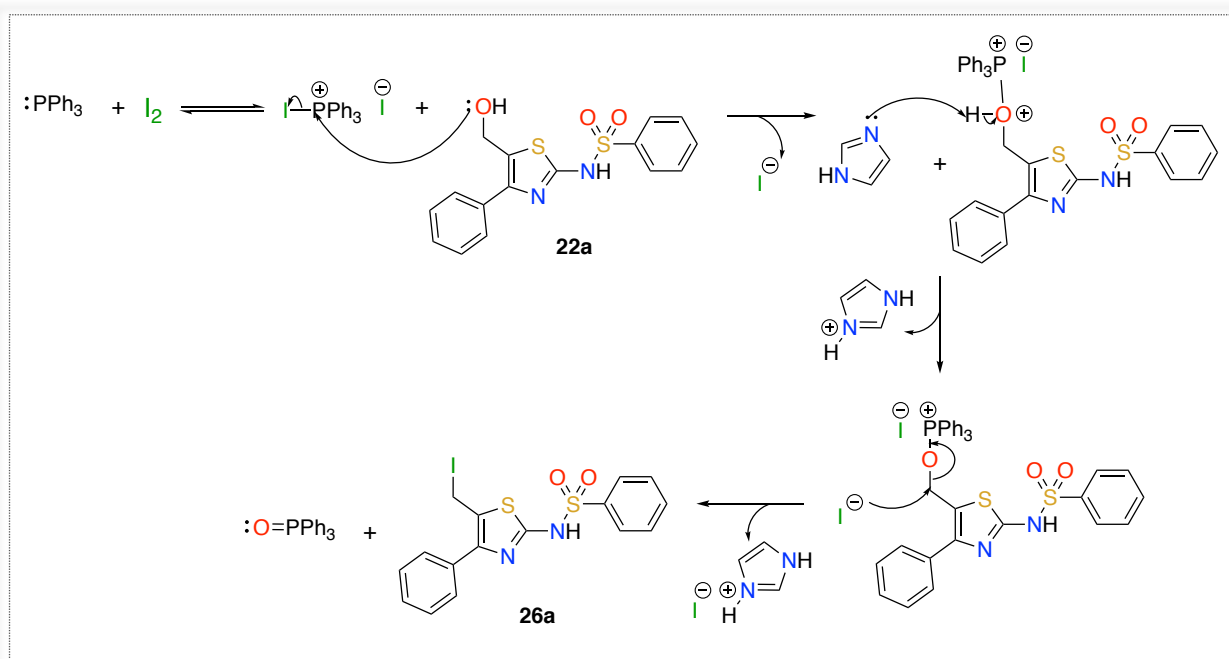
Figure 37: The mechanism of the Appel iodination reaction.

The iodination reaction only succeeded with derivative C and only one compound was obtained for derivative C (compound **26a**) due to more optimisation needed at this step and

difficulties with the reaction conditions. While for both derivative A (compound **24**) and B (compound **25**) a complex mixture was obtained, and the desired product could not be identified. The complex mixture might be a result of using the alcohol derivatives (A =compound **20** and B= compound **21**) without further purification owing to the difficulty in the purification of the alcohols.

At this stage as shown in Figure 38, derivative A and B were not progressed further.
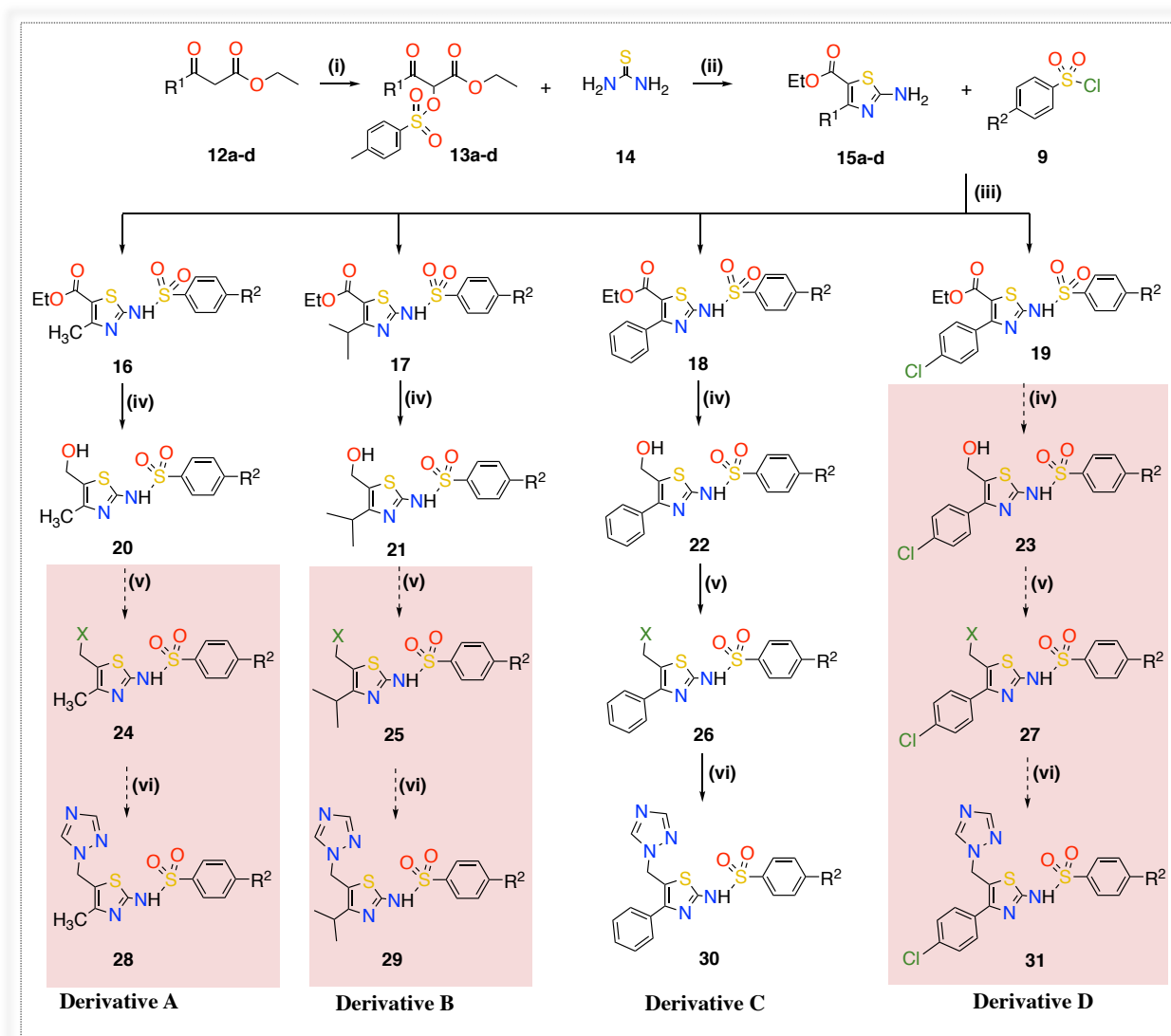
Figure 38: The cut off for derivative A and B within scheme (3).
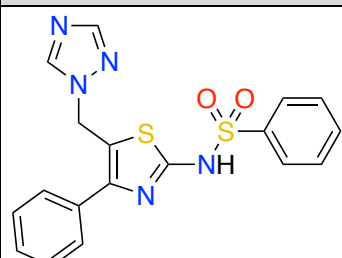
Synthesis of *N*-(5-((1*H*-1,2,4-triazol-1-yl)methyl)-4-phenylthiazol-2-yl)benzenesulfonamide (30):

The final compound of derivative C was obtained by reacting the triazole anion with the previous crude iodinated compound (**30a**). To prepare the triazolate, a solution of dry

acetonitrile and potassium carbonate was heated for 1 h at 45 °C to deprotonate the triazole. The triazole anion was added to the iodinated compound and heated at 70 °C overnight resulting in the displacement of iodide.[95]

After the work up, the crude product was purified by gradient column chromatography and the product confirmed by ^{1}H NMR as two singlet peaks for the triazole ring were observed. The pure compound was obtained in a very low yield since the previous step was crude, and the reaction did not go to completion (Table 18).

Table 18: Yield of the final product (**30a**).

Compound	Structure	Yield (%)	cLog P
30a		5	3.0

2. Second Method:

As shown in Table 17, the alcohols **20a**, **20b** and **21a** of derivatives A and B had very low cLogP = 0.79 – 1.67, which might be a reason for finding the compounds in the aqueous layer even after several extractions. Modifications in scheme (3) for derivatives A-C were needed to improve lipophilicity of the alcohol intermediate, which was a major problem during the synthesis. Moreover, an efficient good leaving group reaction method for the alcohol derivatives will be investigated (Scheme 4).

To synthesise derivatives A-C, an eight-step synthetic pathway was proposed:

1. Koser's reaction with different ethyl acetoacetate derivatives.
2. Hantzsch thiazole synthesis with thiourea.
3. Amine protection using phenyl chloroformate.
4. Reduction reaction with $NaBH_4$.
5. Chlorination reaction using thionyl chloride.
6. Nucleophilic substitution of triazole.
7. Carbamate bond hydrolysis.
8. Sulfonamide linker formation.

Second proposed synthetic pathway of thiazole sulfonamide derivatives:
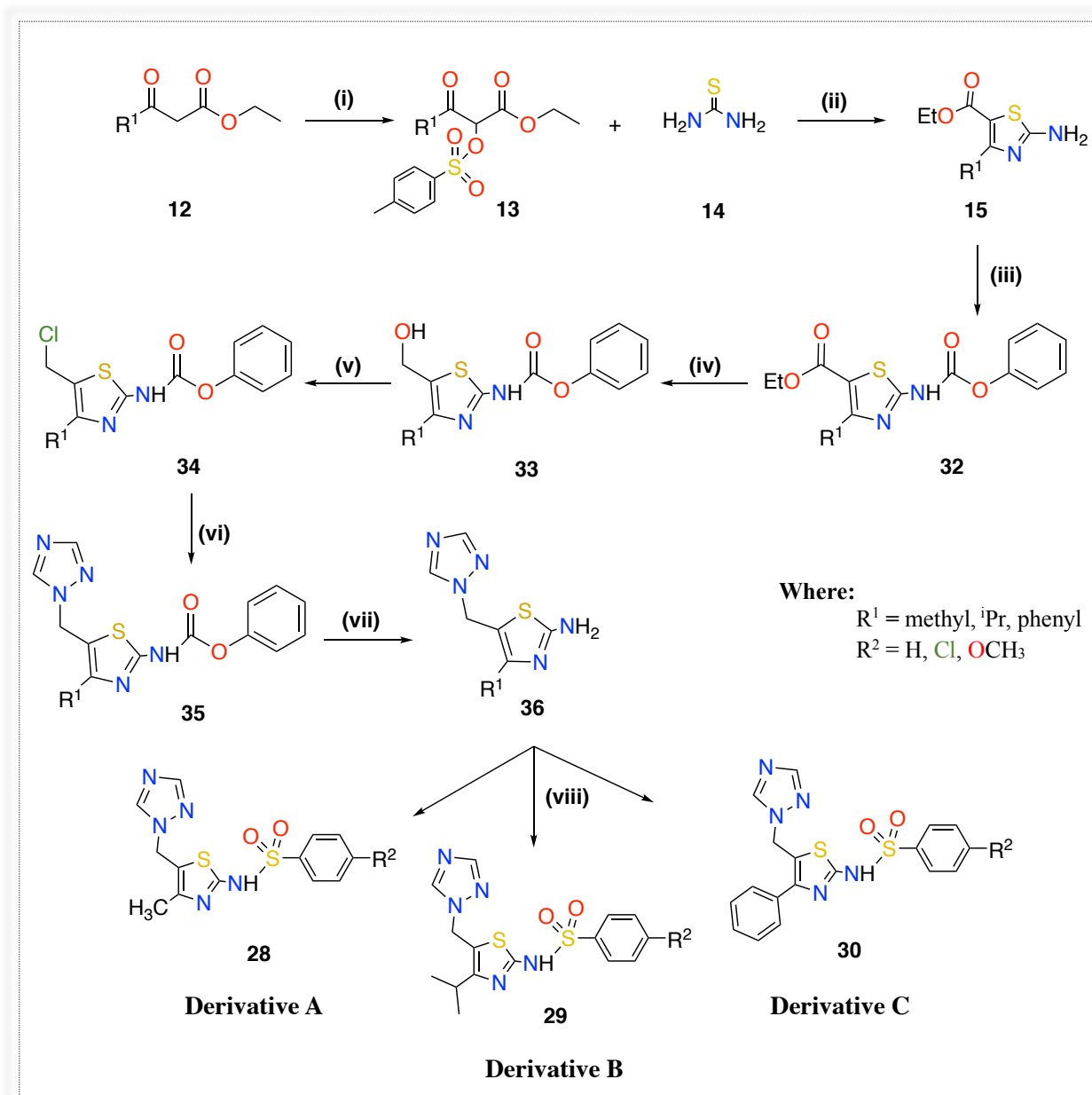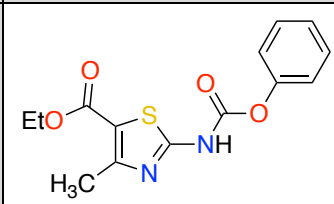
Scheme 4: *Reagents and conditions:* (i) HTIB, CH₃CN 75 °C, o/n (ii) EtOH, reflux at 80 °C, 4 h. (iii) pyridine, phenyl chloroformate, r.t., o/n (iv) THF, NaBH₄, r.t, o/n (v) CH₂Cl₂, SO₂Cl₂, 40 °C, 4 h (vi) (a) CH₃CN, K₂CO₃, triazole, 45 °C, 1 h (b) 70 °C, o/n (vii) piperidine, DMF, r.t., 2 h (vii) pyridine, benzenesulfonyl chloride derivatives, r.t., o/n.

Synthesis of ethyl 4-alkyl/aryl-2-((phenoxycarbonyl)amino)thiazole-5-carboxylate (32):

To solve the lipophilicity issue of derivative A and B, the Fmoc reagent was used first to protect the free amine and increasing Log P of the intermediate. The reaction was carried in dioxane/H$_2$O (1:1) by heating at 60 °C and monitored by TLC using EtOAc/petrolum ether (1:3) eluent system, then the reaction was left overnight. Unfortunately, no reaction occurred between Fmoc and compound **15**. However, the reason for using Fmoc was to improve the stability of the carbamate linker in the reduction of alcoholic intermediate by LiAlH$_4$,[115] which will be done in the next step. The second reagent used was phenyl chloroformate. The reaction involved the addition of phenyl chloroformate into a solution of compound **15** in pyridine at 0°C and the reaction left at room temperature overnight.[111] Only compound **32a** (derivative A) was synthesised first to confirm and optimise the proposed synthetic pathway. Compound **32a** was achieved in a good yield (86%) as a white solid and confirmed by NMR analysis (Table 19).

Table 19: Yield and M.P. of derivative A (**32a**).

Compound	Structure	Yield (%)	M.P (°C)
32a		86	190- 192

Synthesis of phenyl (5-(hydroxymethyl)-4-methylthiazol-2-yl)carbamate (33a):

The reduction of the ester functional group **32a** to produce the alcoholic compound (**33a**) was performed by adding 1.5 equivelants of NaBH$_4$ into a solution of **32a** in THF and the reaction left at room temperature overnight. The reaction was monitored by TLC using EtOAc/petroleum ether (3:1) eluent system, unfortunately no reaction occurred even after increasing NaBH$_4$ equivalents (3 eq.) and heating at 60 °C. At this point, the proposed scheme (4) could not be optimised owing to difficulty in the reduction step.

The only thiazole sulfonamide obtained from the 4 planned derivatives (A-D) was compound **30a** of derivative C, which was evaluated against CaCYP51 strains.
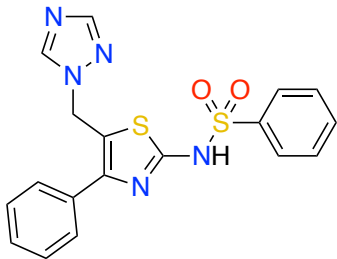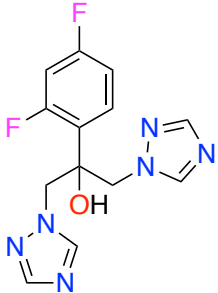
c. Biological evaluation:

1. *C. albicans* susceptibility testing:

The final thiazole sulfonamide compound was evaluated against *C.albicans* wild-type clinical isolate CAI4 and *C.albicans* laboratory strain SC5314. The MIC result for compound **30a** in both strains were very high (>16 µg/mL) compared with fluconazole (Table 20). The minimal antifungal activity could be related to the diffusion or transporter system within the cells.[98]

Table 20: MIC value for compound **30a**.

Code	Compound	MIC (µg/mL)
30a		>16
Fluconazole		0.125

3. New modification on the thiazole sulfonamide derivatives:

Since antifungal results for **30a** were not promising in addition to the difficulties in the synthetic pathway, new modifications on the thiazole sulfonamide derivatives (A-D) were needed and studied computationally to investigate the binding interactions with different amino acids within CaCYP51 active site. From the computational studies, only two derivatives with the aryl group at position 4 of the thiazole ring were considered for synthesis (Table 21).

Table 21: Two derivatives (E and F) of modified thiazole sulfonamide.
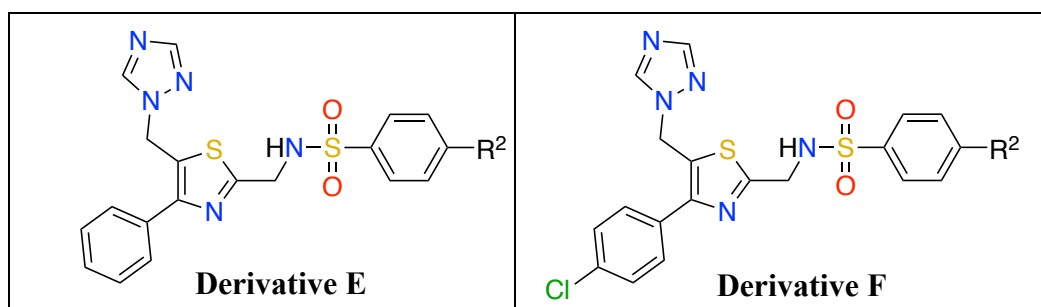
The main idea for the new proposed modification as shown in Figure 39 was:

1. To provide more flexible compounds by adding CH$_2$ at position 2 of the thiazole ring, which might help to improve fit and binding at the access channel.

While two structural features of the previous thiazole sulfonamide derivatives were kept (Figure 39):

2. To maintain the hydrophobic binding at the haem active site's arm by the aryl group at position 4 of the thiazole ring.

3. To increase binding interactions with other amino acids at the access channel by introduction of sulfonamide linker.
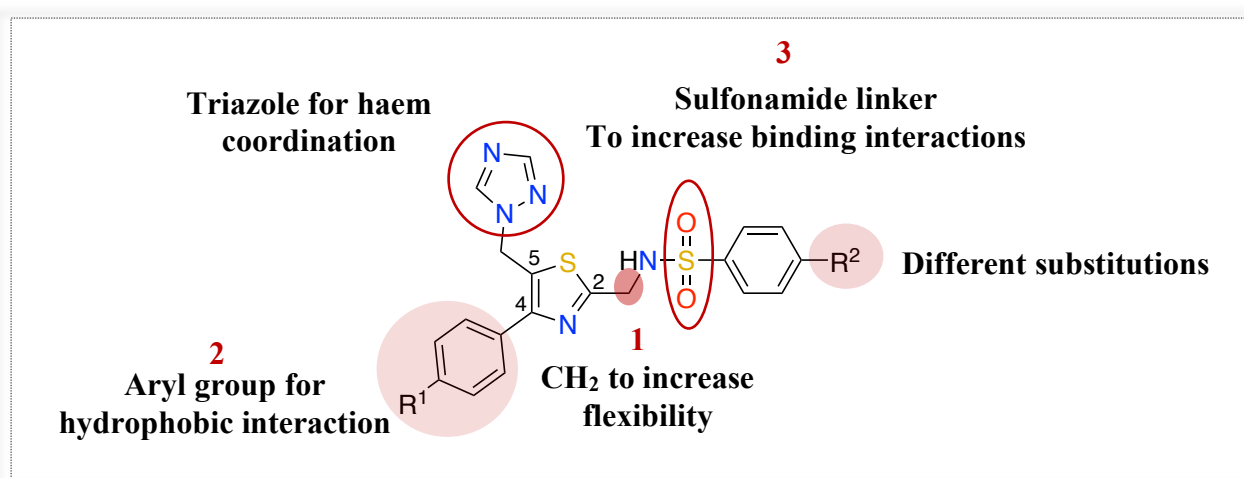
Figure 39: General structure for modified thiazole sulfonamide derivatives.

a. Computational studies:

1. Molecular modelling:

From the docking studies of modified thiazole sulfonamide derivatives, the compounds showed good fitting as well as occupying the access channel, and the distance between the azole nitrogen and the haem iron was approximately 3.33 Å. Binding interactions were through direct and indirect H-bonding with different amino acid residues as well as hydrophobic interctions with 10 amino acids (Figure 40).
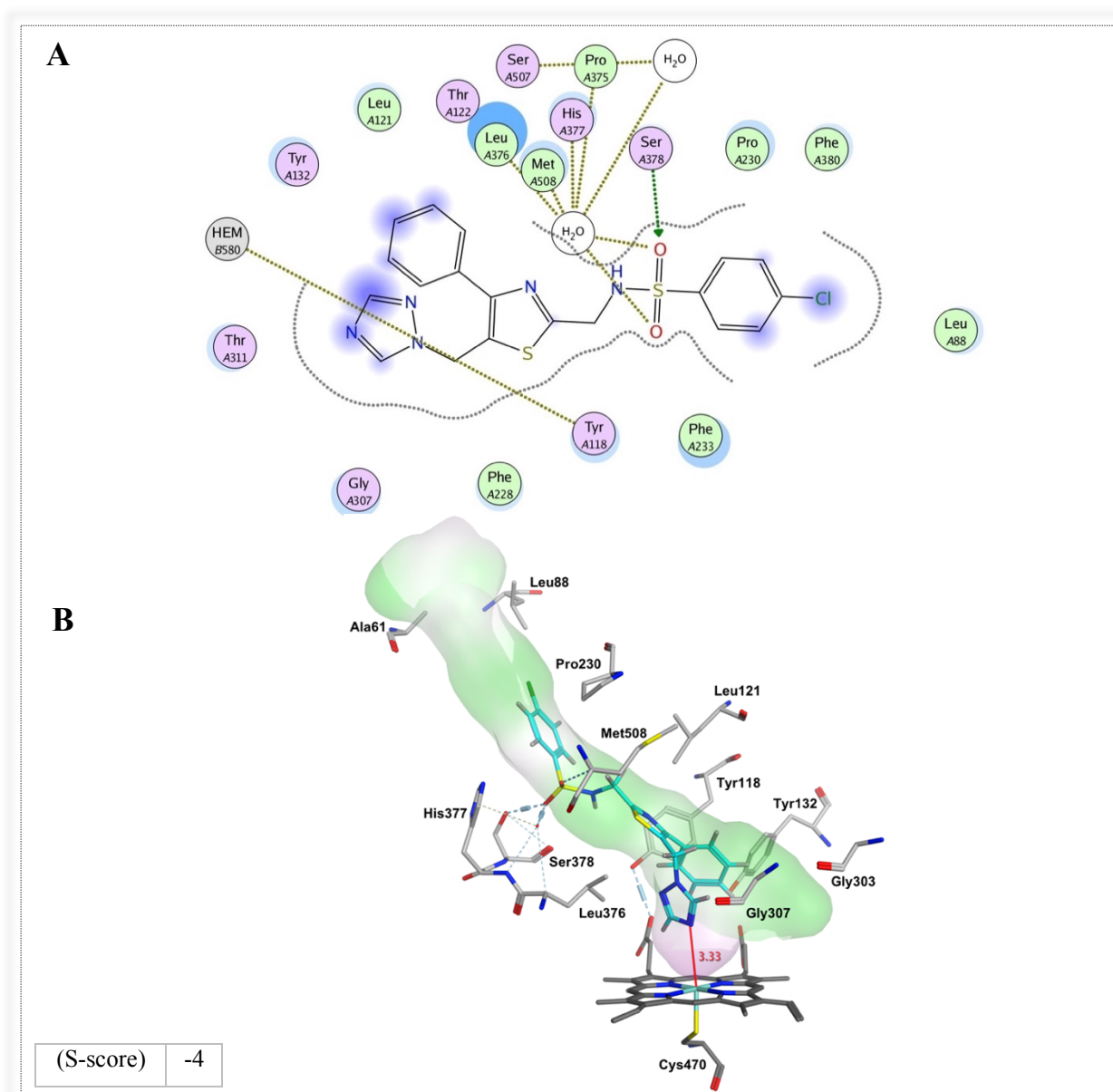
Figure 40: 2D and 3D visualisation of derivative E compound, used as an exemplar. (**A**) 2D ligplot illustrating binding interactions with amino acids in the protein. (**B**) 3D image illustrating key direct H-bonding interactions with Ser378 and through water molecules with Met508, Leu376 and His377.

2. MD simulation:

To confirm the result of the molecular docking for the same obtained pose of derivative E, molecular dynamic simulation was applied. In Figure 41A, the binding profile for derivative E during 200 ns simulation showed direct H-bonding interactions with Ser378, His377 and Met508 and water mediated H-bonding with Ser507 as well as a π-π stacking interaction between the phenyl at position 4 of the thiazole ring and Tyr118. Moreover, the interaction distance between the triazole N and the haem iron was approximately 2.45 Å (Figure 41B).
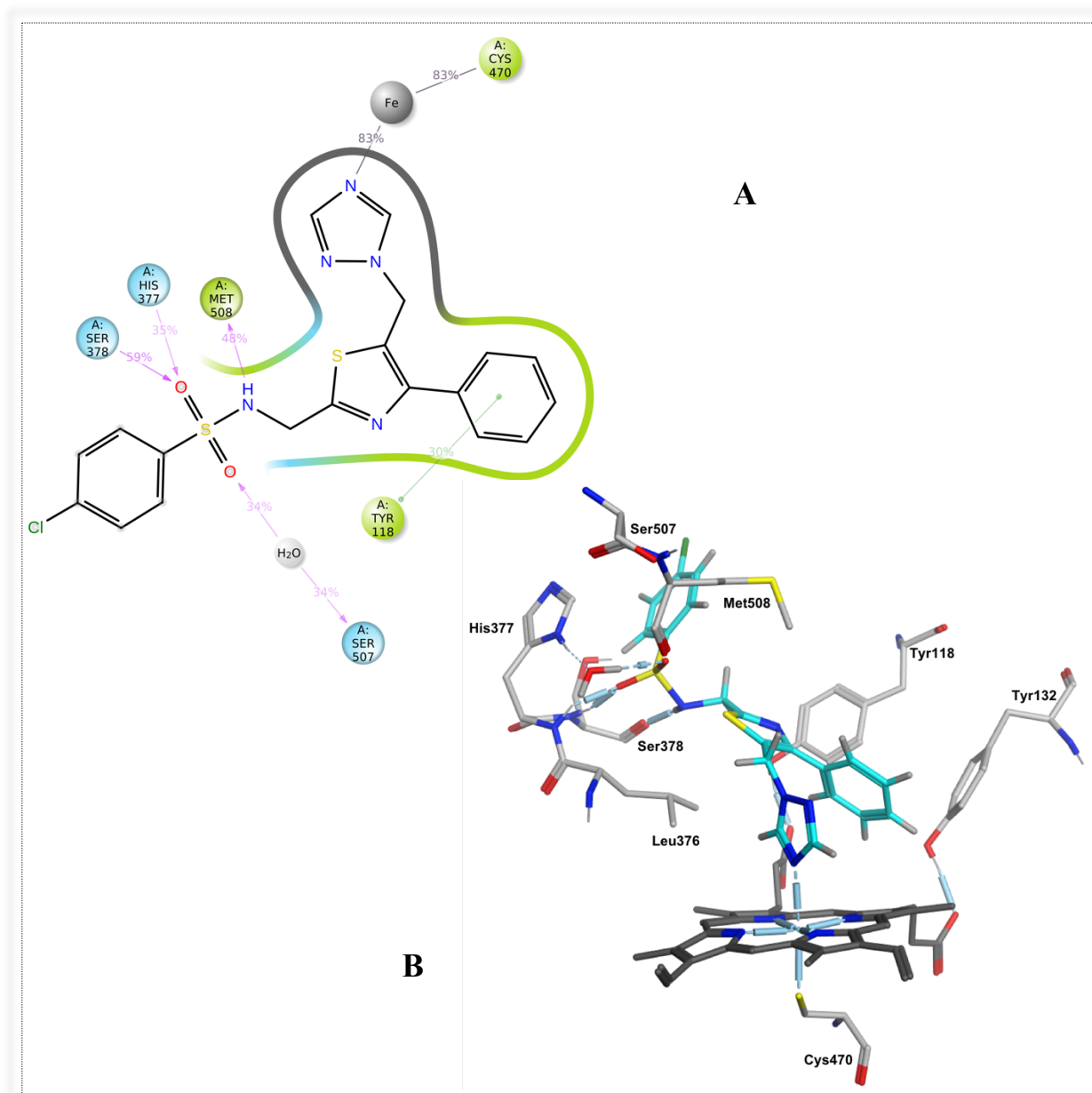
Figure 41: A) 2D ligand interactions of molecular dynamic (MD) simulation of derivative E with amino acids of CaCYP51 active site that occur more than 30% of the simulation time in the selected trajectory (0 through 200 ns). **B)** 3D image showing key binding interactions and position of the triazole ring above the heam with direct binding to Fe^{3+}.

b. Chemistry:

From the results of the docking studies, just two derivatives were chosen for synthesis using the 7 reaction steps pathway (Scheme 5):

1. Lawesson's reaction.
2. Hantzsch thiazole synthesis with thioamide derivative.
3. Hydrolysis of the amine protecting group.
4. Sulfonamide linker formation.
5. Reduction reaction using LiAlH$_4$.
6. Chlorination reaction.
7. Nucleophilic substitution reaction of triazole.

Proposed synthetic scheme of modified thiazole sulfonamide derivatives E and F.
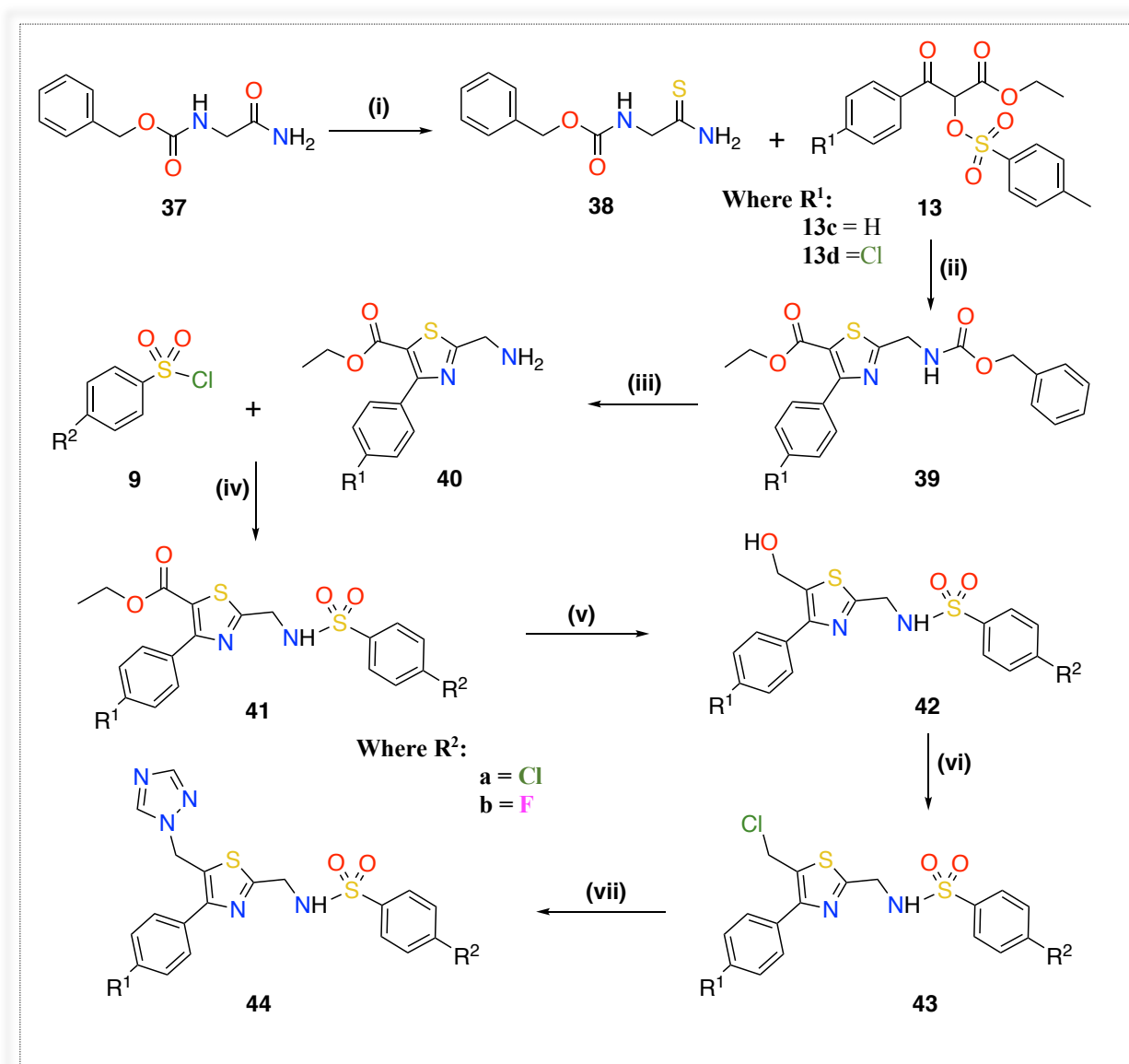
Scheme 5: *Reagents and conditions:* (i) THF, Lawesson's reagent, r.t., 4 h. (ii) DMF/EtOH (2:1), heat at 80 °C o/n. (iii) HBr (in 33% AcOH), r.t., 3 h (iv) pyridine, 80 °C, 3 h, r.t., o/n. (v) THF, LiAlH 4, r.t., o/n. (vi) CH$_2$Cl$_2$, (COCl)$_2$, reflux at 40 °C, 4 h (vii) (a) CH$_3$CN, K$_2$CO$_3$, triazole, 45 °C, 1 h, (b) 70 °C, o/n.

Synthesis of benzyl (2-amino-2-thioxoethyl)carbamate (38):

Lawesson's reagent is a useful thionating agent for ketones, esters and amides, which allows selective transformation.[116] Benzyl(2-amino-2-thioxoethyl) carbamate (**38**) was obtained by adding Lawesson's reagent into a solution of compound **37** in THF, and the mixture was left at room temperature for 4 h.[117]

The reaction mechanism involves a dissociation equilibrium with more reactive dithiophosphine intermediate. Then, the carbonyl O forms a four membered ring and the driving force for the corresponding thioamide (**38**) is the formation of a stable P=O bond from the reactive/unstable ring (Figure 42).[116] The desired product (**38**) was achieved in a good yield (yield = 76 %).
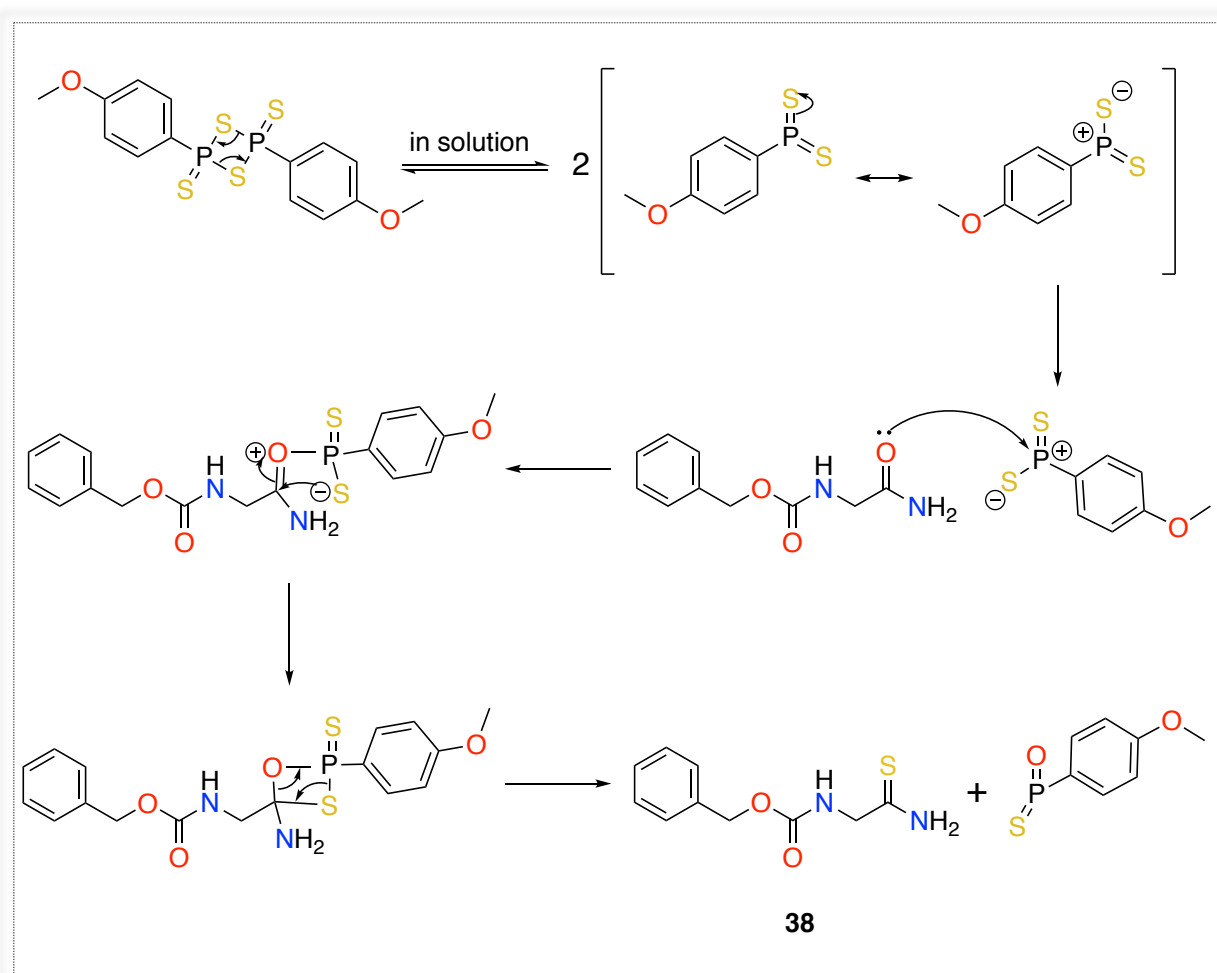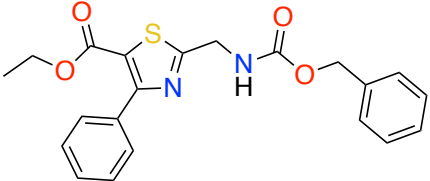
Figure 42: Lawesson's reaction mechanism.

Synthesis of ethyl 2-((((benzyloxy)carbonyl)amino)methyl)-4-phenylthiazole-5-carboxylate (39):

Synthesis of ethyl 2-((((benzyloxy)carbonyl)amino)methyl)-4-phenylthiazole-5-carboxylate (**39c**) was achieved by adding compound (**13a**) into a solution of the thioamide compound (**38**) in a mixture of DMF/EtOH (2:1 v/v), and the reaction was heated at 80 °C overnight. The mechanism involves a cyclisation reaction, similar to compound **3** and **15**, as previously discussed. The purification of this compound was very difficult which affected the yield (Table 22).

Table 22: Yield of compound (**39c**).

Compound	Structure	Yield (%)
39c		29

Unfortunately, the next step, which is a hydrolysis of the carbamate bond in compound (**39c**) to give the free amine, was unsuccessful even with several optimisations of the reaction temperature, time, reagent equivalents and different methods (Figure 43). The first hydrolysis method that failed was the HBr in 33% acetic acid, and the reaction was left at 3 h as well as overnight.[118] The second failed trial was using only acetic acid, and the reaction left for 4 h to 24 h, but only starting material was obtained. On the other hand, reduction of the carbamate bond could be possible using LiAlH$_4$, but this would also reduce the ester, which would complicate the synthetic pathway.
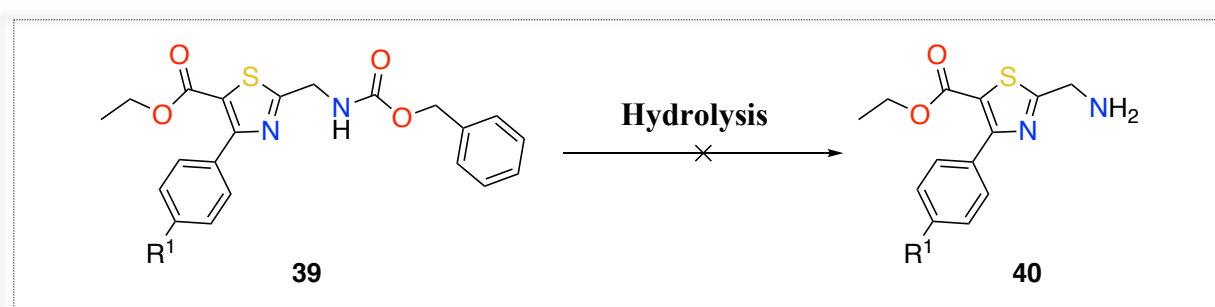
Figure 43: Hydrolysis of Compound (**39**).

Even though the new proposed modifications of the thiazole sulfonamide derivatives showed promising computational results, the proposed synthetic route was not applicable.

4. Conclusion:

The high demand for antifungal drugs to be developed is due to the frequent fluconazole drug resistance that occurs with different antifungal strains, especially for *C. albicans*. Design and synthesis of novel antifungal compounds require a good understanding of the target enzyme, CaCYP51. In this chapter, two type of the thiazole sulfonamide derivatives were designed as shown in Figure 44.
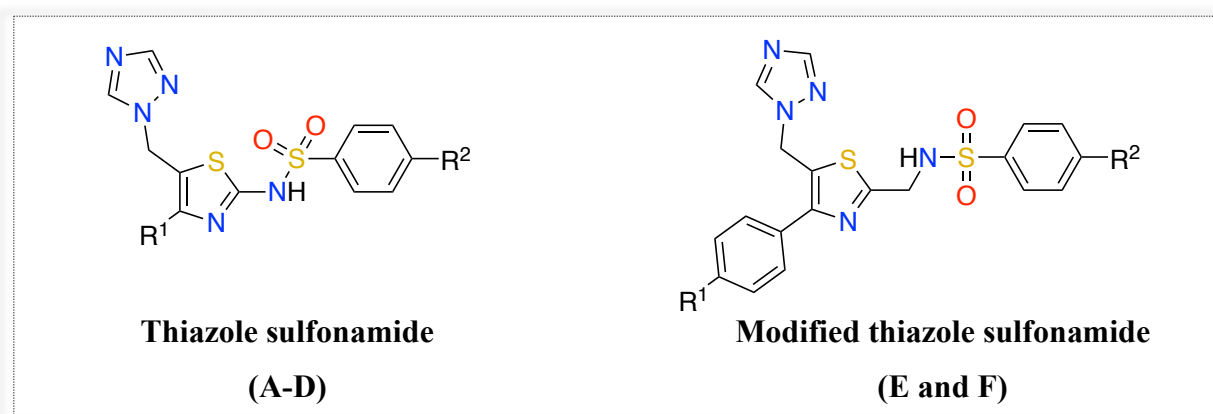
Figure 44: Two different designs of thiazole sulfonamide derivatives.

The computational studies of all thiazole sulfonamide derivatieves (A-F) showed promising binding interactions directly with the amino acids as well as through water molecules. Met 508, Leu376, Ser 378 and His 377 were the key amino acids in the ligand interactions along with the other hydrophobic interactions of the inhibitors with the boundaries of the active site as shown from the MD. Moreover, two methods were explored to achieve the thiazole sulfonamide derivatives (A-D). From the first method, only one compound of derivative C was obtained. Even though compound **30a** was obtained, the synthetic pathway was very difficult specifically at the iodination step (step five), which needed optimisation to obtain completion of the reaction, unfortunately its optimisation was difficult to achieve. The second method was used to synthesise derivative A and B, however the synthetic pathway stopped at the reduction step of the ester to give hydroxy compound (step four) as no reaction was obtained. Similarly, the synthetic route of modified thiazole sulfonamide derivatives (E and F) was cut off at the hydrolysis step of the carbamate bond owing to no reaction occurring.

Even though the computational studies were promising for the thiazole sulfonamide derivatives, the biological result for compound **30a** was negative. One important reason that may explain the negative results in all previous series including chapter II is the rigidity of the designed inhibitors, which might be unfavorable for the transporting system in the extracellular environment of *C. albicans* as well as the efflux system of the fungal cell. Thus, the major idea

from modified thiazole sulfonamide derivatives was to provide a more flexible structure that might improve the activity. Even though the molecular docking and dynamics were promising for the modified thiazole sulfomaide derivatives, the synthetic pathway was not applicable.

Despite the fact that the chemistry of the thiazole sulfonamide derivatives (A-F) did not work, the thiazole nucleus and sulfonamide linker was the building bone of all inhibitors, which was also a common factor in the phenyl thiazole short and extended series (chapter II). The higher polarity of the sulfonamide may be unfavourable for uptake across the lipophilic fungal membrane.

In the next chapter, a new series of novel inhibitors were designed and synthesised in order to provide different/applicable chemistry, more flexible structures that allow the occupancy of the enzyme active site as well as provide direct binding with the haem iron.

5. Experimental

Computational docking, MD simulations and MIC assay were performed as described in Chapter II (p 61 and 79).

General method:

Ethyl 3-oxo-2(tosyloxy)butanoate (13a)[87]

($C_{13}H_{16}O_6S$, M.W. 300.33)

(11)	**(12a)**	**(13a)**
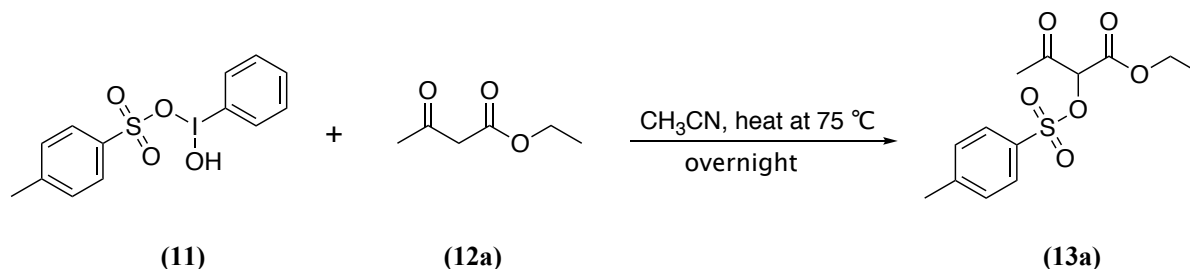
To a solution of HTIB (10.14 g, 25.86 mmol) in dry CH_3CN (30 mL) was added ethyl acetoacetate (**12a**) (3 mL, 23.51 mmol) in portions. The colourless solution was heated overnight at 75 C°. The solvent was evaporated under vacuum and the mixture was extracted with EtOAc (100 mL). The organic layer was washed with H_2O (3 x 50 mL), dried (MgSO₄), and concentrated under reduced pressure. Gradient column chromatography was applied to purify the residue by using a mixture of petroleum ether/ EtOAc (70:30 v/v) as eluent to afford the desired product.

Yield: 3.67 g (52 %) as a pale yellow oil.

R$_f$: 0.33 (5:1 v/v petroleum ether-EtOAc).

^{1}H NMR (DMSO-d₆): δ 7.84 (d, J = 8.3 Hz, 2H, Ar), 7.50 (d, J = 7.9 Hz, 2H, Ar), 5.75 (s, 1H, CH), 4.10 (q, J = 7.1 Hz, 2H, C$\underline{H_2}$CH₃), 2.43 (s, 3H, CH₃), 2.19 (s, 3H, CH₃), 1.13 (t, J = 7.1 Hz, 3H, CH₂C$\underline{H_3}$).

Using this procedure, the following compounds were prepared:

Ethyl 4-methyl-3-oxo-2-(tosyloxy)pentanoate (13b)[87]

($C_{15}H_{20}O_6S$, M.W.328.38)

(11)	**(12b)**	**(13b)**
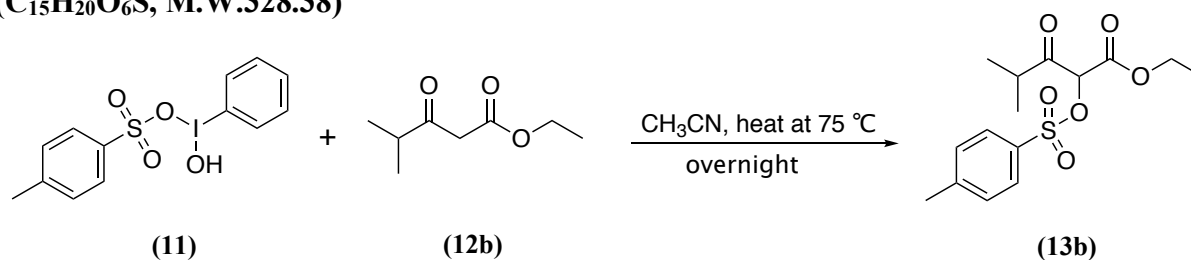
Reagents: ethyl isobutryl acetate (**12b**) (3 mL, 18.58 mmol). The residue was purified by using gradient column chromatography and the pure compound was eluted with 30 % EtOAc in petroleum ether.

Yield: 5.07 g (83 %) as a pale pink oil.

R$_f$: 0.5 (4:1v/v petroleum ether- EtOAc).

^{1}H NMR (DMSO-d$_6$): δ 7.84 (d, J = 8.5 Hz, 2H, Ar), 7.58 (d, J = 7.5 Hz, 2H, Ar), 5.88 (s, C<u>H</u>-Tos), 4.10 (q, J = 7.1 Hz, 2H, C<u>H$_2$</u>CH$_3$), 2.95 (sep, J = 7.0 Hz, 1H, C<u>H</u>(CH$_3$)$_2$), 2.43 (s, 3H, CH$_3$), 1.12 (t, J = 7.1 Hz, 3H, CH$_2$C<u>H$_3$</u>), 0.96 (d, J = 6.8 Hz, 6H, CH(C<u>H$_3$</u>)$_2$).

^{13}C NMR (DMSO-d$_6$): δ 203.3 (C, C=O), 164.4 (C, C=O), 146.2 (C, Ar), 132.3 (C, Ar), 79.4 (<u>C</u>HC=O), 62.8 (CH$_2$), 37.7 (<u>C</u>H(CH$_3$)$_2$), 21.6 (CH$_3$, Ar), 17.7 (CH(<u>C</u>H$_3$)$_2$), 14.1 (CH$_2$<u>C</u>H$_3$).

HPLC (Method B): 98 %, RT = 4.97 min.

HRMS (ESI, m/z): theoretical mass: 351.0878 [M+Na]$^+$, observed mass: 351.0885 [M+Na]$^+$.

Ethyl 3-oxo-3-phenyl-2-(tosyloxy)propanoate (13c)[87]

(C$_{18}$H$_{18}$O$_6$S, M.W. 362.40)

(11)	(12c)	(13c)
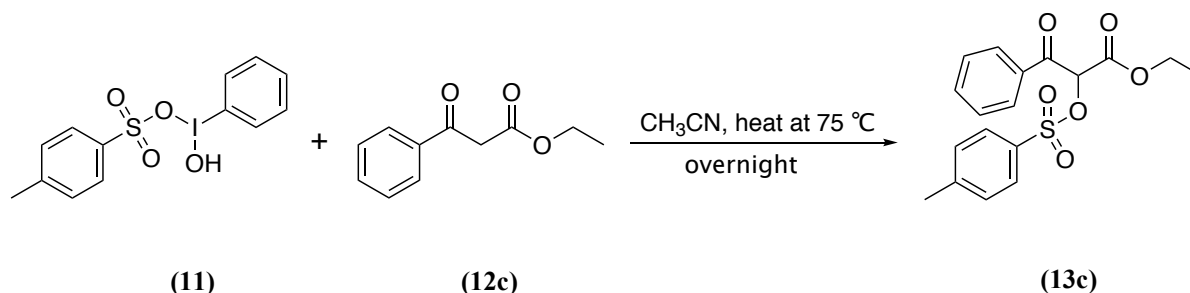
Reagents: ethyl benzyl acetate (**12c**) (3 mL, 17.63 mmol). The residue was purified by gradient column chromatography and the pure compound was eluted with 20 % EtOAc in petroleum ether.

Yield: 5.64 g (88 %) as a yelow oil.

R$_f$: 0.5 (4:1v/v petroleum ether-EtOAc).

^{1}H NMR (DMSO-d$_6$): δ 7.90 (d, J = 7.2 Hz, 2H, Ar), 7.81 (d, J = 8.3 Hz, 2H, Ar), 7.71 (t, J = 7.4 Hz, 1H, para-Ar), 7.53 (t, J = 8.3 Hz, 2H, Ar), 7.45 (d, J = 7.9 Hz, 2H, Ar), 6.59 (s, C<u>H</u>-Tos), 4.09 (q, J = 7.1 Hz, 2H, C<u>H$_2$</u>CH$_3$), 2.41 (s, 3H, CH$_3$), 1.04 (t, J = 7.1 Hz, 3H, CH$_2$C<u>H$_3$</u>).

Ethyl 3-(4-chlorophenyl)-3-oxo-2-(tosyloxy)propanoate (13d)[87]

(C$_{18}$H$_{17}$ClO$_6$S, M.W. 396.84)

(11)   **(12d)**   **(13d)**
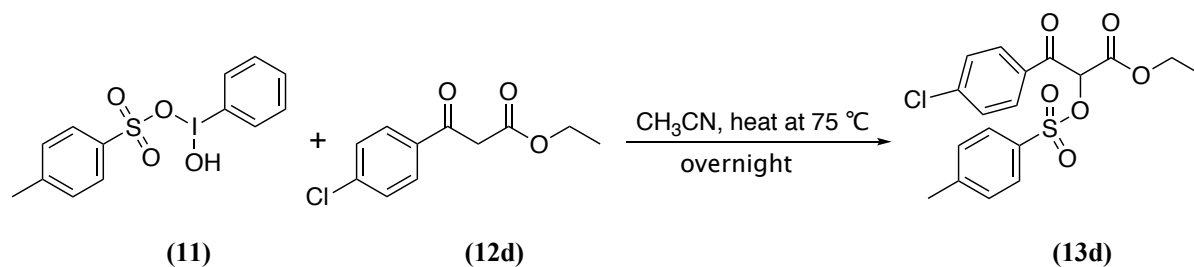
Reagents: ethyl 3-(4-chlorophenyl)-3-oxopropanoate (**12d**) (1.57g 6.9, mmol). The residue was purified by using gradient column chromatography and the pure compound was eluted with 25 % EtOAc in petroleum ether.

Yield: 0.27 g (34 %) as a white powder.

m.p.: 78-80 °C.

R$_f$: 0.4 (4:1v/v petroleum ether-EtOAc).

^{1}H NMR (DMSO-d$_6$): δ 7.94 (d, J = 9.0 Hz, 2H, Ar), 7.81 (d, J = 8.5 Hz, 2H, Ar), 7.62 (d, J = 9.0 Hz, 2H, Ar), 7.45 (d, J = 8.0 Hz, 2H, Ar), 6.62 (s, C$\underline{H}$-Tos), 4.12- 4.07 (m, 2H, C$\underline{H_2}$CH$_3$), 2.41 (s, 3H, CH$_3$), 1.05 (t, J = 7.0 Hz, 3H, CH$_2$C$\underline{H_3}$).

^{13}C NMR (DMSO-d$_6$): δ 188.81(C, C=O), 164.19 (C, C=O), 146.33 (C, Ar), 140.16 (C, Ar), 132.53 (C, Ar), 132.34 (C, Ar), 131.48 (CH, Ar), 130.63 (CH, Ar), 129.51 (CH, Ar), 128.46 (CH, Ar), 77.79 ($\underline{C}$HC=O), 62.97 (CH$_2$), 21.59 (CH$_3$, Ar), 14.06 (CH$_2$$\underline{C}H_3$).

HPLC (Method A): 100 %, RT = 4.77 min.

HRMS (ESI, m/z): theoretical mass: $^{35/37}$Cl 419.0331/421.0331 [M+Na]$^+$, observed mass: $^{35/37}$Cl 419.0330/421.0305 [M+Na]$^+$.

Ethyl 2-amino-4-methylthiazole-5-carboxylate (15a)[119]

(C$_7$H$_{10}$N$_2$O$_2$S, M.W. 186.23)

(1)   **(14)**   **(15a)**
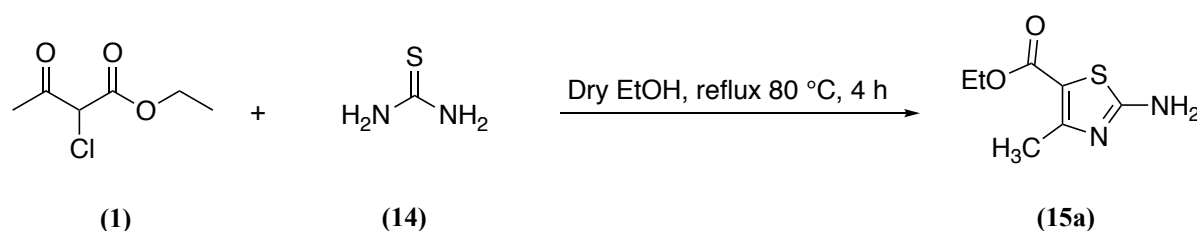
To a solution of ethyl 2-chloroacetoacetate (**1**) (1.29 g, 7.87 mmol) in dry EtOH (15 mL) was added thiourea (**14**) (0.5 g, 6.56 mmol) and the reaction refluxed at 80 °C for 4 h. The reaction mixture was cooled to room temperature, then cold ice/H$_2$O (50 mL) was added to the mixture

and neutralised with aqueous ammonia. The resulting precipitate was collected by filtration and left in the vacuum oven at 40 °C overnight.

Yield: 1.07 g (87 %) as a white fluffy solid.

m.p.: 180-182 °C (Lit. m.p.: 174-176 °C)[109].

R$_f$: 0.22 (2:1 v/v petroleum ether-EtOAc).

^{1}H NMR (DMSO-d$_6$): δ 6.57 (s, 2H, NH$_2$), 4.29 (q, J = 7.1 Hz, 2H, C$\underline{H_2}$CH$_3$), 2.56 (s, 3H, CH$_3$), 1.35 (t, J = 7.1 Hz, 3H, CH$_2$C$\underline{H_3}$).

Using this procedure, the following compounds were prepared:

Ethyl 2-amino-4-isopropylthiazole-5-carboxylate (15b)[119]
(C$_9$H$_{14}$N$_2$O$_2$S, M.W. 214.28)
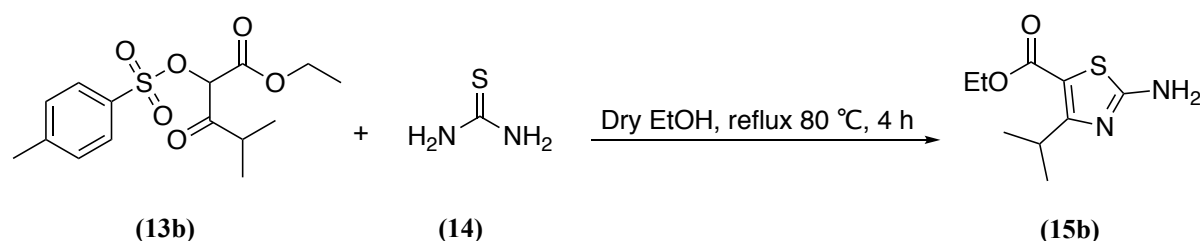
Reagents: ethyl 4-methyl-3-oxo-2-(tosyloxy)pentanoate (**13b**) (1.29 g, 3.93 mmol).

Yield: 0.66 g (94 %) as a white solid.

m.p.: 180-182 °C (Lit. m.p.: 179-181 °C)[109].

R$_f$: 0.45 (2:1 v/v petroleum ether-EtOAc).

^{1}H NMR (DMSO-d$_6$): δ 7.73 (s, 2H, NH$_2$), 4.14 (q, J = 7.1 Hz, 2H, C$\underline{H_2}$CH$_3$), 3.77 (sep, J = 6.9 Hz, 1H, C$\underline{H}$(CH$_3$)$_2$), 1.22 (t, J = 7.1 Hz, 3H, CH$_2$C$\underline{H_3}$), 1.12 (d, J = 6.8 Hz, 6H, CH(C$\underline{H_3}$)$_2$).

Ethyl 2-amino-4-phenylthiazole-5-carboxylate (15c)[119]
(C$_{12}$H$_{12}$N$_2$O$_2$S, M.W. 248.30)
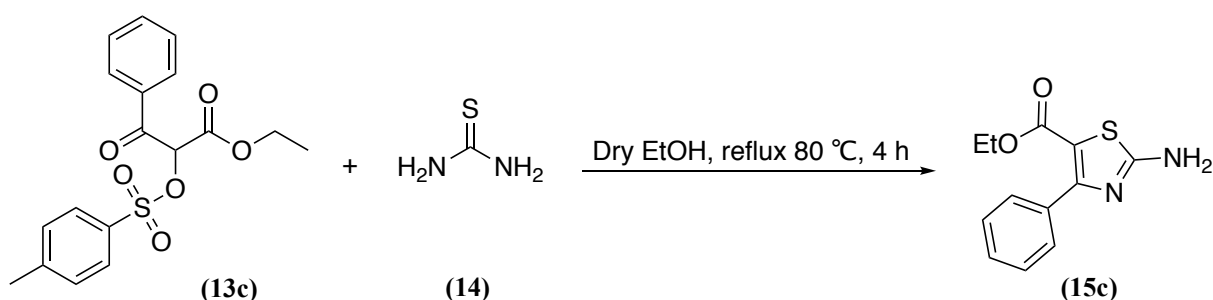
Reagents: ethyl 3-oxo-3-phenyl-2-(tosyloxy) propanoate (**13c**) (0.32 g, 4.14 mmol).

Yield: 0.76 g (74 %) as a faint yellow solid.

m.p.: 168-171 °C (170-172°C)[109].

R$_f$: 0.3 (2:1 v/v petroleum ether-EtOAc).

^{1}H NMR (DMSO-d$_6$): δ 7.83 (s, 2H, N$\underline{H}_2$), 7.64-7.60 (m, 2H, Ar), 7.39-7.36 (m, 3H, Ar), 4.08 (q, J = 7.1 Hz, 2H, C$\underline{H}_2$CH$_3$), 1.14 (t, J = 7.0 Hz, 3H, CH$_2$C$\underline{H}_3$).

Ethyl 2-amino-4-(4-chlorophenyl)thiazole-5-carboxylate (15d)[119]
(C$_{12}$H$_{11}$ClN$_2$O$_2$S, M.W. 282.74)

(13d)   **(14)**   **(15d)**
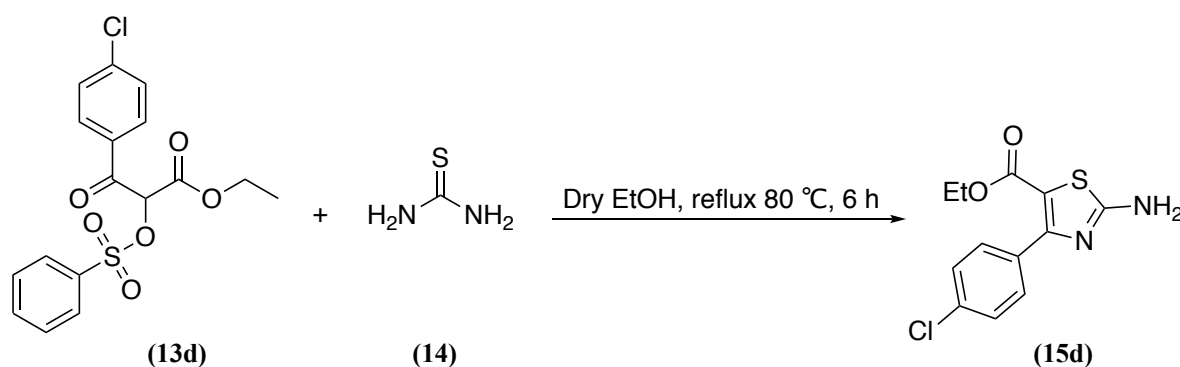
Reagents: ethyl 3-(4-chlorophenyl)-3-oxo-2-(tosyloxy) propanoate (**13d**) (0.34g, 0.86 mmol).

Yield: 0.15 g (60 %) as a pale yellow solid.

m.p.: 194-196 °C (Lit. m.p.: 198-200°C)[110] .

R$_f$: 0.2 (2:1 v/v petroleum ether-EtOAc).

^{1}H NMR (DMSO-d$_6$): δ 7.88 (s, 2H, N$\underline{H}_2$), 7.66 (d, J=8.5 Hz, 2H, Ar), 7.44 (d, J=8.5 Hz, 2H, Ar), 4.08 (q, J = 7.1 Hz, 2H, C$\underline{H}_2$CH$_3$), 1.16(t, J = 7.1 Hz, 3H, CH$_2$C$\underline{H}_3$).

Ethyl 4-methyl-2-(phenylsulfonamido) thiazole-5-carboxylate (16a)[97]
(C$_{13}$H$_{14}$N$_2$O$_4$S$_2$, M. W. 326.39)

(15a)   **(9a)**   **(16a)**
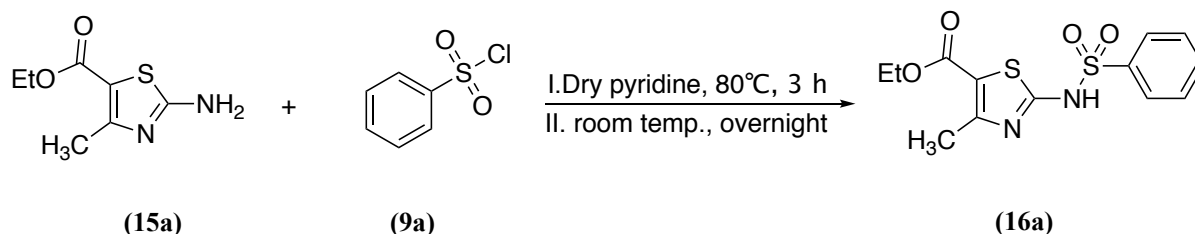
A mixture of ethyl 2-amino-4-methylthiazole-5-carboxylate (**15a**) (1 g, 5.36 mmol) and benzensulfonyl chloride (**9a**) (1.41 g, 8.04 mmol) in dry pyridine (10 mL) was heated at 80 °C for 3 h, then left at room temperature overnight. Then, crushed ice was added to the reaction

mixture and the separated solid product was collected by filtration, washed with H_2O several times, and dried in the vacuum oven at 40 °C overnight.

Yield: 1.5 g (86 %) as a light brown solid.

m.p.: 190-192 °C (Lit. m.p.: 157-158°C)[120].

R$_f$: 0.67 (3:1 v/v EtOAc-petroleum ether).

¹H NMR (DMSO-d₆): δ 13.22 (s, 1H, NH, sulfonamide), 7.82 (d, J = 7.3 Hz, 2H, Ar), 7.65-7.58 (m, 3H, Ar), 4.23 (q, J = 7.1 Hz, 2H, C$\underline{H}_2$CH₃), 2.39 (s, 3H, CH₃), 1.26 (t, J = 7.1 Hz, 3H, CH₂C$\underline{H}_3$).

Using this procedure, the following compounds were prepared:

Ethyl-2-((4-chlorophenyl)sulfonamido)-4-methylthiazole-5-carboxylate (16b)[97]
(C₁₃H₁₃ClN₂O₄S₂, M.W. 360.83)

(15a)   **(9b)**   **(16b)**
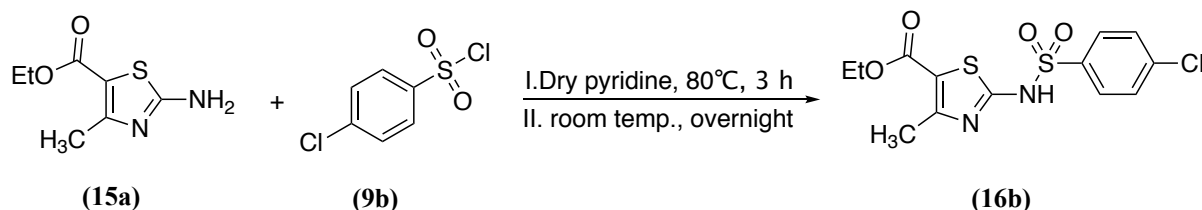
Reagents: ethyl 2-amino-4-methylthiazole-5-carboxylate (**15a**) (1g, 5.36 mmol) and 4-chlorobenzensulfonyl chloride (**9b**) (1.69 g, 8.04 g mmol).

Yield: 1.87 g (96 %) as a light brown solid.

m.p.: 185-187 °C.

R$_f$: 0.57 (3:1 v/v EtOAc-petroleum ether).

¹H NMR (DMSO-d₆): δ 13.32 (s, 1H, NH, sulfonamide), 7.82 (d, J = 8.8 Hz, 2H, Ar), 7.63 (d, J = 8.5 Hz, 2H, Ar), 4.23 (q, J = 7.1 Hz, 2H, C$\underline{H}_2$CH₃), 2.40 (s, 3H, CH₃), 1.26 (t, J = 7.1 Hz, 3H, CH₂C$\underline{H}_3$).

Ethyl 4-isopropyl-2-(phenylsulfonamido) thiazole-5-carboxylate (17a)
(C₁₅H₁₈N₂O₄S₂, M.W. 354.44)

(15b)   **(9a)**   **(17a)**
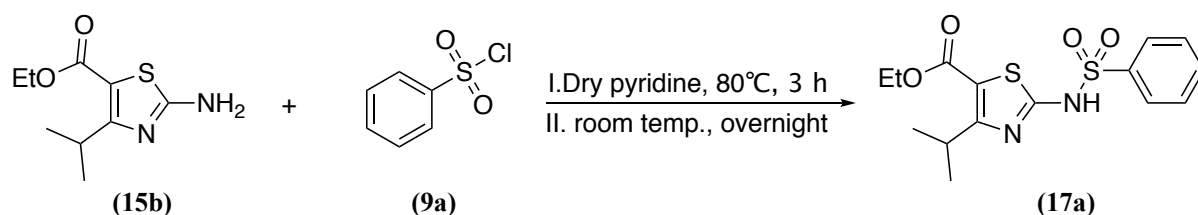
Variation: The compound was extracted with EtOAc (50 mL) and washed with 1M aqueous HCl (2 x 25 mL), brine (2 x 25 mL) and H_2O (2 x 25 mL).

Reagents: ethyl 2-amino-4-isopropylthiazole-5-carboxylate (**15b**) (0.66 g, 3.08 mmol).

Yield: 1.01 g (92%) as a brown oil.

R_f: 0.37 (3:1 v/v EtOAc-petroleum ether).

^{1}H NMR (DMSO-d_6): δ 13.20 (s, 1H, NH), 7.84 (d, J = 7.0 Hz, 2H, Ar), 7.60-7.57 (m, 3H, Ar), 4.24 (q, J = 7.1 Hz, 2H, C$\underline{H_2}$CH$_3$), 3.92 (sep, J = 7.1 Hz, 1H, C$\underline{H}$(CH$_3$)$_2$), 1.27 (t, J = 7.1 Hz, 3H, CH$_2$C$\underline{H_3}$), 1.17 (d, J = 6.2 Hz, 6H, CH(C$\underline{H_3}$)$_2$).

^{13}C NMR (DMSO-d_6): δ 167.54 (C, thiazole), 160.75 (C, C=O), 153.90 (C, thiazole), 142.03 (C, Ar), 133.04 (CH, Ar), 129.66 (CH x 2, Ar), 126.30 (CH x 2, Ar), 106.47 (C, thiazole), 61.65 (CH$_2$), 26.42 ($\underline{C}$H(CH$_3$)$_2$), 20.59 (CH($\underline{C}$H$_3$)$_2$), 14.53 (CH$_3$).

HPLC (Method B): 95 %, RT = 3.31 min.

HRMS (ESI, m/z): theoretical mass: 355.0786 [M+H]$^+$, observed mass: 355.0790 [M+H]$^+$.

Ethyl 4-phenyl-2-(phenylsulfonamido)thiazole-5-carboxylate (18a)
($C_{18}H_{16}N_2O_4S_2$, M.W. 388.46)
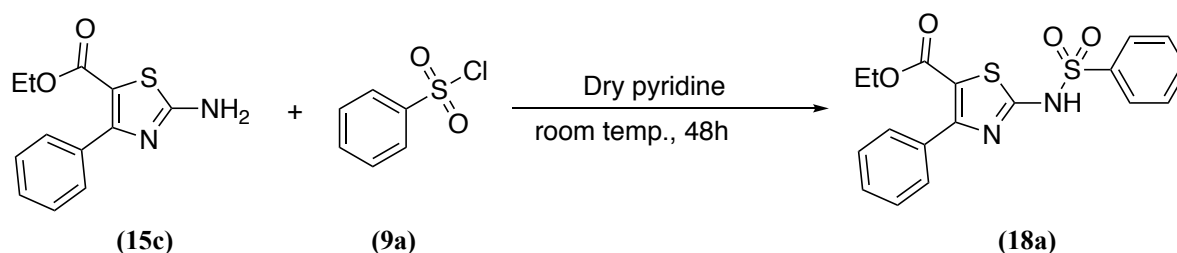
Variation: Reaction stirred at room temperature for 48h. In the work up the compound was extracted with EtOAc (50 mL) and washed with 1M aqueous HCl (2 x 25 mL), brine (2 x 25 mL) and H_2O (2 x 25 mL). Gradient column chromatography was applied to purify the desired product which eluted with petroleum ether-EtOAc 3:2 v/v.

Reagents: ethyl 2-amino-4-phenylthiazole-5-carboxylate (**15c**) (0.56 g, 2.25 mmol).

Yield: 0.53 g (61%) as a white wax (semisolid).

R_f: 0.67 (3:1 v/v EtOAc-petroleum ether).

^{1}H NMR (DMSO-d_6): δ 13.49 (s, 1H, NH), 7.87 (d, J = 7.1 Hz, 2H, Ar), 7.63-7.56 (m, 3H, Ar), 7.59-7.44 (m, 5H, Ar), 4.13 (q, J = 7.1 Hz, 2H, C$\underline{H_2}$CH$_3$), 1.13 (t, J = 7.1 Hz, 3H, CH$_2$C$\underline{H_3}$).

^{13}C NMR (DMSO-d_6): δ 166.96 (C, thiazole), 160.17 (C, C=O), 159.18 (C, thiazole), 142.08 (C, Ar), 135.05 (C, Ar), 133.04 (CH, Ar), 130.78 (CH, Ar), 130.24 (CH x 2, Ar), 129.65 (CH

x 2, Ar), 129.01 (C, thiazole), 128.30 (CH x 2, Ar), 126.34 (CH x 2, Ar), 61.63 (CH$_2$), 14.28 (CH$_3$).

HPLC (Method B): 99 %, RT = 4.96 min.

HRMS (ESI, m/z): theoretical mass: 411.0448 [M+Na]$^+$, observed mass: 411.0452 [M+Na]$^+$.

Ethyl 4-(4-chlorophenyl)-2-(phenylsulfonamido)thiazole-5-carboxylate(19a) (C$_{18}$H$_{15}$ClN$_2$O$_4$S$_2$, M.W. 422.90)

(15d)   **(9a)**   **(19a)**
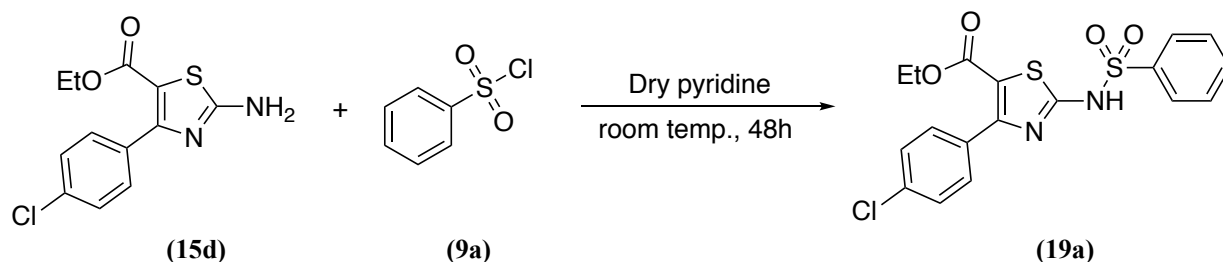
Reagents: ethyl 2-amino-4-(4-chlorophenylthiazole-5-carboxylate (**15d**) (0.37 g, 1.33 mmol). Compound eluted at 40 % EtOAc.

Yield: 0.05 g (8 %) as a beige crystalline solid.

m.p.: 174-176 °C.

R$_f$: 0.25 (3:1 v/v EtOAc-petroleum ether).

^{1}H NMR (DMSO-d$_6$): δ 13.49 (s, 1H, NH), 7.87 (d, J = 7.1 Hz, 2H, Ar), 7.67-7.64 (m, 1H, Ar), 7.62-7.58 (m, 4H, Ar), 7.53 (d, J = 7.8 Hz, 2H, Ar), 4.14 (q, J = 7.1 Hz, 2H, C$\underline{H}_2$CH$_3$), 1.13 (t, J = 7.1 Hz, 3H, CH$_2$C$\underline{H}_3$).

^{13}C NMR (DMSO-d$_6$): δ 166.96 (C, thiazole), 160.17 (C, C=O), 159.18 (C, thiazole), 142.08 (C, Ar), 135.05 (C, Ar), 133.04 (C, Ar), 130.78 (CH, Ar), 130.24 (CH x 2, Ar), 129.65 (CH x 2, Ar), 129.01 (C, thiazole), 128.30 (CH x 2, Ar), 126.34 (CH x 2, Ar), 61.63 (CH$_2$), 14.28 (CH$_3$).

HPLC (Method A): 100 %, RT = 4.71 min.

HRMS (ESI, m/z): theoretical mass: $^{35/37}$Cl 423.0240/425.0240 [M+H]$^+$, observed mass: $^{35/37}$Cl 423.0240/425.0213 [M+H]$^+$.

N-(5-(hydroxymethyl)-4-methylthiazol-2-yl) benzenesulfonamide (20a)

(C$_{11}$H$_{12}$N$_2$O$_3$S$_2$, M.W. 284.35)

(16a) → (20a), LiAlH$_4$, THF, room temp., overnight
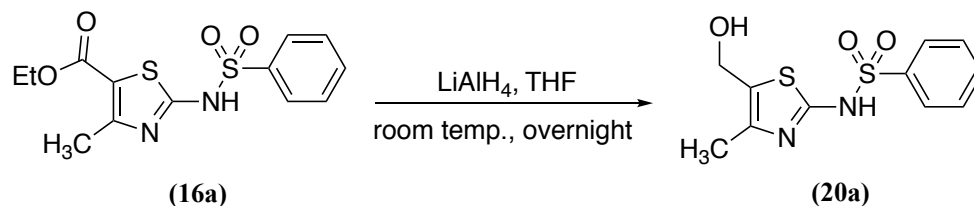
To an ice-cooled stirred solution of ethyl 4-methyl-2-(phenylsulfonamido)thiazole-5-carboxylate (**16a**) (1g, 3.06 mmol) in dry THF (10 mL), was added LiAlH$_4$ (1M in THF, 4.59 mL, 4.59 mmol) dropwise over 30 min. The reaction was left at room temperature with continuous stirring overnight.[87] The resulting mixture was quenched carefully with H$_2$O (20 mL) in an ice-bath until cession of effervescence, then EtOAc (50 mL) was added. The organic layer was washed with H$_2$O (2 x 25 mL), dried (MgSO$_4$) and evaporated under vacuum. The product was used in the next step without further purification.

Yield: 0.24g (27%) as a yellow-orange semi solid.

R$_f$: 0.47 (9.5:0.5 v/v CH$_2$Cl$_2$-MeOH).

^{1}H NMR (DMSO-d$_6$): δ 12.44 (s, 1H, NH), 7.79 (d, J = 7.1 Hz, 2H, Ar), 7.63-7.58 (m, 3H, Ar), 5.35 (t, J = 8.1 Hz, 1H, OH, ex), 4.35 (d, J = 5.1 Hz, 2H, C$\underline{H}_2$), 2.03 (s, 3H, C$\underline{H}_3$).

Using this procedure, the following compounds were prepared:

4-Chloro-N-(5-(hydroxymethyl)-4-methylthiazol-2-yl) benzenesulfonamide (20b)

(C$_{11}$H$_{11}$ClN$_2$O$_3$S$_2$, M.W.318.79)

(16b) → (20b), LiAlH$_4$, THF, room temp., overnight
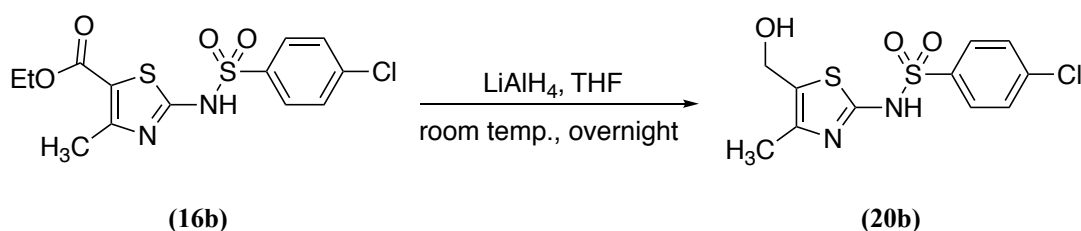
Variations: The resulting mixture was quenched carefully with H$_2$O (20 mL) in an ice-bath until cession of effervescence, then 1M aqueous HCL (20 mL) was added; the compound was extracted with CH$_2$Cl$_2$ (3 x 50 mL), dried (MgSO$_4$) and evaporated under vacuum. The crude product was used without further purification.

Reagents: 4-chloro-N-(5-(hydroxymethyl)-4-methylthiazol-2-yl) benzenesulfonamide (**16b**) (0.5g, 1.38 mmol).

Yield: 0.3g (70%) as a white semisolid.

R$_f$: 0.3 (9.5:0.5 v/v CH$_2$Cl$_2$-MeOH).

^{1}H NMR (DMSO-d$_6$): δ 12.54 (s, 1H, NH), 7.79 (d, J = 8.8 Hz, 2H, Ar), 7.55 (d, J = 8.8 Hz, 2H, Ar), 5.37 (t, J = 6.5 Hz, 1H, OH, ex), 4.35 (d, J = 5.3 Hz, 2H, C$\underline{H}_2$), 2.04 (s, 3H, C$\underline{H}_3$).

N-(5-(Hydroxymethyl)-4-isopropylthiazol-2-yl)benzenesulfonamide (21a)
(C$_{13}$H$_{16}$N$_2$O$_3$S$_2$, M.W. 312.40)

(17a)   **(21a)**
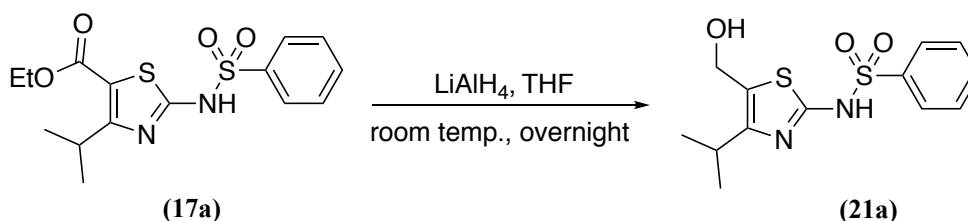
Reagents: Ethyl 4-isopropyl-2-(phenylsulfonamido)thiazole-5-carboxylate (**17a**) (1g, 2.82 mmol). Crude product was used without further purification.

Yield: 0.21 g (23%, crude) as a yellow-orange oil.

R$_f$: 0.3 (9.5:0.5 v/v CH$_2$Cl$_2$-MeOH).

^{1}H NMR (DMSO-d$_6$): δ 12.48 (s, 1H, NH), 7.81 (d, J = 6.8 Hz, 2H, Ar), 7.65-7.56 (m, 3H, Ar), 5.39 (t, J = 5.7 Hz, 1H, OH, ex), 4.38 (d, J = 5.7 Hz, 2H, C$\underline{H}_2$), 3.38 (sep, J = 6.8 Hz, 1H, C$\underline{H}$(CH$_3$)$_2$), 1.11 (d, J = 7.0 Hz, 6H, CH(C$\underline{H}_3$)$_2$).

N-(5-(Hydroxymethyl)-4-phenylthiazol-2-yl)benzenesulfonamide (22a)
(C$_{16}$H$_{14}$N$_2$O$_3$S$_2$, M.W. 346.42)

(18a)   **(22a)**
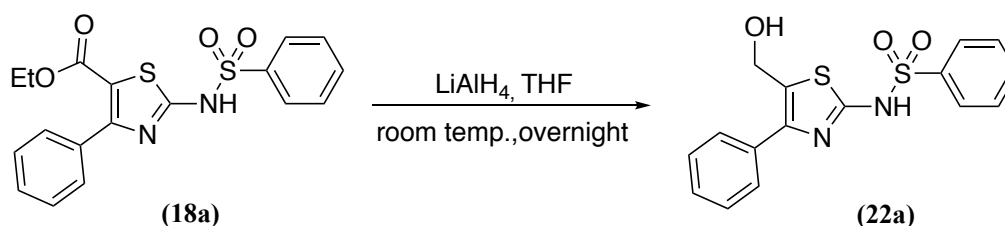
Reagents: Ethyl 4-phenyl-2-(phenylsulfonamido)thiazole-5-carboxylate (**18a**) (0.5g, 1.28 mmol).The crude product was purified using gradient column chromatography and the pure product was eluted with CH$_2$Cl$_2$- MeOH 98:2 v/v.

Yield: 0.24g (54%) as a white solid.

m.p.: 86-88 °C.

R$_f$: (9.5:0.5 v/v CH$_2$Cl$_2$-MeOH).

¹H NMR (DMSO-d₆): δ 12.95 (s, 1H, NH), 7.85 (d, J = 6.8 Hz, 2H, Ar), 7.60-7.56 (m, 3H, Ar), 7.49-7.45 (m, 5H, Ar), 5.68 (t, J = 5.6 Hz, 1H, OH, ex), 4.44 (d, J = 5.4 Hz, 2H, C$\underline{H_2}$).

¹³C NMR (DMSO-d₆): δ 167.58 (C, thiazole), 142.68 (C, thiazole), 129.21 (2 x C, Ar), 132.58 (CH, Ar), 129.73 (CH, Ar), 129.47 (CH x 2, Ar), 129.21 (CH x 2, Ar), 128.74 (CH x 2, Ar), 126.31 (CH x 2, Ar), 122.17 (C, thiazole), 55.83 (CH₂).

HPLC (Method B): 99%, RT = 4.69 min.

HRMS (ESI, m/z): theoretical mass: 369.0343 [M+Na]⁺, observed mass: 369.0344 [M+Na]⁺.

N-(5-(Iodomethyl)-4-phenylthiazol-2-yl)benzenesulfonamide (26a)
($C_{16}H_{13}IN_2O_2S_2$, M.W. 456.32)
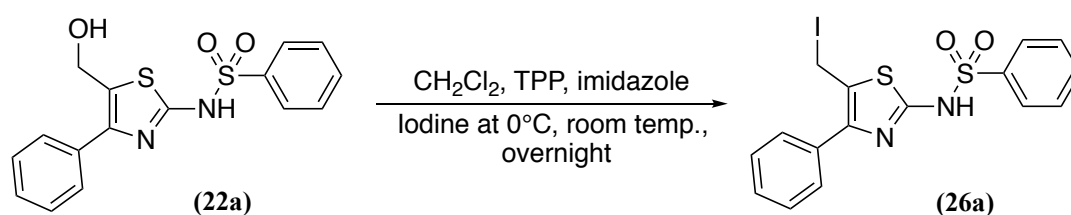
To a solution of triphenylphosphine (TPP) (0.34g, 1.31 mmoL) in dry CH₂Cl₂ (10 mL) was added imidazole (0.09 mL, 1.31 mL). Then, the reaction flask was covered with aluminum foil and cooled in an ice-bath. Four portions of iodine (0.33g, 1.31 mmoL) were added over 20 min, then the reaction warmed to room temperature for 10 min. After that, the solution was cooled to 0°C and the alcohol **22a** (0.35g, 1.01mmoL) was added to the mixture. The reaction was stirred at room temperature overnight.[112] The reaction mixture was diluted with CH₂Cl₂ (50 mL) and washed with H₂O (25 mL), the organic layer was dried (MgSO₄) and evaporated to give an orange oil. The compound was used in the next step without further purifications.

Yield: 0.46g, (100 %, crude) orange oil.

R$_f$: 0.72 (9.5:0.5 v/v CH₂Cl₂-MeOH).

¹H NMR (DMSO-d₆): δ 12.85 (s, 1H, NH), 7.85 (d, J = 6.8 Hz, 2H, Ar), 7.65-7.56 (m, 3H, Ar), 7.48-7.46 (m, 5H, Ar), 4.02 (s, 2H, C$\underline{H_2}$).

N-(5-((1H-1,2,4-triazol-1-yl)methyl)-4-phenylthiazol-2-yl)benzenesulfonamide(30a)
(C₁₈H₁₅N₅O₂S₂, M. W. 397.47)

(26a) → **(30a)**

I. K₂CO₃, triazole, CH₃CN
heat 45 °C, 1 h

II. Heat 70 °C, overnight
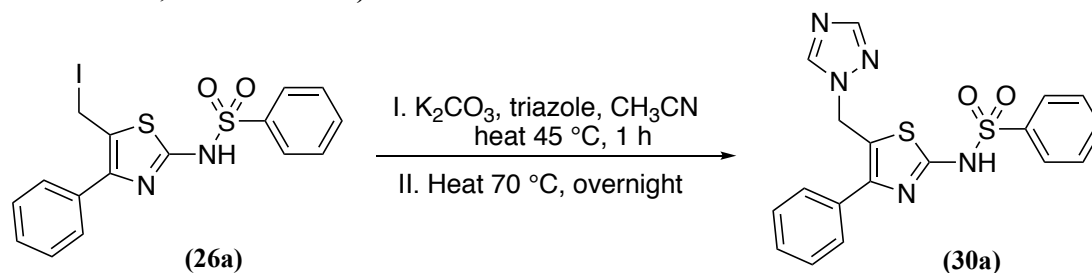
Method: In dry CH₃CN (20 mL), K$_2$CO$_3$ (0.083 g, 0.6 mmol) and triazole (0.28 g, 4 mmol) were added. The suspension was heated at 45 °C for 1 h. After cooling to room temperature, *N*-(5-(iodomethyl)-4-phenylthiazol-2-yl)benzenesulfonamide (**26a**) (0.5 g, 1.1 mmol) was added and the mixture was heated at 70 °C overnight.[87] The solvent was evaporated under vacuum and the residue was extracted with CH$_2$Cl$_2$ (50 mL), washed with brine (3 x 25 mL) and H$_2$O (2 x 25 mL). The organic layer was dried (MgSO$_4$) and evaporated under vacuum. The crude product was purified by gradient column chromatography and the pure compound was eluted with 3.5 % MeOH in CH$_2$Cl$_2$.

Yield: 0.02g (5%) as a pale yellow solid.

m.p.: 192-194 °C.

R$_f$: 0.42 (9.5: 0.5 v/v CH$_2$Cl$_2$-MeOH).

¹H NMR (CDCl₃): δ 8.67 (s, 1H, triazole), 8.50 (s, 1H, NH), 8.04 (s, 1H, triazole), 7.73 (d, *J* = 7.5 Hz, 2H, Ar), 7.64-7.59 (m, 3H, Ar), 7.58-7.47 (m, 5H, Ar), 5.14 (s, 2H, C$\underline{H}_2$).

¹³C NMR (CDCl₃): δ 167.29 (C, thiazole), 151.90 (CH, triazole), 143.32 (CH, triazole), 141.69 (C, thiazole), 136.48 (C, Ar), 132.27 (CH, Ar),130.39 (CH, Ar), 129.34 CH x 2, Ar), 128.80 (CH x 2, Ar), 128.71(CH x 2, Ar), 127.62 (C, thiazole), 126.35 (CH x 2, Ar), 112.38 (C, thiazole), 45,53 (CH₂).

Microanalysis (C₁₈H₁₅N₅O₂S₂): Anal. Calcd: C 54.39 %, H 3.80 %, N 17.61 %. Found: C 54.74 %, H 3.83 %, N 17.24 %.

Ethyl 4-methyl-2-((phenoxycarbonyl)amino)thiazole-5-carboxylate (32)
(C₁₄H₁₄N₂O₄S, M.W. 306.34)

(15a) → **(32)**

Pyridine
room temp.,overnight
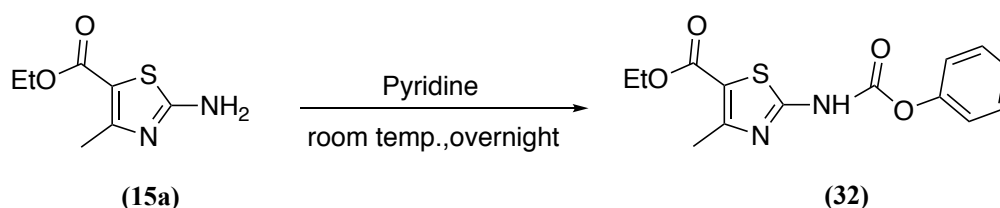
A mixture of ethyl 2-amino-4-methylthiazole-5-carboxylate (**15a**) (0.5 g, 2.68 mmol) and phenyl chloroformate (0.5 g, 3.21 mmol) in dry pyridine (10 mL) was left at room temperature overnight. Then, crushed ice was added to the reaction mixture and the separated solid product was collected by vacuum filtration, washed with H_2O several times, and dried in the vacuum oven at 40 °C overnight.

Yield: 0.02g (5%) as a white solid.

m.p.: 222-224 °C.

R$_f$: 0.6 (2: 1 v/v petrolum ether-EtOAc).

^{1}H NMR (DMSO-d$_6$): δ 12.71 (s, 1H, NH),7.46 (t, J = 7.5 Hz, 2H, Ar),7.33-7.27 (m, 3H, Ar), 4.24 (q, J = 7.6 Hz, 2H, C$\underline{H}_2$CH$_3$), 2.55 (s, 3H, C$\underline{H}_3$), 1.26 (t, J = 7.1 Hz, 3H, CH$_2$C$\underline{H}_3$).

^{13}C NMR (DMSO-d$_6$): δ 176.60 (C, C=O), 162.32 (C, thiazole), 159.51(C, thiazole), 151.12 (C, Ar), 150.45 (C, C=O, Ar), 130.07 (CH x 2, Ar), 126.65 (CH, Ar), 122.16 (CH x 2, Ar), 113.67 (C, thiazole), 61.05 ($\underline{C}$H$_2$), 17.35 ($\underline{C}$H$_3$, thiazole), 14.63 ($\underline{C}$H$_3$).

HPLC (Method A): 100%, RT = 4.7min.

HRMS (ESI, m/z): theoretical mass: 329.0571 [M+Na]$^+$, observed mass: 329.0567 [M+Na]$^+$.

Benzyl (2-amino-2-thioxoethyl)carbamate (38)[117]

($C_{10}H_{12}N_2O_2S$, M.W. 224.28)

(37) **(38)**
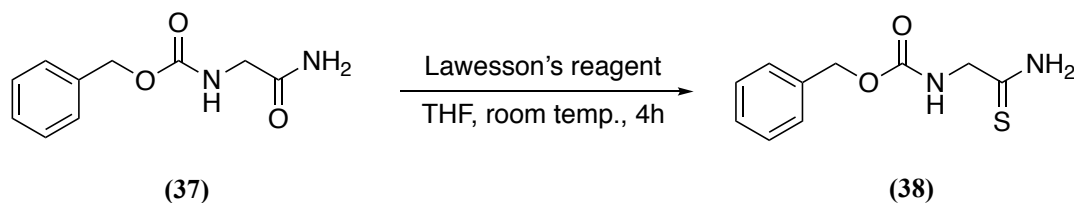
To a solution of Z-Gly-NH$_2$ (**27**) (8.97g, 43.1 mmol) in THF (140 mL) was added (10.5g, 25.95 mmol) of Lawessson's reagent. After stirring for 4 h at 25 °C, the solvent was evaporated under reduced pressure.[117,121] The residue was extracted with EtOAc (100 mL) and washed with 1% aqueous NaOH solution (50 mL). Then, the aqueous layer was extracted with EtOAc (2 x 100 mL) and the combined organic layer washed with brine (3 x 50 mL), dried (MgSO$_4$) and concentrated under reduced pressure to give an orange solid residue, which was washed with diethyl ether to give a white solid pure product.

Yield: 5.27g (80%) as a white solid.

m.p.: 144-146 °C (145- 146 °C)[121].

R$_f$: 0.47 (9.5: 0.5 v/v CH$_2$Cl$_2$-MeOH).

¹H NMR (CDCl₃): δ 9.70 (s, 1H, NH₂), 9.10 (s, 1H, NH₂), 7.54 (t, J = 6.10 Hz, 1H, NH), 7.37-7.31 (m, 5H, Ar), 5.04 (s, 2H, CH₂-Ar), 3.90 (d, J = 6.2 Hz, 2H, CH₂-NH).

Ethyl 2-((((benzyloxy)carbonyl)amino)methyl)-4-phenylthiazole-5-carboxylate (39c)[118] (C₂₁H₂₀N₂O₄S, M.W. 396.46)

(38)   **(13c)**   **(39c)**
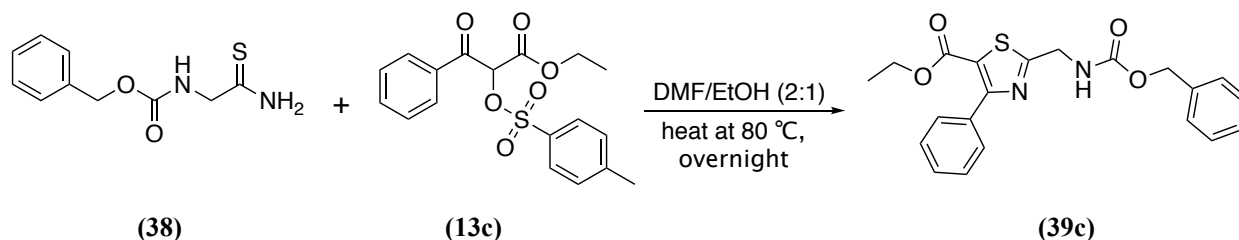
To a stirred solution of enzyl (2-amino-2-thioxoethyl)carbamate (**38**) (0.7g, 3.12 mmol) was added ethyl 3-oxo-3-phenyl-2-(tosyloxy)propanoate (**13c**) (1.69g, 4.68) in a mixture of DMF/EtOH (2:1) (30 mL), then the reaction was heated at 80 °C overnight.[118] After cooling, the solvent was evaporated and the resulted residue dissolved in EtOAc (50 mL), washed with aqueous NaHCO₃ (2x 25 mL), H₂O (2x 25 mL), brine (2x 25 mL) and dried (MgSO₄). The EtOAc was evaporated under reduced pressure to give a dark brown residue, which was purified by gradient column chromatography and the product eluted at 40% EtOAc.

Yield: 0.36g (29 %) as a yellow solid.

m.p.: 126-128 °C (134- 136 °C)[118].

R$_f$: 0.52 (2:1 v/v petroleum ether-EtOAc).

¹H NMR (CDCl₃): δ 8.32 (t, J = 6.0 Hz, 1H, NH), 7.71-7.69 (m, 2H, Ar), 7.45-7.43 (m, 3H, Ar), 7.39-7.36 (m, 5H, Ar), 5.12 (s, 2H, CH₂-Ar), 4.53 (d, J = 6.1 Hz, 2H, CH₂-NH), 4.21(q, J = 7.1 Hz, 2H, CH2CH₃), 1.21 (t, d, J = 7.1 Hz, 3H, CH₂CH₃).

Chapter IV

(Triazole hydroxy-propyl benzamide derivatives)

1. Introduction

The new designed series included a mid-sized series and an extended series in order to provide different/applicable chemistry, more flexible structure, which will allow the occupancy of the "Y-shape" of the enzyme active site as well as direct binding with the haem iron. Even though in the design there is an OH group similar to fluconazole (Figure 7), which in a Tyr132 mutant CaCYP51 strain (e.g. Y132F, Y132H) may result in loss of a key H-bonding interaction at the haem site, the compounds have been designed with functional groups that can form additional binding interactions in the CaCYP51 access channel. The additional binding interactions in the access channel should compensate for the loss of the OH-Tyr132 H-bonding and so retain or improve the binding affinity to CaCYP51. Importantly achieving this goal should also translate to retention of inhibitory activity in Tyr132 resistant strains.

Further development from the phenyl thiazole and thiazole sulfonamide derivatives (series 1 and 2) included the modifications listed below and illustrated in Figure 45, to arrive at the new designed triazole hydroxy-propyl benzamide derivatives (mid-sized and extended):

1. An amide linker in order to improve the flexibility of the compounds.
2. The aryl ring at position 2 of the amide linker is important for the hydrophobic binding at the enzyme active site. R^1 and R^2 are different halide substitutions to explore the structure-activity relationship (SAR).
3. A triazole with a CH_2 linker was kept because of the coordination with the haem iron as well as to obtain better selectivity for CaCYP51.
4. A bulky group after the linker could be a substituted phenyl/ thiazole ring to provide more binding interactions with different amino acids in the enzyme active site.
5. For the extended series, different linkers were added to explore the effects on binding affinity and activity against fungal strains as well as to allow the occupancy of the access channel, which might result in counteracting the fluconazole resistance by forming additional binding interactions with amino acids in the access channel. The linkers investigated were thiourea, amide and urea at position 4 of the benzamide ring.
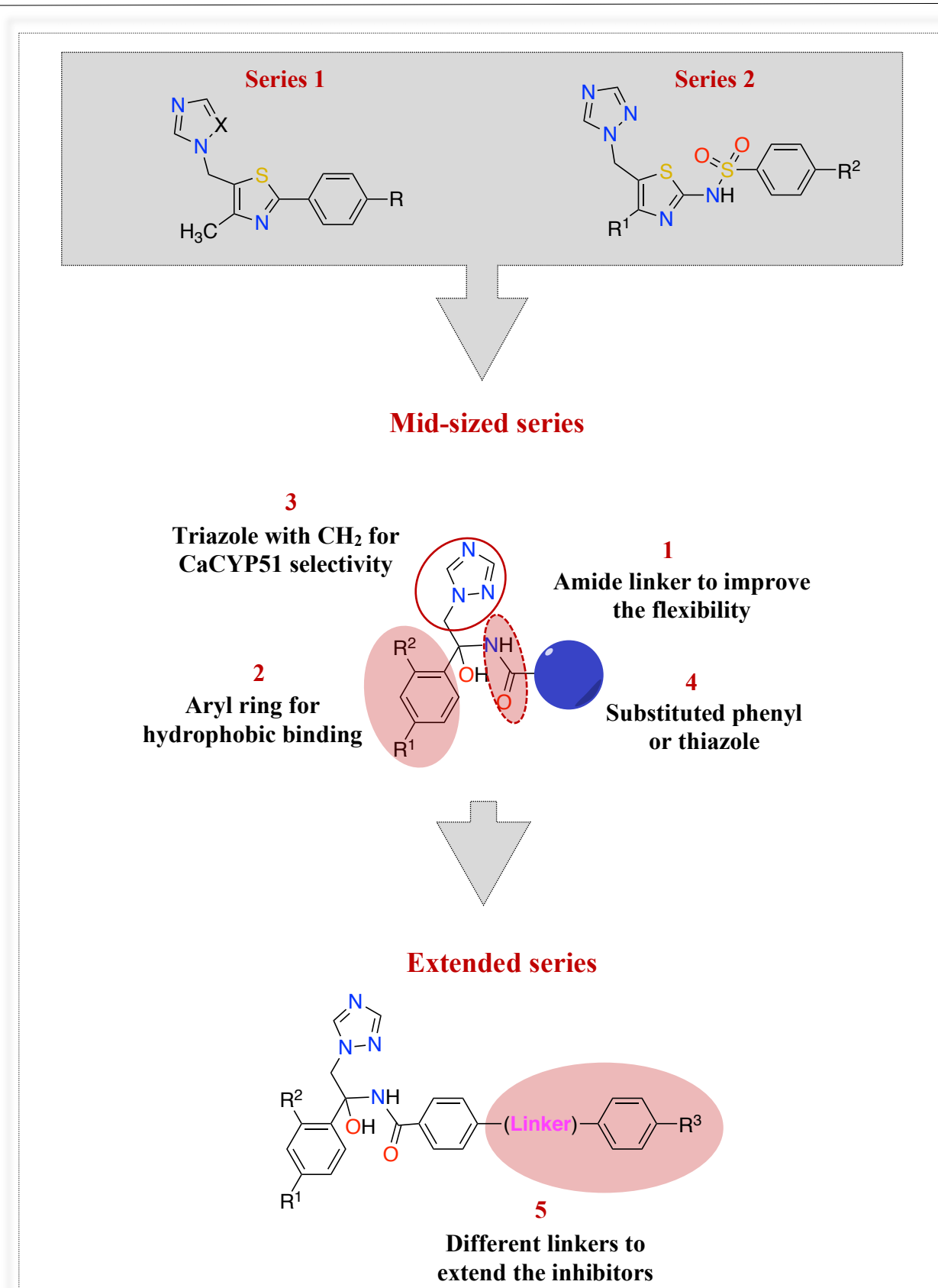
Figure 45: Modification from phenyl thiazole and thiazole sulfonamide derivatives (series 1 and 2) leading to general structures of triazole propyl benzamide mid-sized and extended derivatives.

2. Result and discussion

a. Computational studies:

1. Molecular dynamic simulation (MD):

The design of the novel inhibitors included a stereocentre (a chiral atom), thus the MD simulations of the ligand-CaCYP51complexes included both (*R*)- and (*S*)-configurations. MD simulations were performed on the mid-sized and extended derivatives using wild-type (CaCYP51), and for some of the extended derivatives using the double mutants (Y132H/K143R and Y132F/F145L). The ligand-protein complexes were subjected to 200 ns MD simulation to explore fit and binding interactions.

a. Wild type MD simulation for mid-sized derivatives:

The binding profile of the (*R*)- and (*S*)-configurations of the acetyl derivative (**46b**), is shown (Figure 46) as an example. Both enantiomers of **46b** showed direct binding between the triazole N and the haem iron with ≥ 99% interaction during the 200 ns simulation (Figure 46). Both enantiomers showed a water-mediated binding interaction between the OH and Gly307 and π-π stacking with Tyr132. Only (*S*)-**46b** formed water mediated H-bonding with Met508 and Tyr132 as well as π-π stacking with Phe380 (Figure 46). Similar binding interactions were observed for all mid-sized derivatives.

2D-(*R*)-46b
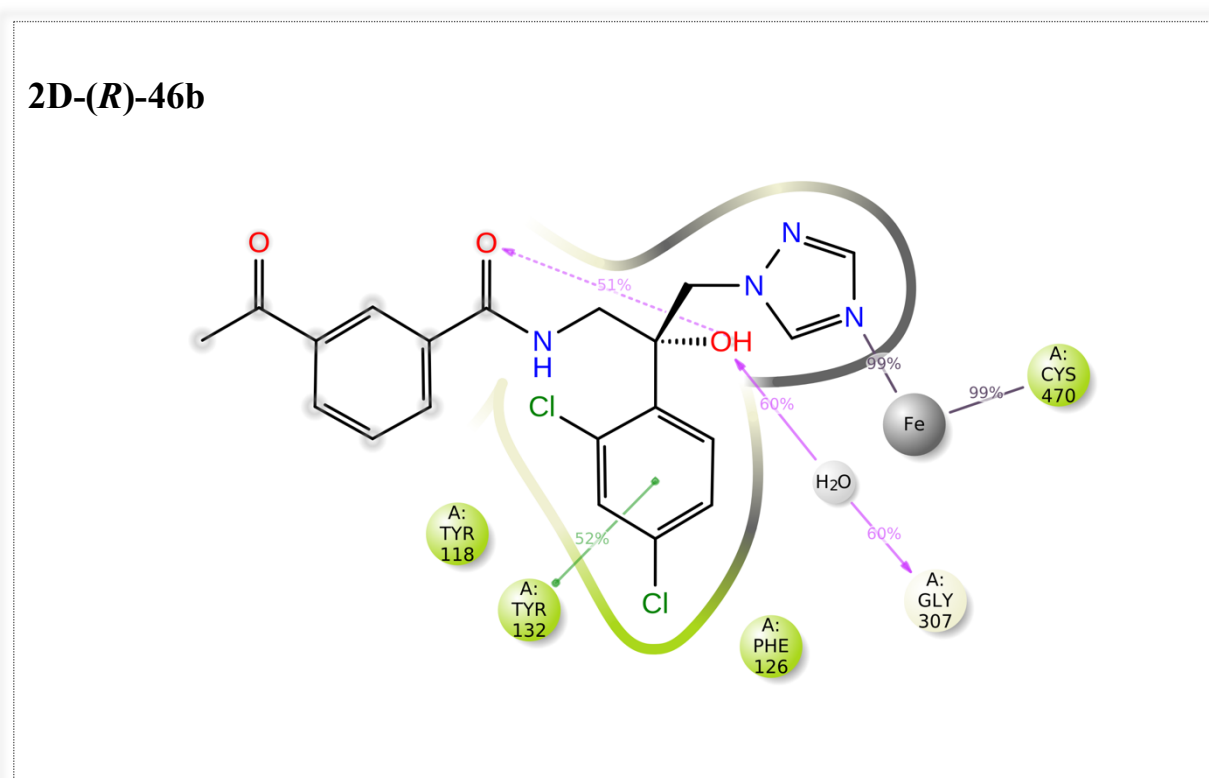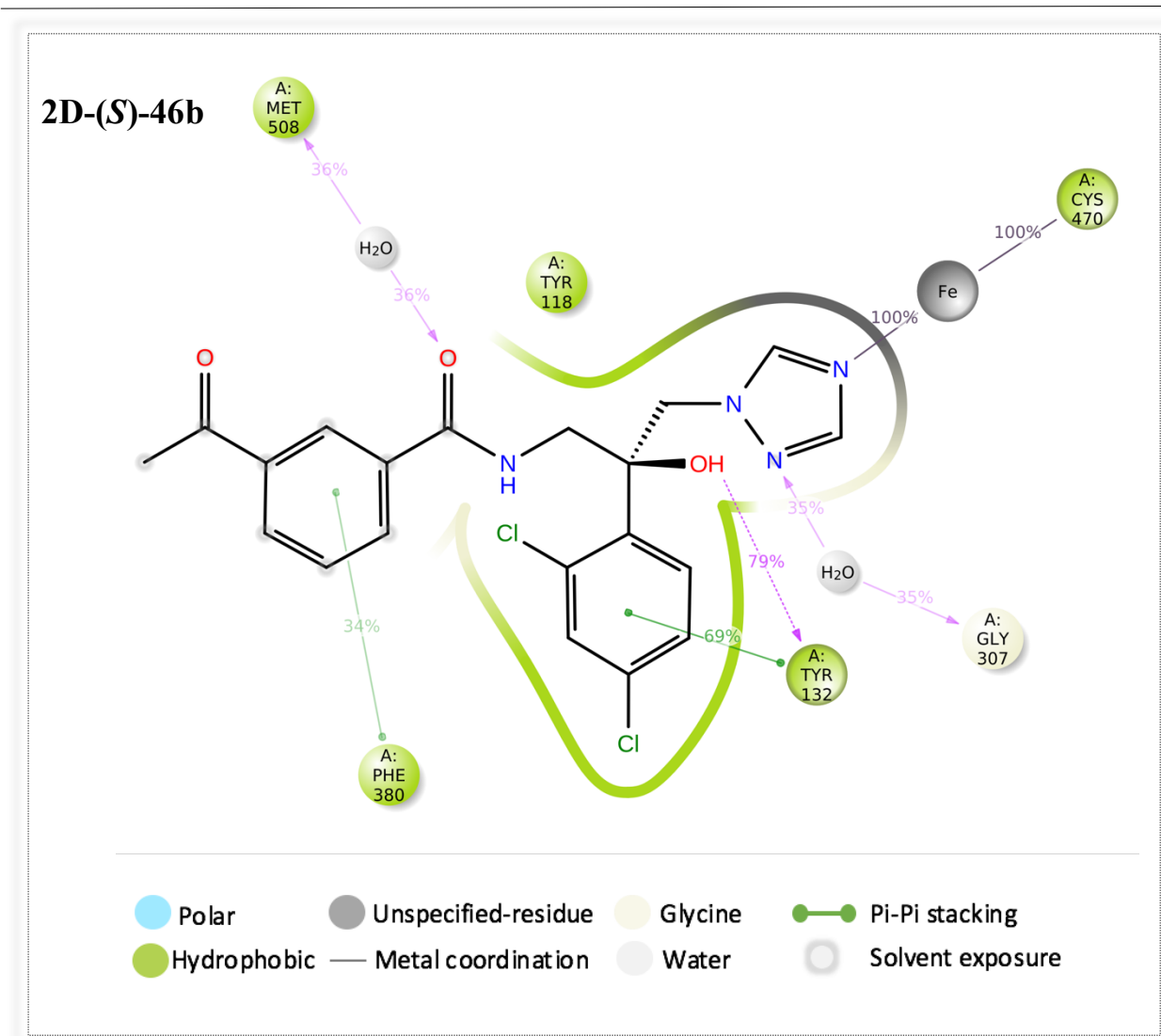
Figure 46: 2D of (*R*)-**46b** and (*S*)-**46b** interactions with CaCYP51 key residues. Interactions that occur more than 30.0% of the simulation time in the selected trajectory (0.00 through 200.00 ns are shown.

As shown in Table 23, the RMSD for the (*R*)-**46b** CaCYP51 complex started at 0.95 Å and rapidly equilibrated with a final RMSD of 1.89 Å at 200 ns. Similarly, the RMSD for (*S*)-**46b** -CaCYP51 complex showed high stability during the 200 ns MD simulation and the ligand RMSD started from 1.56 Å and rapidly reached the equilibrium plateau with a final RMSD of 1.02 Å at 200 ns. The RMSD protein-ligand plot of (*R*)-**46b** and (*S*)-**46b** CaCYP51 complexes illustrated the high stability of the complexes (Figure 47). Again, this stability was observed for all mid-sized derivatives.

Table 23: Protein-ligand complex RMSD (Å) at 0 and 200 ns for (*R*) and (*S*)-**46b**.

Ligand -complex	RMSD (Å) at 0 ns		RMSD (Å) at 200 ns	
	CaCYP51	**Ligand**	**CaCYP51**	**Ligand**
(*R*)-**46b**	1.11	0.95	2.21	1.89
(*S*)-**46b**	1.35	1.56	2.08	1.02
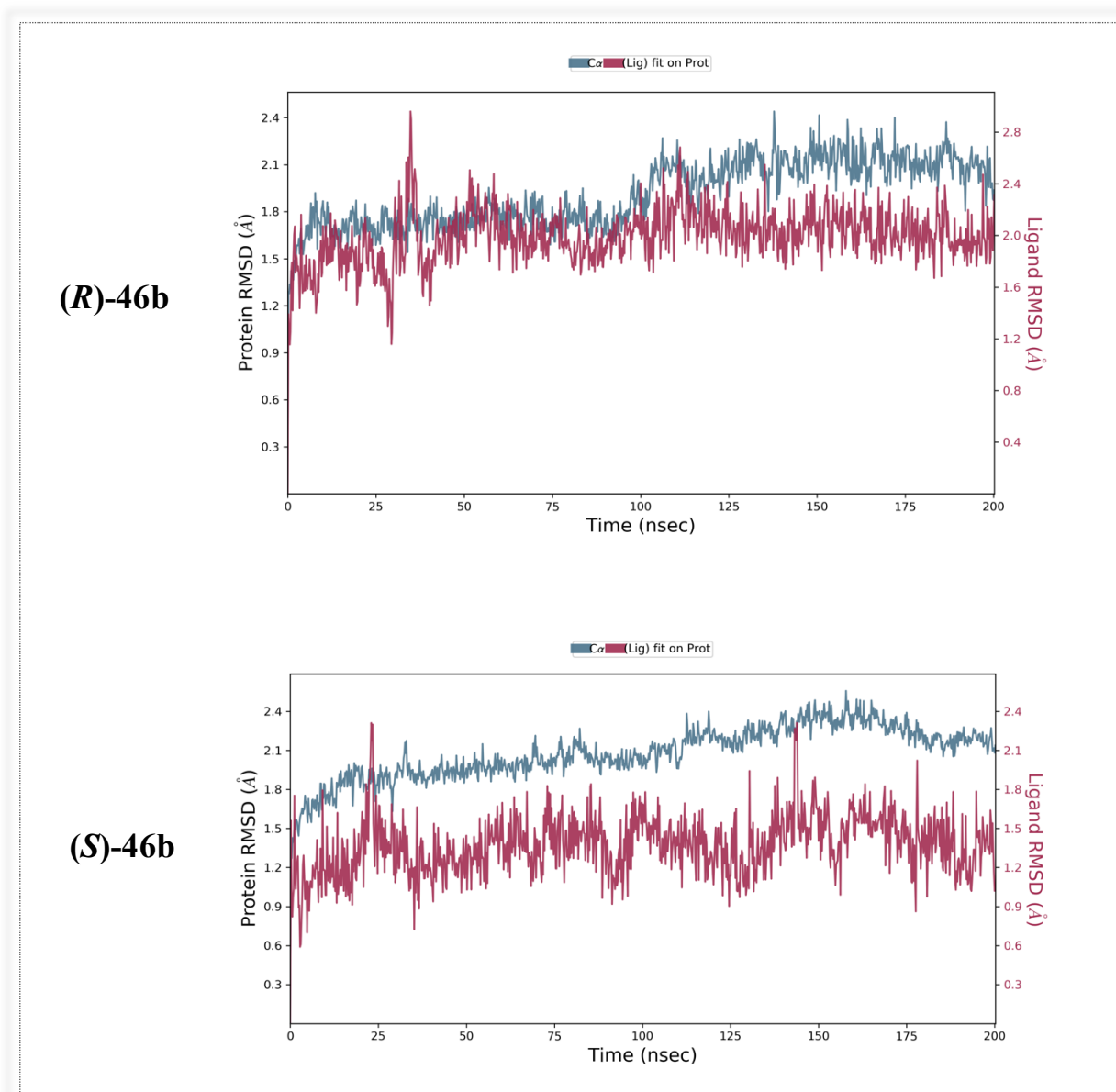
Figure 47: Protein-ligand RMSD of CaCYP51-(*R*)-**46b** and CaCYP51-(*S*)-**46b** complexes over 200 ns MD simulation.

b. Wild type MD simulation for extended derivatives:

For the thiourea and urea derivatives, the ligand-CaCYP51 wild-type complexes (*S*)-enantiomers were the most stable during the 200 ns simulation time and interacted directly with the haem iron. In contrast, for the amide derivatives both (*S*)- and (*R*)-enantiomers were stable. The binding profile for the (*S*)-enantiomers of the thiourea and urea derivatives were similar. Compounds **53a** and **55a** were used as examples for both linkers (Figure 48). Both compounds showed direct binding between the triazole N and the Fe^{3+} with > 99% interactions during the 200 ns MD simulation. Moreover, a direct H-bond interaction between the NH of the linkers and Ser378 was observed as well as hydrophobic interactions with Met508, Pro230, Tyr64 and Tyr118.
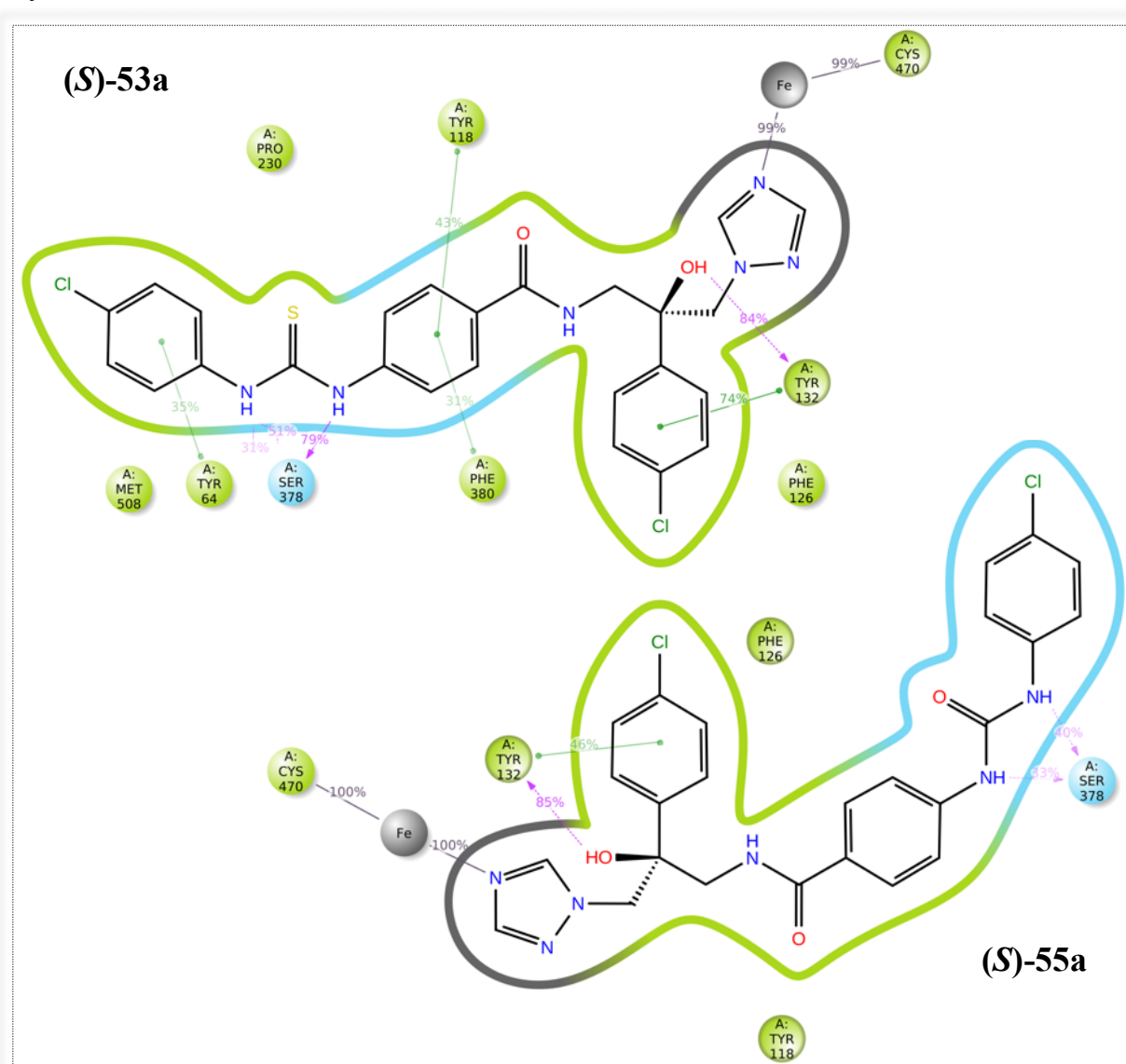
Figure 48: 2D of (*R*)-**53a** and (*S*)-**55a** interactions with CaCYP51 key residues. Interactions that occur more than 30.0% of the simulation time in the selected trajectory (0.00 through 200.00 ns) are shown.

c. Double mutant MD simulation for extended derivatives:

Some of the novel extended compounds showed promising MD results in the double mutant CaCYP51(Y132H/K143R and Y132F/F145L) complexes during the 200 ns MD simulation. In the double mutant Y132H/K143R, the (*R*)- and (*S*)-enantiomers of compound **57c** formed hydrophobic interactions with Tyr118 for both enantiomers, Phe126 for (*S*)-**57c**, and Phe380, Pro230 for (*R*)-**57c** (Figures 49 and 50). The (*S*)-enantiomer formed π-π stacking with His377 while the (*R*)-enantiomer formed π-π stacking with His310 and Phe233. Moreover, the (*S*)-enantiomer showed water mediated H-bonding between the NH of the amide and Ser378. In contrast, the (*R*)-enantiomer showed indirect H-bonding between the carbonyl O and His468, His377, Ser378 and Met508. Importantly, the interaction between the Fe^{3+} and the triazole N in both configurations occurred 100% of the simulation time, suggesting tight binding with the haem active site (Figure 50).
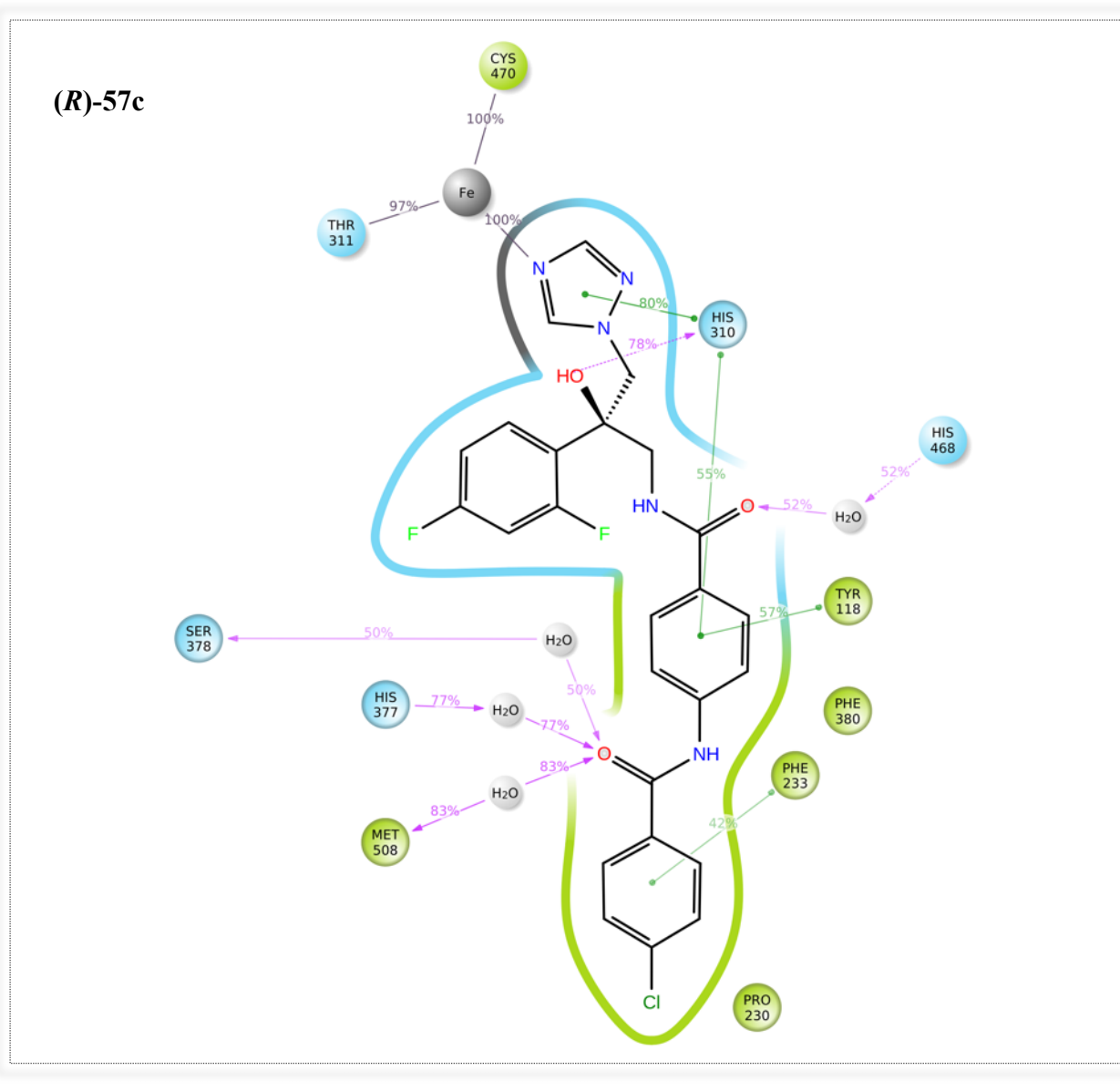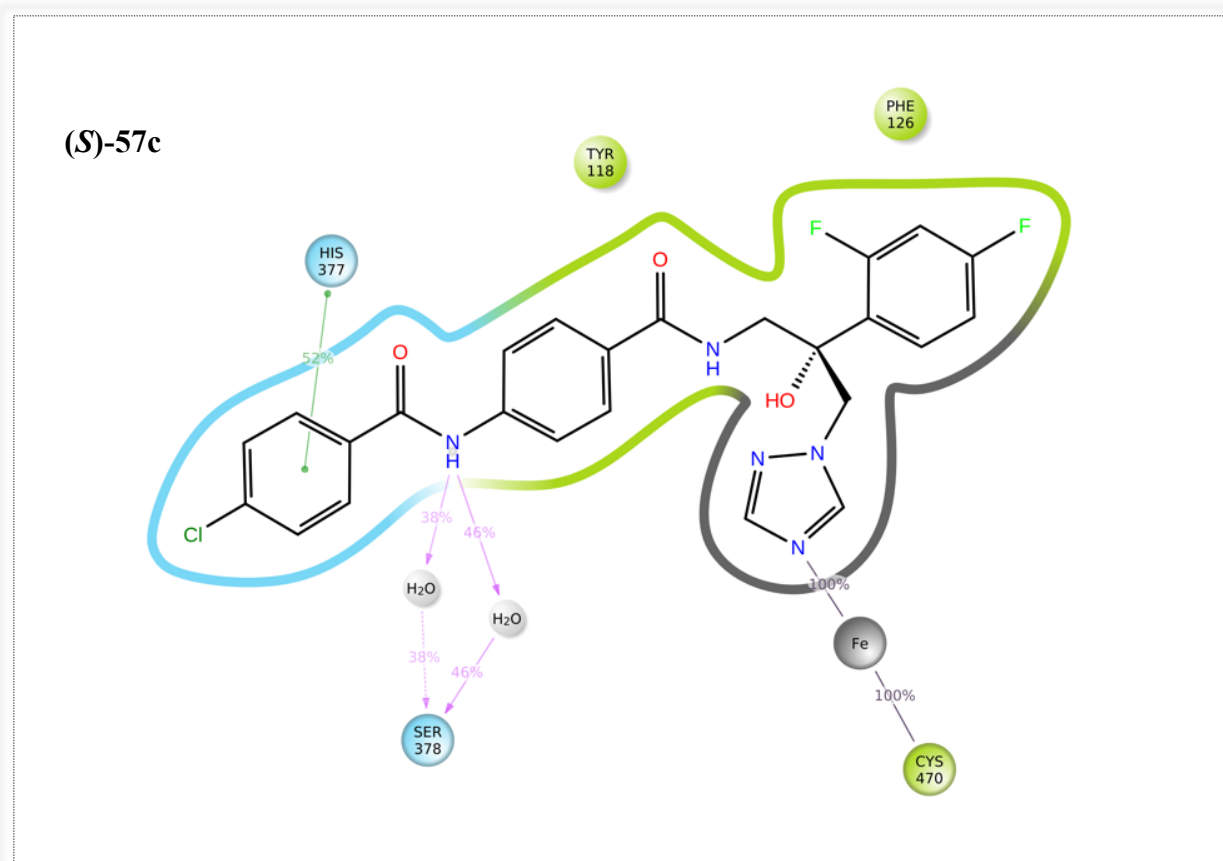
Figure 49: A schematic of detailed ligand atom interactions of (*R*)-and (*S*)-**57c** with the protein residues of the CaCYP51 double mutant Y132H/K143R. Interactions that occur more than 30.0% of the simulation time in the selected trajectory (0.00 through 200.00 ns) are shown.
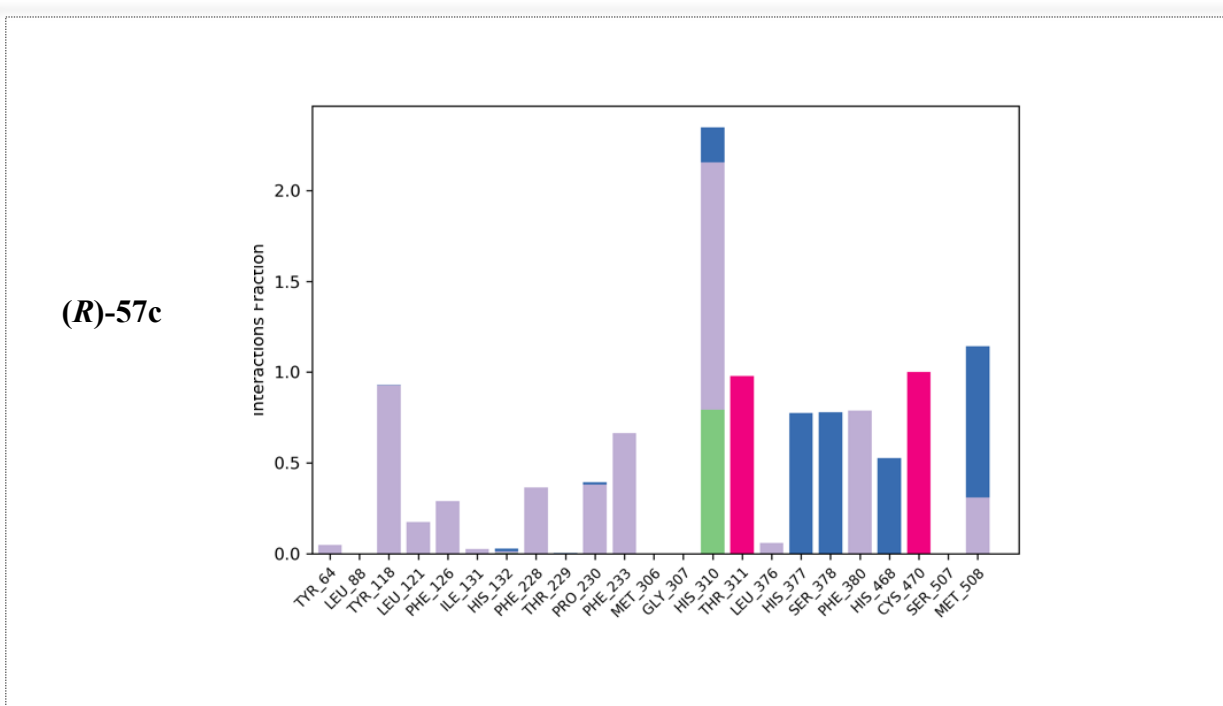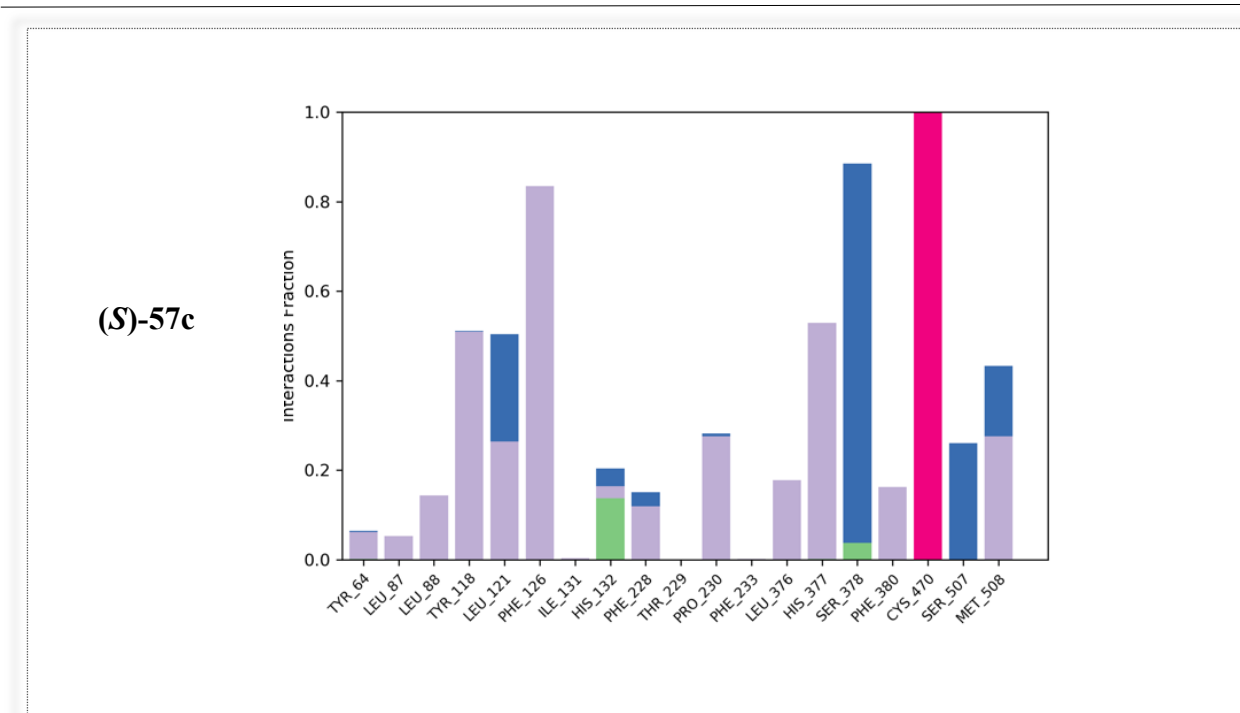
(S)-57c

Figure 50: A schematic of detailed ligand atom interactions of (*R*) and (*S*)- **57c** with the protein residues of the CaCYP51 double mutant Y132H/K143R. Interactions that occur more than 30.0% of the simulation time in the selected trajectory (0.00 through 200.00 ns) are shown. (Hydrophobic (purple), water bridges (blue), H-bonds (green), ionic (pink)).

The most promising configuration of compound **57c** during the molecular dynamic studies of the double mutant Y132F/F145L was the (*R*)-enantiomer. The binding profile of (*R*)-**57c** in the Y132F/F145L mutant showed hydrophobic interactions with Tyr64, Phe132, and Pro230 as well as water mediated H-bonding between the NH of the amide and Ser507 (Figures 51 and 52). In addition, both enantiomers of compound **57c** formed π-π stacking with His377, and with Tyr118 for (*S*)-**57c**. The (*S*)-enantiomer showed a water mediated H-bonding interaction with Ser378 40% of the simulation time (Figures 51 and 52). Interestingly, the interaction between the Fe^{3+} and the triazole N occurred 100% of the simulation time for the (*R*)-**57c** and 52% of the simulation time for (*S*)-**57c**. In the case of (*S*)-**57c**, haem binding was not observed in the final frame.
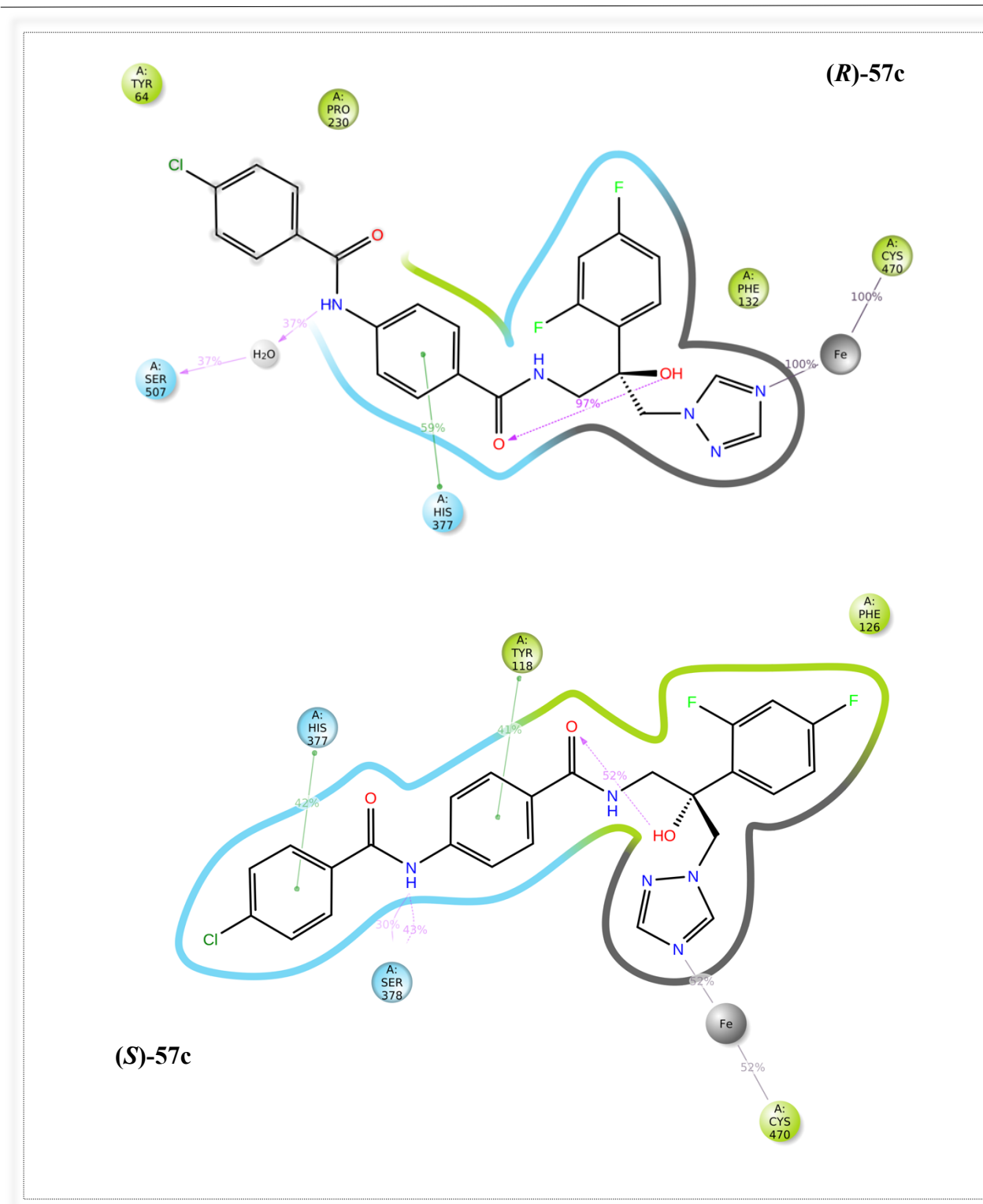
Figure 51: A schematic of detailed ligand atom interactions of (*R*) and (*S*)- **57c** with the protein residues of the CaCYP51 double mutant Y132F/F145L. Interactions that occur more than 30.0% of the simulation time in the selected trajectory (0.00 through 200.00 ns) are shown.
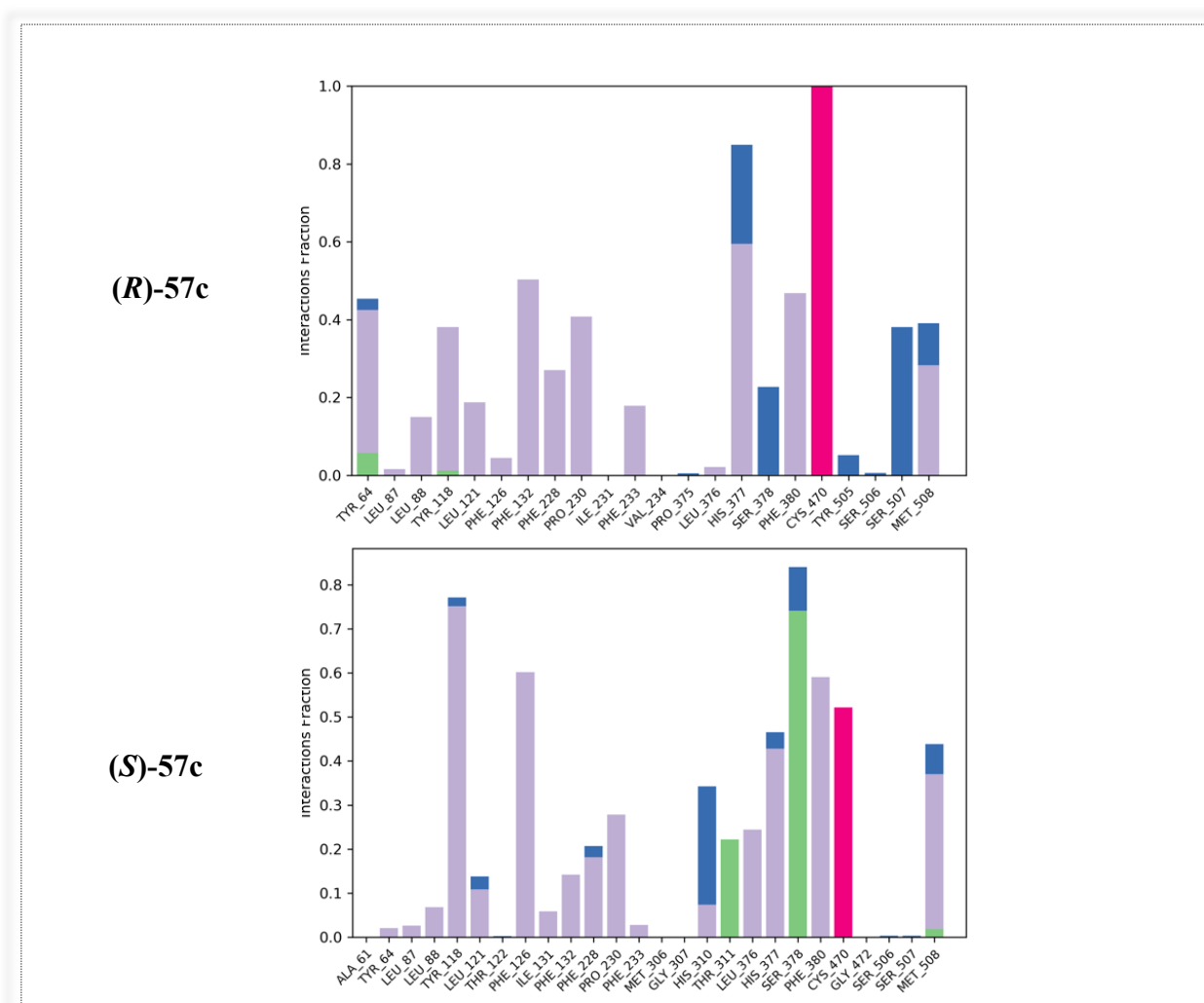
Figure 52: A schematic of detailed ligand atom interactions of the (R)- and (S)-**57c** with the protein residues of the double mutant Y132F/F145L. Interactions that occur more than 30.0% of the simulation time in the selected trajectory (0.00 through 100.00 ns) are shown. (Hydrophobic(purple), water bridges (blue), H-bonds (green), ionic (pink)).

2. Molecular modelling (MOE):

The MOE program was used to visualise the fit and binding interactions of the inhibitors within the CaCYP51 protein after the MD simulation and using the final frame result of the exemplar derivatives that were discussed in the MD section.

a. Wild type (MOE) for mid-sized derivatives:

The binding interactions of the final frame profile of the (*R*)- and (*S*)-enantiomers of the acetyl derivative (**46b**) showed good fit and binding interactions with different amino acids of the wild type CaCYP51 protein. Water mediated H-bonding was observed with Gly307 and Ser378 for (*R*)-(**46b**) and Met508 for (*S*)-(**46b**). Both enantiomers formed multiple hydrophobic interactions with Leu121, Ile131, Thr311, Ile304, Phe380, Leu376, His377 and Phe126 (Figure 53). The 3D visualisation illustrated the binding distance between the triazole N and the haem Fe^{3+}, which was 2.47 Å for (*R*)-**46b** and 2.43 Å for (*S*)-**46b** as shown in Figure 53.
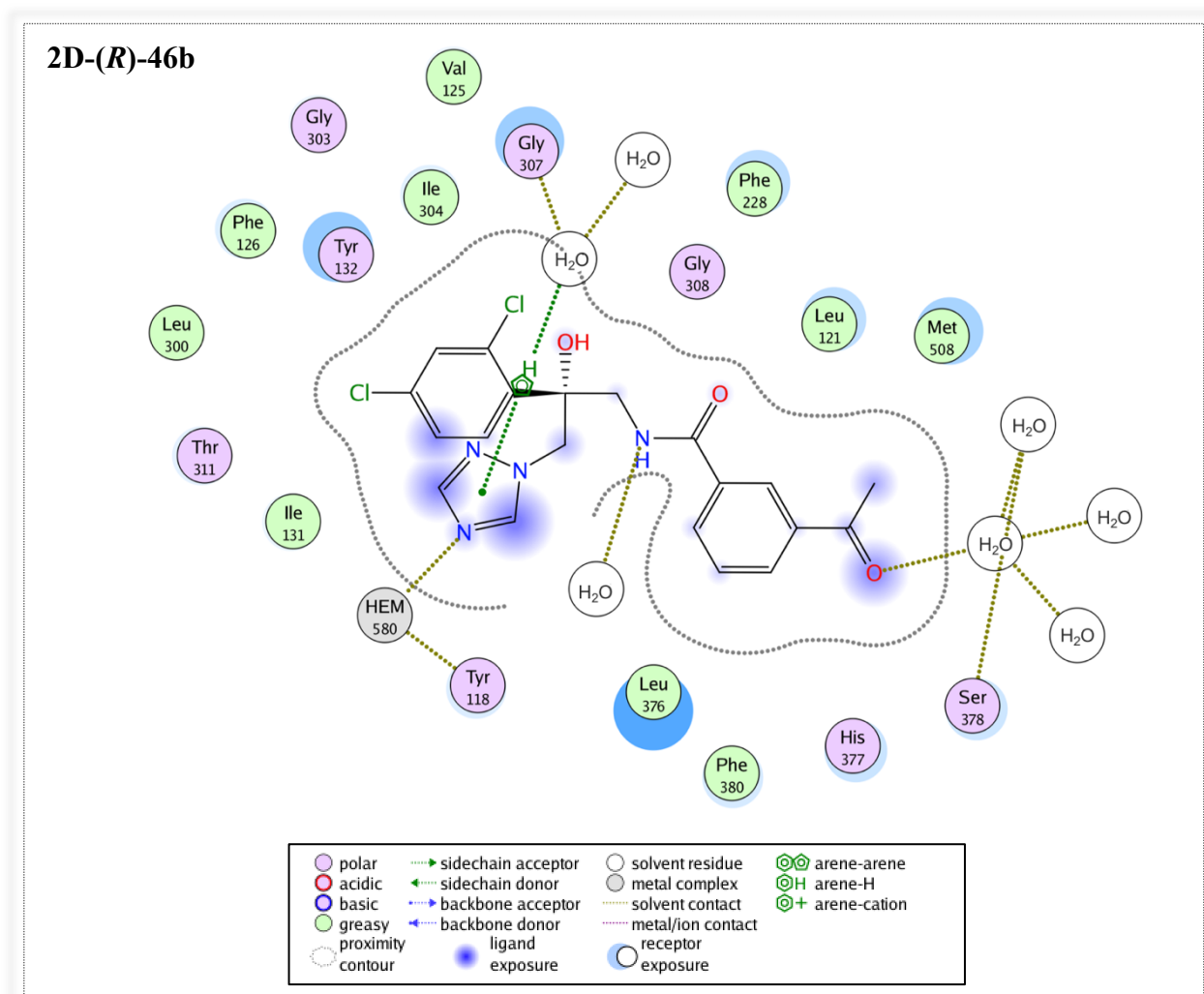
2D-(*S*)-46b
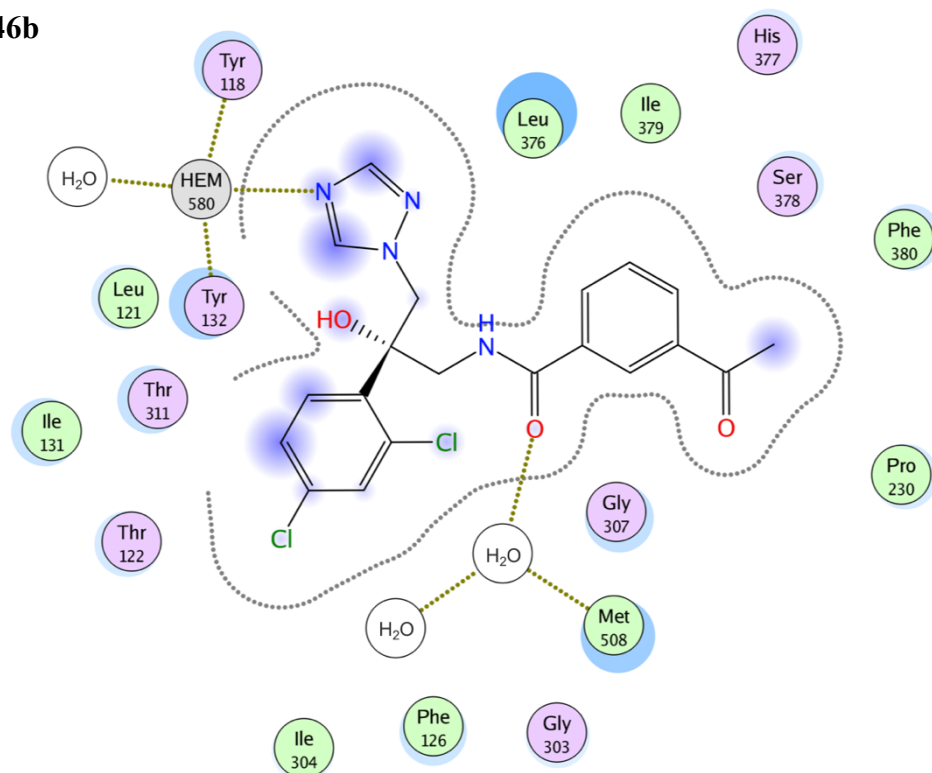
3D-(*R*)-46b
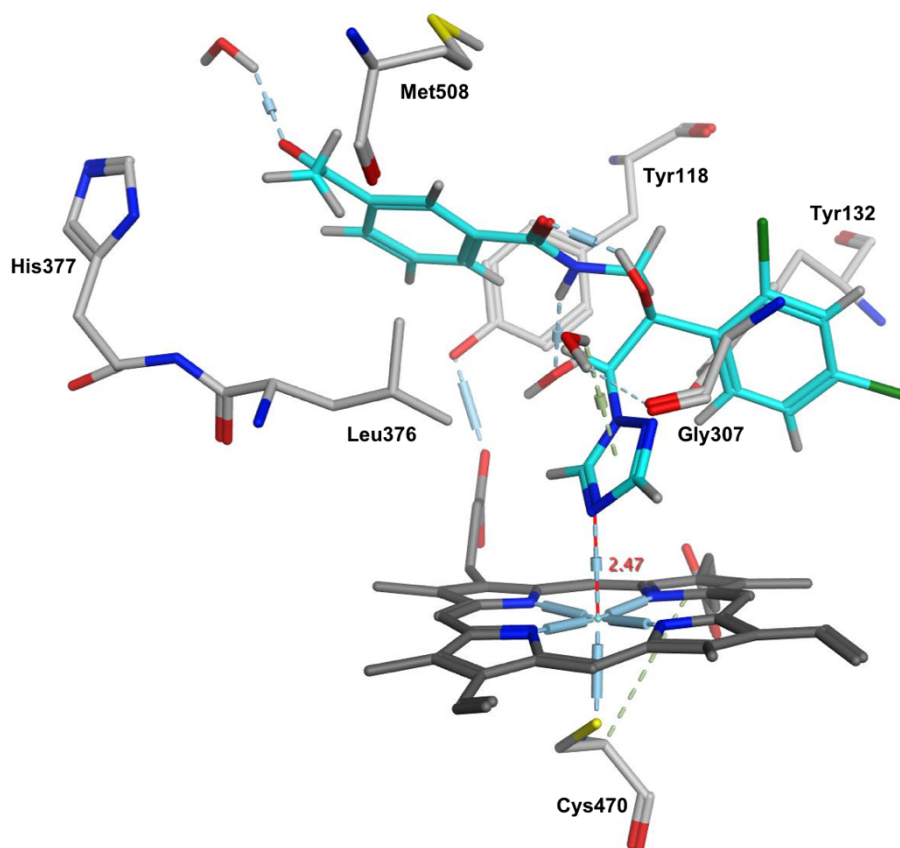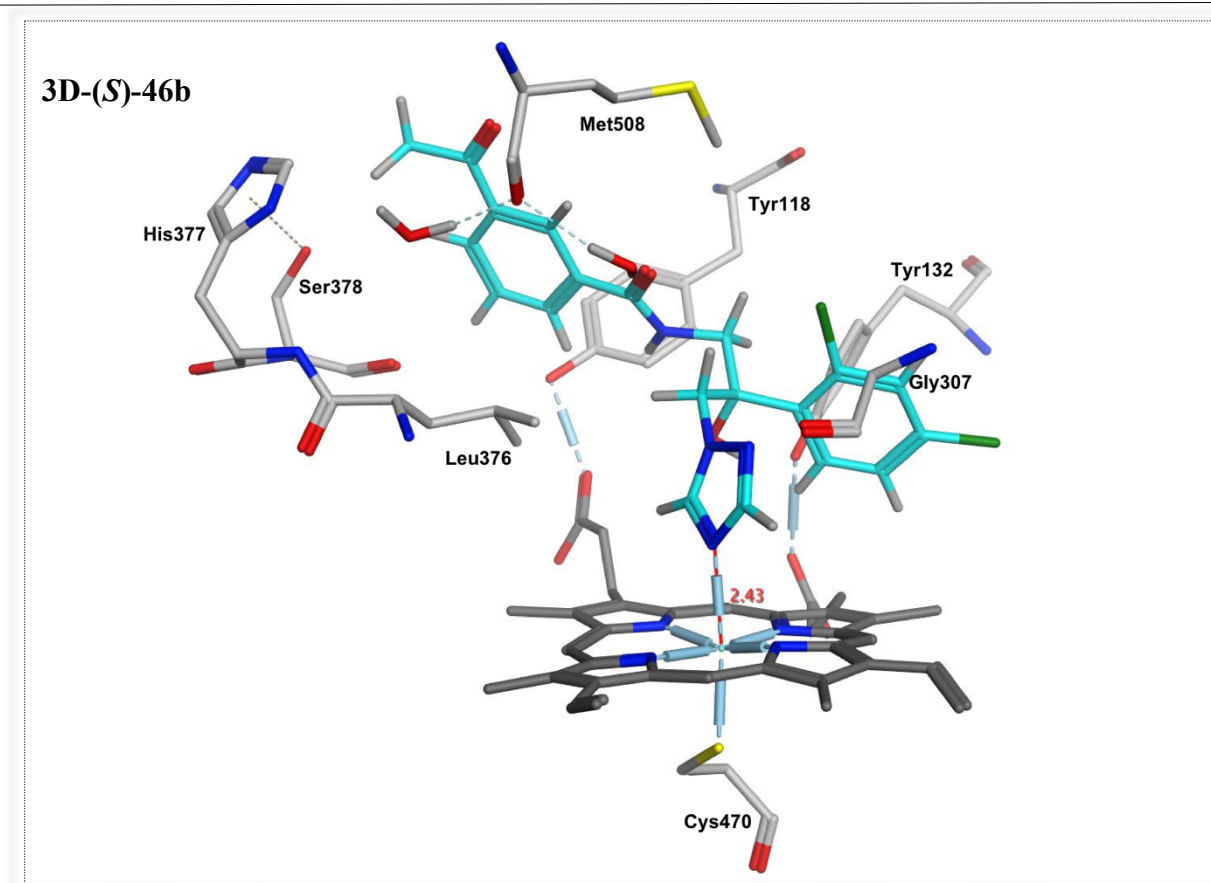
Figure 53: 2D ligplot illustrating binding interactions with amino acids residues of (*R*)- and (*S*)-**46b** MD final frame and 3D image illustrating the perpendicular binding between the N-atom of the triazole and the haem iron with a distance of 2.47 Å for (*R*)-**46b** and 2.43 Å for (*S*)-**46b**.

b. Wild type (MOE) for extended derivatives:

The main aim in the design of the extended series was to allow greater occupancy of the access channel and to overcome resistance arising, in particular, from Tyr132 mutations.

The final frame of the (*S*)-enantiomer of compound **53a** in MOE showed direct binding between the triazole N and the haem Fe^{3+} and water mediated binding interactions between Leu121 and the carbonyl O of the amide group and direct H-bonding between Ser378 and the amide NH as well as another direct hydrogen bonding interaction between the S of the thiourea and Pro230. In addition, the triazole ring formed arene-H binding with Leu376, also multiple hydrophobic interactions with several amino acids within the haem binding pocket and the access channel (Ala61, Tyr64, Tyr505, Leu88, Leu87, Met508, His377, Phe380, Phe228, Phe126, Ile304, Tyr132, Gly307, Ile131, Thr311, Tyr118and Thr122) were observed (Figure 54). As shown in the 3D visualisation in Figure 54, compound **53a** binds perpendicularly with the haem iron and the distance between the triazole nitrogen and the haem iron was 2.40 Å.
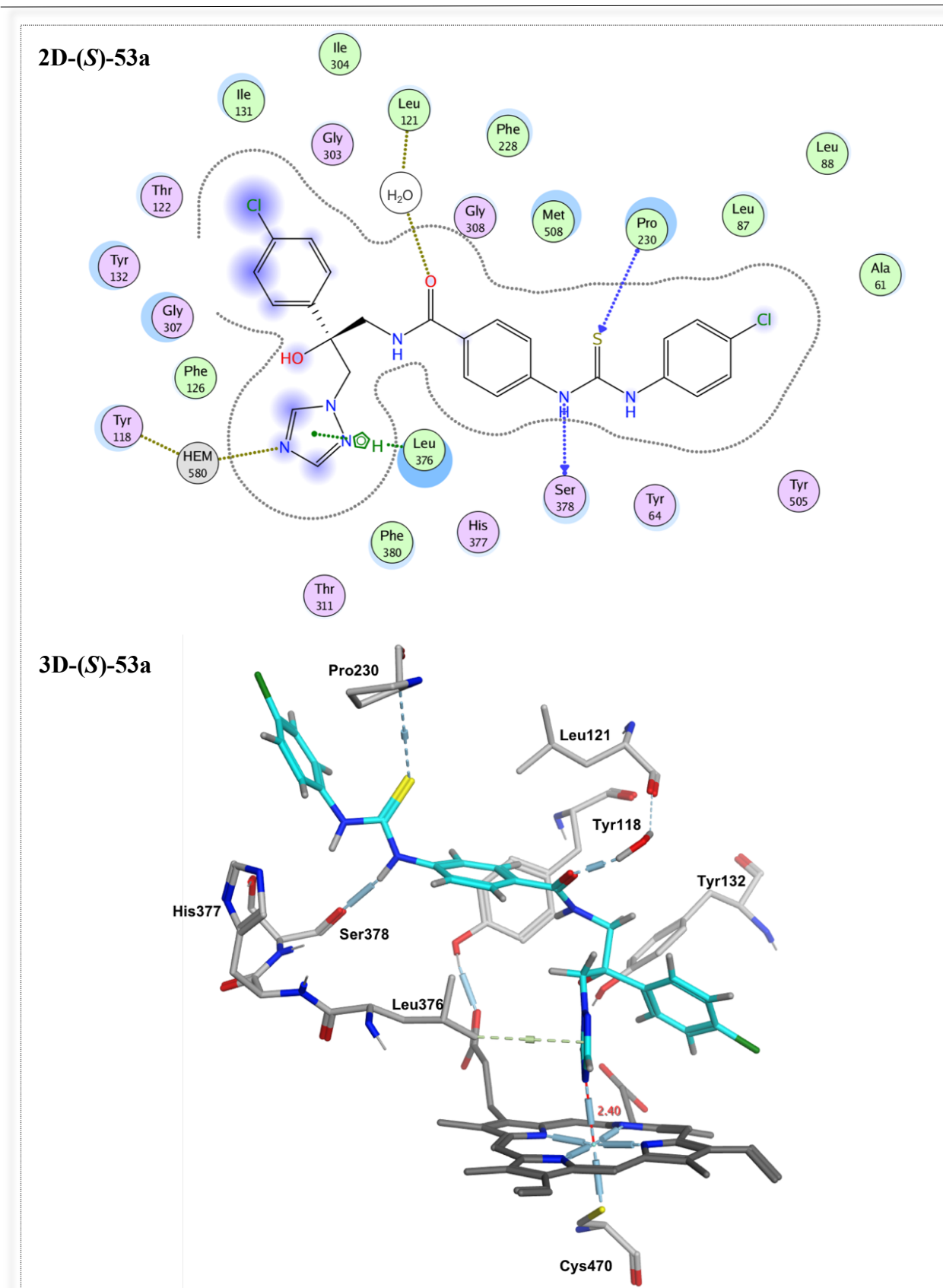
Figure 54: 2D ligplot illustrating binding interactions with CaCYP51 amino acids residues and (*S*)-**53a** MD final frame and 3D image illustrating the perpendicular binding between the N atom of the triazole and the haem iron with a distance of 2.40 Å.

(*S*)-**55a**, with the urea linker showed multiple interactions with water molecules as well as water mediated H-bonding with Ser378, His377 and Met508. Moreover, two direct hydrogen bonds, one between NH of the urea and Ser378 and the other between Tyr132 and the OH at the chiral center were observed. The inhibitor formed hydrophobic interaction with more than 15 amino acids within the haem binding pocket and the access channel (Figure 55). As shown in the 3D visualisation, the distance between the triazole N and the haem iron was 2.47 Å (Figure 55).
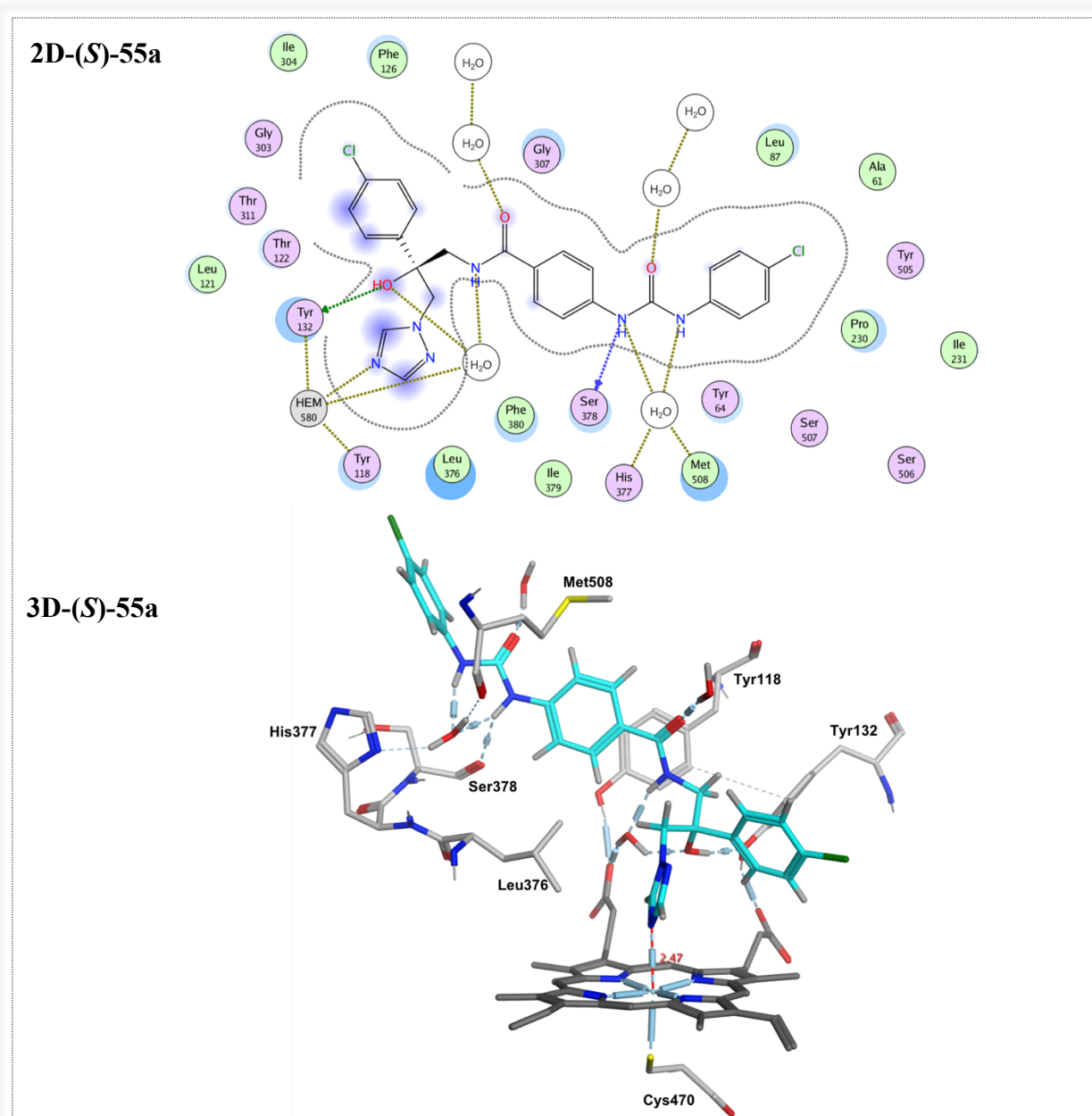
Figure 55: 2D ligplot illustrating binding interactions of CaCYP51 amino acid residues and (*S*)-**55a** MD final frame and 3D image illustrating the perpendicular binding between the N atom of the triazole and the haem iron with a distance of 2.47 Å.

c. Double mutant (MOE) for extended derivatives:

Single, double, triple or even quadruple mutations to CaCYP51 play a significant role in changing the conformation of the enzyme.[13,81,106] A study reported that single mutations such as Ser279 to Phe (S279F) lowered the binding affinity of fluconazole to the haem, and fluconazole lost the key hydrogen bonding with Tyr132.[122] Moreover, double mutations in CaCYP51 such as Y132H/K143R and Y132F/F145L changed the binding affinity to current azole medications especially with fluconazole and increased the IC_{50} value.[14,52] These studies suggested that conformational changes, which occur from different mutations, significantly affect the binding between the triazole nitrogen and haem iron as well as distort the key H-bonding interactions.[14,52,122]

Interestingly, the final frame of the (*R*)-and (*S*)-enantiomers of the amide linker (**57c**) in the double mutant Y132H/K143R showed promising results. Both configurations showed water mediated H-bonding with His468, Thr122 and Met306 for (*R*)-**57c** and with Met508, Ser378 and Ser507 for (*S*)-**57c**. Only the (*R*)-**57c** formed arene-arene interactions with Tyr118 and arene-H binding with Phe233 and Met508. There are 13 amino acids that interacted hydrophobically with (*R*)-**57c**, while there were 20 with (*S*)-**57c** (Figure 56). (*R*)-**57c** showed binding interaction between the triazole N and the haem Fe^{3+} with a distance of 2.36 Å while for (*S*)-**57c** the distance observed was 2.19 Å (Figure 56). This could be a promising design for Y132H/K143R mutant CaCYP51, which would hopefully overcome fluconazole resistance in *C. albicans* mutant strains.
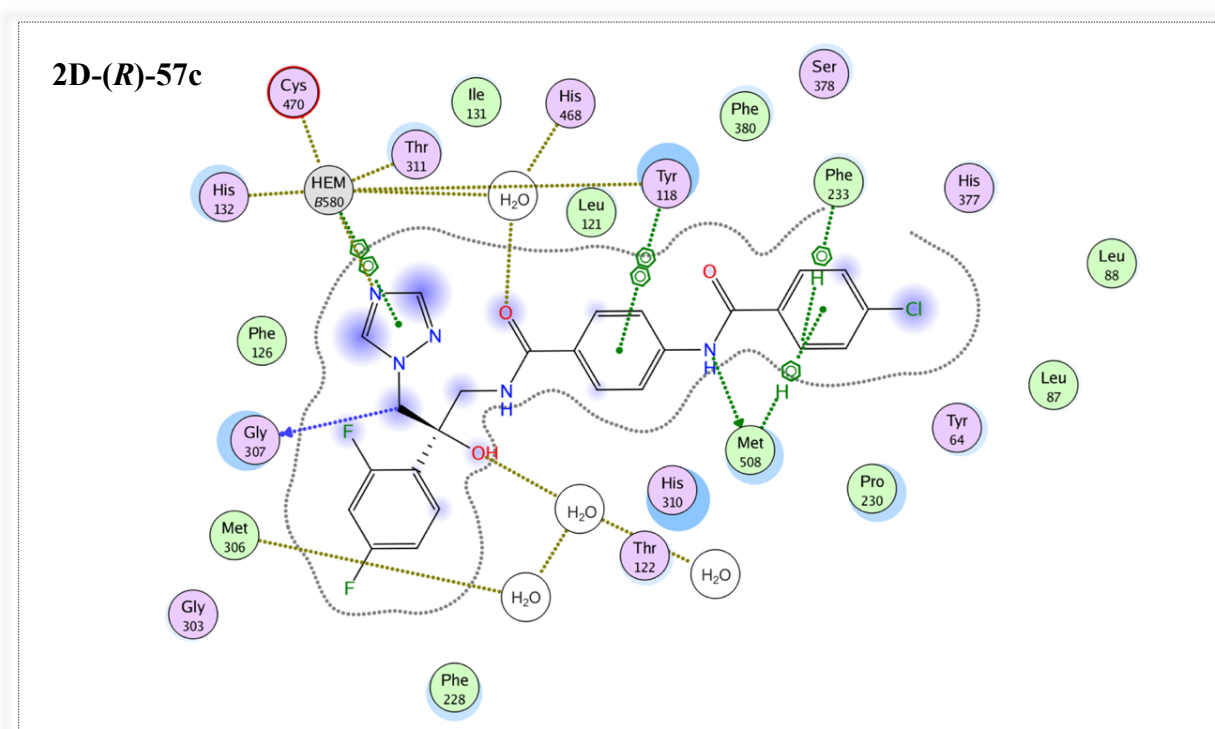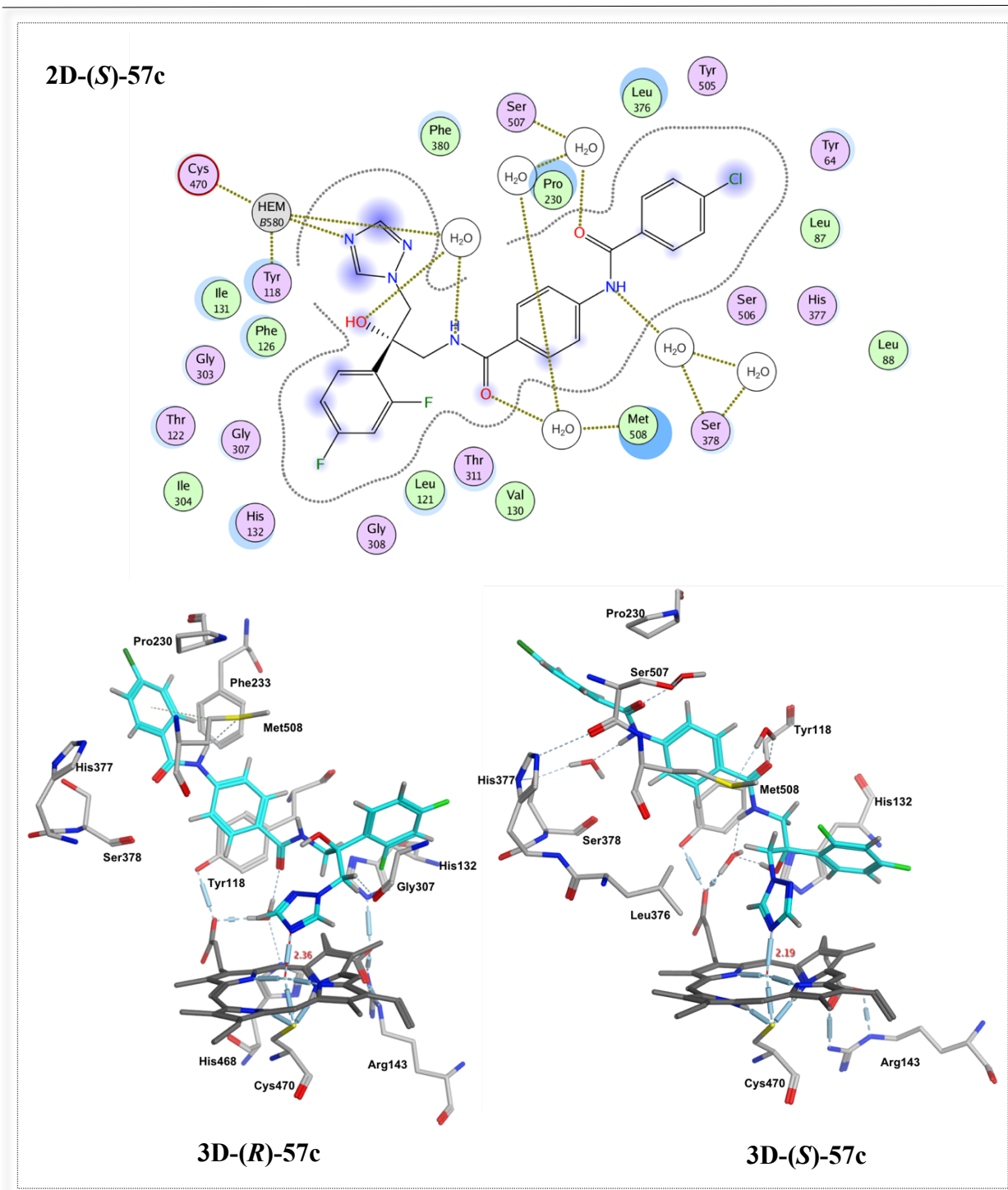
Figure 56: 2D ligplot illustrating binding interactions with the protein residues of the CaCYP51 double mutant Y132H/K143R. (*R*)- and (*S*)-**57c** MD final frame and 3D image illustrating the perpendicular binding between the N atom of the triazole and the haem iron.

On the other hand, (*R*)-**57c** in the double mutant Y132F/F145L was more promising than (*S*)-**57c**. As shown in the 2D and 3D Figures, (*R*)-**57c** binds directly to the haem Fe^{3+} with a distance of 2.29 Å while (*S*)-**57c** lost the binding between the triazole N and the haem iron.

This may be owing to the distortion of the haem as illustrated in Figure 57. (*R*)-**57c** showed water mediated H-bonding with Ser378, Ser507 and Met508 as well as multiple hydrophobic interactions with different amino acids located at the haem binding cavity and at the access channel. Even though the direct binding with the haem iron for (*S*)-**57c** was lost, arene-H binding with Met508 and His377 as well as direct H-bonding with Ser378 was observed (Figure 57)
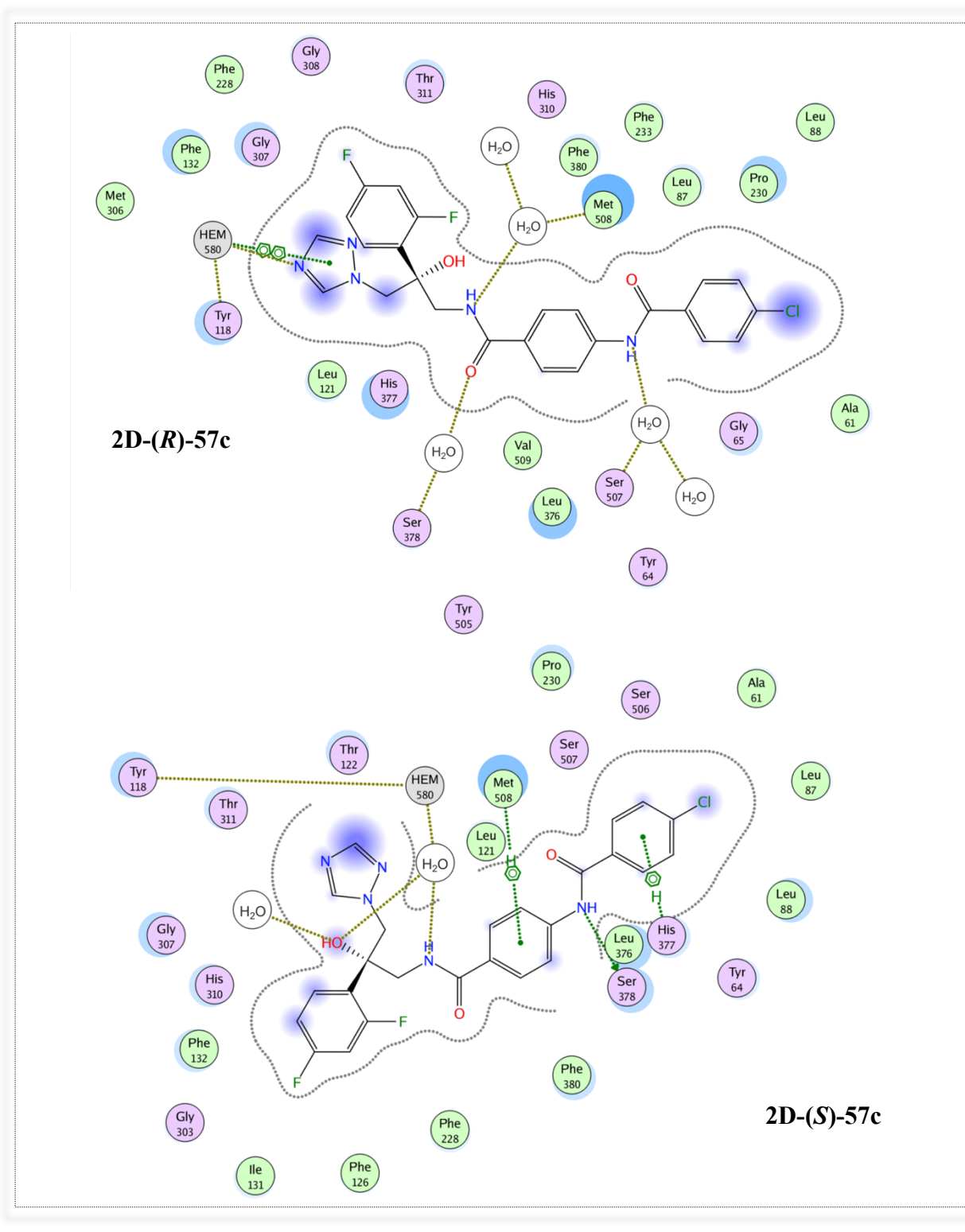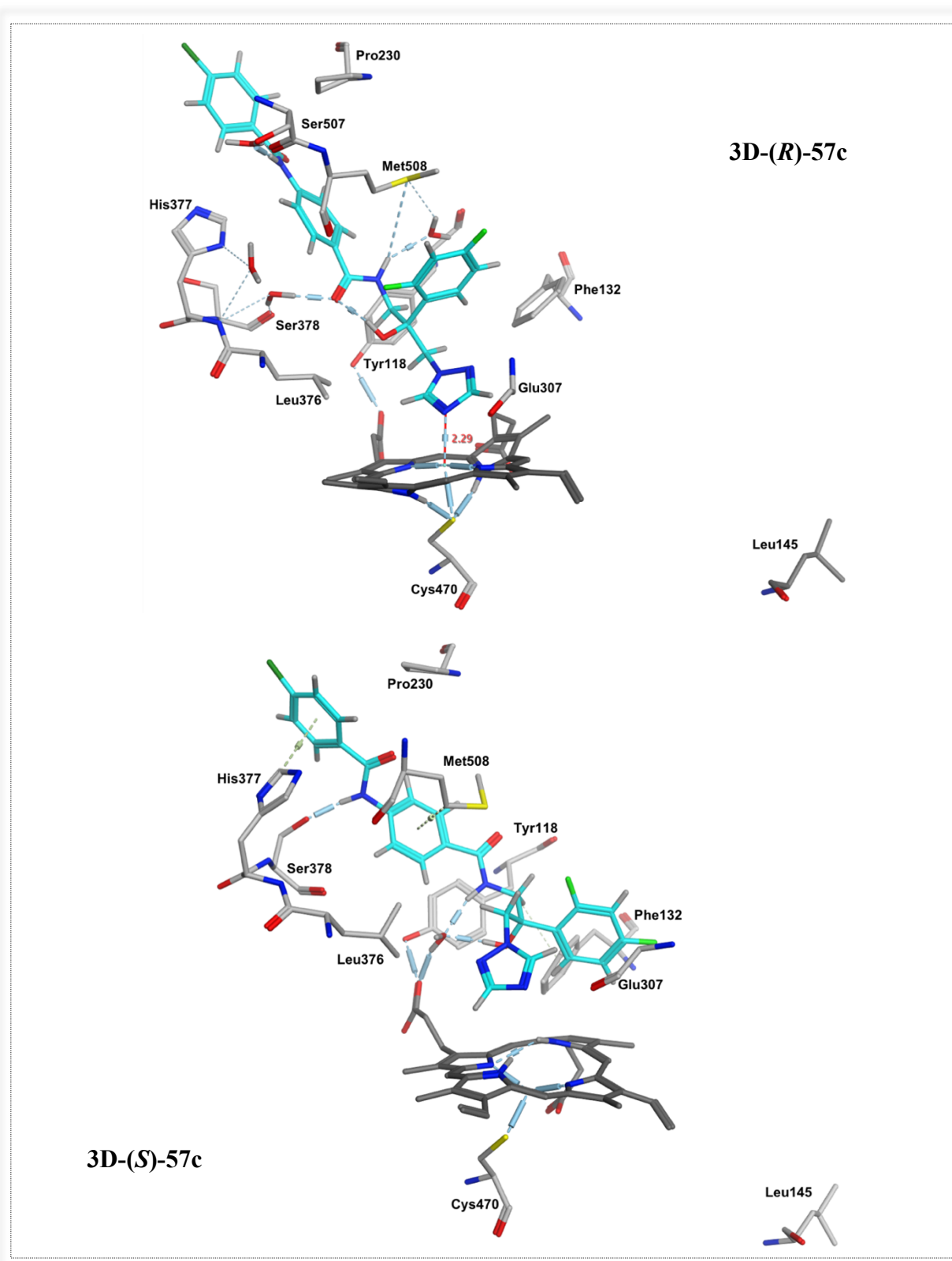
Figure 57: 2D ligplot illustrating binding interactions with the protein residues of the CaCYP51 double mutant Y132F/F145L. (*R*) and (*S*)-**57c** MD final frame and 3D image illustrating the perpendicular binding between the N-atom of the triazole and the haem iron for (*R*)- **57c** only.

b. Chemistry:

1. Mid-sized series synthesis:

Following the promising MD results of the mid-sized series, different derivatives were obtained by five reaction steps (Scheme 6):

1. Nucleophilic substitution reaction

2. Corey-Chaykovsky epoxidation reaction

3. Azide formation

4. Free amine formation by Staudinger reaction

5. Coupling reaction
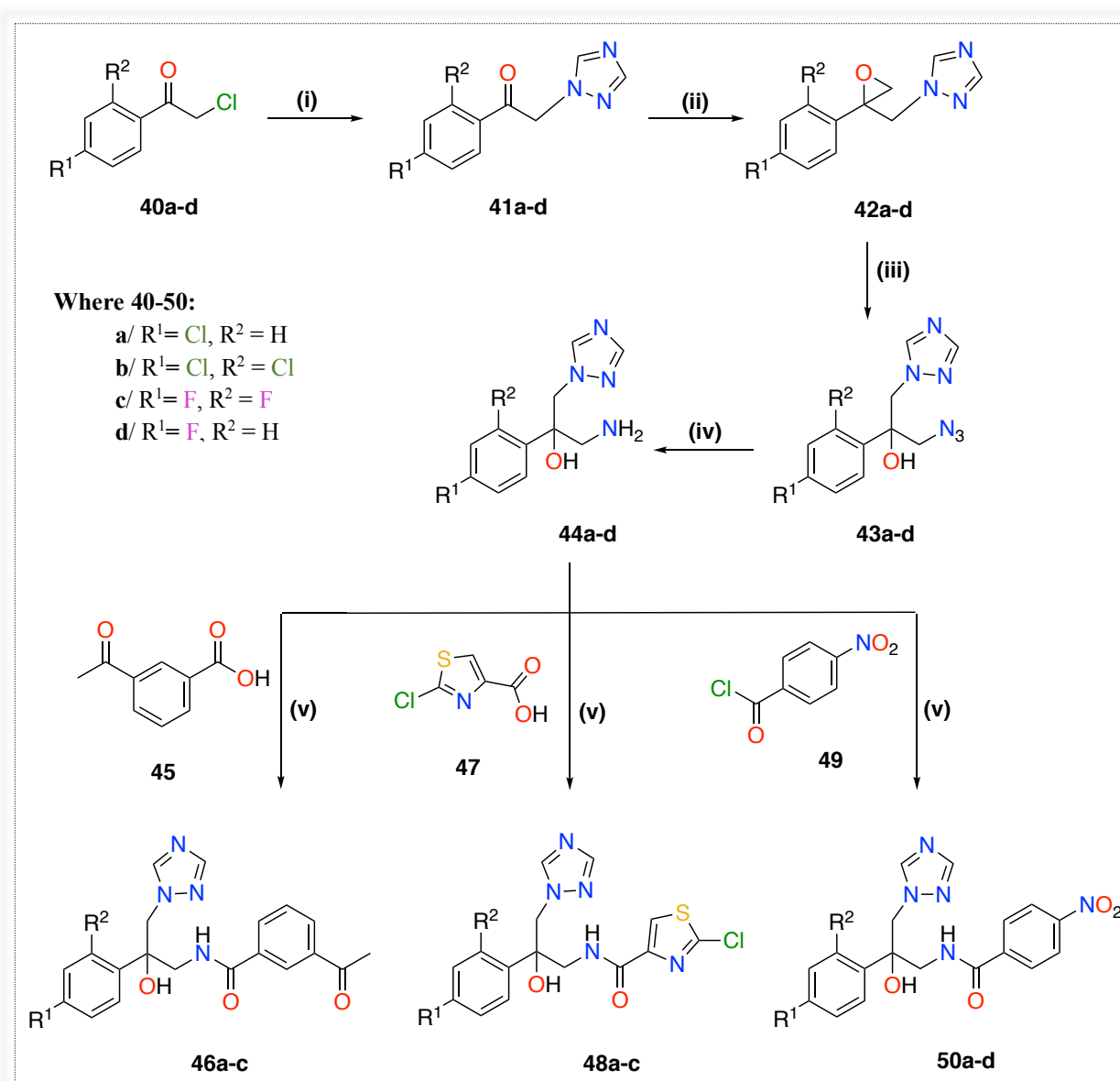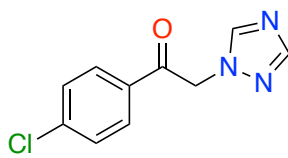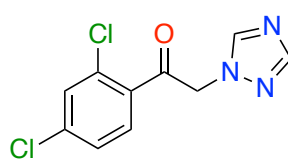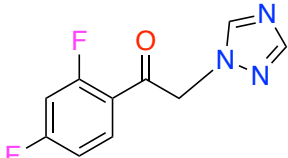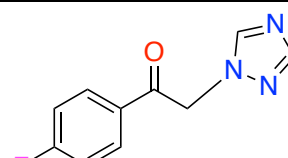
Scheme (6): *Reagents and conditions*: (**i**) 1,2,4-triazole, K_2CO_3, acetonitrile, 0-5 °C 30 min, r.t., 24 h (**ii**) TMSOI, 2M aq. NaOH, toluene, 60 °C, 6 h (**iii**) NaN_3, NH_4Cl, DMF, 60 °C, 2 h, r.t., o/n (**iv**) **a.** Ph_3P, THF, r.t., 1 h **b.** H_2O, 60 °C, 4 h (**v**) CDI, DMF, r.t., o/n.

Synthesis of 1-(substituted phenyl)-2-(1*H*-1,2,4-triazol-1-yl)ethan-1-one (41):

Synthesis of 1-(substituted phenyl)-2-(1*H*-1,2,4-triazol-1-yl)ethan-1-one (**41**) involved an addition of 1,2,4-triazole and activated K_2CO_3 into a solution of a substituted acetophenone (**40**) in acetonitrile.[123] Then, the reaction was stirred vigorously at 0 °C for 30 min and left at room temperature overnight. The reaction did not reach completion even after several optimisations, and the yield for compound (**41a**) was acceptable after recrystallisation. Compound (**41b**) was prepared with the same method but was heated at 80 °C for 4 h, followed by purification by gradient column chromatography giving an improved yield compared with (**41a**).

For the difluoro (**41c**) and fluoro (**41d**), it was necessary to use toluene as a solvent with NaHCO_3 as the base and 4 h reflux with good yields for both compounds (Table 24).[124]

Table 24: Chemistry of the prepared compounds (**41**).

Compound	Structure	Yield (%)	M.P. (Lit. m.p.)
41a		51	148-150 °C (lit. m.p.: 149-150 °C)[123]
41b		60	108- 110°C (lit. m.p.: 160-161 °C)[124]
41c		67	112 -114 °C (lit. m.p.: 104-106 °C)[124]
41d		70	116- 118 °C (lit. m.p. not found)

Synthesis of 1-((2-(substituted phenyl)oxiran-2-yl)methyl)-1*H*-1,2,4-triazole (42):

The synthesis of the epoxide compounds was achieved by a Corey-Chaykovsky epoxidation reaction, which is known as a methylene transfer reagent, using trimethylsulfoxonium iodide (TMSOI).[125] TMSOI was added into a solution of compound (**41**)

followed by 20% aqueous NaOH and heated at 60 ℃.[126] The heating condition for all compounds was for 6h except compound **42c** was heated for 72h. The product (**42**) was not visible under UV so was used directly in the next step without any further purification.

The reaction mechanism includes formation of an ylide by the deprotonation of TMSOI with a strong base (NaOH) to provide the dimethyloxosulfonium methylide (Corey-Chaykovsky reagent). The ylide intermediate acts as a nucleophile to attack the ketone carbonyl carbon and generate O⁻, which acts as a nucleophile. The O⁻ attacks the electrophilic ylide carbon resulting in dimethyl sulfoxide as a byproduct and the epoxide compound (42) (Figure 58).
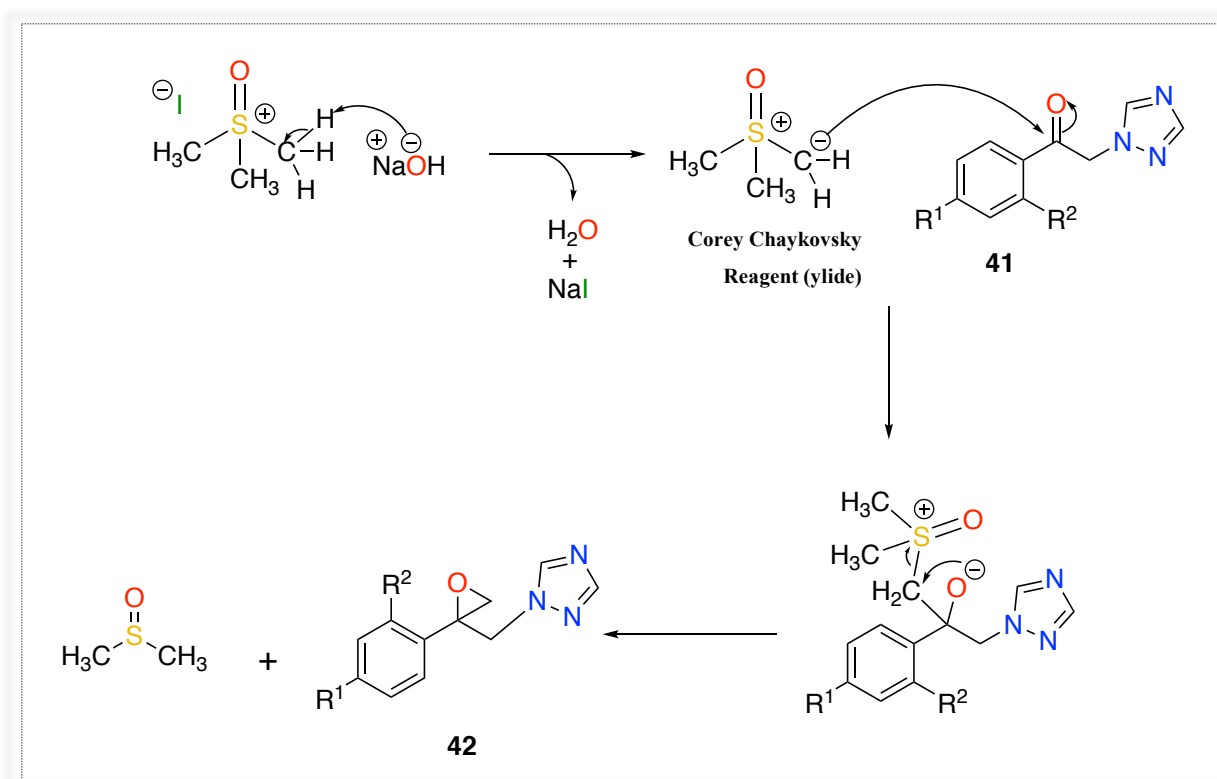
Figure 58: Corey-Chaykovsky epoxidation reaction mechanism.

The structure of the epoxide **42** product was confirmed by ¹H NMR, with two doublet peaks observed for the OCH$_2$ of the epoxide at δ 3.04 (d, J = 4.9 Hz, 1H, OC*Ha*Hb) and 2.87 (d, J = 4.9 Hz, 1H, OCHa*Hb*) of compound **42a** and at δ 3.13 (d, J = 4.7 Hz, 1H, OC*Ha*Hb) and 2.94 (d, J = 4.7 Hz, 1H, OCHa*Hb*) for **42b** (Figure 59).

42a

42b
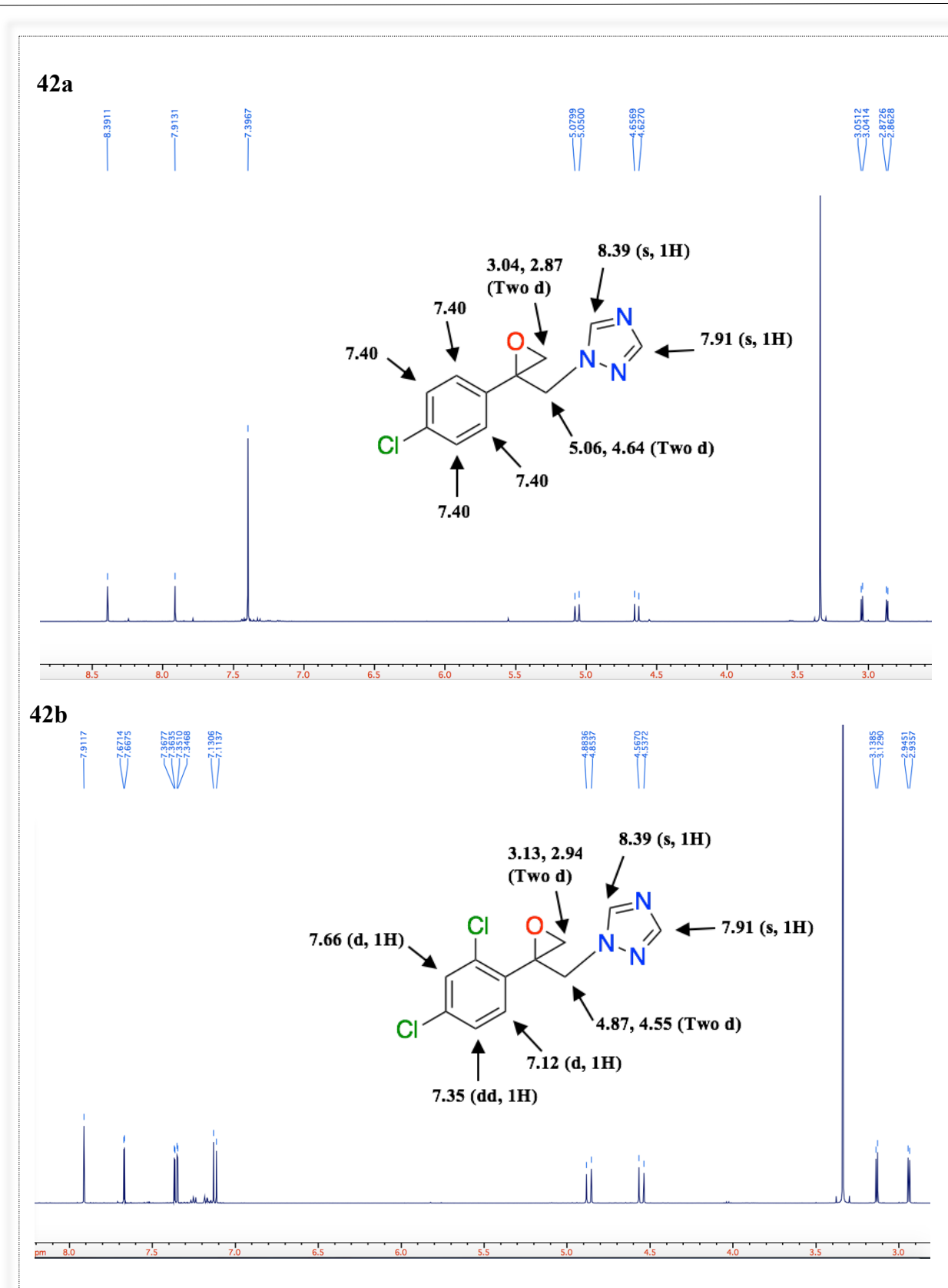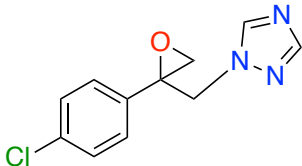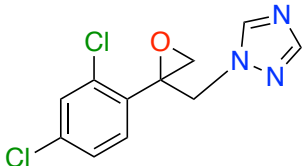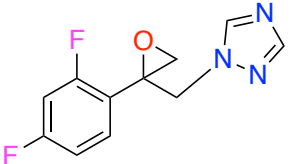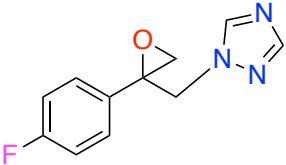
Figure 59: ^{1}H NMR (DMSO-d$_6$/ 500 MHz) for compounds **42a** and **42b**.

All of the epoxides (**42a-d**) were obtained as orange oils and the crude yield was more than 80 % (Table 25).

Table 25: Crude yield of the epoxides (**42**).
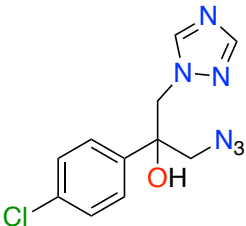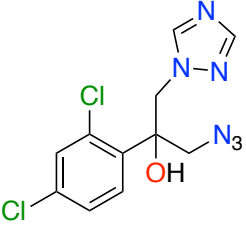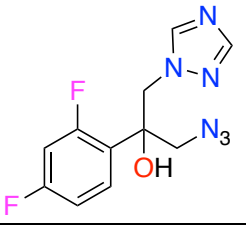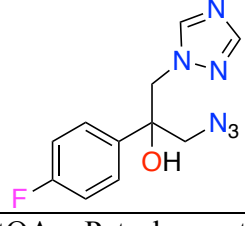
Compound	Structure	Crude yield (%)
42a		95
42b		92
42c		83
42d		92

Synthesis of 1-azido-2-(substituted phenyl)-3-(1*H*-1,2,4-triazol-1-yl)propan-2-ol (43):

The azide compounds (**43**) were obtained on reaction of NaN_3 with the epoxide (**42**) in dry DMF followed by NH_4Cl and heating at 60 ^{o}C for 2 h then overnight at room temperature.[127]

The desired products **43a-d** were achieved in good yields over two steps from **41** as yellow thick oils (Table 26). Interestingly, all derivatives (**43a-d**) have a very weak chromophore, so poorly visible under UV.

Table 26: Chemistry of the azide compounds (**43**).

Compound	Structure	Yield (%)	TLC R_f*
43a		60	0.45
43b		63	0.57
43c		60	0.35
43d		60	0.22

*TLC eluent: (2:1 v/v EtOAc- Petroleum ether)

Synthesis of 1-amino-2-(substituted phenyl)-3-(1*H*-1,2,4-triazol-1-yl)propan-2-ol (44):

Azide reduction to the free amines (**44**) was performed using a Staudinger reaction, which is a very mild condition of azide reduction.[127] TPP was added into a solution of compound **43** in THF and the reaction stirred at room temperature for 1 h. H_2O was added, and the reaction heated at 60 ºC for 4 h.

The mechanism of the Staudinger reaction involves generation of a phosphazide intermediate resulting in loss of N_2 to form an iminophosphorane. Then, adding H_2O during the work up leads to formation of compound **44** and phosphine oxide as a byproduct (Figure 60).
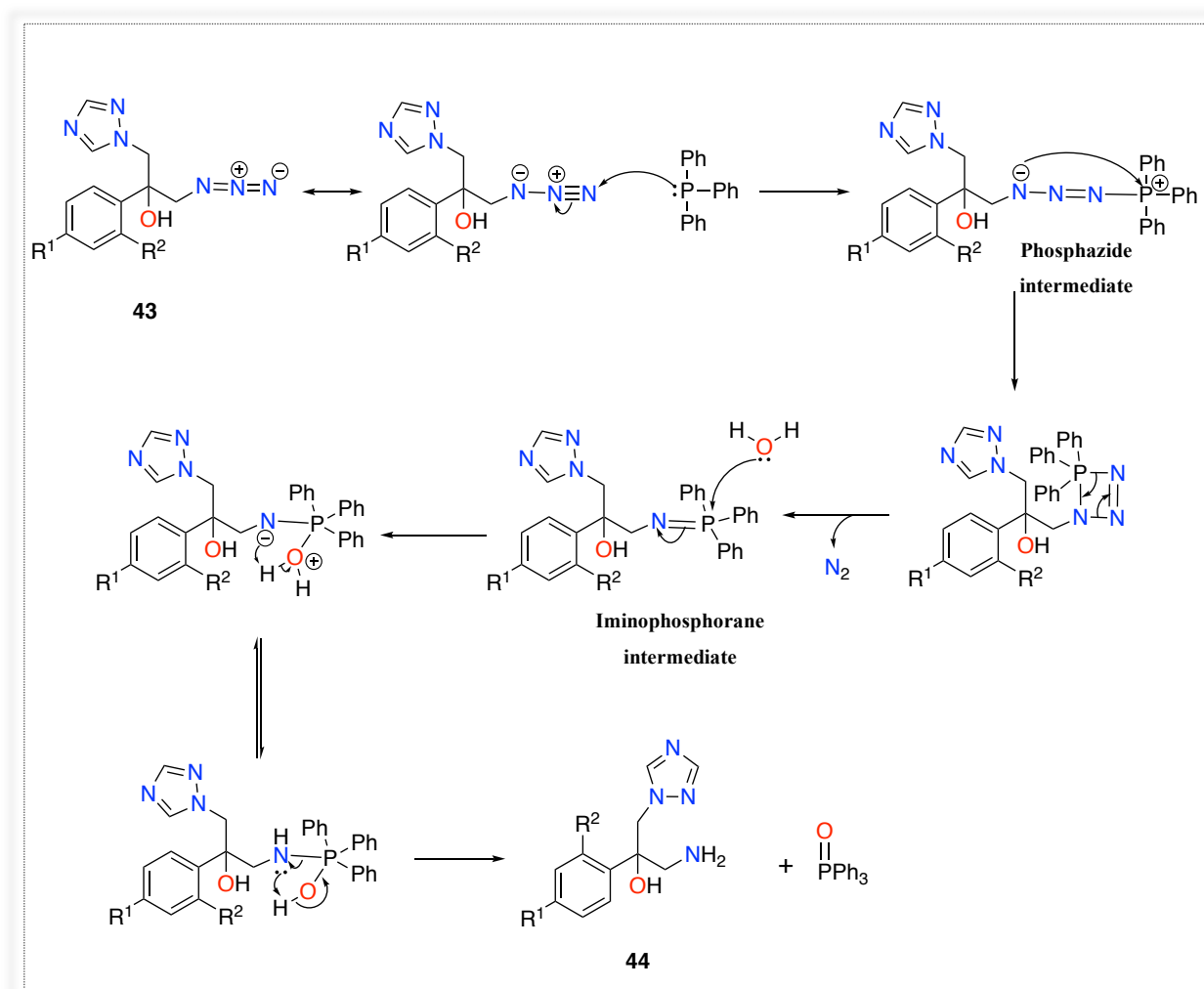
Figure 60: The mechanism of the Staudinger reaction.

All derivatives have a very weak chromophore and were not visible under UV. The structure was confirmed by ^{1}H NMR and used without further purification. The desired free amine compounds were achieved in good yields as white solids (Table 27).

Table 27: Yields and ^{1}H NMR of the free amine compounds (**44**).

Compound	Structure	Yield (%)	^{1}H NMR (DMSO-d$_6$)
44a		91	δ 8.20 (s, 1H, triaz), 7.82 (s, 1H, triaz), 7.39 (d, J = 8.9 Hz, 2H, Ar), 7.33 (d, J = 8.8 Hz, 2H, Ar), 5.53 (brs, 1H, OH, ex), 4.50 (d, J = 14.3 Hz, 1H, C*Ha*Hb-triaz), 4.48 (d, J = 14.3 Hz, 1H, CHa*Hb*-triaz), 3.27 (d, J = 14.3 Hz, 1H, C*Ha*Hb-NH$_2$), 2.94 (d, J = 14.3 Hz, 1H, CHa*Hb*-NH$_2$), 1.56 (brs, 2H, N$\underline{H}_2$).
44b		72	δ 8.29 (s, 1H, triaz), 7.72 (s, 1H, triaz), 7.53 (t, J = 2.1 Hz, 1H, Ar), 7.51 (s, 1H, Ar), 7.30 (dd, J = 2.2, 8.6 Hz, 1H, Ar), 5.79 (s, 1H, OH, ex), 4.87 (d, J = 14.3 Hz, 1H, C*Ha*Hb-triaz), 4.59 (d, J = 14.3 Hz, 1H, CHa*Hb*-triaz), 3.20 (d, J = 13.5 Hz, 1H, C*Ha*Hb-NH$_2$), 3.07 (d, J = 13.5 Hz, 1H, CHa*Hb*-NH$_2$), 1.55 (brs, 2H, N$\underline{H}_2$).
44c		86	δ 8.28 (s, 1H, triaz), 7.73 (s, 1H, triaz), 7.37 (dd, J = 9.0, 15.9 Hz, 1H, Ar), 7.17-7.12 (m, 1H, Ar), 6.86 (ddd, J = 2.8, 8.8, 11.4 Hz, 1H, Ar), 6.23 (brs, 1H, OH-ex), 4.56 (d, J = 14.3 Hz, 1H, C*Ha*Hb-triaz), 4.50 (d, J = 14.3 Hz, 1H, CHa*Hb*-triaz), 3.19 (d, J = 13.5 Hz, 1H, C*Ha*Hb-NH$_2$), 2.91 (d, J = 13.5 Hz, 1H, CHa*Hb*-NH$_2$), 1.88 (s, 2H, N$\underline{H}_2$).
44d		83	δ 8.19 (s, 1H, triaz), 7.82 (s, 1H, triaz), 7.40 (dd, J = 5.5, 9.0 Hz, 2H, Ar), 7.10 (t, J = 9.0 Hz, 2H, Ar), 5.73 (s, 1H, OH, ex), 4.52 (d, J = 14.2 Hz, 1H, C*Ha*Hb-triaz), 4.47 (d, J = 14.2 Hz, 1H, CHa*Hb*-triaz), 3.29 (d, J = 13.9 Hz, 1H, C*Ha*Hb-NH$_2$), 2.82 (d, J = 13.9 Hz, 1H, CHa*Hb*-NH$_2$), 1.76 (br.s, 2H, N$\underline{H}_2$).

From the amines (**44**), the mid-sized derivatives were prepared.

A) Acetyl derivatives:

Synthesis of 3-acetyl-*N*-(2-(substitutedphenyl)-2-hydroxy-3-(1*H*-1,2,4-triazol-1-yl) propyl)benzamide (46):

1,1$^\text{'}$-Carbonyldiimidazole (CDI) is a coupling reagent used to form activated species as acylimidazole.[128] To form the amide liker, activation of the OH group of 3-acetylbenzoic acid

(**45**) is needed to form an acyl leaving group, which will react with the free amine derivatives (**44**). The amides (**46**) were obtained by reaction of 3-acetyl benzoic acid (**45**) with CDI in dry DMF at room temperature for 1 h. Then, a solution of the amine (**44**) in dry DMF was added and the reaction stirred at room temperature overnight to give the amides (**46**).

In this reaction mechanism, imidazole has two roles, first as a base to deprotonate the carboxylic acid of compound **45** and form the anhydride intermediate and second, as a nucleophile to attack the carbonyl carbon of the anhydride intermediate leading to the acylimidazole intermediate and CO_2 byproduct. The amines **44** then attack the acylated derivatives resulting in the formation of amide product **46** and imidazole side product (Figure 61).
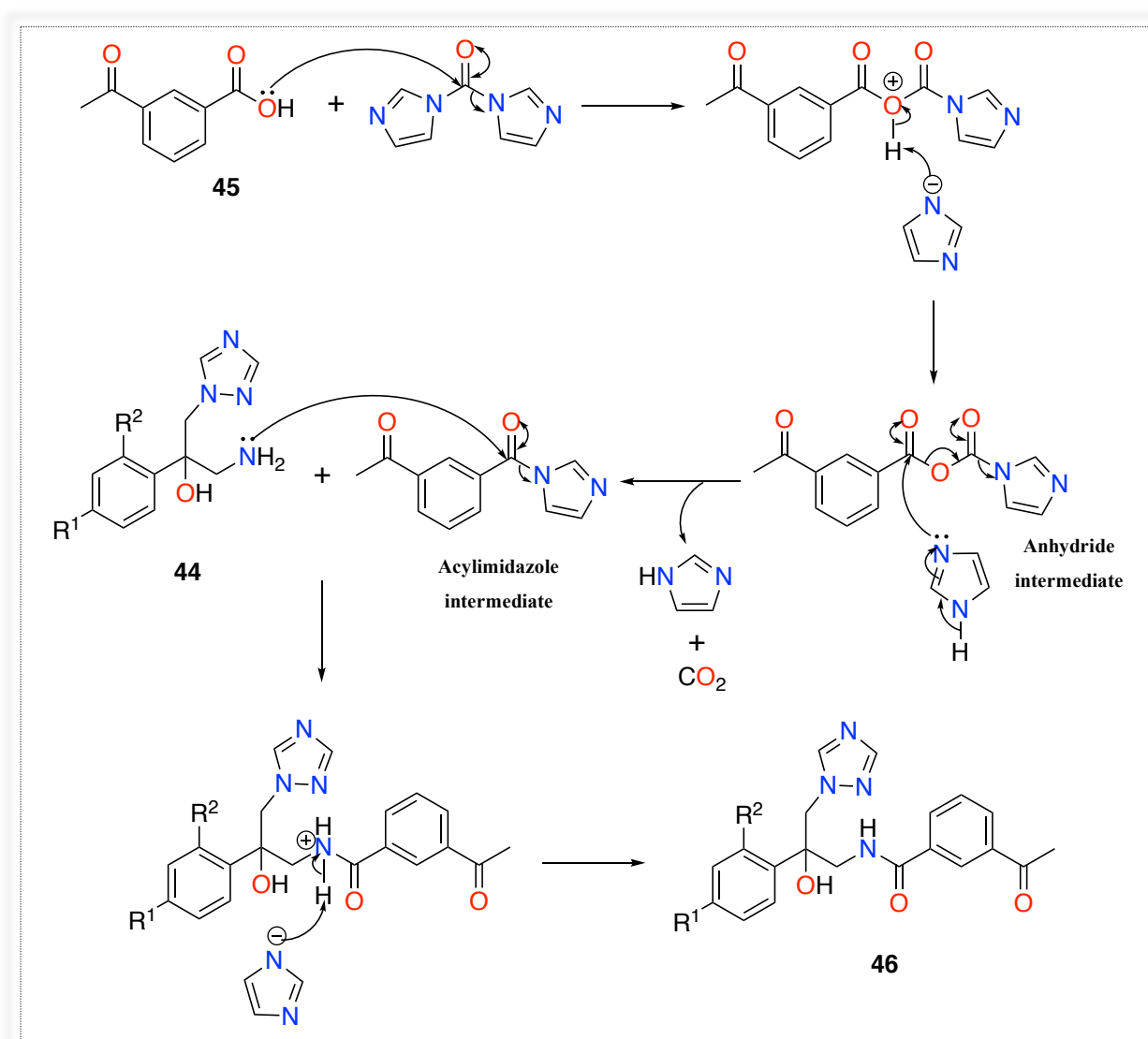
Figure 61: Carboxylic acid activation mechanism by CDI.

All novel amides (**46a-c**) were confirmed using ^{1}H and ^{13}C NMR. The pure compounds showed acceptable yields after purification with gradient column chromatography (Table 28).

Table 28: Yields and HPLC percent of the mid-sized acetyl derivatives (**46**).
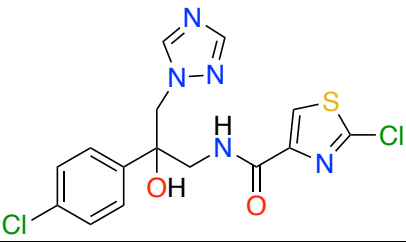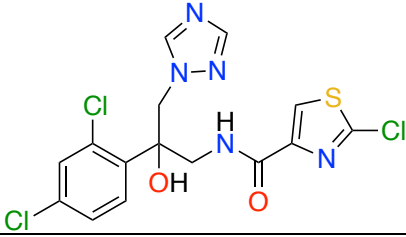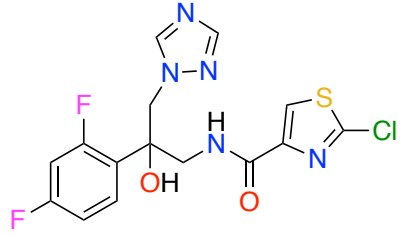
Compound	Structure	Yield (%)	HPLC purity (%)
46a		52	100
46b		45	100
46c		54	100

B) Thiazole derivatives:

Synthesis of 2-chloro-*N*-(2-(substitutedphenyl)-2-hydroxy-3-(1*H*-1,2,4-triazol-1-yl)propyl)thiazole-4-carboxamide (48):

The thiazole derivatives were prepared as described for acetyl derivatives (**46**) using CDI coupling reagent to activate the OH of the 2-chlorothiazole-4-carboxylic acid (**47**) and purified by gradient column chromatography using CH$_2$Cl$_2$/MeOH mobile phase system. The pure thiazoles (**48**) were achieved in good yields and high purity (Table 29).

Table 29: Yields and HPLC percent of the mid-sized thiazole derivatives (**48**).

Compound	Structure	Yield (%)	TLC R$_f$*	HPLC purity (%)
48a		68	0.45	100
48b		68	0.55	100
48c		65	0.42	97

*TLC eluent: (9.5: 0.5 v/v CH$_2$Cl$_2$-MeOH)

C) Nitro-phenyl derivatives:
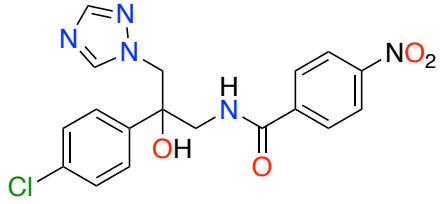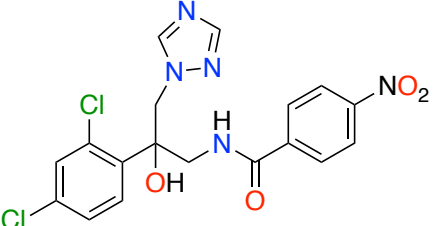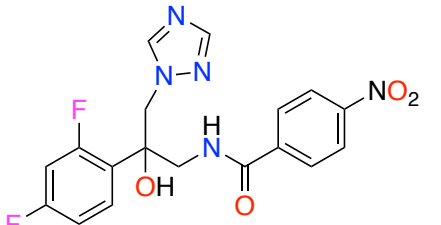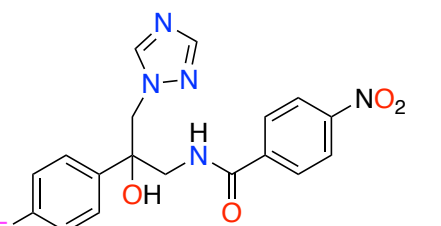
Synthesis of *N*-(2-(substitutedphenyl)-2-hydroxy-3-(1*H*-1,2,4-triazol-1-yl)propyl)-4-nitrobenzamide (50):

N-(2-(substitutedphenyl)-2-hydroxy-3-(1*H*-1,2,4-triazol-1-yl)propyl)-4-nitrobenzamides (**50**) was obtained on reaction of 4-nitrobenzoyl chloride (**49**) with the free amine (**44**) at room temperature overnight.

The crude compounds were purified using gradient column chromatography and the desired products (**50a-d**) achieved in good yields as white solids, and the retention factor ranged from 0.33-0.4 (Table 30).

Table 30: Yields and retention factor of the nitro derivatives (**50**).

Compound	Structure	Yield (%)	TLC R$_f$*
50a		74	0.33
50b		72	0.45
50c		65	0.45
50d		65	0.37

*TLC eluent: (9.5: 0.5 v/v CH_2Cl_2-MeOH)

As the docking result of the short compounds showed very good fit in the CaCYP51 active site, similar to fluconazole, as well as binding interactions with different amino acids, extension of this series was performed to improve the occupancy of the access channel and to provide additional binding interactions.

2. Extended series synthesis:

The nitro derivatives in the mid-sized series, *N*-(2-(substituted phenyl)-2-hydroxy-3-(1*H*-1,2,4-triazol-1-yl)propyl)-4-nitrobenzamide (**50**), provided a route to synthesise new linkers to allow extension (Scheme 7). The reactions involved were:

1. Hydrogenation reaction using Pd/C catalyst
2. Formation of thiourea, urea and amide linkers
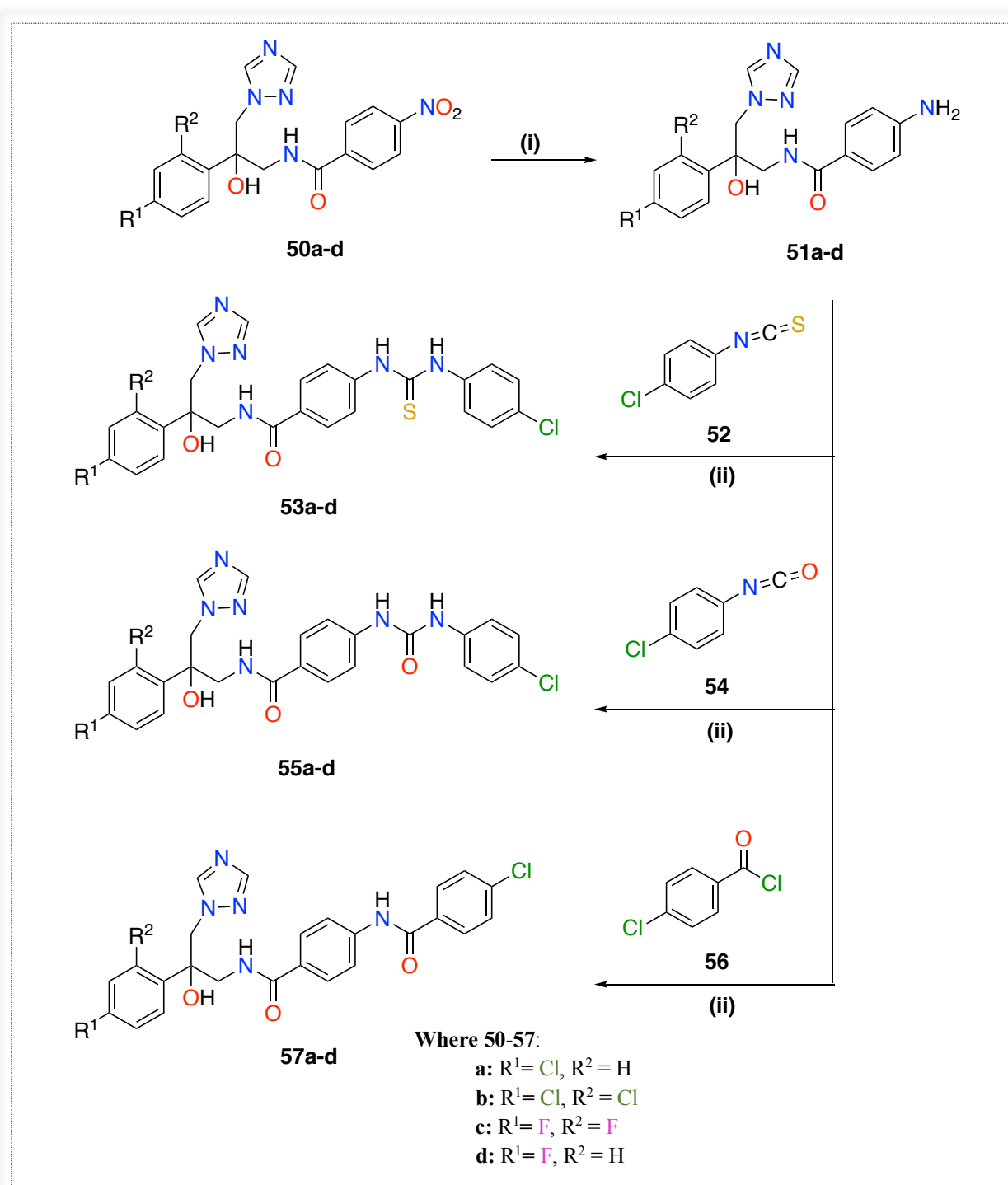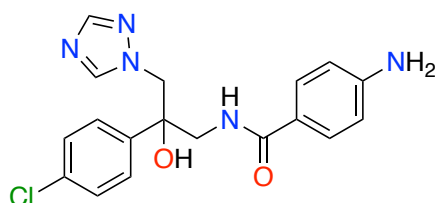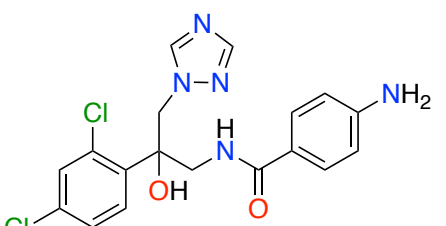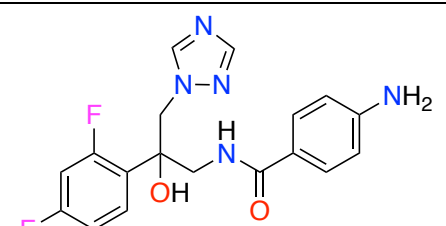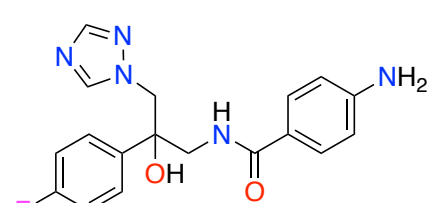
Scheme 7: *Reagents and conditions*: (**i**) H_2, Pd/C, EtOH, r.t., 3 h (**ii**) pyridine, r.t., o/n.

Synthesis of 4-amino-*N*-(2-(substitutedphenyl)-2-hydroxy-3-(1*H*-1,2,4-triazol-1-yl) propyl)benzamide (51):

The nitro derivatives (**50a-d**) were reduced to the amine (**51**) using 10% palladium on carbon (Pd-C) catalyst in dry MeOH. The reaction atmosphere was filled with H_2 using H_2 balloons, and the mixture was stirred at room temperature for 3 h. The crude compounds were purified using gradient column chromatography and the desired free amine derivatives (**51a-d**) achieved in good yields and high purity percent (Table 31).

Table 31: Chemistry of the free amine compound (**51**).

Compound	Structure	Yield (%)	HPLC purity (%)
51a		100	99
51b		100	99
51c		100	100
51d		95	100

Synthesis of the final extended compounds (53, 55, 57) with the thiourea, urea and amide linkers:
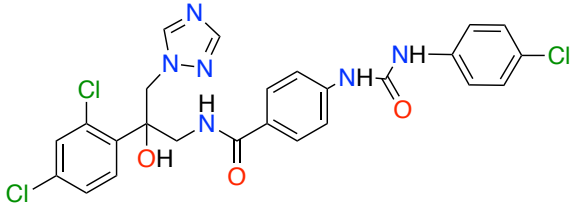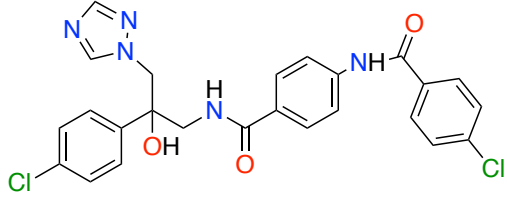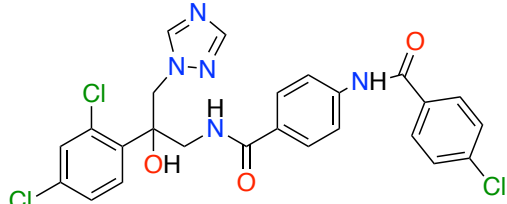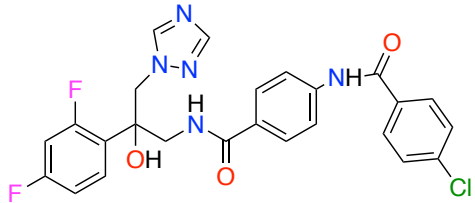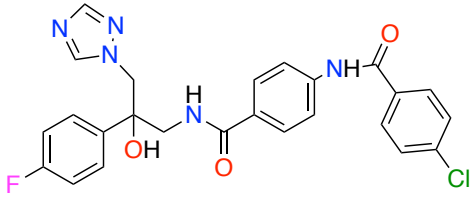
The synthesis of the final compounds (**53,55,57**) with the different linkers was achieved by adding 4-chlorophenyl derivatives (**52**, **54** and **56**) to 4-amino-*N*-(2-(substituted phenyl)-2-hydroxy-3-(1*H*-1,2,4-triazol-1-yl)propyl)benzamide (**51**) in dry pyridine, and the reaction was left at room temperature overnight.

To form the thiourea and urea linkers, 1-chloro-4-isothiocyanatobenzene (**52**) and 1-chloro-4-isocyanatobenzene (**54**) were used as a reactive functional group especially with amines leading to formation of thiourea and urea compounds (**53** and **55**, respectively). While amide compounds (**57a-d**) were obtained using 4-chlorobenzoyl chloride (**56**).

After the work up, the crude products were purified by gradient flash column chromatography and the structure of the final extended compounds (**53**, **55** and **57**) confirmed by ^{1}H and ^{13}C NMR. The extended compounds were achieved in good yields as white solids (Table 32). Two compounds (**53b** and **55b**) showed lower yields than others due to difficulty in purifications.

Table 32: Yield and M.P. of the compounds (**53**, **55** and **57**).

Compound	Structure	Yields (%)	M.P. (°C)
53a		68	146- 148
53b		56	138- 140
55a		63	226-228

55b		52	216- 218
57a		80	222- 224
57b		76	190-192
57c		78	211-213
57d		92	218-220

3. Exploring different moieties:

As discussed previously, the enzyme active site has a structure of two short arms and a long hydrophobic channel, thus the SAR of the two short arms remained the same as compound **44c** since the molecular docking as well as molecular dynamic (MD) of the triazole hydroxy-propyl benzamide compounds showed excellent positioning and fitting in the short arms' active sites. The modification on the compounds will be on the long arm, which occupies the access channel, with the aim to form extra H-bonding with amino acids to counteract resistance arising from mutations at Tyr132. These new moieties included (Figure 62):

1. Fused ring derivatives rather than having a second linker in which the **X**-group could be either C or N and the R-group will be an EDG or EWG to explore binding interaction with different amino acids residue at the hydrophobic channel.

2. Biphenyl derivatives in which the amide linker will be in the meta or para position of the second substituted phenyl ring. The R-group could be OCF_3 or CF_3 to explore CaCYP51 inhibitory activity as well as binding affinity.

1. Fused ring derivatives   **2. Biphenyl derivatives**
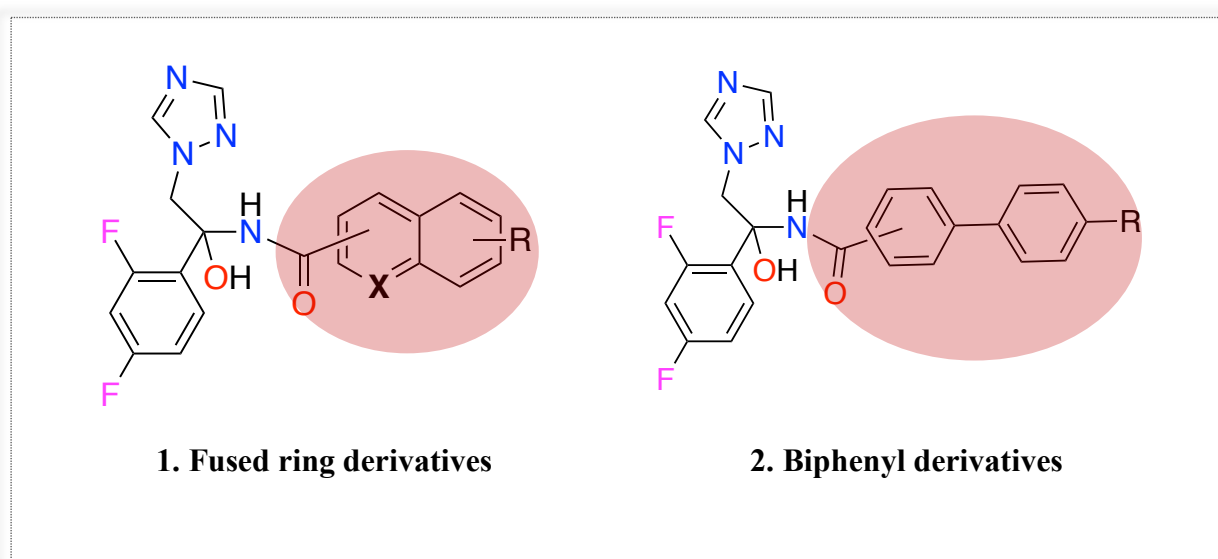
Figure 62: General structures of fused ring and biphenyl derivatives.

A) Fused ring derivatives:

The synthetic pathway of the fused ring derivatives included only one reaction step which was a coupling reaction with compound **44c**. Three compounds of the fused ring

derivatives were synthesized, two of which had a quinoline nucleus and one a naphthalene nucleus (Scheme 8).
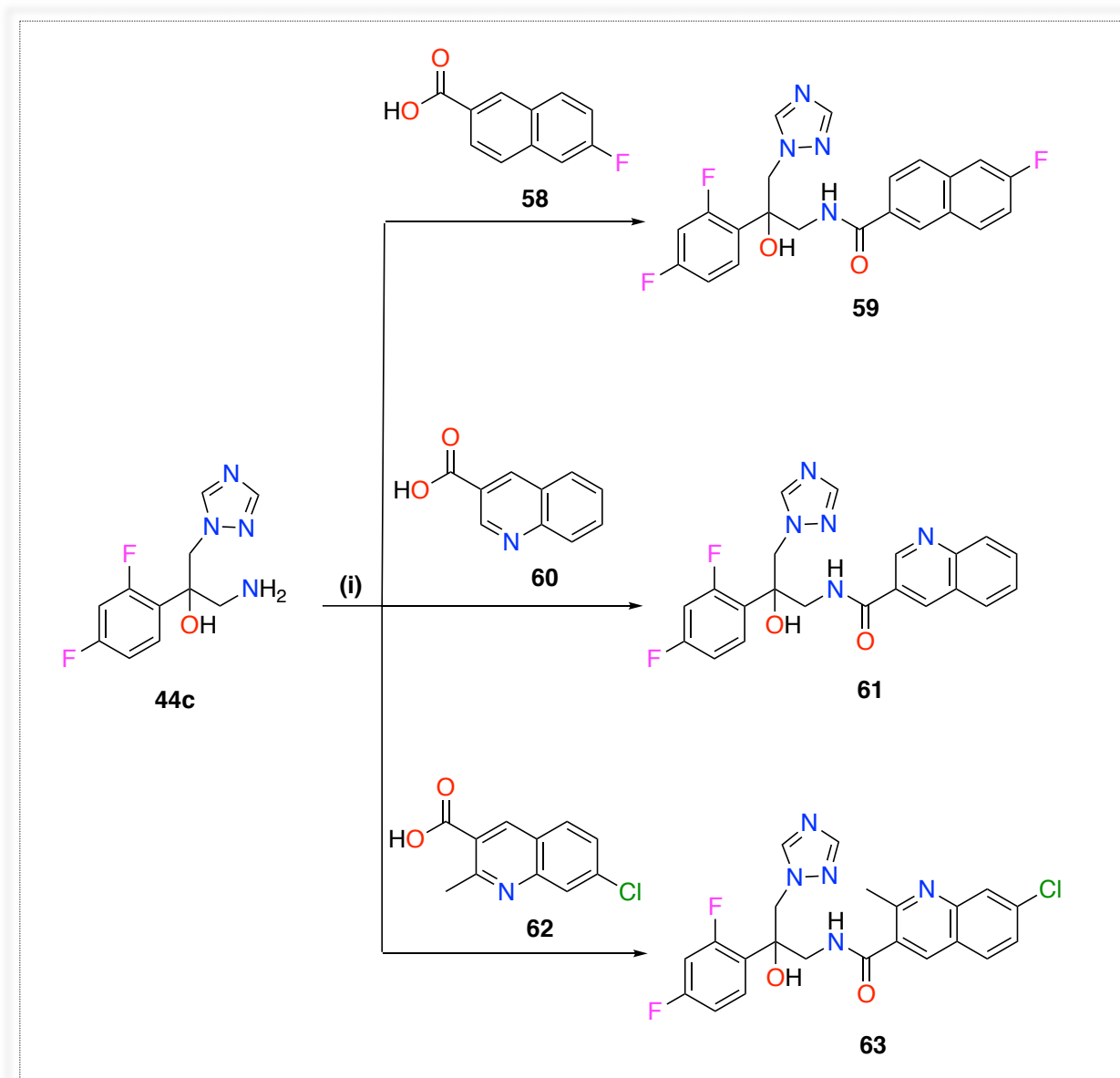
Scheme 8: *Reagents and conditions*: (i) CDI, DMF, r.t, o.n.

Synthesis of fused ring derivatives (59, 61, 63):

The carboxylic acid (**58**, **60**, **62**) was first activated by reaction with CDI in dry DMF at room temperature for 1 h, then compound **44c** was added and the reaction mixture left at room temperature overnight to give the products (**59, 61, 63**) in good yields as white solids (Table 33).

Table 33: Yield, M. P. and HPLC purity of compounds (**59, 61, 63**).

Compound	Structure	Yields (%)	M.P. (°C)	HPLC purity (%)
59		60	195-197	96
61		61	193-195	100
63		63	145-146	100

B) Biphenyl ring derivatives:

To synthesise the *para*-derivatives *N*-(2-(2,4-difluorophenyl)-2-hydroxy-3-(1*H*-1,2,4-triazol-1-yl)propyl)-4'-(trifluoromethyl/trifluoromethoxy)-[1,1'-biphenyl]-4-carboxamide (**69 a-b**) of the biphenyl ring as well as the *meta*-compounds *N*-(2-(2,4-difluorophenyl)-2-hydroxy-3-(1*H*-1,2,4-triazol-1-yl)propyl)-4'-(trifluoromethyl/trifluoromethoxy)-[1,1'-biphenyl]-3-carboxamide (**70a-b**), two reaction steps were used (Scheme 9):

1. Suzuki cross-coupling reaction
2. CDI coupling reaction
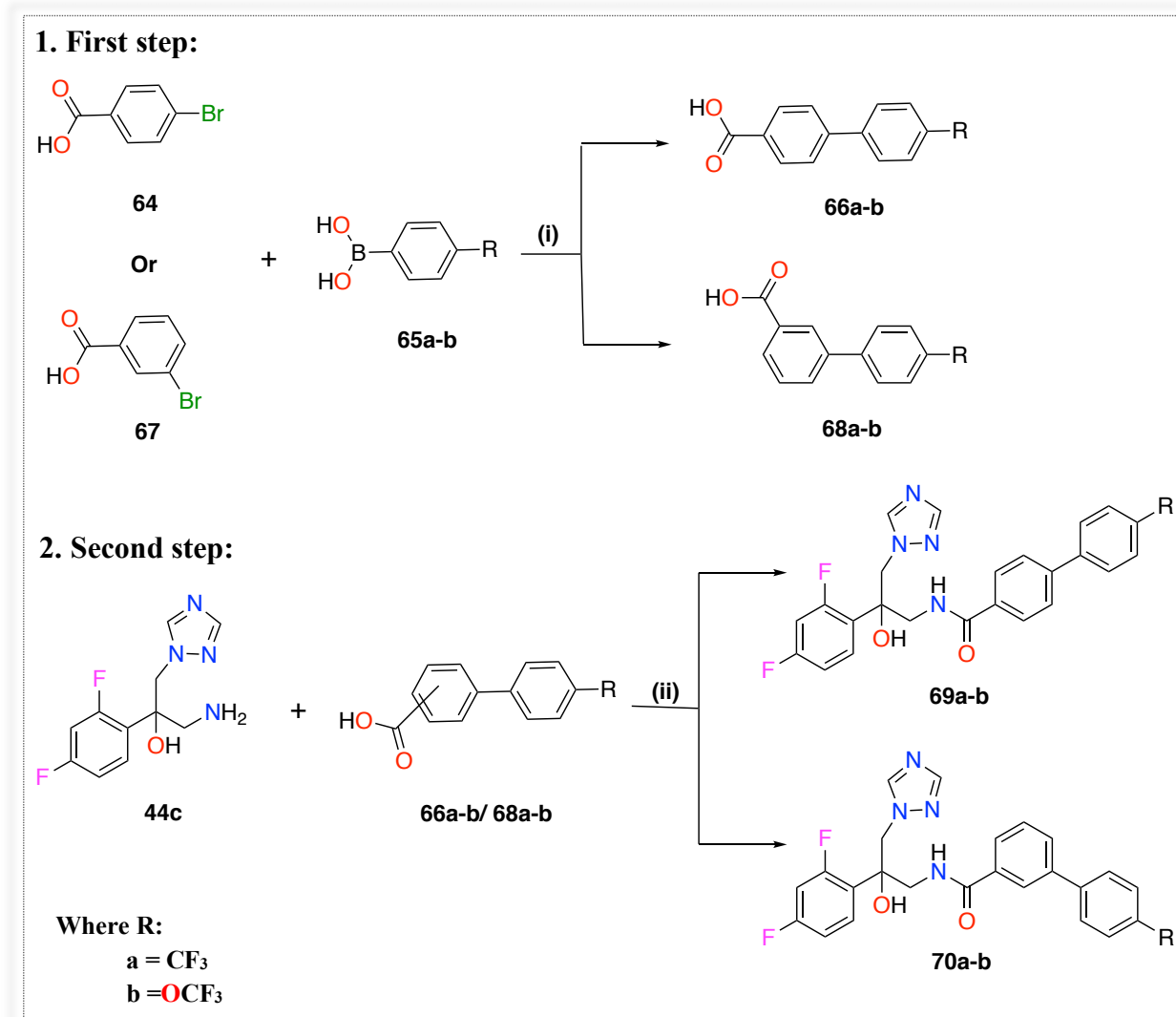
Scheme 9: *Reagents and conditions*: (i) Dioxane/H_2O, Pd(PPh$_3$)$_4$, 104 °C, 6 h (ii) CDI, DMF, r.t., o.n.

Synthesis of 4'-(trifluoromethyl/trifluoromethoxy)-[1,1'-biphenyl]-4/3-carboxylic acid (66,68):

The synthesis of biphenyl intermediates (**66** and **68**) was achieved by a Suzuki cross-coupling reaction. This reaction involved a homogenous palladium, that catalysed the coupling between arylboronic acid and aryl halide, and a base.[129] Compounds **66** and **68** were prepared by reaction of 3/4-bromobenzoic acid (**64/67**), 4-trifluoromethyl/trifluoromethoxy phenylboronic acid (**65**) and 1 mol % of Pd(PPh$_3$)$_4$ in dioxane/H_2O, with K_2CO_3 acting as base. The reaction was heated under reflux for 6 h and after aqueous work up and acidification, the crude product was purified by gradient column chromatography eluting with 2% MeOH in CH_2Cl_2.

The reaction mechanism involved a catalytic cycle with regeneration of the palladium catalyst.[129] There are three main steps in this mechanism (Scheme 10): [129]
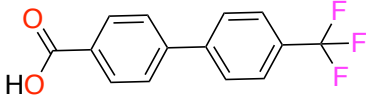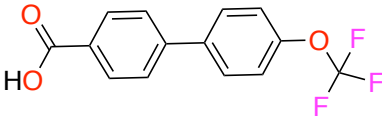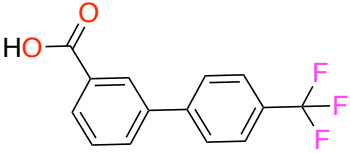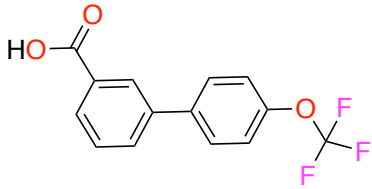
1. Oxidative addition in which the palladium catalyst forms a complex with the aryl halide (**64**, **67**).

2. Transmetalation step, which must include a base (KOH was the base generated in the reaction media after the addition of K_2CO_3 in the presence of H_2O) to activate the arylboronic acid (**65**) and to facilitate the exchange of the aryl group with the palladium complex. The exact mechanism of transmetalation is still unclear.[129]

3. Reductive elimination is a reverse reaction of oxidative addition in organometallic chemistry, which allows regeneration of the palladium catalyst to participate again in the catalytic cycle and generate the biphenyl product (**66**, **68**).
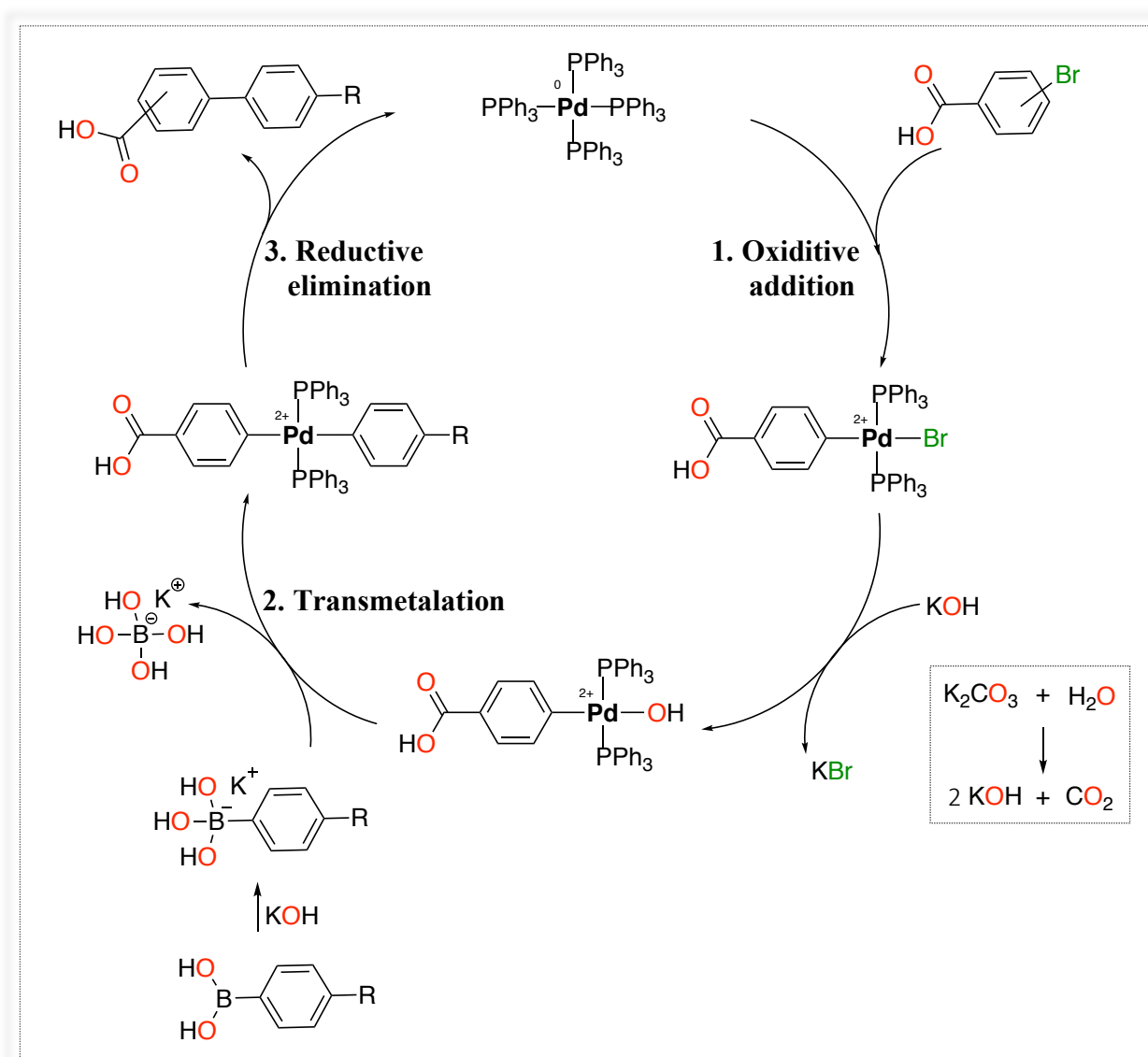
Scheme 10: Suzuki cross-coupling reaction mechanism.

All compounds (**66**, **68**) were characterised by ^{1}H NMR analysis and obtained in good yields (Table 34).
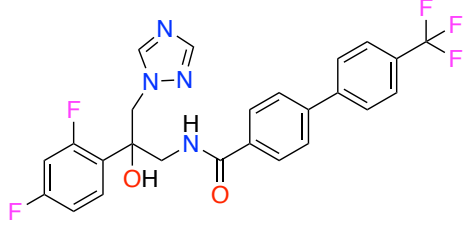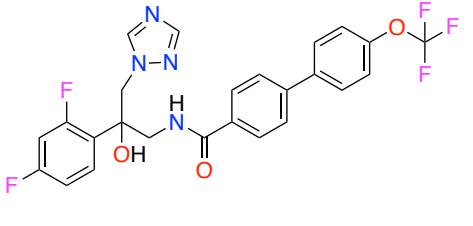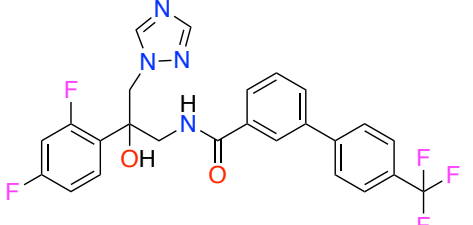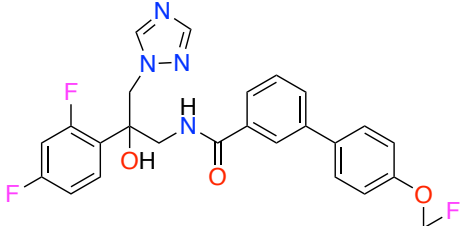
Table 34: Yields and M.P. of compounds **66** and **68**.

Compound	Structure	Yields (%)	M.P. (°C)
66a		82	240-243
66b		85	251-253
68a		90	198-200
68b		83	158-160

Synthesis of *N*-(2-(2,4-difluorophenyl)-2-hydroxy-3-(1*H*-1,2,4-triazol-1-yl)propyl)-4'-(trifluoromethyl/trifluoromethoxy)-[1,1'-biphenyl]-4/3-carboxamide (69 and 70):

The CDI coupling reaction was performed using the same method described for compound **45**. The final compounds **69** and **70** were achieved in good yields as white solids (Table 35).

Table 35: Yields and HPLC purity of compounds (**69** and **70**).

Compound	Structure	Yields (%)	HPLC purity (%)
69a		76	100
69b		65	100
70a		75	100
70b		72	97

c. Biological evaluation:

1. All chloro and dichloro derivatives were evaluated at the Centre for Cytochrome P450 Biodiversity, Swansea University Medical School. Assays were performed by Dr. Josie Parker and Dr. Andrew Warrilow.

A. *C. albicans* susceptibility testing:

All the final compounds of the chloro and dichloro derivatives were screened against *C. albicans* wild-type clinical isolate CAI4 and *C. albicans* laboratory strain SC5314.

The dichloro compounds (**46b**, **48b, 50b** and **51b**) displayed promising antifungal activity against *C. albicans* wild-type strains SC5314 and CA14 compared with chloro derivatives (**46a**, **48a, 50a** and **51a**) as well as with the control fluconazole. The most effective dichloro compounds with MIC < 0.03 μg/mL were the acetyl (**46b**), thiazole (**48b**) and nitro (**50b**) derivatives. This could be explained from cLogP as the more lipophilic compound may be more able to penetrate the lipophilic fungal membrane resulting in better MIC values (Table 36).

The dichloro with the thiourea and urea linker of the extended compounds (**53b**, **55b** and **57b**) was more effective at inhibiting *C. albicans* growth, for example: the dichloro thiourea **53b** showed MIC 0.25 μg/mL compared with the chloro **53a** MIC 4 μg/mL (Table 36). Even though the cLogP of the amide inhibitors (**57a**, cLogP 3.53 and **57b**, cLogP 4.15) was more lipophilic than thiourea (**53a**, cLogP 3.13 and **53b**, cLogP 3.73) and less than urea (**55a**, cLogP 3.86 and **55b**, cLogP 4.46), the mono and dichloro derivatives of the amide linker (**57a** and **57b**) were the most effective over the two linkers as well as the standard fluconazole with MIC < 0.03 μg/mL (Table 36). This could be owing to the high polarity of the thiourea and urea functional group compared with the amide, which may lead to a reduced uptake across the lipophilic fungal membrane.

B. CaCYP51 IC$_{50}$:
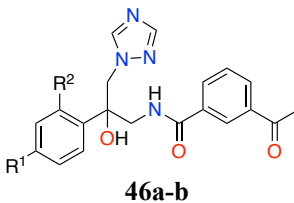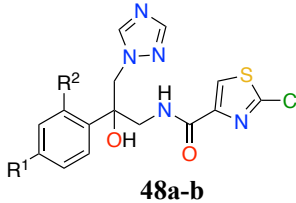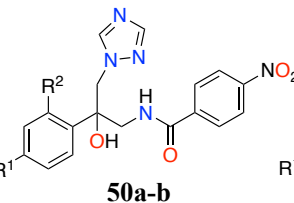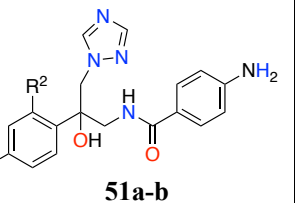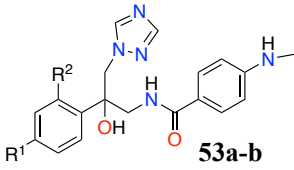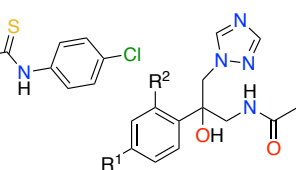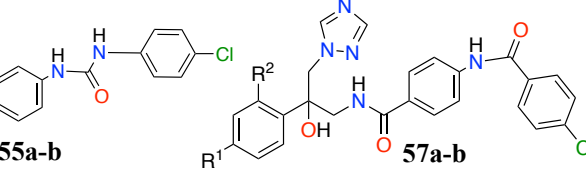
IC$_{50}$ is the concentration of an inhibitor required to inhibit 50% of an enzyme *in vitro*. This research focused on competitive inhibitors that compete with the substrate (lanosterol) to bind to CaCYP51. Derivatives with a MIC less than 1 μg/mL were chosen for IC$_{50}$ testing.

In the mid-sized series (**46a-b**, **48a-b**, **50a-b** and **51a-b**) the dichloro derivatives of the acetyl **46b** and the thiazole **48b** showed optimal inhibitory activity with IC$_{50}$ values of 0.49 and 0.41 μM respectively compared with fluconazole IC$_{50}$ 0.31 μM (Table 36). In addition, the

chloro of the nitro derivative (**50a**), showed promising inhibitory activity with an IC$_{50}$ of 0.79 µM. While the dichloro derivatives of the nitro (**50b**) and free amine (**51b**) showed weaker inhibitory activity (IC$_{50}$ 1.24 and 1.6 µM, respectively). The extended derivatives of the amide linker (**57**) all showed very good inhibitory activity against CaCYP51 (IC$_{50}$ 0.56 µM for **57a** and 0.48 µM for **57b**) (Table 36).

Of all derivatives, compounds **46b**, **48b**, **50a**, **50b**, **55b**, **57a** and **57b** had MIC and IC$_{50}$ values comparable with or lower than fluconazole (Table 36) and that indicates these compounds are promising biochemical candidates for further study as antifungal agents.

Table 36: MIC and IC$_{50}$ values for the chloro and dichloro derivatives of mid-sized and extended compounds.

Compounds	R^1	R^2	MIC (µg/ml)		IC$_{50}$ (µM)	cLogP*
			CA14	SC5314		
46a	Cl	H	0.25	0.25	1.30	1.85
46b	Cl	Cl	<0.03	0.06	0.49	2.46
48a	Cl	H	0.25	0.25	0.77	1.95
48b	Cl	Cl	<0.03	<0.03	0.41	2.55
50a	Cl	H	0.125	0.125	0.79	1.94
50b	Cl	Cl	<0.03	0.49	1.24	2.54
51a	Cl	H	1	1	-	1.05
51b	Cl	Cl	0.25	0.25	1.6	1.66
53a	Cl	H	4	4	-	3.13
53b	Cl	Cl	0.25	0.5	0.67	3.73

55a	Cl	H	1	2	-	3.86
55b	Cl	Cl	0.125	0.125	0.47	4.46
57a	Cl	H	<0.03	<0.03	0.56	3.54
57b	Cl	Cl	<0.03	<0.03	0.48	4.15
Fluconazole			0.125	0.125	0.31	0.86

*cLogP done by Crippen's fragmentation.[103]
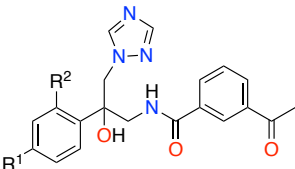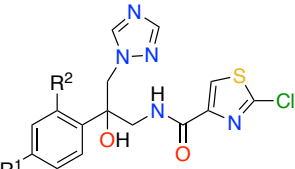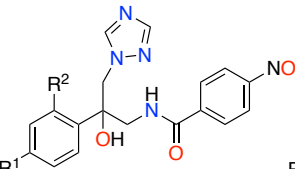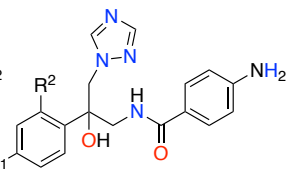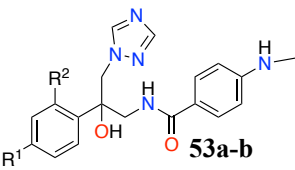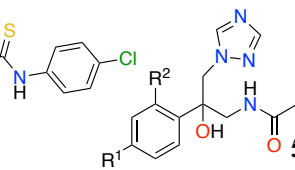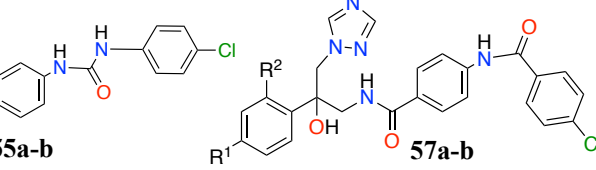
C. Binding affinity:

The novel mid-sized derivatives (**46a-b**, **48a-b**, **50a-b** and **51a-b**) and extended derivatives (**53a-b**, **55a-b** and **57a-b**) with MIC < 1 μg/mL and the control, fluconazole, were evaluated for CaCYP51 binding affinity (K_d) (Table 37).

For the mid-sized series, specifically the dichloro derivatives, the binding affinity for the thiazole (**48b**), nitro (**50b**) and free amine (**51b**) compounds was acceptable compared with fluconazole ($K_d = 60 \pm 40$ nM). For example, the K_d value for compound **48b** was (106 ± 15 nM) and (108 ± 34.4 nM) as well as (159 ± 17.6 nM) for **50b** and **51b**, respectively, which illustrated tight binding with the haem iron (Table 37). Weaker binding affinity for the mono-chloro derivative of the nitro (**50a**) was observed ($K_d = 458 \pm 30$ nM). The binding affinity for the chloro and dichloro of the acetyl derivatives (**46a-b**) as well as the chloro of the thiazole (**48a**) derivative indicated weak binding affinity as shown in Table 37.

For the extended series, the monochloro of the amide derivative (**57a**) showed the tightest binding ($K_d = 46 \pm 7.64$ nM) with CaCYP51 haem Fe^{3+} compared with the mid-sized series as well as fluconazole. Good binding affinity for the dichloro derivative of the thiourea (**53b**) and urea (**55b**) was observed (**53b**, $K_d = 125 \pm 41$ nM and **55b**, $K_d = 137 \pm 14$ nM) (Table 37).

Table 37: Binding affinity (K$_d$) values for the chloro and dichloro derivatives of the mid-sized and extended compounds.

Compounds	R^1	R^2	K$_d$ (nM)
46a	Cl	H	1445 ± 266
46b	Cl	Cl	229 ± 45
48a	Cl	H	635 ± 181
48b	Cl	Cl	106 ± 15
50a	Cl	H	458 ± 30
50b	Cl	Cl	108 ± 34.4
51a	Cl	H	-
51b	Cl	Cl	159 ± 17.6
53a	Cl	H	-
53b	Cl	Cl	125 ± 41.0
55a	Cl	H	-
55b	Cl	Cl	137 ± 14
57a	Cl	H	46 ± 7.64
57b	Cl	Cl	166 ± 39
Fluconazole			60 ± 40

Type II difference binding spectra were observed for both middle-sized and extended derivatives, which were titrated against 5 µM CaCYP51. The spectra illustrated the direct coordination of the triazole N as the sixth axial ligand with the haem Fe^{3+} of CaCYP51 as well as confirming the tight binding to the enzyme (Exemplars are shown in Figure 63) and was comparable with fluconazole binding as previously discussed in Chapter II (p 53).
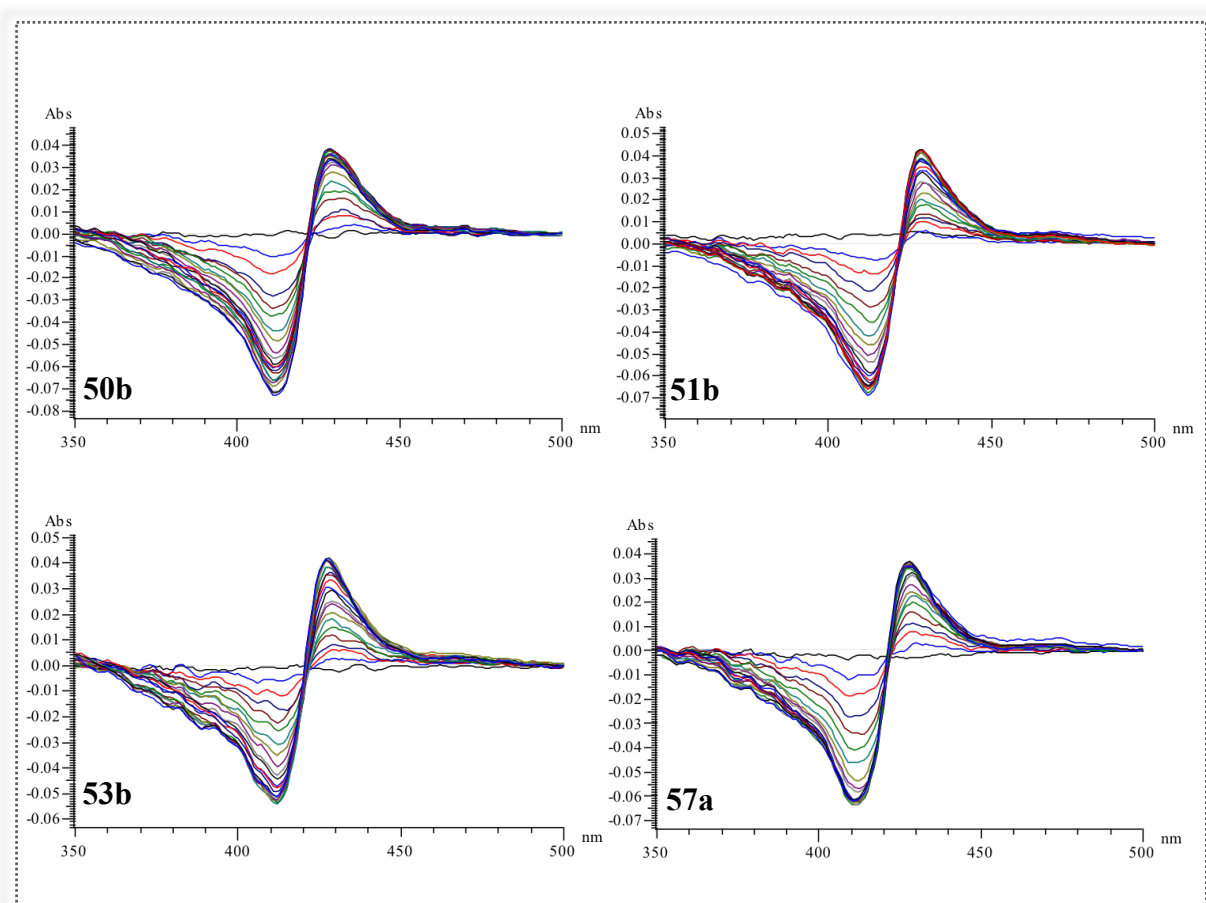
Figure 63: Examples of Type II binding spectra for mid-sized and extended compounds (**50b**, **51b**, **53b** and **57a**).

2. The fluoro and difluoro derivatives of the mid-sized and extended derivatives were evaluated at the Division of Health Sciences, University of Otago in New Zealand. Assays were performed by Dr. Brian Monk, Dr. Mikhail Keniya and Dr. Yasmeen Ruma. Our new collaboration allowed us to achieve the main objective of this project which was evaluating the novel compounds against resistance strains of different *Candida* species.

Saccharomyces cerevisiaeas (*S. cerevisiaeas*) has very high similarity to *Candida* species in the proteins involved as described by Karathia et al.[130] *S. cerevisiaeas* was used as a model organism to screen a large library of the fluoro and difluoro derivatives using disk diffusion assay determine which azole compounds to progress for further testing (MIC, IC_{50} and K_d) against *C. albicans* as well as other *Candida* species.

a) Disk diffusion assay:

The susceptibilities of *S. cerevisiaeas* strains to azole compounds were observed as zones of growth inhibition in agarose diffusion assays.[131] The novel compounds were evaluated against four *S. cerevisiaeas* strains which are:

1. Y2411- host strain expressing native wild type Erg11 and deleted of 7 ABC transporters therefore hypersensitive to azole drugs.[132]

2. Y2300 - overexpresses wild type levels of the native *S. cerevisiae* Erg11.[132]

3. Y2301 - *S. cerevisiae* overexpresses Erg11 with single mutation (Y140F) equivalent to *C. albicans* (Y132F), which showed resistance against fluconazole and voriconazole.[133]

4. Y2513 - *S. cerevisiaie* overexpresses Erg11 with single mutation (Y140H) equivalent to *C. albicans* (Y132H).[133]

All compounds were applied to sterile BBL paper disk with a concentration of 10 nmol/disk, compared with posaconazole (0.5 nmol/disk), and incubated at 30 °C for 48 h.

The hypersensitive strain *S. cerevisiae*-Y2411 was highly susceptible to the fluoro and difluoro of the mid-sized compounds (**46c**, **48c**, **50c-d** and **51c-d**) compared with posaconazole. The diflouro derivative of the thiazole and nitro (**48c** and **50c**, respectively) showed large zone of inhibition in the *S. cerevisiae* that overexpressed ERG11(Y2300) compared with other derivatives as well as with posaconazole. In contrast, all of the mid-sized compounds were ineffective in the single mutant strains (Y2301 and Y2513) compared with posaconazle, which exhibited a very small zone of inhibition as shown in Table 38. However, the reduced inhibitory activity of mid-sized azoles to single mutant strains (Y140F and Y140H) might occur owing to the loss of H-bonding with the mutant Tyr140, which could not be

compensated by forming additional binding interaction at the hydrophobic channel as these inhibitors are more comparable to fluconazole in length.

Table 38: Disk diffusion results of mid-sized derivatives in different *S. cerevisiae* strains.

Compounds / Strains	46c	48c	50c	50d	51c	51d	PCZ[*]
S. cerevisiae-Y2411 Host							
S. cerevisiae-Y2300 ERG11 (overexpressed)							
S. cerevisiae-Y2301 ERG11 (Y140F)							
S. cerevisiae-Y2513 ERG11 (Y140H)							

PCZ[*]=Posaconazole.

For fused ring compounds, the host strain *S. cerevisiae*-Y2411 was highly susceptible to all compounds (**59**, **61**, and **63**) compared with posaconazole. The overexpressed strain with ERG11 was highly susceptible to compound **59** and **61** as well as moderately susceptible to compound **63** compared with posaconazole. In the single mutant strains (Y140F and Y140H), a large zone of inhibition was observed for compound **59** and an intermediate zone for compound **61** compared with posaconazole. Compound **63** was ineffective in both mutant

180

strains (Y2301 and Y2513) as shown in Table 39. However, the steric hindrance at position 2 of compound **63** could play a role in the low susceptibility observed in the ERG11 overexpressed strain owing to reduced interaction with Tyr140. Besides that, reduced inhibitory activity against the mutant strains could occur due to the conformational change at the haem active site leading to loss of susceptibility.

Table 39: Disk diffusion results of fused ring derivatives in different *S. cerevisiae* strains.
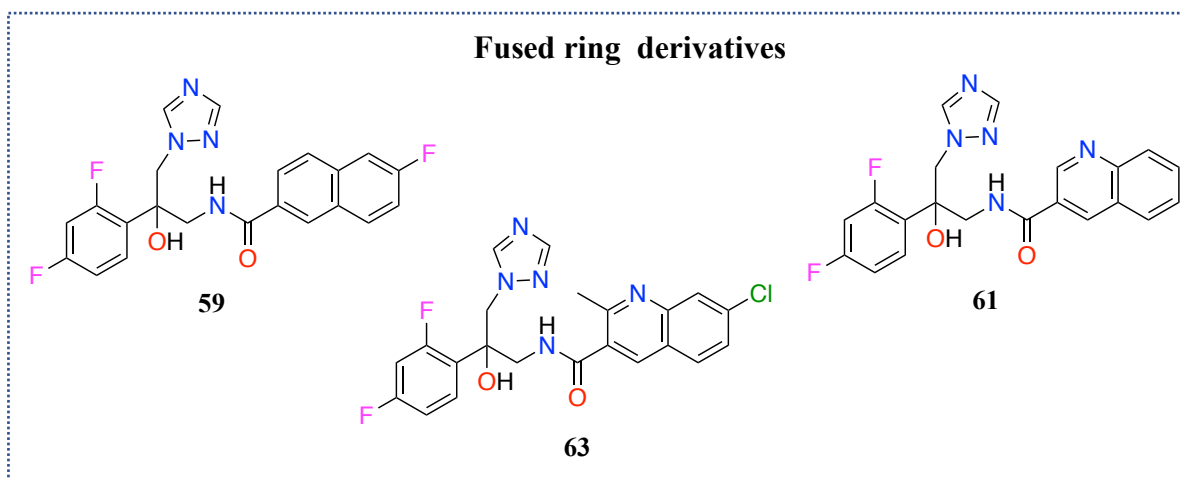
Compounds / Strains	59	61	63	PCZ
S. cerevisiae-Y2411 Host				
S. cerevisiae-Y2300 ERG11 (overexpressed)				
S. cerevisiae-Y2301 ERG11 (Y140F)				
S. cerevisiae-Y2513 ERG11 (Y140H)				

PCZ*=Posaconazole.

Table 40 demonstrated the disk diffusion assay results of extended compounds for the fluoro and difluoro amides linker as well as the *meta*- and *para*-biphenyl derivatives. The hypersensitive strain *S. cerevisiae*-Y2411 in addition to ERG11 overexpressed strain was highly susceptible to the amides (**57c** and **57d**) and biphenyl compounds compared with posaconazole. Moreover, the single mutant strains (Y140F and Y140H) showed good

susceptibility to the difluoro amide (**57c**) and *para*-biphenyl (**69a-b**) derivatives while intermediate susceptibility to the fluoro amide (**57d**) and *meta*-biphenyl (**70a-b**), compared with posaconazole.

Table 40: Disk diffusion results of extended derivatives in different *S. cerevisiae* strains.
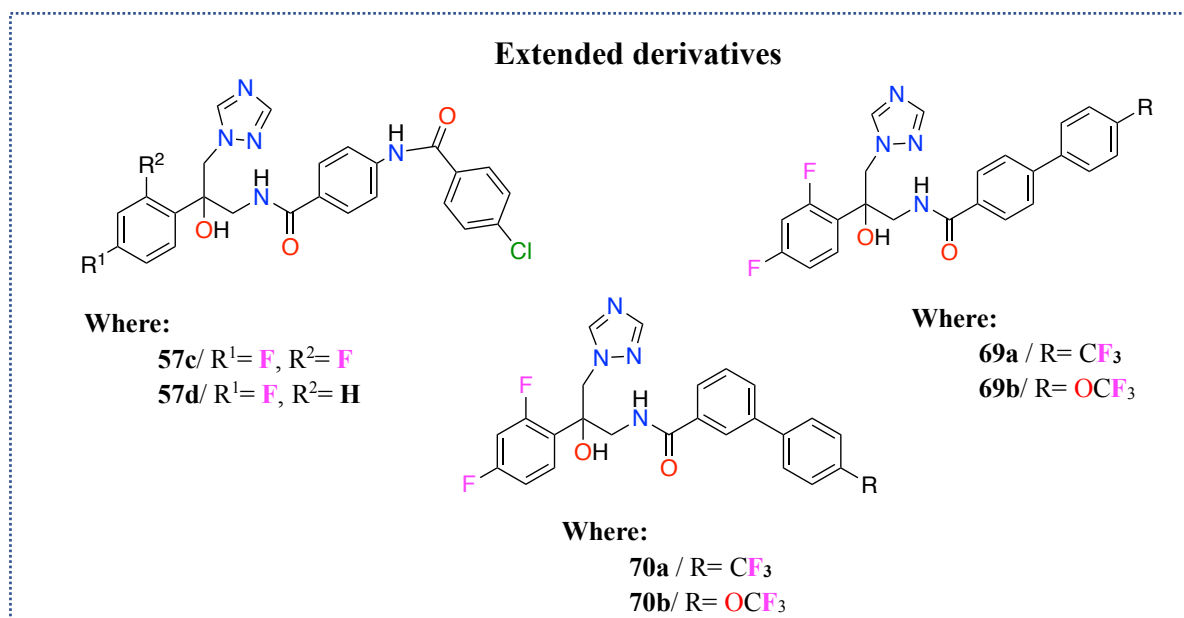
Compounds / Strains	57c	57d	69a	69b	70a	70b	PCZ*
S. cerevisiae-Y2411 Host							
S. cerevisiae-Y2300 ERG11 (overexpressed)							
S. cerevisiae-Y2301 ERG11 (Y140F)							
S. cerevisiae-Y2513 ERG11 (Y140H)							

PCZ*=Posaconazole.

From all derivatives (mid-sized, fused ring and extended series), the most promising compounds in the fused ring (**59**) and extended series (**57c-d**, **69a-b** and **70a-b**) were evaluated against *C. albicans* strains owing to the difficulty/sensitivity of disk diffusion assay as *C.*

albicans always has a blurry appearance in ZOI assay.[133–135] As a result, four *C. albicans* strains were used :

  1. SC5314- a laboratory strain as mentioned in Chapter II.[136]

  2. SGY-243- expresses low CaCdr1, which is one of the efflux pump transporters (ABC family), as mentioned in Chapter I.[137]

  3. Y611/FHB3- overexpresses ABC transporter (CaCdr1 + CaCdr2).[136]

  4. Y419/FR2- overexpresses MFS efflux transporter (CaMdr1),[137] as mentioned in Chapter I.

The disk diffusion assays of novel compounds in *C. albicans* strains involved a comparison with the non-azole drug micafungin, which is one of the echinocandins and has low susceptibility in *C. albicans* strains that overexpressed efflux pump transporters. The main reason for testing the promising compound against overexpress efflux pump strains was to evaluate the role of the transporters on the azoles compound as the current azole treatments show resistance.

  As shown in Figure 64, compound **59** and **69b** were highly active against *C. albicans* wild-type compared with other compounds as well as posaconazole (0.5 nmol/disk) and micafungin (0.4 nmol/disk). In the low CaCdr1 strain, high susceptibility was observed for all compounds (**59**, **57c-d**, **69a-b** and **70a-b**) and posaconazole compared with micafungin. Moreover, *C. albicans* strain with overexpression of CaCdr1 and CaCdr2 was intermediately susceptible to the fused ring compound (**59**) and *para*-biphenyl compound (**69b**) and weak susceptibility was observed for *meta*-biphenyl (**70a-b**). The monoflouro and diflouro amide compounds (**57c-d**) exhibited low inhibition compared with posaconazole and micafungin. This could be explained as the amide compounds (**57c-d**) might be substrats for ABC transporters.[134] On the other hand, *C. albicans* strain with MFS (CaMdr1) overexpression was highly susceptible to compound **59** and **69b** and intermediately susceptible to the rest of the compounds (**57c**, **69a** and **70a-b**) except compound **57d** which showed weak susceptibility compared with posaconazole and micafungin.

  C. glabrata is one of the species that developed resistance against azole treatments as mentioned in Chapter I. Thus, the novel inhibitors were screened against *C. glabrata* (CBS-138, clinical isolate) that overexpressed the ATP binding cassette transporter (CgCdr1).[138] The zone of growth inhibition was large for compounds **59** and **69b** while intermediate for *meta*-biphenyl (**70a-b**), and a small zone of inhibition was observed for compound **69a** compared with micafungin (Figure 64). Similar results observed for *C. albicans* wild-type were expected for wild-type *C. glabrata* disk diffusion testing.
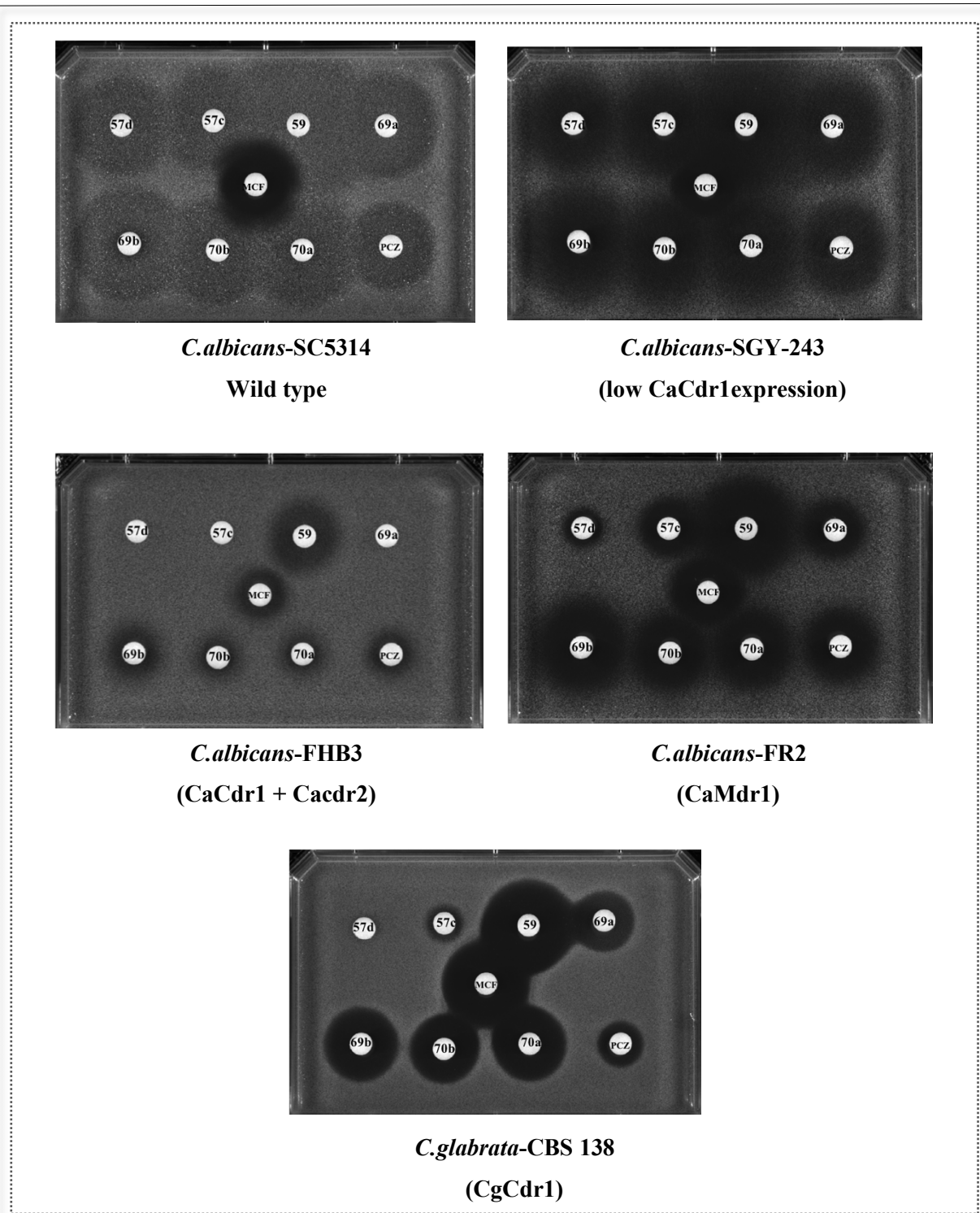
Figure 64: C. albicans and C. glabrata disk diffusion assay results for compound (**57c-d**, **59**, **69a-b** and **70a-b**) showing the zone of inhibition compared to posaconazole (PCZ) and micafungin (MCF).

From all compounds, disk diffusion assays indicated that compounds **59** and **69b** could be promising broad-spectrum azole antifungal treatment for *Candida* species. However, compounds **59**, **57c**, **69b** and **70a-b** were progressed to MIC$_{80}$ testing.

b) MIC$_{80}$ determination for *S. cerevisiaeas* and *Candida* species:

The interpretation of MIC results were always difficult in *Candida* species owing to triazoles fungistatic effects that produce trailing growth.[133,139] Thus, MIC$_{80}$, which is defined as 80% growth inhibition, was used to determine susceptibility values of novel azoles in different yeast species (*S. cerevisiaeas* and *Candida* species).

Five of the novel inhibitors (**59**, **57c**, **69b** and **70a-b**) were screened against four *S. cerevisiaeas,* with different characteristics as mentioned previously, and *C. albicans* wild type SC5314. As shown in Table 41, all five compounds were effective against *S. cerevisiaeas* hypersensitive and ERG11 overexpressed strains, but compound **59** (Y2411-MIC$_{80}$= 15 ± 3 nM and Y2300-MIC$_{80}$= 48 ± 4 nM) was highly effective compared with other compounds as well as posaconazole (Y2411-MIC$_{80}$= 94 ± 15 nM and Y2300-MIC$_{80}$= 281 ± 67 nM). Moreover, the growth of *S. cerevisiaeas* with single mutation (Y140F) was moderately inhibited by diflouro amide (**57c**), fused ring (**59**) and *meta*-biphenyl (**70a-b**) derivatives while good growth inhibition was observed for *para*-biphenyl (**69b**) with MIC$_{80}$ ranging from 93 to 46 nM compared with posaconazole (Y2301-MIC$_{80}$= 191 ± 41 nM). For *S. cerevisiaeas* single mutant (Y140H), compounds **57c** and **69b** showed promising activity compared with other compounds. However, the compound that showed constant and promising activity in all *S. cerevisiaeas* strains was **69b**. This high susceptibility effect in different strains could be related to the chemical structure of compound **69b**, a rigid moiety after the amide linker as well as the functional group OCF$_3$, which might play a role in blocking the enzyme's pocket entrance even if the confirmation of the enzyme changed due to single mutation.

C. albicans wild type SC5314 was very susceptible to fused ring (**59**, MIC$_{80}$= 18 nM) and *para*-biphenyl (**69b**, MIC$_{80}$= 40 nM) compared with other derivatives as well as posaconazole (MIC$_{80}$= 73 nM). Further investigations (MIC$_{80}$, IC$_{50}$ and K$_d$) against C. *albicans* single mutant (Y132F and Y132H), double mutant (Y132H/K143R and Y132F/F145L) and other *Candida* species will be done but owing to the COVI-19 situation, there was some delay in many biological results.

Table 41: MIC$_{80}$ of promising novel inhibitors **59**, **57c**, **69b** and **70a-b**.

Five promising derivatives
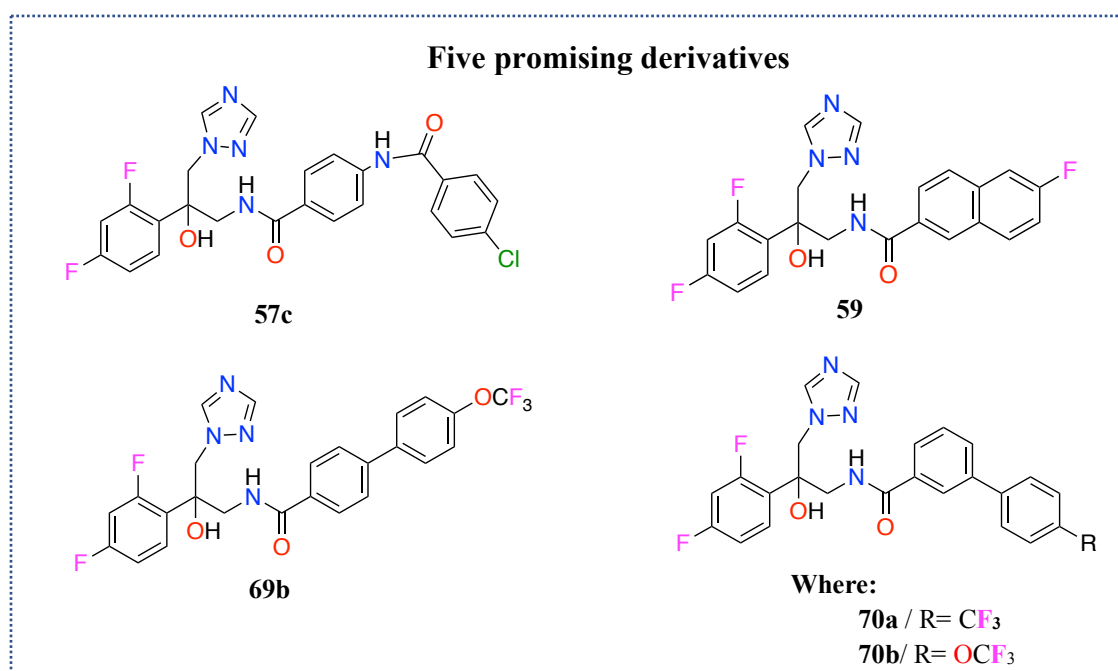
Strains	*S. cerevisiae-* Y2411 Host	*S. cerevisiae-* Y2300 ERG11 (overexpressed)	*S. cerevisiae-* Y2301 ERG11 (Y140F)	*S. cerevisiae-* Y2513 ERG11 (Y140H)	*C. albicans-* SC5314 Wild type
Compounds	MIC$_{80}$ (nM)				
57c	39 ± 14	182 ± 30	123 ± 38	87 ± 4	208 ± 83
59	15 ± 3	48 ± 4	326 ± 48	632 ± 123	18
69b	20	96 ± 29	93 ± 46	78 ± 56	40
70a	30	163 ± 61	419 ± 83	719 ± 1	85
70b	41 ± 15	73 ± 26	411 ± 71	805 ± 121	100
PCZ	94 ± 15	281 ± 67	191 ± 41	147 ± 57	73

3. Conclusion:

The main focus in this chapter was to design and synthesise two series of compounds:

a. Mid-sized series which was slightly longer than fluconazole.

b. Extended series that was comparable with the length of posaconazole.

All azole compounds were computationally investigated in CaCYP51 wild-type as well as in the double mutant CaCYP51(Y132H/K143R and Y132F/F145L) proteins. The novel inhibitors formed direct bonding interaction between the triazole N and the haem Fe^{3+} with a distance less than 3 Å and showed multiple binding interactions with different amino acids in the enzyme pocket. Based on the docking and molecular dynamic studies, the novel extended compounds, especially the amide derivatives (*S*)- **57** and (*R*)-**57**, exhibited promising binding interactions with key amino acids (e.g. His377, Met508, Leu376 and Ser378) in CaCYP51 wild-type as well as in the double mutant CaCYP51 either through direct H-bonding or water mediated interactions. Moreover, the molecular dynamic studies of (*S*)- and (*R*)-biphenyl extended compounds (**69** and **70**) was less promising in forming direct or water mediated interaction compared with amide derivatives (**57**) but exploring different moieties with more rigid structures at the access channel was needed to evaluate the biological effects.

The synthesis of mid-sized series was achieved by five reaction steps with two additional steps for the extended series. The only difficulty during synthesis of the final compounds was purification which slightly affected the yield. However, all final compound structures were confirmed by $^1H/^{13}C$ NMR and purity was confirmed by either HPLC or microanalysis.

The biological testing was done by two teams of collaborators owing to the COVID-19 situation, thus comparing all biological results was difficult due to experimental condition, techniques and MIC_{50} or MIC_{80} concentration used, and the only common factor between the two teams was *C. albicans* SC5314- laboratory strain. As a result, the di-Cl thiazole (**48b**) of the mid-sized series, mono-Cl and di-Cl amide (**57a** and **57b**, respectively) of the extended series were highly active against SC5314 strain with MIC ≤ 0.03 μg/mL for all and with potent IC_{50} (**48b** IC_{50}= 0.41 μM, **57a** IC_{50}= 0.56 μM, **57b** IC_{50}= 0.48 μM), but only compound **57a** showed very tight binding to CaCYP51(**57a** K_d= 46 ± 7.64 nM) while good binding affinity for **48b** (K_d= 106 ± 15 nM) and **57b** (K_d= 166 ± 39 nM,) compared with fluconazole (MIC_{50}= 0.125 μg/ml, IC_{50}= 0.31 μM and K_d= 60 ± 40 nM). On the other hand, the difluoro fused ring derivative (**59**) and *para*-biphenyl (**69b**) were the most active compounds from the rigid

moieties in *C. albicans* SC5314 strain (**59** MIC_{80}=18 nM and **69b** MIC_{80}= 40 nM) compared with posaconazole (MIC_{80}= 73 nM).

Since the MIC values for previous chloro and fluoro compounds (**48b**, **57a-c**, **59**, and **69b**) were promising, determining physicochemical properties was important to assure that compounds were within Lipinsky's range. Table 42 demonstrates the physicochemical properties of the most promising CaCYP51 novel inhibitors and reference antifungal agents. The mid-sized (**48b**) and fused ring (**59**) compounds have much better molecular weight and cLogP compared with fluconazole (FLZ). Thus, compound **48b** and **59** showed more drug like properties even with one extra H-bond donor compared with the clinical azole agents. In contrast, the amide derivatives (**57a-c**) and the biphenyl compound (**69b**) have significant increase in molecular weight in additional to significant increase in cLogP for compound **69b** compared to fluconazole, which leads to violating Lipinsky's range. However, compounds **57** and **69b** showed less violation when compared with posaconazole and oteseconazole (VT-1161). The novel extended compounds (**57** and **69b**) were very close to oteseconazole in all other physicochemical properties except in the number of H-bond donor (nOHNH), which might affect the absorption of the oral drug.[140]

Table 42: Physicochemical properties of promising compounds and clinical antifungal agents.

Compound	MW	cLogP	nON	nOHNH	nrotb	nviol
48b	399.81	2.23	7	2	6	0
57a	510.38	3.79	8	3	8	1
57b	544.83	4.35	8	3	8	1
57c	511.92	3.55	8	3	8	1
59	424.40	3.34	6	2	6	0
69b	518.44	5.39	7	2	9	2
FLZ	306.27	0.87	7	1	5	0
PCZ	700.77	5.38	12	1	12	3
VT-1161	527.39	5.2	7	1	9	2

MW= Molecular weight; nON= H-bond acceptor; nOHNH= H-bond donor; nrotb= number of routable bonds; nviol= number of Lipinsky violations.

However, compounds **59** and **69b** IC_{50} and K_d values are still in progress. Further testing of all promising compounds against *C. albicans* single and double mutant clinical isolates as well as other *Candida* species is in progress. Also, selectivity testing against human CYPs is still in progress. Unfortunately, there was huge delay in all biological testing owing to COVID-19 lockdowns.

In the next chapter, a new series of extended compounds similar to compound **57c** and **69b** but without the hydroxy group at the chiral center were designed and synthesised to overcome fluconazole resistance developed from Tyr132 single or double mutations.

4. Experimental:

Computational docking and MD simulations were performed as described in Chapter II (p 61). The physicochemical properties to compounds were calculated using Molinspiration software.[141]

a. General method:

1-(4-Chlorophenyl)-2-(1H-1,2,4-triazol-1-yl)ethan-1-one (41a)

($C_{10}H_8ClN_3O$, M.W. 221.64)

Dry CH$_3$CN, triazole, K$_2$CO$_3$

0°C for 30 min, room temp., overnight

(40a) **(41a)**
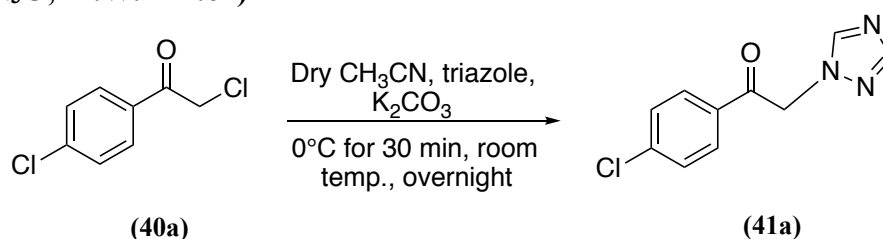
Method: To a cooled (0 °C, ice) solution of 2,4′-dichloroacetophenone (**40a**) (10.0 g, 53 mmol) in acetonitrile (250 mL) was added 1,2,4-triazole (7.307 g, 106 mmol) and K$_2$CO$_3$ (5.33 g, 63 mmol). The reaction was stirred vigorously at 0 °C for 30 min then at room temperature overnight. The orange reaction mixture was filtered to remove inorganics (KCl) and the filtrate concentrated under reduced pressure to give a yellow solid. EtOAc (100 mL) and H$_2$O (50 mL) were added and the mixture stirred at room temperature for 15 min before most of the EtOAc was carefully removed under reduced pressure. The resulting aqueous suspension was filtered, and the residue washed with Et$_2$O to remove any unreacted acetophenone. The crude white solid was recrystallised from EtOH to give the product as a white crystalline solid.

Yield: 5.94 g (51 %) as a white crystalline solid.

m.p.: 148-150 °C (lit. m.p.: 149-150 °C)[123].

Rf: 0.22 (2:1 v/v EtOAc-petroleum ether).

^{1}H NMR (DMSO-d$_6$): δ 8.51 (s, 1H, triaz), 8.07 (d, J = 8.8 Hz, 2H, Ar), 8.03 (s, 1H, triaz), 7.68 (d, J = 8.8 Hz, 2H, Ar), 5.99 (s, 2H, CH$_2$).

1-(2,4-Dichlorophenyl)-2-(1H-1,2,4-triazol-1-yl)ethan-1-one (41b)

($C_{10}H_7Cl_2N_3O$, M.W. 256.09)

Dry toluene, triazole, NaHCO$_3$

reflux for 4h

(40b) **(41b)**
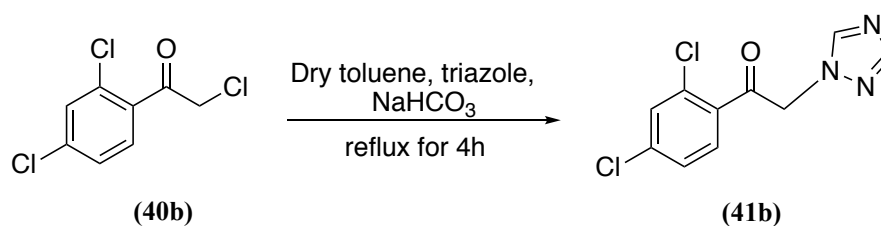
Method: To a solution of 2,2′,4′-trichloroacetophenone (**40b**) (1 g, 4.47 mmol) in dry toluene (30 mL) was added 1,2,4-triazole (0.37 g, 5.37 mmol) and $NaHCO_3$ (0.45 g, 5.37 mmol). The reaction was refluxed for 4 h and left at room temperature overnight. The reaction mixture was extracted with EtOAc (100 mL), and the organic layer was washed with brine (2 x 50 mL), H_2O (2 x 50 mL) and dried ($MgSO_4$). The organic layer was evaporated under reduced pressure to give a brown oil, which was purified by gradient column chromatography and the desired compound was eluted at 3% MeOH in CH_2Cl_2.

Yield: 0.68g (60 %) as a yellow solid.

m.p.: 108-110°C (lit. m.p.: 160-161 °C)[124].

R*f*: 0.5 (9.5: 0.5 v/v CH_2Cl_2-MeOH).

^{1}H NMR (DMSO-d$_6$): δ 8.53 (s, 1H, triaz), 8.02 (s, 1H, triaz), 7.95 (d, *J* = 8.3 Hz, 1H, Ar),7.82 (d, *J* = 1.9 Hz, 1H, Ar), 7.65 (dd, *J* = 2.0, 8.3 Hz, 1H, Ar), 5.85 (s, 2H, CH$_2$).

Using this procedure, the following compounds were prepared:

1-(2,4-Difluorophenyl)-2-(1*H*-1,2,4-triazol-1-yl)ethan-1-one (41c)
(C$_{10}$H$_7$F$_2$N$_3$O, M. Weight. 223.18)

(40c) → Dry Toluene, triazole, NaHCO$_3$, reflux for 4h → (41c)
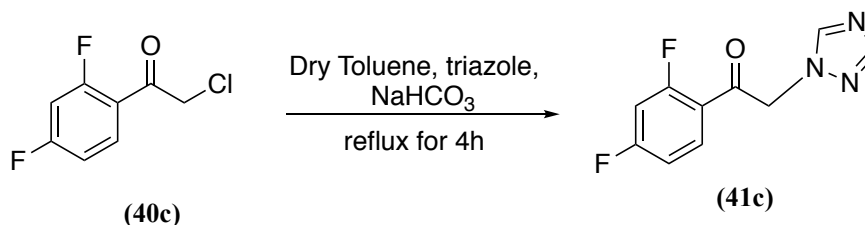
Reagents: 2-chloro-2′,4′-difluoroacetophenone (**41c**) (3 g, 15.74 mmol).

Yield: 2.35 g (67 %) as a white solid.

m.p.: 112-114 °C (lit. m.p.: 104-106 °C)[124].

R*f*: 0.4 (9.5: 0.5 v/v CH_2Cl_2-MeOH).

^{1}H NMR (DMSO-d$_6$): δ 8.49 (s, 1H, triaz), 8.03 (dd, *J* = 8.7, 15.4 Hz, 1H, Ar), 8.02 (s, 1H, triaz), 7.56-7.51 (m, 1H, Ar), 7.31 (ddd, *J* = 2.6, 8.2, 10.6 Hz, 1H, Ar), 5.81 (d, *J* = 3.0 Hz, 2H, C<u>H</u>$_2$).

^{19}F NMR (DMSO-d$_6$): δ -100. 78 (meta-F-Ar), -103.36 (*para*-F-Ar).

1-(4-Fluorophenyl)-2-(1*H*-1,2,4-triazol-1-yl)ethan-1-one (41d)[123]

(C$_{10}$H$_8$FN$_3$O, M.W. 205.19)

(40d) **(41d)**
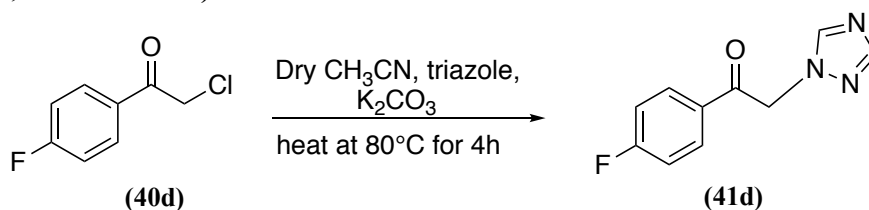
Variation: Heated at 80 °C for 4 h.

Reagents: 2-chloro-4′-fluoro-acetophenone (**41d**) (3.8 g, 22.01 mmol). The residue was purified using column chromatography and the desired compound was eluted at 3 % MeOH.

Yield: 3.19 g (70 %) as a white crystalline solid.

m.p.: 116-118 °C (lit. m.p.: not found).

R*f*: 0.47 (9.5: 0.5 v/v CH$_2$Cl$_2$-MeOH).

^{1}H NMR (DMSO-d$_6$): δ 8.51(s, 1H, triaz), 8.14 (dd, *J* = 5.5, 9.0 Hz, 2H, Ar), 8.02 (s, 1H, triaz), 7.44 (t, *J* = 8.9 Hz, 2H, Ar), 5.99 (s, 2H, C<u>H</u>$_2$-triaz).

F NMR (DMSO-d$_6$): δ -104.32 (*para*-F-Ar).

1-((2-(4-Chlorophenyl)oxiran-2-yl)methyl)-1*H*-1,2,4-triazole (42a)[126]

(C$_{11}$H$_{10}$ClN$_3$O, M.W. 235.67)

(41a) **(42a)**
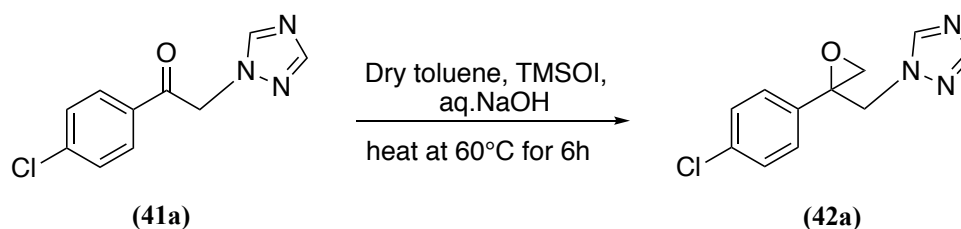
Method: To a solution of 1-(4-chlorophenyl)-2-(1*H*-1,2,4-triazol-1-yl)ethan-1-one (**41a**) (5.0 g, 22.56 mmol) in toluene (250 mL) was added trimethylsulfoxonium iodide (TMSOI) (9.93 g, 45.12 mmol) followed by 20% aqueous NaOH (17.06 mL = 3.41 g, 85.27 mmol) and the reaction heated at 60 ºC for 6 h. TLC (petroleum ether – EtOAc 1:2 v/v) confirmed consumption of starting material. The reaction was diluted with H$_2$O (50 mL) and EtOAc (100 mL). The aqueous layer was extracted with EtOAc (2 x 50 mL), then the combined organic extracts washed with H$_2$O (2 x 50 mL), brine (50 mL), dried (MgSO$_4$) and concentrated under reduced pressure to give the crude product as a dark orange/red oil. This crude product was used directly in the next step without any further purification.

Yield: 5.06 g (95 %, crude) as a dark orange oil.

¹H NMR (DMSO-d₆): δ 8.39 (s, 1H, triaz), 7.91 (s, 1H, triaz), 7.40 (s, 4H, Ar), 5.06 (d, J = 15.0 Hz, 1H, C*Ha*Hb-triaz), 4.64 (d, J = 15.0 Hz, 1H, CHa*Hb*-triaz), 3.04 (d, J = 4.9 Hz, 1H, OC*Ha*Hb), 2.87 (d, J = 4.9 Hz, 1H, OCHa*Hb*).

Using this procedure, the following compounds were prepared:

1-((2-(2,4-Dichlorophenyl)oxiran-2-yl)methyl)-1*H*-1,2,4-triazole (42b)[126]
(C₁₁H₉Cl₂N₃O, M.W. 270.11)

(41b) → (42b)

Dry toluene, TMSOI, aq.NaOH
heat at 60°C for 72h
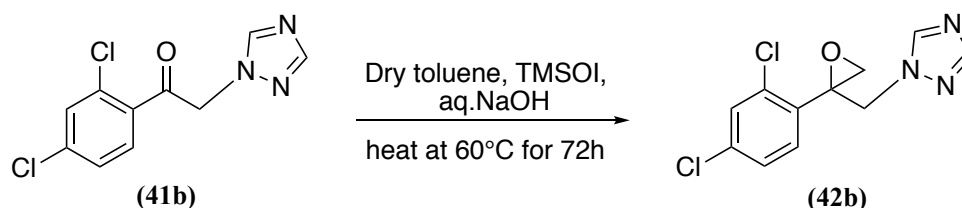
Reagents: 1-(2,4-dichlorophenyl)-2-(1*H*-1,2,4-triazol-1-yl)ethan-1-one (**41b**) (0.68g, 2.65 mmol).

Yield: 0.71 g (92 %, crude) as an orange oil.

R*f*: 0.37 (2:1 v/v EtOAc-petroleum ether).

¹H NMR (DMSO-d₆): δ 8.39 (s, 1H, triaz), 7.91 (s, 1H, triaz), 7.66 (d, J = 1.9 Hz, 1H, Ar), 7.35 (dd, J = 1.9, 8.3 Hz, 1H, Ar), 7.12 (d, J = 8.3 Hz, 1H, Ar), 4.87 (d, J = 15.0 Hz, 1H, C*Ha*Hb-triaz), 4.55 (d, J = 15.0 Hz, 1H, CHa*Hb*-triaz), 3.13 (d, J = 4.7 Hz, 1H, OC*Ha*Hb), 2.94 (d, J = 4.7 Hz, 1H, OCHa*Hb*).

1-((2-(2,4-Difluorophenyl)oxiran-2-yl)methyl)-1*H*-1,2,4-triazole (42c)[126]
(C₁₁H₉F₂N₃O, M.W. 237.21)

(41c) → (42c)

Dry toluene, TMSOI, aq.NaOH
heat at 60°C for 6h
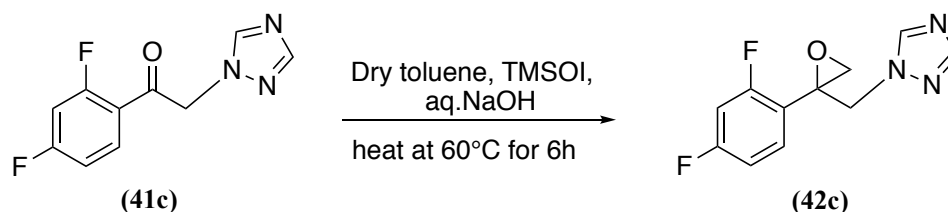
Reagents: 1-(2,4-difluorophenyl)-2-(1*H*-1,2,4-triazol-1-yl)ethan-1-one (**41c**) (1.5g, 6.72 mmol).

Yield: 1.32 g (83 %, crude) as orange oil.

R*f*: 0.42 (2:1 v/v EtOAc-petroleum ether).

¹H NMR (DMSO-d₆): δ 8.39 (s, 1H, triaz), 7.90 (s, 1H, triaz), 7.28 (dd, J = 9.0, 15.1 Hz, 1H, Ar), 7.23-7.18 (m, 1H, Ar), 7.02 (ddd, J = 2.6, 8.5, 10.9 Hz, 1H, Ar), 4.77 (d, J = 15.0 Hz, 1H,

CHaHb-triaz), 4.58 (d, *J* = 15.0 Hz, 1H, CHa*Hb*-triaz), 3.09 (d, *J* = 4.8 Hz, 1H, OC*Ha*Hb), 2.96 (d, *J* = 4.8 Hz, 1H, OCHa*Hb*).

1-((2-(4-Fluorophenyl)oxiran-2-yl)methyl)-1*H*-1,2,4-triazole (42d)[126]
(C₁₁H₁₀FN₃O, M. W. 219.22)

(41d) → **(42d)**

Dry toluene, TMSOI, aq.NaOH

heat at 60°C for 6h
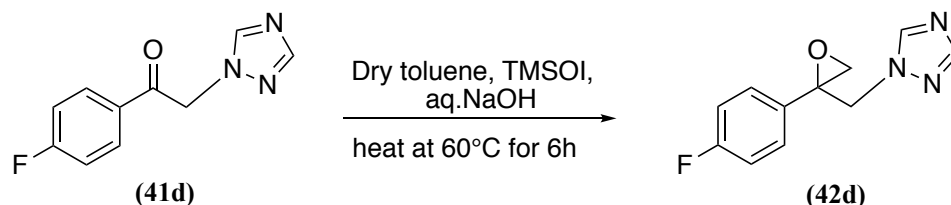
Reagents: 1-(4-fluorophenyl)-2-(1*H*-1,2,4-triazol-1-yl)ethan-1-one (**41d**) (1.65 g, 8.04 mmol).

Yield: 1.63 g (92 %, crude) as a yellow oil.

R*f*: 0.37 (2:1 v/v EtOAc-petroleum ether).

¹H NMR (DMSO-d₆): *δ* 8.38 (s, 1H, triaz), 7.91 (s, 1H, triaz), 7.41 (dd, *J* = 5.5, 9.0 Hz, 2H, Ar), 7.16 (t, *J* = 8.9 Hz, 2H, Ar), 5.02 (d, *J* = 15.0 Hz, 1H, C*Ha*Hb-triaz), 4.6 (d, *J* = 15.0 Hz, 1H, CHa*Hb*-triaz), 3.01 (d, *J* = 4.9 Hz, 1H, OC*Ha*Hb), 2.87 (d, *J* = 4.9 Hz, 1H, OCHa*Hb*).

1-Azido-2-(4-chlorophenyl)-3-(1*H*-1,2,4-triazol-1-yl)propan-2-ol (43a)
(C₁₁H₁₁ClN₆O, M.W. 278.70)

(42a) → **(43a)**

Dry DMF, NaN₃, NH₄Cl

heat at 60°C for 2h room temp., overnight
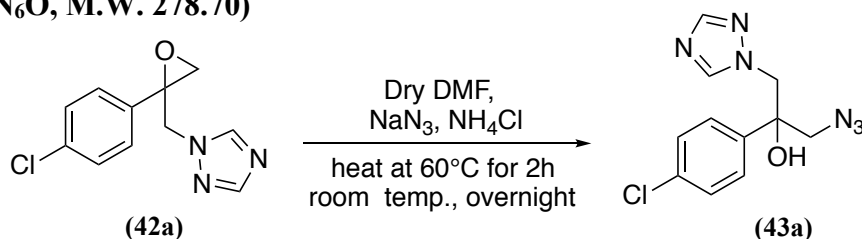
Method: To a solution of crude 1-((2-(4-chlorophenyl)oxiran-2-yl)methyl)-1*H*-1,2,4-triazole (**42a**) (5.06 g, 21.47 mmol) in dry DMF (58 mL) was added NaN₃ (2.72 g, 41.87 mmol) followed by NH₄Cl (1.38 g, 25.76 mmol) and the reaction heated at 60 °C for 2 h then overnight at room temperature. The reaction was quenched by the addition of NaHCO₃ (100 mL) and then extracted with EtOAc (100 mL). The aqueous layer was back extracted with EtOAc (3 x 50 mL) then the combined organic extracts washed with H₂O (100 mL), brine (100 mL), dried (MgSO₄) and concentrated under reduced pressure to give a thick orange-red syrup. The crude product was purified by gradient column chromatography and the product eluted with petroleum ether-EtOAc 4:6 v/v as a thick yellow syrup.

Yield: 3.76 g (60% over two steps from **41a**) as a thick yellow syrup.

R*f*: 0.45 (2:1 v/v EtOAc-petroleum ether).

¹H NMR (DMSO-d₆): *δ* 8.22 (s, 1H, triaz), 7.85 (s, 1H, triaz), 7.42 (d, *J* = 8.9 Hz, 2H, Ar),

7.37 (d, J = 8.9 Hz, 2H, Ar), 6.14 (s, 1H, OH, ex), 4.53 (dd, J = 14.3, 22.0 Hz, 2H, CH$_2$-triaz), 3.65 (dd, J = 12.9, 22.6 Hz, 2H, CH$_2$-N$_3$).

^{13}C NMR (DMSO-d$_6$): δ 151.26 (CH, triaz), 145.58 (CH, triaz), 141.04 (C, Ar), 132.53 (C, Ar), 128.31 (2 x CH, Ar), 128.56 (2 x CH, Ar), 75.94 (C-OH), 57.87 (CH$_2$-triaz), 56.35 (CH$_2$-N$_3$).

HPLC (Method B): 99 %, RT = 4.87 min.

HRMS (ESI, m/z): theoretical mass: 279.0761 [M+H]$^+$, observed mass: 279.0761 [M+H]$^+$.

Using this procedure, the following compounds were prepared:

1-Azido-2-(2,4-dichlorophenyl)-3-(1H-1,2,4-triazol-1-yl)propan-2-ol (43b)[127]
(C$_{11}$H$_{10}$Cl$_2$N$_6$O, M. W. 313.14)

(42b) → **(43b)**
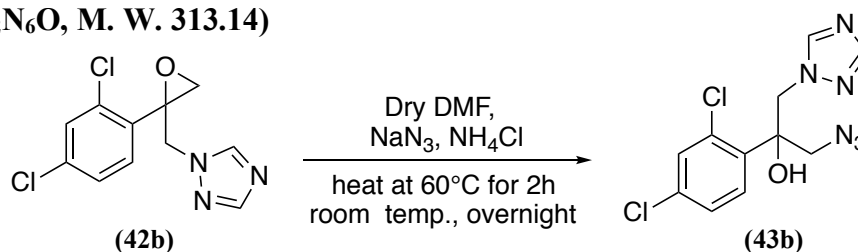
Reagents: 1-((2-(2,4-dichlorophenyl)oxiran-2-yl)methyl)-1H-1,2,4-triazole (0.68g, 2.51 mmol). The residue was purified using gradient column chromatography and the desired compound was eluted with petroleum ether-EtOAc 3:7 v/v.

Yield: 0.52 g (63% over two steps from **41b**) as a thick orange oil.

Rf: 0.57 (2:1 v/v EtOAc- petroleum ether).

^{1}H NMR (DMSO-d$_6$): δ 8.32 (s, 1H, triaz), 7.78 (s, 1H, triaz), 7.58 (t, J = 2.4 Hz, 2H, Ar), 7.37 (dd, J = 2.2, 8.6 Hz, 1H, Ar), 6.46 (s, 1H, OH, ex), 4.85 (d, J = 14. Hz, 1H, CHaHb-triaz), 4.68 (d, J = 14.4 Hz, 1H, CHaHb-triaz), 4.01 (d, J = 13.2 Hz, 1H, CHaHb-N$_3$), 3.73 (d, J = 13.2 Hz, 1H, CHaHb-N$_3$).

1-Azido-2-(2,4-difluorophenyl)-3-(1H-1,2,4-triazol-1-yl)propan-2-ol (43c)[127]
(C$_{11}$H$_{10}$F$_2$N$_6$O, M.W. 280.24)

(42c) → **(43c)**
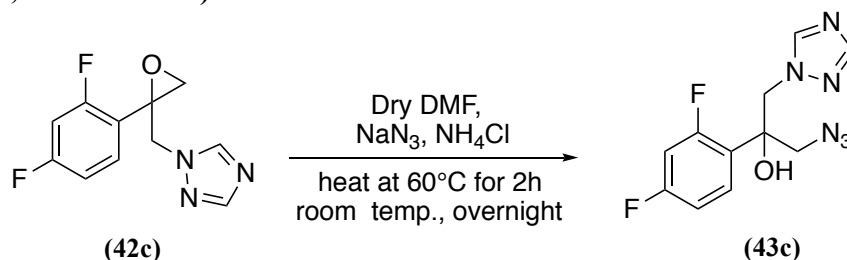
Reagents: 1-((2-(2,4-difluorophenyl)oxiran-2-yl)methyl)-1*H*-1,2,4-triazole (42c) (1.30 g, 5.48 mmol). The residue was purified using gradient column chromatography and the desired compound was eluted with petroleum ether-EtOAc 3:7 v/v.

Yield: 0.93 g (60 % over two steps from **41c**) as a thick colourless oil.

R*f*: 0.35 (2:1 v/v EtOAc-petroleum ether).

¹H NMR (DMSO-d₆): δ 8.30 (s, 1H, triaz), 7.79 (s, 1H, triaz), 7.44 (dd, *J* = 9.1, 15.9 Hz, 1H, Ar), 7.23-7.19 (m, 1H, Ar), 7.03 (ddd, *J* = 2.5, 8.2, 10.8 Hz, 1H, Ar), 6.38 (s, 1H, OH, ex), 4.56 (s, 2H, CH₂-triaz), 3.73 (d, *J* = 13.8 Hz, 1H, C*Ha*Hb-N₃), 3.63 (d, *J* = 13.8 Hz, 1H, CHa*Hb*-N₃).

1-Azido-2-(4-fluorophenyl)-3-(1*H*-1,2,4-triazol-1-yl)propan-2-ol (43d)
(C₁₁H₁₁FN₆O, M.W. 262.25)

(42d)   Dry DMF, NaN₃, NH₄Cl   heat at 60°C for 2h   room temp., overnight   **(43d)**
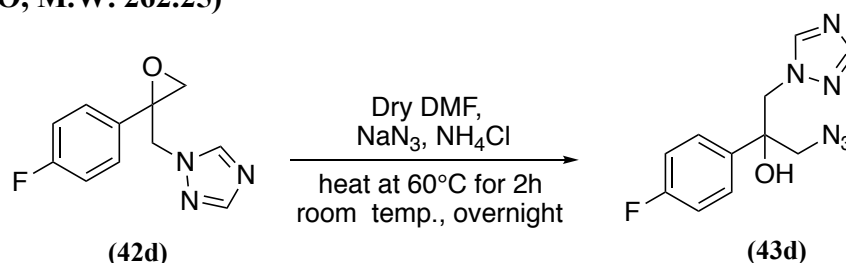
Reagents: 1-((2-(4-fluorophenyl)oxiran-2-yl)methyl)-1*H*-1,2,4-triazole (**42d**) (1.5 g, 6.84 mmol). The residue was purified using gradient column chromatography and the desired compound was eluted with petroleum ether-EtOAc 2:8 v/v.

Yield: 1. 25 g (60 % over two steps from **41d**) as a thick colourless oil.

R*f*: 0.22 (2:1 v/v EtOAc-petroleum ether).

¹H NMR (DMSO-d₆): δ 8.20 (s, 1H, triaz), 7.85 (s, 1H, triaz), 7.44 (dd, *J* = 5.5, 9.0 Hz, 2H, Ar), 7.13 (t, *J* = 8.9 Hz, 2H, Ar), 6.10 (s, 1H, OH, ex), 4.53 (dd, *J* = 14.3, 26.9 Hz, 2H, CH₂-triaz), 3.64 (dd, *J* = 12.9, 25.3 Hz, 2H, CH₂-N₃).

¹³C NMR (DMSO-d₆): δ 161.87 (d, ¹*J*$_{CF}$ = 243.9 Hz, para-CF), 151.22 (CH, triaz), 145.54 (CH, triaz), 138.13 (C, Ar), 128.37 (2 x CH, Ar), 114.99 (2 x CH, Ar), 75.86 (C-OH), 57.59 (CH₂-triaz), 56.48 (CH₂-N₃).

HPLC (Method A): 100 %, RT = 4.17 min.

HRMS (ESI, m/z): theoretical mass: 263.1046 [M+H]⁺, observed mass: 263.1058 [M+H]⁺.

1-Amino-2-(4-chlorophenyl)-3-(1*H*-1,2,4-triazol-1-yl)propan-2-ol (44a)

(C_{11}H_{13}ClN_4O, M.W. 252.70)

(43a)   I. Dry THF, TPP, room temp. 1h / II. H$_2$O heat at 60°C for 4h   **(44a)**
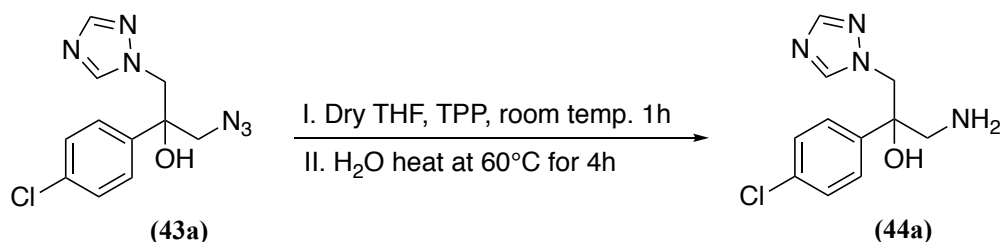
Method: To a solution of 1-azido-2-(4-chlorophenyl)-3-(1*H*-1,2,4-triazol-1-yl)propan-2-ol (**43a**) (2g, 7.81 mmol) in dry THF (20 mL) was added TPP (2.16g, 8.26 mmol) and the reaction stirred at room temperature for 1 h. H$_2$O (1.42 mL, 78.98 mmol) was added and the reaction heated at 60 °C for 4 h. The reaction was concentrated under reduced pressure and 2M aqueous HCl (20 mL) was added to the resulting residue and the reaction stirred at room temperature for 20 min before extracting with CH$_2$Cl$_2$ (4 x 25 mL) to remove excess Ph$_3$P and triphenylphosphine oxide by-product. To the aqueous layer was added 1M aqueous NaOH until basic pH; the free amine was then extracted with EtOAc (2 x 50 mL). The organic layers were combined, dried (MgSO$_4$) and concentrated under reduced pressure to give the product as a colourless syrup, which became a white solid on standing overnight.

Yield: 0.74g (91%) as a white solid.

m.p.: 94-96 °C.

R*f*: 0.36 (9:1 v/v CH$_2$Cl$_2$-MeOH).

¹H NMR (DMSO-d₆): δ 8.20 (s, 1H, triaz), 7.82 (s, 1H, triaz), 7.39 (d, *J* = 8.9 Hz, 2H, Ar), 7.33 (d, *J* = 8.8 Hz, 2H, Ar), 5.53 (brs, 1H, OH, ex), 4.50 (d, *J* = 14.3 Hz, 1H, C*Ha*Hb-triaz), 4.46 (d, *J* = 14.3 Hz, 1H, CHa*Hb*-triaz), 3.27 (d, *J* = 14.3 Hz,, 1H, C*Ha*Hb-NH$_2$), 2.94 (d, *J* = 14.3 Hz,, 1H, CHa*Hb*-NH$_2$), 1.56 (brs, 2H, N<u>H</u>$_2$).

¹³C NMR (DMSO-d₆): δ 150.91 (CH, triaz), 145.28 (CH, triaz), 142.61 (C, Ar), 131.91 (C, Ar), 128.25 (2 x CH, Ar), 128.16 (2 x CH, Ar), 75.82 (C-OH), 56.48 (CH$_2$-triaz), 49.79 (CH$_2$-NH$_2$).

HPLC (Method B): 97 %, RT = 4.84 min.

HRMS (ESI, m/z): theoretical mass: 253.0856 [M+H]⁺, observed mass: 253.0855 [M+H]⁺.

Using this procedure, the following compounds were prepared:

1-Amino-2-(2,4-dichlorophenyl)-3-(1*H*-1,2,4-triazol-1-yl)propan-2-ol (44b) [127]

(C$_{11}$H$_{12}$Cl$_2$N$_4$O, M. W. 287.14)

(43b)   **(44b)**

I. Dry THF, TPP, room temp. 1h

II. H$_2$O heat at 60°C for 4h
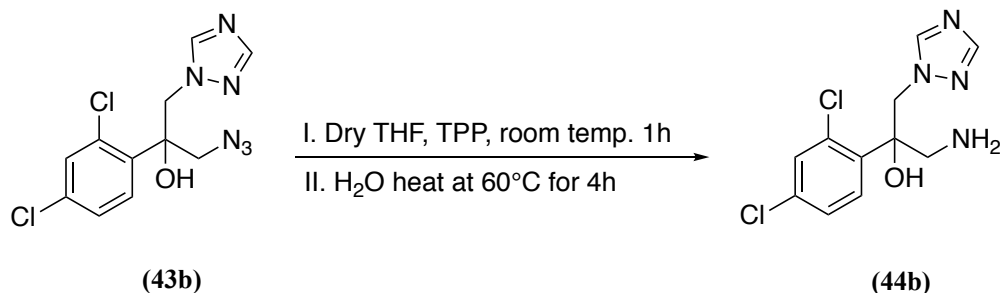
Reagents: 1-azido-2-(2,4-dichlorophenyl)-3-(1*H*-1,2,4-triazol-1-yl)propan-2-ol (**43b**) (0.52g, 1.66 mmoL).

Yield: 0.34g (72%) as a white solid.

m.p.: 78-80 °C (lit. m.p.: 215-216°C)[142].

R*f*: 0.47 (9:1 v/v CH$_2$Cl$_2$-MeOH).

^{1}H NMR (DMSO-d$_6$): δ 8.29 (s, 1H, triaz), 7.72 (s, 1H, triaz), 7.53 (t, *J* = 2.1 Hz, 1H, Ar), 7.51 (s, 1H, Ar), 7.30 (dd, *J* = 2.2, 8.6 Hz, 1H, Ar), 5.79 (s, 1H, OH, ex), 4.87 (d, *J* = 14.3 Hz, 1H, C*Ha*Hb-triaz), 4.59 (d, *J* = 14.3 Hz, 1H, CHa*Hb*-triaz), 3.20 (d, *J* = 13.5 Hz, 1H, C*Ha*Hb-NH$_2$), 3.07 (d, *J* = 13.5 Hz, 1H, CHa*Hb*-NH$_2$), 1.55 (brs, 2H, N<u>H$_2$</u>).

1-Amino-2-(2,4-difluorophenyl)-3-(1*H*-1,2,4-triazol-1-yl)propan-2-ol (44c)[127]

(C$_{11}$H$_{12}$F$_2$N$_4$O, M.W. 254.24)

(43c)   **(44c)**

I. Dry THF, TPP, room temp. 1h

II. H$_2$O heat at 60°C for 4h
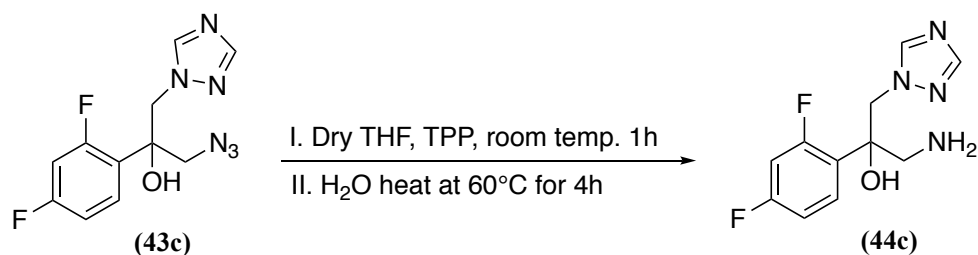
Reagents: 1-azido-2-(2,4-difluorophenyl)-3-(1*H*-1,2,4-triazol-1-yl)propan-2-ol (**43c**) (0.93g, 3.31 mmoL).

Yield: 0.73g (86%) as a white solid.

m.p.: 102-104 °C (lit. mp. 253 °C)[143]

R*f*: 0.38 (9:1 v/v CH$_2$Cl$_2$-MeOH).

^{1}H NMR (DMSO-d$_6$): δ 8.28 (s, 1H, triaz), 7.73 (s, 1H, triaz), 7.37 (dd, *J* = 9.0, 15.9 Hz, 1H, Ar), 7.17-7.12 (m, 1H, Ar), 6.86 (ddd, *J* = 2.8, 8.8, 11.4 Hz, 1H, Ar), 6.23 (brs, 1H, OH-ex), 4.56 (d, *J* = 14.3 Hz, 1H, C*Ha*Hb-triaz), 4.50 (d, *J* = 14.3 Hz, 1H, CHa*Hb*-triaz), 3.19 (d, *J* =

13.5 Hz, 1H, C*Ha*Hb-NH$_2$), 2.91 (d, *J* = 13.5 Hz, 1H, CHa*Hb*-NH$_2$), 1.88 (s, 2H, N$\underline{H}_2$).

1-Amino-2-(4-fluorophenyl)-3-(1*H*-1,2,4-triazol-1-yl)propan-2-ol (44d)

(C$_{11}$H$_{13}$FN$_4$O, M.W. 236.25)

(43d) → I. Dry THF, TPP, room temp. 1h / II. H$_2$O heat at 60°C for 4h → **(44d)**
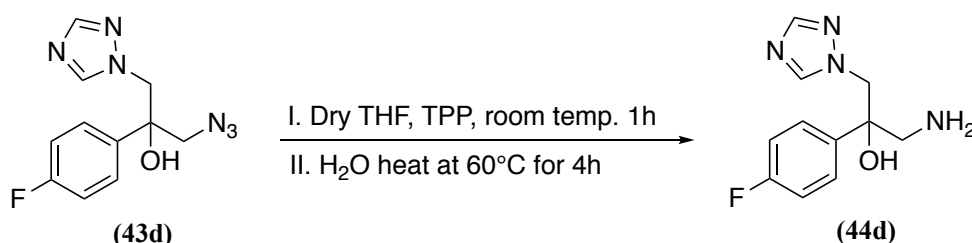
Reagents: 1-azido-2-(4-fluorophenyl)-3-(1*H*-1,2,4-triazol-1-yl)propan-2-ol (**43d**) (0.52g, 1.66 mmoL).

Yield: 0.75g (83%) as a white waxy solid.

R*f*: 0.35 (9:1 v/v CH$_2$Cl$_2$-MeOH).

^{1}H NMR (DMSO-d$_6$): δ 8.19 (s, 1H, triaz), 7.82 (s, 1H, triaz), 7.40 (dd, *J* = 5.5, 9.0 Hz, 2H, Ar), 7.10 (t, *J* = 9.0 Hz, 2H, Ar), 5.73 (s, 1H, OH, ex), 4.52 (d, *J* = 14.2 Hz, 1H, C*Ha*Hb-triaz), 4.47 (d, *J* = 14.2 Hz, 1H, CHa*Hb*-triaz), 3.29 (d, *J* = 13.9 Hz, 1H, C*Ha*Hb-NH$_2$), 2.82 (d, *J* = 13.9 Hz, 1H, CHa*Hb*-NH$_2$), 1,76 (s, 2H, N$\underline{H}_2$).

^{13}C NMR (DMSO-d$_6$): δ 161.57 (d, $^1J_{CF}$ = 242.5 Hz, *para*-CF), 150.89 (CH, triaz), 145.26 (CH, triaz), 139.76 (d, $^4J_{CF}$ = 2.8 Hz, C4-Ar), 128.28 (d, $^3J_{CF}$ = 8.1 Hz, 2 x CH, Ar), 114.88 (d, $^2J_{CF}$ = 23.1 Hz, 2 x CH, Ar), 75.82 (C-OH), 56.64 (CH$_2$-triaz), 50.01 (CH$_2$-NH$_2$).

HPLC (Method A): 94.15 %, RT = 1.43 min.

HRMS (ESI, m/z): theoretical mass: 259.0970 [M+Na]$^+$, observed mass: 259.0967 [M+Na]$^+$.

3-Acetyl-*N*-(2-(4-chlorophenyl)-2-hydroxy-3-(1*H*-1,2,4-triazol-1-yl)propyl)benzamide (46a)

(C$_{20}$H$_{19}$ClN$_4$O$_3$,M.W. 398.85)

(44a) + **(45)** → CDI / DMF room temp., overnight → **(46a)**
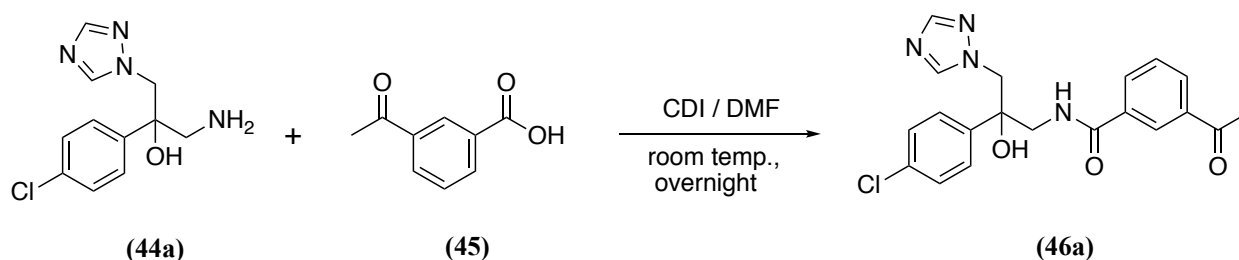
Method: To a solution of 3-acetylbenzoic acid (**45**) (0.14g, 0.88 mmol) in dry DMF (5 mL) was added CDI (0.14g, 0.88 mmol) and the reaction stirred at room temperature for 1 h. Then,

a solution of 1-amino-2-(4-chlorophenyl)-3-(1*H*-1,2,4-triazol-1-yl)propan-2-ol (**44a**) (0.15g, 0.59 mmol) in dry DMF (5 mL) was added and the reaction stirred at room temperature overnight. The reaction mixture was quenched with ice/cooled H_2O (25 mL), then the residue extracted with EtOAc (50 mL), washed with brine (25 mL x 2), and dried ($MgSO_4$). The organic layer was evaporated under reduced pressure to give a light yellow oil. Gradient column chromatography was applied to purify the compound which eluted with 3.5% MeOH in CH_2Cl_2 as a semi solid.

Yield: 0.12 g (52 %) as a white semi solid.

R*f*: 0.4 (9.5: 0.5 v/v CH_2Cl_2-MeOH)

¹H NMR (DMSO-d₆): δ 8.55 (t, J = 5.7 Hz, 1H, NH), 8.27 (d, J = 7.15 Hz, 1H, Ar), 8.26 (s, 1H, triaz), 8.09 (d, J = 7.8 Hz, 1H, Ar), 7.98 (d, J = 8.3 Hz, 1H, Ar), 7.83 (s, 1H, triaz), 7.60 (d, J = 7.8 Hz, 1H, Ar), 7.45 (d, J = 8.8 Hz, 2H, Ar), 7.32 (d, J = 8.8 Hz, 2H, Ar), 6.07 (s, 1H, OH, ex), 4.64 (d, J = 14.3 Hz, 1H, C*Ha*Hb-triaz), 4.59 (d, J = 14.3 Hz, 1H, CHa*Hb*-triaz),, 3.90 (dd, J = 6.80, 14.0 Hz, 1H, C*Ha*Hb-NH), 3.65 (dd, J = 5.3, 14.0 Hz, 1H, CHa*Hb*-NH), 2.61 (s, 3H, C$\underline{H}_3$).

¹³C NMR (DMSO-d₆): δ 197.99 (C, $CH_3C=O$),167.08 (C, C=O, amide), 150.01 (CH, triaz), 145.45 (CH, triaz), 141.40 (C, Ar), 137.19 (C, Ar), 134.92 (C, Ar), 132.31 (CH, Ar), 132.17 (C, C-Cl), 131.41 (CH, Ar), 129.29 (CH, Ar), 128.37 (2 X CH, Ar), 128.09 (2 X CH, Ar), 127.29 (2 X CH, Ar), 76.28 (C-OH), 57.01 (CH_2-triaz), 48.24 (CH_2-NH), 27.30 (CH_3)

HPLC (Method A): 100 %, RT = 4.37 min.

HRMS (ESI, m/z): theoretical mass: $^{35/37}$Cl 399.1224/401.1224 [M+H]⁺, observed mass: $^{35/37}$Cl 399.1225/401.1199 [M+H]⁺.

Using this procedure, the following compounds were prepared:

3-Acetyl-*N*-(2-(2,4-dichlorophenyl)-2-hydroxy-3-(1*H*-1,2,4-triazol-1-yl)propyl)benzamide (46b)

($C_{20}H_{18}Cl_2N_4O_3$, M. W. 433.29)
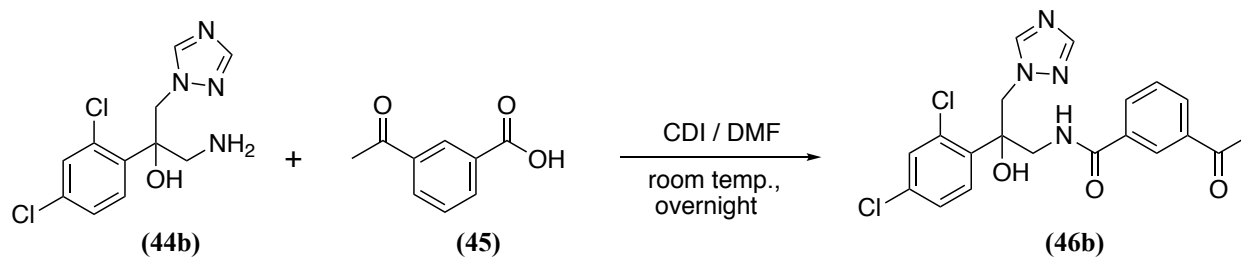
Reagents: 1-amino-2-(2,4-dichlorophenyl)-3-(1*H*-1,2,4-triazol-1-yl)propan-2-ol (**44b**) (0.15g, 0.52 mmoL) and 3-acetyl benzoic acid (**45**) (0.13g, 0.78 mmoL). The residue was purified using column chromatography and the desired compound was eluted with 3.5 % MeOH in CH$_2$Cl$_2$.

Yield: 0.1 g (45 %) as a white solid.

m.p.: 160-162 °C.

R$_f$: 0.45 (9.5: 0.5 v/v CH$_2$Cl$_2$-MeOH)

^{1}H NMR (DMSO-d$_6$): δ 8.72 (t, *J* = 6.0 Hz, 1H, NH), 8.34 (s, 1H, triaz), 8.30 (s, 1H, Ar), 8.10 (d, *J* = 7.8 Hz, 1H, Ar), 8.01 (d, *J* = 8.3 Hz, 1H, Ar), 7.74 (s, 1H, triaz), 7.62-7.57 (m, 3H, Ar), 7.29 (dd, *J* = 2.2, 8.6 Hz, 1H, Ar), 6.35(s, 1H, OH, ex), 5.10 (d, *J* = 14.4 Hz, 1H, C*Ha*Hb-triaz), 4.70 (d, *J* = 14.4 Hz, 1H, CHa*Hb*-triaz), 4.08 (dd, *J* = 5.7, 14.0 Hz, 1H, C*Ha*Hb-NH), 3.97 (dd, *J* = 6.4, 14.0 Hz, 1H, CHa*Hb*-NH), 2.61 (s, 3H, C<u>H$_3$</u>).

^{13}C NMR (DMSO-d$_6$): δ 198.00 (C, CH$_3$C=O),167.58 (C, C=O, amide), 151.02 (CH, triaz), 145.56 (CH, triaz), 138.11 (C, Ar), 137.20 (C, Ar), 134.71 (C, Ar), 133.29 (C, C-Cl), 132.40 (CH, Ar), 131.51 (CH, Ar), 131.50 (C, C-Cl), 130.43 (CH, Ar), 129.30 (2 X CH, Ar), 127.39 (2 X CH, Ar), 76.90 (C-OH), 54.09 (CH$_2$-triaz), 45.95 (CH$_2$-NH), 27.32 (CH$_3$).

HPLC (Method A): 100 %, RT = 4.49 min.

HRMS (ESI, m/z): theoretical mass: $^{35/37}$Cl 433.0834/435.0834 [M+H]$^+$, observed mass: $^{35/37}$Cl 433.0832/435.0806 [M+H]$^+$.

3-Acetyl-*N*-(2-(2,4-difluorophenyl)-2-hydroxy-3-(1*H*-1,2,4-triazol-1-yl)propyl)benzamide (46c)

(C$_{20}$H$_{18}$F$_2$N$_4$O$_3$, M.W. 400.39)
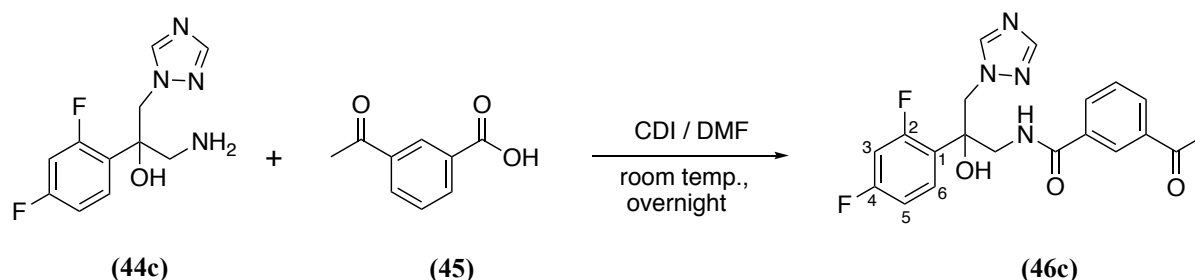
Reagents: 1-amino-2-(2,4-difluorophenyl)-3-(1*H*-1,2,4-triazol-1-yl)propan-2-ol (**44c**) (0.2g, 0.78 mmol) and 3-acetyl benzoic acid (**45**) (0.19g, 1.17mmoL). The residue was purified using gradient column chromatography and the desired compound was eluted with 3% MeOH in CH$_2$Cl$_2$.

Yield: 0.17g (54 %) as a white semisolid.

R*f*: 0.35 (9.5:0.5 v/v CH_2Cl_2-MeOH).

^{1}H NMR (DMSO-d$_6$): δ 8.37 (t, J = 6.0 Hz, 1H, NH), 8.34 (s, 1H, triaz), 8.30 (s, 1H, Ar), 8.09 (d, J = 7.8 Hz, 1H, Ar), 8.00 (d, J = 8.3 Hz, 1H, Ar), 7.75 (s, 1H, triaz), 7.61 (t, J = 7.8 Hz, 1H, Ar), 7.41 (dd, J = 9.0, 15.9 Hz, 1H, Ar), 7.21-7.16 (m, 1H, Ar), 6.93 (ddd, J = 2.6, 8.5, 11.0 Hz, 1H, Ar), 6.24 (s, 1H, OH, ex), 4.73 (d, J = 14.4 Hz, 1H, C*Ha*Hb-triaz), 4.60 (d, J = 14.4 Hz, 1H, CHa*Hb*-triaz), 3.84 (d, J = 14.0 Hz, 1H, C*Ha*Hb-NH), 3.77 (d, J = 14.0 Hz, 1H, CHa*Hb*-NH), 2.61 (s, 3H, C$\underline{H}_3$).

^{19}F NMR (DMSO-d$_6$): δ -106. 77 (*para*-F-Ar), -112.08 (*meta*-F-Ar).

^{13}C NMR (DMSO-d$_6$): δ 197.99 (C, C=O), 167.32 (C, C=O), 162.28 (dd, $^3J_{CF}$ = 12.6 Hz, $^1J_{CF}$ =246.0 Hz, C, C2-Ar),159.60 (dd, $^3J_{CF}$ = 12.5 Hz, $^1J_{CF}$ =247.3 Hz, C, C4-Ar), 150.99 (CH, triaz), 145.44 (CH, triaz), 137.20 (C, Ar), 134.79 (C, Ar), 132.34 (CH, Ar), 131.46 (CH Ar), 130.44 (dd, $^3J_{CF}$ = 6.1 Hz, $^3J_{CF}$ = 9.6 Hz, CH, C6-Ar), 129.29 (CH, Ar), 127.31 (CH, Ar), 125.20 (dd, $^4J_{CF}$ = 3.5 Hz, $^2J_{CF}$ =13.23 Hz, C, C1-Ar), 111.15 (dd, $^4J_{CF}$ = 3.1 Hz, $^2J_{CF}$ = 20.6 Hz, CH, C5-Ar), 104.41 (t, $^2J_{CF}$ = 26.2 Hz, CH, C3-Ar), 75.57 (C-OH), 55.53 (CH$_2$-triaz), 47.09 (CH$_2$-NH$_2$), 27.31 (CH$_3$).

HPLC (Method A): 100 %, RT = 4.26 min.

HRMS (ESI, m/z): theoretical mass: 401.1425 [M+H]$^+$, observed mass: 401.1425 [M+H]$^+$.

2-Chloro-*N*-(2-(4-chlorophenyl)-2-hydroxy-3-(1*H*-1,2,4-triazol-1-yl)propyl)thiazole-4-carboxamide (48a)

(C$_{15}$H$_{13}$Cl$_2$N$_5$O$_2$S, M.W. 398.26)
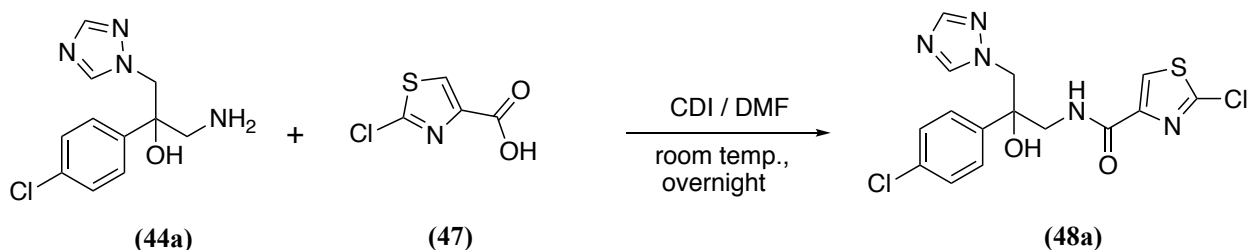
Reagents: 1-amino-2-(2,4-dichlorophenyl)-3-(1*H*-1,2,4-triazol-1-yl)propan-2-ol (**44a**) (0.16g, 0.63 mmoL) and 2-chlorothiazole-4-carboxylic acid (**47**) (0.15g, 0.95 mmol). The residue was purified by using gradient column chromatography and the pure compound was eluted with 3.5 % MeOH in CH_2Cl_2.

Yield: 0.17 g (68 %) as a white semisolid.

R$_f$: 0.45 (9.5: 0.5 v/v CH_2Cl_2-MeOH).

^{1}H NMR (DMSO-d$_6$): δ 8.23 (s, 1H, thiazole), 8.22 (s, 1H, triaz), 8.10 (t, J = 5.2 Hz, 1H, NH), 7.84 (s, 1H, triaz), 7.41 (d, J = 8.8 Hz, 2H, Ar), 7.32 (d, J = 8.8 Hz, 2H, Ar), 6.12 (s, 1H, OH,

ex), 4.53 (s, 2H, C$\underline{H_2}$-triaz), 3.96 (dd, *J* = 7.3, 14.0 Hz, 1H, C*Ha*Hb-NH), 3.58 (dd, *J* = 5.1, 14.0 Hz, 1H, CHa*Hb*-NH).

¹³C NMR (DMSO-d₆): δ 160.06 (C, C=O, amide), 151.44 (C, C-Cl), 151.13 (CH, triaz), 147.72 (C, Ar), 145.45 (CH, triaz), 141.28 (C, thiazole), 132.28 (C, Ar), 128.30 (2 X CH, Ar), 128.19 (2 X CH, Ar), 128.03 (CH, thiazole), 75.72 (C-OH), 57.26 (CH₂-triaz), 47.22 (CH₂-NH).

HPLC: 100 %, RT = 4.52 min.

HRMS (ESI, m/z): theoretical mass: ³⁵/³⁷Cl 398.0245/400.0245 [M+H]⁺, observed mass: ³⁵/³⁷Cl 398.0242/400.0214 [M+H]⁺.

2-Chloro-*N*-(2-(2,4-dichlorophenyl)-2-hydroxy-3-(1*H*-1,2,4-triazol-1-yl)propyl)thiazole-4-carboxamide (48b)

(C₁₅H₁₂Cl₃N₅O₂S, M. W. 432.70)
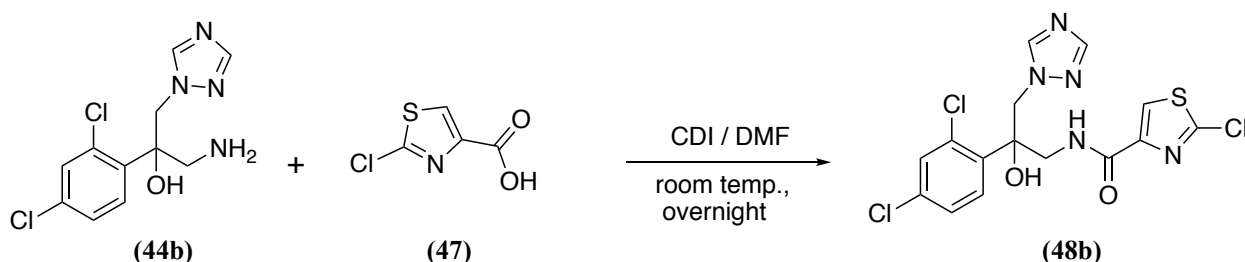
Reagents: 1-amino-2-(2,4-dichlorophenyl)-3-(1*H*-1,2,4-triazol-1-yl)propan-2-ol (**44b**)(0.15g, 0.52 mmoL) and 2-chlorothiazole-4-carboxylic acid (**47**) (0.13g, 0.78 mmol). The residue was purified by gradient column chromatography and the pure compound was eluted with 2.5 % MeOH in CH₂Cl₂.

Yield: 0.15 g (68 %) as a pale yellow wax.

R*f*: 0.55 (9.5: 0.5 v/v CH₂Cl₂-MeOH).

¹H NMR (DMSO-d₆): δ 8.32 (s, 1H, thiazole), 8.26 (t, *J* = 5.9 Hz, 1H, NH), 8.25 (s, 1H, triaz), 7.72 (s, 1H, triaz), 7.54 (d, *J* = 7.7 Hz, 2H, Ar), 7.29 (dd, *J* = 2.2, 8.6 Hz, 1H, Ar), 6.33 (s, 1H, OH, ex), 5.03 (d, *J* = 14.4 Hz, 1H, C*Ha*Hb-triaz), 4.64 (d, *J* = 14.4 Hz, 1H, CHa*Hb*-triaz), 4.05 (dd, *J* = 6.7, 14.0 Hz, 1H, C*Ha*Hb-NH), 3.99 (dd, *J* = 5.8, 14.0 Hz, 1H, CHa*Hb*-NH).

¹³C NMR (DMSO-d₆): δ 160.43 (C, C=O, amide), 151.45 (C, C-Cl), 151.03 (CH, triaz), 147.67 (C, Ar), 145.58 (CH, triaz), 137.98 (C, thiazole), 133.35 (C, C-Cl), 132.07 (C, C-Cl), 131.49 (CH, Ar), 130.47 (CH, Ar), 128.18 (CH, thiazole), 127.30 (CH, Ar), 76.27 (C-OH), 54.14 (CH₂-triaz), 45.06 (CH₂-NH).

HPLC (Method A): 100 %, RT = 4.63 min.

HRMS (ESI, m/z): theoretical mass: ³⁵/³⁷Cl 431.9855/433.9855 [M+H]⁺, observed mass:

2-Chloro-*N*-(2-(2,4-difluorophenyl)-2-hydroxy-3-(1*H*-1,2,4-triazol-1-yl)propyl)thiazole-4-carboxamide (48c)

(C$_{15}$H$_{12}$ClF$_2$N$_5$O$_2$S, M.W. 399.80)
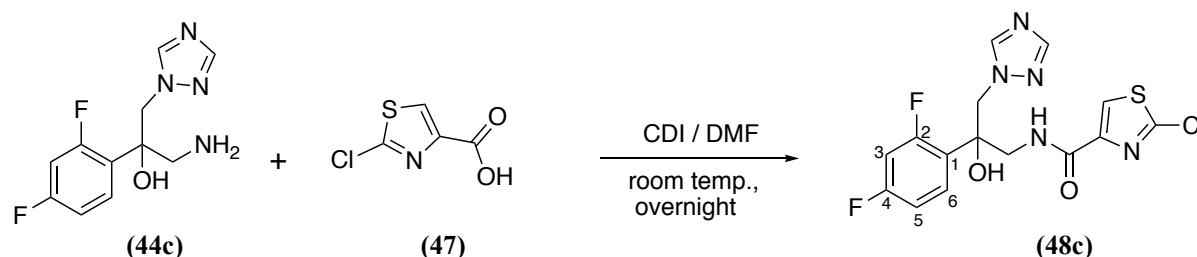
Reagents: 1-amino-2-(2,4-difluorophenyl)-3-(1*H*-1,2,4-triazol-1-yl)propan-2-ol (**44c**) (0.2g, 0.78 mmol) and 2-chlorothiazole-4-carboxylic acid (**47**) (0.19g, 1.17 mmol). The residue was purified by gradient column chromatography and the desired compound was eluted with 2% MeOH in CH$_2$Cl$_2$.

Yield: 0.20g (65 %) as a white solid.

m.p.: 182-184 °C.

R*f*: 0.42 (9.5:0.5 v/v CH$_2$Cl$_2$-MeOH).

^{1}H NMR (DMSO-d$_6$): δ 8.32 (s, 1H, thiazole), 8.30 (t, *J* = 6.2 Hz, 1H, NH), 8.24 (s, 1H, triaz), 7.73 (s, 1H, triaz), 7.38 (dd, *J* = 9.0, 15.9 Hz, 1H, Ar), 7.19-7.15 (m, 1H, Ar), 6.93 (ddd, *J* = 2.4, 8.3, 10.9 Hz, 1H, Ar), 6.24 (s, 1H, OH, ex), 4.66 (d, *J* = 14.4 Hz, 1H, C*Ha*Hb-triaz), 4.54 (d, *J* = 14.4 Hz, 1H, CHa*Hb*-triaz), 3.85 (dd, *J* = 6.9, 14.0 Hz, 1H, C*Ha*Hb-NH), 3.74 (dd, *J* = 5.8, 13.9 Hz, 1H, CHa*Hb*-NH).

^{19}F NMR (DMSO-d$_6$): *δ* -106. 88 (*para*-F-Ar), -111.95 (*meta*-F-Ar).

^{13}C NMR (DMSO-d$_6$): *δ* 162.30 (dd, $^3J_{CF}$ = 12.7 Hz, $^1J_{CF}$ =246.1 Hz, C, C2-Ar), 160.34 (C, C=O), 159.68 (dd, $^3J_{CF}$ = 12.5 Hz, $^1J_{CF}$ =247.3 Hz, C, C4-Ar), 151.42 (C, thiazole), 151.01 (CH, triaz), 147.72 (C, thiazole), 145.46 (CH, triaz), 130.50 (dd, $^3J_{CF}$ = 6.1 Hz, $^3J_{CF}$ =9.6 Hz, CH, C6-Ar), 128.10 (CH, Ar), 125.12 (dd, $^4J_{CF}$ = 3.5 Hz, $^2J_{CF}$ =13.4 Hz, C, C1-Ar), 111.19 (dd, $^4J_{CF}$ = 3.0 Hz, $^2J_{CF}$ = 20.4 Hz, CH, C5-Ar), 104.43 (t, $^2J_{CF}$ = 27.9 Hz, CH, C3-Ar), 75.02 (C-OH), 55.57 (CH$_2$-triaz), 46.16 (CH$_2$-NH$_2$).

HPLC (Method A): 97.1%, RT = 4.42 min.

HRMS (ESI, m/z): theoretical mass: $^{35/37}$Cl 422.0265/424.0265 [M+Na]$^+$, observed mass: $^{35/37}$Cl 422.0262/424.0234 [M+Na]$^+$.

N-(2-(4-chlorophenyl)-2-hydroxy-3-(1H-1,2,4-triazol-1-yl)propyl)-4-nitrobenzamide (50a)

(C$_{18}$H$_{16}$ClN$_5$O$_4$, M.W. 401.81)
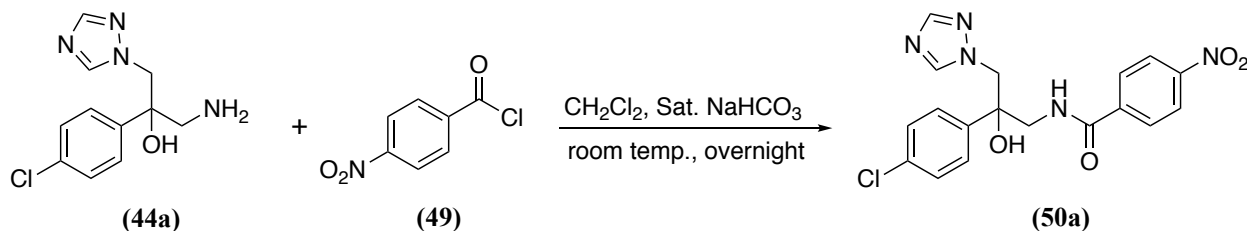
Method: Dichloromethane (3 mL) and sat. aqueous NaHCO$_3$ (6 mL) were stirred vigorously and chilled in an ice bath. 4-Nitrobenzoyl chloride (**49**) (0.22g, 1.19 mmol) was added, followed immediately by 1-amino-2-(4-chlorophenyl)-3-(1H-1,2,4-triazol-1-yl)propan-2-ol (**44a**) (0.20g, 0.79 mmol). Stirring was continued at room temperature overnight. The solvent was evaporated under reduced pressure then the suspension was extracted with EtOAc (2 x 25 mL), dried (MgSO$_4$), and the organic layer was evaporated to give the crude product, which was purified by gradient column chromatography and the desired compound eluted with 3% MeOH in CH$_2$Cl$_2$.

Yield: 0.24g (74 %) as a white solid.

m.p.: 228-230 °C.

Rf: 0.33 (9.5:0.5 v/v CH$_2$Cl$_2$-MeOH).

^{1}H NMR (DMSO-d$_6$): δ 8.62 (t, J = 6.0 Hz, 1H, NH), 8.28 (d, J = 9.0 Hz, 2H, Ar), 8.25 (s, 1H, triaz), 7.95 (d, J = 9.0 Hz, 2H, Ar), 7.83 (s, 1H, triaz), 7.45 (d, J = 8.7 Hz, 2H, Ar), 7.32 (d, J = 8.7 Hz, 2H, Ar), 5.99 (s, 1H, OH, ex), 4.62 (d, J = 14.4 Hz, 1H, C*Ha*Hb-triaz), 4.59 (d, J = 14.4 Hz, 1H, CHa*Hb*-triaz), 3.90 (dd, J = 6.8, 13.9 Hz, 1H, C*Ha*Hb-NH), 3.64 (dd, J = 5.3, 13.9 Hz, 1H, CHa*Hb*-NH).

^{13}C NMR (DMSO-d$_6$): δ 166.07 (C, C=O), 151.03 (CH, triaz), 149.48 (C, C-NO$_2$), 145.45 (CH, triaz), 141.26 (C, Ar), 140.32 (C, Ar), 132.20 (C, C-Cl), 129.27 (2 X CH, Ar), 128.35 (2 X CH, Ar), 128.09 (2 X CH, Ar), 123.91 (2 X CH, Ar), 76.11 (C-OH), 56.91 (CH$_2$-triaz), 48.14 (CH$_2$-NH).

HPLC (Method B): 99 %, RT = 4.84 min.

HRMS (ESI, m/z): theoretical mass: $^{35/37}$Cl 402.0969/404.0969 [M+H]$^+$, observed mass: $^{35/37}$Cl 402.0969/404.0945 [M+H]$^+$.

Using this procedure, the following compounds were prepared:

***N*-(2-(2,4-Dichlorophenyl)-2-hydroxy-3-(1*H*-1,2,4-triazol-1-yl)propyl)-4-nitrobenzamide (50b)**

(C_{18}H_{15}Cl_2N_5O_4, M. W. 436.25)
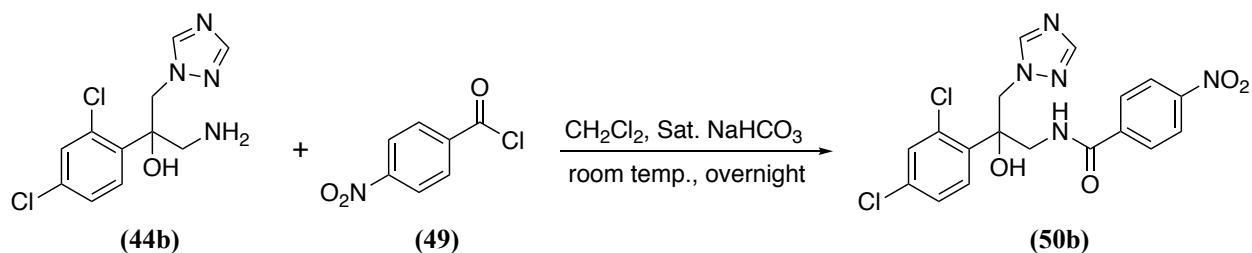
Reagents: 1-amino-2-(2,4-dichlorophenyl)-3-(1*H*-1,2,4-triazol-1-yl)propan-2-ol (44b) (0.34g, 1.18 mmoL) and 4-nitrobenzoyl chloride (**49**) (0.33g, 1.77 mmol). The residue was purified by gradient column chromatography and the desired compound was eluted with 3% MeOH in CH₂Cl₂.

Yield: 0.36g (72 %) as a white solid.

m.p.: 240-242 °C.

R*f*: 0.45 (9.5:0.5 v/v CH₂Cl₂-MeOH).

¹H NMR (DMSO-d₆): δ 8.78 (t, *J* = 6.0 Hz, 1H, NH), 8.33 (s, 1H, triaz), 8.29 (d, *J* = 8.9 Hz, 2H, Ar), 7.98 (d, *J* = 8.7 Hz, 2H, Ar), 7.74 (s, 1H, triaz), 7.57 (s, 1H, Ar), 7.55 (d, *J* = 2.2 Hz, 1H, Ar), 7.29 (dd, *J* = 2.2, 8.6 Hz, 1H, Ar), 6.26 (s, 1H, OH, ex), 5.10 (d, *J* = 14.4 Hz, 1H, C*Ha*Hb-triaz), 4.71 (d, *J* = 14.4 Hz, 1H, CHa*Hb*-triaz), 4.07 (dd, *J* = 5.8, 13.9 Hz, 1H, C*Ha*Hb-NH), 4.00 (dd, *J* = 6.4, 13.9 Hz, 1H, CHa*Hb*-NH).

¹³C NMR (DMSO-d₆): δ 166.49 (C, C=O), 151.05 (CH, triaz), 149.55 (C, C-NO₂), 145.56 (CH, triaz), 140.15 (C, Ar), 137.97 (C, Ar), 133.33 (C, C-Cl), 132.11 (C, C-Cl), 131.49 (CH, Ar), 130.45 (CH, Ar), 129.36 (2 X CH, Ar), 127.26 (CH, Ar), 123.93 (2 X CH, Ar), 76.73 (C-OH), 54.02 (CH₂-triaz), 45.81 (CH₂-NH).

HPLC (Method B): 99 %, RT = 4.68 min.

HRMS (ESI, m/z): theoretical mass: ³⁵/³⁷Cl 436.0579/438.0579 [M+H]⁺, observed mass: ³⁵/³⁷Cl 436.0578/438.0554 [M+H]⁺.

N-(2-(2,4-Difluorophenyl)-2-hydroxy-3-(1H-1,2,4-triazol-1-yl)propyl)-4-nitrobenzamide (50c)

(C₁₈H₁₅F₂N₅O₄, M. Weight. 403.35)
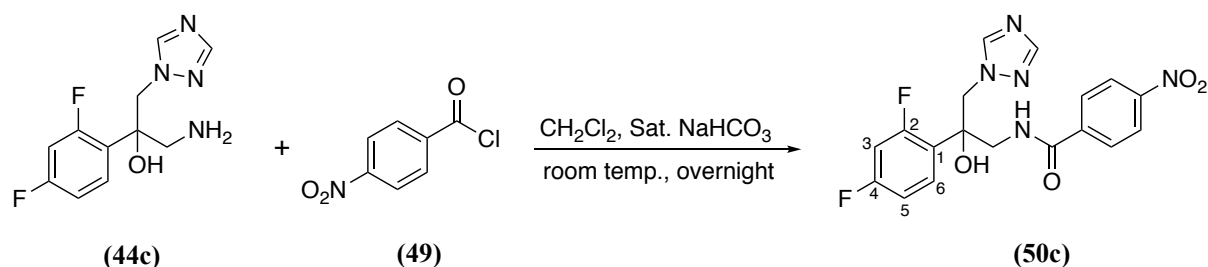
Reagents: 1-amino-2-(2,4-difluorophenyl)-3-(1H-1,2,4-triazol-1-yl)propan-2-ol (**44c**) (0.83g, 3.26 mmoL) and 4-nitrobenzoyl chloride (**49**) (0.90g, 4.89 mmol). The residue was purified by gradient column chromatography and the desired compound was eluted with 4% MeOH in CH$_2$Cl$_2$.

Yield: 0.86g (65 %) as a white solid.

m.p.: 232-234 °C.

Rf: 0.45 (9.5:0.5 v/v CH$_2$Cl$_2$-MeOH).

^{1}H NMR (DMSO-d$_6$): δ 8.79 (t, J = 6.0 Hz, 1H, NH), 8.33 (s, 1H, triaz), 8.29 (d, J = 9.0 Hz, 2H, Ar), 7.97 (d, J = 9.0 Hz, 2H, Ar), 7.75 (s, 1H, triaz), 7.41 (dd, J = 9.0, 15.9 Hz, 1H, Ar), 7.20-7.15 (m, 1H, Ar), 6.93 (ddd, J = 2.5, 8.4, 10.9 Hz, 1H, Ar), 6.15 (s, 1H, OH, ex), 4.73 (d, J = 14.4 Hz, 1H, C*Ha*Hb-triaz), 4.61 (d, J = 14.4 Hz, 1H, CHa*Hb*-triaz), 3.85 (dd, J = 6.6, 13.9 Hz, 1H, C*Ha*Hb-NH), 3.77 (dd, J = 5.7, 13.8 Hz, 1H, CHa*Hb*-NH).

^{13}C NMR (DMSO-d$_6$): δ 166.23 (C, C=O), 162.30 (dd, $^3J_{CF}$ = 12.6 Hz, $^1J_{CF}$ =243.1 Hz, C, C2-Ar), 159.63 (dd, $^3J_{CF}$ = 12.2 Hz, $^1J_{CF}$ =247.7 Hz, C, C4-Ar), 151.02 (CH, triaz), 149.51 (C, C-NO$_2$), 145.44 (CH, triaz), 140.22 (C, Ar), 130.47 (dd, $^3J_{CF}$ = 5.8 Hz, $^3J_{CF}$ =9.7 Hz, CH, C6-Ar), 129.26 (2 X CH, Ar), 125.48 (dd, $^4J_{CF}$ = 3.5 Hz, $^2J_{CF}$ =13.0 Hz, C, C1-Ar), 123.92 (2 X CH, Ar), 111.14 (dd, $^4J_{CF}$ = 3.0 Hz, $^2J_{CF}$ = 20.5 Hz, CH, C5-Ar), 104.41 (t, $^2J_{CF}$ = 28.0 Hz, CH, C3-Ar), 75.40 (C-OH), 55.43 (CH$_2$-triaz), 47.01 (CH$_2$-NH$_2$).

HPLC (Method A): 100 %, RT = 4.37 min.

HRMS (ESI, m/z): theoretical mass: 404.1170 [M+H]$^+$, observed mass: 404.1173 [M+H]$^+$.

N-(2-(4-Fluorophenyl)-2-hydroxy-3-(1H-1,2,4-triazol-1-yl)propyl)-4-nitrobenzamide (50d)

(C$_{18}$H$_{16}$FN$_5$O$_4$, M.W. 385.36)
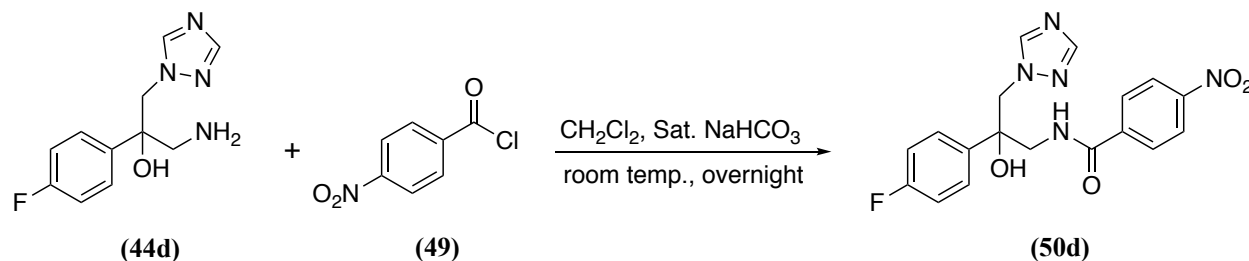
Reagents: 1-amino-2-(4-fluorophenyl)-3-(1H-1,2,4-triazol-1-yl)propan-2-ol (**44d**) (0.75g, 3.17 mmoL) and 4-nitrobenzoyl chloride (**49**) (0.88g, 4.76 mmol). The residue was purified using column chromatography and the desired compound was eluted with 3% MeOH in CH$_2$Cl$_2$.

Yield: 0.8g (65 %) as a white solid.

m.p.: 213-215 °C.

R*f*: 0.37 (9.5:0.5 v/v CH$_2$Cl$_2$- MeOH).

^{1}H NMR (DMSO-d$_6$): δ 8.60 (t, *J* = 5.65 Hz, 1H, NH), 8.28 (d, *J* = 9.0 Hz, 2H, Ar), 8.24 (s, 1H, triaz), 7.94 (d, *J* = 9.0 Hz, 2H, Ar), 7.83 (s, 1H, triaz), 7.46 (dd, *J* = 5.5, 9.0 Hz, 2H, Ar), 7.08 (t, *J* = 8.9 Hz, 2H, Ar), 5.96 (s, 1H, OH, ex), 4.63 (d, *J* = 14.4 Hz, 1H, C*Ha*Hb-triaz), 4.60 (d, *J* = 14.4 Hz, 1H, CHa*Hb*-triaz), 3.90 (dd, *J* = 6.8, 13.9 Hz, 1H, C*Ha*Hb-NH), 3.64 (dd, *J* = 5.3, 13.9 Hz, 1H, CHa*Hb*-NH).

^{13}C NMR (DMSO-d$_6$): δ 166.02 (C, C=O), 161.70(d, $^1J_{CF}$ = 243.1 Hz, C, C1-Ar), 151.02 (CH, triaz), 149.46 (C, C-NO$_2$), 145.43 (CH, triaz), 140.36 (C, Ar), 138.36 (d, $^4J_{CF}$ = 2.5 Hz, C, C4-Ar), 129.25 (2 X CH, Ar), 128.43 (d, $^3J_{CF}$ = 8.1 Hz, 2 x CH, Ar), 123.91 (2 X CH, Ar),114.85 (d, $^2J_{CF}$ = 21.1 Hz, 2 x CH, Ar), 76.06 (C-OH), 57.07 (CH$_2$-triaz), 48.22 (CH$_2$-NH$_2$).

HPLC (Method A): 100 %, RT = 4.33 min.

HRMS (ESI, m/z): theoretical mass: 386.1264 [M+H]$^+$, observed mass: 386.1261 [M+H]$^+$.

4-Amino-*N*-(2-(4-chlorophenyl)-2-hydroxy-3-(1*H*-1,2,4-triazol-1-yl)propyl)benzamide (51a)

(C₁₈H₁₈ClN₅O₂, M.W. 371.83)

(50a)   **(51a)**
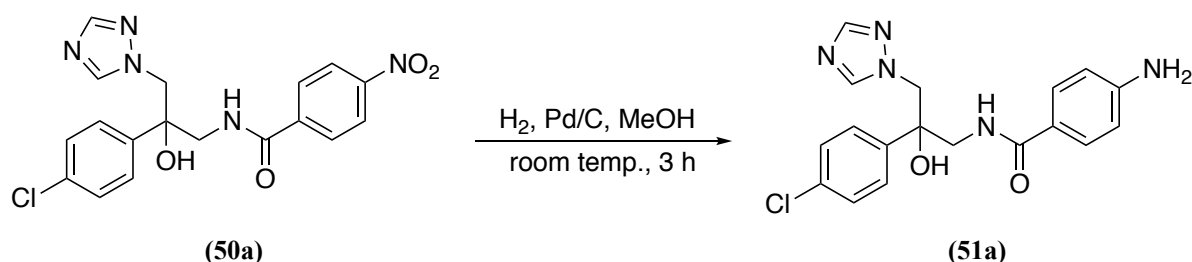
Method: To a solution of *N*-(2-(4-chlorophenyl)-2-hydroxy-3-(1*H*-1,2,4-triazol-1-yl)propyl)-4-nitrobenzamide (**50a**) (0.44g, 1.09 mmol) in dry MeOH (15 mL) was added 10 % Pd/C (44 mg). Then, the reaction atmosphere was filled with H₂ using H₂ balloons, and the mixture was stirred at room temperature for 3 h. The suspension was filtered through a pad of celite and the solvent was evaporated under reduced pressure to give the crude product, which was purified by column chromatography and the desired compound eluted at 3% MeOH in CH₂Cl₂.

Yield: 0.40g (100 %) as an off-white wax.

R*f*: 0.42 (9.5: 0.5 v/v CH₂Cl₂-MeOH)

¹H NMR (DMSO-d₆): δ 8.25 (s, 1H, triaz), 7.99 (t, *J* = 6.0 Hz, 1H, NH), 7.82 (s, 1H, triaz), 7.48 (d, *J* = 8.7 Hz, 2H, Ar), 7.41 (d, *J* = 8.7 Hz, 2H, Ar), 7.31 (d, *J* = 8.7 Hz, 2H, Ar), 6.51 (d, *J* = 8.7 Hz, 2H, Ar), 6.40 (s, 1H, OH, ex), 5.67 (brs, 2H, N*H*₂), 4.53 (d, *J* = 14.3 Hz, 1H, C*Ha*Hb-triaz), 4.49 (d, *J* = 14.3 Hz, 1H, CHa*Hb*-triaz), 3.79 (dd, *J* = 6.6, 13.9 Hz, 1H, C*Ha*Hb-NH), 3.60 (dd, *J* = 5.1, 13.9 Hz, 1H, CHa*Hb* -NH).

¹³C NMR (DMSO-d₆): δ 168.38 (C, C=O), 152.49 (C, C-NH₂), 150.41 (CH, triaz), 145.45 (CH, triaz), 141.73 (C, Ar), 132.07 (C, C-Cl), 129.41 (2 X CH, Ar), 128.41 (2 X CH, Ar), 128.08 (2 X CH, Ar), 120.44 (C,Ar), 112.91 (2 X CH, Ar), 76.53 (C-OH), 57.33 (CH₂-triaz), 48.39 (CH₂-NH).

HPLC (Method B): 99 %, RT = 4.68 min.

HRMS (ESI, m/z): theoretical mass: ³⁵ᐟ³⁷Cl 394.1046/396.1046[M+Na]⁺, observed mass: ³⁵ᐟ³⁷Cl 394.1047/396.1024 [M+Na]⁺.

Using this procedure, the following compounds were prepared:

4-Amino-*N*-(2-(2,4-dichlorophenyl)-2-hydroxy-3-(1*H*-1,2,4-triazol-1-yl)propyl) benzamide (51b)

(C$_{18}$H$_{17}$Cl$_2$N$_5$O$_2$, M.W. 406.27)

(50b)   **(51b)**
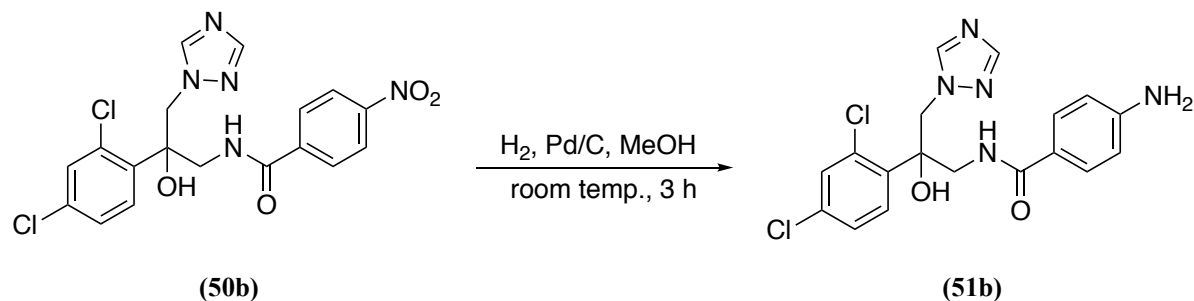
Reagents: *N*-(2-(2,4-dichlorophenyl)-2-hydroxy-3-(1*H*-1,2,4-triazol-1-yl)propyl)-4-nitrobenzamide (**50b**) (0.44g, 1.09 mmol). The residue was purified by gradient column chromatography and the desired compound was eluted with 2.5% MeOH in CH$_2$Cl$_2$.

Yield: 0.32g (100 %) as a pale yellow oil.

R$_f$: 0.37 (9.5: 0.5 v/v CH$_2$Cl$_2$-MeOH)

^{1}H NMR (DMSO-d$_6$): δ 8.34 (s, 1H, triaz), 8.20 (t, *J* = 5.9 Hz, 1H, NH), 7.73 (s, 1H, triaz), 7.58 (d, *J* = 8.6 Hz, 1H, Ar), 7.55 (d, *J* = 2.2 Hz, 1H, Ar), 7.50 (d, *J* = 8.7 Hz, 2H, Ar), 7.27 (d, *J* = 2.2 Hz, 1H, Ar), 6.87 (s, 1H, OH, ex), 6.54 (d, *J* = 8.7 Hz, 2H, Ar), 5.70 (brs, 2H, N<u>H</u>$_2$), 4.99 (d, *J* = 14.3 Hz, 1H, C*Ha*Hb-triaz), 4.64 (d, *J* = 14.3 Hz, 1H, CHa*Hb*-triaz), 3.95 (d, *J* = 14.5 Hz, 1H, C*Ha*Hb-NH), 3.91 (d, *J* = 14.5 Hz, 1H, CHa*Hb*-NH).

^{13}C NMR (DMSO-d$_6$): δ 169.23 (C, C=O), 152.66 (C, C-NH$_2$), 150.95 (CH, triaz), 145.61 (CH, triaz), 138.47 (C, Ar), 133.21 (C, C-Cl), 131.96 (C, C-Cl), 131.66 (CH, Ar), 130.30 (CH, Ar), 129.59 (2 X CH, Ar), 127.29 (2 X CH, Ar), 120.01 (C,Ar), 112.89 (2 X CH, Ar), 77.21 (C-OH), 54.33 (CH$_2$-triaz), 46.39 (CH$_2$-NH).

HPLC (Method B): 99 %, RT = 4.69 min.

HRMS (ESI, m/z): theoretical mass: $^{35/37}$Cl 428.0656/430.0656 [M+Na]$^+$, observed mass: $^{35/37}$Cl 428.0660/430.0633 [M+Na]$^+$.

4-Amino-*N*-(2-(2,4-difluorophenyl)-2-hydroxy-3-(1*H*-1,2,4-triazol-1-yl) propyl) benzamide (51c)

(C$_{18}$H$_{17}$F$_2$N$_5$O$_2$, M.W. 373.36)
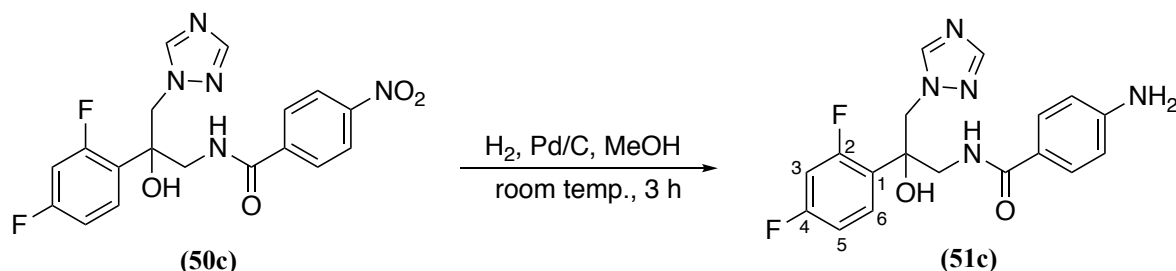
Reagents: *N*-(2-(2,4-difluorophenyl)-2-hydroxy-3-(1*H*-1,2,4-triazol-1-yl)propyl)-4-nitrobenzamide (**50c**) (0.48g, 1.19 mmoL). The residue was purified by gradient column chromatography and the desired compound was eluted with 2.5 % MeOH in CH$_2$Cl$_2$.

Yield: 0.44g (100 %) as an off-white semisolid.

R*f*: 0.35 (9.5:0.5 v/v CH$_2$Cl$_2$- MeOH).

^{1}H NMR (DMSO-d$_6$): δ 8.33 (s, 1H, triaz), 8.20 (t, *J* = 6.0 Hz, 1H, NH), 7.73 (s, 1H, triaz), 7.50 (d, *J* = 8.7 Hz, 2H, Ar), 7.40 (dd, *J* = 9.0, 15.9 Hz, 1H, Ar), 7.20-7.15 (m, 1H,Ar), 6.93 (ddd, *J* = 2.4, 8.3, 10.9 Hz, 1H, Ar), 6.67 (s, 1H, OH, ex), 5.69 (s, 2H, NH$_2$), 4.64 (d, *J* = 14.4 Hz, 1H, C*Ha*Hb-triaz), 4.53 (d, *J* = 14.3 Hz, 1H, CHa*Hb*-triaz), 3.73 (dd, *J* = 5.5, 14.2 Hz, 1H, C*Ha*Hb-NH), 3.70 (dd, *J* = 6.3, 14.3 Hz, 1H, CHa*Hb*-NH).

^{13}C NMR (DMSO-d$_6$): δ 168.90 (C, C=O), 162.23 (dd, $^3J_{CF}$ = 12.5 Hz, $^1J_{CF}$ =245.4 Hz, C, C2-Ar), 159.46 (dd, $^3J_{CF}$ = 12.5 Hz, $^1J_{CF}$ =247.5 Hz, C, C4-Ar), 152.58 (C, C-NH$_2$), 151.02 (CH, triaz), 145.44 (CH, triaz), 140.22 (C, Ar), 130.44 (dd, $^3J_{CF}$ = 6.2 Hz, $^3J_{CF}$ =9.6 Hz, CH, C6-Ar), 129.50 (2 X CH, Ar), 125.48 (dd, $^4J_{CF}$ = 3.5 Hz, $^2J_{CF}$ =13.0 Hz, C, C1-Ar), 120.17 (C, Ar), 112.89 (2 X CH, Ar),111.19 (dd, $^4J_{CF}$ = 3.0 Hz, $^2J_{CF}$ = 17.7 Hz, CH, C5-Ar), 104.36 (t, $^2J_{CF}$ = 27.8 Hz, CH, C3-Ar), 75.85 (C-OH), 55.77 (CH$_2$-triaz), 47.47 (CH$_2$-NH$_2$).

HPLC (Method A): 100 %, RT = 4.04 min.

HRMS (ESI, m/z): theoretical mass: 374.1428 [M+H]$^+$, observed mass: 374.1430 [M+H]$^+$.

4-Amino-*N*-(2-(4-fluorophenyl)-2-hydroxy-3-(1*H*-1,2,4-triazol-1-yl)propyl)benzamide (51d)

(C$_{18}$H$_{18}$FN$_5$O$_2$, M.W. 355.37)

(50d)   H$_2$, Pd/C, MeOH   room temp., 3 h   **(51d)**
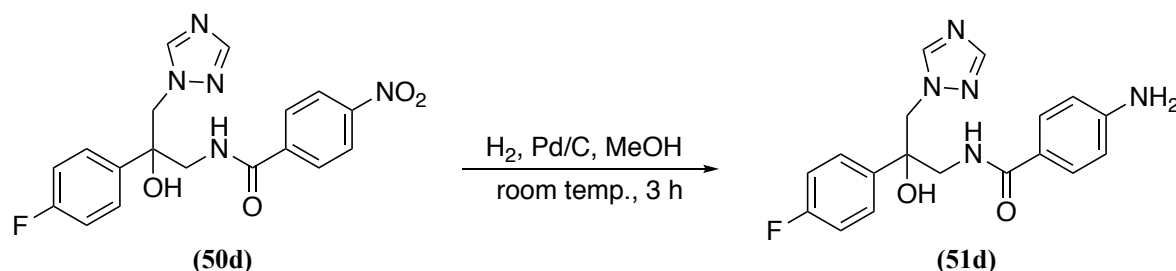
Reagents: *N*-(2-(4-fluorophenyl)-2-hydroxy-3-(1*H*-1,2,4-triazol-1-yl)propyl)-4-nitrobenzamide (**50d**) (0.47g, 1.21 mmoL). The residue was purified by gradient column chromatography and the desired compound was eluted with 2.5% MeOH in CH$_2$Cl$_2$.

Yield: 0.4g (95 %) as a white semisolid.

R*f*: 0.37 (9.5:0.5 v/v CH$_2$Cl$_2$-MeOH).

^{1}H NMR (DMSO-d$_6$): δ 8.22 (s, 1H, triaz), 7.95 (t, *J* = 5.6 Hz, 1H, NH), 7.82 (s, 1H, triaz), 7.47 (d, *J* = 9.0 Hz, 2H, Ar), 7.42 (dd, *J* = 5.5, 9.0 Hz, 2H, Ar), 7.07 (t, *J* = 8.9 Hz, 2H, Ar), 6.5 (d, *J* = 8.8 Hz, 2H, Ar), 6.34 (s, 1H, OH, ex), 5.66 (s, 2H, NH$_2$), 4.54 (d, *J* = 14.3 Hz, 1H, C*Ha*Hb-triaz), 4.50 (d, *J* = 14.3 Hz, 1H, CHa*Hb*-triaz), 3.79 (dd, *J* = 6.6, 14.2 Hz, 1H, C*Ha*Hb-NH), 3.60 (dd, *J* = 5.2, 14.2 Hz, 1H, CHa*Hb*-NH).

^{13}C NMR (DMSO-d$_6$): δ 168.34 (C, C=O), 161.64 (d, $^1J_{CF}$ = 243.1 Hz, C1-Ar), 152.46 (C, Ar), 150.94 (CH, triaz), 145.39 (CH, triaz), 138.80 (d, $^4J_{CF}$ = 2.5 Hz, C4-Ar), 129.37 (2 X CH, Ar), 128.45 (d, $^3J_{CF}$ = 8.1 Hz, 2 x CH, Ar), 120.49 (C, Ar), 114.83 (d, $^2J_{CF}$ = 21.0 Hz, 2 x CH, Ar), 112.91 (2 X CH, Ar), 76.47 (C-OH), 57.49 (CH$_2$-triaz), 48.45 (CH$_2$-NH$_2$).

HPLC (Method A): 100 %, RT = 3.97 min.

HRMS (ESI, m/z): theoretical mass: 356.1523 [M+H]$^+$, observed mass: 356.1523 [M+H]$^+$.

N-(2-(4-chlorophenyl)-2-hydroxy-3-(1*H*-1,2,4-triazol-1-yl)propyl)-4-(3-(4-chlorophenyl)thioureido)benzamide (53a)

(C$_{25}$H$_{22}$Cl$_2$N$_6$O$_2$S, M.W. 541.45)

(51a)   **(52)**   Pyridine room temp., overnight   **(53a)**
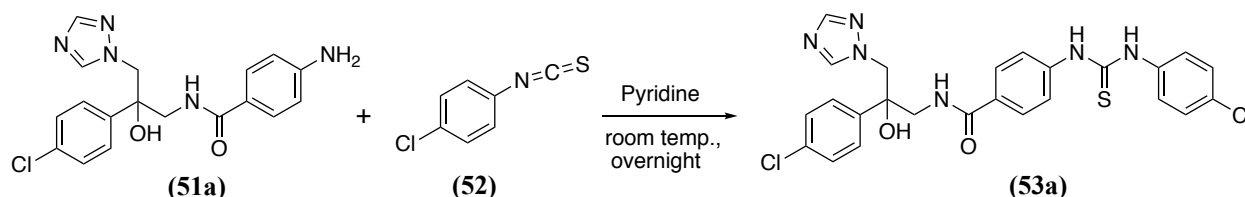
Method: To a cooled (0°C, ice bath) solution of 4-amino-*N*-(2-(4-chlorophenyl)-2-hydroxy-3-(1*H*-1,2,4-triazol-1-yl)propyl)benzamide (**51a**) (0.16g, 043 mmol) in dry pyridine (5 mL) was

added 4-chlorophenyl isothiocyanate (**52**) (0.11g, 064 mmol) in portions,[59, 61] the reaction stirred at room temperature overnight. The solvent was evaporated, and the resulting oil was extracted with EtOAc (50 mL), washed with 1M aq. HCl (25 mL), H_2O (2 x 25 mL), and dried ($MgSO_4$). The organic layer was evaporated under reduced pressure to give a crude yellow-orange oil. The desired product was purified by gradient column chromatography and the desired product eluted with 3.5 % MeOH in CH_2Cl_2.

**Yield:** 0.15 g (68 %) as a white solid.

m.p.: 146-148 °C.

R$_f$: 0.23 (9.5: 0.5 v/v CH_2Cl_2-MeOH)

^{1}H NMR (DMSO-d$_6$): δ 10.05 (s, 1H, NH-thiourea), 10.00 (s, 1H, NH-thiourea), 8.22 (t, J = 6.0 Hz, 1H, NH-CH$_2$), 8.20 (s, 1H, triaz), 7.84 (s, 1H, triaz), 7.70 (d, J = 8.9 Hz, 2H, Ar), 7.55 (dd, J = 8.8, 21.2 Hz, 4H, Ar), 7.43 (d, J = 7.1 Hz, 2H, Ar), 7.39 (d, J = 8.9 Hz, 2H, Ar), 7.33-7.19 (m, 2H, Ar), 6.05 (s, 1H, OH, ex), 5.74 (d, J = 14.3 Hz, 1H, C*Ha*Hb-triaz), 4.55 (d, J = 14.3 Hz, 1H, CHa*Hb*-triaz), 3.86 (dd, J = 6.7, 14.0 Hz, 1H, C*Ha*Hb-NH), 3.63 (dd, J = 5.2, 14.1 Hz, 1H, CHa*Hb*-NH).

^{13}C NMR (DMSO-d$_6$): δ 179.97 (C, C=S), 167.33 (C, C=O), 150.96 (CH, triaz), 145.38 (CH, triaz), 142.70 (C, Ar), 142.45 (C, Ar), 141.48 (C, Ar), 138.75 (C, C-Cl), 132.14 (C, C-Cl), 129.85 (C, Ar), 129.84 (2 X CH, Ar), 128.23 (2 X CH, Ar), 128.17 (2 X CH, Ar), 126.24 (2 X CH, Ar), 125.74 (2 X CH, Ar), 122.74 (2 X CH, Ar), 76.48 (C-OH), 57.40 (CH$_2$-triaz), 48.35 (CH$_2$-NH).

HPLC (Method B): 99 %, RT = 4.78 min.

HRMS (ESI, m/z): theoretical mass: $^{35/37}$Cl 541.0980/543.0980 [M+H]$^+$, observed mass: $^{35/37}$Cl 541.0971/543.0945 [M+H]$^+$.

Using this procedure, the following compounds were prepared:

4-(3-(4-Chlorophenyl)thioureido)-*N*-(2-(2,4-dichlorophenyl)-2-hydroxy-3-(1*H*-1,2,4-triazol-1-yl)propyl)benzamide (53b)

(C$_{25}$H$_{21}$Cl$_3$N$_6$O$_2$S, M.W. 575.89)
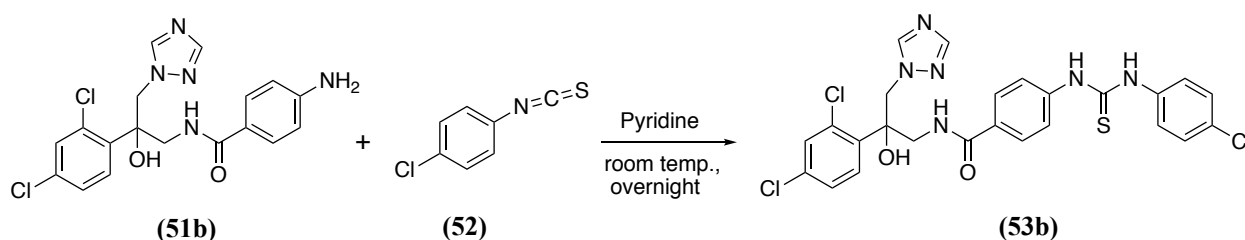
(51b)   (52)   (53b)

Reagents: 4-amino-*N*-(2-(2,4-dichlorophenyl)-2-hydroxy-3-(1*H*-1,2,4-triazol-1-yl)propyl) benzamide (**51b**) (0.17g, 0.41 mmol) and 4-chlorophenyl isothiocyanate (**52**)(0.1g, 0.62 mmol).

Yield: 0.13g (56 %) as a white solid.

m.p.: 138-140 °C.

R$_f$: 0.32 (9.5: 0.5 v/v CH$_2$Cl$_2$-MeOH)

^{1}H NMR (DMSO-d$_6$): δ 10.06 (s, 1H, NH-thiourea), 10.03 (s, 1H, NH-thiourea), 8.47 (t, *J* = 6.0 Hz, 1H, NH-CH$_2$), 8.34 (s, 1H, triaz), 7.74 (s, 1H, triaz), 7.73(d, *J* = 8.8 Hz, 2H, Ar), 7.58-7.56 (m, 4H, Ar), 7.51 (d, *J* = 8.9 Hz, 2H, Ar), 7.39 (d, *J* = 8.9 Hz, 2H, Ar), 7.29 (dd, *J* = 2.3, 8.7, 1H, Ar), 6.46 (s, 1H, OH-ex), 5.05 (d, *J* = 14.4 Hz, 1H, C*Ha*Hb-triaz), 4.68 (d, *J* = 14.4 Hz, 1H, CHa*Hb*-triaz), 4.02 (dd, *J* = 5.7, 14.2 Hz, 1H, C*Ha*Hb-NH), 3.97 (dd, *J* = 6.5, 14.2 Hz, 1H, CHa*Hb*-NH).

^{13}C NMR (DMSO-d$_6$): δ 179.90 (C, C=S), 168.02 (C, C=O), 151.01 (CH, triaz), 145.59 (CH, triaz), 142.89 (C, Ar), 138.76 (C, Ar), 138.19 (C, C-Cl), 133.26 (C, C-Cl), 132.17 (C, C-Cl), 132.04 (C, C-Cl), 131.54 (CH, Ar), 130.41 (CH, Ar), 128.81 (2 X CH, Ar), 128.32 (2 X CH, Ar), 127.27 (CH, Ar), 125.72 (2 X CH, Ar), 122.70 (2 X CH, Ar), 76.99 (C-OH), 54.18 (CH$_2$-triaz), 46.05 (CH$_2$-NH).

Microanalysis (C$_{25}$H$_{21}$Cl$_3$N$_6$O$_2$S): Anal. Calcd: C 52.13 %, H 3.68 %, N 14.59 %. Found: C 52.29 %, H 3.82 %, N 14.71 %.

_N_-(2-(4-chlorophenyl)-2-hydroxy-3-(1_H_-1,2,4-triazol-1-yl)propyl)-4-(3-(4-chlorophenyl) ureido)benzamide (55a)

(C$_{25}$H$_{22}$Cl$_2$N$_6$O$_3$, M.W. 525.39)
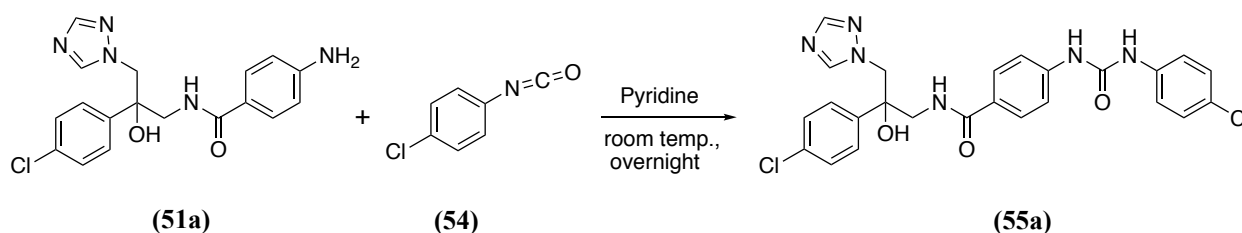
(51a) **(54)** **(55a)**

Reagents: 4-amino-*N*-(2-(4-chlorophenyl)-2-hydroxy-3-(1*H*-1,2,4-triazol-1-yl)propyl)benzamide (**51a**) (0.16g, 0.43 mmol) and 4-chlorophenyl isocyanate (**54**) (0.1g, 0.64 mmol). The desired product was purified by gradient column chromatography and the desired product eluted with 6 % MeOH in CH$_2$Cl$_2$.

Yield: 0.14g (63 %) as a white solid.

m.p.: 226-228 °C.

R$_f$: 0.35 (9.5: 0.5 v/v CH$_2$Cl$_2$-MeOH)

^{1}H NMR (DMSO-d$_6$): δ 8.99 (s, 1H, NH-urea), 8.90 (s, 1H, NH-urea), 8.25 (s, 1H, triaz), 8.22 (t, J = 6.0 Hz, 1H, NH-CH$_2$), 7.83 (s, 1H, triaz), 7.54 (dd, J = 3.2, 8.9 Hz, 2H, Ar), 7.48 (m, 4H, Ar), 7.43 (d, J = 8.8 Hz, 2H, Ar), 7.34-7.28 (m, 4H, Ar), 6.16 (s, 1H, OH-ex), 4.60 (d, J = 14.3 Hz, 1H, C*Ha*Hb-triaz), 4.56 (d, J = 14.3 Hz, 1H, CHa*Hb*-triaz), 3.85 (dd, J = 6.7, 14.1 Hz, 1H, C*Ha*Hb-NH), 3.63 (dd, J = 5.2, 14.1 Hz, 1H, CHa*Hb*-NH).

^{13}C NMR (DMSO-d$_6$): δ 167.51 (C, C=O), 152.63 (C, C=O), 151.00 (CH, triaz), 145.45 (CH, triaz), 143.01 (C, Ar), 142.50 (C, Ar), 141.52 (C, Ar), 138.88 (C, C-Cl), 132.12 (C, C-Cl), 129.10 (C, Ar), 128.80 (2 X CH, Ar), 128.38 (2 X CH, Ar), 128.09 (2 X CH, Ar), 120.34 (2 X CH, Ar), 117.66 (2 X CH, Ar), 76.337 (C-OH), 57.14 (CH$_2$-triaz), 48.24 (CH$_2$-NH).

Microanalysis (C$_{25}$H$_{22}$Cl$_2$N$_6$O$_3$): Anal. Calcd: C 57.15 %, H 4.22 %, N 15.99 %. Found: C 57.53 %, H 4.28 %, N 15.94 %.

4-(3-(4-Chlorophenyl)ureido)-N-(2-(2,4-dichlorophenyl)-2-hydroxy-3-(1H-1,2,4-triazol-1-yl)propyl)benzamide (55b)

(C$_{25}$H$_{21}$Cl$_3$N$_6$O$_3$, M. W. 559.83)
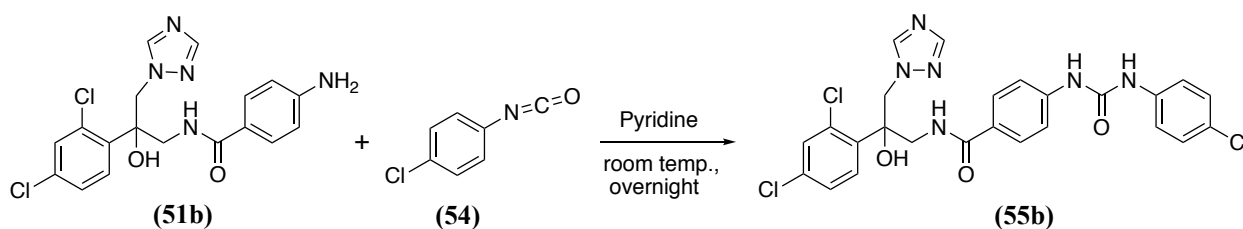
Reagents: 4-amino-N-(2-(2,4-dichlorophenyl)-2-hydroxy-3-(1H-1,2,4-triazol-1-yl)propyl) benzamide (**51b**) (0.16g, 0.43 mmol) and 4-chlorophenyl isocyanate (**54**) (0.1g, 0.64 mmol). The desired product was purified by gradient column chromatography and the desired product eluted with 6 % MeOH in CH$_2$Cl$_2$.

Yield: 0.11g (52 %) as a white solid.

m.p.: 216-218 °C.

R$_f$: 0.37 (9.5: 0.5 v/v CH$_2$Cl$_2$-MeOH)

^{1}H NMR (DMSO-d$_6$): δ 9.06 (s, 1H, NH-urea), 8.97 (s, 1H, NH-urea), 8.42 (t, J = 6.0 Hz, 1H, NH-CH$_2$), 8.34 (s, 1H, triaz), 7.72 (d, J = 11.0 Hz, 2H, Ar), 7.70 (s, 1H, triaz), 7.57 (dd, J = 8.6, 11.0 Hz, 2H, Ar), 7.51- 7.47 (m, 4H, Ar), 7.33 (d, J = 8.9 Hz, 2H, Ar), 7.28 (dd, J = 2.2, 8.6 Hz, 1H, Ar), 6.53 (s, 1H, OH, ex), 5.05 (d, J = 14.3 Hz, 1H, C*Ha*Hb-triaz), 4.67 (d, J =

14.3 Hz, 1H, CHa*Hb*-triaz), 4.02 (dd, *J* = 5.5, 14.1 Hz, 1H, C*Ha*Hb-NH), 3.95 (dd, *J* = 6.3, 14.1 Hz, 1H, CHa*Hb*-NH).

¹³C NMR (DMSO-d₆): δ 168.21 (C, C=O), 152.66 (C, C=O), 151.00 (CH, triaz), 145.45 (CH, triaz), 143.18 (C, Ar), 138.90 (C, Ar), 138.25 (C, C-Cl), 133.25 (C, C-Cl), 132.02 (C, C-Cl), 131.55 (CH, Ar), 131.24 (CH, Ar), 130.04 (CH, Ar), 129.10 (2 X CH, Ar), 128.93 (CH, Ar), 127.27 (CH, Ar), 120.35 (2 X CH, Ar), 117.64 (2 X CH, Ar), 77.03 (C-OH), 54.19 (CH₂-triaz), 46.12 (CH₂-NH).

Microanalysis (C₂₅H₂₁Cl₃N₆O₃): Anal. Calcd: C 53.64 %, H 3.78 %, N 15.00 %. Found: C 53.84 %, H 3.68 %, N 14.63 %.

4-Chloro-*N*-(4-((2-(4-chlorophenyl)-2-hydroxy-3-(1*H*-1,2,4-triazol-1-yl)propyl) carbamoyl)phenyl)benzamide (57a)

(C₂₅H₂₁Cl₂N₅O₃, M.W. 510.38)

(51a)   **(56)**   **(57a)**
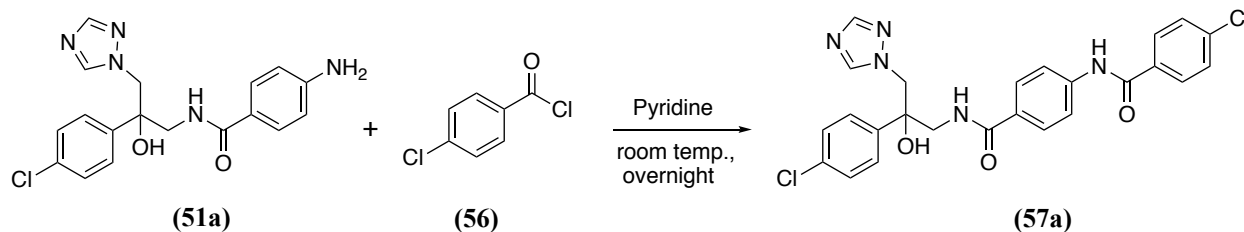
Reagents: 4-amino-*N*-(2-(4-chlorophenyl)-2-hydroxy-3-(1*H*-1,2,4-triazol-1-yl)propyl)benzamide (51a) (0.15g, 0.42 mmol) and 4-chlorobenzoyl chloride (**56**) (0.1g, 0.64 mmol). The desired product was purified by gradient column chromatography and the desired product eluted with 6 % MeOH in CH₂Cl₂.

Yield: 0.16g (80 %) as a white solid.

m.p.: 222-224 °C.

R*f*: 0.33 (9.5: 0.5 v/v CH₂Cl₂-MeOH)

¹H NMR (DMSO-d₆): δ 10.50 (s, 1H, NH-amide), 8.28 (t, *J* = 6.0 Hz, 1H, NH-CH₂), 8.26 (s, 1H, triaz), 7.99 (d, *J* = 8.8 Hz, 2H, Ar), 7.84 (s, 1H, triaz), 7.83 (dd, *J* = 3.8, 8.9 Hz, 2H, Ar), 7.76 (d, *J* = 8.9 Hz, 2H, Ar), 7.62 (d, *J* = 8.8 Hz, 2H, Ar), 7.44 (d, *J* = 8.8 Hz, 2H, Ar), 7.33-7.27 (m, 2H, Ar), 6.14 (s, 1H, OH-ex), 4.60 (d, *J* = 14.4 Hz, 1H, C*Ha*Hb-triaz), 4.57 (d, *J* = 14.4 Hz, 1H, CHa*Hb*-triaz), 3.86 (dd, *J* = 6.8, 14.1 Hz, 1H, C*Ha*Hb-NH), 3.64 (dd, *J* = 5.3, 14.1 Hz, 1H, CHa*Hb*-NH).

¹³C NMR (DMSO-d₆): δ 167.38 (C, C=O), 165.13 (C, C=O), 151.00 (CH, triaz), 145.45 (CH, triaz), 142.26 (C, Ar), 141.49 (C, Ar), 137.10 (C, C-Cl), 133.76 (C, Ar), 132.14 (C, C-Cl), 130.17 (2 X CH, Ar), 129.34 (C, Ar), 128.97 (2 X CH, Ar), 128.53 (2 X CH, Ar), 128.09 (2 X

CH, Ar), 126.25 (2 X CH, Ar), 119.91 (2 X CH, Ar), 76.33 (C-OH), 57.10 (CH$_2$-triaz), 48.24 (CH$_2$-NH).

Microanalysis (C$_{25}$H$_{21}$Cl$_2$N$_5$O$_3$): Anal. Calcd: C 58.83 %, H 4.15 %, N 13.72 %. Found: C 58.78 %, H 4.07 %, N 13.68 %.

4-Chloro-*N*-(4-((2-(2,4-dichlorophenyl)-2-hydroxy-3-(1*H*-1,2,4-triazol-1-yl)propyl) carbamoyl)phenyl)benzamide (57b)

(C$_{25}$H$_{20}$Cl$_3$N$_5$O$_3$, M. W. 544.82)
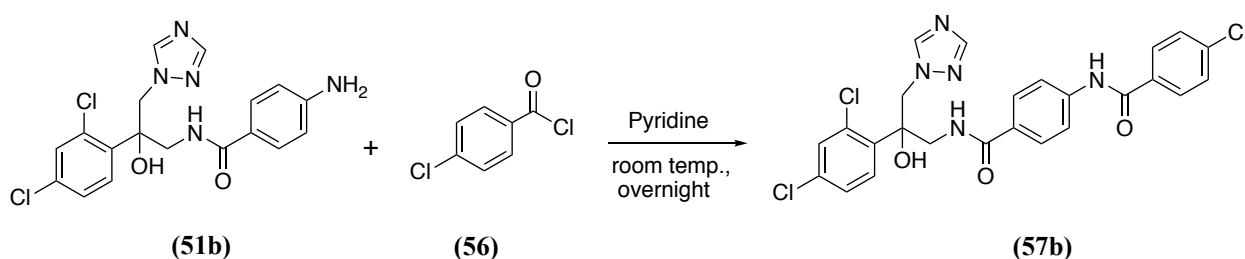
(51b)   **(56)**   **(57b)**

Reagents: 4-amino-*N*-(2-(2,4-dichlorophenyl)-2-hydroxy-3-(1*H*-1,2,4-triazol-1-yl)propyl) benzamide (**51b**) (0.16g, 0.39 mmol) and 4-chlorobenzoyl chloride (**56**) (0.16g, 0.6 mmol). The desired product was purified by gradient column chromatography and the desired product eluted with 5 % MeOH in CH$_2$Cl$_2$.

Yield: 0.16 g (76 %) as a white solid.

m.p.: 190-192 °C.

R$_f$: 0.32 (9.5: 0.5 v/v CH$_2$Cl$_2$-MeOH)

¹H NMR (DMSO-d$_6$): δ 10.51 (s, 1H, NH-amide), 8.49 (t, *J* = 5.9 Hz, 1H, NH-CH$_2$), 8.35 (s, 1H, triaz), 7.99 (d, *J* = 8.6 Hz, 2H, Ar), 7.84 (d, *J* = 8.8 Hz, 2H, Ar), 7.79 (d, *J* = 8.8 Hz, 2H, Ar), 7.74 (s, 1H, triaz), 7.62 (d, *J* = 8.6 Hz, 2H, Ar), 7.57 (dd, *J* = 8.6, 13.4 Hz, 2H, Ar), 7.29 (dd, *J* = 2.2, 8.6 Hz, 1H, Ar), 6.50 (s, 1H, OH, ex), 5.07 (d, *J* = 14.3 Hz, 1H, C*Ha*Hb-triaz), 4.68 (d, *J* = 14.3 Hz, 1H, CHa*Hb*-triaz), 4.04 (dd, *J* = 5.5, 14.0 Hz, 1H, C*Ha*Hb-NH), 3.97 (dd, *J* = 6.5, 14.0 Hz, 1H, CHa*Hb*-NH).

¹³C NMR (DMSO-d$_6$): δ 168.02 (C, C=O), 165.14 (C, C=O), 151.00 (CH, triaz), 145.58 (CH, triaz), 142.38 (C, Ar), 138.21 (C, Ar), 137.11 (C, C-Cl), 133.75 (C, C-Cl), 133.26 (C, C-Cl), 132.04 (C, Ar), 131.55 (CH, Ar), 130.41 (CH, Ar), 130.17 (X CH, Ar), 129.06 (C, Ar), 128.98 (2 X CH, Ar), 128.65 (2 X CH, Ar), 127.27 (CH, Ar), 119.89 (2 X CH, Ar), 76.99 (C-OH), 54.16 (CH$_2$-triaz), 46.68(CH$_2$-NH).

Microanalysis (C$_{25}$H$_{20}$Cl$_3$N$_5$O$_3$): Anal. Calcd: C 54.39 %, H 3.65 %, N 12.68 %. Found: C 54.05 %, H 3.80 %, N 12.31 %.

4-Chloro-*N*-(4-((2-(2,4-difluorophenyl)-2-hydroxy-3-(1*H*-1,2,4-triazol-1-yl)propyl)

carbamoyl)phenyl)benzamide (57c)

(C$_{25}$H$_{20}$ClF$_2$N$_5$O$_3$, M.W. 511.91)

(51c)   **(56)**   **(57c)**
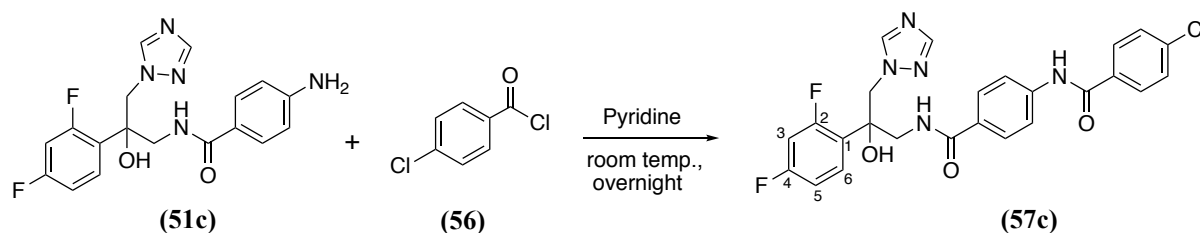
Reagents: 4-amino-*N*-(2-(2,4-difluorophenyl)-2-hydroxy-3-(1*H*-1,2,4-triazol-1-yl) propyl) benzamide (**51c**) (0.25g, 0.66 mmoL) and 4-chlorobenzoyl chloride (**56**) (0.17g, 1.0 mmol). The desired product was purified by gradient column chromatography and the desired product eluted with 4 % MeOH in CH$_2$Cl$_2$.

Yield: 0.26g (78%) as a white solid.

m.p.: 211-213 °C.

R*f*: 0.37 (9.5:0.5 v/v CH$_2$Cl$_2$-MeOH).

^{1}H NMR (DMSO-d$_6$): δ 10.50 (s, 1H, NH), 8.48 (t, *J* = 6.0 Hz, 1H, NH), 8.34 (s, 1H, triaz), 7.99 (d, *J* = 8.8 Hz, 2H, Ar), 7.84 (d, *J* = 9.0 Hz, 2H, Ar), 7.78 (d, *J* = 9.0 Hz, 2H, Ar), 7.75 (s, 1H, triaz), 7.62 (d, *J* = 8.8 Hz, 2H, Ar), 7.42 (dd, *J* = 9.0, 15.9 Hz, 1H, Ar), 7.21-7.16 (m, 1H,Ar), 6.93 (ddd, *J* = 2.4, 8.4, 10.9 Hz, 1H, Ar), 6.34 (s, 1H, OH, ex), 4.71 (d, *J* = 14.4 Hz, 1H, C*Ha*Hb-triaz), 4.58 (d, *J* = 14.4 Hz, 1H, CHa*Hb*-triaz), 3.81 (dd, *J* = 6.1, 14.4 Hz, 1H, C*Ha*Hb-NH), 3.77 (dd, *J* = 5.7, 14.4 Hz, 1H, CHa*Hb*-NH).

^{13}C NMR (DMSO-d$_6$): δ 167.73 (C, C=O), 165.14 (C, C=O), 162.27 (dd, $^3J_{CF}$ = 13.4 Hz, $^1J_{CF}$ =246.8 Hz, C, C2-Ar),159.56 (dd, $^3J_{CF}$ = 12.3 Hz, $^1J_{CF}$ =247.1 Hz, C, C4-Ar), 150.97 (CH, triaz), 145.45 (CH, triaz), 142.32 (C, Ar), 137.11 (C, Ar), 133.76 (C, Ar), 130.53 (dd, $^3J_{CF}$ = 6.3 Hz, $^3J_{CF}$ =9.5 Hz, CH, C6-Ar), 130.17 (2 X CH, Ar), 129.19 (C, Ar), 128.98 (2 X CH, Ar), 128.58 (2 X CH, Ar), 125.29 (dd, $^4J_{CF}$ = 3.4 Hz, $^2J_{CF}$ =13.0 Hz, C, C1-Ar), 119.91 (2 X CH, Ar),111.17 (dd, $^4J_{CF}$ = 3.3 Hz, $^2J_{CF}$ = 20.7 Hz, CH, C5-Ar), 104.39 (t, $^2J_{CF}$ = 27.9 Hz, CH, C3-Ar), 75.66 (C-OH), 55.59 (CH$_2$-triaz), 47.17 (CH$_2$-NH$_2$).

HPLC (Method A): 100 %, RT = 4.6 min.

HRMS (ESI, m/z): theoretical mass: $^{35/37}$Cl 512.1301/514.1301 [M+H]$^+$, observed mass: $^{35/37}$Cl 512.1304/514.1284 [M+H]$^+$.

4-Chloro-*N*-(4-((2-(4-fluorophenyl)-2-hydroxy-3-(1*H*-1,2,4-triazol-1-yl)propyl) carbamoyl) phenyl)benzamide (57d)

(C₂₅H₂₁ClFN₅O₃, M.W. 493.92)
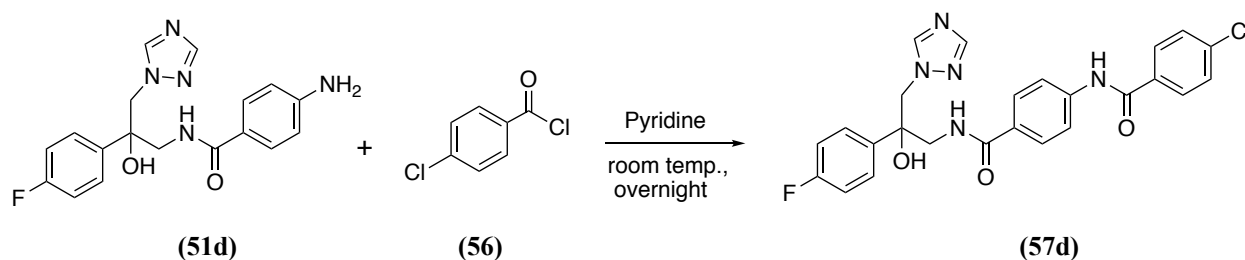
Reagents: 4-amino-*N*-(2-(4-fluorophenyl)-2-hydroxy-3-(1*H*-1,2,4-triazol-1-yl)propyl)benzamide (**51d**) (0.19g, 0.53mmoL) and 4-chlorobenzoyl chloride (**56**) (0.14g, 0.8 mmol). The desired product was purified by gradient column chromatography and the desired product eluted with 5 % MeOH in CH₂Cl₂.

Yield: 0.24g (92 %) as a white solid.

**m.p.:** 218-220 °C.

R*f*: 0.37 (9.5:0.5 v/v CH₂Cl₂-MeOH).

¹H NMR (DMSO-d₆): δ 10.50 (s, 1H, NH), 8.26 (t, *J* = 5.6 Hz, 1H, NH), 8.24 (s, 1H, triaz), 7.97 (d, *J* = 8.8 Hz, 2H, Ar), 7.83 (s, 1H, triaz), 7.82 (d, *J* = 5.6 Hz, 2H, Ar), 7.76 (d, *J* = 8.9 Hz, 2H, Ar), 7.62 (d, *J* = 8.8 Hz, 2H, Ar), 7.46 (dd, *J* = 5.5, 9.0 Hz, 2H, Ar), 7.09 (t, *J* = 8.9 Hz, 2H, Ar), 6.10 (s, 1H, OH, ex), 4.60 (d, *J* = 14.3 Hz, 1H, C*Ha*Hb-triaz), 4.57 (d, *J* = 14.3 Hz, 1H, CHa*Hb*-triaz), 3.86 (dd, *J* = 6.7, 14.0 Hz, 1H, C*Ha*Hb-NH), 3.64 (dd, *J* = 5.3, 14.0 Hz, 1H, CHa*Hb*-NH).

¹³C NMR (DMSO-d₆): δ 167.35 (C, C=O), 165.13 (C, C=O), 161.69 (d, ¹J_{CF} = 242.8 Hz, C, C1-Ar), 150.99 (CH, triaz), 145.42 (CH, triaz), 142.24 (C, Ar), 138.59 (d, ⁴J_{CF} = 2.5 Hz, C, C4-Ar), 137.10 (C, Ar), 133.76 (C, Ar), 130.17 (2 X CH, Ar), 129.38 (C, Ar), 128.97 (2 X CH, Ar), 128.51(2 X CH, Ar), 128.44 (d, ³J_{CF} = 8.1 Hz, 2 x CH, Ar), 119.91 (2 X CH, Ar), 114.85 (d, ²J_{CF} = 21.0 Hz, 2 x CH, Ar), 76.28 (C-OH), 57.28 (CH₂-triaz), 48.31 (CH₂-NH₂).

HPLC (Method A): 100 %, RT = 4.6 min.

HRMS (ESI, m/z): theoretical mass: ³⁵ᐟ³⁷Cl 494.1395/496.1395 [M+H]⁺, observed mass: ³⁵ᐟ³⁷Cl 494.1393/ 496.1376 [M+H]⁺.

 Using compound (46) procedure, the following compounds were prepared:

***N*-(2-(2,4-Difluorophenyl)-2-hydroxy-3-(1*H*-1,2,4-triazol-1-yl)propyl)-6-fluoro-2-naphthamide (59)**

(C$_{22}$H$_{17}$F$_3$N$_4$O$_2$, M. W. 426.40)
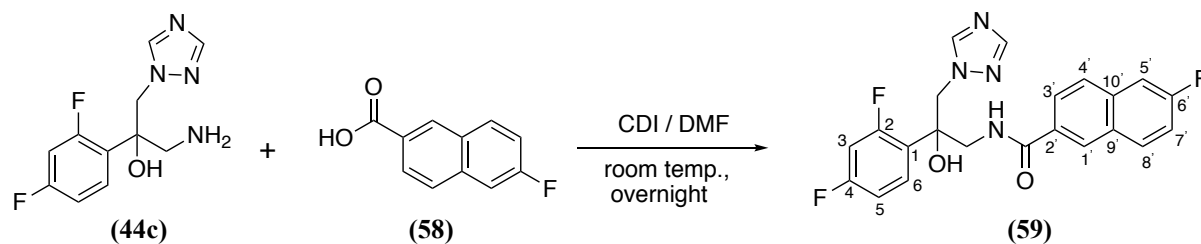
Reagents: 6-fluoro-2-naphthoic acid (**58**) (0.22g, 1.17 mmol) and 1-amino-2-(2,4-difluorophenyl)-3-(1*H*-1,2,4-triazol-1-yl)propan-2-ol (**44c**) (0.2g, 0.78 mmol). The desired product was purified by gradient column chromatography and the desired product eluted with 2.5 % MeOH in CH$_2$Cl$_2$.

Yield: 0.20g (60 %) as a white solid.

m.p.: 195-197 °C.

R$_f$: 0.37 (9.5: 0.5 v/v CH$_2$Cl$_2$-MeOH).

¹H NMR (DMSO-d$_6$): δ 8.69 (t, *J* = 6.0 Hz, 1H, NH), 8.42 (s, 1H, Ar), 8.35 (s, 1H, triaz), 8.10 (dd, *J* = 5.8, 9.1 Hz 1H, Ar), 7.96 (d, *J* = 9.0 Hz, 1H, Ar), 7.88 (d, *J* = 8.8 Hz, 1H, Ar), 7.77 (dd, *J* = 2.6, 19.2 Hz, 1H, Ar), 7.75 (s, 1H, triaz), 7.51 (ddd, *J* = 2.7, 8.9, 11.5 Hz, 1H, Ar), 7.43 (dd, *J* = 9.0, 15.9 Hz, 1H, Ar), 7.21-7.17 (m, 1H, Ar), 6.94 (ddd, *J* = 2.8, 8.7, 11.3 Hz, 1H, Ar), 6.32 (s, 1H, OH, ex), 4.74 (d, *J* = 14.4 Hz, 1H, C*Ha*Hb-triaz), 4.62 (d, *J* = 14.4 Hz, 1H, CHa*Hb*-triaz), 3.86 (dd, *J* = 6.2, 14.1 Hz, 1H, C*Ha*Hb-NH), 3.82 (dd, *J* = 5.8, 14.1 Hz, 1H, CHa*Hb*-NH).

¹⁹F NMR (DMSO-d$_6$): δ -106.76 (*para*-F-Ar), -112.09 (2F, *meta*-F-Ar and naph-F).

¹³C NMR (DMSO-d$_6$): δ 167.97 (C, C=O), 162.39 (d, $^1J_{CF}$ = 246.2 Hz, C, C6'-Ar), 160.9 (dd, $^3J_{CF}$ = 12.7 Hz, $^1J_{CF}$ =245.4 Hz, C, C2-Ar), 159.21 (dd, $^3J_{CF}$ = 12.5 Hz, $^1J_{CF}$ =247.4 Hz, C, C4-Ar), 150.9 (CH, triaz), 145.44 (CH, triaz), 135.62 (d, $^3J_{CF}$ = 9.9 Hz, C, C10'-Ar), 132.38 (dd, $^3J_{CF}$ = 9.3 Hz, CH, C8'-Ar), 131.22 (d, $^4J_{CF}$ = 2.7 Hz, C, C9'-Ar), 130.53 (dd, $^3J_{CF}$ = 6.1Hz, $^3J_{CF}$ = 9.5 Hz, CH, C6-Ar), 129.67 (C, C2'-Ar), 128.27 (CH, Ar), 127. 82 (d, $^4J_{CF}$ = 5.3 Hz, CH, C4'-Ar), 125.67 (CH, Ar), 125.25 (dd, $^4J_{CF}$ = 3.3 Hz, $^2J_{CF}$ =12.8 Hz, C, C4-Ar), 117.51 (d, $^2J_{CF}$ = 25.4 Hz, CH, C7'-Ar), 111.26 (d, $^2J_{CF}$ =20.7 Hz, CH, C5'-Ar) 111.18 (dd, $^4J_{CF}$ = 3.1 Hz, $^2J_{CF}$ =20.7 Hz, CH, C5-Ar), 104.42 (t, $^2J_{CF}$ = 27.1 Hz, CH, C3-Ar), 75.62 (C-OH), 55.57 (CH$_2$-triaz), 47.20 (CH$_2$-NH$_2$).

HPLC: 96 %, RT = 4.59 min.

HRMS (ESI, m/z): theoretical mass: 449.1201 [M+Na]⁺, observed mass: 449.1199 [M+Na]⁺.

N-(2-(2,4-Difluorophenyl)-2-hydroxy-3-(1*H*-1,2,4-triazol-1-yl)propyl)quinoline-3-carboxamide (61)

(C₂₁H₁₇F₂N₅O₂, M.W. 409.40)
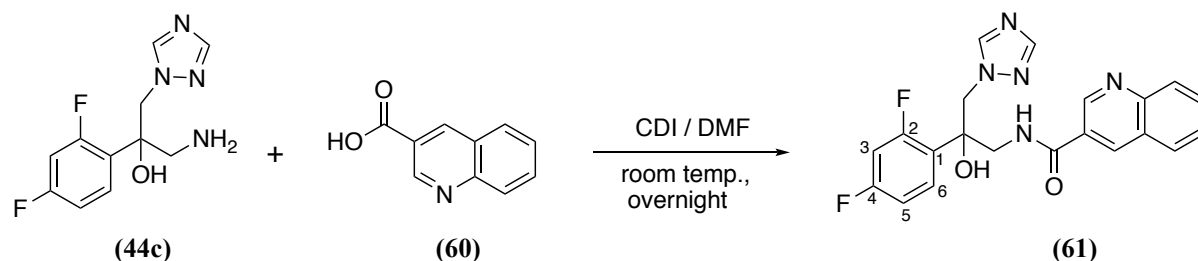
Reagents: Quinoline-3-carboxylic acid (**60**) (0.20g, 1.17 mmol) and 1-amino-2-(2,4-difluorophenyl)-3-(1*H*-1,2,4-triazol-1-yl)propan-2-ol (**44c**) (0.2g, 0.78 mmol). The desired product was purified by gradient column chromatography and the desired product eluted with 3 % MeOH in CH₂Cl₂.

Yield: 0.19g (61 %) as a white solid.

m.p.: 193-195 °C.

R*f*: 0.3 (9.5: 0.5 v/v CH₂Cl₂-MeOH).

¹H NMR (DMSO-d₆): δ 9.18 (d, *J* = 2.2 Hz, 1H, Ar), 8.87 (t, *J* = 6.1 Hz, 1H, NH), 8.75 (d, *J* = 2.2 Hz, 1H, Ar), 8.35 (s, 1H, triaz), 8.07 (d, *J* = 9.8 Hz, 2H, Ar), 7.88- 7.85 (m, 1H, Ar), 7.76 (s, 1H, triaz), 7.71-7.68 (m, 1H, Ar), 77.44 (dd, *J* = 9.0, 15.9 Hz, 1H, Ar), 7.22-7.17 (m, 1H, Ar), 6.94 (ddd, *J* = 2.5, 8.7, 10.9 Hz, 1H, Ar), 6.22 (s, 1H, OH, ex), 4.77 (d, *J* = 14.4 Hz, 1H, C*Ha*Hb-triaz), 4.65 (d, *J* = 14.4 Hz, 1H, CHa*Hb*-triaz), 3.86 (dd, *J* = 6.2, 13.8 Hz, 1H, C*Ha*Hb-NH), 3.83 (dd, *J* = 6.2, 13.8 Hz, 1H, CHa*Hb*-NH).

¹⁹F NMR (DMSO-d₆): δ -106.77 (*para*-F-Ar), -112.05 (*meta*-F-Ar).

¹³C NMR (DMSO-d₆): δ 165.51 (C, C=O), 162.32 (dd, ³*J*₍CF₎ = 12.6 Hz, ¹*J*₍CF₎ =245.9 Hz, C, C2-Ar), 159.6 (dd, ³*J*₍CF₎ = 12.5 Hz, ¹*J*₍CF₎ =247.7 Hz, C, C4-Ar), 151.0 (CH, triaz), 149.32 (CH, Ar), 148.92 (C, Ar), 145.44 (CH, triaz), 136.16 (CH, Ar), 131.72 (CH, Ar), 130.53 (dd, ³*J*₍CF₎ = 6.1 Hz, ³*J*₍CF₎ = 9.5 Hz, CH, C6-Ar), 129.54 (CH, Ar), 129.21 (CH, Ar), 127. 90 (CH, Ar), 127.22 (C, Ar), 126.87 (C, Ar), 125.16 (dd, ⁴*J*₍CF₎ = 3.5 Hz, ²*J*₍CF₎ =13.0 Hz, C, C1-Ar), 111.19 (dd, ⁴*J*₍CF₎ = 2.6 Hz, ²*J*₍CF₎ = 20.5 Hz, CH, C5-Ar), 104.44 (t, ²*J*₍CF₎ = 28.0 Hz, CH, C3-Ar), 75.55 (C-OH), 55.46 (CH₂-triaz), 46.97 (CH₂-NH₂).

HPLC: 100 %, RT = 4.34 min.

HRMS (ESI, m/z): theoretical mass: 410.1428 [M+H]⁺, observed mass: 410.1427 [M+H]⁺.

7-Chloro-*N*-(2-(2,4-difluorophenyl)-2-hydroxy-3-(1*H*-1,2,4-triazol-1-yl)propyl)-2-methylquinoline-3-carboxamide (63)

(C$_{22}$H$_{18}$ClF$_2$N$_5$O$_2$, M.W. 457.87)
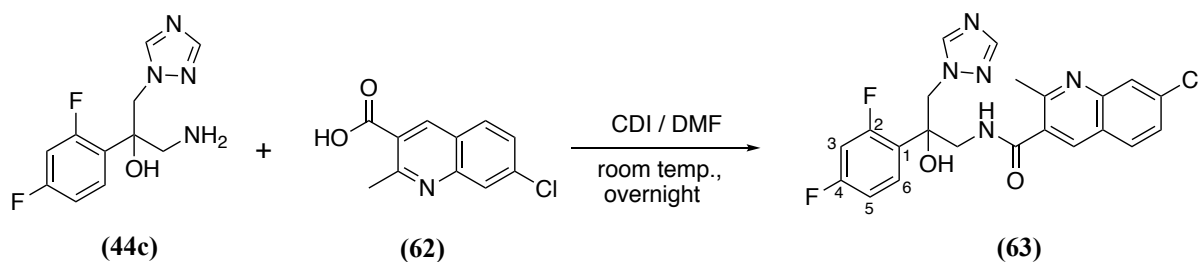
Reagents: 7-chloro-2-methylquinoline-3-carboxylic acid (**62**) (0.17g, 0.78 mmol) and 1-amino-2-(2,4-difluorophenyl)-3-(1*H*-1,2,4-triazol-1-yl)propan-2-ol (**44c**) (0.2g, 0.78 mmol). The desired product was purified by gradient column chromatography and the desired product eluted with 3 % MeOH in CH$_2$Cl$_2$.

Yield: 0.22g (63 %) as a white solid.

m.p.: 145-146 °C.

R*f*: 0.45 (9.5: 0.5 v/v CH$_2$Cl$_2$-MeOH).

^{1}H NMR (DMSO-d$_6$): δ 8.62 (t, *J* = 6.0 Hz, 1H, NH), 8.36 (s, 1H, triaz), 8.20 (s, 1H, Ar), 7.99 (d, *J* = 11.2 Hz, 1H, Ar), 7.98 (s, 1H, Ar), 7.79 (s, 1H, triaz), 7.62 (dd, *J* = 2.2, 9.0 Hz, 1H, Ar), 77.46 (q, *J* = 9.0 Hz, 1H, Ar), 7.23-7.18 (m, 1H, Ar), 7.00 (ddd, *J* = 2.5, 8.5, 11.0 Hz, 1H, Ar), 6.17 (s, 1H, OH, ex), 4.74 (d, *J* = 14.4 Hz, 1H, C*Ha*Hb-triaz), 4.66 (d, *J* = 14.4 Hz, 1H, CHa*Hb*-triaz), 4.00 (dd, *J* = 7.0, 13.9 Hz, 1H, C*Ha*Hb-NH), 3.67 (dd, *J* = 5.3, 13.9 Hz, 1H, CHa*Hb*-NH).

^{19}F NMR (DMSO-d$_6$): δ -106.69 (*para*-F-Ar), -112.07 (*meta*-F-Ar).

^{13}C NMR (DMSO-d$_6$): δ 168.74 (C, C=O), 162.43 (dd, $^3J_{CF}$ = 12.9 Hz, $^1J_{CF}$ = 245.8 Hz, C, C2-Ar), 159.71 (dd, $^3J_{CF}$ = 12.0 Hz, $^1J_{CF}$ = 247.8 Hz, C, C4-Ar), 151.07 (CH, triaz), 147.72 (C, Ar), 145.50 (CH, triaz), 135.39 (C, Ar), 135.09 (CH, Ar), 130.99 (C, Ar), 130.78 (dd, $^3J_{CF}$ = 6.0 Hz, $^3J_{CF}$ = 9.7 Hz, CH, C6-Ar), 130.48 (CH, Ar), 127. 53 (CH, Ar), 127.24 (CH, Ar), 125.02 (dd, $^4J_{CF}$ = 3.6 Hz, $^2J_{CF}$ = 13.0 Hz, C, C1-Ar), 111.11 (dd, $^4J_{CF}$ = 3.0 Hz, $^2J_{CF}$ = 20.4 Hz, CH, C5-Ar), 104.44 (t, $^2J_{CF}$ = 27.8 Hz, CH, C3-Ar), 75.31 (C-OH), 55.50 (CH$_2$-triaz), 46.51 (CH$_2$-NH$_2$), 23.50 (CH$_3$).

HPLC: 100 %, RT = 4.51 min.

HRMS (ESI, m/z): theoretical mass: $^{35/37}$Cl 458.1195/460.1195 [M+H]$^+$, observed mass: $^{35/37}$Cl 458.1192/460.1169 [M+H]$^+$.

4'-(Trifluoromethyl)-[1,1'-biphenyl]-4-carboxylic acid (66a)

($C_{14}H_9F_3O_2$, M.W. 266.22)

(64)　　　　　　**(65a)**　　　　　　　　　　　　　　**(66a)**
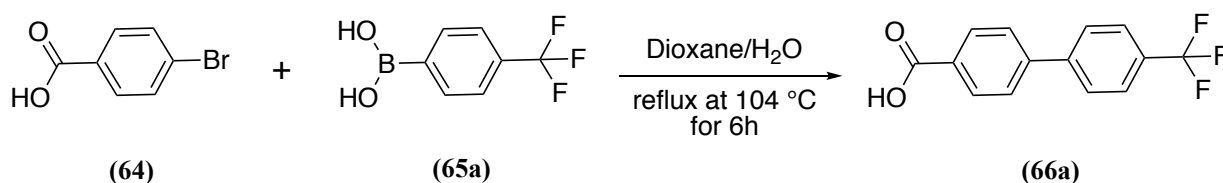
Method: Under nitrogen atmosphere, 4-bromobenzoic acid (**64**) (0.3g, 1.49 mmol), 4-trifluoromethyl phenylboronic acid (**65a**) (0.42g, 2.23 mmol) and 1 mol % of Pd(PPh$_3$)$_4$ (0.17mg) were dissolved in a mixture solution of dioxane/H$_2$O (10:1 v/v). Then, K$_2$CO$_3$ (0.41g, 2.93 mmol) was added and the mixture heated under reflux for 6 h. The reaction mixture was cooled to room temperature and the dioxane was evaporated. After that, H$_2$O (20 mL) was added and the solution was adjusted to pH 1-3 with 2N aqueous HCl, then extracted with EtOAc (3 x 50 mL) and dried (MgSO$_4$). The organic layer was evaporated under reduced pressure to give a crude light gray semisolid. The residue was purified by gradient column chromatography and the desired product was eluted with 2% MeOH in CH$_2$Cl$_2$.

Yield: 0.32g (82 %) as a white solid.

m.p.: 240-243 °C.

R$_f$: 0.42 (9.5: 0.5 v/v CH$_2$Cl$_2$-MeOH).

^{1}H NMR (DMSO-d$_6$): δ 13.07 (s, 1H, OH), 8.06 (d, J = 8.7 Hz, 2H, Ar), 7.87 (dd, J = 5.2, 8.7 Hz, 4H, Ar), 7.71 (d, J = 8.7 Hz, 2H, Ar).

^{19}F NMR (DMSO-d$_6$): δ -60.92 (C$\underline{F}_3$).

 Using this procedure, the following compounds were prepared:

4'-(Trifluoromethoxy)-[1,1'-biphenyl]-4-carboxylic acid (66b)

($C_{14}H_9F_3O_3$, M.W. 282.22)

(64)　　　　　　**(65b)**　　　　　　　　　　　　　**(66b)**
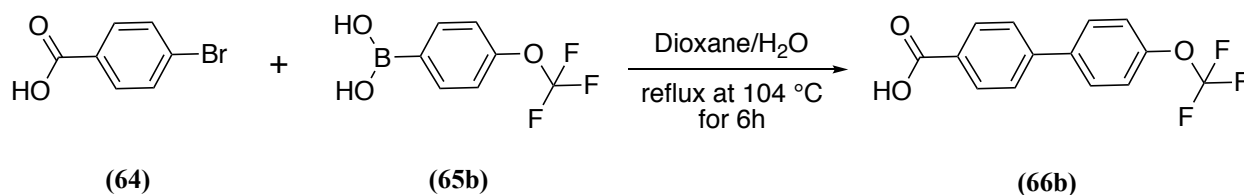
Reagents: 4-bromobenzoic acid (**64**) (0.3g, 1.49 mmol) and 4-trifluoromethoxy phenylboronic acid (**65b**) (0.46g, 2.23 mmol).

Yield: 0.36g (85 %) as a white solid.

m.p.: 251-253 °C.

R$_f$: 0.47 (9.5: 0.5 v/v CH$_2$Cl$_2$-MeOH)

^{1}H NMR (DMSO-d$_6$): δ 13.03 (s, 1H, OH), 8.03 (d, J = 8.7 Hz, 2H, Ar), 7.86 (d, J = 8.9 Hz, 2H, Ar), 7.82 (d, J = 8.7 Hz, 2H, Ar), 7.49 (d, J = 8.0 Hz, 2H, Ar).

^{19}F NMR (DMSO-d$_6$): δ -56.74 (C$\underline{F}_3$).

4'-(Trifluoromethyl)-[1,1'-biphenyl]-3-carboxylic acid (68a)
(C$_{14}$H$_9$F$_3$O$_2$, M.W. 266.22)
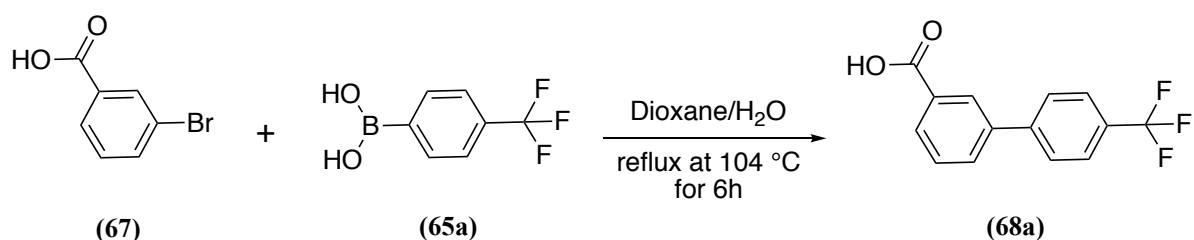
(67)   (65a)   (68a)

Reagents: 3-bromobenzoic acid (**67**) (0.3g, 1.49 mmol) and 4-trifluoromethyl phenylboronic acid (**65a**) (0.42g, 2.23 mmol). The residue was purified by gradient column chromatography and the desired product was eluted with 2.5 % MeOH in CH$_2$Cl$_2$.

Yield: 0.35g (90 %) as a white solid.

m.p.: 198-200 °C.

R$_f$: 0.45 (9.5: 0.5 v/v CH$_2$Cl$_2$-MeOH).

^{1}H NMR (DMSO-d$_6$): δ 13.18 (s, 1H, OH), 8.24 (s, 1H, Ar), 8.02-7.99 (m, 2H, Ar), 7.94 (d, J = 8.0 Hz, 2H, Ar), 7.84 (d, J = 8.1 Hz, 2H, Ar), 7.65 (t, J = 7.7 Hz, 1H, Ar).

^{19}F NMR (DMSO-d$_6$): δ -60.96 (C$\underline{F}_3$).

4'-(Trifluoromethoxy)-[1,1'-biphenyl]-3-carboxylic acid (68b)
(C$_{14}$H$_9$F$_3$O$_3$, M.W. 282.22)
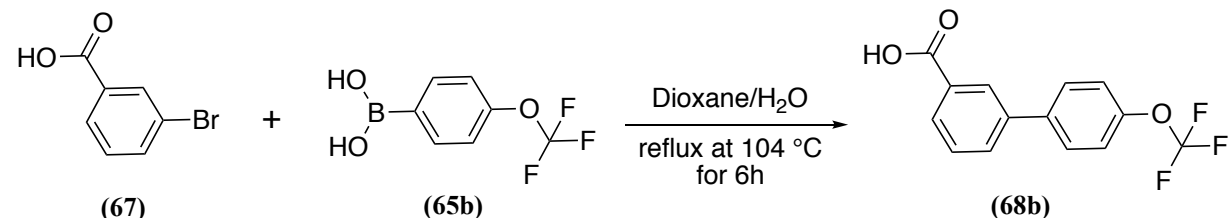
(67)   (65b)   (68b)

Reagents: 3-bromobenzoic acid (**67**) (0.3g, 1.49 mmol) and 4-trifluoromethoxy phenylboronic acid (**65b**) (0.46g, 2.23 mmol). The residue was purified by gradient column chromatography and the desired product was eluted with 2.5 % MeOH in CH$_2$Cl$_2$.

Yield: 0.35g (83 %) as a beige solid.

m.p.: 158-160 °C.

R$_f$: 0.35 (9.5: 0.5 v/v CH$_2$Cl$_2$-MeOH).

^{1}H NMR (DMSO-d$_6$): δ 13.13 (s, 1H, OH), 8.19 (s, 1H, Ar), 7.95 (dd, J = 7.7, 15.9 Hz, 2H, Ar), 7.84 (d, J = 8.9 Hz, 2H, Ar), 7.62 (t, J = 7.7 Hz, 1H, Ar), 7.47 (d, J = 7.9 Hz, 2H, Ar).

^{19}F NMR (DMSO-d$_6$): δ -56.74 (C$\underline{F}_3$).

^{13}C NMR (DMSO-d$_6$): δ 167.55 (C, C=O), 148.60 (C, Ar), 139.53 (C, Ar), 139.02 (C, Ar), 132.06 (C, Ar), 131.69 (CH, Ar), 129.89 (CH, Ar), 129.24 (2 x CH, Ar), 129.11 (CH), 127.89 (CH), 122.00 (2 x CH, Ar), 120.56 (q, $^1J_{CF3}$ = 256.24 Hz, C, CF$_3$).

HPLC: 100 %, RT = 4.81 min.

HRMS (ESI, m/z): theoretical mass: 281.0426 [M-H]$^-$, observed mass: 281.0431 [M-H]$^-$.

Using compound (46) procedure, the following compounds were prepared:

***N*-(2-(2,4-Difluorophenyl)-2-hydroxy-3-(1*H*-1,2,4-triazol-1-yl)propyl)-4'-(trifluoromethyl)-[1,1'-biphenyl]-4-carboxamide (69a)**
(C$_{25}$H$_{19}$F$_5$N$_4$O$_2$, M.W. 502.45)
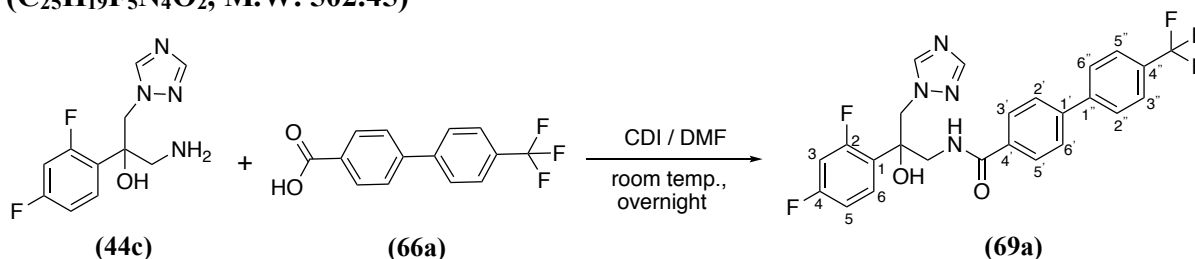
Reagents: 4'-(trifluoromethyl)-[1,1'-biphenyl]-4-carboxylic acid (**66a**) (0.2g, 0.78 mmol) and 1-amino-2-(2,4-difluorophenyl)-3-(1*H*-1,2,4-triazol-1-yl)propan-2-ol (**44c**) (0.15g, 0.58 mmol). The residue was purified by gradient column chromatography and the desired product was eluted with 2.5 % MeOH in CH$_2$Cl$_2$.

Yield: 0.3g (76 %) as a white solid.

m.p.: 211-213 °C.

R$_f$: 0.37 (9.5: 0.5 v/v CH$_2$Cl$_2$-MeOH).

^{1}H NMR (DMSO-d$_6$): δ 8.61 (t, J = 6.0 Hz, 1H, NH), 8.35 (s, 1H, triaz), 7.94 (d, J = 8.1 Hz, 2H, Ar), 7.89 (d, J = 8.9 Hz, 2H, Ar), 7.83 (dd, J = 5.7, 7.8 Hz, 4H, Ar), 7.75 (s, 1H, triaz), 7.42 (dd, J = 9.0, 15.9 Hz, 1H, Ar), 7.21-7.16 (m, 1H, Ar), 6.93 (ddd, J = 2.7, 8.6, 11.1 Hz, 1H, Ar), 6.29 (s, 1H, OH, ex), 4.73 (d, J = 14.4 Hz, 1H, C*Ha*Hb-triaz), 4.60 (d, J = 14.4 Hz, 1H, CHa*Hb*-triaz), 3.85 (dd, J = 6.5, 14.0 Hz, 1H, C*Ha*Hb-NH), 3.79 (dd, J = 5.7, 14.0 Hz, 1H,

CHa*Hb*-NH).

^{19}F NMR (DMSO-d$_6$): δ -60.96 (C$\underline{F}_3$), -106. 79 (*para*-F-Ar), -112.15 (*meta*-F-r).

^{13}C NMR (DMSO-d$_6$): δ 167.61 (C, C=O), 162.28 (dd, $^3J_{CF}$ = 12.1 Hz, $^1J_{CF}$ = 245.5 Hz, C, C2-Ar), 159.60 (dd, $^3J_{CF}$ = 12.2 Hz, $^1J_{CF}$ = 247.2 Hz, C, C4-Ar), 150.9 (CH, triaz), 145.57 (CH, triaz), 143.57 (C, Ar), 141.77 (C, Ar), 134.05 (C, Ar), 130.51 (dd, $^3J_{CF}$ = 6.2 Hz, $^3J_{CF}$ = 9.6 Hz, CH, C6-Ar), 128.82 (d, $^2J_{CF3}$ = 31.9 Hz, C, C4''-Ar), 128.69 (2 x CH, Ar), 128.57 (2 x CH, Ar), 127. 42 (2 x CH, Ar), 126.30 (q, $^3J_{CF3}$ = 3.5 Hz, 2 x CH, C3''and C5''-Ar), 125.22 (dd, $^4J_{CF}$ = 3.4 Hz, $^2J_{CF}$ = 12.9 Hz, C, C1-Ar), 124.64 (q, $^1J_{CF3}$ = 256.18 Hz, C, CF$_3$), 111.16 (dd, $^4J_{CF}$ = 2.4 Hz, $^2J_{CF}$ = 20.6 Hz, CH, C5-Ar), 104.41 (t, $^2J_{CF}$ = 26.3 Hz, CH, C3-Ar), 75.64 (C-OH), 55.57 (CH$_2$-triaz), 47.08 (CH$_2$-NH$_2$).

HPLC: 100 %, RT = 4.76 min.

HRMS (ESI, m/z): theoretical mass: 503.1506 [M+H]$^+$, observed mass: 503.1503 [M+H]$^+$.

N-(2-(2,4-Difluorophenyl)-2-hydroxy-3-(1H-1,2,4-triazol-1-yl)propyl)-4'-(trifluoromethoxy)-[1,1'-biphenyl]-4-carboxamide (69b)

(C$_{25}$H$_{19}$F$_5$N$_4$O$_3$, M.W. 518.44)
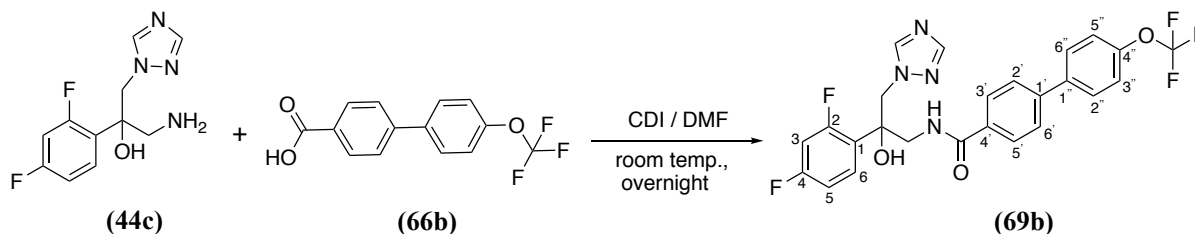
Reagents: 4'-(trifluoromethoxy)-[1,1'-biphenyl]-4-carboxylic acid (**66b**) (0.22g, 0.78 mmol) and 1-amino-2-(2,4-difluorophenyl)-3-(1H-1,2,4-triazol-1-yl)propan-2-ol (**44c**) (0.2g, 0.78 mmol). The residue was purified by gradient column chromatography and the desired product was eluted with 2.5 % MeOH in CH$_2$Cl$_2$.

Yield: 0.26g (65 %) as a white solid.

m.p.: 208-210 °C.

R$_f$: 0.35 (9.5: 0.5 v/v CH$_2$Cl$_2$-MeOH).

^{1}H NMR (DMSO-d$_6$): δ 8.59 (t, J = 6.0 Hz, 1H, NH), 8.35 (s, 1H, triaz), 7.85 (q, J = 8.7 Hz, 4H, Ar), 7.77 (d, J = 8.7 Hz, 2H, Ar), 7.75 (s, 1H, triaz), 7.47 (d, J = 7.9 Hz, 2H, Ar), 7.42 (dd, J = 9.0, 15.9 Hz, 1H, Ar), 7.21- 7.16 (m, 1H, Ar), 6.93 (ddd, J = 2.4, 8.3, 10.9 Hz, 1H, Ar), 6.30 (s, 1H, OH, ex), 4.72 (d, J = 14.4 Hz, 1H, C*Ha*Hb-triaz), 4.60 (d, J = 14.4 Hz, 1H, CHa*Hb*-triaz), 3.84 (dd, J = 6.5, 14.0 Hz, 1H, C*Ha*Hb-NH), 3.79 (dd, J = 5.7, 14.0 Hz, 1H, CHa*Hb*-NH).

^{19}F NMR (DMSO-d$_6$): δ -56.69 (C$\underline{F_3}$), -106. 81 (*para*-F-Ar), -112.12 (*meta*-F-Ar).

^{13}C NMR (DMSO-d$_6$): δ 167.70 (C, C=O), 162.29 (dd, $^3J_{CF}$ = 12.4 Hz, $^1J_{CF}$ = 245.3 Hz, C, C2-Ar), 159.60 (dd, $^3J_{CF}$ = 12.7 Hz, $^1J_{CF}$ = 247.2 Hz, C, C4-Ar), 150.9 (CH, triaz), 148.72 (C, Ar), 145.46 (CH, triaz), 141.94 (C, Ar), 138.88 (C, Ar), 133.81 (C, Ar), 130.51 (dd, $^3J_{CF}$ = 6.0 Hz, $^3J_{CF}$ = 9.5 Hz, CH, C6-Ar), 129.30 (2 x CH, Ar), 128.51 (2 x CH, Ar), 127. 15 (2 x CH, Ar), 125.23 (dd, $^4J_{CF}$ = 3.5 Hz, $^2J_{CF}$ = 13.3 Hz, C, C1-Ar), 123.20 (q, $^1J_{CF3}$ = 256.23 Hz, C, CF$_3$), 121.97 (2 x CH, Ar), 111.16 (dd, $^4J_{CF}$ = 2.8 Hz, $^2J_{CF}$ = 20.7 Hz, CH, C5-Ar), 104.40 (t, $^2J_{CF}$ = 28.1 Hz, CH, C3-Ar), 75.61 (C-OH), 55.57 (CH$_2$-triaz), 47.09 (CH$_2$-NH$_2$).

HPLC: 100 %, RT = 4.78 min.

HRMS (ESI, m/z): theoretical mass: 519.1455 [M+H]$^+$, observed mass: 519.1453 [M+H]$^+$.

N-(2-(2,4-Difluorophenyl)-2-hydroxy-3-(1*H*-1,2,4-triazol-1-yl)propyl)-4'-(trifluoromethyl)-[1,1'-biphenyl]-3-carboxamide (70a)

(C$_{25}$H$_{19}$F$_5$N$_4$O$_2$, M. W. 502.45)

(44c) + **(68a)** → **(70a)**
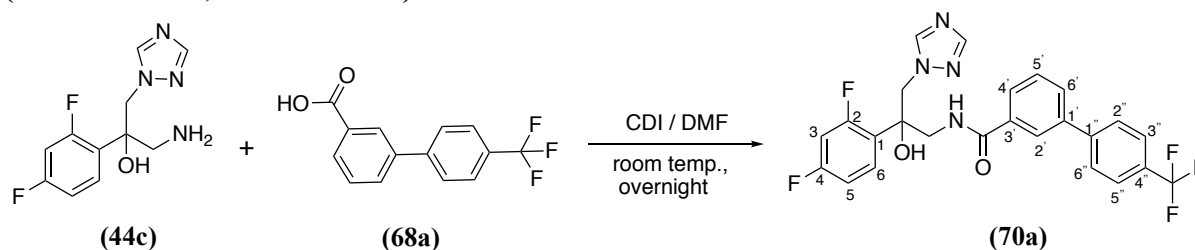
Reagents: 4'-(trifluoromethyl)-[1,1'-biphenyl]-3-carboxylic acid (**68a**) (0.24g, 0.90 mmol) and 1-amino-2-(2,4-difluorophenyl)-3-(1*H*-1,2,4-triazol-1-yl)propan-2-ol (**44c**) (0.23g, 0.90 mmol). The residue was purified by gradient column chromatography and the desired product was eluted with 3 % MeOH in CH$_2$Cl$_2$.

Yield: 0.34g (75 %) as a white solid.

m.p.: 92-94 °C.

R$_f$: 0.42 (9.5: 0.5 v/v CH$_2$Cl$_2$-MeOH).

^{1}H NMR (DMSO-d$_6$): δ 8.72 (t, *J* = 6.0 Hz, 1H, NH), 8.35 (s, 1H, triaz), 8.09 (s, 1H, Ar), 7.94 (d, *J* = 8.1 Hz, 2H, Ar), 7.90 (d, *J* = 7.7 Hz, 1H, Ar), 7.86 (d, *J* = 8.2 Hz, 2H, Ar), 7.81 (d, *J* = 8.2 Hz, 1H, Ar), 7.75 (s, 1H, triaz), 7.59 (t, *J* = 7.7 Hz, 1H, Ar), 7.43 (dd, *J* = 9.0, 15.9 Hz, 1H, Ar), 7.21-7.17 (m, 1H, Ar), 6.94 (ddd, *J* = 2.5, 8.4, 10.9 Hz, 1H, Ar), 6.27 (s, 1H, OH, ex), 4.74 (d, *J* = 14.4 Hz, 1H, C*Ha*Hb-triaz), 4.61 (d, *J* = 14.4 Hz, 1H, CHa*Hb*-triaz), 3.85 (d, *J* = 6.0, 13.9 Hz, 1H, C*Ha*Hb-NH), 3.79 (d, *J* = 6.0, 13.9 Hz, 1H, CHa*Hb*-NH).

^{19}F NMR (DMSO-d$_6$): δ -60.90 (C$\underline{F_3}$), -106. 80 (*para*-F-Ar), -112.08 (*meta*-F-Ar).

^{13}C NMR (DMSO-d$_6$): δ 167.87 (C, C=O), 162.34 (dd, $^3J_{CF}$ = 12.3 Hz, $^1J_{CF}$ = 245.6 Hz, C,

C2-Ar), 159.65 (dd, $^3J_{CF}$ = 12.2 Hz, $^1J_{CF}$ = 247.6 Hz, C, C4-Ar), 151.01 (CH, triaz), 145.72 (CH, triaz), 143.92 (C, Ar), 139.01 (C, Ar), 135.25 (C, Ar), 130.50 (dd, $^3J_{CF}$ = 6.0 Hz, $^3J_{CF}$ = 9.7 Hz, CH, C6-Ar), 130.40 (CH, Ar), 129.69 (CH, Ar), 128.63 (d, $^2J_{CF3}$ = 31.8 Hz, C, C4''-Ar), 128.11 (3 x CH, Ar), 127. 95 (CH, Ar), 126.31 (q, $^3J_{CF3}$ = 3.3 Hz, 2 x CH, C3''and C5''-Ar), 125.24 (dd, $^4J_{CF}$ = 3.3 Hz, $^2J_{CF}$ = 13.2 Hz, C, C1-Ar), 124.66 (q, $^1J_{CF3}$ = 256.4 Hz, C, CF$_3$), 111.18 (dd, $^4J_{CF}$ = 2.8 Hz, $^2J_{CF}$ = 20.7 Hz, CH, C5-Ar), 104.42 (t, $^2J_{CF}$ = 28.0 Hz, CH, C3-Ar), 75.64 (C-OH), 55.52 (CH$_2$-triaz), 47.12 (CH$_2$-NH$_2$).

HPLC: 100 %, RT = 4.77 min.

HRMS (ESI, m/z): theoretical mass: 503.1506 [M+H]$^+$, observed mass: 503.1505 [M+H]$^+$.

N-(2-(2,4-Difluorophenyl)-2-hydroxy-3-(1H-1,2,4-triazol-1-yl)propyl)-4'-(trifluoromethoxy)-[1,1'-biphenyl]-3-carboxamide (70b)

(C$_{25}$H$_{19}$F$_5$N$_4$O$_3$, M.W. 518.44)

(44c)   **(68b)**   CDI / DMF
room temp.,
overnight   **(70b)**
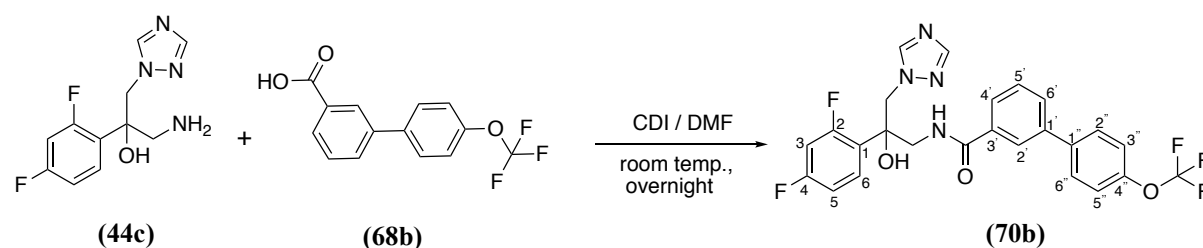
Reagents: 4'-(trifluoromethoxy)-[1,1'-biphenyl]-3-carboxylic acid (**68b**) (0.22g, 0.78 mmol) and 1-amino-2-(2,4-difluorophenyl)-3-(1H-1,2,4-triazol-1-yl)propan-2-ol (**44c**) (0.2g, 0.78 mmol). The residue was purified by gradient column chromatography and the desired product was eluted with 2 % MeOH in CH$_2$Cl$_2$.

Yield: 0.27g (72 %) as a pale yellow oil.

R$_f$: 0.4 (9.5: 0.5 v/v CH$_2$Cl$_2$-MeOH).

^{1}H NMR (DMSO-d$_6$): δ 8.69 (t, J = 6.1 Hz, 1H, NH), 8.35 (s, 1H, triaz), 8.03 (s,1H, Ar), 7.83 (d, J = 8.9 Hz, 3H, Ar), 7.77 (d, J = 8.4 Hz, 1H, Ar), 7.75 (s, 1H, triaz), 7.56 (t, J = 7.7 Hz, 1H, Ar), 7.49 (d, J = 8.0 Hz, 2H, Ar), 7.42 (dd, J = 9.0, 15.9 Hz, 1H, Ar), 7.21-7.17 (m, 1H, Ar), 6.94 (ddd, J = 2.7, 8.6, 11.2 Hz, 1H, Ar), 6.28 (s, 1H, OH, ex), 4.73 (d, J = 14.4 Hz, 1H, C*Ha*Hb-triaz), 4.60 (d, J = 14.4 Hz, 1H, CHa*Hb*-triaz), 3.84 (d, J = 6.2, 14.3 Hz, 1H, C*Ha*Hb-NH), 3.78 (d, J = 5.7, 14.3 Hz, 1H, CHa*Hb*-NH).

^{19}F NMR (DMSO-d$_6$): δ -56.74 (C$\underline{F}_3$), -106. 81 (para-F-Ar), -112.09 (meta-F-Ar).

^{13}C NMR (DMSO-d$_6$): δ 167.95 (C, C=O), 162.29 (dd, $^3J_{CF}$ = 12.7 Hz, $^1J_{CF}$ = 245.9 Hz, C, C2-Ar), 159.60 (dd, $^3J_{CF}$ = 12.0 Hz, $^1J_{CF}$ = 247.0 Hz, C, C4-Ar), 150.9 (CH, triaz), 148.55 (C, Ar), 145.44 (CH, triaz), 139.27 (C, Ar), 139.16 (C, Ar), 135.13 (C, Ar), 130.50 (dd, $^3J_{CF}$ = 6.2

Hz, $^3J_{CF}$ = 9.7 Hz, CH, C6-Ar), 130.18 (CH, Ar), 129.58 (CH, Ar), 129.24 (2 x CH, Ar), 127. 40 (CH, Ar), 126.17 (CH, Ar), 125.24 (dd, $^4J_{CF}$ = 3.6 Hz, $^2J_{CF}$ = 13.3 Hz, C, C1-Ar), 123.04 (q, $^1J_{CF3}$ = 256.2 Hz, C, CF_3), 121.99 (2 x CH, Ar), 111.18 (dd, $^4J_{CF}$ = 2.7 Hz, $^2J_{CF}$ = 20.6 Hz, CH, C5-Ar), 104.42 (t, $^2J_{CF}$ = 28.1 Hz, CH, C3-Ar), 75.65 (C-OH), 55.52 (CH_2-triaz), 47.20 (CH_2-NH_2).

HPLC: 97 %, RT = 4.79 min.

HRMS (ESI, m/z): theoretical mass: 519.1455 [M+H]$^+$, observed mass: 519.1453 [M+H]$^+$.

b. Biological evaluation:

1. Evaluation of chloro and dichloro compounds was performed at the Center for Cytochrome P450 Biodiversity, Swansea University Medical School by Dr. Josie Parker and Dr. Andrew Warrilow. MIC and K_d assays were performed as described in Chapter II (p 61 and 79).

A. CaCYP51 IC$_{50}$ determination:

C. albicans CYP51 was overexpressed in *E.coli* and purified.[144] CYP51 reconstitutions assays were performed.[145] The final reaction volume was 500 μL, containing; 1 μM *C. albicans* CYP51, 2 μM *Homo sapiens* cytochrome P450 reductase (CPR) (UniProtKB accession number P16435), 60 μM lanosterol, 50 μM dilaurylphosphatidylcholine, 4% w/v 2-hydroypropyl-cyclodextrin, 0.4 mg/mL isocitrate dehydrogenase, 25 mM trisodium isocitrate, 50 mM NaCl, 5 mM $MgCl_2$, and 40 mM MOPS (morpholinepropanesulfonic acid, pH 7.2). Antifungal compounds were added in 2.5 μL DMSO. The reaction was started by the addition of 4 mM NADPH-tetrasodium salt. Samples were shaken for 15 min at 37 °C and sterol metabolites extracted with ethyl acetate and derivatised with BSTFA.

2. The fluoro and difluoro derivatives were evaluated at the Division of Health Sciences, University of Otago in New Zealand. Assays were performed by Dr. Brian Monk, Dr. Mikhail Keniya and Dr. Yasmeen Ruma.

A. Disk diffusion assay:

The susceptibilities of *S. cerevisiaeas* and *Candida* species strains to azole compounds were observed as zones of growth inhibition in agarose diffusion assays.[131] The disk diffusion assays were carried out as described by Keniya et al.[135] Complete Supplement Mixture (CSM) agarose (0.6 % agarose [wt/vol]; 20 mL Synthetic defined medium (SD); pH 6.8-7) was solidified in a rectangular Petri dish which was overlaid with CSM agarose (0.6% [wt/vol]; 5 ml; pH 6.8-7) seeded with yeast cells at an optical density (OD$_{600}$) of 0.008 (118,000 cells per 1 mL of overlay). Then, azole compounds with a concentration of 10 nmol/disk were applied to sterile BBL paper disks (Becton Dickinson Co., Sparks, MD), which were then placed on the overlays. Cell growth was assessed after incubation at 30°C for 48 h.

B. MIC$_{80}$ determination for *S. cerevisiaeas* and *C. albicans* strains:

The MIC assay were carried out as described by Keniya et al.[133,135] MIC$_{80}$s for novel inhibitors, MCF and PCZ were determined in 96-well microtiter plates using SD buffered to pH 6.8 for S. cerevisiae constructs while pH 7 for *C. albicans*. Cells were seeded at an OD$_{600}$ of 0.005 (1.5 x 104 CFU), and the plates were incubated at 30°C with shaking at 200 rpm for 48 h for *S. cerevisiae* strains and 24 h for *C. albicans*. Cell growth was assessed by measuring the OD$_{600}$ using a Synergy 2 multimode plate reader (BioTek Instruments, VT, USA). Each MIC$_{80}$ was determined using triplicate measurements for pools of 4 clones of each strain, in three separate experiments.

Chapter V

(Triazole propanamide derivatives)

1. Introduction:

The promising biological results of the triazole hydroxy-propyl benzamide derivatives (chapter IV) encouraged us to design novel extended inhibitors similar to compound **57c** and **69** but without a hydroxyl group at the chiral center of the short arm. Removing the OH group may show good activity in *Candida* species that develop resistance from recognising azole compounds containing a hydroxyl group. A few modifications on compound **57c** and **69** were indicated (Figure 65):

1. The amide group with the CH_2 was reversed and the OH group replaced with a hydrogen in both compounds (**57c** and **69**) to explore the activity and binding affinity against CaCYP51.

2. Exploring different moieties at the phenyl ring located after the second amide linker for compound **57c** to explore additional binding interaction at the access channel. R could be EDG or EWG or no substitution.

3. Maintaining the substituted biphenyl ring (CF_3 and OCF_3) similar to compound **69**.
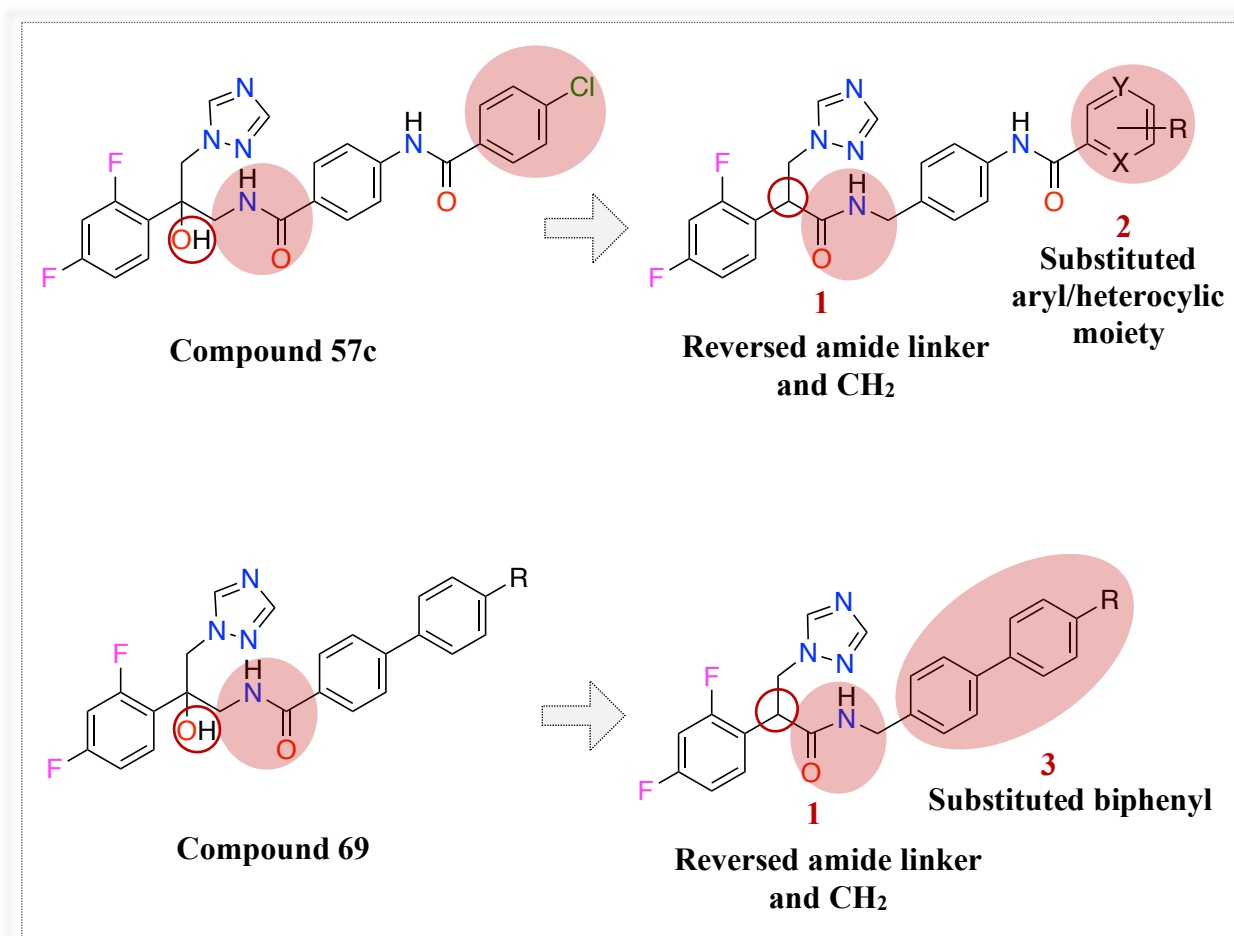
Figure 65: General structure of new series, triazole propanamide derivatives, after modification of compounds **57c** and **69**.

2. Results and discussion:

a. Computational studies (MD):

To perform the molecular dynamic simulation studies, the favourable pose of the protein-ligand complex was obtained from MOE, then subjected to 200 ns molecular dynamic simulations using the Desmond programe of Maestro. Of note, only MD data results are presented in this chapter owing to the more accurate data generated from MD simulations as both the CaCYP51 protein and the inhibitor can move during the simulation time to form a stable protein-ligand complex to identify key binding interactions with amino acid residues.

The binding profile of *para*-biphenyl (**80a-d**) and substituted amide (**85a-f**) derivatives in the wild-type were similar in forming a coordination interaction between the haem Fe^{3+} and the triazole N. Moreover, only the (*R*)-configuration was promising for amide compounds while both (*S*)- and (*R*)-configurations looked promising for biphenyl derivatives. All derivatives formed direct or indirect hydrogen bonding and hydrophobic interactions at the access channel as well as π-π stacking binding interactions with different amino acids such as His377, Met508, Ser378, Leu376, Tyr505 and Trp57.

Compound **80d** was used as an exemplar for *para*-biphenyl derivatives to illustrate binding interactions during the 200 ns simulation time. In the 2D ligand interactions, both enantiomers showed 100% binding interaction with the haem Fe^{3+} as well as more than 65% interaction with Tyr132 through a water molecule (Figure 66A). The 3D visualisation in MOE for the final frame demonstrated hydrophobic binding interactions with Met508, His377, Leu376, Ser378, Tyr64, Leu87 and Pro230 for both configurations while H-arene binding interaction with Met508 was observed for (*S*)-**80d** (Figure 66B). In addition, (*S*)- **80d** was shown to bind perpendicularly with the haem iron and the distance between the triazole nitrogen and the haem iron was 2.36 Å while (*R*)-**80d** was found to bind slightly sloped with a distance of 2.46 Å (Figure 66B). In Figure 67, the protein-ligand RMSD plot of (*S*)-**80d** and (*R*)-**80d** CaCYP51 complexes illustrated high stability of the complexes during the 200 ns simulation time.

A

2D-(*S*)-80d

2D-(*R*)-80d

Polar   Unspecified-residue   Glycine   Pi-Pi stacking

Hydrophobic   — Metal coordination   Water   Solvent exposure
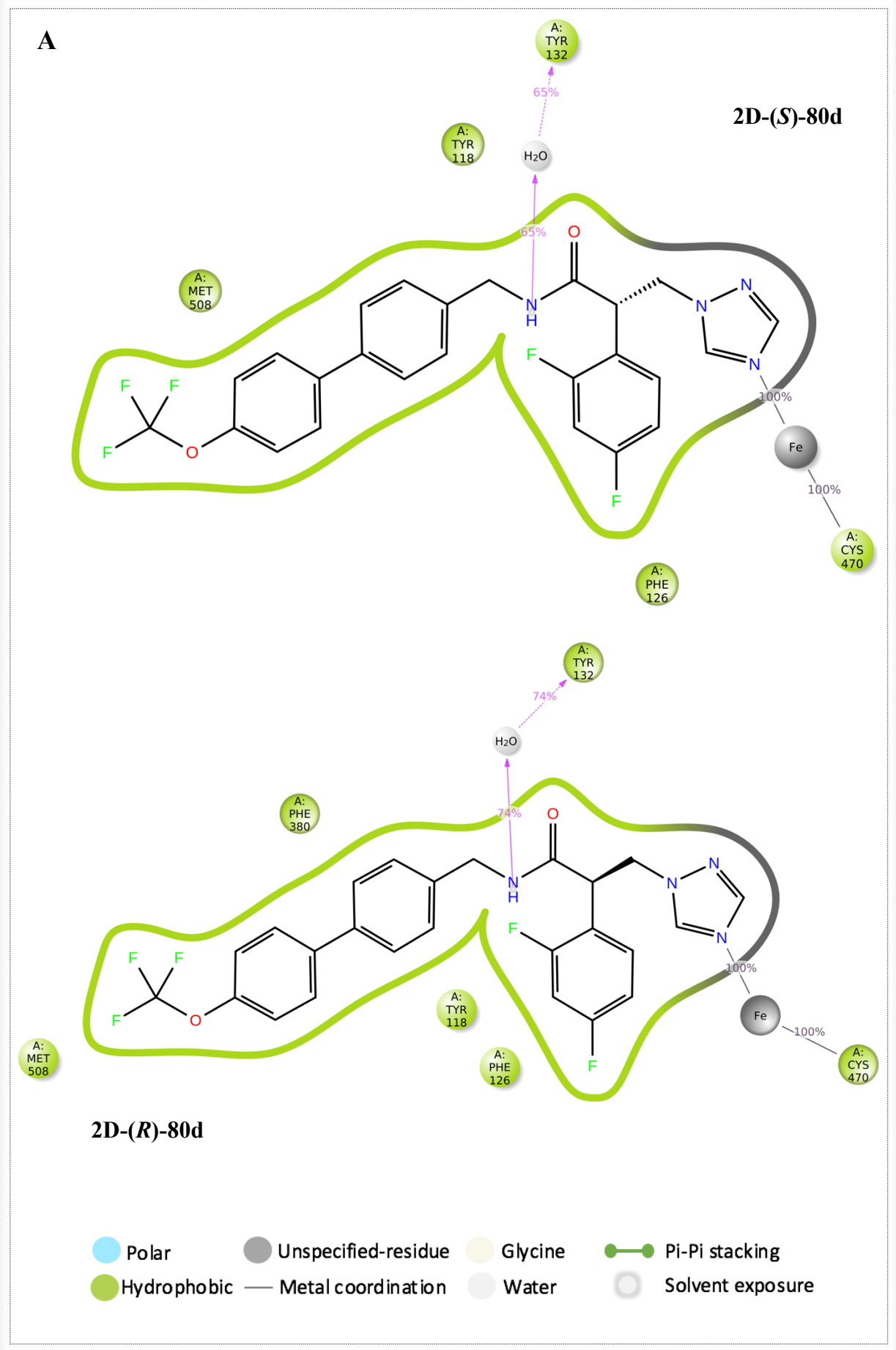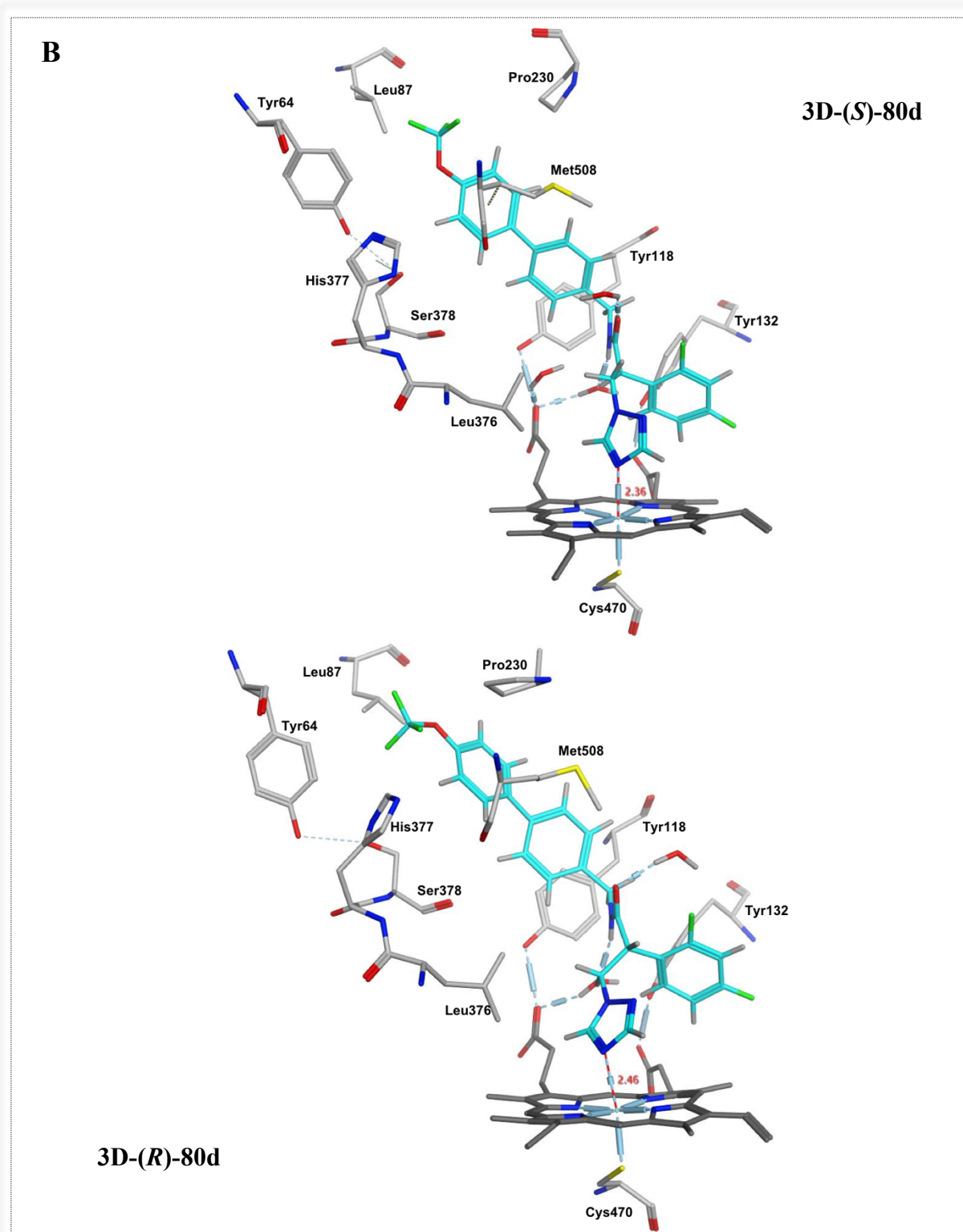
Figure 66: A) 2D of (*S*)-**80d** and (*R*)-**80d** interactions with CaCYP51 key residues. Interactions that occur more than 30.0% of the simulation time in the selected trajectory (0.00 through 200.00 ns are shown. **B**) 3D image illustrating binding between the N-atom of the triazole and the haem iron for (*S*)-**80d** and (*R*)-**80d**.
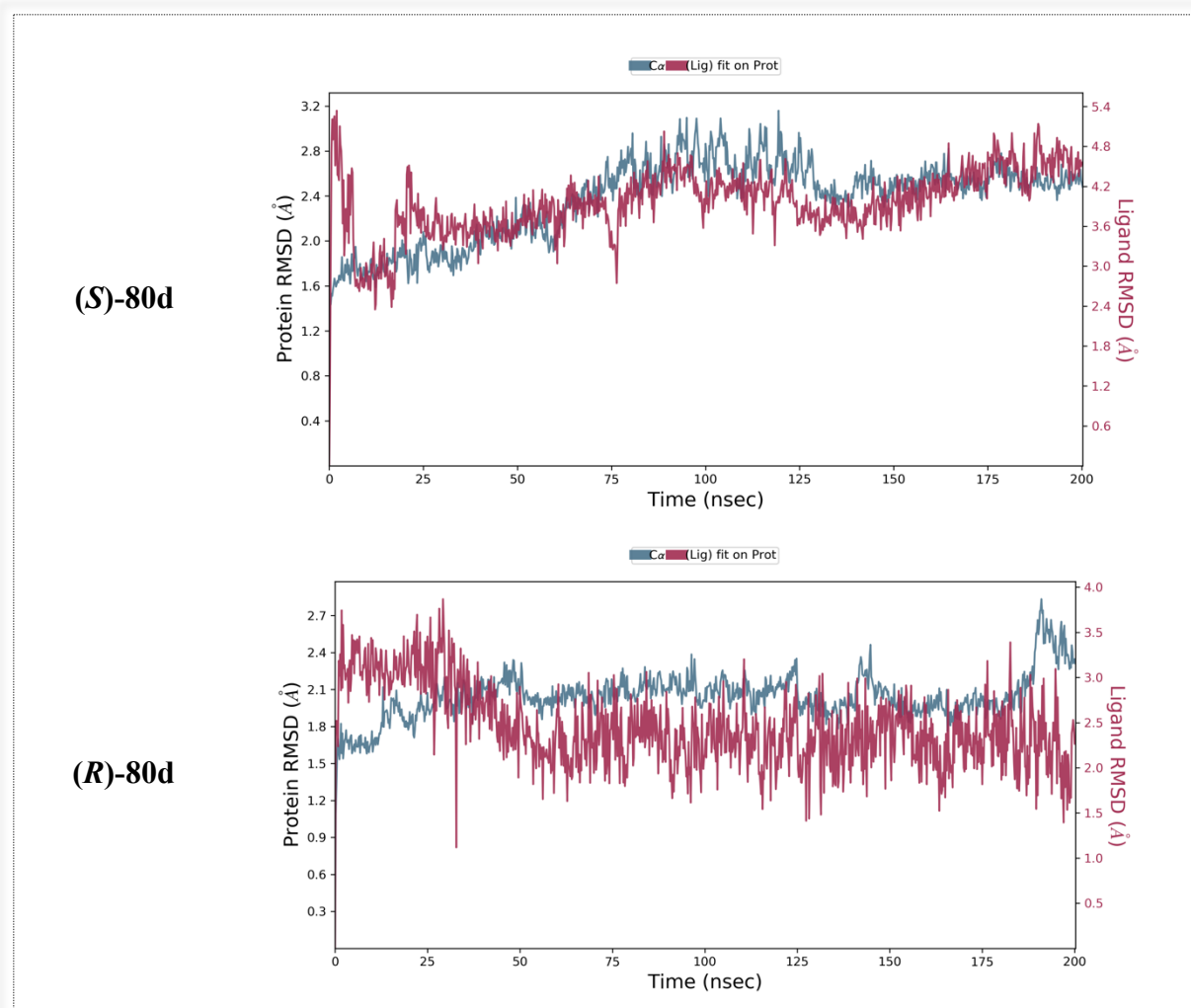
Figure 67: Protein-ligand RMSD of CaCYP51-(*S*)-**80d** and CaCYP51-(*R*)-**80d** complexes over 200 ns MD simulation.

An example of the amide derivatives was compound **85f** with a pyrazine substitution. The 2D ligand interactions showed 99% binding interaction with the haem Fe^{3+} as well as more than 53% direct H-bonding with Ser378 and $\geq$ 51% π-π stacking with Tyr118 and His377 for both configurations during the 200 ns simulation time. Only (*R*)-**85f** exhibited additional binding interaction through a water molecule with Tyr132 (65%) and Tyr505 (48%) during the simulation time as shown in Figure 68A. Moreover, the loss of direct binding with the heam iron was observed for the (*S*)-**85f** final frame in MOE and the triazole ring was positioned flat above the haem with a distance of 2.63 Å while (*R*)-**85f** was shown to bind perpendicularly with a distance of 2.67 Å (Figure 68B). Both configurations showed hydrophobic interactions with His37, Leu376 and Leu121 but (*R*)-**85f** formed water mediated H-bonding between the haem porphyrin and amide N as well as between the sp^2 of the pyrazine N and Tyr505. In addition, direct hydrogen bonding between the amide NH and Ser378 was observed for (*R*)-

85f as shown in Figure 68B. However, the MD for all amide derivatives (**85a-f**) was similar in which the (*R*)-configuration preserved the direct binding with Fe^{3+} during the 200 ns simulation time and had an advantage in binding interactions with different amino acids.
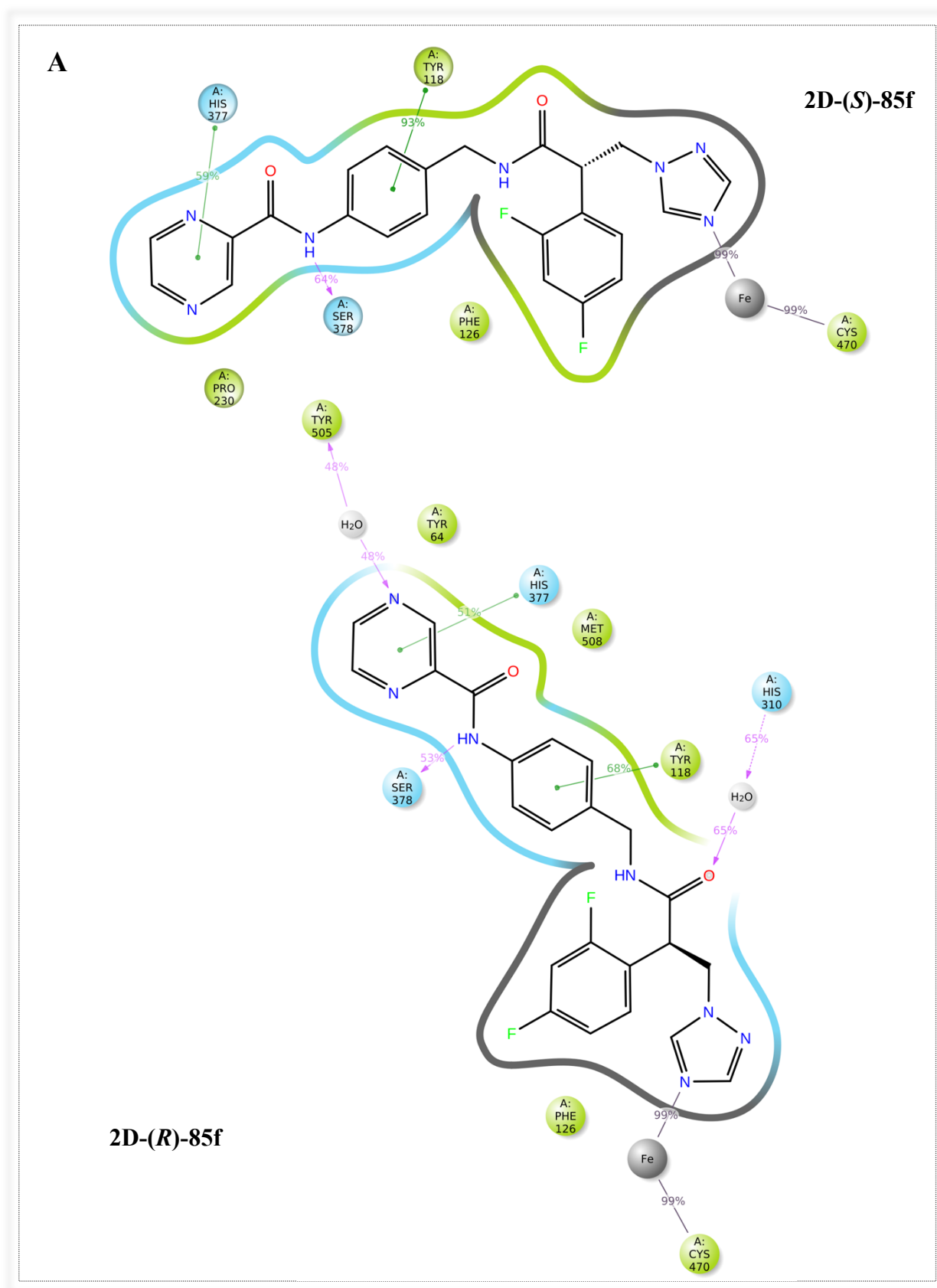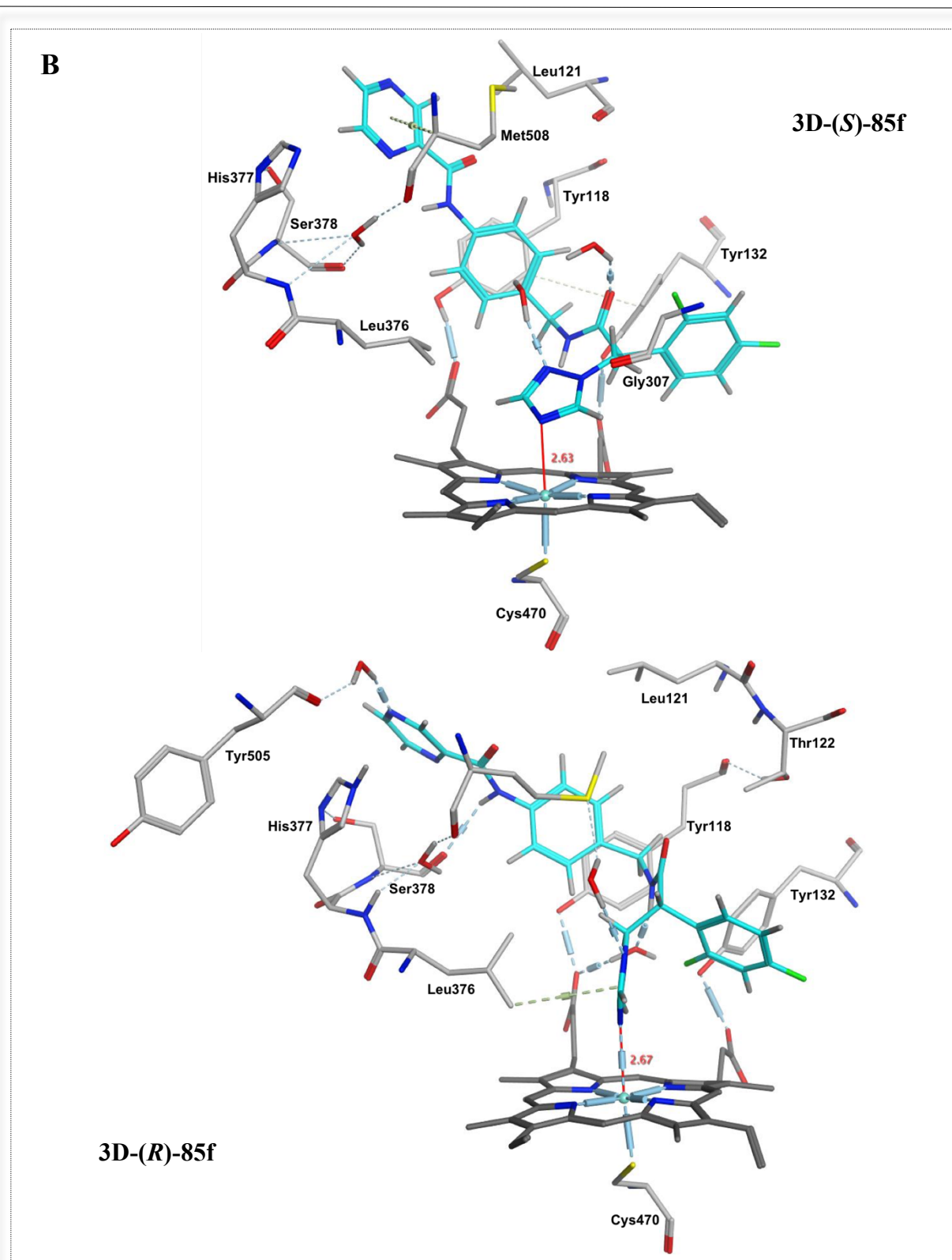
Figure 68: A) 2D of (*S*)-**85f** and (*R*)-**85f** interactions with CaCYP51 key residues. Interactions that occur more than 30.0% of the simulation time in the selected trajectory (0.00 through 200.00 ns are shown. **B)** 3D image illustrating binding between the N-atom of the triazole and the haem iron for (*S*)-**85f** and (*R*)-**85f**.

b. Chemistry:

To synthesise the novel triazole propanamide derivatives, two synthetic pathways were optimised to achieve the final compounds in good yields and high purity.

1. **First synthetic pathway:**

A few compounds of the triazole propanamide with the biphenyl nucleus were synthesised through six reaction steps (Scheme 11):

1.1. Esterification reaction.

1.2. Hydroxymethyl addition to α-carbon.

1.3. Mesylation reaction.

1.4. Nucleophilic substitution of triazole.

1.5. Ester hydrolysis.

1.6. Coupling reaction using CDI.
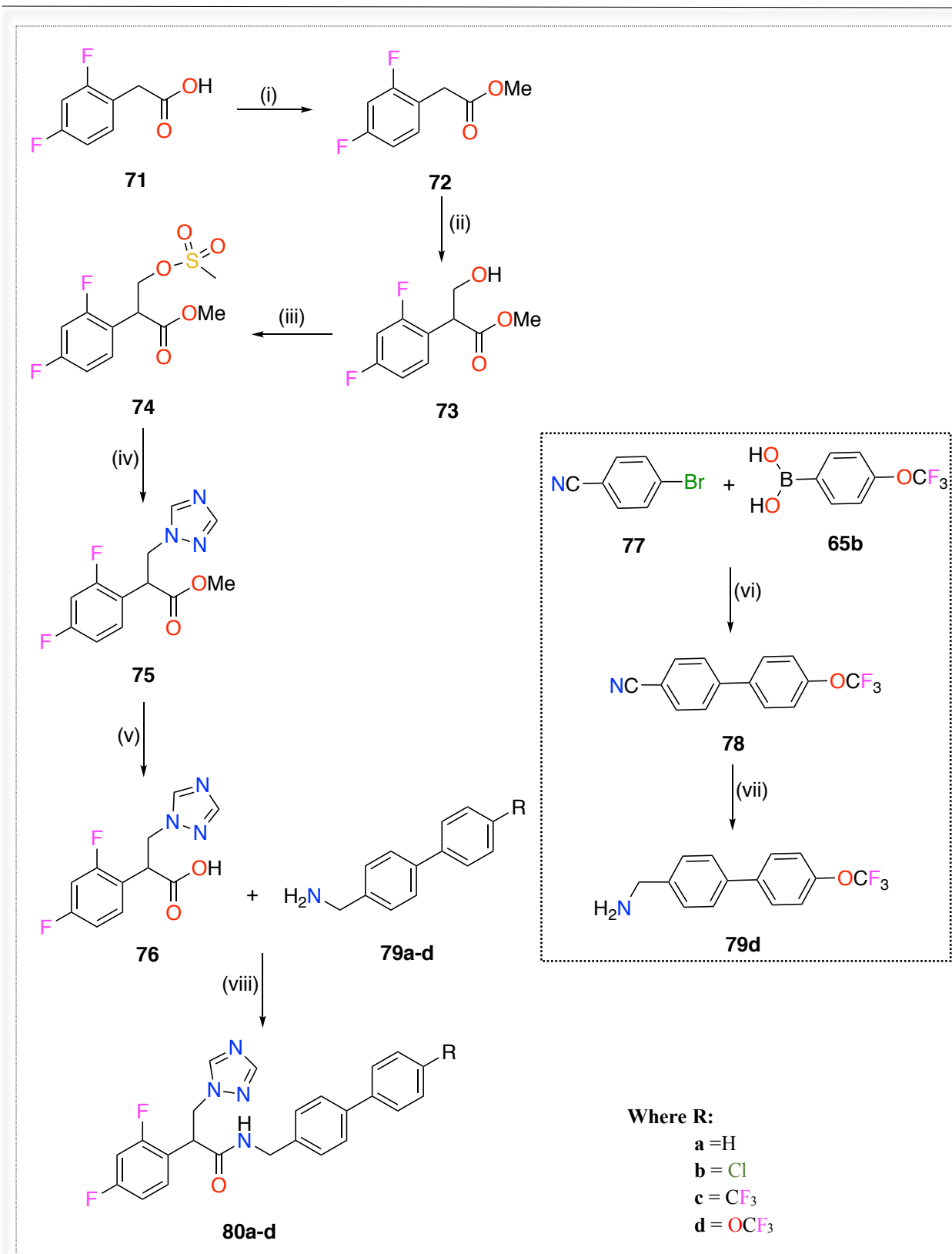
Scheme 11: *Reagents and conditions:* (**i**) SOCl₂, MeOH, 60 °C, 3 h (**ii**) DMSO, NaOCH₃, paraformaldehyde, r.t., 4 h (**iii**) CH₂Cl₂, Et₃N, CH₃SO₂Cl, r.t., o/n (**iv**) (a) CH₃CN, K₂CO₃, triazole, 45 °C, 1 h (b) 70 °C, o/n (**v**) THF, LiOH, r.t., 1 h (**vi**) Dioxane/H₂O, Pd(PPh₃), 104 °C, 6 h (**vii**) THF, LiAlH₄, 0 °C, 5 h (**viii**) DMF, CDI, r.t., o/n.

Synthesis of methyl 2-(2,4-difluorophenyl)acetate (72):

To synthesise methyl 2-(2,4-difluorophenyl)acetate (**72**), an esterification reaction was performed by reacting compound (**71**) with $SOCl_2$ in MeOH and the reaction heated at 60 °C for 3 h.[146] The reaction mechanism involved a nucleophilic attack of the OH lone pair of the carboxylic acid on the sulfur to form a good leaving group, which was displaced by MeOH to form the desired ester as shown in Figure 69. Compound (**72**) was confirmed by ^{1}H NMR and achieved in a good yield (91%) as a yellow oil
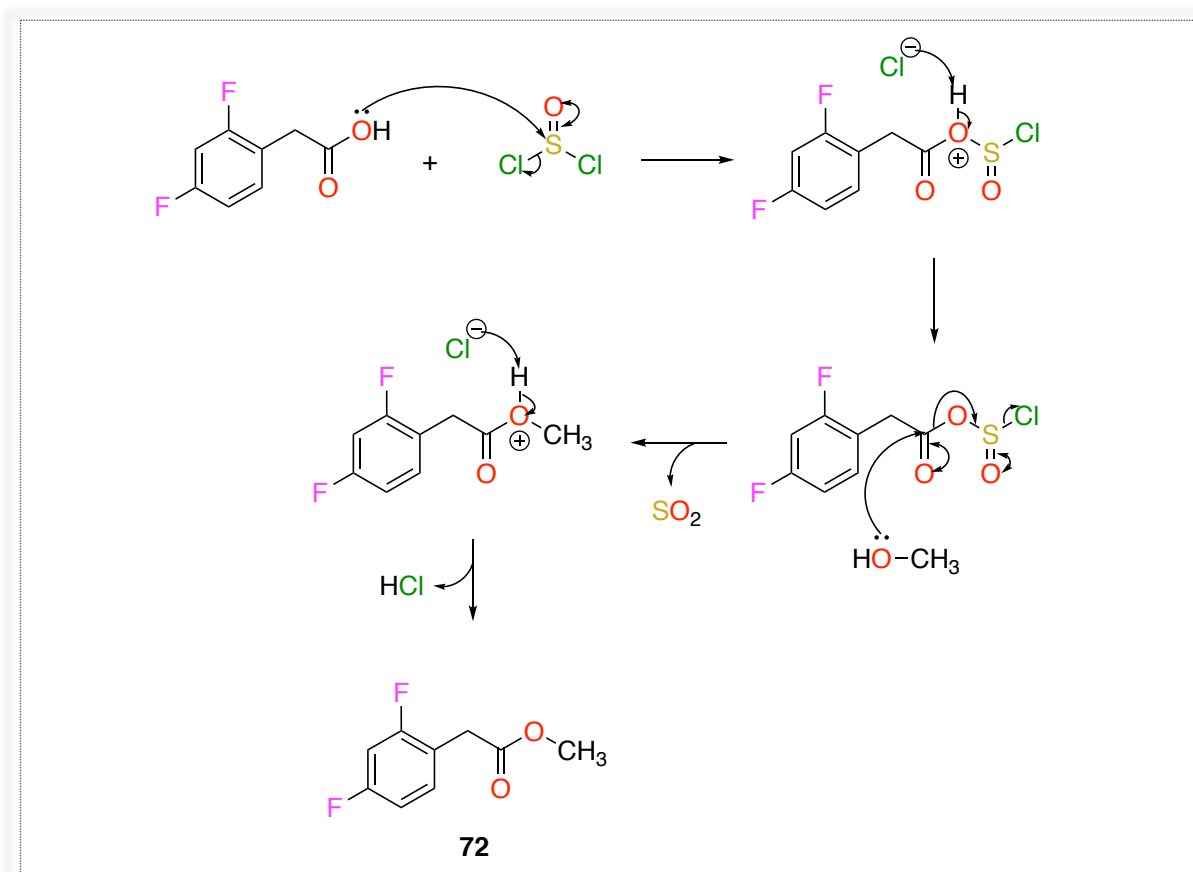
Figure 69: Esterification mechanism.

Synthesis of methyl 2-(2,4-difluorophenyl)-3-hydroxypropanoate (73):

The addition of hydroxymethyl to the α-carbon of compound (**72**) was achieved by adding sodium methoxide to a solution of methyl 2-(2,4-difluorophenyl) acetate (**72**) in dry DMSO at 0 °C, followed by paraformaldehyde and the reaction mixture was stirred at room temperature for 4 h.[147] The reaction mechanism involved a deprotonation of the acidic proton at the α-carbon by sodium methoxide, then the carbanion intermediate attacks the carbonyl C of the paraformaldehyde to add CH_2-OH moiety resulting in compound (**73**) as shown in Figure 70.
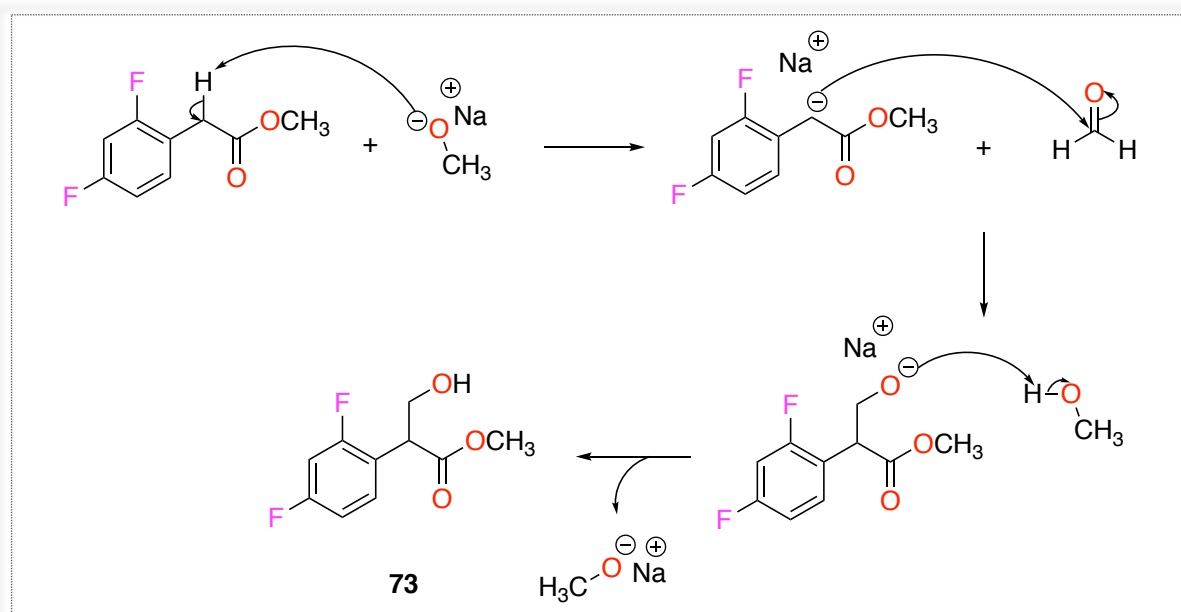
Figure 70: Reaction mechanism of hydroxy-methyl addition.

After workup, the residue was purified by gradient column chromatography and the desired oily product was obtained in a good yield (78%). To confirm synthesis of hydroxymethyl compound (**73**), ^{1}H and ^{13}C NMR was applied. In the ^{1}H NMR a triplet peak for OH appeared at δ 5.06 and two doublet of doublet peaks for each proton of CH$_2$ appeared at δ 3.98 and δ 3.93 as shown in Table 43. ^{13}C NMR confirmed the additional carbon of CH$_2$ which appeared at δ 62.29 as well as the CH carbon (δ 46.51).

Table 43: Yield and NMR data for compound (**73**)
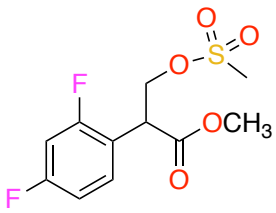
Compound (73)	
Structure	
Yield (%)	78
^{1}**H NMR (DMSO-d₆)**	δ 7.44 (q, J = 8.7 Hz, 1H, Ar), 7.23 (t, J = 10.6 Hz, 1H, Ar), 7.08 (t, J = 8.5 Hz, 1H, Ar), 5.06 (t, J = 5.5 Hz, 1H, OH-ex), 3.98 (dd, J = 7.4, 13.7 Hz, 1H, CH$_2$), 3.93 (dd, J = 4.7, 10.4 Hz, 1H, CH$_2$), 3.68 (m, 1H, CH), 3.62 (s, 3H, CH$_3$).

13C NMR (DMSO-d6)	δ 172.08 (C, C=O), 162.23 (dd, $^3J_{CF}$ = 12.6 Hz, $^1J_{CF}$ = 160.0 Hz, C, C2-Ar), 160.27 (dd, $^3J_{CF}$ = 12.2 Hz, $^1J_{CF}$ =161.8 Hz, C, C4-Ar), 131.32 (dd, $^3J_{CF}$ = 5.5 Hz, $^3J_{CF}$ = 9.62 Hz, CH, C6-Ar), 120. 61 (dd, $^4J_{CF}$ = 4.1 Hz, $^2J_{CF}$ =15.3 Hz, CH, C1-Ar), 112.00 (dd, $^4J_{CF}$ = 3.5 Hz, $^2J_{CF}$ = 21.0 Hz, CH, C5 -Ar), 104.27 (t, $^2J_{CF}$ = 26.7 Hz, CH, C3-Ar), 62.29 ($\underline{C}H_2$), 52.41($\underline{C}H_3$), 46.51 ($\underline{C}H$).

Synthesis of methyl 2-(2,4-difluorophenyl)-3-((methylsulfonyl)oxy)propanoate (74):

The alcoholic functional group in the previous compound (**73**) was converted into a good leaving group using methane sulfonyl chloride reagent (MsCl). The mesylated compound (**74**) was achieved by reacting compound (**73**) with MsCl in the presence of Et₃N. The reaction was stirred at 0 °C for 1 h then at room temperature overnight.[148] The product was purified by gradient column chromatography to yield 84 % as a colorless oily product (Table 44).

Table 44: Yield and R$_f$ of compound (**74**).

Compound	Structure	Yield (%)	TLC R$_f$*
74		84	0.55

*TLC eluent (petroleum ether-EtOAc 1:1 v/v).

Synthesis of methyl 2-(2,4-difluorophenyl)-3-(1*H*-1,2,4-triazol-1-yl)propanoate (75):

As mentioned previously in chapter II, the nucleophilic substitution reaction of the triazole was performed by reacting triazole with K₂CO₃ for 1 h at 45 ºC. After the mixture cooled to room temperature, methyl 2-(2,4-difluorophenyl)-3-((methylsulfonyl)oxy) propanoate (**74**) was added and heated at 70 ºC for 4 h then room temperature overnight. The product (**75**) was obtained as a yellow oil (yield 85%) after purification with column chromatography. Compound **75** was confirmed by ¹H NMR as two singlet peaks of the triazole CH appeared at δ 8.35 and 7.90 as shown in Figure 71.
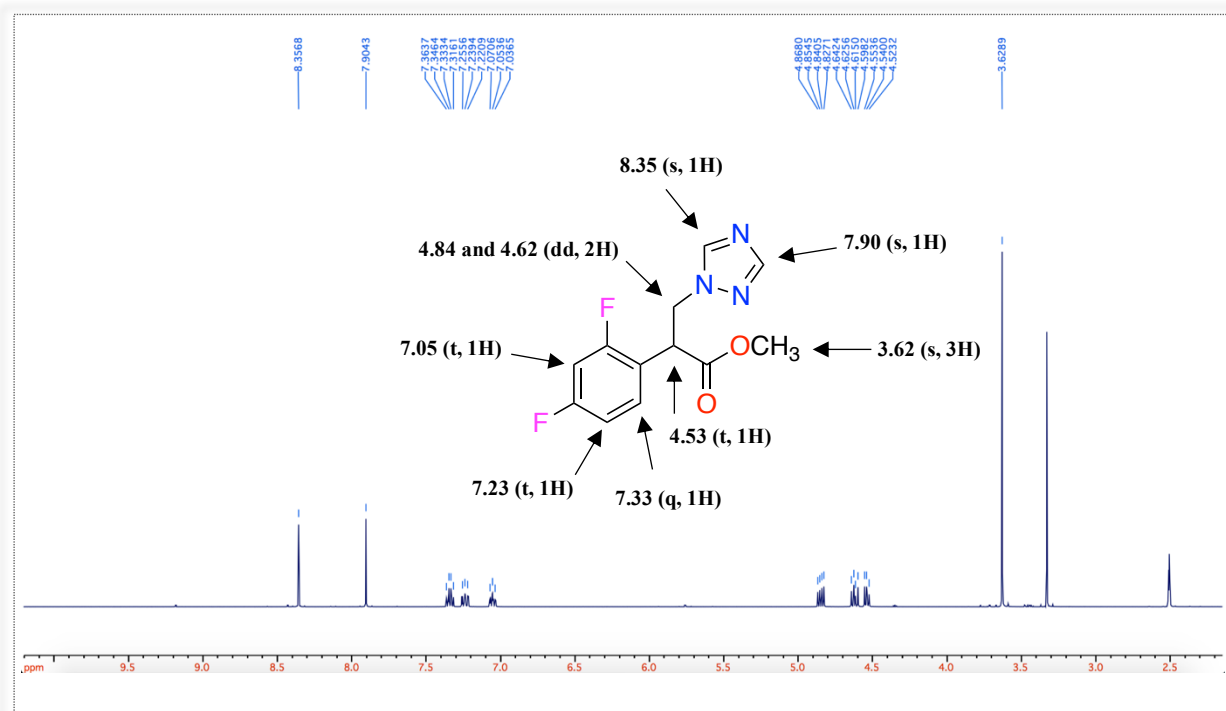
Figure 71: ^{1}H NMR (DMSO-d[6]/500 MHz) spectrum for compound **75**.

However, the synthesis of the tetrazole derivative from compound (**74**) was not successful as the alkene byproduct was formed with a yield of 85%. Formation of the alkene was not expected owing to the acidity of the tetrazole nucleus[149] as well as the presence of the mesylate good leaving group, but the resulting tetrazole anion could deprotonate the acidic proton at the α-carbon leading to the alkene byproduct (Figure 72).
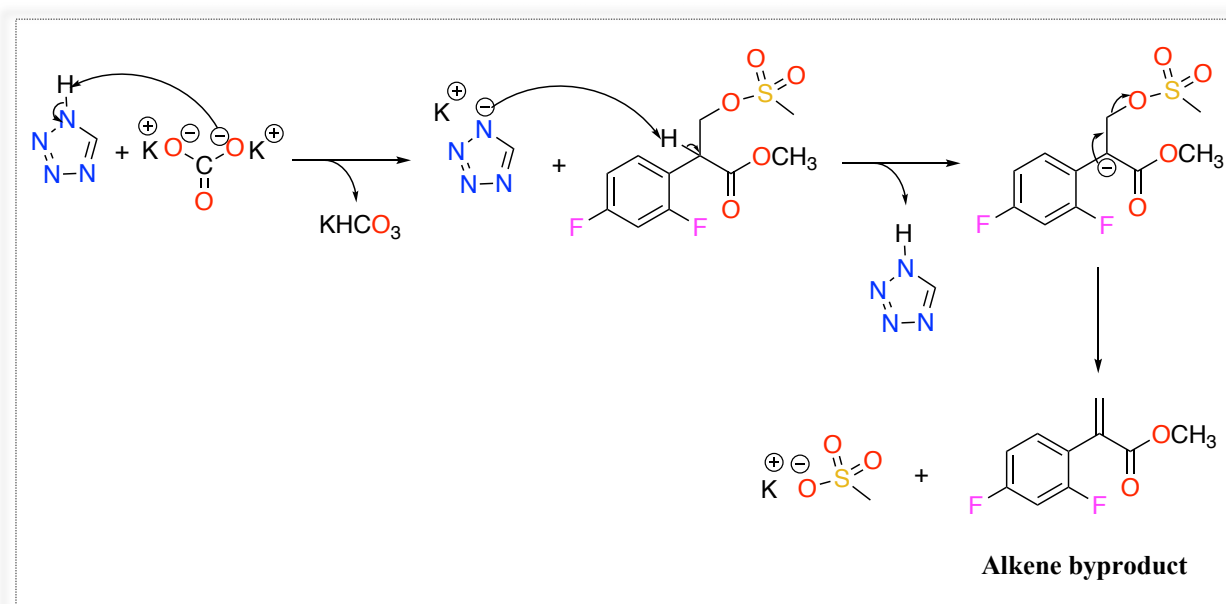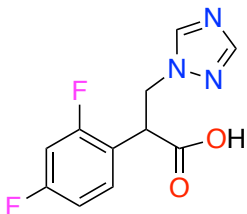
Figure 72: Proposed reaction mechanism of alkene byproduct formation.

Synthesis of 2-(2,4-difluorophenyl)-3-(1*H*-1,2,4-triazol-1-yl)propanoic acid (76):

The synthesis of 2-(2,4-difluorophenyl)-3-(1*H*-1,2,4-triazol-1-yl)propanoic acid (**76**) involved an ester hydrolysis by reacting compound **75** with lithium hydroxide monohydrate in H_2O at room temperature for 1 h. After workup, a white powder was achieved in good yield (Table 45).

Table 45: Yield and melting point (M.P.) of compound (**76**).
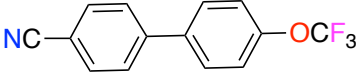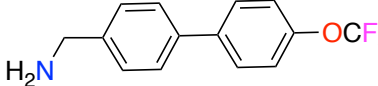
Compound	Structure	Yield (%)	M.P. (ºC)
76		73	193- 195

Synthesis of *N*-((4'-substituted-[1,1'-biphenyl]-4-yl)methyl)-2-(2,4-difluorophenyl)-3-(1*H*-1,2,4-triazol-1-yl)propanamide (80a-d):

The final compounds of the biphenyl derivative were attempted by activating the OH of compound **76** using CDI reagent as discussed in chapter IV for compound **46**. Then, the acylimidazole intermediate was reacted with the free amine of compound **79** to form the desired product (**80**).
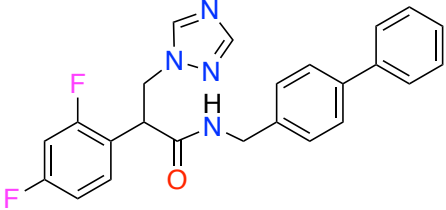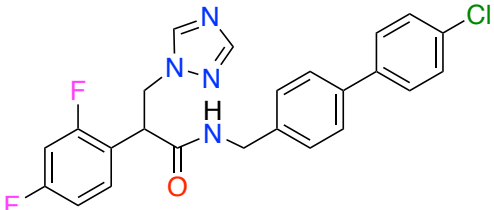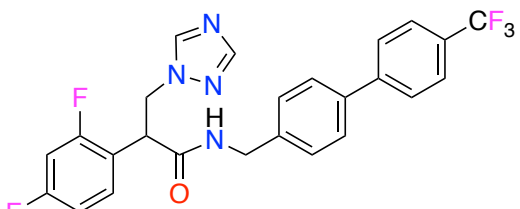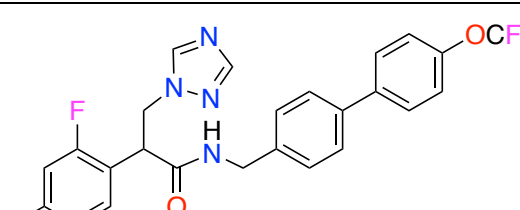
Compounds **79a-c** were commercially available, compound **79d** was prepared by two reaction steps. The first step was Suzuki coupling, as mentioned previously in chapter IV for compound **66**, in which 4-bromobenzonitrile (**77**) was reacted with 4-trifluromethoxyphenylboronic acid (**65b**) and 1 mol % Pd(PPh₃) in dioxane/H_2O in the presence of K_2CO_3 as a base.[150] The desired compound (**78**) was achieved in an excellent yield (93%) as a yellow solid (Table 46). The second step was a reduction of the nitrile functional group in compound (**78**) to the free amine derivative (**79d**), which was performed by adding LiALH₄ dropwise to a solution of compound **78** in THF at -40 ºC for 30 min, then the reaction mixture was left at 0 ºC for 5 h.[151] The crude white solid (approximately 83%) was used in the next step without further purification owing to difficulty in the purification as the compound has solubility issue.

Table 46: Compound (**78**) and (**79d**) chemistry.

Compound	Structure	Yield (%)	M.P. (ºC) (Lit. M.P.)
78	NC—◯—◯—OCF₃	93	53- 54 (51)[152]
79d	H₂N—◯—◯—OCF₃	83	-

The unsubstituted biphenyl derivative (**80a**) is not optimal for drug like properties owing to metabolic stability, however it was synthesised to confirm the reaction method. All biphenyl final compounds were confirmed by ^{1}H/^{13}C NMR and achieved in good yields with high purity as shown in Table 47.

Table 47: Yield and HPLC/EA purity of compound (**80a-d**).

Compound	Structure	Yield (%)	HPLC purity (%)/*EA
80a		66	100
80b		55	100
80c		54	100
80d		40	*EA: Anal. Calcd: C 59.76 %, H 3.81 %, N 11.15 %. Found: C 59.72 %, H 3.69 %, N 11.18 %.

*EA= Elemental analysis

2. Second synthetic pathway:

This synthetic pathway was applied to extend the novel compounds by a second amide linker in order to occupy the hydrophobic channel of wildtype/mutant CaCYP51 as well as to block the entrance of the natural substrate, which would hopefully circumvent resistance by forming additional binding interactions with different amino acids. To synthesise compounds **85a-f**, three reaction steps were involved starting from the carboxylic acid derivative (**76**) (Scheme 12):

1.7. Coupling reaction using tris(trifluoromethyl)borate.

1.8. Hydrogenation reaction using Pd/C catalyst.

1.9. Amide linker formation.

Where:
a/ Z= Cl, X=C, Y=C, R= Cl
b/ Z= Cl, X=C, Y=C, R= OCH₃
c/ Z= Cl, X= C, Y= C, R= CN
d/ Z= OH, X=C, Y=C, R= acetyl
e/ Z= Cl, X=H, Y=N, R= H
f/ Z= OH, X= N, Y=N, R= H
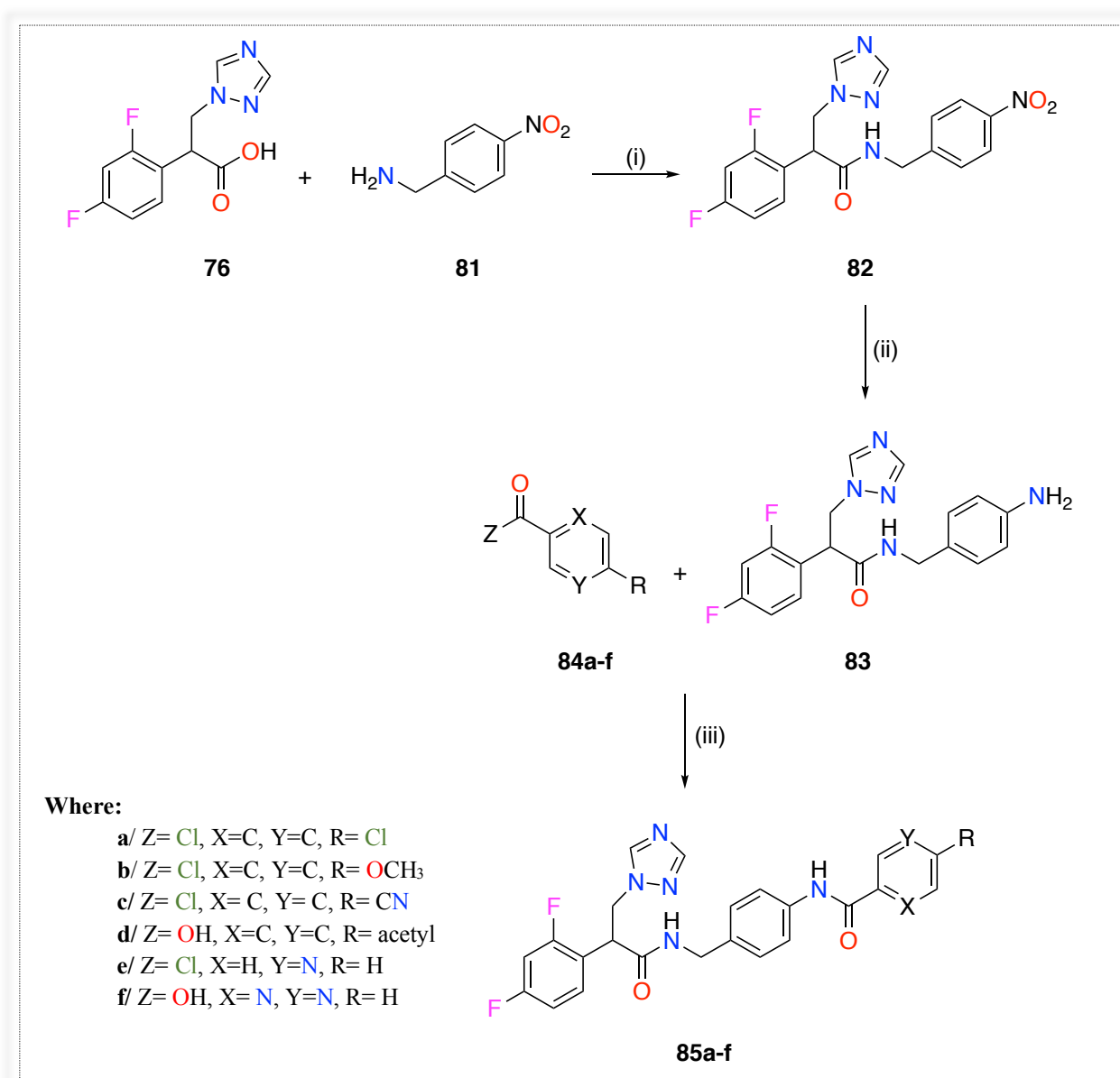
Scheme 12: *Reagents and conditions:* (**i**) CPME, B(OCH₂CF₃)₃, 100 °C, o/n (**ii**) H₂, Pd/C, MeOH, r.t., 3 h (**iii**) Pyridine, r.t., o/n.

Synthesis of 2-(2,4-difluorophenyl)-*N*-(4-nitrobenzyl)-3-(1*H*-1,2,4-triazol-1-yl) propenamide (82):

To synthesise 2-(2,4-difluorophenyl)-*N*-(4-nitrobenzyl)-3-(1*H*-1,2,4-triazol-1-yl) propenamide (**82**), an amidation reaction with CDI coupling reagent was first applied to achieve the desired product but unfortunately a complicated TLC was obtained. The second reagent was used tris(2,2,2-trifluoroethyl)borate (B(OCH$_2$CF$_3$)$_3$) in which the reagent was added to a solution of compound **76** and 4-nitrobenzylamine (**81**) in cyclopentyl methyl ether (CPME) and the mixture was stirred at 100 °C overnight.[153]

The reaction mechanism involved activation of the OH of compound **76** to form the borate leaving group, which can be displaced by the free amine of compound **81** to produce H$_2$O as a byproduct and the desired compound (**82**) (Figure 73).
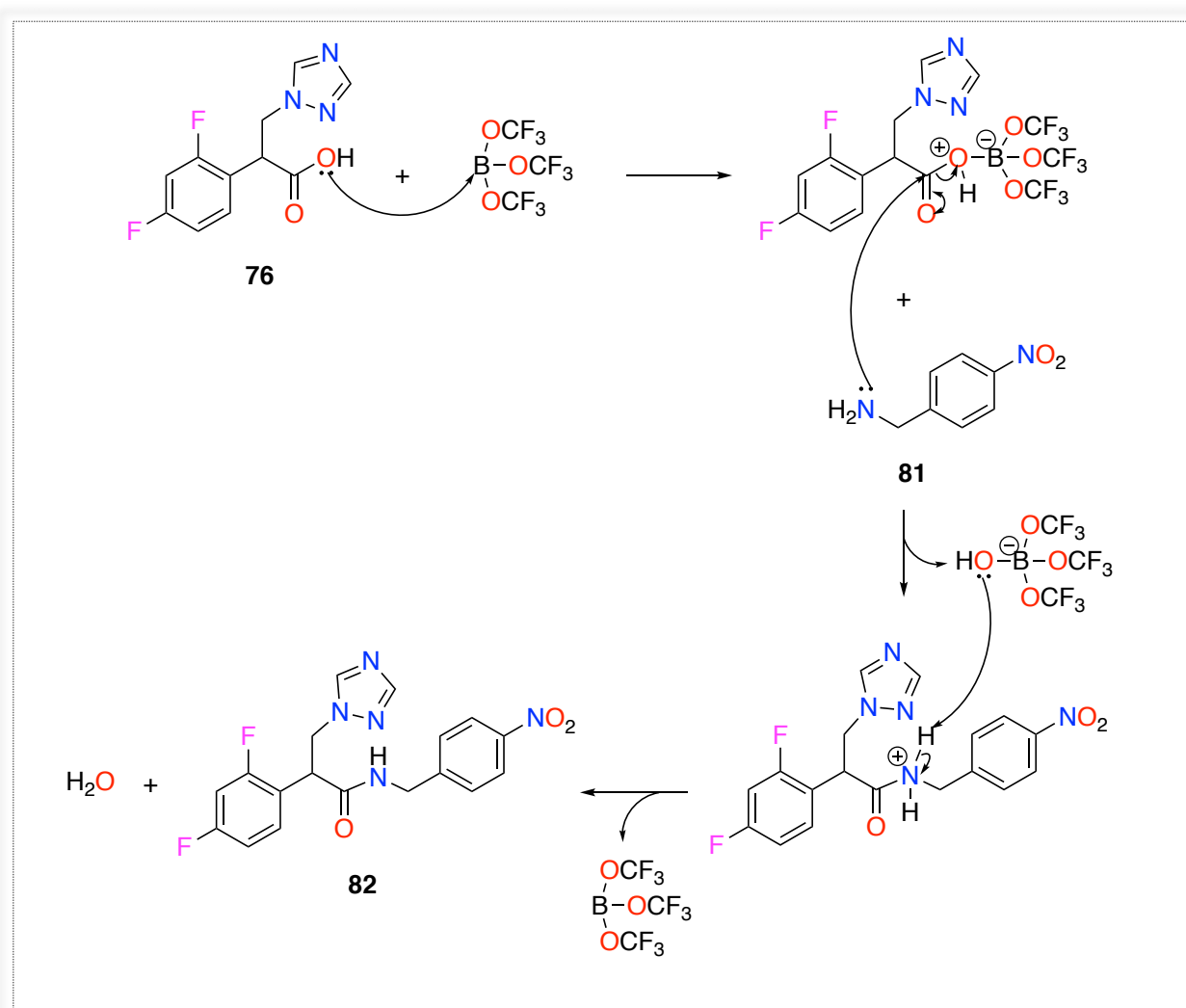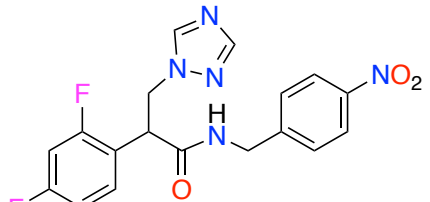
Figure 73: Amidation reaction mechanism.

A solid phase workup using resins was carried out by adding Amberlyst A-26(OH) (COOH scavenger), Amberlyst 15 (free amine scavenger) and Amberlite IRA743 (boron scavenger) together to the mixture and stirred for 30 min.[154] Then, the mixture was dried (MgSO$_4$), filtered to remove resins and MgSO$_4$, and the filtrate was concentrated *in vacuo*. The crude product was purified by gradient column chromatography to yield a faint yellow solid (Table 48).

Table 48: Chemistry of compound (**82**).

Compound	Structure	Yield (%)	M.P. (°C)
82		67	178- 180

Synthesis of *N*-(4-aminobenzyl)-2-(2,4-difluorophenyl)-3-(1*H*-1,2,4-triazol-1-yl) propenamide (83):
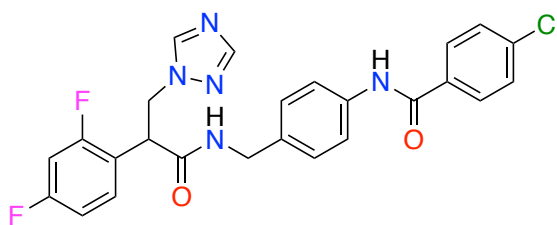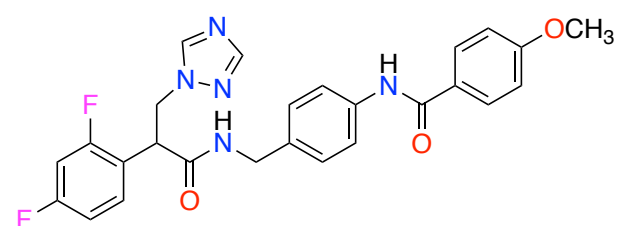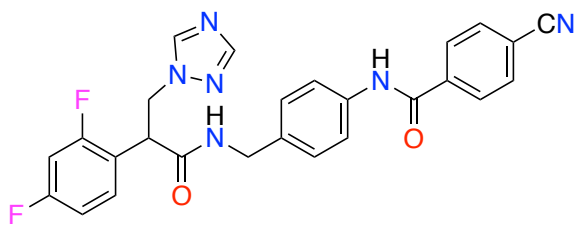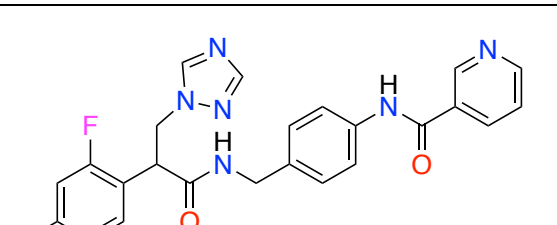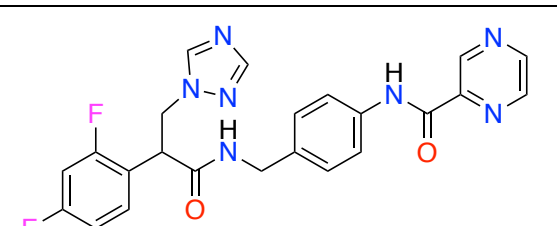
The nitro compound **82** was reduced by hydrogenation using Pd/C as described in chapter II for compound **8**. The free amine derivative **83** was confirmed by ¹H NMR (singlet for N<u>H</u>$_2$ at δ 4.92), and the desired product was achieved in an excellent yield (93 %) as a white solid.

Synthesis of substituted *N*-(4-((2-(2,4-difluorophenyl)-3-(1*H*-1,2,4-triazol-1-yl) propanamido)methyl)phenyl)benz/nicotin/pyrazin-amide (85):

The final compounds (**85a-f**) were synthesised by reacting compound **83** with the acid chloride derivatives (**84a-f**) in pyridine at room temperature overnight. An additional step before the amide coupling reaction was applied for compounds **85d** and **85f**, which was preparing the acid chloride derivative by adding SOCl$_2$ to a solution of the carboxylic acid compound (**84d** and **84f**) in CH$_2$Cl$_2$. Then, the reaction mixture was heated at 40 °C for 4 h and after evaporation used in the amide coupling step without further purifications.

All novel compounds were achieved in good yields after purification with column chromatography, as shown in Table 49, except compound **85d**. The purification was challenging and difficult as the TLC of the final compound (**85d**) was very complicated; moreover; the very low yield (12%) of the acetyl derivative (**85d**) could be owing to the stability of the acetyl derivative in the chlorination and coupling steps.

Table 49: Yields and HPLC purity of the final compounds (**85a-f**).

Compound	Structure	Yield (%)	HPLC purity (%)
85a		68	100
85b		72	100
85c		80	100
85d		12	100
85e		77	100
85f		68	100

c. Biological evaluation:

All novel compounds will be evaluated at the Division of Health Sciences, University of Otago in New Zealand. Assays will be performed by Drs. Brian Monk, Mikhail Keniya and Yasmeen Ruma. Same strategy of biological evaluations used in Chapter IV will be applied to this series.

3. Conclusion:

The non-hydroxy derivatives of the *para*-biphenyl (**80a-d**) and amide (**85a-f**) derivatives showed promising docking results but one favorable conformation was observed for amide derivatives. The synthesis of *para*-biphenyl derivatives (**80a-d**) was achieved with six reaction steps with an additional two steps for amide (**85a-f**) compounds. The acetyl derivative **85d** was obtained in very low yield (12%) owing to purification difficulties as well as stability issue with the chlorinated compound. However, all synthesised compounds were sent for biological evaluation at University of Otago in New Zealand. The biological results of the non-hydroxy derivatives against *C. albicans* wild-type and mutant strains as well as other *Candida* species will be compared with the hydroxy derivatives in chapter IV to provide a clear SAR for future design.

4. Experimental:

Computational docking and MD simulations were performed as described in Chapter II (p 61).

General method:

Methyl 2-(2,4-difluorophenyl) acetate (72)

($C_9H_8F_2O_2$, M.W.186.16)

(71) → **(72)**

Reagents: MeOH, $SOCl_2$, heat at 60 °C, 3h
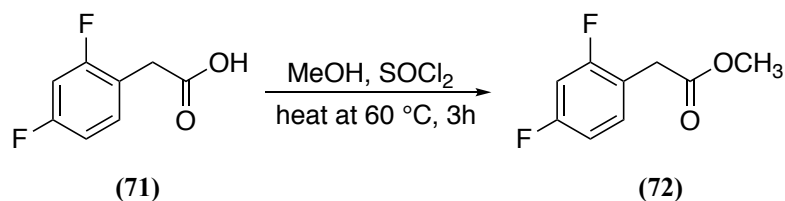
Method: To a colourless solution of 2-(2,4-difluorophenyl) acetic acid (**71**) (1.5g, 8.71mmol) in dry MeOH (15 mL) was added $SOCl_2$ (1.26 mL, 17.42 mmol) dropwise while cooling in an ice- bath. The mixture was heated to 60 °C for 3 h. After evaporation, the residue was dissolved in EtOAc (70 mL), washed with aqueous $NaHCO_3$ (3 x 35 mL), H_2O (3 x 35 mL) and brine (35 mL), dried ($MgSO_4$), and concentrated under vacuum to give the product that was used in the next step without further purification.

Yield: 1.48g (91 %) as a yellow oil.

Rf = 0.65 (petroleum ether-EtOAc 3:1 v/v).

^{1}H NMR (DMSO-d_6): δ 7.42 (dd, J = 8.7, 15.4 Hz, 1H, Ar), 7.23 (ddd, J = 2.6, 9.5, 10.3 Hz, 1H, Ar), 7.06 (ddd, J = 2.7, 8.5, 11.1 Hz, 1H, Ar), 3.73 (s, 2H, C$\underline{H}_2$), 3.63 (s, 3H, C$\underline{H}_3$).

^{19}F NMR (DMSO-d_6): δ -106.76 (*para*-F-Ar), -112.09 (*meta*-F-Ar).

Methyl 2-(2,4-difluorophenyl)-3-hydroxypropanoate (73)

($C_{10}H_{10}F_2O_3$, M.W. 216.18)

(72) → **(73)**

Reagents: DMSO, $NaOCH_3$, paraformaldehyde, room temp., overnight
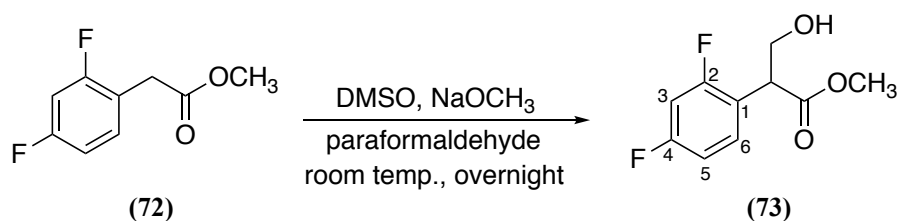
Method: To a stirred solution of methyl 2-(2,4-difluorophenyl) acetate (**72**) (1.39g, 7.46 mmol) in dry DMSO (20 mL) was added sodium methoxide (0.02g, 0.37 mmol) at 0 °C.

Paraformaldehyde (0.23g, 7.84 mmol) was then added and the reaction mixture was stirred at room temperature for 4 h. The reaction mixture was diluted with EtOAc (70 mL), washed with water (3 x 35 mL), brine (35 mL), dried (MgSO$_4$) and evaporated *in vacuo* to afford the crude product. The crude material was purified by gradient column chromatography eluting with petroleum ether-EtOAc 60:40 v/v.

Yield: 1.26g (78%) as colourless oil.

Rf = 0.5 (petroleum ether-EtOAc 1:1 v/v).

^{1}H NMR (DMSO-d$_6$): δ 7.44 (dd, J = 8.7, 15.3 Hz, 1H, Ar), 7.23 (ddd, J = 2.6, 9.3, 10.6 Hz, 1H, Ar), 7.08 (ddd, J = 2.7, 8.5, 10.0 Hz, 1H, Ar), 5.06 (t, J = 5.5 Hz, 1H, OH-ex), 3.98 (dd, J = 7.4, 13.7 Hz, 1H, C*Ha*Hb), 3.93 (dd, J = 6.0, 10.4 Hz, 1H, CHa*Hb*), 3.70- 3.66 (m, 1H, C$\underline{H}$), 3.62 (s, 3H, C$\underline{H_3}$).

^{13}C NMR (DMSO-d$_6$): δ 172.08 (C, C=O), 162.23 (dd, $^3J_{CF}$ = 12.6 Hz, $^1J_{CF}$ = 160.0 Hz, C, C2-Ar), 160.27 (dd, $^3J_{CF}$ = 12.2 Hz, $^1J_{CF}$ = 161.8 Hz, C, C4-Ar), 131.32 (dd, $^3J_{CF}$ = 5.5 Hz, $^3J_{CF}$ = 9.6 Hz, CH, C6-Ar), 120. 61 (dd, $^4J_{CF}$ = 4.1 Hz, $^2J_{CF}$ = 15.3 Hz, CH, C1-Ar), 112.00 (dd, $^4J_{CF}$ = 3.5 Hz, $^2J_{CF}$ = 21.0 Hz, CH, C5-Ar), 104.27 (t, $^2J_{CF}$ = 26.7 Hz, CH, C3-Ar), 62.29 ($\underline{C}$H$_2$), 52.41($\underline{C}$H$_3$), 46.51 ($\underline{C}$H).

HPLC (Method A): 100 %, RT = 4.23 min.

HRMS (ESI, m/z): theoretical mass: 239.0495 [M+Na]$^+$, observed mass: 239.0499 [M+Na]$^+$.

Methyl 2-(2,4-difluorophenyl)-3-((methylsulfonyl)oxy) propanoate (74)
(C$_{11}$H$_{12}$F$_2$O$_5$S, M. W. 294.27)
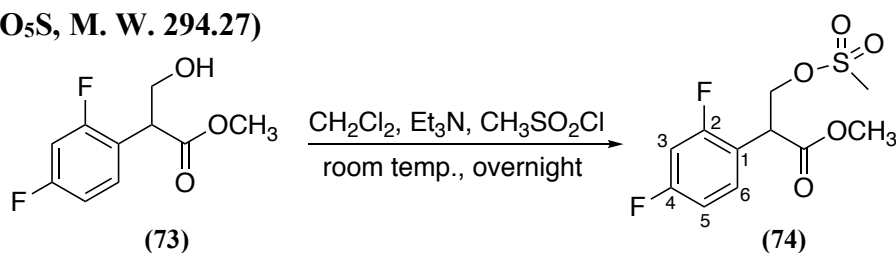
Method: To an ice-cooled suspension of methyl 2-(2,4-difluorophenyl)-3-hydroxypropanoate (**73**) (2.94g, 13.59 mmoL) in dry CH$_2$Cl$_2$ (25 mL), was added Et$_3$N (2.84 mL, 20.39 mmoL) followed by methane sulfonyl chloride (2.63 mL, 33.99 mmoL) dropwise. The reaction was stirred at 0 °C for 1 h then at room temperature overnight. After evaporation, the reaction was diluted with EtOAc (100 mL), washed with H$_2$O (2 x 50 mL), dried (MgSO$_4$) and evaporated under vacuum. The product was purified by gradient column chromatography and the desired product was eluted with 40 % EtOAc in petroleum ether.

Yield: 3.39g (84%) as a colourless oil.

Rf = 0.55 (petroleum ether-EtOAc 1:1 v/v).

^{1}H NMR (DMSO-d$_6$): δ 7.48 (dd, J = 8.7, 15.3 Hz, 1H, Ar), 7.31 (ddd, J = 2.5, 9.4, 10.6 Hz, 1H, Ar), 7.13 (ddd, J = 2.6, 8.5, 10.2 Hz, 1H, Ar), 4.70 (dd, J = 6.8, 10.1 Hz, 1H, C*Ha*Hb), 4.50 (dd, J = 7.0, 10.1 Hz, 1H, CHa*Hb*), 4.41 (t, J = 6.9 Hz, 1H, C<u>H</u>), 3.66 (s, 3H, OC<u>H</u>$_3$), 3.16 (s, 3H, C<u>H</u>$_3$).

^{13}C NMR (DMSO-d$_6$): δ 170.34 (C, C=O), 162.57 (dd, $^3J_{CF}$ = 12.6 Hz, $^1J_{CF}$ = 206.7 Hz, C, C2-Ar), 160.60 (dd, $^3J_{CF}$ = 12.6 Hz, $^1J_{CF}$ = 207.9 Hz, C, C4-Ar), 131.94 (dd, $^3J_{CF}$ = 5.3 Hz, $^3J_{CF}$ = 9.63 Hz, CH, C6-Ar), 118.88 (dd, $^4J_{CF}$ = 3.7 Hz, $^2J_{CF}$ = 15.1 Hz, CH, C1-Ar), 112.40 (dd, $^4J_{CF}$ = 3.5 Hz, $^2J_{CF}$ = 21.2 Hz, CH, C5-Ar), 104.71 (t, $^2J_{CF}$ = 26.2 Hz, CH, C3-Ar), 69.10 (<u>C</u>H$_2$), 52.96 (O<u>C</u>H$_3$), 43.56 (<u>C</u>H), 37.03 (<u>C</u>H$_3$).

HPLC (Method A): 92.57 %, RT = 4.29 min.

HRMS (ESI, m/z): theoretical mass: 317.0271 [M+Na]$^+$, observed mass: 317.0269 [M+Na]$^+$.

Methyl 2-(2,4-difluorophenyl)-3-(1*H*-1,2,4-triazol-1-yl) propanoate (75)
(C$_{12}$H$_{11}$F$_2$N$_3$O$_2$, M. W. 267.24)
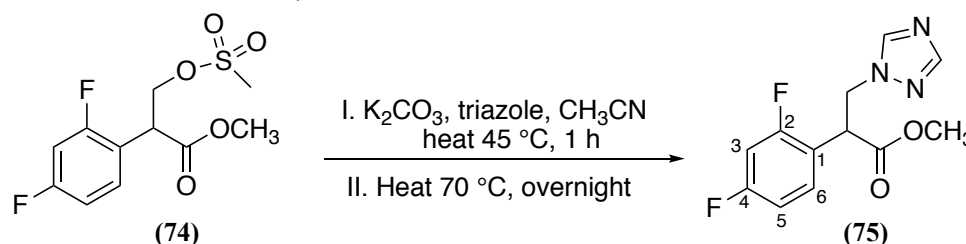
Method: To a stirred solution of triazole (0.17g, 2.54 mmoL) in dry CH$_3$CN (2 mL) was added K$_2$CO$_3$ (0.35g, 2.54 mmoL), and the mixture was heated for 1 h at 45 °C. After coolin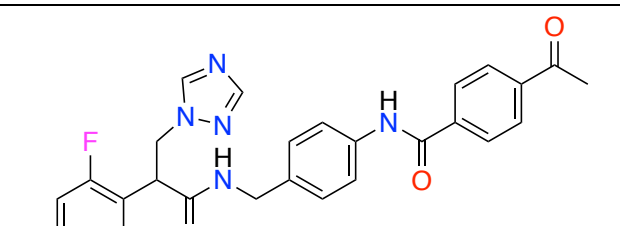g to room temperature, methyl 2-(2,4-difluorophenyl)-3-((methylsulfonyl)oxy) propanoate (**74**) (0.5g, 1.69 mmoL) was added and the reaction was heated at 70 °C for 4 h then stirred at room temperature overnight. The solvent was evaporated under vacuum and the residue was extracted with EtOAc (50 mL), washed with brine (3 x 25 mL) and H$_2$O (3 x 25 mL). The organic layer was dried (MgSO$_4$) and evaporated under vacuum to give the crude product, which was purified by gradient column chromatography and the desired product was eluted with 2 % MeOH in CH$_2$Cl$_2$.

Yield: 0.38g (85%) as a yellow oil.

R*f* = 0.52 (CH$_2$Cl$_2$-MeOH 9.5:0.5 v/v).

^{1}H NMR (DMSO-d$_6$): δ 8.35 (s, 1H, triaz), 7.90 (s, 1H, triaz), 7.33 (dd, J = 8.7, 15.2 Hz, 1H, Ar), 7.23 (ddd, J = 2.7, 9.3, 10.8 Hz, 1H, Ar), 7.05 (ddd, J = 2.7, 8.5, 10.0 Hz, 1H, Ar), 4.84 (dd, J = 6.8, 13.7 Hz, 1H, C*Ha*Hb), 4.62 (dd, J = 8.4, 13.7 Hz, 1H, CHa*Hb*), 4.53 (t, J = 6.8 Hz, 1H, C<u>H</u>), 3.62 (s, 3H, OC<u>H</u>$_3$).

^{13}C NMR (DMSO-d$_6$): δ 170.93 (C, C=O), 162.47 (dd, $^3J_{CF}$ = 12.1 Hz, $^1J_{CF}$ = 198.9 Hz, C, C2-Ar), 160.50 (dd, $^3J_{CF}$ = 12.2 Hz, $^1J_{CF}$ = 200.1 Hz, C, C4-Ar), 152.01 (CH, triaz), 145.07 (CH, triaz), 131.77 (dd, $^3J_{CF}$ = 5.4 Hz, $^3J_{CF}$ = 9.57 Hz, CH, C6-Ar), 119.48 (dd, $^4J_{CF}$ = 3.7 Hz, $^2J_{CF}$ = 15.0 Hz, CH, C1-Ar), 112.28 (dd, $^4J_{CF}$ = 3.6 Hz, $^2J_{CF}$ = 21.1 Hz, CH, C5-Ar), 104.48 (t, $^2J_{CF}$ = 26.2 Hz, CH, C3-Ar), 52.91 (CH$_3$), 49.47 (CH$_2$), 44.37 (CH).

HPLC (Method A): 100 %, RT = 4.20 min.

HRMS (ESI, m/z): theoretical mass: 268.0897 [M+H]$^+$, observed mass: 268.0903 [M+H]$^+$.

2-(2,4-Difluorophenyl)-3-(1H-1,2,4-triazol-1-yl) propanoic acid (76)

(C$_{11}$H$_9$F$_2$N$_3$O$_2$, M.W. 253.21)
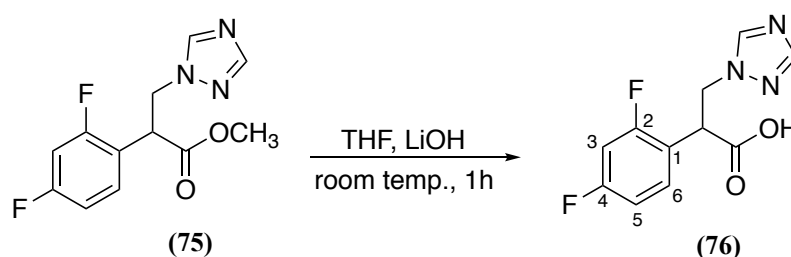
(75)   THF, LiOH / room temp., 1h   **(76)**

Method: To a stirred solution of methyl 2-(2,4-difluorophenyl)-3-(1H-1,2,4-triazol-1-yl) propanoate (**75**) (0.7g, 2.65 mmoL) in dry THF (8 mL) was added a solution of LiOH . H$_2$O (0.28g, 6.62 mmoL) in H$_2$O (2.4 mL) dropwise at 0 °C and the resulting mixture stirred at room temperature for 1 h. The reaction mixture was acidified (pH 3) with 2N aqueous HCl and extracted with EtOAc (3 x 50 mL). The combined organic layers were washed with brine (3 x 25 mL), water (25 mL), dried (MgSO$_4$) and evaporated under vacuum to give a white powder which was washed with Et$_2$O.

Yield: 0.49g (73%) as a white solid.

m.p.: 193-195 °C

Rf = 0.12 (CH$_2$Cl$_2$-MeOH 9.5:0.5 v/v).

^{1}H NMR (DMSO-d$_6$): δ 13.02 (brs, 1H, OH), 8.35 (s, 1H, triaz), 7.90 (s, 1H, triaz), 7.34 (dd, J = 8.6, 15.1 Hz, 1H, Ar), 7.22 (ddd, J = 2.6, 9.4, 10.5 Hz, 1H, Ar), 7.04 (ddd, J = 2.5, 8.5, 10.9 Hz, 1H, Ar), 4.81 (dd, J = 6.8, 13.7 Hz, 1H, C*Ha*Hb), 4.55 (dd, J = 8.5, 13.7 Hz, 1H, CHa*Hb*), 4.42 (t, J = 8.4 Hz, 1H, CH).

^{13}C NMR (DMSO-d$_6$): δ 171.89 (C, C=O), 162.42 (dd, $^3J_{CF}$ = 12.2 Hz, $^1J_{CF}$ = 172.8 Hz, C, C2-Ar), 160.45 (dd, $^3J_{CF}$ = 12.6 Hz, $^1J_{CF}$ = 174.5 Hz, C, C4-Ar), 151.93 (CH, triaz), 144.99 (CH, triaz), 131.64 (dd, $^3J_{CF}$ = 5.5 Hz, $^3J_{CF}$ = 9.6 Hz, CH, C6-Ar), 120.15 (dd, $^4J_{CF}$ = 3.7 Hz, $^2J_{CF}$ =15.1 Hz, CH, C1-Ar), 112.14 (dd, $^4J_{CF}$ = 3.5 Hz, $^2J_{CF}$ = 21.4 Hz, CH, C5-Ar), 104.49 (t,

$^2J_{CF}$ = 26.1 Hz, CH, C3-Ar), 49.66 (CH$_2$), 44.63 (CH).

HPLC (Method A): 100 %, RT = 3.97 min.

HRMS (ESI, m/z): theoretical mass: 254.0741 [M+H]$^+$, observed mass: 254.0740 [M+H]$^+$.

N-([1,1'-biphenyl]-4-ylmethyl)-2-(2,4-difluorophenyl)-3-(1H-1,2,4-triazol-1-yl) propenamide (80a)

(C$_{24}$H$_{20}$F$_2$N$_4$O, M. W. 418.45)
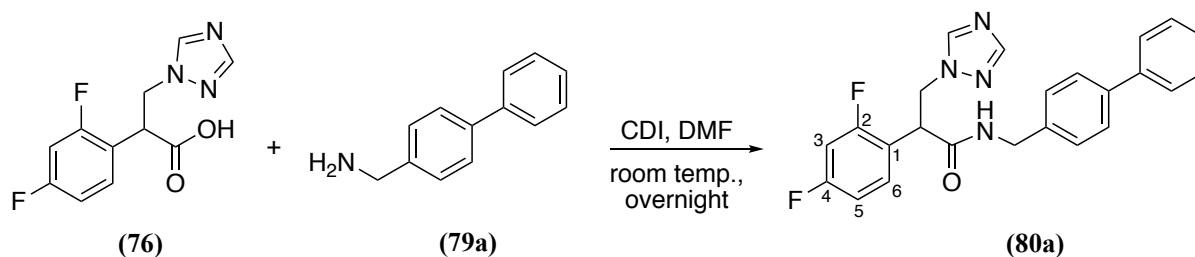
(76)   (79a)   (80a)

Method: Chapter IV compound **46**.

Reagents: 2-(2,4-difluorophenyl)-3-(1H-1,2,4-triazol-1-yl)propanoic acid (**76**) (0.15g, 0.59 mmol) and [1,1'-biphenyl]-4-yl-methanamine (**79a**) (0.13g, 0.71 mmol). The residue was purified by gradient column chromatography and the desired compound eluted with 2.5 % MeOH in CH$_2$Cl$_2$.

Yield: 0.16g (66 %) as a white solid.

m.p.: 194-195 °C

Rf = 0.37 (CH$_2$Cl$_2$-MeOH 9.5:0.5 v/v).

^{1}H NMR (DMSO-d$_6$): δ 8.77 (t, J = 5.9 Hz, 1H, NH), 8.35 (s, 1H, triaz), 7.98 (s, 1H, triaz), 7.63 (d, J = 7.2 Hz, 2H, Ar), 7.58 (dd, J = 8.7, 15.3 Hz, 1H, Ar), 7.54 (d, J = 8.4 Hz, 2H, Ar), 7.45 (t, J = 7.3 Hz, 2H, Ar), 7.35 (ttt, J = 1.2, 1.7, 1.3 Hz, 1H, Ar), 7.23 (ddd, J = 2.6, 9.3, 10.4 Hz, 1H, Ar), 7.12 (d, J = 8.5 Hz, 2H, Ar), 7.11 (ddd, J = 2.5, 8.4, 10.9 Hz, 1H, Ar), 4.81 (dd, J = 7.8, 12.7 Hz, 1H, CHaHb-triaz), 4.52-4.44 (m, 2H, CHCHaHb-triaz), 4.31 (dd, J = 6.2, 15.4 Hz, 1H, CHaHb-NH), 4.20 (dd, J = 5.6, 15.4 Hz, 1H, CHaHb-NH).

^{13}C NMR (DMSO-d$_6$): δ 169.60 (C, C=O), 162.29 (dd, $^3J_{CF}$ = 12.2 Hz, $^1J_{CF}$ = 189.9 Hz, C, C2-Ar), 160.32 (dd, $^3J_{CF}$ = 12.6 Hz, $^1J_{CF}$ = 191.6 Hz, C, C4-Ar), 152.03 (CH, triaz), 145.06 (CH, triaz), 140.34 (C, Ar), 139.14 (C, Ar), 138.61 (C, Ar), 130.96 (dd, $^3J_{CF}$ = 5.2 Hz, $^3J_{CF}$ = 9.9 Hz, CH, C6-Ar), 129.36 (CH x 2, Ar), 127.94 (CH x 2, Ar), 127.78 (CH, Ar), 127.01 (CH x 2, Ar), 126.95 (CH x 2, Ar), 120.66 (dd, $^4J_{CF}$ = 3.9 Hz, $^2J_{CF}$ =15.0 Hz, CH, C1-Ar), 112.017 (dd, $^4J_{CF}$ = 3.5 Hz, $^2J_{CF}$ =21.0 Hz, CH, C5-Ar), 104.38 (t, $^2J_{CF}$ = 26.3 Hz, CH, C3-Ar), 50.53 (CH$_2$-triaz), 44.06 (CH), 42.32 (CH$_2$-NH).

HPLC (Method A): 100 %, RT = 4.69 min.

HRMS (ESI, m/z): theoretical mass: 441.1502 [M+Na]$^+$, observed mass: 441.1498 [M+Na]$^+$.

Using this procedure, the following compounds were prepared:

N-((4'-chloro-[1,1'-biphenyl]-4-yl) methyl)-2-(2,4-difluorophenyl)-3-(1*H*-1,2,4-triazol-1-yl)propenamide (80b)

(C$_{24}$H$_{19}$ClF$_2$N$_4$O, M.W. 452.89)
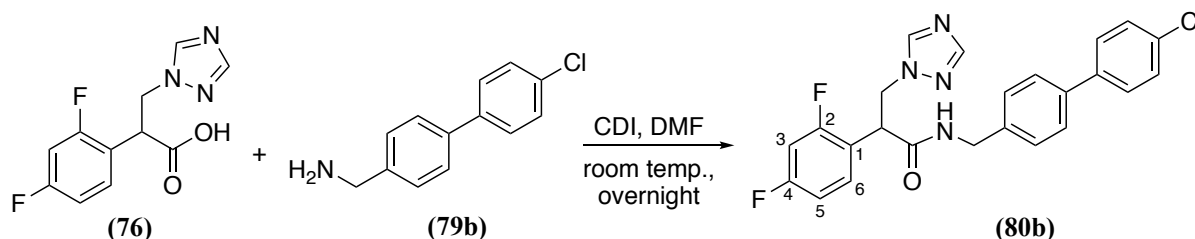
Reagents: 2-(2,4-difluorophenyl)-3-(1*H*-1,2,4-triazol-1-yl)propanoic acid (**76**) (0.15g, 0.59 mmol) and (4'-chloro-[1,1'-biphenyl]-4-yl)methanamine (**79b**) (0.15g, 0.71 mmol). The residue was purified by gradient column chromatography and the desired compound eluted with 2 % MeOH in CH$_2$Cl$_2$.

Yield: 0.14 g (53 %) as a white solid.

m.p.: 198-200 °C

R*f* = 0.4 (CH$_2$Cl$_2$-MeOH 9.5:0.5 v/v).

^{1}H NMR (DMSO-d$_6$): δ 8.78 (t, *J* = 5.9 Hz, 1H, N*H*), 8.35 (s, 1H, triaz), 7.98 (s, 1H, triaz), 7.66 (d, *J* = 8.7 Hz, 2H, Ar), 7.57 (dd, *J* = 8.7, 15.3 Hz, 1H, Ar), 7.55 (d, *J* = 8.4 Hz, 2H, Ar), 7.50 (d, *J* = 8.7 Hz, 2H, Ar), 7.23 (ddd, *J* = 2.6, 9.4, 10.5 Hz, 1H, Ar), 7.11 (d, *J* = 8.4 Hz, 2H, Ar), 7.10 (ddd, *J* = 2.4, 8.4, 10.0 Hz, 1H, Ar), 4.81 (dd, *J* = 7.8, 12.8 Hz, 1H, C*Ha*Hb-triaz), 4.52-4.44 (m, 2H, C*H*CHa*Hb*-triaz), 4.31 (dd, *J* = 6.2, 15.4 Hz, 1H, C*Ha*Hb-NH), 4.20 (dd, *J* = 5.6, 15.4 Hz, 1H, CHa*Hb*-NH).

^{13}C NMR (DMSO-d$_6$): δ 169.62 (C, C=O), 162.29 (dd, $^3J_{CF}$ = 12.5 Hz, $^1J_{CF}$ = 190.7 Hz, C, C2-Ar), 160.32 (dd, $^3J_{CF}$ = 12.1 Hz, $^1J_{CF}$ = 192.6 Hz, C, C4-Ar), 152.03 (CH, triaz), 145.06 (CH, triaz), 139.13 (C, Ar), 139.06 (C, Ar), 137.76 (C, Ar), 132.65 (C, Ar), 130.96 (dd, $^3J_{CF}$ = 5.2 Hz, $^3J_{CF}$ = 9.9 Hz, CH, C6-Ar), 129.30 (CH x 2, Ar), 128.76 (CH x 2, Ar), 127.99 (CH x 2, Ar), 126.90 (CH x 2, Ar), 120.66 (dd, $^4J_{CF}$ = 3.8 Hz, $^2J_{CF}$ = 15.1 Hz, CH, C1-Ar), 112.017 (dd, $^4J_{CF}$ = 3.5 Hz, $^2J_{CF}$ = 21.1 Hz, CH, C5-Ar), 104.38 (t, $^2J_{CF}$ = 26.5 Hz, CH, C3-Ar), 50.53 (*C*H$_2$-triaz), 44.06 (*C*H), 42.29 (*C*H$_2$-NH).

HPLC (Method A): 100 %, RT = 4.80 min.

HRMS (ESI, m/z): theoretical mass: $^{35/37}$Cl 451.1137/453.1137 [M-H]⁻, observed mass: $^{35/37}$Cl 451.1142/453.1120 [M-H]⁻.

2-(2,4-Difluorophenyl)-3-(1_H_-1,2,4-triazol-1-yl)-_N_-((4'-(trifluoromethyl)-[1,1'-biphenyl]-4-yl) methyl) propenamide (80c)

(C₂₅H₁₉F₅N₄O, M.W. 486.45)
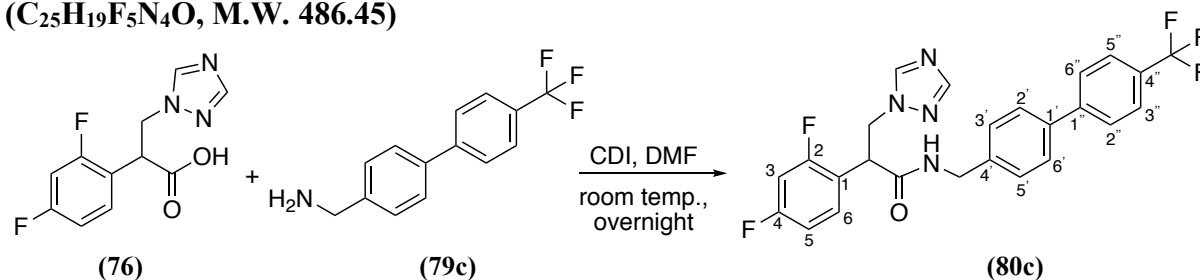
Reagents: 2-(2,4-difluorophenyl)-3-(1_H_-1,2,4-triazol-1-yl)propanoic acid (**76**) (0.15g, 0.59 mmol) and (4'-(trifluoromethyl)-[1,1'-biphenyl]-4-yl)methanamine (**79c**) (0.20 g, 0.71 mmol). The residue was purified by gradient column chromatography and the desired compound eluted with 2 % MeOH in CH₂Cl₂.

Yield: 0.15 g (54 %) as a white solid.

m.p.: 197-198 °C.

R_f_ = 0.42 (CH₂Cl₂-MeOH 9.5:0.5 v/v).

¹H NMR (DMSO-d₆): δ 8.80 (t, _J_ = 5.9 Hz, 1H, N_H_), 8.35 (s, 1H, triaz), 7.98 (s, 1H, triaz), 7.86 (d, _J_ = 8.2 Hz, 2H, Ar), 7.80 (d, _J_ = 8.2 Hz, 2H, Ar), 7.63 (d, _J_ = 8.4 Hz, 2H, Ar), 7.58 (dd, _J_ = 8.7, 15.3 Hz, 1H, Ar), 7.23 (ddd, _J_ = 2.6, 9.4, 10.4 Hz, 1H, Ar), 7.15 (d, _J_ = 8.4 Hz, 2H, Ar), 7.11 (ddd, _J_ = 2.4, 8.4, 10.7 Hz, 1H, Ar), 4.81 (dd, _J_ = 7.9, 12.9 Hz, 1H, C_Ha_Hb-triaz), 4.52- 4.44 (m, 2H, C_H_CHa_Hb_-triaz), 4.33 (dd, _J_ = 6.2, 15.5 Hz, 1H, C_Ha_Hb-NH), 4.22 (dd, _J_ = 5.6, 15.5 Hz, 1H, CHa_Hb_-NH).

¹³C NMR (DMSO-d₆): δ 169.65 (C, C=O), 162.29 (dd, ³_J_CF = 12.5 Hz, ¹_J_CF =191.1 Hz, C, C2-Ar), 160.32 (dd, ³_J_CF = 12.6 Hz, ¹_J_CF = 193.4 Hz, C, C4-Ar), 152.02 (CH, triaz), 145.06 (CH, triaz), 144.32 (C, Ar), 139.80 (C, Ar), 137.50 (C, Ar), 130.96 (dd, ³_J_CF = 5.0 Hz, ³_J_CF = 10.1 Hz, CH, C6-Ar), 128.16 (d, ²_J_CF3 = 31.9 Hz, C, C4''-Ar), 128.06 (CH x 2, Ar), 127.78 (CH x 2, Ar), 127.33 (CH x 2, Ar), 126.20 (q, ³_J_CF3 = 3.7 Hz, CH x 2, C3''and C5''-Ar), 123.29 (q, ¹_J_CF = 203.1 Hz, CF₃), 120.62 (dd, ⁴_J_CF = 3.8 Hz, ²_J_CF =15.3 Hz, CH, C1-Ar), 112.018 (dd, ⁴_J_CF = 3.6 Hz, ²_J_CF = 21.5 Hz, CH, C5-Ar), 104.38 (t, ²_J_CF = 26.5 Hz, CH, C3-Ar), 50.51 (_C_H₂-triaz), 44.06 (_C_H), 42.28 (_C_H₂-NH).

HPLC (Method A): 100 %, RT = 4.79 min.

HRMS (ESI, m/z): theoretical mass: 487.1557 [M+H]⁺, observed mass: 487.1553 [M+H]⁺.

4'-(Trifluoromethoxy)-[1,1'-biphenyl]-4-carbonitrile (78)

(C₁₄H₈F₃NO, M.W. 263.22)

Method: Chapter IV compound (**66**).

Reagents: 4-bromobenzonitrile (**77**) (0.5g, 2.74 mmol), (4-(trifluoromethoxy) phenyl) boronic acid (**65b**) (0.67g, 3.29 mmol), 1 mol % of Pd(PPh₃)₄ (31 mg) and K₂CO₃ (0.75g, 5.48 mmol). The residue was purified by gradient column chromatography and the desired compound eluted with 20 % EtOAc in petroleum ether.

Yield: 0.67 g (93 %) as a yellow solid.

m.p.: 53-54 °C (lit. m.p. 51°C)[152].

R*f* = 0.75 (petroleum ether- EtOAc 3:1 v/v).

¹H NMR (DMSO-d₆): δ 7.93 (d, *J* = 8.7 Hz, 2H, Ar), 7.90 (d, *J* = 9.2 Hz, 2H, Ar), 7.89 (d, *J* = 9.0 Hz, 2H, Ar), 7.51 (d, *J* = 8.0 Hz, 2H, Ar).

(4'-(Trifluoromethoxy)-[1,1'-biphenyl]-4-yl)methanamine (79d)

(C₁₄H₁₂F₃NO, M.W. 267.25)

Method: LiAlH₄ in 1M THF (6.83 mL, 6.83 mmol) was added to a solution of 4'-(trifluoromethoxy)-[1,1'-biphenyl]-4-carbonitrile (**78**) (0.6g, 2.27 mmol) in THF (30 mL) while stirring at -40 °C for 30 min. The reaction mixture was left at 0 °C for 5 h, then (1 mL) H₂O was added to decompose any remaining LiAlH₄. Then, 1N aq.NaOH (0.25 mL) was added and the mixture stirred for 30 min at room temperature. The reaction mixture was filtered through a pad of celite, washed with EtOAc and the filtrate was evaporated under vaccuo. H₂O (25 mL) was added to the concentrated mixture and extracted with EtOAc (3 x 50 mL), dried (MgSO₄) and evaporated under reduced pressure. The crude white solid was used in the next step without further purification.

Yield: 0.5g (83 % crude yield) as a white solid.

m.p.: 142-144 °C.

R*f* = 0.17 (CH$_2$Cl$_2$-MeOH 9.5:0.5 v/v).

¹H NMR (DMSO-d₆): δ 8.60 (s, 2H, NH$_2$), 7.91 (d, *J* = 8.5 Hz, 2H, Ar), 7.85 (d, *J* = 9.0 Hz, 2H, Ar), 7.78 (d, *J* = 8.9 Hz, 2H, Ar), 7.67 (d, *J* = 8.4 Hz, 2H, Ar), 4.86 (s, 2H, C*H*$_2$).

2-(2,4-Difluorophenyl)-3-(1*H*-1,2,4-triazol-1-yl)-*N*-((4'-(trifluoromethoxy)-[1,1'-biphenyl]-4-yl) methyl)propenamide (80d)

(C$_{25}$H$_{19}$F$_5$N$_4$O$_2$, M.W. 502.45)

Method: Chapter IV compound **46**.

Reagents: 2-(2,4-difluorophenyl)-3-(1*H*-1,2,4-triazol-1-yl)propanoic acid (**76**) (0.3g, 1.18 mmol) and (4'-(trifluoromethoxy)-[1,1'-biphenyl]-4-yl)methanamine (**79d**) (0.37 g, 1.42 mmol). The residue was purified by gradient column chromatography and the desired compound eluted with 3 % MeOH in CH$_2$Cl$_2$. A faint minor impurity spot was observed just above the major spot on TLC therefore the compound was purified further by recrystallisation from EtOH resulting in a white crystalline solid.

Yield: 0.24 g (40 %) as a white solid.

m.p.: 160-162 °C

R*f* = 0.55 (CH$_2$Cl$_2$-MeOH 9.5:0.5 v/v).

¹H NMR (DMSO-d₆): δ 8.79 (t, *J* = 5.9 Hz, 1H, NH), 8.36 (s, 1H, triaz), 7.98 (s, 1H, triaz), 7.76 (d, *J* = 8.9 Hz, 2H, Ar), 7.60- 7.56 (m, 1H, Ar), 7.57 (d, *J* = 8.4 Hz, 2H, Ar), 7.44 (dd, *J* = 0.9, 8.8 Hz, 2H, Ar), 7.23 (ddd, *J* = 2.7, 9.4, 10.5 Hz, 1H, Ar), 7.13 (d, *J* = 8.5 Hz, 2H, Ar), 7.11 (ddd, *J* = 2.4, 8.5, 10.8 Hz, 1H), 4.81 (dd, *J* = 7.9, 12.9 Hz, 1H, C*Ha*Hb-triaz), 4.52- 4.44 (m, 2H, C*H*CHa*Hb*-triaz), 4.32 (dd, *J* = 6.2, 15.4 Hz, 1H, C*Ha*Hb-NH), 4.21 (dd, *J* = 5.7, 15.4 Hz, 1H, CHa*Hb*-NH).

¹³C NMR (DMSO-d₆): δ 169.65 (C, C=O), 162.1 (dd, ³*J*$_{CF}$ = 12.1 Hz, ¹*J*$_{CF}$ = 246.1 Hz, C, C2-Ar), 160.32 (dd, ³*J*$_{CF}$ = 12.1 Hz, ¹*J*$_{CF}$ = 251.4 Hz, C, C4-Ar), 152.0 (CH, triaz), 148.21 (C, Ar), 145.1 (CH, triaz), 139.7 (C, Ar), 137.2 (C, Ar), 137.7 (C, Ar), 130.96 (dd, ³*J*$_{CF}$ = 5.2 Hz, ³*J*$_{CF}$ = 9.8 Hz, CH, C6-Ar), 128.9 (CH x 2, Ar), 128.0 (CH x 2, Ar), 127.1 (CH x 2, Ar), 121.9 (CH

x 2, Ar), 120.7 (dd, $^4J_{CF}$ = 3.6 Hz, $^2J_{CF}$ = 15.3 Hz, CH, C1-Ar), 120.58 (q, $^1J_{CF}$ = 256.1 Hz, CF$_3$), 112.18 (dd, $^4J_{CF}$ = 3.5 Hz, $^2J_{CF}$ = 21.3 Hz, CH, C5-Ar), 104.39 (t, $^2J_{CF}$ = 26.0 Hz, CH, C3-Ar), 50.5 (CH$_2$-triaz), 44.1 (CH), 42.3 (CH$_2$-NH).

Microanalysis (C$_{25}$H$_{19}$F$_5$N$_4$O$_2$): Anal. Calcd: C 59.76 %, H 3.81 %, N 11.15 %. Found: C 59.72 %, H 3.69 %, N 11.18 %.

2-(2,4-Difluorophenyl)-*N*-(4-nitrobenzyl)-3-(1*H*-1,2,4-triazol-1-yl)propenamide (82)

(C$_{18}$H$_{15}$F$_2$N$_5$O$_3$, M. W. 387.35)
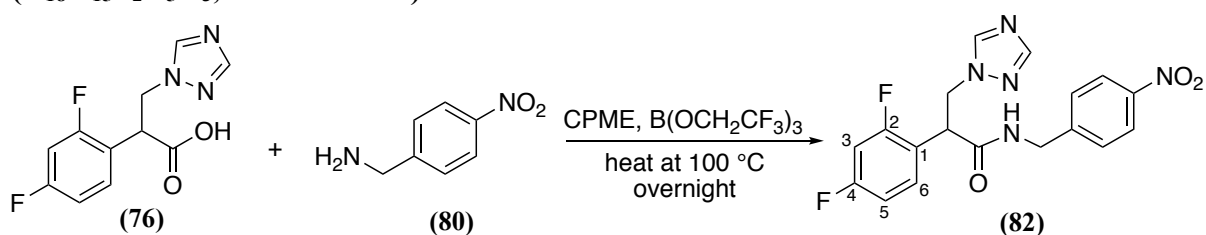
Method: Tris(2,2,2-trifluoroethyl)borate (B(OCH$_2$CF$_3$)$_3$) (0.40 mL, 1.80 mmol) was added to a solution of 2-(2,4-difluorophenyl)-3-(1*H*-1,2,4-triazol-1-yl)propanoic acid (**76**) (0.23g, 0.90 mmol) and 4-nitrobenzylamine (**81**) (0.15g, 0.99 mmol) in CPME (4 mL). The resulting mixture was then stirred at 100 °C overnight. Upon completion the reaction mixture was diluted with EtOAc (8 mL) and H$_2$O (1 mL). Amberlyst A-26(OH) (300 mg), Amberlyst 15 (300 mg) and Amberlite IRA743 (300 mg) were added together to the mixture and it was stirred for 30 min. The mixture was then dried (MgSO$_4$), filtered to remove resins and MgSO$_4$ and washed with EtOAc (3 x 20 mL). The filtrate was concentrated *in vacuo* and an orange oil residue was obtained. The crude product was purified by gradient column chromatography to yield a faint yellow solid with 2.5 % MeOH in CH$_2$Cl$_2$.

Yield: 0.23g (67%) as a yellow solid.

m.p.: 178-180 °C.

R*f* = 0.42 (CH$_2$Cl$_2$-MeOH 9.5:0.5 v/v).

^{1}H NMR (DMSO-d$_6$): δ 8.90 (t, *J* = 5.9 Hz, 1H, N*H*), 8.35 (s, 1H, triaz), 8.12 (d, *J* = 8.8 Hz, 2H, Ar), 8.00 (s, 1H, triaz), 7.54 (dd, *J* = 8.7, 15.0 Hz, 1H, Ar), 7.26 (d, *J* = 8.9 Hz, 2H, Ar), 7.25 (ddd, *J* = 2.6, 8.9, 10.0 Hz, 1H, Ar), 7.11 (ddd, *J* = 2.8, 8.5, 10.0 Hz, 1H, Ar), 4.81 (dd, *J* = 8.4, 13.2 Hz, 1H, C*Ha*Hb-triaz), 4.53-4.45 (m, 2H, C*H*CHa*Hb*-triaz), 4.41 (dd, *J* = 6.2, 16.0 Hz, 1H, C*Ha*Hb-NH), 4.26 (dd, *J* = 5.5, 16.0 Hz, 1H, CHa*Hb*-NH).

^{13}C NMR (DMSO-d$_6$): δ 169.92 (C, C=O), 162.30 (dd, $^3J_{CF}$ = 12.6 Hz, $^1J_{CF}$ = 198.9 Hz, C, C2-Ar), 160.33 (dd, $^3J_{CF}$ = 12.2 Hz, $^1J_{CF}$ = 200.3 Hz, C, C4-Ar), 152.09 (CH, triaz), 147.54 (C,

Ar), 146.84 (C, Ar), 145.10 (CH, triaz), 130.92 (dd, $^3J_{CF}$ = 5.0 Hz, $^3J_{CF}$ = 9.4 Hz, CH, C6-Ar), 128.24 (CH x 2, Ar), 123.80 (CH x 2, Ar), 120.43 (dd, $^4J_{CF}$ = 3.7 Hz, $^2J_{CF}$ = 15.0 Hz, CH, C1-Ar), 112.24 (dd, $^4J_{CF}$ = 3.3 Hz, $^2J_{CF}$ = 21.1 Hz, CH, C5-Ar), 104.44 (t, $^2J_{CF}$ = 26.2 Hz, CH, C3-Ar), 50.42 ($\underline{C}H_2$-triaz), 43.99 ($\underline{C}H$), 42.21 ($\underline{C}H_2$-NH).

HPLC (Method A): 100 %, RT = 4.35 min.

HRMS (ESI, m/z): theoretical mass: 388.1221[M+H]$^+$, observed mass: 388.1221[M+H]$^+$.

N-(4-aminobenzyl)-2-(2,4-difluorophenyl)-3-(1H-1,2,4-triazol-1-yl) propenamide (83)

(C$_{18}$H$_{17}$F$_2$N$_5$O, M. W. 357.36)
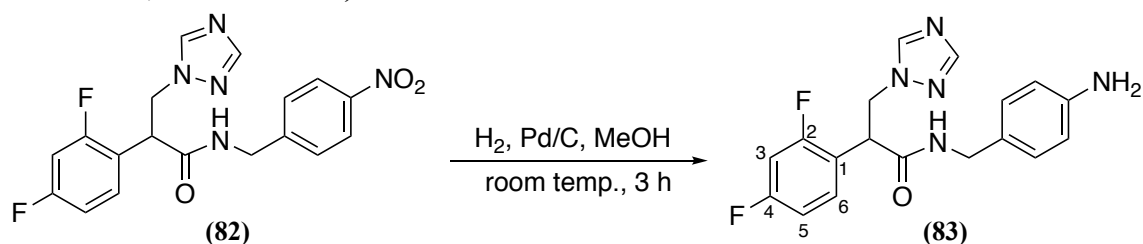
Method: Chapter II compound **8**.

Reagents: 2-(2,4-difluorophenyl)-N-(4-nitrobenzyl)-3-(1H-1,2,4-triazol-1-yl)propenamide (**82**) (0.18g, 0.46 mmol) and 10 % Pd-C (20 mg). The residue was purified by gradient column chromatography and the desired compound eluted with 3 % MeOH in CH$_2$Cl$_2$.

Yield: 0.15g (93%) as a white solid.

m.p.: 147-149 °C.

Rf = 0.3 (CH$_2$Cl$_2$-MeOH 9.5:0.5 v/v).

^{1}H NMR (DMSO-d$_6$): δ 8.53 (t, J = 5.8 Hz, 1H, N$\underline{H}$), 8.33 (s, 1H, triaz), 7.92 (s, 1H, triaz), 7.56 (dd, J = 8.7, 15.3 Hz, 1H, Ar), 7.20 (ddd, J = 2.7, 9.4, 10.5 Hz, 1H, Ar), 7.08 (ddd, J = 2.4, 8.5, 11.2 Hz, 1H, Ar), 6.69 (d, J = 8.5 Hz, 2H, Ar), 6.43 (d, J = 8.5 Hz, 2H, Ar), 4.92 (s, 2H, N$\underline{H}_2$), 4.76 (dd, J = 5.1, 15.7 Hz, 1H, CHaHb-triaz), 4.45- 4.40 (m, 2H, CHCHaHb-triaz), 4.07 (dd, J = 6.0, 15.0 Hz, 1H, CHaHb-NH), 3.98 (dd, J = 5.6, 15.0 Hz, 1H, CHaHb-NH).

^{13}C NMR (DMSO-d$_6$): δ 169.17 (C, C=O), 162.50 (dd, $^3J_{CF}$ = 12.2 Hz, $^1J_{CF}$ = 182.7 Hz, C, C2-Ar), 160.27 (dd, $^3J_{CF}$ = 12.0 Hz, $^1J_{CF}$ = 184.6 Hz, C, C4-Ar), 151.93 (CH, triaz), 147.95 (C, Ar), 144.99 (CH, triaz), 130.94 (dd, $^3J_{CF}$ = 5.2 Hz, $^3J_{CF}$ = 9.53 Hz, CH, C6-Ar), 128.39 (CH x 2, Ar), 126.07 (C, Ar), 120.82 (dd, $^4J_{CF}$ = 3.6 Hz, $^2J_{CF}$ = 15.0 Hz, CH, C1-Ar), 114.05 (CH x 2, Ar), 112.06 (dd, $^4J_{CF}$ = 3.5 Hz, $^2J_{CF}$ = 21.3 Hz, CH, C5-Ar), 104.29 (t, $^2J_{CF}$ = 26.5 Hz, CH, C3-Ar), 50.59 ($\underline{C}H_2$-triaz), 44.05 ($\underline{C}H$), 42.40 ($\underline{C}H_2$-NH).

HPLC (Method A): 100 %, RT = 3.77 min.

HRMS (ESI, m/z): theoretical mass: 358.1479 [M+H]$^+$, observed mass: 358.1480 [M+H]$^+$.

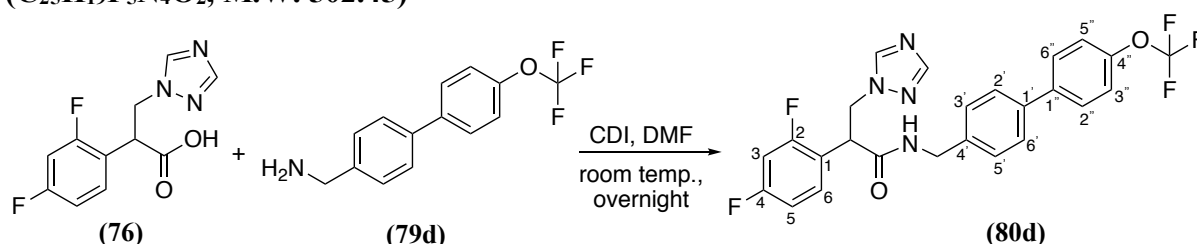**4-Chloro-*N*-(4-((2-(2,4-difluorophenyl)-3-(1*H*-1,2,4-triazol-1-yl)propanamido)methyl) phenyl)benzamide (85a)**

(C$_{25}$H$_{20}$ClF$_2$N$_5$O$_2$, M. W. 495.91)
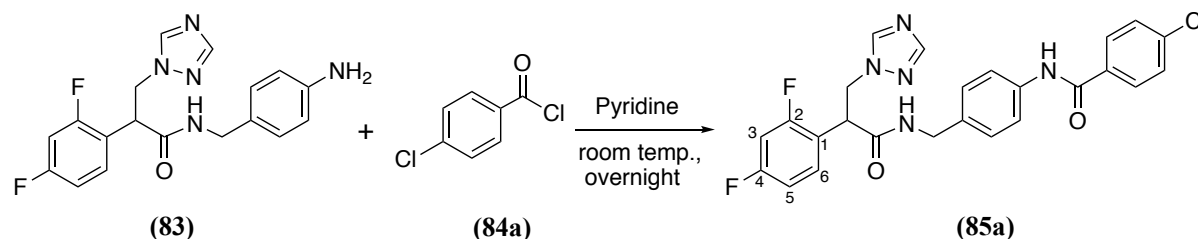
Method: Chapter II compound **10**.

Reagents: *N*-(4-aminobenzyl)-2-(2,4-difluorophenyl)-3-(1*H*-1,2,4-triazol-1-yl)propenamide (**83**) (0.12g, 0.33 mmol) and 4-chlorobenzoyl chloride (**84a**) (0.06 mL, 0.50 mmol). The residue was purified by gradient column chromatography and the desired compound eluted with 3 % MeOH in CH$_2$Cl$_2$.

Yield: 0.11g (68%) as a white solid.

m.p.: 206-208 °C.

R*f* = 0.5, (CH$_2$Cl$_2$-MeOH 9.5:0.5 v/v).

^{1}H NMR (DMSO-d$_6$): δ10.26 (s, 1H, NH), 8.73 (t, *J* = 5.9 Hz, 1H, N<u>H</u>), 8.36 (s, 1H, triaz), 7.98 (d, *J* = 8.8 Hz, 2H, Ar), 7.95 (s, 1H, triaz), 7.63 (d, *J* = 8.5 Hz, 2H, Ar), 7.60 (d, *J* = 8.8 Hz, 2H, Ar), 7.56 (dd, *J* = 8.7, 15.3 Hz, 1H, Ar), 7.23 (dd, *J* = 2.7, 9.4, 10.5 Hz, 1H, Ar), 7.10 (ddd, *J* = 2.4, 8.4, 11.5 Hz, 1H, Ar), 6.99 (d, *J* = 8.5 Hz, 2H, Ar), 4.81 (dd, *J* = 7.3, 12.3 Hz, 1H, C*Ha*Hb-triaz), 4.50-4.43 (m, 2H, C*H*CHa*Hb*-triaz), 4.25 (dd, *J* = 6.1, 15.2 Hz, 1H, C*Ha*Hb-NH), 4.14 (dd, *J* = 5.6, 15.2 Hz, 1H, CHa*Hb*-NH).

^{13}C NMR (DMSO-d$_6$): δ 169.51 (C, C=O), 164.70 (C, C=O), 162.28 (dd, $^3J_{CF}$ = 12.4 Hz, $^1J_{CF}$ = 188.7 Hz, C, C2-Ar), 160.31 (dd, $^3J_{CF}$ = 12.5 Hz, $^1J_{CF}$ = 190.4 Hz, C, C4-Ar), 151.98 (CH, triaz), 145.05 (CH, triaz), 138.06 (C, Ar), 136.82 (C, Ar), 134.76 (C, Ar), 134.01 (C, Ar), 130.95 (dd, $^3J_{CF}$ = 5.2 Hz, $^3J_{CF}$ = 9.54 Hz, CH, C6-Ar), 130.04 (CH x 2, Ar), 128.90 (CH x 2, Ar), 127.58 (CH x 2, Ar), 120.71(CH x 2, Ar), 120.67 (dd, $^4J_{CF}$ = 2.26 Hz, $^2J_{CF}$ = 12.2 Hz, CH, C1-Ar), 112.06 (dd, $^4J_{CF}$ = 3.4 Hz, $^2J_{CF}$ = 21.0 Hz, CH, C5-Ar), 104.37 (t, $^2J_{CF}$ = 26.0 Hz, CH, C3-Ar), 50.51 (<u>C</u>H$_2$-triaz), 44.06 (<u>C</u>H), 42.22 (<u>C</u>H$_2$-NH).

HPLC (Method A): 100 %, RT = 4.57 min.

HRMS (ESI, m/z): theoretical mass: 518.1171/520.1171 [M+Na]$^+$, observed mass: 518.1169/520.1148 [M+Na]$^+$.

Using this procedure, the following compounds were prepared:

N-(4-((2-(2,4-difluorophenyl)-3-(1*H*-1,2,4-triazol-1-yl)propanamido)methyl)phenyl)-4-methoxybenzamide (85b)

($C_{26}H_{23}F_2N_5O_3$, M.W. 491.50)
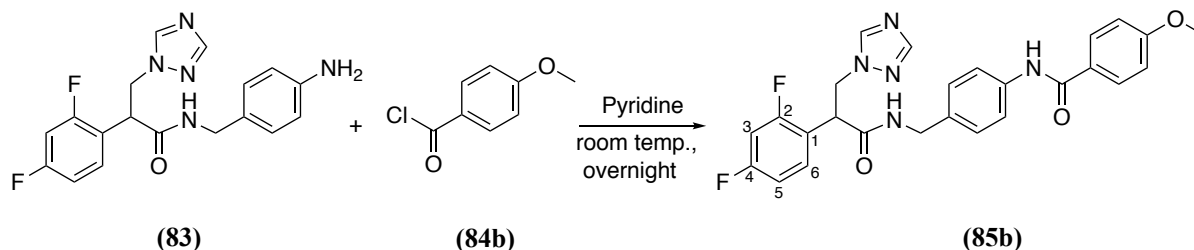
(83)   **(84b)**   **(85b)**

Reagents: *N*-(4-aminobenzyl)-2-(2,4-difluorophenyl)-3-(1*H*-1,2,4-triazol-1-yl)propenamide **(83)** (0.15g, 0.41 mmol) and 4-methoxybenzoyl chloride **(84b)** (0.08 mL, 0.62 mmol). The residue was purified by gradient column chromatography and the desired compound eluted with 3 % MeOH in CH_2Cl_2.

Yield: 0.13g (72%) as a white solid.

m.p.: 222-224 °C.

R*f* = 0.4 (CH_2Cl_2-MeOH 9.5:0.5 v/v).

^{1}H NMR (DMSO-d$_6$): δ10.04 (s, 1H, NH), 8.72 (t, *J* = 5.9 Hz, 1H, N*H*), 8.36 (s, 1H, triaz), 7.99-7.93 (m, 3H, triaz + Ar), 7.63 (d, *J* = 8.6 Hz, 2H, Ar), 7.57 (dd, *J* = 8.7, 15.3 Hz, 1H, Ar), 7.23 (ddd, *J* = 2.7, 9.4, 10.5 Hz, 1H, Ar), 7.10 (ddd, *J* = 2.4, 8.4, 10.7 Hz, 1H, Ar), 7.05 (d, *J* = 8.9 Hz, 2H, Ar), 6.97 (d, *J* = 8.5 Hz, 2H, Ar), 4.81 (dd, *J* = 7.2, 12.1 Hz, 1H, C*Ha*Hb-triaz), 4.50- 4.43 (m, 2H, C*H*CHa*Hb*-triaz), 4.24 (dd, *J* = 6.1, 15.2 Hz, 1H, C*Ha*Hb-NH), 4.14 (dd, *J* = 5.6, 15.2 Hz, 1H, CHa*Hb*-NH), 3.84 (s, 3H, C*H₃*).

^{13}C NMR (DMSO-d$_6$): δ 169.49 (C, C=O), 165.17 (C, C=O), 162.32 (C, Ar), 162.28 (dd, $^3J_{CF}$ = 12.2 Hz, $^1J_{CF}$ = 188.0 Hz, C, C2-Ar), 160.32 (dd, $^3J_{CF}$ = 12.4 Hz, $^1J_{CF}$ = 190.0 Hz, C, C4-Ar), 151.98 (CH, triaz), 145.05 (CH, triaz), 138.46 (C, Ar), 134.29 (C, Ar), 130.96 (dd, $^3J_{CF}$ = 5.0 Hz, $^3J_{CF}$ = 9.8 Hz, CH, C6-Ar), 129.99 (CH x 2, Ar), 127.53 (CH x 2, Ar), 127.34 (C, Ar), 120.70 (dd, $^4J_{CF}$ = 3.6 Hz, $^2J_{CF}$ = 14.8 Hz, CH, C1-Ar), 120.62 (CH x 2, Ar), 114.03 (CH x 2, Ar), 112.14 (dd, $^4J_{CF}$ = 3.4 Hz, $^2J_{CF}$ = 21.1 Hz, CH, C5-Ar), 104.36 (t, $^2J_{CF}$ = 26.5 Hz, CH, C3-Ar), 55.88 (O*C*H₃), 50.52 (*C*H₂-triaz), 44.07 (*C*H), 42.23 (*C*H₂-NH).

HPLC (Method A): 100 %, RT = 4.44 min.

HRMS (ESI, m/z): theoretical mass: 514.1666 [M+Na]$^+$, observed mass: 514.1660 [M+Na]$^+$.

4-Cyano-*N*-(4-((2-(2,4-difluorophenyl)-3-(1*H*-1,2,4-triazol-1-yl)propanamido)methyl)

phenyl)benzamide (85c)

(C₂₆H₂₀F₂N₆O₂, M.W. 486.48)
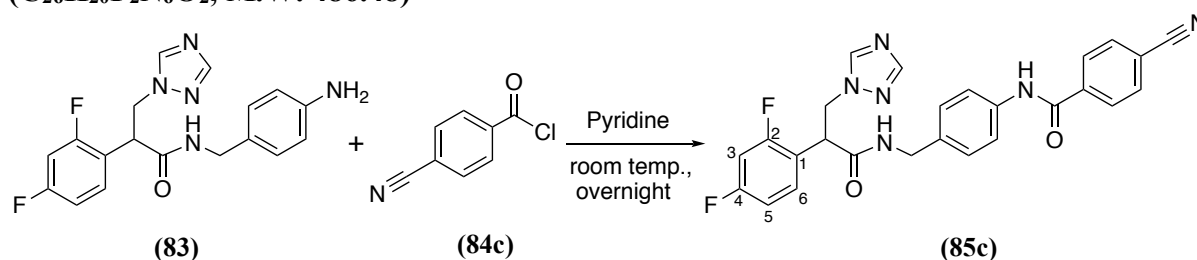
Reagents: *N*-(4-aminobenzyl)-2-(2,4-difluorophenyl)-3-(1*H*-1,2,4-triazol-1-yl)propenamide (**83**) (0.16g, 0.44 mmol) and 4-cyanobenzoyl chloride (**84c**) (0.11g, 0.67 mmol). The residue was purified by gradient column chromatography and the desired compound eluted with 3 % MeOH in CH₂Cl₂.

Yield: 0.17g (80%) as a white solid.

m.p.: 200-201 °C.

R*f* = 0.32 (CH₂Cl₂-MeOH 9.5:0.5 v/v).

¹H NMR (DMSO-d₆): δ10.44 (s, 1H, NH), 8.73 (t, *J* = 5.9 Hz, 1H, N$\underline{H}$), 8.36 (s, 1H, triaz), 8.10 (d, *J* = 8.7 Hz, 2H, Ar), 8.02 (d, *J* = 8.7 Hz, 2H, Ar), 7.64 (d, *J* = 8.6 Hz, 2H, Ar), 7.57 (dd, *J* = 8.7, 15.2 Hz, 1H, Ar), 7.23 (ddd, *J* = 2.7, 9.4, 10.5 Hz, 1H, Ar), 7.10 (ddd, *J* = 2.4, 8.4, 11.6 Hz, 1H, Ar), 7.00 (d, *J* = 8.7 Hz, 2H, Ar), 4.81 (dd, *J* = 7.4, 12.4 Hz, 1H, C*Ha*Hb-triaz), 4.50- 4.43 (m, 2H, C*H*CHa*Hb*-triaz), 4.25 (dd, *J* = 6.1, 15.2 Hz, 1H, C*Ha*Hb-NH), 4.14 (dd, *J* = 5.6, 15.2 Hz, 1H, CHa*Hb*-NH).

¹³C NMR (DMSO-d₆): δ 169.53 (C, C=O), 164.42 (C, C=O), 162.28 (dd, ³*J*$_{CF}$ = 12.5 Hz, ¹*J*$_{CF}$ = 188.8 Hz, C, C2-Ar), 160.32 (dd, ³*J*$_{CF}$ = 12.7 Hz, ¹*J*$_{CF}$ = 191.4 Hz, C, C4-Ar), 151.98 (CH, triaz), 145.06 (CH, triaz), 139.33 (C, Ar), 137.83 (C, Ar), 135.08 (C, Ar), 132.91 (CH x 2, Ar), 130.96 (dd, ³*J*$_{CF}$ = 5.1 Hz, ³*J*$_{CF}$ = 9.8 Hz, CH, C6-Ar), 128.95 (CH x 2, Ar), 127.63 (CH x 2, Ar), 120.76 (CH x 2, Ar), 120.67 (dd, ⁴*J*$_{CF}$ = 5.4 Hz, ²*J*$_{CF}$ = 16.4 Hz, CH, C1-Ar), 118.78 ($\underline{C}$N), 114.27 (C, Ar), 112.15 (dd, ⁴*J*$_{CF}$ = 3.4 Hz, ²*J*$_{CF}$ = 21.0 Hz, CH, C5-Ar), 104.37 (t, ²*J*$_{CF}$ = 26.3 Hz, CH, C3-Ar), 50.52 ($\underline{C}$H₂-triaz), 44.07 ($\underline{C}$H), 42.21 ($\underline{C}$H₂-NH).

HPLC (Method A): 100 %, RT = 4.38 min.

HRMS (ESI, m/z): theoretical mass: 509.1513 [M+Na]⁺, observed mass: 509.1509 [M+Na]⁺.

4-Acetyl-*N*-(4-((2-(2,4-difluorophenyl)-3-(1*H*-1,2,4-triazol-1-yl)propanamido)methyl)

phenyl) benzamide (85d)

(C$_{27}$H$_{23}$F$_2$N$_5$O$_3$, M.W. 503.51)
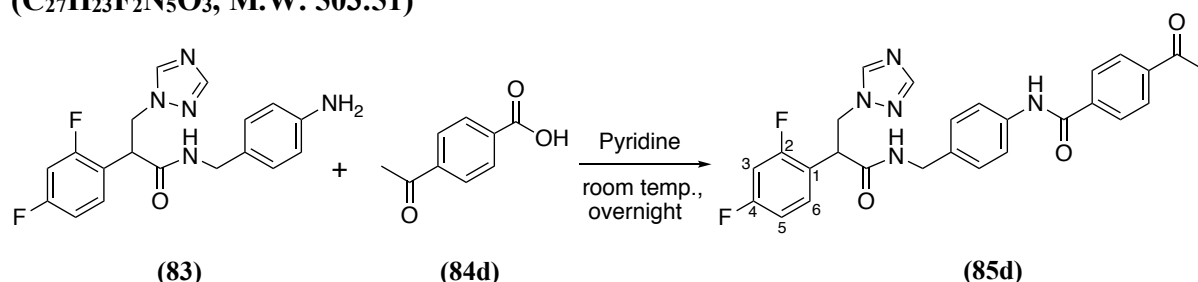
Variations: To an ice-cooled solution of 4-acetylbenzoic acid (**84d**) (0.11g, 0.67 mmol) in CH$_2$Cl$_2$ (10 mL) was added SOCl$_2$ (0.09 mL, 1.34 mmol) and the reaction was heated at 40 °C for 4 h to form 4-acetylbenzoyl chloride.

Reagents: *N*-(4-aminobenzyl)-2-(2,4-difluorophenyl)-3-(1*H*-1,2,4-triazol-1-yl) propenamide (**83**) (0.14 g, 0.39 mmol). The residue was purified by gradient column chromatography and the desired compound eluted with 4 % MeOH in CH$_2$Cl$_2$.

Yield: 0.023g (12%) as a faint beige solid.

m.p.: 220-222 °C.

R*f* = 0.3 (CH$_2$Cl$_2$-MeOH 9.5:0.5 v/v).

^{1}H NMR (DMSO-d$_6$): δ10.37 (s, 1H, NH), 8.73 (t, *J* = 5.9 Hz, 1H, N<u>H</u>), 8.36 (s, 1H, triaz), 8.07 (q, *J* = 8.8 Hz, 4H, Ar), 7.95 (s, 1H, triaz), 7.65 (d, *J* = 8.5 Hz, 2H, Ar), 7.57 (dd, *J* = 8.7, 15.3 Hz, 1H, Ar), 7.23 (ddd, *J* = 2.7, 9.4, 10.4 Hz, 1H, Ar), 7.10 (ddd, *J* = 2.4, 8.4, 10.9 Hz, 1H, Ar), 7.00 (d, *J* = 8.7 Hz, 2H, Ar), 4.81 (dd, *J* = 7.3, 12.3 Hz, 1H, C*Ha*Hb-triaz), 4.51-4.43 (m, 2H, C*H*CHa*Hb*-triaz), 4.25 (dd, *J* = 6.1, 15.2 Hz, 1H, C*Ha*Hb-NH), 4.14 (dd, *J* = 5.6, 15.3 Hz, 1H, CHa*Hb*-NH), 2.64 (s, 3H, C<u>H$_3$</u>).

^{13}C NMR (DMSO-d$_6$): δ 198.20 (C, C=O), 169.53 (C, C=O), 165.04 (C, C=O), 162.29 (dd, $^3J_{CF}$ = 12.0 Hz, $^1J_{CF}$ = 187.1 Hz, C, C2-Ar), 160.32 (dd, $^3J_{CF}$ = 12.7 Hz, $^1J_{CF}$ = 191.1 Hz, C, C4-Ar), 151.98 (CH, triaz), 145.06 (CH, triaz), 139.27 (C, Ar), 139.10 (C, Ar), 138.00 (C, Ar), 134.90 (C, Ar), 130.95 (dd, $^3J_{CF}$ = 5.4 Hz, $^3J_{CF}$ = 9.7 Hz, CH, C6-Ar), 128.63 (CH x 2, Ar), 128.43 (CH x 2, Ar), 127.60 (CH x 2, Ar), 120.76 (CH x 2, Ar), 120.67 (dd, $^4J_{CF}$ = 2.26 Hz, $^2J_{CF}$ = 12.2 Hz, CH, C1-Ar), 112.15 (dd, $^4J_{CF}$ = 3.4 Hz, $^2J_{CF}$ = 21.1 Hz, CH, C5-Ar), 104.37 (t, $^2J_{CF}$ = 26.5 Hz, CH, C3-Ar), 50.51 (<u>C</u>H$_2$-triaz), 44.07 (<u>C</u>H), 42.22 (<u>C</u>H$_2$-NH), 27.46 (<u>C</u>H$_3$).

HPLC (Method A): 100 %, RT = 4.38 min.

HRMS (ESI, m/z): theoretical mass: 504.1847 [M+H]$^+$, observed mass: 504.1843 [M+H]$^+$.

N-(4-((2-(2,4-difluorophenyl)-3-(1H-1,2,4-triazol-1-yl)propanamido)methyl)phenyl) nicotinamide (85e)

(C$_{24}$H$_{20}$F$_2$N$_6$O$_2$, M. W. 462.46)
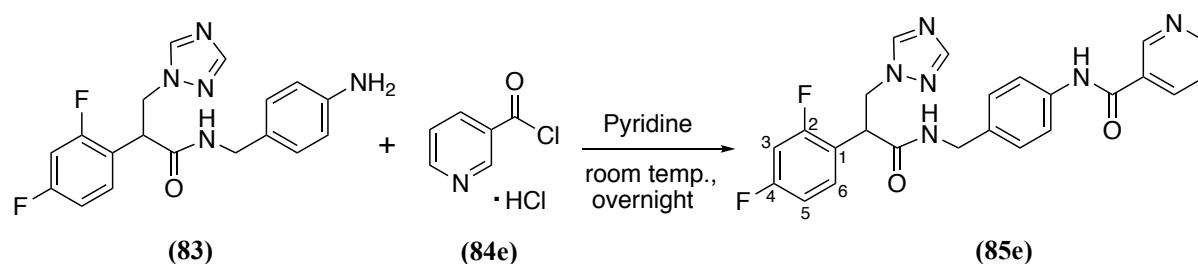
Reagents: N-(4-aminobenzyl)-2-(2,4-difluorophenyl)-3-(1H-1,2,4-triazol-1-yl)propenamide (**83**) (0.14g, 0.39 mmol) and nicotynoylchloride hydrochloride (**84e**) (0.10g, 0.58 mmol). The residue was purified by gradient column chromatography and the desired compound eluted with 4 % MeOH in CH$_2$Cl$_2$.

Yield: 0.14g (77 %) as a white solid.

m.p.: 204-206 °C.

Rf = 0.27 (CH$_2$Cl$_2$-MeOH 9.5:0.5 v/v).

^{1}H NMR (DMSO-d$_6$): δ10.39 (s, 1H, NH), 9.10 (d, J = 2.3 Hz, 1H, CH-pyridine), 8.76 (d, J = 1.6, 4.7 Hz, 1H, CH-pyridine), 8.73 (t, J = 5.9 Hz, 1H, NH), 8.36 (s, 1H, triaz), 8.28 (tt, J = 1.7, 2.3 Hz, 1H, CH-pyridine), 7.95 (s, 1H, triaz), 7.64 (d, J = 8.6 Hz, 2H, Ar), 7.60-7.55 (m, 2H, Ar), 7.23 (ddd, J = 2.7, 9.4, 10.4 Hz, 1H, Ar), 7.10 (ddd, J = 2.4, 8.4, 10.9 Hz, 1H, Ar), 7.01 (d, J = 8.6 Hz, 2H, Ar), 4.81 (dd, J = 7.3, 12.3 Hz, 1H, CHaHb-triaz), 4.51-4.43 (m, 2H, CHCHaHb-triaz), 4.25 (dd, J = 6.6, 15.2 Hz, 1H, CHaHb-NH), 4.15 (dd, J = 5.6, 15.2 Hz, 1H, CHaHb-NH).

**^{13}C NMR (DMSO-d$_6$):** δ 169.53 (C, C=O), 164.33 (C, C=O), 162.29 (dd, $^3J_{CF}$ = 12.3 Hz, $^1J_{CF}$ = 188.7 Hz, C, C2-Ar), 160.32 (dd, $^3J_{CF}$ = 12.6 Hz, $^1J_{CF}$ = 190.6 Hz, C, C4-Ar), 152.54 (CH, pyridine), 151.98 (CH, triaz), 149.10 (CH, pyridine), 145.06 (CH, triaz), 137.93 (C, Ar), 135.86 (CH, pyridine), 134.93 (C, Ar), 130.96 (dd, $^3J_{CF}$ = 5.2 Hz, $^3J_{CF}$ = 9.9 Hz, CH, C6-Ar), 130.95 (C, Ar), 127.63 (CH x 2, Ar), 123.93 (CH, pyridine), 120.69 (dd, $^4J_{CF}$ = 3.9 Hz, $^2J_{CF}$ = 10.0 Hz, CH, C1-Ar), 120.68 (CH x 2, Ar), 112.14 (dd, $^4J_{CF}$ = 3.4 Hz, $^2J_{CF}$ = 21.0 Hz, CH, C5-Ar), 104.37 (t, $^2J_{CF}$ = 26.2 Hz, CH, C3-Ar), 50.52 (CH$_2$-triaz), 44.07 (CH), 42.21 (CH$_2$-NH).

HPLC (Method A): 100 %, RT = 4.23 min.

HRMS (ESI, m/z): theoretical mass: 463.1703 [M+H]$^+$, observed mass: 463.1693 [M+H]$^+$.

N-(4-((2-(2,4-difluorophenyl)-3-(1H-1,2,4-triazol-1-yl)propanamido)methyl)phenyl) pyrazine-2-carboxamide (85f)

(C₂₃H₁₉F₂N₇O₂, M. W. 463.45)
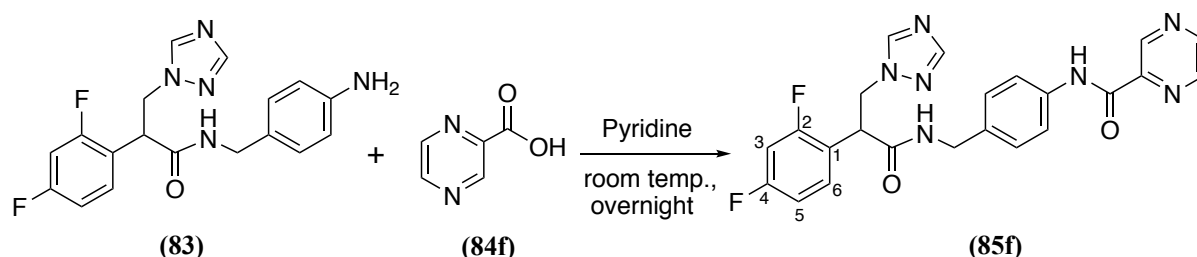
Variations: To an ice-cooled solution of pyrazine-2-carboxylic acid (**84f**) (0.1g, 0.8 mmol) in CH₂Cl₂ (10 mL) was added SOCl₂ (0.11 mL, 1.61 mmol) and the reaction was heated at 40 °C for 4 h to form pyrazine-2-carbonyl chloride.

Reagents: N-(4-aminobenzyl)-2-(2,4-difluorophenyl)-3-(1H-1,2,4-triazol-1-yl)propenamide (**83**) (0.15g, 0.41 mmol). The residue was purified by gradient column chromatography and the desired compound eluted with 3 % MeOH in CH₂Cl₂.

Yield: 0.13g (68 %) as a white solid.

m.p.: 202-204 °C.

Rf = 0.4 (CH₂Cl₂-MeOH 9.5:0.5 v/v).

^{1}H NMR (DMSO-d₆): δ10.68 (s, 1H, NH), 9.29 (d, J = 1.5 Hz, 1H, C$\underline{H}$-pyrazine), 8.93 (d, J = 2.5 Hz, 1H, C$\underline{H}$-pyrazine), 8.81 (dd, J = 1.5, 2.5 Hz, 1H, C$\underline{H}$-pyrazine), 8.73 (t, J = 5.9 Hz, 1H, N$\underline{H}$), 8.36 (s, 1H, triaz), 7.95 (s, 1H, triaz), 7.77 (d, J = 8.6 Hz, 2H, Ar), 7.56 (dd, J = 8.7, 15.3 Hz, 1H, Ar), 7.23 (ddd, J = 2.7, 9.4, 10.4 Hz, 1H, Ar), 7.10 (ddd, J = 2.4, 8.4, 10.9 Hz, 1H, Ar), 7.02 (d, J = 8.6 Hz, 2H, Ar), 4.81 (dd, J = 6.5, 11.5 Hz, 1H, CHaHb-triaz), 4.50- 4.44 (m, 2H, CHCHaHb-triaz), 4.25 (dd, J = 6.1, 15.2 Hz, 1H, CHaHb-NH), 4.15 (dd, J = 5.6, 15.2 Hz, 1H, CHaHb-NH).

^{13}C NMR (DMSO-d₆): δ 169.53 (C, C=O), 162.29 (dd, $^3J_{CF}$ = 12.6 Hz, $^1J_{CF}$ = 187.1 Hz, C, C2-Ar), 162.02 (C, C=O), 160.32 (dd, $^3J_{CF}$ = 12.1 Hz, $^1J_{CF}$ = 189.8 Hz, C, C4-Ar), 151.98 (CH, triaz), 148.13 (CH, pyrazine), 145.51 (C, Ar), 145.05 (CH, triaz), 144.47 (CH, pyrazine), 143.67 (CH, pyrazine), 137.26 (C, Ar), 135.22 (C, Ar), 130.96 (dd, $^3J_{CF}$ = 5.1 Hz, $^3J_{CF}$ = 9.6 Hz, CH, C6-Ar), 127.67 (CH x 2, Ar), 120.85 (CH x 2, Ar), 120.70 (dd, $^4J_{CF}$ = 2.26 Hz, $^2J_{CF}$ = 12.2 Hz, CH, C1-Ar), 112.14 (dd, $^4J_{CF}$ = 3.4 Hz, $^2J_{CF}$ = 21.2 Hz, CH, C5-Ar), 104.36 (t, $^2J_{CF}$ = 26.4 Hz, CH, C3-Ar), 50.51 (C$\underline{H}$₂-triaz), 44.07 (C$\underline{H}$), 42.24 (C$\underline{H}$₂-NH).

HPLC (Method A): 100 %, RT = 4.29 min.

HRMS (ESI, m/z): theoretical mass: 464.1646 [M+H]⁺, observed mass: 464.1642 [M+H]⁺.

Chapter VI

(Conclusion)

♦ **Conclusion:**

The aim of this project was to design and synthesise novel CaCYP51 inhibitors owing to frequent drug resistance of azole antifungals in different *Candida* species, specifically *C. albicans*. For compounds design, fluconazole was used as a pharmacophore to build our novel inhibitors. Computational studies were performed to provide a preliminary idea about the conformation, key amino acid interactions and direct binding between the imidazole/triazole nitrogen and the haem iron. The synthetic pathways for all series involved 4 to 8 reaction steps, and compounds were achieved after several optimisations of the reaction conditions or routes. Different purification methods and analyses were performed for all new compounds or intermediates with structures confirmed by ^{1}H, ^{19}F and ^{13}C NMR.

The biological activity of the thiazole backbone in Chapter II and III was negative (MIC > 16 μg/mL compared with fluconazole 0.125 μg/mL) against wildtype antifungal strains even though the computational studies were promising. In contrast, the extended triazole hydroxy benzamide derivatives, especially the (*S*)- and (*R*)-enantiomers of the amide derivative (**57**)**,** in Chapter IV, exhibited excellent binding profile in MOE and MD studies for both CaCYP51 wild type as well as in double mutant (Y132H/K143R and Y132F/F145L) homology models. MOE/MD studies of the fused ring (**59**, **61** and **63**) and biphenyl (**69** and **70**) derivatives were less promising in both configurations compared with thiourea, urea and amide derivatives. However, the extended derivatives, specifically amide (**57**), fused ring (**59**), *para*-(**69**) and *meta*- (**70**) biphenyl extended compounds (Figure 74), showed promising activity against *C. albicans* wildtype as well as against *S. cerevisiae* (MIC, IC$_{50}$, K$_d$, disk diffusion).

The disk diffusion assay results in *S. cerevisiae* single mutant (Y140F and Y140H) strains were promising for the difluoro compounds, in particular the amide (**57c**), fused ring (**59**) and *para*-biphenyl (**69**), while compounds **57c** and **69b** showed the most promising MIC for *S. cerevisiaeas* single mutant (Y140F and Y140H) strains. The difluoro derivatives were examined against *C. albicans* strains that overexpressed CaCdr1, CaCdr2 and CaMdr1 to evaluate efficacy with compounds **59** and **69b** found to be the most effective against *C. albicans* strains overexpressing efflux pump.
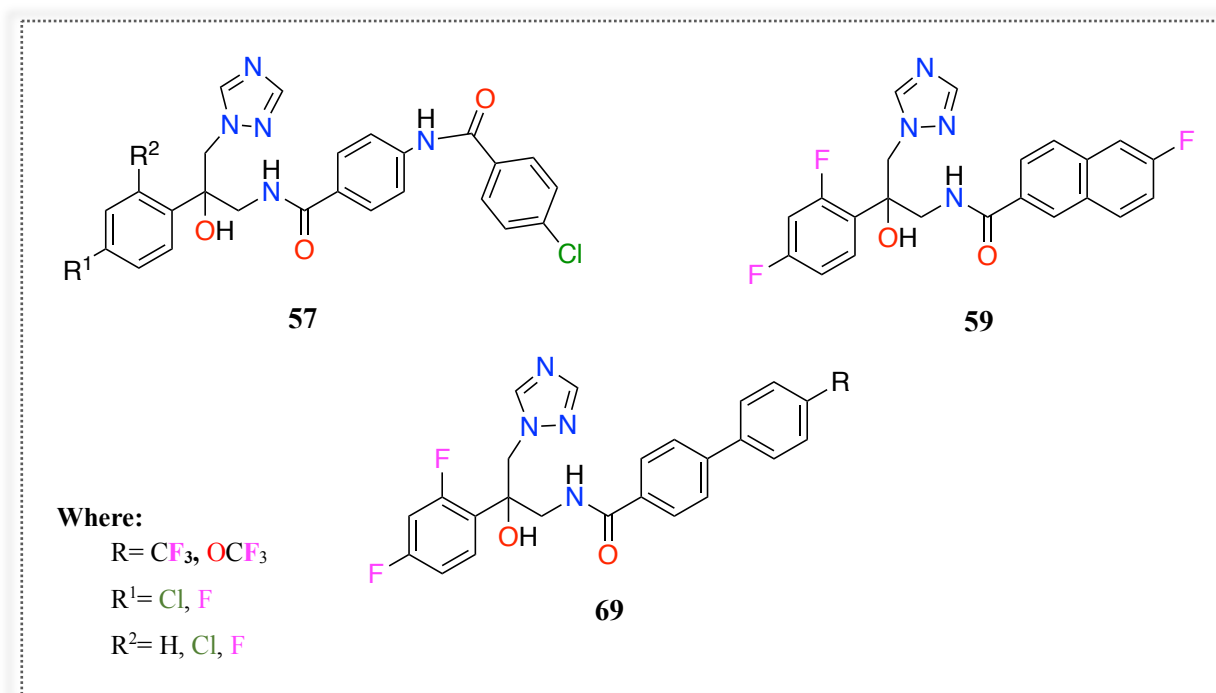
Figure 74: The most promising compounds from all series.

In Chapter V, which included the triazole non-hydroxy propanamide derivatives, the *para*-biphenyl (**80a-d**) compounds showed promising computational results for both (*S*)- and (*R*)-configurations while only the (*R*)-configuration was promising in the substituted amide (**85a-f**) compounds. The novel inhibitors (**80** and **85**) have been sent for biological testing with results still to be received.

Considering the computational studies as well as the antifungal data obtained, it is possible to drive some SAR required for CaCYP51 inhibitors (Figure 75):
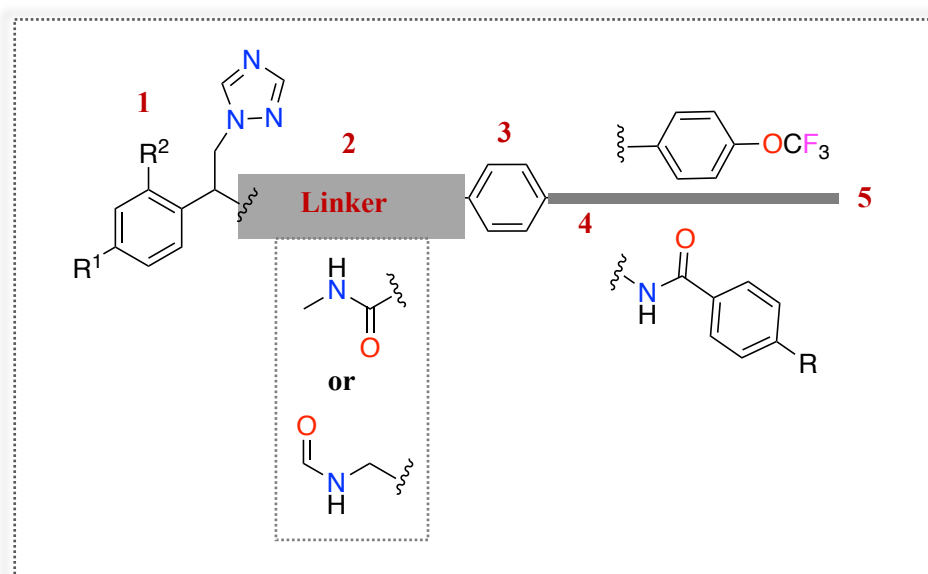
Figure 75: Hypothesised SAR required for CaCYP51 inhibitors, numbers explained in the text.

1. Substituted phenyl at the short arm and CH_2-triazole are important for haem active site binding, position and orientation.

2. Amide is the best linker between the groups that sit in the short arm of the enzyme active site and the extended moieties that fit in the enzyme access channel.

3. Aromatic as a central nucleus to provide more rigid structure with reduced flexibility in the access channel.

4. Less polar functional groups (e.g. amide) or hydrophobic moieties (biphenyl/fused ring) to improve antifungal activity as good activity was observed for compounds with Log P between 3 and 5, which improves uptake across the fungal cell wall.

5. *Para*-substitution with OCF_3 at the lateral chain could block the enzyme entrance through additional binding interactions and/or potentially form a steric block to prevent access of lanosterol i.e. the addition of the OCF_3 enhances the competitive inhibition of the designed inhibitors.

This project has resulted in the generation of promising series of compounds with specific features that showed good biological activity against *C. albicans* as well as the model strain *S. cerevisiae.* Future work will include:

1. Testing all promising compounds against CaCYP51 double mutant strains as well as against different clinical *Candida* species and fungal strains such as *Aspergillus*, *Pneumocysti* and *Cryptococcus*.

2. Selectivity testing for CaCYP51 over human CYP51 and also against a CYP panel, to include CYP2D6 and CYP3A4, to avoid side effects and toxicity.

3. Find a synthetic route to obtain tetrazole derivatives, similar to Chapters IV and V, for better selectivity against hCYP51 as well as better antifungal activity compared with triazole inhibitors.

References

(1)   Engelkirk, P. G.; Duben, E. J. Microbial Diversity. In *Burton's microbiology for the health science*; Wolters Kluwer Health Lippincot Williams and wilkins: Baltimore, **2011**; pp 74–81.

(2)   Bongomin, F.; Gago, S.; Oladele, R.; Denning, D. Global and multi-national prevalence of fungal diseases estimate precision. *J. Fungi* **2017**, *3* (4), 1–29.

(3)   Sanglard, D. Emerging Threats in Antifungal-Resistant Fungal Pathogens. *Front. Med.* **2016**, *3* (1), 1–10.

(4)   Centre for Disease Control and Protection. Fungal diseases and COVID-19. https://www.cdc.gov/fungal/covid-fungal.html (accessed Apr 16, **2021**).

(5)   Nucci, M.; Barreiros, G.; Guimaraes, L. F.; Deriquehem, V. A. S.; Castineiras, A. C.; Nouer, S. A. Increased incidence of candidemia in a tertiary care hospital with the COVID-19 pandemic. *Mycoses.* **2021**, *64* (2), 152–156.

(6)   Koehler, P.; Cornely, O. A.; Bottiger, B. W.; Dusse, F.; Eichenauer, A.; Fuchs, F.; Hallek, M.; Jung, N.; Klein, F.; et al. COVID-19 associated pulmonary aspergillosis. *Mycoses.* **2020**, *63*, 528–534.

(7)   Benedetti, M. F.; Alava, K. H.; Sagardia, J.; Cadena, R. C.; Laplume, D.; Capece, P.; Posse, G.; Nusblat, A. D.; Cuestas, M. L. COVID-19 associated pulmonary aspergillosis in ICU patients: report of five cases from Argentina. *Med. Mycol. Case Rep.* **2021**, *31*, 24–28.

(8)   Mohamed, A.; Rogers, T. R.; Talento, A. F. COVID-19 associated invasive pulmonary aspergillosis: diagnostic and therapeutic challenges. *J. of Fungi.* **2020**, *6* (115), 1-14.

(9)   Posteraro, B.; Torelli, R.; Vella, A.; Leone, P. M.; De Angelis, G.; De Carolis, E.; Ventura, G.; Sanguinetti, M.; Fantoni, M. Pan-echinocandin-resistant *Candida glabrata* bloodstream infection complicating COVID-19: a fatal case report. *J. Fungi.* **2020**, *6* (163), 1–11.

(10)   Whaley, S. G.; Berkow, E. L.; Rybak, J. M.; Nishimoto, A. T.; Barker, K. S.; Rogers, P. D. Azole antifungal resistance in *Candida albicans* and emerging non-*albicans candida* species. *Front. Microbiol.* **2017**, *7* (1), 1–12.

(11)   Araujo, D.; Henriques, M.; Silva, S. Portrait of *Candida* species biofilm regulatory network genes. *Trends Microbiol.* **2017**, *25* (1), 62–75.

(12)   Centre for Disease Control and Protection. Types of Fungal Diseases http://www.cdc.gov/fungal/diseases/ (accessed Jan 15, **2019**).

(13)   Parker, J. E.; Warrilow, A. G. S.; Price, C. L.; Mullins, J. G. L.; Kelly, D. E.; Kelly, S. L. Resistance to antifungals that target CYP51. *J. Chem. Biol.* **2014**, *7* (4), 143–161.

(14)   Flowers, S. A.; Colon, B.; Whaley, S. G.; Schuler, M. A.; David Rogers, P. Contribution of clinically derived mutations in *ERG11* to azole resistance in *Candida albicans*. *Antimicrob. Agents Chemother.* **2015**, *59* (1), 450–460.

(15)   Mayer, F. L.; Wilson, D.; Hube, B. *Candida albicans* pathogenicity mechanisms. *Virulence* **2013**, *4* (2), 119–128.

(16)   Medscape. Candidiasis https://emedicine.medscape.com/article/213853-overview (accessed Oct 27, **2018**).

(17)   Rodrigues, M. L.; Carlos Chagas, I.; Oswaldo Cruz, F. The multifunctional fungal ergosterol. *Ammerican Soc. Microbiligy.* **2018**, *9* (5), 1–5.

(18)   Dupont, S.; Lemetais, G.; Ferreira, T.; Cayot, P.; Gervais, P.; Beney, L. Ergosterol biosynthesis: a fungal pathway for life on land? *Evolution (N. Y).* **2012**, *66* (9), 2961–2968.

(19)   Lv, Q. Z.; Yan, L.; Jiang, Y. Y. The synthesis, regulation, and functions of sterols in *Candida albicans*: well-known but still lots to learn. *Virulence* **2016**, *7* (6), 649–659.

(20)   Choi, J. Y.; Podust, L. M.; Roush, W. R. Drug strategies targeting CYP51 in neglected tropical diseases. *Chem. Rev.* **2014**, *114*, 11242–11271.

(21)   Sanglard, D.; Ischer, F.; Parkinson, T.; Falconer, D.; Bille, J. *Candida albicans* mutations in the ergosterol biosynthetic pathway and resistance to several antifungal agents. *Antimicrob. Agents Chemother.* **2003**, *47* (8), 2404–2412.

(22)   Onyewu, C.; Blankenship, J. R.; Del Poeta, M.; Heitman, J. Ergosterol biosynthesis inhibitors become fungicidal when combined with calcineurin inhibitors against

Candida albicans, *Candida glabrata*, and *Candida krusei*. *Antimicrob. Agents Chemother.* **2003**, *47* (3), 956–964.

(23) Gachotte, D.; Pierson, C. A.; Lees, N. D.; Barbuch, R.; Koegel, C.; Bard, M. A yeast sterol auxotroph (*erg25*) is rescued by addition of azole antifungals and reduced levels of heme. *Biochemistry.* **1997**, *94*, 11173-11178.

(24) Foye, W. O.; Lemke, T. L.; Williams, D. A.; Roche, V. F.; Zito, W. S. Foyes´s principles of medicinal chemistry. *Wolters Kluwer,Lippincott Williams and Wilkins.* **2008**, 606–609.

(25) Hargrove, T. Y.; Friggeri, L.; Wawrzak, Z.; Qi, A.; Hoekstra, W. J.; Schotzinger, R. J.; York, J. D.; Peter Guengerich, F.; Lepesheva, G. I. Structural analyses of *Candida albicans* sterol 14α-demethylase complexed with azole drugs address the molecular basis of azole-mediated inhibition of fungal sterol biosynthesis. *J. Biol. Chem.* **2017**, *292* (16), 6728–6743.

(26) Centre for Disease Control and Protection. Candidiasis https://www.cdc.gov/fungal/diseases/candidiasis/index.html (accessed Oct 28, **2018**).

(27) Nobile, C. J.; Johnson, A. D. *Candida albicans* biofilms and human disease. *Annu. Rev. Microbiol.* **2015**, *69* (1), 71–92.

(28) Vazquez, L. Citation: Vazquez L. Antifungal prophylaxis in immunocompromised patients. *Mediterr J Hematol Infect Dis.* **2016**, *8* (1), 2016040.

(29) Centre for Disease Control and Protection. Risk and prevention of invasive candidiasis, fungal diseases https://www.cdc.gov/fungal/diseases/candidiasis/invasive/risk-prevention.html (accessed May 3, **2021**).

(30) Pappas, P. G.; Lionakis, M. S.; Arendrup, M. C.; Ostrosky-Zeichner, L.; Kullberg, B. J. Invasive candidiasis. *Nat. Rev. Dis. Prim.* **2015**, *373* (1), 1445–1456.

(31) Nogrady, T.; Weaver, D. F. *Medicinal chemistry a molecular and biochemical approach*; Oxford University Press: New York, **2005**; 581-588.

(32) Ben-Ami, R. Treatment of invasive candidiasis: a narrative review. *J. Fungi* **2018**, *4* (97), 1–18.

(33)   Seneviratne, C. J.; Rosa, E. A. R. Antifungal drug discovery: new theories and new therapies. *Frontiers in Microbiology*. **2016**, *7*, 1-131.

(34)   Dixon, D. M.; Walsh, T. J. Antifungala agents. *In Medical Microbilogy*; University of Texas Medical Branch; Galveston, TX, **1996**; 1-7.

(35)   Park, N. H.; Shin, K. H.; Kang, M. K. Antifungal and antiviral agents. In *Pharmacology and Therapeutics for Dentistry*. **2017**; 488–503.

(36)   Alves P. J.; Bailao, A. M.; Amaral, A. C.; Taborda, C. P.; Domiraci, P., J.; Borges, C. L.; Pereira, M. Antifungal resistance, metabolic routes as drug targets, and new antifungal agents: an overview about endemic dimorphic fungi. *Hindawi*. **2017**, 1–16.

(37)   Gintjee, T. J.; Donnelley, M. A.; Thompson, G. R. Aspiring antifungals: review of current antifungal pipeline developments. *J. Fungi* **2020**, *6* (1), 28.

(38)   Nicola, A. M.; Albuquerque, P.; Paes, H. C.; Fernandes, L.; Costa, F. F.; Kioshima, E. S.; Abadio, A. K. R.; Bocca, A. L.; Felipe, M. S. Antifungal drugs: new insights in research & development. *Pharmacol. Ther.* **2019**, *195*, 21–38.

(39)   Park, N. H.; Shin, K. H.; Kang, M. K. Antifungal and antiviral agents. In *Pharmacology and Therapeutics for Dentistry*. **2017**, 488–503.

(40)   Bartlett, J. G. Guidelines for treatment of candidiasis. *Infect. Dis. Clin. Pract.* **2004**, *12* (4), 245–246.

(41)   Shuter, J. Antifungal and antiviral agents: a review. *Cancer Invest.* **1999**, *17* (2), 145–152.

(42)   Perlin, D. S. Echinocandin resistance in *Candida*. *Clinical Infectous Disease.* **2015,** 1-16.

(43)   DrugBank Online. Ibrexafungerp: Uses, Interactions, Mechanism of Action https://go.drugbank.com/drugs/DB12471 (accessed Sep 26, **2021**).

(44)   Medical Xpress. New drug for vaginal yeast infections approved by FDA https://medicalxpress.com/news/2021-06-drug-vaginal-yeast-infections-fda.html (accessed Sep 26, **2021**).

(45)   Baxter, R.; Hastings, N.; Law, A.; Glass, E. J. . Antifungal agents. In *Foyes′s principles of medicinal chemistry*. **2013**, 1159–1174.

(46)   Odds, F. C.; Brown, A. J. P.; Gow, N. A. R. Antifungal agents: mechanisms of action. *Trends Microbiol.* **2003**, *11* (6), 272–279.

(47)   Thummel, K. E.; Kunze, K. L.; Shen, D. D. Enzyme-catalyzed processes of first-pass hepatic and intestinal drug extraction. *Advanced Drug Delivery Reviews.* **1997**, 99–127.

(48)   Darkes, M. J. M.; Scott, L. J.; Goa, K. L.; Abdel-Rahman, S. M.; Roberts, D. T. Terbinafine a review of its use in onychomycosis in adults. *Adis Drug Eval.* **2003**, *4* (1), 39–65.

(49)   Mandal, S. M.; Rao Juvvadi, P.; Yan, L.; Wang, Y.; Jiang, Y.; Zhang, J.; Li, L.; Lv, Q. The fungal CYP51s: their functions, structures, related drug resistance, and inhibitors. *Front. Microbiol.* **2019**, *10* (691), 1–17.

(50)   Jordan, P. Corporate overview and oteseconazole market opportunity advancing women's health. *Mycovia Pharmaceuticals.* **2020**, 1–24.

(51)   Mycovia pharmaceuticals. A study of oral VT-1161 for the treatment of acute vaginal candidiasis (Yeast Infection) in patients with recurrent vaginal candidiasis https://clinicaltrials.gov/ct2/show/NCT03840616 (accessed Jun 11, **2020**).

(52)   Warrilow, A. G.; Nishimoto, A. T.; Parker, J. E.; Price, C. L.; Flowers, S. A.; Kelly, D. E.; Rogers, P. D.; Kelly, S. L. The evolution of azole resistance in *Candida albicans* sterol 14α-demethylase (CYP51) through incremental amino acid substitutions. *Antimicrob. Agents Chemother.* **2019**, *63* (5), 1–16.

(53)   Fothergill, A. W.; Sutton, D. A.; Mccarthy, D. I.; Wiederhold, N. P. Impact of new antifungal breakpoints on antifungal resistance in *Candida* species. *J. Clin. Microbiol.* **2014**, *52* (3), 994–997.

(54)   Pfaller, M. A.; Diekema, D. J.; Sheehan, D. J. Interpretive breakpoints for fluconazole and *Candida* revisited: a blueprint for the future of antifungal susceptibility testing. *Clin. Microbiol. Rev.* **2006**, *19* (2), 435–447.

(55)   Eksi, F.; Gayyurhan, D.; Balci, I.; Joshi, A.; Ouwehand, A. In vitro susceptibility of

Candida species to four antifungal agents assessed by the reference broth microdilution method. *Sci. World J.* **2013**, 1–6.

(56) Prasad, R.; Rawal, M. K.; De Koning, H. P. Efflux pump proteins in antifungal resistance. *Front. Pharmacol.* **2014**, *5* (202), 1–13.

(57) Caruana, C. The electrochemical proton gradient. *WikiLectures*. **2006**, 1-2.

(58) Martel, C. M.; Parker, J. E.; Bader, O.; Weig, M.; Gross, U.; Warrilow, A. G. S.; Rolley, N.; Kelly, D. E.; Kelly, S. L. Identification and characterization of four azole-resistant erg3 mutants of *Candida albicans*. *Antimicrob. Agents Chemother.* **2010**, *54* (11), 4527–4533.

(59) Eddouzi, J.; Parker, J. E.; Vale-Silva, L. A.; Coste, A.; Ischer, F.; Kelly, S.; Manai, M.; Sanglard, D. Molecular mechanisms of drug resistance in clinical *Candida* species isolated from Tunisian hospitals. *Antimicrob. Agents Chemother.* **2013**, *57* (7), 3182–3193.

(60) Sanglard, D.; Oise Ischer, F.; Koymans, L.; Bille, J. Amino acid substitutions in the cytochrome P450 lanosterol 14-demethylase (CYP51A1) from azole-resistant *Candida albicans* clinical isolates contribute to resistance to azole antifungal agents. *Antimicrob. Agents Chemother.* **1998**, *42* (2), 241–253.

(61) Omura, T.; Sato, R.; Heppel, L. A.; Cantoni, G. L. A new cytochrome in liver microsomes. *Comp. Biochem.* **1962**, *237* (4), 1375-1376.

(62) Guengerich, F. P.; Waterman, M. R.; Egli, M. Feature review recent structural insights into cytochrome P450 function. *Trends Pharmacol. Sci.* **2016**, *37*, 625–640.

(63) McKinnon, R. A. Cytochrome P450 part 1: multiplicity and function. *Aust. J. Hosp. Pharm.* **2000**, *30* (2), 54–56.

(64) Furge, L. L.; Guengerich, F. P. Cytochrome P450 enzymes in drug metabolism and chemical toxicology: an introduction. *Biochem. Mol. Biol. Educ.* **2006**, *34* (2), 66–74.

(65) Lewis, D. F. V. *Guide to Cytochrome P450 Structure and Function*; Taylor & Francis, **2001**; 50-59.

(66)   Cook, D. J.; Finnigan, J. D.; Cook, K.; Black, G. W.; Charnock, S. J. *Cytochromes P450: History, Classes, Catalytic Mechanism, and Industrial Application*; Taylor and Francis, UK, **2016**; 105-126.

(67)   Rendic, S.; Guengerich, F. P. Survey of human oxidoreductases and cytochrome P450 enzymes involved in the metabolism of xenobiotic and natural chemicals. *Chem. Res. Toxicol.* **2015**, *28* (1), 38–42.

(68)   Lewis, D. F. V. *Guide to Cytochromes P450*; Taylor & Francis, **1996**; 1-330.

(69)   Froy, O. Cytochrome P450 and the biological clock in mammals. *Curr Drug Metab* **2009**, *10* (2), 104–115.

(70)   Meunier, B.; De Visser, S. P.; Shaik, S. Mechanism of oxidation reactions catalyzed by cytochrome P450 enzymes. *Chem. Rev.* **2004**, *104*, 3947–3980.

(71)   Werck-Reichhart, D.; Feyereisen, R. Protein family review cytochromes P450: a success story. *Genome Biol.* **2000**, *1* (6), 1–9.

(72)   Omura, T.; Sato, R. The carbon monoxide-binding pigment of liver microsomes. *J. Biol. Chem.* **1964**, *239* (7), 2370–1378.

(73)   Lewis, D. F. V; Hlavica, P. Interactions between redox partners in various cytochrome P450 systems: functional and structural aspects. *Biochim. Biophys.* **2000**, *1460*, 353–374.

(74)   Paul R.; Montellano, O.; James, D. J. Cytochrome P450: structure, mechanism, and biochemistry; *Kluwer Academic Plenum.* **2005**, *21*(2), 183-230.

(75)   Huang, X.; Groves, J. T. Oxygen activation and radical transformations in heme proteins and metalloporphyrins. *Chem. Rev.* **2018**, *118*, 2491–2553.

(76)   Guengerich, F. P. Mechanisms of cytochrome P450 substrate oxidation: minireview. *J Biochem Mol. Toxicol.* **2007**, *21* (4), 163–168.

(77)   Choi, J. Y.; Roush, W. R. Structure based design of CYP51 inhibitors. *Curr. Top. Med. Chem.* **2017**, *17* (1), 30–39.

(78)   Hargrove, T. Y.; Friggeri, L.; Wawrzak, Z.; Sivakumaran, S.; Yazlovitskaya, E. M.;

Hiebert, S. W.; Guengerich, F. P.; Waterman, M. R.; Lepesheva, G. I. Human sterol 14α-demethylase as a target for anticancer chemotherapy: towards structure-aided drug design. *J. Lipid Res.* **2016**, *57* (8), 1552–1563.

(79)   Giraud, F.; Guillon, R.; Loge, C.; Pagniez, F.; Picot, C.; Borgne, M. Le; Pape, P. Le. Synthesis and structure-activity relationships of 2-phenyl-1-[(pyridinyl- and piperidinylmethyl)Amino]-3-(1*H*-1,2,4-triazol-1-yl)propan-2-ols as antifungal agents. *Bioorganic Med. Chem. Lett.* **2009**, *19* (2), 301–304.

(80)   Warrilow, A. G.; Nishimoto, A. T.; Parker, J. E.; Price, C. L.; Flowers, S. A.; Kelly, D. E.; David Rogers, P.; Kelly, S. L. The evolution of azole resistance in *Candida albicans* sterol 14α-demethylase (CYP51) through incremental amino acid substitutions. *Antimicrob. Agents Chemother.* **2019**, *63* (5), 1–16.

(81)   Sagatova, A. A.; Keniya, M. V; Wilson, R. K.; Sabherwal, M.; Tyndall, J. D. A.; Monk, B. C. Triazole resistance mediated by mutations of a conserved active site tyrosine in fungal lanosterol 14α-demethylase. *Nat. Publ. Gr.* **2016**, 1–11.

(82)   Zhang, J.; Li, L.; Lv, Q.; Yan, L.; Wang, Y.; Jiang, Y. The fungal CYP51s: their functions, structures, related drug resistance, and inhibitors. *Frontiers in Microbiology.* **2019**, *10*, 1-17.

(83)   Hargrove, T. Y.; Friggeri, L.; Wawrzak, Z.; Qi, A.; Hoekstra, W. J.; Schotzinger ¶, R. J.; York, J. D.; Guengerich, F. P.; Lepesheva, G. I. Structural analyses of *Candida albicans* sterol 14α-demethylase complexed with azole drugs address the molecular basis of azole-mediated inhibition of fungal sterol biosynthesis. *J. Biol. Chem.* **2017**, *292* (16), 6728–6743.

(84)   Marichal, P.; Koymans, L.; Willemsens, S.; Bellens, D.; Verhasselt, P.; Luyten, W.; Borgers, M.; Ramaekers, F. C. S.; Odds, F. C.; Bossche, H. Vanden. Contribution of mutations in the cytochrome P450 14α-demethylase (Erg11p, Cyp51p) to azole resistance in *Candida albicans*. *Microbilogy.* **1999**, *145*, 2701-2713.

(85)   Morio, F.; Loge, C.; Besse, B.; Hennequin, C.; Le Pape, P. Screening for amino acid substitutions in the *Candida albicans* Erg11 protein of azole-susceptible and azole-resistant clinical isolates: new substitutions and a review of the literature. *Diagn.*

Microbiol. Infect. Dis. **2010**, *66*, 373–384.

(86) Sheng, C.; Zhang, W. New lead structures in antifungal drug discovery. *Curr. Med. Chem.* **2011**, *18* (5), 733–766.

(87) Kishk, S.; Simons, C. Pharmaceutical Bio-Technology, Drug Design, Synthesis, and Biological Evaluation of Novel Anti-Infective Drugs, School of pharmacy and pharmaceutical sciences, Cardiff University, **2018**.

(88) RCSB http://www.rcsb.org/pdb/results/results.do?qrid=541319A5&tabtoshow=Current (accessed Jan 28, **2019**).

(89) Mahmood Dar, A. A concise review on the synthesis of pyrazole heterocycles. *J. of Nuclear Medicine and Radiation Therapy.* **2015**, *6* (5), 1–5.

(90) Patonay, T.; Levai, A.; Riman, E.; Varma, R. S. Microwave-induced, solvent-free transformations of benzoheteracyclanones by HTIB (Koser's reagent). *ARKAT USA.* **2004**, *7*, 183–195.

(91) Neuman, R. C. *Oxidation and Reduction from Organic Chemistry*; University of California; Riversied, CA, **2008**, 1-38.

(92) Libretext Chemistry. Reduction of carbonyls to alcohols using metal hydrides https://chem.libretexts.org/Bookshelves/Organic_Chemistry/Supplemental_Modules_(Organic_Chemistry)/Aldehydes_and_Ketones/Reactivity_of_Aldehydes_and_Ketones/Reduction_of_Carbonyls_to_Alcohols_Using_Metal_Hydrides (accessed Feb 8, **2019**).

(93) Li, Z.; Liu, C.; Xu, X.; Qiu, Q.; Su, X.; Dai, Y.; Yang, J.; Li, H.; Shi, W.; Liao, C.; et al. Discovery of phenylsulfonyl acetic acid derivatives with improved efficacy and safety as potent free fatty acid receptor 1 agonists for the treatment of type 2 diabetes. *Eur. J. Med. Chem.* **2017**, *138*, 458–479.

(94) Li, Z.; Qiu, Q.; Xu, X.; Wang, X.; Jiao, L.; Su, X.; Pan, M.; Huang, W.; Qian, H. Design, synthesis and structure-activity relationship studies of new thiazole-based free fatty acid receptor 1 agonists for the treatment of type 2 diabetes. *Eur. J. Med. Chem.* **2016**, *113*,

246–257.

(95) Taban, I. M.; Elshihawy, H. E. A. E.; Torun, B.; Zucchini, B.; Williamson, C. J.; Altuwairigi, D.; Ngu, A. S. T.; McLean, K. J.; Levy, C. W.; Sood, S. Novel aryl substituted pyrazoles as small molecule inhibitors of cytochrome P450 CYP121A1: synthesis and antimycobacterial evaluation. *J. Med. Chem.* **2017**, *60* (24), 10257–10267.

(96) Bhabak, K. P.; Arenz, C. Novel amide- and sulfonamide-based aromatic ethanolamines: effects of various substituents on the inhibition of acid and neutral ceramidases. *Bioorganic Med. Chem.* **2012**, *20* (20), 6162–6170.

(97) Wydysh, E. A.; Medghalchi, S. M.; Vadlamudi, A.; Townsendd, C. A. Design and synthesis of small molecule glycerol 3-phosphate acyltransferase inhibitors. *J. Med. Chem.* **2009**, *52* (10), 3317–3327.

(98) Al-Fattani, M. A.; Douglas, L. J. Penetration of candida biofilms by antifungal agents. *Antimicrob. Agents Chemother.* **2004**, *48* (9), 3291–3297.

(99) Peng, C. C.; Cape, J. L.; Rushmore, T.; Crouch, G. J.; Jones, J. P. Cytochrome P450 2C9 type II binding studies on quinoline-4-carboxamide analogs. *J Med Chem.* **2008**, *51* (24), 8000–8011.

(100) Warrilow, A. G. S.; Martel, C. M.; Parker, J. E.; Melo, N.; Lamb, D. C.; David Nes, W.; Kelly, D. E.; Kelly, S. L. Azole binding properties of *Candida albicans* sterol 14α-demethylase (CaCYP51). *Antimicrob. Agents Chemother.* **2010**, *54* (10), 4235–4245.

(101) Genheden, S.; Reymer, A.; Saenz, M. P.; Eriksson, L. A. Computational chemistry and molecular modelling basics. *The Royal Society of Chemistry.* **2017**, *3*, 1-38.

(102) Schrödinger release 2020-1: Desmond molecular dynamics system, D. E. Shaw research, New York, NY, 2020. Maestro-desmond interoperability tools, Schrödinger, New York, NY, **2020**. [Https://Www.Schrodinger.Com/Desmond/].

(103) Ghose, A. K.; Crippen, G. M. Atomic physicochemical parameters for three-dimensional-structure-directed quantitative structure-activity relationships. 2. modeling dispersive and hydrophobic interactions. *J. chem. Inf. Comput. Sci.* **1987**, *27*, 21-35.

(104) Abhale, Y. K.; Shinde, A.; Keshav.; Deshmukh, K.; Nawale, L.; Dhiman, S.; Pravin,

M. Synthesis, antitubercular and antimicrobial potential of some new thiazole substituted thiosemicarbazide derivatives. *Med. Chem. Res.* **1955**, *26*, 2557–2567.

(105) JH, R.; B, A.; D, A.; Al, E. Reference method for broth dilution antifungal susceptibility testing of yeasts. *Clinical Laboratory Standatds Institution.* **2008**, *28* (14), 1–7.

(106) Binjubair, F. A.; Parker, J. E.; Warrilow, A. G.; Puri, K.; Braidley, P. J.; Tatar, E.; Kelly, S. L.; Kelly, D. E.; Simons, C. Small-molecule inhibitors targeting sterol 14α-demethylase (CYP51): synthesis, molecular modelling and evaluation against *Candida albicans*. *ChemMedChem.* **2020**, *15* (14), 1294–1309.

(107) Perricone, U.; Gulotta, M. R.; Lombino, J.; Parrino, B.; Cascioferro, S.; Diana, P.; Cirrincione, G.; Padova, A. An overview of recent molecular dynamics applications as medicinal chemistry tools for the undruggable site challenge. *The Royal Society of Chemistry.* **2018**, 920–936.

(108) Dong, J.; Chen, S.; Li, R.; Cui, W.; Jiang, H.; Ling, Y.; Yang, Z.; Hu, W. Imidazole-based pinanamine derivatives: discovery of dual inhibitors of the wild-type and drug-resistant mutant of the influenza A virus. *Eur. J. Med. Chem.* **2016**, *108*, 605–615.

(109) S. Kuarm, B.; V. Madhav, J.; Rajitha, B. Xanthan sulfuric acid: an efficient bio-supported and recyclable solid acid catalyst for the synthesis of 2-aminothiazole-5-carboxylates and 2-aminoselenazole-5-carboxylates. *Lett. Org. Chem.* **2011**, *8* (8), 549–553.

(110) Lee, L. F.; Schleppnik, F. M.; Howe, R. K. Syntheses and reactions of 2-halo-5-thiazolecarboxylates. *J. Heterocycl. Chem.* **1985**, *22* (6), 1621–1630.

(111) Sherif, A.F.; Rostoma, b.; Hassan, M.; Faidallah, C.; Mohammed, F.; Radwan, A. Bifunctional ethyl 2-amino-4-methylthiazole-5-carboxylate derivatives: synthesis and *in vitro* biological evaluation as antimicrobial and anticancer agents. *Eur. J. Med. Chem.* **2014**, *76*, 170–181.

(112) Szanti-Pinter, E.; Wouters, J.; Gomory, A.; Saghy, E.; Szoke, E.; Helyes, Z.; Kollar, L.; Skoda-Foldes, R. Synthesis of novel 13α-18-norandrostane-ferrocene conjugates via homogeneous catalytic methods and their investigation on TRPV1 receptor activation. *Steroids.* **2015**, *104*, 284–293.

(113) Atmuri, N. Preparation of *N*-(Boc)-allylglycine methyl ester using a zinc-mediated, palladium-catalyzed cross-coupling reaction. *Org. Synth.* **2015**, *92* (1), 103–116.

(114) Clarke, M.; O'neil, H. Thieno[3,2] pyridine, furo[3,2] pyrimidine, and pyrrolo[3,2-d] pyrimidines useful for treating respiratory syncitial virus infections. Patent WO2016/018697 A1, Februeary 4, **2016**.

(115) Orgainc chemistry. Amino protecting groups stability. https://www.organic-chemistry.org/protectivegroups/amino.shtm (accessed Jan 28, **2021**).

(116) Ozturk, T.; Ertas, E.; Mert, O. Use of Lawesson's reagent in organic syntheses. *Am. Chem. Soc.* **2007**, *107*, 5210–5278.

(117) Koerber, K.; Massiot, G. Total synthesis of nosiphetide. *J. Heterocycl. Chem.* **1995**, *32*, 1309–1315.

(118) Casagrande, M.; Barteselli, A.; Basilico, N.; Parapini, S.; Taramelli, D.; Sparatore, A. Synthesis and antiplasmodial activity of new heteroaryl derivatives of 7-chloro-4-aminoquinoline. *Bioorganic Med. Chem.* **2012**, *20* (19), 5965–5979.

(119) World international property organization. Thiazole derivatives as stearoyl CoA desaturase inhibitors. WO2010007482, December 3, **2008**.

(120) Dovlatyan, V. V.; Eliazyan, K. A.; Pivazyan, V. A.; Kazaryan, E. A.; Engoyan, A. P. Thiazolecarboxylic acid derivatives. 1. *N*-substituted 2-amino-4-methylthiazole-5-carboxylic acid derivatives. *Chem. Heterocycl. Compd.* **2004**, *40* (1), 84–89.

(121) Culbertson, T. P.; Domagala, J. M.; Peterson, P.; Bongers, S.; Nichols, J. B. New 7-substituted quinolone antibacterial agents: the synthesis of 1-ethyl-1,4-dihydro-4-oxo-7-(2-thiazolyl and 4-thiazolyl)-3-quinolinecarboxylic acids. *J. Heterocycl. Chem.* **1987**, *24* (6), 1509–1520.

(122) Warrilow, A. G. S.; Mullins, J. G. L.; Hull, C. M.; Parker, J. E.; Lamb, D. C.; Kelly, D. E.; Kelly, S. L. S279 point mutations in *Candida albicans* sterol 14α-demethylase (CYP51) reduce *in vitro* inhibition by fluconazole. *Antimicrob. Agents Chemother.* **2012**, *56* (4), 2099–2107.

(123) Sekimata, K.; Han, S. Y.; Yoneyama, K.; Takeuchi, Y.; Yoshida, S.; Asami, T. A

specific and potent inhibitor of brassinosteroid biosynthesis possessing a dioxolane ring. *J. Agric. Food Chem.* **2002**, *50*, 3486–3490.

(124) Roman, G.; Vlahakis, J. Z.; Vukomanovic, D.; Nakatsu, K.; Szarek, W. A. Heme oxygenase inhibition by 1-aryl-2-(1*H*-imidazol-1-yl/1*H*-1,2,4-triazol-1-yl)ethanones and their derivatives. *ChemMedChem.* **2010**, *5* (9), 1541–1555.

(125) Molinaro, C.; Guilbault, A.-A.; Kosjek, B. Resolution of 2,2-disubstituted epoxides via biocatalytic azidolysis. *Biotransformations Org. Chem.* **1994**, *33* (1), 1083.

(126) Wang, Y.; Damu, G. L. V; Lv, J. S.; Geng, R. X.; Yang, D. C.; Zhou, C. H. Design, synthesis and evaluation of clinafloxacin triazole hybrids as a new type of antibacterial and antifungal agents. *Bioorganic Med. Chem. Lett.* **2012**, *22*, 5363–5366.

(127) Pore, V. S.; Agalave, S. G.; Singh, P.; Shukla, P. K.; Kumar, V.; Siddiqi, M. I. Design and synthesis of new fluconazole analogues. *Org. Biomol. Chem.* **2015**, *13*, 6551.

(128) Montalbetti, C. N.; Falque, V. Amide bond formation and peptide coupling. *Tetrahedron.* **2005**, *61* (46), 10827–10852.

(129) Soloducho, J.; Olech, K.; Swist, A.; Zajac, D.; Cabaj, J. RecentaAdvances of modern protocol for C-C bonds-the Suzuki cross-coupling. *Adv. Chem. Eng. Sci.* **2013**, *03* (03), 19–32.

(130) Hiren, K.; Ester V.; Albert S.; Rui, A. *Saccharomyces cerevisiaeas* a model organism: a comparative study. *PLoS One.* **2011**, *6* (2), 1–10.

(131) Laboratory methodologies for bacterial antimicrobial susceptibility testing. *OIE Terrestrial Manual.* **2012**, 1-11.

(132) Keniya, M. V.; Ruma, Y. N.; Tyndall, J. D. A.; Monk, B. C. Heterologous expression of full-length lanosterol 14α-demethylases of prominent fungal pathogens *Candida albicans* and *Candida glabrata* provides tools for antifungal discovery. *Antimicrob. Agents Chemother.* **2018**, *62* (11), 1–15.

(133) Monk, B. C.; Keniya, M. V.; Sabherwal, M.; Wilson, R. K.; Graham, D. O.; Hassan, H. F.; Chen, D.; Tyndall, J. D. A. Azole resistance reduces susceptibility to the tetrazole antifungal VT-1161. *Antimicrob. Agents Chemother.* **2019**, *63* (1), 1–19.

(134) Lamping, E.; Monk, B. C.; Niimi, K.; Holmes, A. R.; Tsao, S.; Tanabe, K.; Niimi, M.; Uehara, Y.; Cannon, R. D. Characterization of three classes of membrane proteins involved in fungal azole resistance by functional hyperexpression in *Saccharomyces cerevisiae*. *Eukaryot. Cell*. **2007**, *6* (7), 1150–1165.

(135) Keniya, M. V.; Fleischer, E.; Klinger, A.; Cannon, R. D.; Monk, B. C. Inhibitors of the *Candida albicans* major facilitator superfamily transporter Mdr1p responsible for fluconazole resistance. *PLoS ONE.* **2015**, 1–16.

(136) Marr, K. A.; Lyons, C. N.; Ha, K.; Rustad, T. R.; White, T. C. Inducible azole resistance associated with a heterogeneous phenotype in *Candida albicans*. *Antimicrob. Agents Chemother.* **2001**, *45* (1), 52–59.

(137) Kelly, R.; Miller, S. M.; Kurtz, M. B.; Kirsch, D. R. Directed mutagenesis in *Candida albicans*: one-step gene disruption to isolate Ura3 mutants. *Mol. Cell. Biol.* **1987**, *7* (1), 199–208.

(138) Niimi, M.; Nagai, Y.; Niimi, K.; Wada, S.; Cannon, R. D.; Uehara, Y.; Monk, B. C. Identification of two proteins induced by exposure of the pathogenic fungus *Candida glabrata* to fluconazole. *J. Chromatogr. B*. **2002**, *782*, 245–252.

(139) Zomorodian, K.; Bandegani, A.; Mirhendi, H.; Pakshir, K.; Alinejhad, N.; Fard, A. P. In vitro susceptibility and trailing growth effect of clinical isolates of *Candida* species to azole drugs. *Jundishapur J. Microbiol* **2016**, *9* (2), 1-6.

(140) Benet, L. Z.; Hosey, C. M.; Ursu, O.; Oprea, T. I. BDDCS, the rule of 5 and drugability. *Adv Drug Deliv Rev.* **2016**, *101*, 89–98.

(141) Molinspiration. Calculation of molecular properties and bioactivity score https://www.molinspiration.com/cgi-bin/properties (accessed Sep 1, **2021**).

(142) Giraud, F.; Loge, C.; Pagniez, F.; Crepin, D.; Le Pape, P.; Le Borgne, M. Design, synthesis, and evaluation of 1-(*N*-benzylamino)-2-phenyl-3-(1*H*-1,2,4-triazol-1-yl)propan-2-ols as antifungal agents. *Bioorganic Med. Chem. Lett.* **2008**, *18* (6), 1820–1824.

(143) Borate, H.; Sawargave, S.; Maujan, S. A short synthesis of 3,6-disubstituted-*N*-2-

thienyl/aryl-indoles. *Tetrahedron Lett.* **2009**, *50*, 6562–6566.

(144) Warrilow, A. G. S.; Martel, C. M.; Parker, J. E.; Melo, N.; Lamb, D. C.; David Nes, W.; Kelly, D. E.; Kelly, S. L. Azole binding properties of *Candida albicans* sterol 14α-demethylase (CaCYP51). *Antimicrob. Agents Chemother.* **2010**, *54* (10), 4235–4245.

(145) Warrilow, A. G.; Parker, J. E.; Kelly, D. E.; Kelly, S. L. Azole affinity of sterol 14α-demethylase (CYP51) enzymes from *Candida albicans* and homo sapiens. *Antimicrob. Agents Chemother.* **2013**, *57* (3), 1352–1360.

(146) Xie, J.; Yang, F.; Zhang, M.; Lam, C.; Qiao, Y.; Xiao, J.; Zhang, D.; Ge, Y.; Fu, L.; Xie, D. Antiproliferative activity and SARs of caffeic acid esters with mono-substituted phenylethanols moiety. *Bioorganic Med. Chem. Lett.* **2017**, *27* (2), 131–134.

(147) Andrews, M. D.; Bagal, S. K.; Gibson, K. R.; Omoto, K.; Ryckmans, T.; Skerratt, S. E.; Stupple, P. A. Pyrrolo [2, 3 -d] pyrimidine derivatives as inhibitors of tropomyosin-related kinases. WO2012137089A1, October 11, **2012**.

(148) Marcotullio, M. C.; Campagna, V.; Sternativo, S.; Costantino, F.; Curini, M. A new, simple synthesis of *N*-tosyl pyrrolidines and piperidines. *Synthesis (Stuttg).* **2006**, 16, 2760–2766.

(149) Varala, R.; Babu, B. H. A click chemistry approach to tetrazoles: recent advances. *Mol. Docking.* **2018**, 51-75.

(150) Zhao, D.; Zhao, S.; Zhao, L.; Zhang, X.; Wei, P.; Liu, C.; Hao, C.; Sun, B.; Su, X.; Cheng, M. Discovery of biphenyl imidazole derivatives as potent antifungal agents: design, synthesis, and structure-activity relationship studies. *Bioorganic Med. Chem.* **2017**, *25* (2), 750–758.

(151) Hu, X.; Wan, B.; Liu, Y.; Shen, J.; Franzblau, S. G.; Zhang, T.; Ding, K.; Lu, X. Identification of pyrazolo[1,5- a]pyridine-3-carboxamide diaryl derivatives as drug resistant antituberculosis agents. *ACS Med. Chem. Lett.* **2019**, *10* (3), 295–299.

(152) Emsley, J. W.; Celebre, G.; De Luca, G.; Longeri, M.; Lucchesini, F. A comparison of the structure, flexibility and mesogenic properties of 4-methoxy-4′-cyanobiphenyl and the α,α,α-trifluorinated derivative. *Liq. Cryst.* **1994**, *16* (6), 1037–1049.

(153) Karaluka, V.; Lanigan, R. M.; Murray, P. M.; Badland, M.; Sheppard, T. D. B(OCH$_2$ CF$_3$)$_3$-mediated direct amidation of pharmaceutically relevant building blocks in cyclopentyl methyl ether. *Org. Biomol. Chem.* **2015**, *13*, 10888–10894.

(154) Sabatini, M. T.; Boulton, L. T.; Sheppard, T. D. Borate esters: simple catalysts for the sustainable synthesis of complex amides. *Sci. Adv.* **2017**, *3*, 1–8.